

The effect of L-arginine supplementation on an *in vitro* model of cellular metabolism which underpins metabolic disorders

2023

Saranya Sathiyavasan

A thesis submitted to the University of Kent for the degree of Doctor of Biochemistry

School of Biosciences

Division of Natural Sciences

University of Kent

Declaration

I hereby declare that the project work entitled “The effect of L-arginine supplementation on an *in vitro* model of cellular metabolism which underpins metabolic disorders” submitted to the University of Kent, is a record of an original work done by me under the supervision of Professor Mark Smales at the School of Biosciences, Division of Natural Sciences, University of Kent, and this project work is submitted in the fulfilment of the requirements for the award of the degree of Doctor of Biochemistry . The results embodied in this thesis have not been submitted to any other University or Institute for the award of any degree or diploma.

Ms. Saranya Sathiyavasan

Date 30 April, 2023

Acknowledgment

First of all, I would like to thank almighty God, for letting me through all the difficulties. I have experienced your guidance day by day. You are the one who let me finish my degree. I will keep on trusting you for my future.

Undertaking this PhD has been a truly challenging experience for me and it would not have been possible to do without the support and guidance that I received from many people. At this juncture, I have many people to thank with open arms for their help and probably words will fall short.

No words of thanks can sum up the gratitude that I owe to Professor Mark Smales, who has always been a key person for me in inculcating a learning attitude toward cutting-edge research since my post-graduate study. Without his continuous support, guidance and constant feedback my study would not have been achievable. I would also like to express my sincere gratitude for his moral support to lift me up to continue my study when I went through some difficult situations during my study period. My gratitude goes to Dr. Mark Shepherd for being a second supervisor and helping me during my PhD study period, especially in Griess assay. Thanks are due to Dr. Andrew Lawrence, who helped me with the HPLC analysis, as well as to Dr. Dave Beal, who helped me with the LC-MS experiment.

It is my pleasure to thank Joanne Roobol for her training, support and encouragement throughout my PhD program. My siblings are far away from me, but I can still remember their love and care from you. Jo, thank you so much for your moral support too. I would like to reserve in memory lane and extend a special thanks to Dr. Emma Jane Hargreaves and Dr. Tanya Knight, who went above and beyond to train and assist me with my work at the beginning of my study. I would also like to thank all of the past and present members of Smales's lab for their support in the lab, and their friendship, all of whom have made studying at Kent a great experience.

I give additional thanks to the Eastern University, Sri Lanka as well as extend my thanks to the Accelerating Higher Education and Development Program (AHEAD) Operation, a World Bank funded project to accelerate higher education expansion and development in Sri Lanka, for the award of PhD Scholarship Grant that partially funded my PhD study.

It is impossible for me to express how grateful I am to my dear husband Prashath Perinpasivanantha. It means a lot to me that you sacrifice your life for my study. The love, care and support you gave me throughout my study period made me confident that I could complete my studies successfully. I feel that I truly bless to have a husband like you. Finally, I would also like to give thanks to my and my husband's family members as a whole for their continuous support and understanding when undertaking my study in abroad.

Thanks to everyone.

Abstract

L-arginine (Arg) is a semi-essential amino acid in mammals. L-Arg metabolism in the cell can give rise to urea production and L-ornithine via arginase activity or nitric oxide (NO) and L-citrulline production via nitric oxide synthase (NOS). NO is produced by three isoenzymes of NOS, neuronal NOS (nNOS) and endothelial NOS (eNOS) are isoforms constitutively expressed, inducible NOS (iNOS) is mainly expressed during inflammatory responses. NO is an important intra- and inter-cellular signalling molecule, that regulates lipid and glucose metabolism. Synthesis of NO requires a number of co-factors including tetrahydrobiopterin (BH₄). The biological availability of NO is affected by the NOS inhibitor; N^G-nitro-L-arginine methyl ester (L-NAME) and the NO donor; S-nitroso-N-acetyl-DL-penicillamine (SNAP). This study was conducted to investigate the impact of addition of different concentrations of exogenous L-Arg to cultured model cell systems and on the NOS signalling pathway. The experiments were conducted with cell models to define the direct effects of L-Arg and its catabolic products on specific cell signalling pathway in insulin-sensitive cells; mouse liver epithelial cultured model BNL CL2 (a hepatocyte cell model) and mouse adipocyte cells; 3T3 L1. The cells were cultured in two different additional exogenous concentrations of L-Arg (400 and 800 μM) in L-Arg deficient media or control complete DMEM media (contains 250 μM L-Arg itself and maintained without excess L-Arg treatment) with 10% FBS and the cellular response investigated 24 and 72 h after the L-Arg additions. qRT-PCR was used to determine the mRNA levels of key transcripts for enzymes involved in the metabolism of L-Arg and downstream metabolic pathways whilst Western blotting was undertaken for proteins analysis. NO production was also determined with Griess reagent and residual cell culture supernatant amino acid concentrations (L-Arg, L-Cit and L-Orn) measured by HPLC. To further investigate NO production, the impact of the NOS inhibitor L-NAME (4 mM), external NO donor SNAP (100 μM), and NOS co-factor BH₄ (40 μM) was also analysed. Finally, stably constitutively over-expressing iNOS 3T3 L1 cells were generated and the impact of culturing in elevated exogenous L-Arg (0, 400 and 800 μM) investigated.

The culture viability and number of viable cells were similar upon the addition of exogenous L-Arg whilst the mRNA levels of AMPK and ACC-1 were increased in both cell types, whilst that of CPT-1 was increased in 3T3 L1 cells and decreased in BNL CL2 cells. The protein expression and activation of AMPK and ACC-1 was increased in liver cells in response to increased extracellular L-Arg in a concentration and time dependent manner, explaining the increased energy metabolism in arginine-treated BNL CL2 cells. In this cell model phosphorylated ACC-1, a downstream target of AMPK, increased in response to L-Arg supplementation, resulting in inactivation of ACC-1 and an increase in the activity of CPT-1. The activation of AMPK and ACC-1 was decreased in 3T3 L1 adipose cells in response to L-Arg supplementation, however, there was an increase in the activity of CPT-1 that reportedly facilitates the transport of long-chain fatty acids from the cytosol to mitochondria for oxidation. L-Arg addition also impacted on the level of post-translational modification of proteins involved in cholesterol synthesis, HMGCR and SREBP-2 and a lipogenic regulator SREBP-1 in liver cells (BNL CL2, increased) and adipose cells (3T3 L1, decreased) compared to the control. A hall mark of L-Arg metabolism; NO in the form of NO₂⁻ in cell culture supernatant, was elevated in 800 μM L-Arg cultured samples after 24 h in BNL CL2 cells. However, in 3T3 L1 cells, the amount of NO₂⁻ was elevated in 400 μM (at 72 h) and 800 μM L-Arg (at 24 h) cultures. L-NAME significantly inhibited NO production from liver and adipose cells in a time-dependent manner and subsequently impacted AMPK and ACC expression. L-Arg supplementation also affected mRNA and protein levels of AMPK and ACC-1 in the cells grown in the presence of BH₄ and SNAP. Associated with these changes were changes in the concentration of L-Arg, L-Cit and L-Orn in the culture media. Interestingly there were elevated iNOS mRNA levels in the control, 0 μM and untreated at T=0 samples in comparison to low mRNA levels in the L-Arg supplemented samples. Construction of iNOS in-frame with a V5 tag enabled generation of cell pools over-expressing the iNOS-V5 tagged protein but surprisingly there appeared to be little impact on cell growth or L-Arg metabolism. In conclusion, this study provides new insights into how excess L-Arg in cell culture media impacts NO production and cell signalling pathways in model *in-vitro* cultured liver and adipocyte cells. Collectively, these results show that excess L-Arg is sensed by the cell which then regulates AMPK and ACC-1 expression in response. The findings could have implications in modulation of signalling pathways for treating obesity and obesity induced diabetic mellitus. Inhibition of NO synthesis moderately attenuated the arginine-stimulated increases of AMPK and ACC-1 in BNL CL2 cells whilst regulation of the L-Arg/NOS/NO pathway by BH₄ and SNAP impacted the mRNA and protein expression of AMPK and ACC-1, and consequently culture supernatant nitrite. These data suggest that modulation of the L-Arg-NO pathway may provide a potentially novel means to impact metabolism that underpins generation of fat mass and such a hypothesis could be tested in the future.

Table of Contents

Declaration.....	2
Acknowledgment.....	i
Abstract.....	ii
List of Figures and Captions.....	viii
List of Tables.....	xvii
Abbreviations.....	xviii
Chapter-1 Introduction.....	1
1.1. Background to the study.....	1
1.2. Regulation of the L-arginine/NO pathway.....	2
1.3. A myriad of cellular impacts; the miracle molecule ‘nitric oxide’ and metabolic control.....	4
1.4. The factory of nitric oxide production, ‘Nitric oxide synthase’.....	6
1.4.1. The structure of NOS.....	6
1.4.2. Isoforms of NOS.....	7
1.4.3. The modification, and biological roles of NOS.....	8
1.5. Key sites of metabolism and NO regulation.....	9
1.5.1. Adipose tissue.....	9
1.5.2. The liver.....	12
1.5.3. Muscle.....	13
1.6. The L-arginine metabolic pathway and signalling molecules.....	15
1.6.1. Downstream targets of the L-arginine/NO mechanistic pathway.....	15
1.7. The need for further elucidation of the L-arginine-NOS/NO axis and signalling pathways.....	23
1.7.1.....	23
1.8. Hypothesis of the work in this thesis.....	23
1.9. Main and specific objectives of the work.....	24
Chapter-2 Establishment of BNL CL2 and 3T3 L1 cell culture models and assessment of the impact of exogenous L-arginine addition on cell signalling pathways.....	25
2.1. Introduction.....	25
2.2. Materials and Methods.....	25
2.2.1. Establishment of cell culture models for analysing culture viability and viable cell numbers.....	25
2.2.2. RNA extraction and quantitative real-time PCR (qRT-PCR) for transcript mRNA analysis.....	27
2.2.3. Protein and post-translational modification (phosphorylation) analysis.....	28

2.2.4. Nitric oxide /Nitrite measurement by Griess Assay	35
2.2.5. Analysis of L-arginine, L-ornithine and L-citrulline by HPLC.....	36
2.2.6. Analysis of L-arginine, L-citrulline and L-ornithine adducts with OPA derivatising agent by liquid chromatography– mass spectrometry (LC–MS)	39
2.2.7. Statistical analysis	39
2.3. Results.....	40
2.3.1. Impact of L-Arg addition on culture viability and viable cell numbers in BNL CL2 cells.....	40
2.3.2. qRT-PCR analysis of targets genes and assays upon culturing of BNL CL2 cells in different exogenous L-arginine concentrations.....	43
2.3.3. Monitoring protein and post-translational phosphorylation expression in response to L-Arg supplementation	48
2.3.4. Determination of nitric oxide/nitrite measurements by Griess Assay in BNL CL2 cells grown in different concentrations of exogenous L-arginine.....	71
2.3.5. Impact of L-Arg addition on culture viability and viable cell numbers in 3T3 L1 cells.....	73
2.3.6. qRT-PCR analysis of targets genes upon culturing of 3T3 L1 cells in different exogenous L-arginine concentrations	76
2.3.7. Monitoring protein and post-translational phosphorylation expression in response to L-Arg supplementation	82
2.3.8. Determination of nitric oxide / nitrite measurements by Griess Assay in 3T3 L1 cells grown in different concentrations of exogenous L-arginine.....	104
2.3.9. Confirmation of the formation of the expected L-arginine, L-ornithine and L-citrulline adducts for amino acid analysis by liquid chromatography–mass spectrometry (LC-MS)	106
2.3.10. HPLC analysis of residue L-arginine, L-ornithine and L-citrulline in the cell culture media of BNL CL2 cells cultured in different initial L-arginine concentrations by HPLC	112
2.3.11. HPLC analysis of residue L-arginine, and L-ornithine and L-citrulline in the cell culture media of 3T3 L1 cells cultured in different initial L-arginine concentrations by HPLC	117
2.4. Discussion	121
2.4.1. The impact of exogeneous L-arginine supplementation on BNL CL2 cells	121
2.4.2. The impact of exogeneous L-arginine supplementation on 3T3 L1 cells	131
2.4.3. Overall conclusions from the work presented in this chapter	137
Chapter-3 AMPK and ACC-1 cell signalling upon addition of exogenous L-arginine and NOS inhibitors, co-factors and NO donors to BNL CL2 and 3T3 L1 cells	139
3.1. Introduction	139
3.2. Materials and Methods	139

3.2.1. Preparation of stock solutions of L-arginine, N ^o -nitro-L-arginine methyl ester hydrochloride (L-NAME), 5,6,7,8-tetrahydrobiopterin (BH ₄) and S-nitroso-N-acetyl-DL-penicillamine (SNAP) solution	139
3.2.2. Establishment of cell culture models for investigating AMPK and ACC-1 cell signalling upon addition of exogenous L-Arg and L-NAME; BH ₄ ; co-factor and SNAP to BNL CL2 and 3T3 L1 cells	140
3.2.3. RNA extraction and quantitative real-time PCR (qRT-PCR) for transcript mRNA analysis	143
3.2.4. Protein and post-translational modification (phosphorylation) analysis	144
3.2.5. Nitric oxide /Nitrite measurement by Griess Assay	145
3.2.6. Analysis of L-arginine, L-ornithine and L-citrulline by HPLC	145
3.2.7. Statistical analysis	145
3.3. Results	146
3.3.1. qRT-PCR analysis of targets genes (AMPK and ACC-1) upon culturing of BNL CL2 cells in different exogenous L-Arg concentrations and L-NAME (4 mM), BH ₄ (40 μM) and SNAP (100 μM)	146
3.3.2. Monitoring protein expression (AMPK and ACC-1) in response to L-Arg supplementation to BNL CL2 cells with L-NAME (4 mM), BH ₄ (40 μM) and SNAP (100 μM) additions	152
3.3.3. Determination of nitric oxide / nitrite measurements by Griess Assay in BNL CL2 cells in different concentrations of exogenous L-arginine with L-NAME (4 mM), BH ₄ (40 μM) and SNAP (100 μM).	166
3.3.4. HPLC analysis of residue L-arginine, and L-ornithine and L-citrulline in the cell culture media of BNL CL2 cells cultured in different initial L-arginine concentrations with L-NAME (4 mM), BH ₄ (40 μM) and SNAP (100 μM)	170
3.3.5. qRT-PCR analysis of targets genes (AMPK and ACC-1) upon culturing of 3T3 L1 cells in different exogenous L-arginine concentrations and L-NAME (4 mM), BH ₄ (40 μM) and SNAP (100 μM)	181
3.3.6. Monitoring protein expression (AMPK and ACC-1) in response to L-Arg supplementation to 3T3 L1 cells with L-NAME (4 mM), BH ₄ (40 μM) and SNAP (100 μM)	185
3.3.7. Determination of nitric oxide /nitrite by Griess Assay in 3T3 L1 cells grown in different concentrations of exogenous L-arginine with L-NAME (4 mM), BH ₄ (40 μM) and SNAP (100 μM).	199
3.3.8. HPLC analysis of residue L-arginine, L-ornithine and L-citrulline in the cell culture media of 3T3 L1 cells cultured in different initial L-arginine with L-NAME (4 mM), BH ₄ (40 μM) and SNAP (100 μM)	203
3.4. Discussion	213
3.4.1. BNL CL2 cells grown in different concentrations of exogenous L-arginine with L-NAME (4 mM), BH ₄ (40 μM) and SNAP (100 μM) additions	213
3.4.2. Overall conclusions from the work conducted with BNL CL2 cells	219
3.4.3. 3T3 L1 cells grown in different concentrations of exogenous L-arginine with L-NAME (4 mM), BH ₄ (40 μM) and SNAP (100 μM) additions	219
3.4.4. Overall conclusions from the work conducted with 3T3 L1 cells in this chapter	223

Chapter-4 Generation of 3T3 L1 cells stably over-expressing iNOS and the impact upon cell signalling in the presence or absence of elevated exogenous L-arginine	224
4.1. Introduction	224
4.2. Materials and Methods	224
4.2.1. Establishment of iNOS constructs for iNOS transcript analysis	224
4.2.2. Establishment of iNOS -V5 tagged construct for protein analysis.....	235
4.2.3. Nitric oxide /Nitrite measurement by Griess Assay	240
4.2.4. Analysis of L-arginine, L-ornithine and L-citrulline by HPLC.....	240
4.2.5. Statistical analysis	240
4.3. Results.....	241
4.3.1. Generation of iNOS constructs.....	241
4.3.2. Transient transfection of the iNOS constructs and subsequent iNOS transcript analysis	245
4.3.3. Stable iNOS 3T3 L1 cell pools: The impact of L-Arg addition on culture viability and viable cell numbers	247
4.3.4. qRT-PCR analysis of iNOS, AMPK and β -actin genes upon culturing of stably expressing iNOS-3T3 L1 cells in different exogenous L-arginine concentrations.....	250
4.3.5. Generation of iNOS -V5 tagged construct for transient protein analysis.....	252
4.3.6. Analysis of transient protein expression of iNOS-V5 and a control eGFP	253
4.3.7. Immunofluorescence analysis of transiently expressed iNOS-V5 in 3T3 L1 cells	254
4.3.8. Nitric oxide (as NO_2^-) measurement in stably expressing iNOS-3T3 L1 cells upon culturing in different concentrations of L-Arg.....	256
4.3.9. HPLC amino acid analysis in stably expressing iNOS-3T3 L1 cells upon culturing in different concentrations of L-Arg	257
4.4. Discussion	260
4.4.1. Trouble shooting of endogenously induced iNOS transcript expression	260
4.4.2. Over and constitutive expression of iNOS	260
Chapter-5 Overall Summary and Future Directions.....	262
5.1. Overall Summary and Discussion	262
5.2. Future directions.....	266
References.....	271
Appendices	283
Appendix I. Multialignment of NOS isoforms	283
Appendix II. Composition / formulation of complete DMEM and No L-Arg SILAC DMEM	289
Appendix III. Sequencing results for iNOS-CDS and iNOS-UTR inserts	290

Appendix IV. Sequencing results for iNOS-CDS-in-frame-V5 insert296

List of Figures and Captions

Figure 1.1.1. Chemical structure of L-arginine, L-citrulline and L-ornithine.....	1
Figure 1.1.2. A schematic overview diagram showing the L-arginine metabolism axis interconnected with different biological synthesis processes.	2
Figure 1.2.1. Schematic outlining the interconversion of L-arginine to L-citrulline that is catalysed by nitric oxide synthase (NOS) enzyme and appropriate cofactors.	3
Figure 1.2.2. A schematic diagram showing the biosynthetic pathway for production of NO from L -arginine.	3
Figure 1.3.1. Working model of the systemic effects of NO on obesity and metabolism.	4
Figure 1.4.1. Schematic illustrating the structural organization of different human nitric oxide synthase isoforms.	6
Figure 1.5.1. White and brown adipocytes.	10
Figure 1.5.2. Integrative metabolic pathways in the liver, skeletal muscle and adipose tissue.	14
Figure 1.6.1. Schematic outlining the L-arginine metabolic pathway and subsequent cellular processes impacted.	15
Figure 1.6.2. AMPK-mTOR signalling pathway.	22
Figure 2.2.1. Schematic diagram outlining L-arginine supplementation of medium for BNL CL2 or 3T3 L1 cell growth.	27
Figure 2.2.2. Principle of nitrite quantitation using the Griess reaction	36
Figure 2.2.3. Chemical reaction between OPA and primary amino acid to form an adduct (OPA-ME-AA).....	37
Figure 2.3.1. Cell growth profile of BNL CL2 cells with different concentrations of L-arginine and the control.	41
Figure 2.3.2. Culture viability profile of BNL CL2 cells grown in different concentrations of L-arginine and the control.	42
Figure 2.3.3. Relative mRNA expression of AMPK and ACC-1 in BNL CL2 cells cultured in different concentrations of L-arginine and the control.	45
Figure 2.3.4. Relative mRNA expression of CPT-1 and HMGCR in BNL CL2 cells cultured in different concentrations of L-arginine and the control.	46
Figure 2.3.5. Relative mRNA expression of SREBP-1 and SREBP-2 in BNL CL2 cells cultured in different concentrations of L-arginine and the control.	47
Figure 2.3.6. Western blot comparison for target proteins and phosphorylated proteins expression in BNL CL2 cells cultured at 0 μ M L-Arg concentration for 24 and 72 h and untreated at T=0.	48
Figure 2.3.7. Western blot comparison for target proteins and phosphorylated proteins expression in BNL CL2 cells cultured at the control complete DMEM for 24 and 72 h.....	49
Figure 2.3.8. Western blot comparison for target proteins and phosphorylated proteins expression in BNL CL2 cells cultured at 400 μ M L-Arg concentration for 24 and 72 h.	50

Figure 2.3.9. Western blot comparison for target proteins and phosphorylated proteins expression in BNL CL2 cells cultured at 800 μ M L-Arg concentration for 24 and 72 h.	51
Figure 2.3.10. Western blot comparison for HMGCR expression in BNL CL2 cells cultured at 0, 400 and 800 μ M L-Arg concentration and the control for 24 and 72 h and untreated at T=0.	52
Figure 2.3.11. Western blot comparison for SREBP-1 expression in BNL CL2 cells cultured at 0, 400 and 800 μ M L-Arg concentration and the control for 24 and 72 h and untreated at T=0.	53
Figure 2.3.12. Western blot comparison for SREBP-2 expression in BNL CL2 cells cultured at 0, 400 and 800 μ M L-Arg concentration and the control for 24 and 72 h and untreated at T=0.	54
Figure 2.3.13. Relative protein expression and a western blot across concentration with time for AMPK α protein and AMPK α -P in BNL CL2 cells.	56
Figure 2.3.14. Relative protein expression and a western blot across concentration with time for ACC-1 protein and ACC-1-P in BNL CL2 cells.	58
Figure 2.3.15. Relative protein expression and western blots across concentration with time for CPT-1 protein and mTOR in BNL CL2 cells.	61
Figure 2.3.16. Relative protein expression and a western blot across concentration with time for eEF2 protein and eEF2-P in BNL CL2 cells.	63
Figure 2.3.17. Relative protein expression and a western blot across concentration with time for eIF α protein and eIF α -P in BNL CL2 cells.	65
Figure 2.3.18. Relative protein expression and a western blot across concentration with time for precursor and mature of HMGCR in BNL CL2 cells.	67
Figure 2.3.19. Relative protein expression and a western blot across concentration with time for precursor and mature of SREBP-1 in BNL CL2 cells.	69
Figure 2.3.20. Relative protein expression and a western blot across concentration with time for precursor and mature of SREBP-2 in BNL CL2 cells.	71
Figure 2.3.21. The effect of exogenous L-arginine concentration on nitrite production in BNL CL2 cells.	72
Figure 2.3.22. Cell growth profile of 3T3 L1 cells with different concentrations of L-arginine and the control.	74
Figure 2.3.23. Culture viability profile of 3T3 L1 cells grown in different concentrations of L-arginine and the control.	75
Figure 2.3.24. Relative mRNA expression of AMPK and ACC-1 in 3T3 L1 cells cultured in different concentrations of L-arginine and the control.	78
Figure 2.3.25. Relative mRNA expression of CPT-1 and HMGCR in 3T3 L1 cells cultured in different concentrations of L-arginine and the control.	79
Figure 2.3.26. Relative mRNA expression of SREBP-1 and SREBP-2 in 3T3 L1 cells cultured in different concentrations of L-arginine and the control.	81
Figure 2.3.27. Western blot comparison for target proteins and phosphorylated proteins expression in 3T3 L1 cells cultured at 0 μ M L-Arg concentration for 24 and 72 h and untreated at T=0.	82

Figure 2.3.28. Western blot comparison for target proteins and phosphorylated proteins expression in 3T3 L1 cells cultured at the control complete DMEM for 24 and 72 h.	83
Figure 2.3.29. Western blot comparison for target proteins and phosphorylated proteins expression in 3T3 L1 cells cultured at 400 μ M L-Arg concentration for 24 and 72 h.	84
Figure 2.3.30. Western blot comparison for target proteins and phosphorylated proteins expression in 3T3 L1 cells cultured at 800 μ M L-Arg concentration for 24 and 72 h.	85
Figure 2.3.31. Western blot comparison for HMGCR expression in 3T3 L1 cells cultured at 0, 400 and 800 μ M L-Arg concentration and the control for 24 and 72 h and untreated at T=0.	86
Figure 2.3.32. Western blot comparison for SREBP-1 protein expression in 3T3 L1 cells cultured at 0, 400 and 800 μ M L-Arg concentration and the control for 24 and 72 h and untreated at T=0.	87
Figure 2.3.33. Western blot comparison for SREBP-2 protein expression in 3T3 L1 cells cultured at 0, 400 and 800 μ M L-Arg concentration and the control for 24 and 72 h and untreated at T=0.	88
Figure 2.3.34. Relative protein expression and a western blot across concentration with time for AMPK α protein and AMPK α -P in 3T3 L1 cells.	90
Figure 2.3.35. Relative protein expression and a western blot across concentration with time for ACC-1 protein and ACC-1-P in 3T3 L1 cells.	92
Figure 2.3.36. Relative protein expression and western blots across concentration with time for CPT-1 protein and mTOR in 3T3 L1 cells.	94
Figure 2.3.37. Relative protein expression and a western blot across concentration with time for eEF2 protein and eEF2-P in 3T3 L1 cells.	96
Figure 2.3.38. Relative protein expression and a western blot across concentration with time for eIF2 α protein and eIF2 α -P in 3T3 L1 cells.	98
Figure 2.3.39. Relative protein expression and a western blot across concentration with time for precursor and mature of HMGCR in 3T3 L1 cells.	100
Figure 2.3.40. Relative protein expression and a western blot across concentration with time for precursor and mature of SREBP-1 in 3T3 L1 cells.	102
Figure 2.3.41. Relative protein expression and a western blot across concentration with time for precursor and mature of SREBP-2 in 3T3 L1 cells.	104
Figure 2.3.42. The effect of exogenous L-arginine concentration on nitrite production in 3T3 L1 cells.	105
Figure 2.3.43. Schematic reaction mechanism and mass spectrum for formation of L-arginine adduct in positive polarity and negative polarity.	108
Figure 2.3.44. Liquid chromatogram for standard amino acids mix.	108
Figure 2.3.45. Schematic reaction mechanism, HPLC chromatogram and mass spectrum for formation of L-ornithine adduct in positive polarity.	109
Figure 2.3.46. Schematic reaction mechanism, HPLC chromatogram and mass spectrum for formation of L-arginine adduct in positive polarity.	110

Figure 2.3.47. Schematic reaction mechanism, HPLC chromatogram and mass spectrum for formation of L-citrulline adduct in positive polarity.	111
Figure 2.3.48. Relative and absolute quantification of residual serum L-Arg in BNL CL2 cells cultured in different L-Arg concentrations and the control for 24 and 72 h.	113
Figure 2.3.49. Relative and absolute quantification of residual serum L-Cit in BNL CL2 cells cultured in different L-Arg concentrations and the control for 24 and 72 h.	115
Figure 2.3.50. Relative and absolute quantification of residual serum L-Orn in BNL CL2 cells cultured in different L-Arg concentrations and the control for 24 and 72 h.	116
Figure 2.3.51. Relative and absolute quantification of residual serum L-Arg in 3T3 L1 cells cultured in different L-Arg concentrations and the control for 24 and 72 h.	118
Figure 2.3.52. Relative and absolute quantification of residual serum L-Cit in 3T3 L1 cells cultured in different L-Arg concentrations and the control for 24 and 72 h.	119
Figure 2.3.53. Relative and absolute quantification of residual serum L-Orn in 3T3 L1 cells cultured in different L-Arg concentrations and the control for 24 and 72 h.	121
Figure 2.4.1. Comparison of relative AMPK mRNA and protein expression in BNL CL2 cells cultured in different exogenous L-arginine amounts for different times.	123
Figure 2.4.2. Comparison of relative CPT-1 mRNA and protein expression in BNL CL2 cells cultured in different exogenous L-arginine amounts for different times.	124
Figure 2.4.3. Comparison of relative ACC-1 mRNA and protein expression in BNL CL2 cells cultured in different exogenous L-arginine amounts for different times.	125
Figure 2.4.4. Comparison of relative SREBP-1 mRNA and protein expression in BNL CL2 cells cultured in different exogenous L-arginine amounts for different times.	126
Figure 2.4.5. Comparison of relative HMGCR mRNA and protein expression in BNL CL2 cells cultured in different exogenous L-arginine amounts for different times.	127
Figure 2.4.6. Comparison of relative SREBP-2 mRNA and protein expression in BNL CL2 cells cultured in different exogenous L-arginine amounts for different times.	128
Figure 2.4.7. Comprised urea cycle pathway.	129
Figure 2.4.8. Comparison of relative AMPK mRNA and protein expression in 3T3 L1 cells cultured in different exogenous L-arginine amounts for different times.	131
Figure 2.4.9. Comparison of relative ACC-1 mRNA and protein expression in 3T3 L1 cells cultured in different exogenous L-arginine amounts for different times.	132
Figure 2.4.10. Comparison of relative CPT-1 mRNA and protein expression in 3T3 L1 cells cultured in different exogenous L-arginine amounts for different times.	133
Figure 2.4.11. Comparison of relative SREBP-1 mRNA and protein expression in 3T3 L1 cells cultured in different exogenous L-arginine amounts for different times.	134

Figure 2.4.12. Comparison of relative HMGCR mRNA and protein expression in 3T3 L1 cells cultured in different exogenous L-arginine amounts for different times.	135
Figure 2.4.13. Comparison of relative SREBP-2 mRNA and protein expression in 3T3 L1 cells cultured in different exogenous L-arginine amounts for different times.	136
Figure 2.4.14. The urea cycle of rat white adipose tissue.	137
Figure 3.2.1. Schematic diagram outlining L-arginine and L-NAME (4 mM) supplementation of medium into BNL CL2 or 3T3 L1 cell cultures.	141
Figure 3.2.2. Schematic diagram outlining L-arginine and BH ₄ (40 μM) supplementation into medium for BNL CL2 or 3T3 L1 cell cultures.	142
Figure 3.2.3. Schematic diagram outlining L-arginine and SNAP (100 μM) supplementation into medium for BNL CL2 or 3T3 L1 cell cultures.	143
Figure 3.3.1. Relative mRNA expression of AMPK and ACC-1 in BNL CL2 cells cultured in different concentrations of L-arginine and the control with L-NAME (4 mM).	147
Figure 3.3.2. Relative mRNA expression of AMPK and ACC-1 in BNL CL2 cells cultured in different concentrations of L-arginine and the control with BH ₄ (40 μM).	149
Figure 3.3.3. Relative mRNA expression of AMPK and ACC-1 in BNL CL2 cells cultured in different concentrations of L-arginine and the control with SNAP (100 μM).	151
Figure 3.3.4. Western blot comparison for AMPK and ACC-1 protein expressions in BNL CL2 cells cultured in different concentrations of L-arginine and the control with L-NAME (4 mM).	153
Figure 3.3.5. Relative protein expression and western blot comparisons (with or without L-NAME) for AMPK protein in BNL CL2 cells cultured in different concentrations of L-arginine and the control with L-NAME (4 mM).	155
Figure 3.3.6. Relative protein expression and western blot comparisons (with or without L-NAME) for ACC-1 protein in BNL CL2 cells cultured in different concentrations of L-arginine and the control with L-NAME (4 mM).	157
Figure 3.3.7. Western blot comparison for AMPK and ACC-1 protein expressions in BNL CL2 cells cultured in different concentrations of L-arginine and the control with BH ₄ (40 μM).	158
Figure 3.3.8. Relative protein expression and western blot comparisons (with or without BH ₄) for AMPK protein in BNL CL2 cells cultured in different concentrations of L-arginine and the control with BH ₄ (40 μM).	160
Figure 3.3.9. Relative protein expression and western blot comparisons (with or without BH ₄) for ACC-1 protein in BNL CL2 cells cultured in different concentrations of L-arginine and the control with BH ₄ (40 μM).	162
Figure 3.3.10. Western blot comparison for AMPK and ACC-1 protein expressions in BNL CL2 cells cultured in different concentrations of L-arginine and the control with SNAP (100 μM).	163
Figure 3.3.11. Relative protein expression and western blot comparisons for AMPK protein in BNL CL2 cells cultured in different concentrations of L-arginine and the control with SNAP (100 μM).	164

Figure 3.3.12. Relative protein expression and western blot comparisons for ACC-1 protein in BNL CL2 cells cultured in different concentrations of L-arginine and the control with SNAP (100 μ M).....	165
Figure 3.3.13. The effect of exogenous L-arginine concentration and iNOS inhibitor, L-NAME addition on nitrite production in BNL CL2 cells.....	167
Figure 3.3.14. The effect of exogenous L-arginine concentration and co-factor of iNOS, BH ₄ addition on nitrite production in BNL CL2 cells.....	168
Figure 3.3.15. The effect of exogenous L-arginine concentration and external NO donor, SNAP addition on nitrite production in BNL CL2 cells.....	170
Figure 3.3.16. Relative and absolute quantification of residual serum L-Arg in BNL CL2 cells cultured in different L-Arg concentrations and the control with L-NAME (4 mM) for 24 and 72 h.	171
Figure 3.3.17. Relative and absolute quantification of residual serum L-Cit in BNL CL2 cells cultured in different L-Arg concentrations and the control with L-NAME (4 mM) for 24 and 72 h.	172
Figure 3.3.18. Relative and absolute quantification of residual serum L-Orn in BNL CL2 cells cultured in different L-Arg concentrations and the control with L-NAME (4 mM) for 24 and 72 h.	173
Figure 3.3.19. Relative and absolute quantification of residual serum L-Arg in BNL CL2 cells cultured in different L-Arg concentrations and the control with BH ₄ (40 μ M) for 24 and 72 h.....	174
Figure 3.3.20. Relative and absolute quantification of residual serum L-Cit in BNL CL2 cells cultured in different L-Arg concentrations and the control with BH ₄ (40 μ M) for 24 and 72 h.....	176
Figure 3.3.21. Relative and absolute quantification of residual serum L-Orn in BNL CL2 cells cultured in different L-Arg concentrations and the control with BH ₄ (40 μ M) for 24 and 72 h.	177
Figure 3.3.22. Relative and absolute quantification of residual serum L-Arg in BNL CL2 cells cultured in different L-Arg concentrations and the control with SNAP (100 μ M) for 6 and 24 h.	178
Figure 3.3.23. Relative and absolute quantification of residual serum L-Cit in BNL CL2 cells cultured in different L-Arg concentrations and the control with SNAP (100 μ M) for 6 and 24 h.	179
Figure 3.3.24. Relative and absolute quantification of residual serum L-Orn in BNL CL2 cells cultured in different L-Arg concentrations and the control with SNAP (100 μ M) for 6 and 24 h.	180
Figure 3.3.25. Relative mRNA expression of AMPK and ACC-1 in 3T3 L1 cells cultured in different concentrations of L-arginine and the control with L-NAME (4 mM).	182
Figure 3.3.26. Relative mRNA expression of AMPK and ACC-1 in 3T3 L1 cells cultured in different concentrations of L-arginine and the control with BH ₄ (40 μ M).....	183
Figure 3.3.27. Relative mRNA expression of AMPK and ACC-1 in 3T3 L1 cells cultured in different concentrations of L-arginine and the control with SNAP (100 μ M).	185
Figure 3.3.28. Western blot comparison for AMPK and ACC-1 protein expressions in 3T3 L1 cells cultured in different concentrations of L-arginine and the control with L-NAME (4 mM).....	186

Figure 3.3.29. Relative protein expression and western blot comparisons (with or without L-NAME) for AMPK protein in 3T3 L1 cells cultured in different concentrations of L-arginine and the control with L-NAME (4 mM).	188
Figure 3.3.30. Relative protein expression and western blot comparisons (with or without L-NAME) for ACC-1 protein in 3T3 L1 cells cultured in different concentrations of L-arginine and the control with L-NAME (4 mM).	189
Figure 3.3.31. Western blot comparison for AMPK and ACC-1 protein expressions in 3T3 L1 cells cultured in different concentrations of L-arginine and the control with BH ₄ (40 μM).	191
Figure 3.3.32. Relative protein expression and western blot comparisons (with or without BH ₄) for AMPK protein in 3T3 L1 cells cultured in different concentrations of L-arginine and the control with BH ₄ (40 μM).....	193
Figure 3.3.33. Relative protein expression and western blot comparisons (with or without BH ₄) for ACC-1 protein in 3T3 L1 cells cultured in different concentrations of L-arginine and the control with BH ₄ (40 μM).	195
Figure 3.3.34. Western blot comparison for AMPK and ACC-1 protein expressions in 3T3 L1 cells cultured in different concentrations of L-arginine and the control with SNAP (100 μM).....	196
Figure 3.3.35. Relative protein expression and western blot comparison for AMPK protein in 3T3 L1 cells cultured in different concentrations of L-arginine and the control with SNAP (100 μM).....	197
Figure 3.3.36. Relative protein expression and western blot comparison for ACC-1 protein in 3T3 L1 cells cultured in different concentrations of L-arginine and the control with SNAP (100 μM).....	198
Figure 3.3.37. The effect of exogenous L-arginine concentration and iNOS inhibitor, L-NAME addition on nitrite production in 3T3 L1 cells.	200
Figure 3.3.38. The effect of exogenous L-arginine concentration and co-factor of iNOS, BH ₄ addition on nitrite production in 3T3 L1 cells.	201
Figure 3.3.39. The effect of exogenous L-arginine concentration and external NO donor, SNAP addition on nitrite production in 3T3 L1 cells.	202
Figure 3.3.40. Relative and absolute quantification of residual serum L-Arg in 3T3 L1 cells cultured in different L-Arg concentrations and the control with L-NAME (4 mM) for 24 and 72 h.	204
Figure 3.3.41. Relative and absolute quantification of residual serum L-Cit in 3T3 L1 cells cultured in different L-Arg concentrations and the control with L-NAME (4 mM) for 24 and 72 h.	205
Figure 3.3.42. Relative and absolute quantification of residual serum L-Orn in 3T3 L1 cells cultured in different L-Arg concentrations and the control with L-NAME (4 mM) for 24 and 72 h.	206
Figure 3.3.43. Relative and absolute quantification of residual serum L-Arg in 3T3 L1 cells cultured in different L-Arg concentrations and the control with BH ₄ (40 μM) for 24 and 72 h.....	207
Figure 3.3.44. Relative and absolute quantification of residual serum L-Cit in 3T3 L1 cells cultured in different L-Arg concentrations and the control with BH ₄ (40 μM) for 24 and 72 h.....	208
Figure 3.3.45. Relative and absolute quantification of residual serum L-Orn in 3T3 L1 cells cultured in different L-Arg concentrations and the control with BH ₄ (40 μM) for 24 and 72 h.....	209

Figure 3.3.46. Relative and absolute quantification of residual serum L-Arg in 3T3 L1 cells cultured in different L-Arg concentrations and the control with SNAP (100 μ M) for 6 and 24 h.	210
Figure 3.3.47. Relative and absolute quantification of residual serum L-Cit in 3T3 L1 cells cultured in different L-Arg concentrations and the control with SNAP (100 μ M) for 6 and 24 h.	211
Figure 3.3.48. Relative and absolute quantification of residual serum L-Orn in 3T3 L1 cells cultured in different L-Arg concentrations and the control with SNAP (100 μ M) for 6 and 24 h.	212
Figure 3.4.1. Comparison of relative AMPK (A) and ACC-1 (B) mRNA and protein expression in BNL CL2 cells cultured in iNOS inhibitor, L-NAME (4 mM) in different exogenous L-arginine amounts for different times..	214
Figure 3.4.2. Comparison of relative AMPK (A) and ACC-1 (B) mRNA and protein expression in BNL CL2 cells cultured in co-factor of iNOS, BH ₄ (40 μ M) in different exogenous L-arginine amounts for different times. ...	216
Figure 3.4.3. Comparison of relative AMPK (A) and ACC-1 (B) mRNA and protein expression in BNL CL2 cells cultured in SNAP, as external NO donor (100 μ M) in different exogenous L-Arg amounts for different times.	217
Figure 3.4.4. Comparison of relative AMPK (A) and ACC-1 (B) mRNA and protein expression in 3T3 L1 cells cultured in iNOS inhibitor, L-NAME (4 mM) in different exogenous L-arginine amounts for different times..	220
Figure 3.4.5. Comparison of relative AMPK (A) and ACC-1 (B) mRNA and protein expression in 3T3 L1 cells cultured in co-factor of iNOS, BH ₄ (40 μ M) in different exogenous L-arginine amounts for different times. ...	221
Figure 3.4.6. Comparison of relative AMPK (A) and ACC-1 (B) mRNA and protein expression in 3T3 L1 cells cultured in SNAP, as external NO donor (100 μ M) in different exogenous L-arginine amounts for different times.	222
Figure 4.2.1. The positive control plasmid pBS-iNOS sourced from Addgene.....	225
Figure 4.2.2. The mammalian expression vector pcDNA TM 3.1/Hygro(+).	226
Figure 4.2.3. The FastDigest enzyme cleavage sites.	228
Figure 4.3.1. Agarose gel analysis of the amplified products of Phusion high fidelity DNA polymerase PCR of iNOS gene +/- UTR sequences.	241
Figure 4.3.2. Agarose gel electrophoresis images of iNOS and pcDNA3.1hygro restriction enzyme digest products.....	242
Figure 4.3.3. Generated pcDNA 3.1/ Hygro-iNOS construct with CDS sequence of iNOS.	243
Figure 4.3.4. Generated pcDNA 3.1/ Hygro-iNOS construct including the UTR sequence of iNOS.	243
Figure 4.3.5. Colonies for transformation.....	244
Figure 4.3.6. Agarose gel analysis of PCR products from colony-screening-PCR.	244
Figure 4.3.7. Agarose gel analysis of Apal fast digest enzyme digestion of plasmid DNAs.	245
Figure 4.3.8. Relative quantitation of iNOS transcript (Red curve) and reference gene; β -actin transcript (Green curve) amounts.....	246
Figure 4.3.9. Agarose gel analysis for the amplicon products of qRT-PCR of iNOS or β -actin transcripts.	247

Figure 4.3.10. Cell growth profile of stably expressing and empty vector 3T3 L1 cells with different concentrations of L-arginine and the control.	248
Figure 4.3.11. Culture viability profile of stably expressing and empty vector 3T3 L1 cells with different concentrations of L-arginine and the control.	250
Figure 4.3.12. Relative mRNA expression of iNOS and AMPK in stably expressing iNOS and empty vector 3T3 L1 cells cultured in different concentrations of L-arginine and the control.....	251
Figure 4.3.13. Generated iNOS-in-frame-3.1/V5-His-TOPO Hygro (iNOS-V5 tagged plasmid) construct.....	252
Figure 4.3.14. Agarose gel analysis for single-colony PCR screening and restriction digestion products of plasmid DNA of iNOS-V5 tagged plasmid.	253
Figure 4.3.15. Western blot of transient expression of iNOS-V5 tagged protein in BNL CL2 (A) and 3T3 L1 cells (B).	254
Figure 4.3.16. Western blot analysis of transient expression of eGFP protein in BNL CL2 and 3T3 L1 cells. ...	254
Figure 4.3.17. Combined immunofluorescent images of endogenous AMPK and ACC-1 proteins and V5 tagged iNOS protein in 3T3 L1 cells transfected with iNOS-V5-tagged plasmid and 3.1/V5-His-TOPO empty vector.	255
Figure 4.3.18. The effect of exogenous L-arginine concentration on nitrite production in stably expressing iNOS and the control empty vector 3T3 L1 cells.	256
Figure 4.3.19. The residual plasma L-Arg concentration in stably expressing iNOS and empty vector 3T3 L1 cells grown in excess exogenous L-Arg.....	258
Figure 4.3.20. The residual plasma L-Orn concentration in stably expressing iNOS and empty vector 3T3 L1 cells grown in excess exogenous L-Arg.....	259
Figure 5.1.1. Putative cell signalling pathway of L-Arg/NOS/NO and regulation of this pathway by the modulators L-NAME, BH ₄ and SNAP in liver cells.	265
Figure 5.1.2. Putative cell signalling pathway of L-Arg/NOS/NO and regulation of this pathway by the modulators L-NAME, BH ₄ and SNAP in adipose cells.....	266
Figure 5.1.3. Series of reaction and oxidized congeners of NO.	267

List of Tables

Table 2.2.1. Primers used for real-time qPCR analysis of the target genes listed and size of amplicon expected	30
Table 2.2.2. List of antibodies used and sourced from different companies for Western blotting.	34
Table 2.2.3. HPLC gradient program for separation of L-Arg, L-Cit and L-Orn at flow rate 1.1 mL/min.	38
Table 2.2.4. LC-MS gradient used to identify the derivatisation adducts of amino acids (OPA-ME-AA) at a flow rate 1.5 mL/min.....	39
Table 2.3.1. Comparison of expected mass of the adducts with the experimental mass	106
Table 2.4.1. Selected amino acids concentration in growth media with 10 % FBS.....	130
Table 4.2.1. Components for preparing Lysogeny broth	224
Table 4.2.2. The reaction mixtures components for Phusion high fidelity DNA polymerase PCR.....	227
Table 4.2.3. The reaction mix components for double digest of plasmid or PCR product	229
Table 4.2.4. The reaction mix components for ligation of inserts and vector.....	230
Table 4.2.5. The sequencing primers used in PCR colony screening	231
Table 4.2.6. The reaction mixtures components for Go-Taq DNA polymerase PCR.....	232
Table 4.2.7. Primers used for real-time qPCR analysis of the target iNOS gene listed and size of amplicon expected	234
Table 4.2.8. The reaction mixtures components for iTaq™ Universal SYBR Green One-Step qRT-PCR.....	234
Table 4.3.1. Comparison of Ct cycle numbers for the transient expression of iNOS gene transcript and endogenous expression of reference gene β -actin in transfected BNL CL2 and 3T3 L1 cells	246
Table 5.1.1. Comparison of formulation of complete DMEM and no L-Arg DMEM SILAC media	289
Table 5.1.2. The composition of fetal bovine serum.....	289
Table 5.1.3. Specification and properties of V5 epitope tag	296

Abbreviations

3T3 L1	Mouse adipocytes spontaneously immortalized cell line
ACC	Acetyl-CoA carboxylase
AMPK	5' adenosine monophosphate-activated protein kinase
ANOVA	Analysis of variance
ATP	Adenosine triphosphate
BAT	Brown adipose tissues
BGHR	Bovine growth hormone terminator reverse sequencing primer
BH ₄	(6R)-5,6,7,8-tetrahydrobiopterin
BNL CL2	Mouse hepatocytes spontaneously immortalized cell line
BSA	Bovine serum albumin
CAM	Calmodulin
CDS	Coding sequence
CO ₂	Carbon dioxide
CPT-1	Carnitine palmitoyl transferase-1
DMEM	Dulbecco's modified Eagle medium
DMSO	Dimethyl sulfoxide
DNA	Deoxyribonucleic acid
dNTP	Deoxynucleoside triphosphate
DTT	Dithiothreitol
ecNOS	Endothelial constitutive nitric oxide synthase
EDTA	Ethylene diamine tetra acetic acid
ECL	Enhanced Chemiluminescence
E. Coli	Escherichia coli
eEF2	Eukaryotic elongation factor 2
eEF2K	Elongation factor 2 kinase
eGFP	Enhanced green fluorescent protein
EGTA	Ethylene glycol tetra acetic acid
eIF2	Eukaryotic initiation factor 2
eNOS	Endothelial nitric oxide synthase
FBS	Fetal bovine serum
FFA	Free fatty acids
HMGCR	hydroxy-methylglutaryl coenzyme A reductase
HPLC	High-performance liquid chromatography
IgG	Immunoglobulin G
iNOS	Inducible nitric oxide synthase
L-Arg	L-Arginine
L-Cit	L-Citrulline
LC-MS	Liquid chromatography–mass spectrometry
L-NAME	N ^G -nitro-L-arginine methylester
L-Orn	L-Ornithine
LPS	Lipopolysaccharide
mRNA	Messenger RNA
mTOR	Mammalian target of Rapamycin
NaCl	Sodium chloride
NaF	Sodium fluoride
Na ₃ VO ₄	Sodium orthovanadate
NCBI	National Center for Biotechnology Information
NED	N-(1-naphtyl)-ethylenediamine dihydrochloride
nNOS	Neuronal
NOS	Nitric oxide synthase
NO	Nitric oxide
NO ₂ ⁻	Nitrite

OPA	o-Phthalaldehyde
Opti-MEM	Improved minimal essential medium/ Reduced-serum medium
ORF	Open reading frame
PBS	Phosphate-buffered saline
pBS-iNOS	Plasmid of bacterial strain iNOS
pcDNA	Plasmid cloning DNA
PCR	Polymerase chain reaction
PMSF	Phenylmethylsulfonyl fluoride
qRT-PCR	Quantitative reverse transcription PCR
RIPA	Radioimmunoprecipitation assay buffer
RNA	Ribonucleic acid
SDS-PAGE	Sodium dodecyl-sulfate polyacrylamide gel electrophoresis
SILAC DMEM	Stable isotope labeling with amino acids in cell culture DMEM
SNAP	S-nitroso-N-acetyl-DL-penicillamine
SREBP	Sterol regulatory element binding proteins
TAE	Tris-acetate-EDTA
TAG	Triacylglycerols
TBS	Tris-buffered saline
TBS-T	Tris-buffered saline, 0.1% Tween 20
TG	Triglycerides
T _m	Melting temperature
T _a	Annealing temperature
UTR	Untranslated region
WAT	White adipose tissues

Chapter-1 Introduction

1.1. Background to the study

The 20 amino acids are the key building blocks of proteins and peptides, but also play a role in other metabolic pathways in cells. The study here focuses on eukaryotic cells, specifically mammalian cells (mouse liver and mouse adipose cells), and amino acid metabolism involving the amino acid L-arginine. In mammalian cells amino acids are traditionally defined as nutritionally essential (EAA, cannot be synthesized by the cell) or non-essential amino acids (NEAA). Traditionally EAA include cysteine, histidine, isoleucine, leucine, lysine, methionine, phenylalanine, threonine, tryptophan, tyrosine, and valine (Wu, 2014). Cysteine and tyrosine are sometimes not considered EAAs as they can be synthesized from methionine and phenylalanine but there is no direct synthesis of these (Wu, 2014). Some of the NEAA, particularly arginine, glutamate, glutamine, glycine, and proline are also important in regulating cellular properties such as gene expression, and cell signalling. Thus, particular amino acids regulate major metabolic pathways that are essential for maintenance, proliferation, reproduction and immunity of cells besides their role as building blocks of polypeptides (M. Wang *et al.*, 2014).

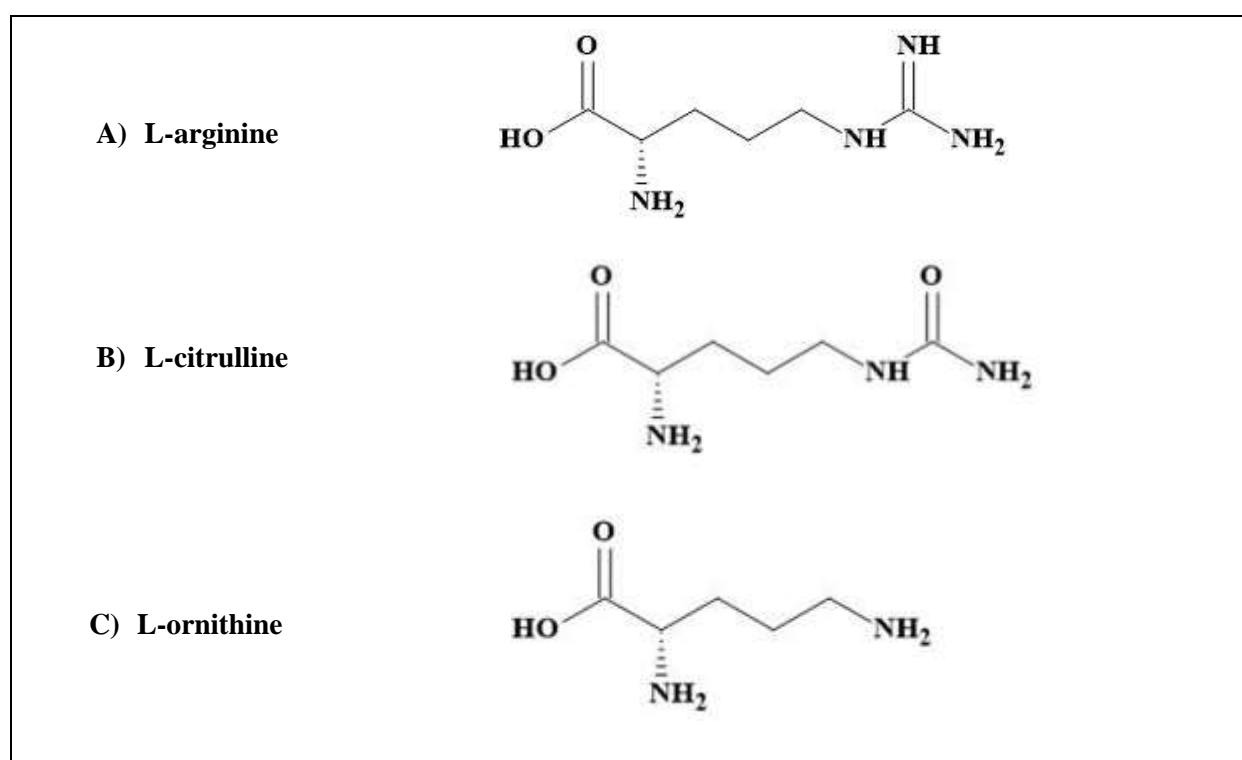


Figure 1.1.1. Chemical structure of L-arginine, L-citrulline and L-ornithine

(A) The chemical structure representing the stereochemistry of L-arginine. The configuration of the chiral L- α -amino acid is L-isomer of arginine, that is L-arginine. The amino acid side-chain of arginine consists of a 3-carbon aliphatic straight chain, the distal end of which is capped by a guanidinium group, which has a pKa of 13.8, and is therefore always protonated and positively charged at physiological pH. Because of the conjugation between the double bond and the nitrogen lone pairs, the positive charge is delocalized, enabling the formation of multiple hydrogen bonds (Fitch *et al.*, 2015). (B) The chemical structure representing the stereochemistry of L-Cit, an α -amino acid. L-Arg undergoes deimination to give L-Cit, converting the positively charged guanidinium moiety into a neutral urea group (Wu *et al.*, 2019). (C) The chemical structure representing the stereochemistry of L-Orn, an α -amino acid. L-Cit consists a side-chain ω -amino group, which is potentially able to coordinate a metal ion in addition to the α -amino group. The ω -NH₂ and α -NH₂ groups are separated by three methylene residues in L-Orn (Conato *et al.*, 2000).

L-arginine (L-Arg, Error! Reference source not found..1) is considered a semi-essential amino acid with a variety of physiological effects on the cell and cell signalling (Sansbury and Hill, 2014). Arginine can be sourced from three main sources; dietary, recycling of amino acids during protein degradation, and from being synthesised from precursor compounds. The most common dietary sources of arginine are meat, fish, dairy products and nuts (Singh *et al.*, 2019). Arginine is also interconvertible with glutamate and proline; however, it is also an important intermediate in the synthesis of, or control of, the production of agmatine, creatine, nitric oxide (NO), polyamines and urea (**Fig 1.1.2**) alongside being a key amino acid in the building of proteins and peptides.

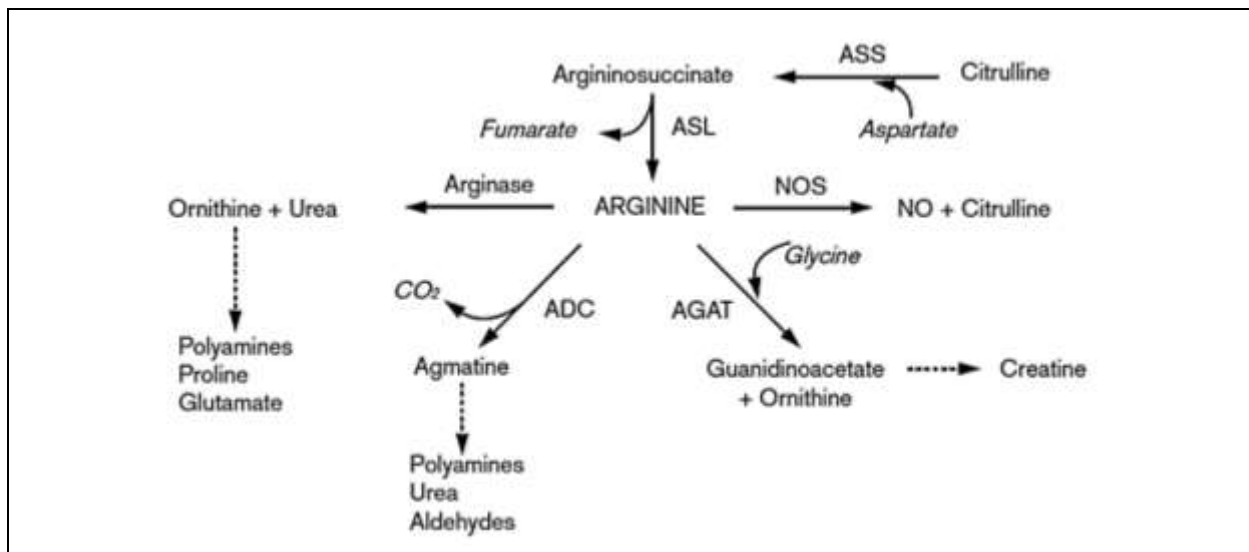


Figure 1.1.2. A schematic overview diagram showing the L-arginine metabolism axis interconnected with different biological synthesis processes.

The key amino acid L-arginine can be interchanged to different amino acids through different metabolic pathways, and is an important intermediate in biological pathways. Arginine is obtained from food, body protein, and *de novo* synthesis from citrulline. Arginine is the substrate for synthesis of proteins, NO and citrulline, urea and ornithine, creatine, and agmatine. Argininosuccinate synthase catalyzes the coupling of citrulline and aspartate to form argininosuccinate, the immediate precursor of arginine and then argininosuccinate lyase catalyze argininosuccinate to produce fumarate and arginine. Abbreviations: ADC, Arginine decarboxylase; AGAT, arginine : glycine amidino transferase; ASL, argininosuccinate lyase; ASS, argininosuccinate synthetase; NO, nitric oxide; NOS, nitric oxide (Morries, 2004).

1.2. Regulation of the L-arginine/NO pathway

L-arginine metabolism in the cell can give rise to urea production and ornithine via arginase activity or nitric oxide and L-citrulline production via nitric oxide synthase (NOS) (**Fig 1.2.1**) (Rath *et al.*, 2014). The homodimers of three NOS isoforms catalyse oxidation of L-arginine via a two-step process. Firstly, L-arginine is hydroxylated to the intermediate N^G-hydroxyl-L-arginine then, secondly, further oxidation produces L-citrulline and NO (**Fig 1.2.2**) (Baldelli *et al.*, 2014; Balligand and Cannon, 1997). The major locations of arginine synthesis in the body are the liver (Osowska *et al.*, 2004) and kidneys (Lau *et al.*, 2000; Brosnan and Brosnan, 2004), of which the kidneys are the vital site for *de-novo* arginine synthesis. Generally, arginine is biologically synthesised in the liver by the urea cycle, then arginine subsequently is a substrate used to produce ornithine and urea in the presence of arginase enzyme.

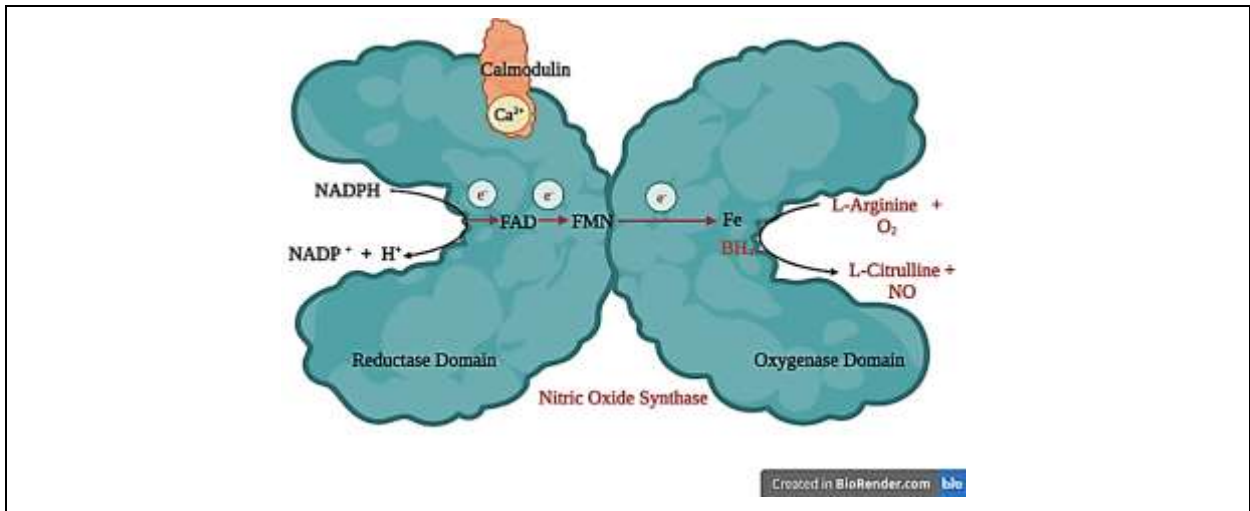


Figure 1.2.1. Schematic outlining the interconversion of L-arginine to L-citrulline that is catalysed by nitric oxide synthase (NOS) enzyme and appropriate cofactors.

There are two domains in the NOS enzyme; a reductase domain and an oxygenase domain. NADPH provides an electron which is carried through the redox carriers FAD and FMN to the oxygenase domain, where they couple with Fe ion and BH₄ at the active site of the NOS enzyme to catalyse the reaction of L-arginine and oxygen to produce L-citrulline and NO (Alderton, Cooper and Knowles, 2001). The flow of electrons throughout the reductase domain depends on Ca²⁺ and CaM binding (Tengan, Rodrigues and Godinho, 2012).

Liver contains an exceptionally high arginase activity to hydrolyse the endogenously synthesised arginine (enhanced arginase-induced arginine utilisation), and there is no net biosynthesis of arginine in the liver from the urea cycle (Osowska *et al.*, 2004; Wu *et al.*, 2013; Wijnands *et al.*, 2015). Citrulline is not taken up by the liver and is spontaneously transported to the kidneys where it is captured and metabolised to arginine, and thereby is a good source or substrate for arginine production (Osowska *et al.*, 2004). The flux of arginine to the liver is controlled by the intestine, where dietary arginine is converted to citrulline. However, the enzymes that metabolise citrulline to arginine (argininosuccinate synthetase and argininosuccinate lyase) are present at very low concentrations in the intestine (Osowska *et al.*, 2004; Cai *et al.*, 2016). As a result, citrulline synthesised by enterocytes cannot be used *in situ* and therefore is captured by the kidneys (approximately 80% of citrulline released by the gut) to be recycled to arginine. This is then circulated in the blood and taken up by the tissues which have a demand for arginine for protein synthesis and other biochemical functions (Osowska *et al.*, 2004). There are structural similarities between L-citrulline and L-arginine, therefore it is important to eliminate L-citrulline promptly to prevent its build-up which can inhibit the enzyme active centre competitively (Cai *et al.*, 2016).

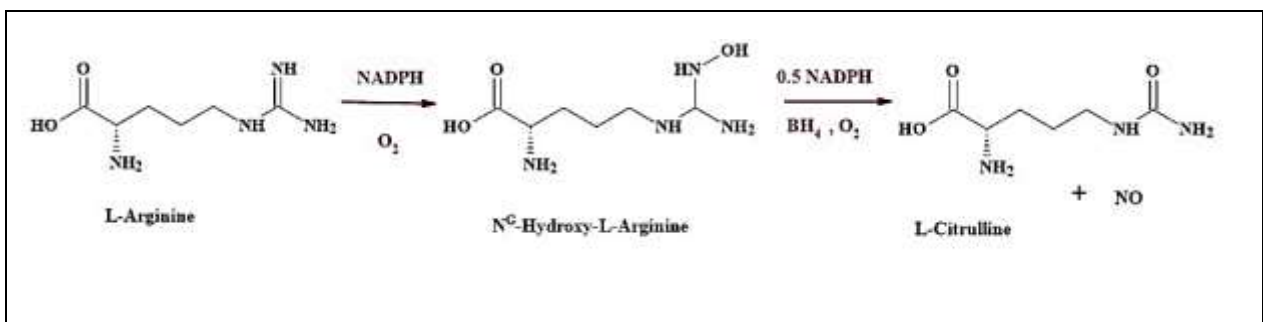
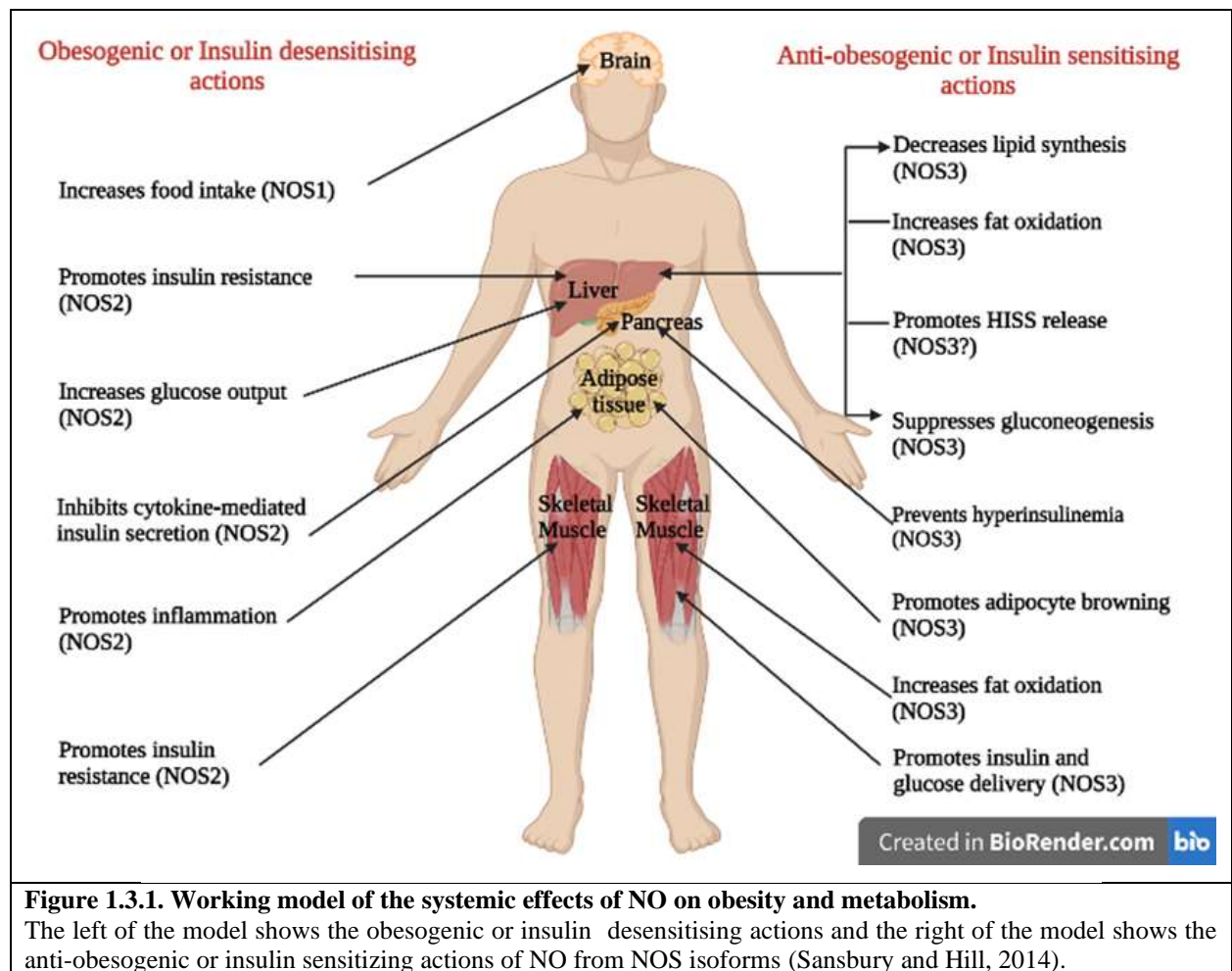


Figure 1.2.2. A schematic diagram showing the biosynthetic pathway for production of NO from L-arginine. At first L-arginine is hydroxylated to the intermediate N^G-hydroxyl-L-arginine then, secondly, further oxidation produces L-citrulline and NO.

Nitric oxide (NO) is synthesised by 3 isoforms of NOS and oxygen, from L-arginine and requires a number of co-factors including tetrahydrobiopterin [(6R)-5,6,7,8-tetrahydrobiopterin] (BH₄), flavin adenine dinucleotide (FAD), flavin mononucleotide (FMN) and nicotinamide adenine dinucleotide phosphate (NADPH) (Tengan, Rodrigues and Godinho, 2012) (**Fig 1.2.1**). BH₄ is an essential cofactor of NOS, playing a crucial role in regulating endothelial NO synthesis (Kohli *et al.*, 2018; Yvette C. Luiking, Engelen and Deutz, 2011). BH₄ itself is synthesized from GTP via the GTP-cyclohydrolase-I (GTP-CH) pathway (Yvette C. Luiking, Engelen and Deutz, 2011). Previous studies have shown that NO synthesis can be regulated by phosphorylated NOS, the presence/concentration of arginine and the cofactor BH₄ (Wu and Meininger, 2002). Besides these cellular modes of regulation of NO production by co-factors, NO is modulated by a range of NOS inhibitors such as N^G-nitro-L-arginine methylester (L-NAME), N^G-monomethyl-L-arginine (L-NMMA) and N^G-nitro-L-arginine (L-NNA) (Hon, Lee and Khoo, 2015).

1.3. A myriad of cellular impacts; the miracle molecule ‘nitric oxide’ and metabolic control

As described above, nitric oxide is an important intra- and inter-cellular (McAdam *et al.*, 2012; Sansbury and Hill, 2014) signalling molecule that regulates nutrient metabolism (Frühbeck and Gómez-Ambrosi, 2001).



Physiological levels of NO (25 to 35 μmol) (Pahlavani *et al.*, 2017) stimulate glucose uptake and oxidation as well as fatty acid oxidation in insulin-sensitive tissues (muscle, heart, liver and adipose), inhibit the synthesis of glucose, glycogen and fat in target tissues (e.g. liver and adipose) and enhance lipolysis in adipocytes

(Jobgen *et al.*, 2006) (**Fig.1.3.1**). The production of NO occurs in nearly all cells and tissues of mammals, particularly adipocytes, endothelial cells, cardiac cells, neurons, hepatocytes, myotubes and phagocytic cell (Lee *et al.*, 2003; Wu *et al.*, 2015).

A simple search in PubMed (02/01/2023) using the term “NO in metabolic disorders” returned 127,911 articles of which 47,258 articles were published in the last decade. These data illustrate the wide scientific interest in, and numerous functions of, NO in a variety of research fields around physiological pathways, pathologic process and pharmaceutical treatment based on NO function (Tengan, Rodrigues and Godinho, 2012).

NO is a gaseous, inorganic, uncharged, diatomic molecule and a free radical with one unpaired electron. The lipophilic (lipophilic of NO analysed by solvation properties of NO using solvation descriptors and water–solvent partition coefficients; Abraham *et al.*, 2000), high diffusible and permeable features of NO facilitate its diffusion through cell membranes until it reaches its destination cell or tissue, where it may initiate a specific biological effect (Tengan, Rodrigues and Godinho, 2012). In contrast to other second messenger molecules, NO does not directly couple with intracellular or extracellular receptors in order to elicit its biological functions (Baldelli *et al.*, 2014). Interestingly, NO is synthesised on demand in specific destinations because it has short half-life (5 s) (Tengan, Rodrigues and Godinho, 2012).

Oxidative metabolite products of NO are nitrites and nitrates whose formation swiftly deactivates NO and which are diffused into circulation. As such, the previous existence of NO in circulation can be measured indirectly by determining the concentrations of nitrite and nitrate present and these are frequently used as indicators of the NO concentration (Hon, Lee and Khoo, 2015). NO also regulates intracellular cGMP levels that are increased via the stimulation of soluble guanylate cyclase, which then binds to the iron in the haem centre, and as such the concentration of cGMP is also proportional to the presence of NO (Hon, Lee and Khoo, 2015).

The fate of a number of possible NO redox forms, including NO^+ , NO^\cdot and NO^- have roles in cell signalling through involvement in a range of different chemical reactions within the cell (Hon, Lee and Khoo, 2015). Lipid peroxidation-free radicals impact carbon-carbon double bond in lipids (Ayala, Muñoz and Argüelles, 2014) and nitration of tyrosine residues in proteins are indirectly interconnected to peroxynitrite, a highly reactive molecule, produced by NO reaction with a superoxide anion (Hon, Lee and Khoo, 2015).

In addition to the well-established roles of NO in various signalling cascades, NO regulates some enzymes due to its ability to activate soluble guanylate cyclase (sGC) and inhibit cytochrome c oxidase via the interaction of NO with haem (Baldelli *et al.*, 2014). The enzymes catalyse reactions in the respiratory cycle; mitochondrial respiratory complexes, the tricarboxylic acid (TCA) cycle; aconitase and DNA synthesis pathways are at least in part modulated by coupling of NO to non- haem iron and iron-sulphur centres present in many enzymes (Baldelli *et al.*, 2014) (Hon, Lee and Khoo, 2015). There is a potential of NO to combine with the haem groups of cytochromes, the consequence of this being a decreased rate of metabolism and reduction in the capability of oxidation of these enzymes (Clemens, 1999).

1.4. The factory of nitric oxide production, ‘Nitric oxide synthase’

1.4.1. The structure of NOS

The well described three isoforms of NOS originate from three different genes and at the nucleotide sequence level these share around 51-57% identity (Wu and Morris, 2008; Tengan, Rodrigues and Godinho, 2012). Dimerization of the NOS enzyme is required to stimulate its function. There are two subunits in the NOS enzyme, an N-terminal oxygenase subunit consisting of binding sites for L-arginine, BH₄ and haem (Fe) and the C-terminal reductase subunit containing binding sites for the crucial cofactors FMN, FAD, NADPH and calmodulin (Tengan, Rodrigues and Godinho, 2012; Baldelli *et al.*, 2014). Both subunits are held together by a zinc ion, which is bound by two cysteines ligands from each subunit to build the dimeric complex. Calmodulin binds to a linker region between the two domains and is necessary for NOS activity (Feng, 2012) (**Fig 1.2.1 and 1.4.1**). However, there are some specific different features present in the isoforms nNOS and eNOS. In the nNOS isoform there is a 250 amino acid N-terminal sequence addition in skeletal muscle, named the PDZ domain (postsynaptic density protein 95/discs large/ZO-1 homology domain), which facilitates the enzymes present in sarcolemma in skeletal muscle. The eNOS isoform has sites for myristoylation and palmitoylation located in the N-terminal for acylation by myristate and palmitate, which is obligatory for the subcellular localization of eNOS in the caveolae of endothelial cells (Tengan, Rodrigues and Godinho, 2012).

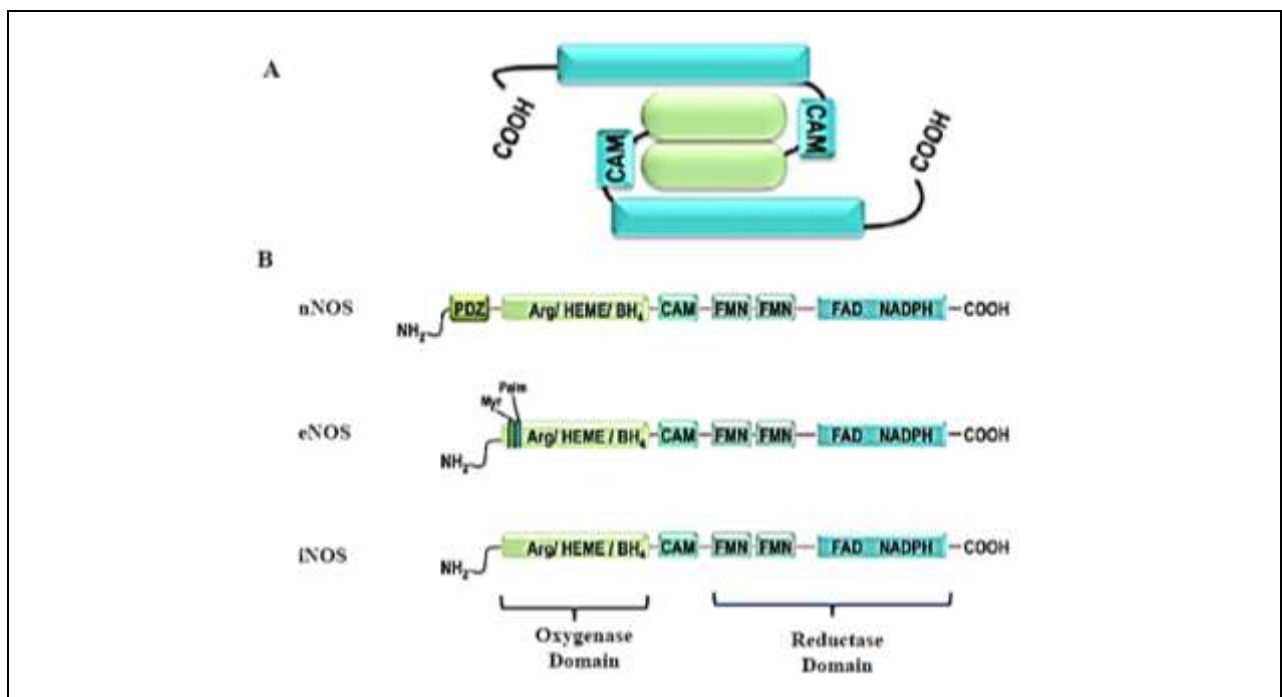


Figure 1.4.1. Schematic illustrating the structural organization of different human nitric oxide synthase isoforms.

(A) The dimeric conformation of nitric oxide synthases (NOS) with both oxygenase and reductase domains. (B) Core structural differences within the three NOS isoforms with specific features of nNOS (PDZ domain) and eNOS (sites for myristoylation (Myr) and palmitoylation (Palm) shown). Noticeably, all isoforms contain the oxygenase domain consisting of binding sites for L-arginine (Arg), Haem and tetrahydrobiopterin (BH₄) and the reductase domain consisting of binding sites for calmodulin (CAM), FMN, FAD and NADPH. iNOS is denoted induced NOS enzyme (Tengan, Rodrigues and Godinho, 2012).

The regulation of NOS, including limiting/activating its activity, expression and localisation are complicated and multifactorial because of numerous physiological roles of NOS crosstalk with many signalling pathways,

expression specificity of NOS to tissues and different isoforms of NOS (Tengan, Rodrigues and Godinho, 2012). Some of these mechanisms are discussed in more detail for each isoform below.

1.4.2. Isoforms of NOS

The isozymes of NOS have sequence variations and this has an impact on the biological mechanisms by which they act (De Vera, Geller and Billiar, 1995). As described above, three isoforms of nitric oxide synthase (NOS) are known; calcium-dependent and membrane associated endothelial NOS (eNOS or NOS3), calcium-dependent neuronal NOS (nNOS or NOS1) (Alderton, Cooper and Knowles, 2001), and calcium-independent cytosolic inducible NOS (iNOS or NOS2) (Alderton, Cooper and Knowles, 2001; Sessa, 2004; Balligand, Feron and Dessy, 2009; De Vera, Geller and Billiar, 1995). eNOS and nNOS are expressed constitutively at low amounts in a variety of cell types and tissues and are controlled by the level of Ca^{2+} binding with calmodulin (Wu and Morris, 2008; Tengan, Rodrigues and Godinho, 2012). However, iNOS is not expressed, or very low level, in cells or tissues under ‘normal’ condition (Wu and Morris, 2008) and instead its expression is induced under appropriate conditions (Alderton, Cooper and Knowles, 2001). The initial purification and characterisation of iNOS was successfully carried out from murine macrophages (Cinelli *et al.*, 2020). Further, iNOS is not modulated by Ca^{2+} (Tengan, Rodrigues and Godinho, 2012). It should be noted that there are two types of nomenclature commonly used for naming NOS isoforms; numerical and descriptive nomenclatures. The former nomenclature denotes NOS isoforms as nNOS being type I, iNOS as type II and eNOS as type III. The later nomenclature labels NOS isoforms based on the interaction of Ca^{2+} , here Ca^{2+} is denoted by a letter “c”, therefore neuronal and endothelial isoforms are named as ncNOS and ecNOS, respectively (Tengan, Rodrigues and Godinho, 2012).

iNOS expression can be induced by cytokines and endotoxin. iNOS expresses in many cell types in large amounts and can be either cytoprotective or cytotoxic in cells (De Vera, Geller and Billiar, 1995) including hepatocytes, macrophages (Vos *et al.*, 1999; Sass *et al.*, 2001), smooth muscle, chondrocytes (Vos *et al.*, 1999) and cardiac myocytes (Cinelli *et al.*, 2020). Kupffer cells, the macrophage cells of the liver, that have been activated by lipopolysaccharide (LPS), lead to the activation and production of inflammatory mediators such as NO by iNOS (Mustafa and Olson, 1999; Wang *et al.*, 1999). The main stimulators of iNOS expression are tumour necrosis factor (TNF), interleukin- 1β (IL- 1β), interferon- γ (IFN- γ) and lipopolysaccharide (LPS). LPS is a weak inducer for iNOS when it is applied alone. Some non-immune cells need combinations of these inducers to initiate NO synthesis (Cinelli *et al.*, 2020). For example, a previous study reported that in mouse skeletal muscle NO is not produced by these inducers when applied alone to the cells, however combinations of these inducers, such as IFN- γ and TNF or IL-1 (or with all three cytokines) stimulated NO production in the cells (Cinelli *et al.*, 2020). The stimulation and expression of iNOS therefore has cell specificity and species specificity. For instance, iNOS expression in rat and mouse glial cells can be stimulated by the solitary effect of LPS, but it cannot stimulate iNOS in human cells (Cinelli *et al.*, 2020).

Neuronal NOS (nNOS) is a constitutively active form of NOS and has a much wider tissue expression, although it is most highly expressed in the brain whilst also being expressed in skeletal muscle, testis, lung and kidney, and at low levels in heart, adrenal gland and the retina. nNOS is encoded by the gene NOS1

located on chromosome 12q24.22, consisting of 29 exons and there being a minimum ten transcript variants including nNOS μ , nNOS β and nNOS δ . The variant nNOS μ was discovered at first in mouse skeletal and cardiac muscles, but later was observed in other parts of the human body; aorta, bladder, colon, corpus cavernosum and placenta (Tengan, Rodrigues and Godinho, 2012). As discussed earlier, nNOS contains an extra PDZ motif localised at the N-terminus, thereby nNOS can interact with the PDZ motif of other proteins. This communication between the PDZ motifs of proteins govern the subcellular localisation and activity of nNOS (Baldelli *et al.*, 2014).

Endothelial NOS (eNOS), also known as constitutive NOS (cNOS), is primarily expressed in endothelial cells. However, eNOS is also expressed in bone marrow-derived cells such as leukocytes, red blood cells and platelets (Dick *et al.*, 2020). The localization of eNOS is not defined clearly although it is generally localised to the plasma membrane and cytoplasm (Jobgen *et al.*, 2006). It is thought that most eNOS is located in the caveolae, where it is bound to caveolin, a resident coat protein (Albrecht *et al.*, 2003). Caveolae is a lipid raft, involved in small invaginations of the plasma membrane in many vertebrate cell types, especially in endothelial cells, adipocytes and embryonic notochord cells (Bastiani and Parton, 2010). The functionality of the eNOS dimer is mainly controlled by the co-factor BH₄ (Jobgen *et al.*, 2006). The discovery of the interaction between eNOS expression with mitochondrial markers in skeletal muscle resulted in the proposal of a close relationship between eNOS and mitochondria. In addition to all the well-known isoforms of NOS, a study to analyse eNOS in rat liver and brain using gold labelling and electron microscopy resulted in the authors suggesting that a mitochondrial NOS (mtNOS) might be eNOS or another form of NOS with substantial homology to the eNOS form (Tengan, Rodrigues and Godinho, 2012).

1.4.3. The modification, and biological roles of NOS

Phosphorylation of eNOS at numerous sites impacts its activity such that either positive (stimulatory) or negative regulation can be imparted by this post-translational modification. So far seven phosphorylation sites of eNOS have been categorized, with stimulatory sites (2; S615, S1177), inhibitory sites (3; S114, T495, Y657) and two remaining sites (Y81, S633) where the effect on eNOS activity, if any, is not yet known. Interestingly, upon phosphorylation at S1177 and S615 of eNOS residue by AMPK, this activates eNOS. External stimuli (Akt/ PKA; protein kinase B signalling) and the internal metabolic state of AMPK in the cell regulates eNOS activity. Metformin, a drug broadly used to treat type 2 diabetes, has recently been shown to stimulate the AMPK (Hawley *et al.*, 2002). However, such AMPK activation was not observed in eNOS knockout mice when treated with metformin and further to this, physical activities in eNOS knockout mice did not activate AMPK (Cunningham, Sheldon and Rector, 2020). Surprisingly, NO donors activate phosphorylation of AMPK. These findings support the hypothesis that the beneficial effect of eNOS in metabolic pathways are exerted in an AMPK-dependent manner and eNOS may play a vital role in cellular signalling when energy or metabolic signals are imbalanced, such as in obesity (Cunningham, Sheldon and Rector, 2020).

The eNOS/NO pathway has well-known roles in metabolic disorders and mitochondrial dynamics (Cunningham, Sheldon and Rector, 2020). eNOS knockout mice form insulin resistance in liver and marginal tissues and when they are fed with a high-fat diet develop fat content in liver compared to wild type. Obese

patients with a range of degrees of obesity have shown notable dysfunction of eNOS. In a nut shell, eNOS has a major role in metabolic disorders (Cunningham, Sheldon and Rector, 2020).

Extracellular L-arginine is required for optimal NO synthesis by eNOS and iNOS in rat superior mesenteric artery rings and was optimal at a concentration of L-arginine close to the plasma level. These results provide showed that extracellular L-arginine can enhance endothelium function only when the endothelium is impaired or when iNOS has been induced. The L-arginine/NO pathway is sensitive to extracellular L-arginine concentration, thus altering the extracellular L-arginine concentration regulates the production of NO (MacKenzie and Wadsworth, 2003). It has also been reported that induced macrophages produced NO and this is dependent on the exogenous supply of L-arginine (Kuo, 1998).

1.5. Key sites of metabolism and NO regulation

Three key main organs and tissue; liver, adipose and muscle regulate key metabolic pathways. The enzymes present in these organ's tissues catalyse the storage, usage or generation of specific fuels. Mechanisms of metabolic control in these tissues are interconnected with other tissues (Honka *et al.*, 2018) (**Fig 1.5.2**).

1.5.1. Adipose tissue

Adipose tissue is a mature connective tissue type, under the loose connective tissue. This consists of adipocytes, derived form of fibroblasts (Ye *et al.*, 2022). The cellular process of differentiation of preadipocytes into mature adipocytes is called as adipogenesis, which modulates the development of adipose tissue and energy balance. A vital regulator for adipogenesis at the transcriptional stage is peroxisome proliferator-activated receptor γ (PPAR γ), a member of the nuclear-receptor superfamily (Luo and Liu, 2018). Adipose tissues are located with the areolar connective tissue in places such as the deeper coat of skin, heart and kidneys, yellow bone marrow, cushioning joints and in the eye socket (Tortora and Derrickson, 2019).

During vertebrate evolution, multicellular organisms formed adipocytes as an additional energy storage depot. Prominent adipocytes are found in mammals, birds, reptiles, amphibians and fish. However, the localization of the adipocytes are different (Rosen and Spiegelman, 2011). Conventional adipose storage places are found in more mammals. Large structural adipocytes can have only a moderate or low contribution to energy balance, for instance, fat pads of the heels, fingers and toes and the periorbital fat supporting the eyes (Giorgino, Laviola and Eriksson, 2005). Some adipocytes are associated with the skin and referred to as subcutaneous fat. Herniation of subcutaneous fat within fibrous connective tissue forms 'cellulite'. Other adipose tissue depots are found for example wrapping around the heart and other organs, aligned with the intestinal mesentery and in the retroperitoneum. Among these are those referred to as visceral fat, channelled to the hepatic-portal vein and associated with diseases such as obesity and type 2 diabetes. The distribution of fat in the human body is considered more important in terms of health and disease than the total amount of fat (Giorgino, Laviola and Eriksson, 2005).

Besides the different localizations of fat cells, there are two major traditional structural classification based on their distinct colour. These are brown adipose tissues (BAT) and white adipose tissues (WAT) (Richard, 2000; Giorgino, Laviola and Eriksson, 2005). The differences between brown and white adipocytes are based on

their structural arrangement, size and arrangement of organelles within the cells (Fitzgerald *et al.*, 2018; de sa *et al.*, 2017) (**Fig 1.5.1**). WAT is mostly found in adults, with a single large fat drop, and due to this fat drop, the cytoplasm and nucleus are pushed to one of the pole sides of the cell (Fitzgerald *et al.*, 2018; Tortora and Derrickson, 2019). WAT in humans is important in storing energy (Song, Xiaoli and Yang, 2018), hormonal secretion and signalling and sensitizing insulin (Richard, 2000).

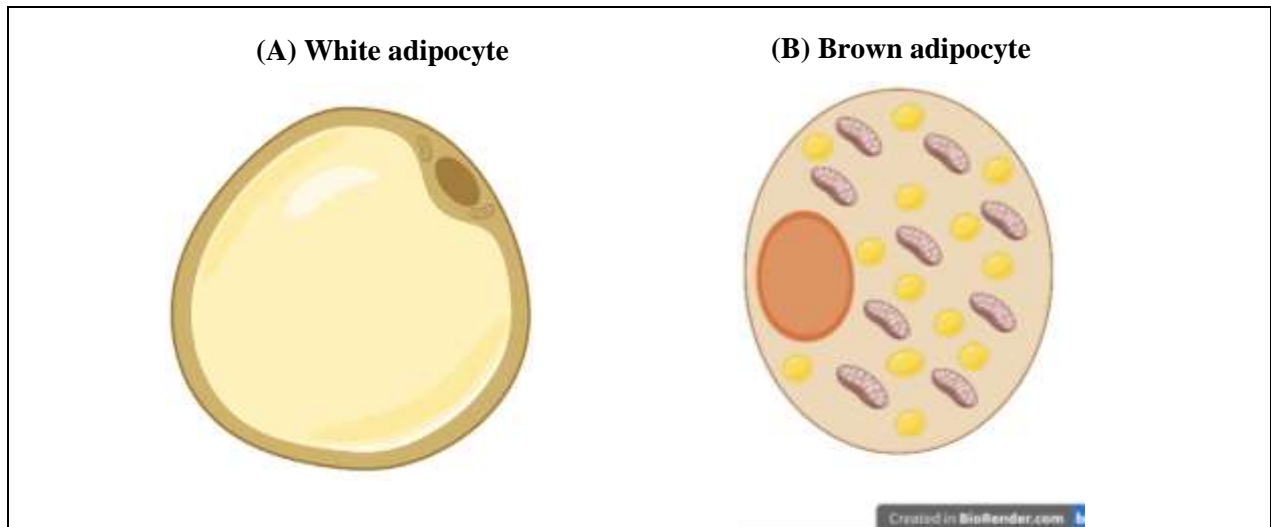


Figure 1.5.1. White and brown adipocytes.

(A) White adipocyte, a spherical shape, consists of significant size of lipid droplet that occupies a large proportion of the cytoplasm and displaces the nucleus and cell organelles to the edge of the cell. White colour appearance is formed in white adipocyte because of the massive lipid content. (B) Brown adipocyte, an ovoid shape, consists of numerous droplets of lipids and mitochondria, which has cytochromes (Fitzgerald *et al.*, 2018).

BAT is localized in evolutionarily higher hierarchy mammals only (Giorgino, Laviola and Eriksson, 2005). BAT are found in abundance in small mammals (example small mammalian hibernators; chipmunks, dormice, hamsters, hedgehogs and bats) as well as in newborns of larger mammals (around heart and great vessels), including humans (Sell, Deshaies and Richard, 2004; Giorgino, Laviola and Eriksson, 2005). However, BAT localizes in less amounts in human adults (Tortora and Derrickson, 2019), and is found in supraclavicular and thoracic regions of human adults (Cypess *et al.*, 2009). Structurally, brown adipocytes are multilocular fat storage cells with high spreading of mitochondria and consist of low amounts of lipid when compared to WAT (Giorgino, Laviola and Eriksson, 2005). BAT are darker in colour because of the surplus blood supply and the high spreading of mitochondria with pigments (Fitzgerald *et al.*, 2018; Tortora and Derrickson, 2019). BAT disperse energy in the form of heat to regulate the body temperature of the human baby (Tortora and Derrickson, 2019).

Adipocytes are also the specific storage depot for triacylglycerols (TAG) or triglycerides (TG), which are centrally localized as a fat droplet (Tortora and Derrickson, 2019). Pro-long food refrainment and continuous physical activity create energy deprivation in the human body (Song, Xiaoli and Yang, 2018). This energy demand condition is fulfilled by the energy storage from triacylglycerols (Richard, 2000). It should be noted that adipose tissue is not only a passive energy source, but also a complex endocrine organ. The secreted hormones from adipose tissue circulate and communicate metabolic messages to other metabolically active

organs such as muscle, liver, pancreas and brain through hormonal mechanisms, thereby controlling systemic metabolism (Richard, 2000; Kershaw and Flier, 2004; Luo and Liu, 2018). Notably, the functions of adipocytes are organized by endocrine and non-endocrine mechanisms of adipocytes (Rosen and Spiegelman, 2011).

The endocrinology of adipose tissue can be divided into two. These are (i) protein secretion, which has an impact on metabolic activity of distal cell and tissue, and (ii) as metabolic enzymes of steroid hormone synthesis (Kershaw and Flier, 2004). Adipose tissue maintains glucose and lipid metabolism by secretion of regulatory hormones such as adipokines (preadipocytes-derived proteins). Some named adipokines are leptin and adiponectin and lipokines (Richard, 2000; Oh *et al.*, 2005). Leptin, a satiety hormone and encoded by the obesity (*ob*) gene regulates energy homeostasis by preventing hunger. The satiety effect of leptin is attained by overcoming the blood–brain barrier and directing the hypothalamus, a primary hunger centre modulating food consumption and forming body weight in order to control the mass of adipose tissue by reducing food consumption and regulating glucose and fat metabolism (Luo and Liu, 2018). Therefore, leptin plays a vital part in food balance and disbursement of energy in adipose tissue.

Apart from energy, fat and nutrient balance, adipose tissue has functions in the immune response, blood pressure control, haemostasis, bone mass, thyroid and reproductive function (Trayhurn, 2005), heat reduction, supporting and protecting the internal organs (Tortora and Derrickson, 2019). The blood circulation network in the adipose tissue is prominently different for an obese person (high number of blood vessels) than a lean person (fewer blood vessels). Therefore, the former person has the vulnerability for high blood pressure (Tortora and Derrickson, 2019). Any defects in adipose tissue function impact on the homeostasis of glucose and lipid amount in the human body lead to metabolic abnormal diseases such as obesity and obesity accompanied diseases (type 2 diabetes mellitus) (Richard, 2000), cardiovascular disease (CVD), non-alcoholic fatty liver disease (NAFLD) and several types of cancer (Richard, 2000; Song, Xiaoli and Yang, 2018). The role of adipose tissue in obesity has stimulated research based on understanding adipose tissue and its physiology (Mokdad *et al.*, 2003; Bray and Bellanger, 2006). Indeed, understanding the roles of adipocytes in glucose and energy homeostasis has led to the production of drugs for the treatment of metabolic abnormalities such as obesity and type 2 diabetes.

1.5.1.1. Adipose tissue and the NOS/NO pathway

Adipogenesis, the intake of glucose by the stimulation of insulin and degradation of lipids in adipose tissue is regulated by NO. If NOS activity is reduced, glucose uptake is severely diminished (Roy, Perreault and Marette, 1998). This has also been shown in 3T3-L1 adipocyte cell lines, used as a model to investigate adipocyte-NO responses, nitric oxide induces glucose uptake via insulin-independent GLUT4 translocation (Tanaka *et al.*, 2003).

Constitutive nitric oxide synthases (mainly eNOS) is found in both WAT and BAT adipose tissue (Kikuchi-Utsumi Kazue *et al.*, 1987; Engeli *et al.*, 2004). The cytoplasm and nucleus of BAT adipose tissue contain eNOS, and short and long term expression of eNOS is stimulated by insulin and high intracellular calcium

concentrations (Engeli *et al.*, 2004). NO production by adipocyte eNOS is used to balance the glucose and insulin amounts in WAT (Engeli *et al.*, 2004). Indeed, the phosphorylation of eNOS results in a decline in NO production and this is a major root cause of insulin resistance in diet-induced obese mice (Xia *et al.*, 2016).

1.5.2. The liver

The liver is one of the major organs in the human body (Liu *et al.*, 2017). The functional unit of the liver are hepatocytes; modified epithelial cells, which play a variety of roles in metabolism, secretion and in endocrinology of the human body. There are two blood drainage systems join with the liver named as hepatic artery and hepatic portal vein. The former carries oxygen-rich blood and delivers it to the liver. And the latter brings nutrient-enriched blood with a surplus amount of absorbed metabolites of carbohydrates, lipids and proteins, pharmacological compounds and if possible carries micro-organisms and toxic compounds from the intestinal system (**Fig 1.5.2**) (Liu *et al.*, 2017; Tortora and Derrickson, 2019). The liver synthesises proteins, removes waste material from the body, produces cholesterol, stores and releases glucose and metabolises many medicinal drugs (Hon, Lee and Khoo, 2015).

Metabolic homeostasis and energy metabolism are regulated by the liver (Liu *et al.*, 2017). Glucose, fatty acids and amino acid metabolism in the liver collectively called hepatic metabolism are strongly regulated by factors such as nutrient availability, hormones and signalling molecules. Metabolic imbalance and signalling interruption in the liver leads to metabolic disorders such as diabetic mellitus (Liu *et al.*, 2017). One of the functions of liver is to help maintain the glucose homeostasis in the body. Carbohydrate-rich meal consumption and digestion creates a spike in glucose, which is absorbed by the liver and stored as glucose polymers; glycogen and triglycerides. Massive glucose influx to the liver leads to the synthesis of fatty acids from glucose. If glucose levels decrease in the body the liver releases glucose from glycogen (glycogenolysis) and this glucose circulates in the body and reaches the tissues where it is oxidized to produce energy. During high demand for glucose, when more glucose is required than storage as glycogen, the liver synthesises glucose from fatty acids and amino acids (gluconeogenesis) (Liu *et al.*, 2017).

The liver is involved in lipid metabolism including ATP production by breaking down of fatty acids, lipoprotein and cholesterol synthesis, using cholesterol for bile synthesis, transportation of fatty acids, triglycerides and cholesterol recycling (Rui, 2016). Free fatty acids are absorbed by the liver cells from the digestive sap. In the hepatocytes, esterification of these free fatty acids with glycerol-3-phosphate forms triacylglycerols (TAG) or combine with cholesterol to form the cholesterol esters, storage form in the lipid droplets or adjoin with protein to form the one of the lipoproteins very-low-density lipoprotein (VLDL), which is circulated in blood from the liver (Liu *et al.*, 2017).

1.5.2.1. The Liver and the NOS/NO pathway

The liver is impacted by NO and mis-regulation can lead to acute or chronic conditions (Hon, Lee and Khoo, 2015). The distribution of nitric oxide synthases (eNOS and iNOS), by *in situ* hybridization in normal and cirrhotic human liver, shows that the distribution of eNOS is consistent with hepatocytes and localised in the endothelium of hepatic arteries, terminal hepatic venules, sinusoids and in biliary epithelium. The distribution of iNOS was also in hepatocytes and detected primarily in the periportal zone of the liver acinus (McNaughton

et al., 2002). iNOS is released from nearly all cell types of liver; hepatocytes, Kupffer cells, hepatic endothelial cells and Ito cells. It has been discussed previously in this chapter, that a combination of cytokines is necessary to induce iNOS in many human cells. However, interleukin-1 β (IL-1 β) alone is sufficient to induce iNOS mRNA in human liver cells, confirming that iNOS is stimulated rapidly in hepatocytes compared to other cells (Hon, Lee and Khoo, 2015). Nevertheless, the amount of NO in these cells is determined by the type of stimuli and cells (Hon, Lee and Khoo, 2015). Interestingly, protein synthesis in liver cells is repressed in the cell secretome from Kupffer cells in hepatocytes upon stimulation of iNOS and NO production (Clemens, 1999).

1.5.3. Muscle

The major function of the muscular system is to provide support for physical movement (Tortora and Derrickson, 2019). There are two major structural classifications for the muscle. They are striated muscle which consists of skeletal muscle (attached with the skeleton system or bone) and heart muscle (exclusively found in heart), and non-striated muscle - smooth muscle (found in the walls of hollow system gastrointestinal tract, uterus and stomach).

One of the major glycogen depots in the human body is in skeletal muscle. During vigorous physical activity, muscle glycogen is broken down and used to produce ATP (Harvey and Ferrier, 2011). Acute fasting does not affect the glycogen amount in muscle whereas chronic fasting reduces the amount of glycogen. However, the feed and fast cycle heavily impacts the liver glycogen capacity. Replacing of glycogen occurs after being used during strenuous exercise (Harvey and Ferrier, 2011). Glycogenolysis (breakdown of glycogen into glucose) happens in skeletal muscle during physical activity (McGee, 2013).

Glucose and free fatty acids are used up for the production of ATP in skeletal muscle. However, utilization of these sources for the generation of ATP depends on the individual's metabolic condition such as fed or fasting condition (Colberg *et al.*, 1995). In adipose tissue, plasma free fatty acids (FFA) levels are increased during fasting because of lipolysis while glucose uptake in skeletal muscle is reduced. This increase in FFAs are utilized consequently as a primary source for ATP production in skeletal muscle (Cahová, Vavřínková and Kazdová, 2007).

During a fed state, insulin secretion is stimulated by higher plasma glucose levels, which boosts glucose uptake by skeletal muscles. The consequences of this are a reduced rate of lipolysis in adipose tissue and a decrease in plasma FFAs. To promote glucose oxidation in skeletal muscle, the ability to swap substrates between fasted and fed states is vital. Subsequently, it has been reported that the muscle of individuals with insulin-resistance or diabetes does not have the ability to shift the substrates between fed and fasting states. This metabolic inflexibility may lead to the development of insulin resistance (DeFronzo and Tripathy, 2009).

1.5.3.1. Muscle and the NOS/NO pathway

All isoforms of NOS are present in various depots in skeletal muscle fibre, which are involved in production of NO. Of those isoforms, nNOS is considered to be a major NO production source, but the muscle nNOS isoform is not the same found in brain (Tengan, Rodrigues and Godinho, 2012; Baldelli *et al.*, 2014). Splicing variants of nNOS have vital roles in modulation of major muscle functions such as blood flow, muscle

contraction and metabolic activity of muscle. Among the variants of nNOS, nNOS μ is considered as the principal source for NO production in skeletal muscle (Tengan, Rodrigues and Godinho, 2012; Baldelli *et al.*, 2014).

NO is also involved in the mitochondrial biogenesis pathway, where PGC-1 α is the key signalling molecule. Several lines of evidence demonstrate that stimulation of mitochondrial biogenesis by NO donors produce ATP through oxidative phosphorylation. A study with primary skeletal muscle cultures of rat reported that supplementation of NO donor; S-nitroso-N-acetylpenicillamine (SNAP) increased the amount of mitochondrial biogenesis and function (Tengan, Rodrigues and Godinho, 2012). During physical activities phosphorylation of nNOS μ at Ser1451 is stimulated by AMPK phosphorylation, which may account for the induction of nNOS μ , increasing in NO synthesis and mitochondrial biogenesis and glucose up take. Upon phosphorylation by AMPK, both nNOS μ and eNOS are activated and this nNOS μ and eNOS activation is regulated by NOS inhibitors and NO donors (Tengan, Rodrigues and Godinho, 2012; Baldelli *et al.*, 2014).

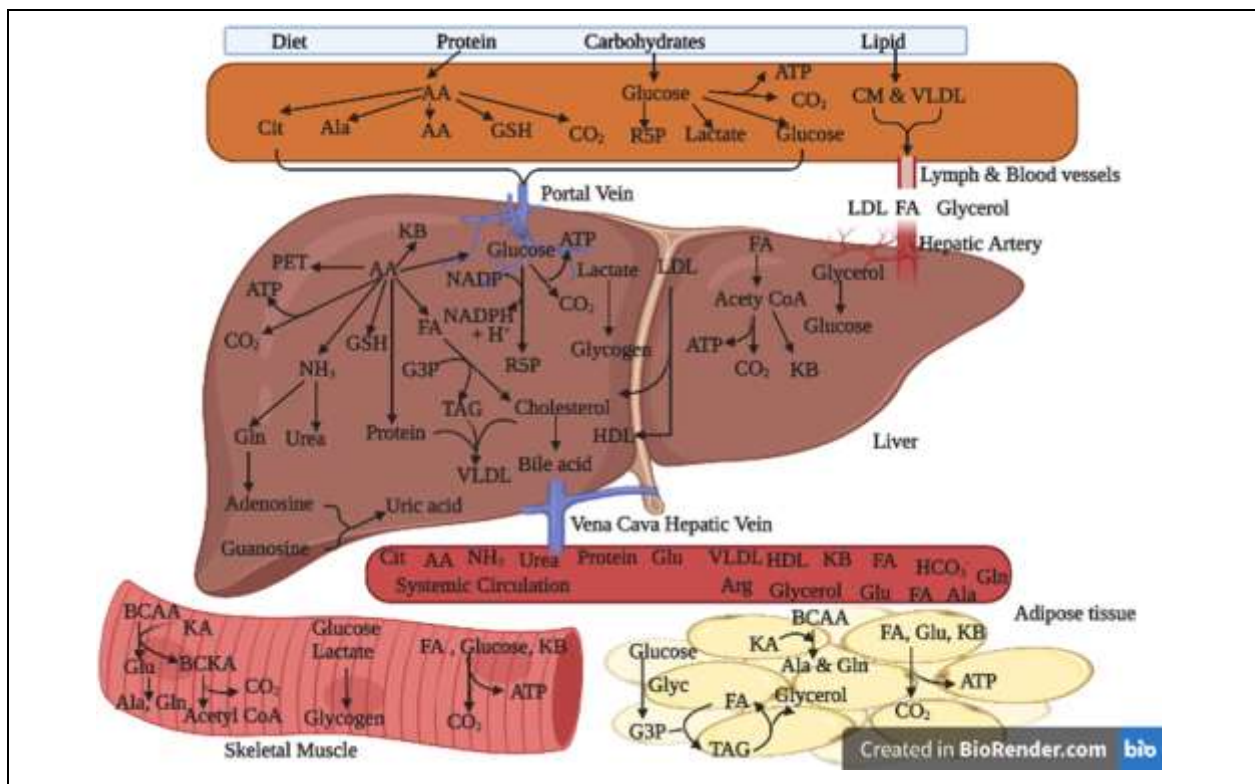


Figure 1.5.2. Integrative metabolic pathways in the liver, skeletal muscle and adipose tissue.

Integrated metabolic pathway of macronutrient molecules in mammals. Proteins, carbohydrates and lipids are sourced for the production of energy through multifaceted metabolic pathways that are interconnected between the insulin sensitizing tissues such as liver, adipose and muscle. In post-prandial stage, digested sap of macronutrient molecules is piped to the liver via hepatic portal circulatory system and the metabolites of amino acids, glucose and fatty acids synthesized in numerous tissues reach the systemic circulation and reach the destination tissues or cells where there is a demand for it. Abbreviations: AA, amino acids; Ala, alanine; Arg, arginine; BCAA, branched-chain amino acids; BCKA, branched-chain α -ketoacid; Cit, citrulline; CM, chylomicrons; FA, fatty acids; Gln, glutamine; Glu, glutamate; GSH, glutathione; G3P, glycerol-3 phosphate; KA, α -ketoacids (pyruvate and α -ketoglutarate); KB, ketone bodies, PET, peptide; and R5P, ribulose-5-phosphate.

1.6. The L-arginine metabolic pathway and signalling molecules

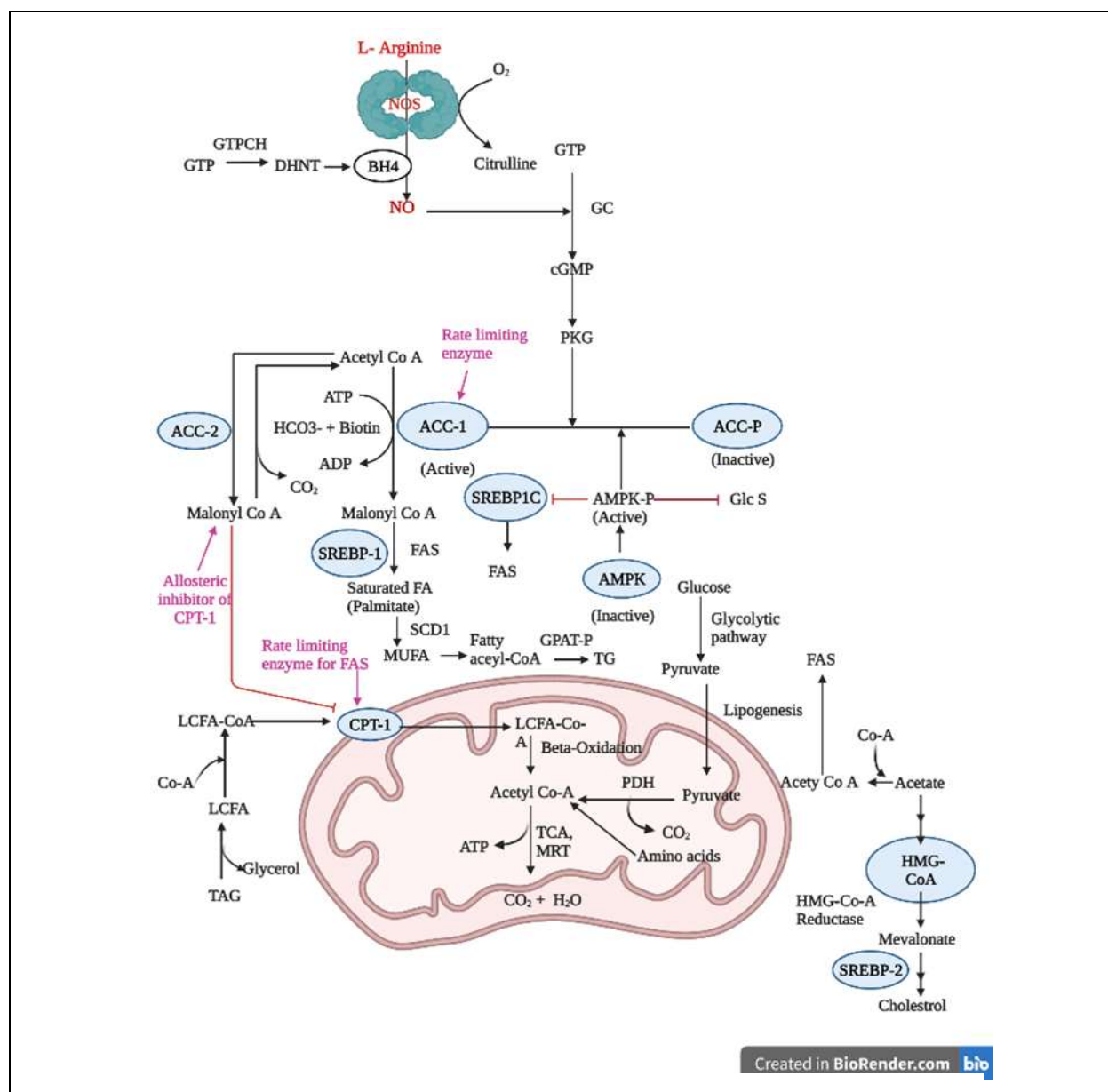


Figure 1.6.1. Schematic outlining the L-arginine metabolic pathway and subsequent cellular processes impacted.

Physiological levels of NO enhance oxidation of fatty acids, glucose and amino acids through cGMP/AMPK-dependent multiple pathways. Abbreviations: NOS, nitric oxide synthase; NO, nitric oxide; FAS, fatty acid synthase; GC, guanylyl cyclase; GlcS, glucose synthase; PKG, protein kinase G; Glyc, glycolysis; GTP, guanosine triphosphate; GMP, guanosine-3',5'-monophosphate; GTPCH, guanosine triphosphate cyclohydrolase-I; MRT, mitochondrial respiration chain; PDH, pyruvate dehydrogenase; SREBP, sterol regulatory element binding proteins; SCD1, stearoyl-CoA desaturase 1; TG, triacylglycerol; FA, fatty acid; ACC, acetyl-CoA carboxylase; GPAT, glycerol-3-phosphate acyltransferase; ACC, acetyl-CoA carboxylase; HMGCR, hydroxy-methylglutaryl coenzyme A reductase; LCFA, long chain fatty acid; TCA, tricarboxylic acid cycle; ATP, adenosine tri phosphate; AMPK, AMP activated protein kinase.

1.6.1. Downstream targets of the L-arginine/NO mechanistic pathway

There are important cellular signalling pathways that respond to L-arginine and NO concentrations and that were monitored during the subsequent studies reported in this thesis (**Fig 1.6.1**). Key downstream targets are described in more detail here, and their relationship to NO and L-arginine.

1.6.1.1. 5'-Adenosine monophosphate-activated protein kinase (AMPK)

AMPK is a heterotrimeric protein complex consisting of 3 subunits; α , β and γ in mammals (Wang *et al.*, 2016). Based on the functional characteristics of AMPK, the subunits are described as either the catalytic subunit or regulatory subunits. The catalytic subunit is AMPK- α with a molecular weight 63 kDa and the two regulatory subunits are AMPK- β and AMPK- γ with molecular weights of 43 kDa and 38 kDa, respectively (Dolinsky and Dyck, 2006). The α subunit has two isoforms; $\alpha 1$ and $\alpha 2$ with a kinase motif located at the N terminal, where upstream kinases phosphorylate the Thr172 residue of AMPK. The expression of the $\alpha 1$ subunit is broadly observed across tissue types (Wang *et al.*, 2016). The predominant form of AMPK $\alpha 2$ is expressed in skeletal and cardiac muscle at a high level. This isoform is also expressed in the liver and at lower levels in other tissues. Likewise, AMPK $\beta 2$ is expressed predominantly in skeletal and cardiac muscle, but it is also found at lower levels in many other tissues. The restricted expression of AMPK $\gamma 2$ and AMPK $\gamma 3$ is in skeletal and cardiac tissue (Garcia and Shaw, 2017).

AMPK activity depends on which tissue it is expressed in and is dysregulated in type 2 diabetic conditions (Garcia and Shaw, 2017). AMPK is activated upon an increase in the intracellular AMP/ATP ratio (López-Lluch *et al.*, 2008). AMPK is activated upon phosphorylation at Thr172 by its two major upstream kinases, liver kinase B1 (LKB1) and calcium/calmodulin-dependent kinase kinase (CAMKK β), in response to stimuli that increase intracellular AMP/ADP kinases (Cantó and Auwerx, 2013; Muraleedharan and Dasgupta, 2022). As AMPK plays an important role in regulating glucose and fatty acid metabolism in animals (Kahn *et al.*, 2005; Baldelli *et al.*, 2014), the net effects of activated AMPK are hepatic fatty acid oxidation, suppression of cholesterol and triglyceride synthesis and lipogenesis (Elhanati *et al.*, 2013), control of insulin resistance, obesity and mitochondrial biogenesis (López-Lluch *et al.*, 2008). A further consequence of AMPK activation is the attenuation of ATP-consuming pathways (including lipogenesis and gluconeogenesis) and the activation of ATP-producing pathways (including fatty acid and glucose oxidation) (Kahn *et al.*, 2005; Dzamko *et al.*, 2008). Major sources of energy, glucose and lipids and their synthesis and storage, are therefore prohibited by AMPK. Glucose transporters GLUT4 and GLUT1 levels and translocation are regulated by TBC1D1 (TBC domain family, member 1) protein and TXNIP (thioredoxin-interacting protein) respectively, which are phosphorylated by AMPK, whereby this increases glucose uptake (Grahame, 2013; Wu *et al.*, 2012). Upon phosphorylation of PFKFB2 (6-phosphofructo-2-kinase), AMPK controls glycolysis in some tissues, whereas glucose storage in the form of glycogen in macrophages and cardiac muscle is inhibited by impeding numerous isoforms of glycogen synthase (Grahame, 2013; Zois and Harris, 2016).

Gluconeogenesis, *de-novo* synthesis of glucose, is inhibited by AMPK by phosphorylation and nuclear elimination of CRTC2 (cyclic-AMP-regulated transcriptional co-activator 2) and class II HDACs (histone deacetylases), which are essential co-factors for the transcription of gluconeogenic genes (Garcia and Shaw, 2017). Furthermore, transcription factors which activate gene expression of the glycolytic and lipogenic pathways are inhibited by AMPK phosphorylation. Indeed, transcription factors SREBP-1, a master transcriptional regulator of lipid synthesis (Kohjima *et al.*, 2008), HNF4 α (hepatocyte nuclear factor-4 α) (Chang *et al.*, 2016) and ChREBP (carbohydrate-responsive element binding protein) (Uyeda, Yamashita and Kawaguchi, 2002) are regulated by AMPK.

As outlined above, important lipid regulators are regulated themselves via AMPK. Overall cellular lipid metabolism is controlled by AMPK by direct phosphorylation of ACC-1 and ACC-2, thereby decreasing fatty acid synthesis whilst at the same time increasing fatty acid oxidation by releasing the suppression of CPT-1 by malonyl-CoA, which is synthesized at the mitochondria outer membrane by ACC-2 (Garcia and Shaw, 2017; Srivastava *et al.*, 2012). In the cell, AMPK also facilitates pre-programming of lipid and sterol synthesis by phosphorylating and inhibiting HMGCR, which together impact ACC-1 and ACC-2. Absorption and release of lipids is also promoted by AMPK phosphorylating lipases, including hormone-sensitive lipase (HSL) and adipocyte-triglyceride lipase (ATGL) (Srivastava *et al.*, 2012; Kim *et al.*, 2016).

Both AMPK and the mammalian Target of Rapamycin (mTOR, sometimes referred to as mechanistic target of rapamycin) are evolutionarily conserved master regulatory kinases that function to modulate extensive cellular and systemic metabolism (Sukumaran, Choi and Dasgupta, 2020). Direct inhibition of mTORC1 complex by AMPK mainly inhibits protein synthesis. Two key mechanisms are regulated by phosphorylation of AMPK to control activity of mTORC1. One is the activation of TSC2 (tuberous sclerosis complex 2), which is a repressor of mTORC1, and the other is the negative regulation of Raptor (regulatory-associated protein of mTOR), which is a subunit of the mTORC1 complex (Sukumaran, Choi and Dasgupta, 2020; Gwinn *et al.*, 2014). In addition to this regulation of mTOR by AMPK, phosphorylation of TIF-IA (transcription initiation factor IA), which is a transcription factor for RNAPolymerase I (Pol I), by AMPK inhibits and controls protein synthesis by blocking ribosomal RNA synthesis (Hoppe *et al.*, 2009).

Phosphorylation and activation of eEF2K (eukaryotic elongation factor 2 kinase), an inhibitor of translation elongation during protein synthesis, by AMPK diminishes protein synthesis (Johanns *et al.*, 2017). It has been reported that mTORC1 is also a vital regulator of eEF2K (Johanns *et al.*, 2017; Hizli *et al.*, 2013). In addition to being directly phosphorylated by mTORC1 or S6K1, multiple downstream targets of AMPK are negatively regulated by AMPK phosphorylation. As a result, AMPK and mTOR limit anabolism and catabolism by flipping main metabolic switches on and off within the cell (Sukumaran, Choi and Dasgupta, 2020).

Amino acids have been shown to be important regulators of AMPK activity (Leclerc and Rutter, 2004). Exposure to excess nutrients such as branched chain amino acids (BCAA) downregulated AMPK activity (Coughlan *et al.*, 2015). It has been reported that arginine-mediated cellular pathways and accumulation of glucose were regulated by AMPK when human umbilical vein endothelial cells were incubated with 100 μ M arginine for acute (2 h) and chronic (7 days) periods with or without other modulating agents for AMPK/arginine mechanistic pathways. The same study also suggested that AMPK provokes its downstream NO production by modulating eNOS activity and thereby control glucose accumulation through cellular transport (Mohan *et al.*, 2013).

1.6.1.2. Acetyl-CoA carboxylase (ACC)

There are two major isoforms of acetyl-CoA carboxylase (ACC); ACC-1 (or ACC α) and ACC-2 (or ACC β), which are encoded by two different genes *ACACA* and *ACACB* respectively in human. The proteins that derive from these two genes have molecular weights of 265 kDa and 280 kDa, respectively (Widmer *et al.*, 1996; Abu-Elheiga *et al.*, 2000; Abu-Elheiga *et al.*, 2003). Lipogenic tissues (liver and adipose) have high expression

of ACC-1 with the expression being modulated at both the transcriptional and post-translational (by phosphorylation and dephosphorylation at specific serine residues) levels. Citrate and palmitoyl-CoA are also allosteric inhibitors of ACC-1. The levels and activities of ACC-1 are induced by high-carbohydrate and low-fat foods, while long term food deprivation or fasting and diabetic conditions decreases the activity of ACC-1 through downregulation of its expression at the transcript (mRNA) level and/or upregulation of its phosphorylation (Abu-Elheiga *et al.*, 2000). ACC-2 activity is regulated in a similar manner. Immunogens of ACC-1 and ACC-2 are different, even though there is 70% sequence similarity between the polypeptide chains. Thus, anti-ACC-1 antibodies do not detect ACC-2 and vice versa. The ACC-2 isoform is found in liver and is a major carboxylase in striated muscular systems like heart and skeletal muscles (Abu-Elheiga *et al.*, 2000).

ACC responds to and elicits changes in glucose, insulin and insulin like growth factors (IGFs) and modulates gluconeogenesis, glucose transport and insulin sensitivity (Baur *et al.*, 2006). Previous studies have reported that the regulatory pathway of fatty acid synthesis is controlled by ACC-1; a cytosolic enzyme involved in fatty acetyl Co-A synthesis and triglyceride synthesis, whereas ACC-2 is localized in the mitochondria and inhibits the oxidation of fatty acids (Romero, Sabater and Fernández-lópez, 2015). Two major pathways are regulated by ACC, the fatty acid synthesis and oxidation pathways by the catalytic carboxylation of acetyl-CoA to malonyl-CoA during the synthesis of fatty acids or allosteric inhibition of CPT-1 (Munday, 2002). The primary and secondary sites for *de-novo* fatty acid synthesis in both human and rodents are liver and adipose tissue, respectively (Letexier *et al.*, 2003; Luo and Liu, 2016; Bergen and Mersmann, 2018). A precursor for *de-novo* fatty acid synthesis is malonyl-CoA, the rate-limiting enzyme for fatty acid synthesis and the main substrate of fatty acid synthase. The malonyl-CoA synthesized by ACC-1 and ACC-2 is used for fatty acid synthesis and functions as an allosteric inhibitor of carnitine palmitoyl transferase I (CPT-I) (Sujobert and Tamburini, 2016; Lee *et al.*, 2011), a rate-controlling enzyme for fatty acid oxidation (Laloties, Bizelis and Rogdakis, 2010; Viollet *et al.*, 2006). Malonyl-CoA is a vital regulatory factor of fatty acid oxidation in the liver. ACC-2 is phosphorylated at Ser219 by AMPK and the consequence of this phosphorylation is inhibition of ACC-2 activity (O'Neill *et al.*, 2014). The inhibition of ACC-2 causes reduced malonyl-CoA, sequentially promotes CPT-1, leading to the increased transport of acyl-CoA to mitochondria and the β -oxidation. Accelerated or overexpression of CPT-1 expression induces HMGCo-A expression via the Ketogenesis pathway.

1.6.1.3. Sterol regulatory element-binding transcription factors (SREBP-1 and 2)

Sterol regulatory element-binding transcription factors (SREBPs) comprise a family of membrane-bound transcription factors with three isoforms (SREBP-1a, SREBP-1c and SREBP-2) (Ye and DeBose-Boyd, 2011; Kim *et al.*, 2006), which modulate the expression of enzymes involved in the synthesis of fatty acids, triglycerides, phospholipids and cholesterol. Of the SREBP family isoforms, SREBP-1a and SREBP-1c facilitate the transcription of genes involved in fatty acid uptake, fatty acid synthesis and triglycerides synthesis (Elhanati *et al.*, 2013). SREBP-2, on-the-other-hand, stimulates the transcription of genes involved in cholesterol biosynthesis (Elhanati *et al.*, 2013). The predominant transcript form of SREBP-1 in the liver is SREBP-1c which is found ten times more than its counterpart SREBP-1a. The SREBP-2 transcript is found in cells and tissues at a more-or-less constant level (Ye and DeBose-Boyd, 2011). SREBP-1 and SREBP-2

transcript expressions are different in adipose tissue, liver and skeletal muscle (Raghow *et al.*, 2008; Laplante and Sabatini, 2012).

Proteolytic cleavage of SREBPs activates the inactive precursor form of ER bound SREBPs with molecular weight 125 kDa. The full length of SREBP-1 is cleaved into an NH₂-terminal fragment, molecular weight 68 kDa, by S1P (site 1 protease) and S2P (site 2 protease) proteases (Zhao, Lin and Wang, 2022) and SCAP (SREBP cleavage-activating protein) to activate SREBP-1s. Active SREBP-2 is approximately 62 kDa and is also cleaved by proteases to make it transcriptionally active (Li and Wu, 2021). The mature form of SREBPs translocate to the nucleus, where they stimulate lipogenic gene expression in the liver (Raghow *et al.*, 2008) by binding to a sterol response element (SRE) in the promoter region of target genes, activating their transcription. Accumulation of sterols in ER membranes triggers binding of Scap to one of two retention proteins called Insigs, which blocks incorporation of Scap-SREBP complexes into ER transport vesicles. As a result, SREBPs no longer translocate to the Golgi apparatus, the transcriptionally active N-terminal domain cannot be released from the membrane, and transcription of all target genes declines (DeBose-Boyd, 2008). The main regulator of SREBP-1 is insulin (Raghow *et al.*, 2008). The end product, fatty acids inhibit SREBP-1 activity (by feedback inhibition). However, SREBP-2 transcription is not inhibited by the polyunsaturated fatty acids (PUFA). Unsaturated fatty acids not only inhibited SREBP-1 transcription but also suppressed SREBP-1 proteolytic activation (Ye and DeBose-Boyd, 2011).

Nuclear accumulation of SREBP-1 and the expression of lipogenic genes are rapidly induced by insulin treatment or constitutive Akt activation. Growth factors such as insulin increase Akt activity, thereby facilitating mTORC1 activation by directly phosphorylating the tuberous sclerosis complex 1 or 2 (TSC1 or 2). Support for this mechanism has come from previous work that showed that rapamycin (a potent and specific mTOR inhibitor) diminishes the expression of many down regulated target genes of SREBP-1, including ACC, fatty acid synthase (FAS) and stearoyl-CoA desaturase 1 (SCD-1) (Laplante and Sabatini, 2012) (**Fig 1.6.1** and **Fig 1.6.2**).

Several post-translational modifications of SREBP-1 are suppressed by AMPK. AMPK phosphorylates SREBP-1c at Ser372, suppressing the proteolytic cleavage of precursor SREBP-1c into mature SREBP-1c (Li *et al.*, 2011). SREBP-2 is the primary transcriptional regulator in cholesterol metabolism. AMPK decreases the nuclear translocation of SREBP-2 in hepatic cells. Importantly, eNOS activation plays a role in mediating the activation of SREBP. Activation of eNOS generates O⁻ and superoxide (O₂⁻) which with NO are responsible for the activation of SREBP (Gharavi *et al.*, 2006). NO alone is unable to activate SREBP, therefore coupling of NO with sufficient amount of O₂⁻ is mandatory for the activation and regulation of SREBP (Gharavi *et al.*, 2006).

1.6.1.4. 3-Hydroxy-3-methylglutaryl-CoA reductase (HMGCR)

3-Hydroxy-3-methylglutaryl coenzyme A reductase (HMGCR) is a trans membrane glycoprotein in the endoplasmic reticulum (ER) in mammals and is comprised of 887 or 888 amino acids in total with two adjoining domains with a molecular weight of 97 kDa (Liscum *et al.*, 1985; DeBose-Boyd, 2008). The N-terminal domain has 339 amino acids with 8 membrane spanning loops while the C-terminal has 548-amino

acids and protrudes into the cytosolic region. The C-terminal domain is the catalytic domain where all enzymatic reactions take place (DeBose-Boyd, 2008). The enzymatically active catalytic fragment is formed from the cleavage of HMGCR bound with ER membrane vesicles by endogenous protease and releases a soluble 53 kDa fragment of HMGCR (Liscum *et al.*, 1985).

HMGCR is a major rate-limiting enzyme in the synthesis of cholesterol and catalyses the conversion of HMG-CoA to mevalonate (Göbel *et al.*, 2019), the precursor form of isoprenoid groups that are combined into many end-products such as cholesterol (DeBose-Boyd, 2008). Several transcriptional and post-translational regulatory mechanisms control HMGCR and the cholesterol synthesis pathway (Göbel *et al.*, 2019). The equilibrium between the phosphorylation and dephosphorylation of HMGCR enzyme regulates its activity with the enzyme being inactivated by phosphorylation. Whilst phosphorylation of AMPK at Thr172 activates AMPK, a consequence of this is inactivation of HMGCR by AMPK phosphorylation at Ser871 (Wang *et al.*, 2018; Loh *et al.*, 2019). An *in-vivo* study of AMPK-HMGCR signalling in mice with a Ser871-alanine (Ala) knock-in mutation confirmed that synthesis of both cholesterol and triglyceride during carbohydrate rich fed condition is controlled by the AMPK-HMGCR signalling pathway, where AMPK plays a master role in mevalonate and fatty acid synthesis pathways to reduce the detrimental effect of a high carbohydrate diet (Loh *et al.*, 2019). Relevant to this study, a study with genetically-engineered eNOS deficient mice confirmed that acute L-arginine and eNOS activity is a deleterious condition. However, supplementation of simvastatin (an HMGCR inhibitor) alongside L-arginine upregulated eNOS protein, consequently augmented the eNOS-dependent cerebral blood flow in the normal and ischemic brain (Yamada *et al.*, 2000). Further, it has been reported that eNOS expression is upregulated when human saphenous vein endothelial cells are treated with oxidized low-density lipoprotein (50 mg/mL) and with HMGCR inhibitors (simvastatin and lovastatin) (Laufs *et al.*, 1998).

1.6.1.5. Mammalian target of Rapamycin (mTOR)

Rapamycin was discovered from the bacterial strain *Streptomyces hygroscopicus* (Mohamed, Elkhateeb and Daba, 2022). Extracellular signals are linked to intracellular responses in mammalian cells by a vital regulator, mammalian target of rapamycin (mTOR), which is in the phosphoinositide 3-kinase based family (PI3K). mTOR is a serine threonine kinase and regulates protein synthesis, ribosome biogenesis and cell proliferation in mammalian cells. There are two catalytic subunits with two different protein complexes, mTOR complex 1 (mTORC1) and 2 (mTORC2). mTORC1 contains 3 major subunits; mTOR, Raptor; a regulatory protein that facilitates substrate binding and subcellular localization of mTORC1, and target of rapamycin complex subunit LST8, also known as mammalian lethal with SEC13 protein 8 (mLST8) (Wang *et al.*, 2009; Betz and Hall, 2013). There are two inhibitory subunits in mTORC1, the proline-rich Akt substrate of 40 kDa (PRAS40) subunit, a physiological substrate of mammalian target of rapamycin complex 1 and DEP subunit consisting of mTOR-interacting protein (DEPTOR), an endogenous regulator of mTORC1 and mTORC2 (Laplante and Sabatini, 2009) (Saxton and Sabatini, 2017).

The major subunit for the activation of the mTOR complex is raptor; phosphorylation of raptor is stimulated by insulin and inhibited by rapamycin (Wang *et al.*, 2009). It has been reported that L-arginine enhances

protein synthesis by impacting the degree of phosphorylation of mTOR observed (Thr2446) in a NO-dependent manner in muscle cells when a C2C12 muscle cell model was cultured with excess L-arginine (1 mM). A sufficient intracellular amino acid pool is mandatory to activate mTORC1. mTORC1 is activated by Rheb, located on the surface of lysosomes, whereas mTORC1 is regulated by a protein complex known as TSC via its inhibitory action on Rheb. L-arginine regulates the TSC2-Rheb signalling pathway to activate mTORC1 leading to growth of the cells. The mTORC1 sensing L-arginine pathway is vital during cell development (Carroll *et al.*, 2016). Thus, nutrient and energy sensing and growth control in cells are regulated by AMPK and mTOR in an opposite but interconnected manner. AMPK turns on during high energy demand or lack of nutrients and inhibits growth of the cells, whereas mTOR turns on when there is appropriate nutrient availability and facilitates growth of cells (González *et al.*, 2020).

1.6.1.6. Eukaryotic initiation factor 2 (eIF2)

Eukaryotic initiation factor 2 (eIF2) is a heterotrimer that consists of 3 subunits; α , β and γ (Komar and Merrick, 2020; Andaya *et al.*, 2012). eIF2 is involved in the early step of eukaryotic protein synthesis. Translation of an mRNA requires correct assembly of the translational functional unit consisting of the mRNA, initiator tRNA (Met-tRNA) and ribosome, requiring coordination between eIFs and the hydrolysis of both GTP and ATP. A ternary complex (TC) initially forms with Met-tRNA and GTP coupled with the heterotrimeric initiation factor (eIF2). The activity of eIF2 is controlled by phosphorylation of the α subunit by one of four kinases; eIF2 α K1- the mammalian ortholog of the yeast general control non-derepressing kinase-2 (mGCN2), eIF2 α K2 - the haem-regulated inhibitor (HRI), eIF2 α K3 - the protein kinase dsRNA-activated (PKR), and eIF2 α K4 - the PKR-like endoplasmic reticulum kinase (PERK) (Kimball and Jefferson, 2004). Phosphorylation of the α subunit of eIF2 stabilizes and controls the eIF2/GDP/eIF2B complex and prevents GDP/GTP exchange reaction because of increased affinity binding between phosphorylated eIF2 α and eIF2B, thus impairing the recycling of eIF2 and leading to universal inhibition of translation (Langland and Jacobs, 2004; Montero *et al.*, 2008). Phosphorylation on Ser-52 residue by the GCN2 protein kinase occurs in response to amino acid starvation.

It has been reported that both NO donors and the expression of iNOS decreases total protein synthesis non-specifically as a result of the phosphorylation of eIF2 α and inhibition of the 80S initiation complex formation (Kim *et al.*, 1998). A follow up study was conducted to explain the mechanism of NO and increased phosphorylation of eIF2 α using diffusible gases nitric oxide (NO) and carbon monoxide (CO) in rabbit reticulocyte lysate upon activation of HRI. Noticeably, CO decreased NO-stimulated HRI activation, even though NO is known as a more effective activator of HRI. Further to this, using NO producers in NT2 neuroepithelial and C2C12 myoblast cells also increase eIF2 α phosphorylation levels (Uma, Yun and Matts, 2001). Some amino acids have the ability to regulate gene expression by controlling translation of mRNA at the initiation stage. One of the eIF2 α kinases; mGCN2 potentially modulates translation of mRNA by availability of all essential amino acids. Further, control of mRNA translation can also happen selectively through mTOR signalling pathways, such as eIF4B phosphorylation by activated S6K1 (S6K1 is activated by mTOR) and enhanced eIF4F assembly by phosphorylation of the eIF4E binding proteins by mTOR (**Fig 1.6.2**).

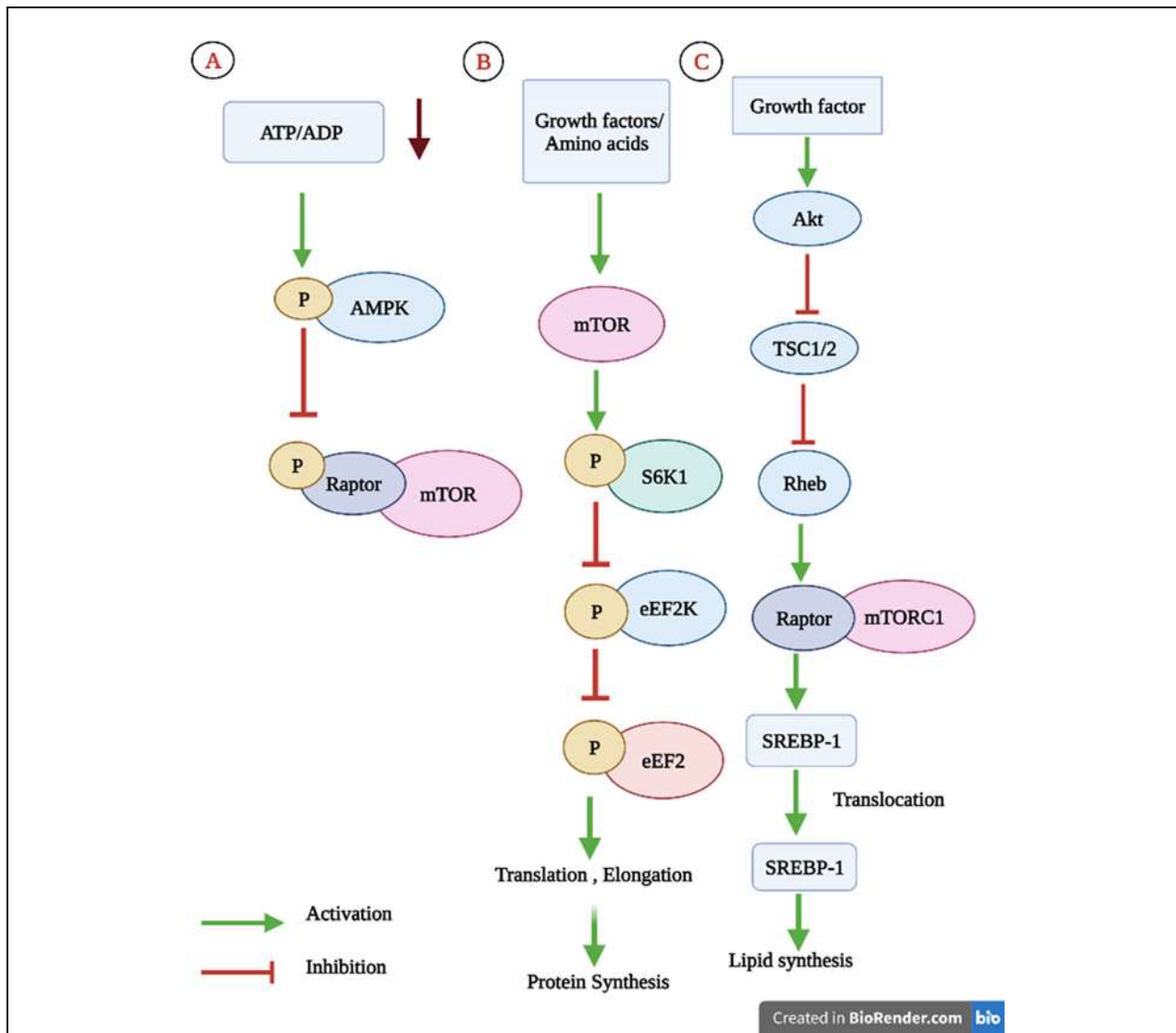


Figure 1.6.2. AMPK-mTOR signalling pathway.

(A) Energy deprivation (low ATP:ADP ratio) activates AMPK, direct phosphorylation of Raptor by activated AMPK diminishes mTORC1 activity during energy deprivation. (B) Activation of mTORC1 by growth factors or amino acids promotes protein synthesis via the phosphorylation of S6K1. The stimulation of S6K1 activity by mTORC1 leads to increases in cap-dependent translation and elongation and the translation of ribosomal proteins through regulation of the activity of many proteins, such as eukaryotic elongation factor 2 kinase (eEF2K). (C) Growth factors such as insulin increases Akt activity, thereby facilitates mTORC1 activation by directly phosphorylating the tuberous sclerosis complex 1 or 2 (TSC1 or 2) and consequently activates SREBP-1 by Akt pathway (Laplante and Sabatini, 2009; Laplante and Sabatini, 2012).

1.6.1.7. Eukaryotic elongation factor 2 (eEF2)

Elongation factor 2 protein belongs to the GTPase super family and is formed from 857 amino acids with molecular weight of 95.3 kDa (Kaul, Pattan and Rafeequi, 2011). There are 5 domains of this protein, which are folded to form 3 structural subunits; domains I-II, the N-terminal block; domains IV-V, the C-terminal block; domain III, bridging between N and C terminal blocks by flexible covalent bonding (Laurberg *et al.*, 2000). The mechanical energy needed for the dynamic process of translocation of the mRNA to tRNA complex through the ribosome from the A-site to the P-site of the ribosome is gained from eEF2-dependent GTP hydrolysis (Taylor *et al.*, 2007; Kaul, Pattan and Rafeequi, 2011). Translocation of tRNAs from the A (aminoacyl) site to the P (peptidyl) site to the E (exit) site is associated with the pre- and post-translocational

conformational changes of the ribosome which is catalysed by eEF2, incorporated with the GTP hydrolysis and coupling of phosphate (Sengupta *et al.*, 2011; Spahn *et al.*, 2004).

Phosphorylation and dephosphorylation of eEF2 is facilitated by a specific kinase; eEF2 kinase (eEF2K). Upon activation of eEF2K, this phosphorylates eEF2 at Thr56 residue and deactivates eEF2 therefore preventing its contact with ribosome leading to decrease the rate of elongation of polypeptide chain (Kaul, Pattan and Rafeequi, 2011; Xie *et al.*, 2019). eEF2K is inactivated by mTORC1 signalling pathway, thereby increasing protein elongation when nutrient conditions are favourable (**Fig 1.6.2**) (Xie *et al.*, 2019).

1.7. The need for further elucidation of the L-arginine-NOS/NO axis and signalling pathways

The metabolic consequences of excess L-arginine on the NOS/NO signalling pathway in different tissues is not fully mapped. This is somewhat surprising as L-arginine is taken as a dietary supplement to help control body mass/fat matter (McKnight *et al.*, 2010). Further, the importance of the L-arginine/NOS/NO pathway in insulin sensitizing metabolic pathways has been established *in-vivo* using diabetic and obese animal models. Therefore, in this study, *in-vitro* cell culture models including BNL CL2 (mouse hepatocytes) and 3T3 L1 (mouse adipocytes) have been used to investigate the role of L-arginine/NOS/NO in regulation of glucose and fatty acid metabolism and signalling in liver cells (BNL CL2) and adipocytes (3T3 L1) by mapping the responses of key genes and proteins in these pathways that are involved in L-arginine and NO induced signalling cascades.

1.7.1 Why new treatments are needed to treat diabetes and obesity

Semaglutide is marketed under the brand name of Ozempic for treatment of diabetes and Wegovy for treatment of obesity. However, these drugs caused some side effects (Food and Drug Administration, 2021). New approaches in managing and preventing diabetes in obese individuals must be studied and investigated based on less side effects and cost effective. Previous studies demonstrated that L-Arg can reduce plasma glucose levels, improving glucose tolerance in rats. L-Arg supplementation was also shown to reduce adiposity and improve insulin sensitivity in animal models of obesity as well as in patients with diabetes and obesity (Forzano *et al.*, 2023). In this study, I aimed to investigate the direct effect of L-Arg in insulin sensitive cells (mouse liver cells and mouse adipose cells) and demonstrate the impact of L-Arg and L-Arg/NO metabolism on specific cell signalling pathway. L-Arg is relatively very low-cost food supplement and also, we can increase the bioavailability of L-Arg by diet.

1.8. Hypothesis of the work in this thesis

This study was conducted to test the hypothesis that excess L-arginine treatment regulates glucose and fatty acid metabolism in insulin-sensitive tissues such as liver cells and adipocytes by modulating the expression of key target genes and proteins which are involved in the metabolism of energy substrates in an NO dependent manner. Specifically, that excess L-arginine modulates energy metabolism by enhancing NO production, by activating the major energy sensing and downstream gene AMPK, via the AMPK/NOS/NO pathway.

1.9. Main and specific objectives of the work

As outlined above, the objectives of the study are to investigate the impact of exogenous L-arginine addition on cell signalling in *in-vitro* cultured cell models. In particular, the work set out to investigate the impact of addition of exogenous arginine to several cultured model cell systems and on specific signalling pathways. Of particular interest was the NOS signalling pathway and how this responds to different concentrations of L-arginine alongside characterisation of the general impact on cell fitness (e.g. culture viability). The study also set out to investigate how exogenously overexpressed iNOS impacts regulation of downstream targets at the transcript level in the presence of exogenous L-arginine addition in BNL CL2 and/or 3T3 L1 cells. Key metabolites of L-arginine (L-citrulline and L-ornithine) and the nitrite amount present in cells was also analysed as a functional readout in the study. The specific objectives were therefore;

- To determine whether the presence of excess L-arginine in cell culture media impacted the L-arginine/NOS/NO pathway of BNL CL2 and 3T3 L1 cells and any impact on the proliferation of the cells and activation of AMPK
- To determine the transcript and protein expression of key genes in the L-arginine-NOS-NO signalling pathway as indicators of the molecular mechanisms activated upon sensing high L-arginine by liver or adipose cultured cells that may be related to the beneficial effect of taking supplementary arginine for control of obesity and obesity induced diabetic conditions
- To investigate how stably over-expressed iNOS impacts the L-arginine/iNOS/NO pathway and subsequent signalling pathways
- To investigate and determine nitrite concentrations in cells cultured in different L-arginine concentrations as a readout of NO production
- To investigate the effect and mechanism of action of the modulators such as nitric oxide synthase inhibitor; N^G-nitro-L-arginine-methylester (L-NAME), co-factor of NOS; tetrahydrobiopterin (BH₄) and external NO donor; S-Nitroso-N-acetylpenicillamine (SNAP) on metabolic pathways of L-Arg in BNL CL2 and 3T3 L1 cells
- To analyse residual amounts of selected amino acids (L-Arg, L-Cit and L-Orn) which are derived from L-Arg metabolic pathways, when cells are grown in different concentrations of L-Arg, modulators of the L-Arg metabolic pathways or overexpression of iNOS

Collectively these objectives will help map the cellular responses to sensing excess L-arginine concentrations in cultured cell systems that may help define how supplementary L-arginine impacts dietary control and/or liver and adipose cellular responses.

Chapter-2 Establishment of BNL CL2 and 3T3 L1 cell culture models and assessment of the impact of exogenous L-arginine addition on cell signalling pathways

2.1. Introduction

L-arginine is a precursor for synthesis of urea, polyamines, proline and nitric oxide (NO) as outlined in the main introduction to this study. Nitric oxide (NO) has been implicated in several cellular processes as a signalling molecule. L-arginine is metabolised in the cell to generate nitric oxide (NO) and citrulline via the enzyme nitric oxide synthase (NOS). The goal of the work in this chapter was to establish model systems to study the impact of L-arginine on cell signalling to allow investigation of the molecular mechanisms responsible for the L-Arg/NOS/NO metabolic pathways in insulin sensitive cells including liver cells; BNL CL2 and adipocyte cells; 3T3 L1. Once the cell systems had been established, the work in this chapter describes investigations of the impact of excess L-arginine of the metabolic signalling pathways.

2.2. Materials and Methods

2.2.1. Establishment of cell culture models for analysing culture viability and viable cell numbers

2.2.1.1. Culturing of adherent BNL CL2 and 3T3 L1 cell lines

BNL CL2 and 3T3 L1 cell lines were used as model systems, obtained from two different sources. 3T3 L1 cells were a generous gift from Dr Arcidiacono Biagio, University of Catanzaro 'Magna Graecia', Italy. BNL CL2 cells were a generous gift from Associate Prof of Medicine Dimiter Avtanski, Zucker School of Medicine at Hofstra/Northwell, Hempstead, New York. The BNL CL2 cell line is a mouse hepatocyte epithelial insulin-sensitive cell (Li *et al.*, 2019; Molinaro *et al.*, 2020; Leclercq *et al.*, 2007) whilst the 3T3 L1 cell line is a mouse adipocyte (mouse embryonic fibroblast) insulin-sensitive cell (Li *et al.*, 2019; Søndergaard & Jensen, 2016). The base medium for growth of both cell lines was Dulbecco's Modified Eagle's Medium (DMEM, Thermo Fisher Scientific, Cat. No: 41966). To prepare complete growth medium, foetal bovine serum (FBS, Sigma, Cat. No: F7524, Non-USA origin) was added to a final concentration of 10% (v/v). During passaging cells were maintained in vented T25 tissue culture flasks (Sarstedt, Germany) in complete growth medium (10 mL) and incubated in a static incubator (Thermo Forma, Thermo Fisher) at 37°C, 5% CO₂. Both cell lines were routinely passaged every 3-4 days. For experiments, cells were used 2 or 3 days after passage when they were in growth phase.

2.2.1.2. Preparation of stock solutions of L-arginine and growth medium with varying L-arginine concentrations

Commercially available DMEM media for Stable Isotope Labelling using Amino Acids (SILAC, Thermo Scientific, Cat. No: 88364), which is deficient in both L-lysine and L-arginine, was used to generate growth medium with varying L-Arg concentrations. Foetal bovine serum (FBS, Sigma, Cat. No: F7524, Non-USA origin) was added to a final concentration of 10% (v/v). L-lysine-HCl (Sigma, Cat. No: L-8662) was also added to give the same concentration of L-lysine (146 mg/L) as in the complete DMEM basal media described in **2.2.1.1** (and in **appendix II**). This media was termed L-Arg deficient media, containing no exogenously

added L-Arg (although FBS could contain unspecified concentrations of L-Arg, the amount of L-Arg in the media was determined by HPLC after FBS addition as undetectable and hence this media was considered L-Arg deficient (0 μ M). L-Arg (0.125 g, Sigma, A5006) was added to the SILAC L-Arg deficient DMEM media (10 mL) to obtain an L-Arg stock solution (71.75 mM). This was then diluted as required with the L-Lys and FBS containing SILAC media to generate different L-Arg concentration containing mediums.

2.2.1.3. Establishment of cell culture models for investigating cell fitness as determined by cell culture growth and viability parameters

BNL CL2 cells or 3T3 L1 cells were inoculated into a T125 tissue culture flask (Sarstedt, Germany) in complete DMEM (10% (v/v) FBS) in a total of 30 mL and the cells incubated for 2-3 days at 37°C, 5% CO₂. Cells were then observed under a light microscopy (Zeiss, Germany) to confirm around 90-95% confluency, at which time the media was removed and cells were washed with pre-warmed (37°C) phosphate-buffered saline (PBS) (Oxoid, Cat. No: BR0014G). For trypsinisation of cells, pre-warmed 0.05% trypsin-EDTA (Gibco, Cat. No: 11580626, 3 mL) was added and incubated for 5 min at 37°C, 5% CO₂ followed by addition of pre-warmed DMEM with 10% (v/v) FBS media (7 mL). A cell count was then performed using a Vi-CELL cell viability analyser (Beckman Coulter, Life sciences, USA) to determine viable cell concentrations (cells/mL) and culture viability (%). BNL CL2 cells were then seeded into 6-well tissue culture plates (Greiner Bio-One) at 2×10^5 viable cells/well in 2 mL of complete DMEM media.

The cells were then incubated in a static incubator (Thermo Forma, Thermo Fisher) for 24 h at 37°C, 5% CO₂. After 24 h, the media was replaced with media of different concentrations of L-arginine (0, 400 and 800 μ M) or the control complete DMEM with 10% (v/v) FBS (2 mL/ well) as in **Fig 2.2.1**. Complete DMEM is meant to contain 398.10 μ M of L-arginine hydrochloride according to the media formulation from the company (Thermo Fisher) (**Appendix II**), however this was measured as only 250 μ M using the HPLC method used and described in this study. Thus the 400 and 800 μ M culture conditions represent a 1.6 and 3.2-fold increase in exogenous L-arginine concentration compared to the complete DMEM controls. Cells and cell culture supernatant was then harvested at time points; 24, 48, 72 and 120 h post addition of L-Arg media of different concentrations. Briefly, the cell culture media (2 mL) was collected from the cell cultures and frozen at -20°C. Then, the cells were washed with pre-warmed PBS (2 mL) and subsequently trypsinised with pre-warmed 0.05% Trypsin-EDTA (Gibco, Cat. No: 11580626, 0.5 mL) for 5 min at 37°C, 5% CO₂. After trypsinisation, L-Arg deficient DMEM media for SILAC (1 mL) was added to the cells to stop trypsin activity. Cell suspension of the samples (1 mL) was used to measure culture viability (%) and the viable number of cells/mL ($\times 10^6$) using a Vi-CELL cell viability analyzer (Beckman Coulter, Life sciences, USA).

(Preliminary experiments were undertaken to find the more effective concentration of L-Arg using different concentration of L-Arg starting from 25 μ M to 1000 μ M and the time point at which the activity of L-Arg was maximum using different time points starting from 6 h to 120 h.)

2.2.2. RNA extraction and quantitative real-time PCR (qRT-PCR) for transcript mRNA analysis

Cells grown as described in section 2.2.1.3 but the cells were harvested at T=0; untreated samples (24 h after incubation of the cells and collected before L-Arg addition) and then samples were harvested 24 and 72 h after L-Arg addition. Cells were then washed with pre-warmed PBS (2 mL/well) followed by lysis using RLT (RNA lysis buffer) lysis buffer (350 μ L, Qiagen) and total RNA lysates were pipetted off into Eppendorf tubes (1.5 mL) and snap frozen in dry-ice and stored at -80°C or immediately further processed. Collected RNA lysates at T=0, 24 and/or 72 h were homogenised using a QIAshredder kit (Qiagen, Cat. No: 79654) to reduce viscosity of the cell lysates. Extraction of total RNA was then achieved using the commercially available RNeasy Mini Kit (Qiagen, Cat. No: 74104) following the protocol of the manufacturer. The quantity and quality of extracted RNA were then determined using a Thermo Nano Drop ND 1000 Spectrophotometer (Thermo Scientific, USA) by measuring absorbance at 260 and 280 nm, at this specific wavelength, nucleic acids absorb ultraviolet (UV) light. For pure DNA samples, the maximum absorbance occurs over a broad peak at around 260 nm; at 280 nm it only absorbs about half as much UV light compared to 260 nm. Extracted total RNA was treated for contaminating DNAase using RQ1 RNase-Free DNase kit (Promega, Cat. No: M6101). Diluted RNA (90.91 ng/ μ L) and then stored at -80°C until required for analysis.

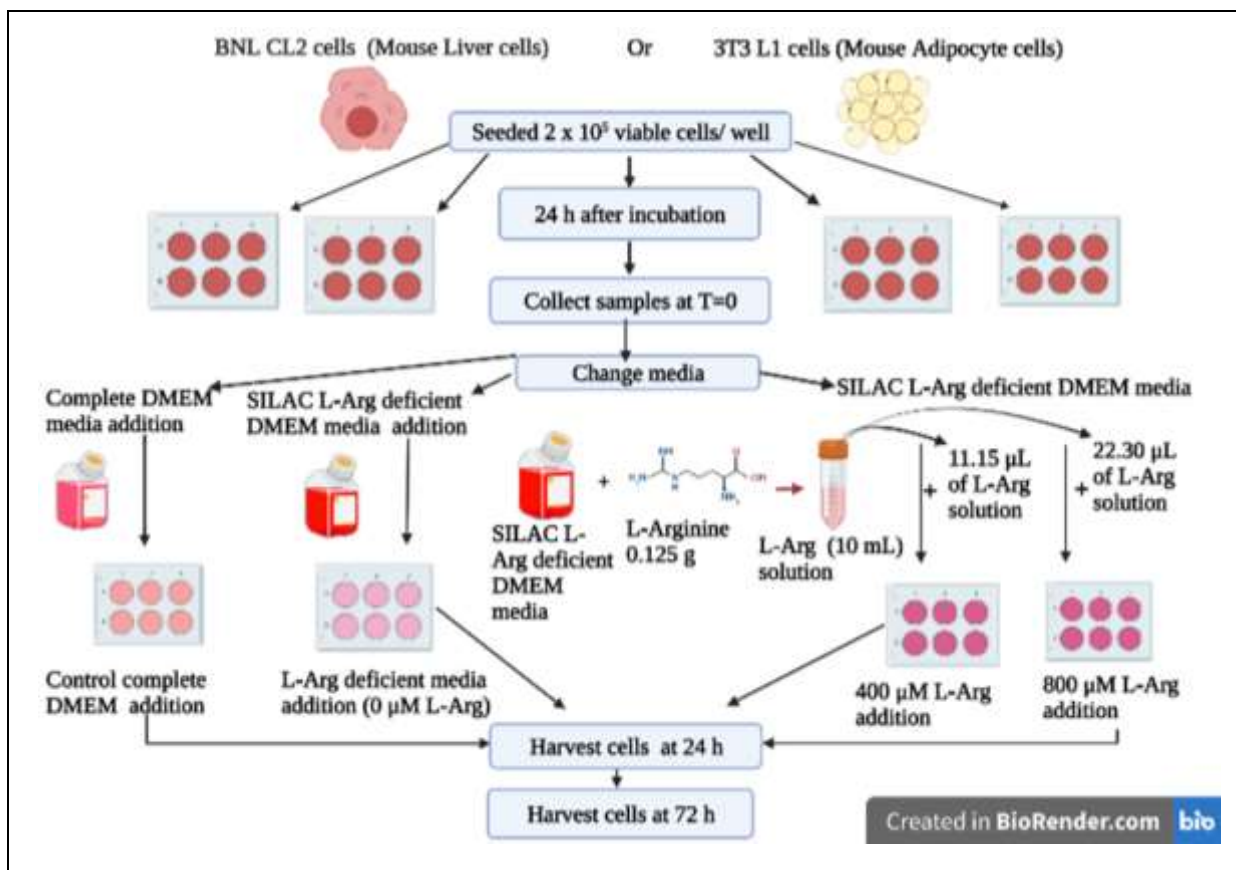


Figure 2.2.1. Schematic diagram outlining L-arginine supplementation of medium for BNL CL2 or 3T3 L1 cell growth.

Cells were maintained with different extracellular concentrations of L-arginine (0, 400 and 800 μ M) in SILAC L-Arg deficient media or the control complete DMEM with 10% FBS (2 mL/ well). Samples were collected 24 and 72 h post addition of L-arginine for analysis.

2.2.2.1. qRT-PCR methods

Primers were designed to target genes of interest within the region of two exons either side of an intron of a size less than 500 bp using UniProt, Ensembl, BLAST and OligoPerfect bioinformatics tools. Primers were selected within a region of high similarity (ideally 100%) to detect all splice variants/isoforms of genes of interest. The amplicon size was designed to be between 100 and 163 bp for efficient qPCR amplification. Primers (forward and reverse) were diluted to obtain 200 nM stock solutions of each. Primers designed for PCR amplification of target genes of interest are described in **Table 2.2.1**, which is explained in results section **2.3.2**.

qRT-PCR amplification of target sequences and the housekeeping control (β -actin) was undertaken using the commercially available iTaq™ Universal SYBR Green One-Step Kit (Bio-Rad, Cat. No: 1725151). The concentration of RNA of samples was adjusted to be 90.91 ng/ μ L for all reactions. Reaction mixtures for qRT-PCR were then prepared following the protocol provided by the manufacturer for a final reaction volume of 12.5 μ L. A DNA engine opticon 2 system for real-time PCR detection thermocycler (Bio-Rad) was used for amplification and for producing melting curve profiles of the amplicons using the following parameters.

qRT-PCR conditions (one-step):

Initial denaturation: 95°C, 1 min.

39 cycles:

Denaturation: 95°C for 10 sec

Annealing and extension: 60°C for 30 sec

Melting profile from 65°C to 95°C read every 0.5°C, hold 2 sec

2.2.3. Protein and post-translational modification (phosphorylation) analysis

2.2.3.1. Total protein extraction

Samples for protein analysis were generated by culturing cells as described in section **2.2.1.3**, but the cells were harvested at T=0; untreated samples (24 h after incubation of the cells and collected before L-Arg addition) and then samples were harvested 24 and 72 h after L-Arg addition. Samples for analysis were collected by removing the media and then washing the cells twice with chilled PBS (2 mL/well) or TBS (2 mL/well). PBS (2 mL/well) was used to wash the cells to be lysed for total protein analysis and TBS (2 mL/well) was used to wash the cells to be lysed for phosphorylated protein analysis as the presence of phosphate ions in PBS may interfere with the signal from the phosphorylated target. Plates were then kept on ice and lysis buffer added to the cells. Three different lysis buffers were used to obtain best signals of the target proteins from the cell lysates; (1) regular lysis buffer, (2) modified radioimmunoprecipitation (RIPA) lysis buffer, and (3) lysis buffer for phosphorylated protein analysis. Regular lysis buffer consisted of ice-cold 20 mM HEPES-NaOH, pH 7.2, containing 100 mM NaCl, 1% (w/v) Triton X-100 (Sigma, Cat. No: 9002-93-1) and cComplete™ mini protease inhibitor cocktail (Roche, Cat. No 11836153001, 1 tablet/10 mL lysis buffer). The modified RIPA lysis buffer contained the same regular lysis buffer components with 10 mM sodium β -glycerophosphate, 50 mM NaF, 1 mM activated sodium orthovanadate (Na_3VO_4), 0.2 mM phenylmethylsulfonyl fluoride (PMSF), 10 μ g/ml leupeptin and 2 μ g/mL pepstatin added. The lysis buffer

for phosphorylated protein extraction and analysis contained the same modified RIPA lysis buffer components with the addition of 1 mM ethylenediaminetetraacetic acid (EDTA), 1 mM dithiothreitol (DTT) and 1 mM ethylene glycol tetraacetic acid (EGTA). During harvesting, lysis buffer (200 μ L/well) was added and after 10 min on ice the cells were dislodged from the flask by using a cell scraper and the cell lysates (approximately 200 μ L) obtained. The cell lysates were centrifuged at 17,000 g for 10 min and then the collected protein extract kept at -80°C until required for analysis.

2.2.3.2. Bradford assay to determine protein concentration in samples

Bradford reagent (500 mL) was prepared consisting of 120 mM Coomassie blue G250 (Fisher, Cat. No: C/P541/46), 15% (v/v) ethanol and 8.5% (v/v) phosphoric acid. Following 10 minutes of stirring the reagent was filtered through filter paper (Whatman No.54) using a vacuum manifold and was collected into a dark bottle. Bradford reagent (1 mL) was added to 50 μ L of diluted samples (diluent: sample was 48:2 μ L) with a blank of 50 μ L of water. The samples were then briefly vortexed, left for 10 min and then the absorbance read on a calibrated spectrophotometer (Eppendorf BioPhotometer, Germany) at 595 nm. A series of known bovine serum albumin concentrations were used to generate a standard curve to calculate unknown protein concentrations.

Table 2.2.1. Primers used for real-time qPCR analysis of the target genes listed and size of amplicon expected

Target	Gene	NCBI ID	Forward primer oligo	Reverse primer oligo	Amplicon size (bp)
ACC-1	<i>Acaca</i>	NM_133360.3	GGGTCAAGTCCTTCCTGCTC	TTCCACACACGAGCCATTCA	139
AMPK	<i>Prkaal</i>	NM_001013367.3	GGATCCATCAGCAACTATCG	TCGACTCCTCCCCTGTCGAC	120
β -actin	<i>Actb</i>	NM_007393.5	AGCTGAGAGGGAAATTGTGCG	GCAACGGAAACGCTCATT	163
CPT-1	<i>Cpt1a</i>	NM_013495.2	TGTCTGAGCCATGGAGGTTG	ACACCATAGCCGTCATCAGC	133
HMGCR	<i>Hmgcr</i>	NM_001360165.1	ATGACATTCTTCCCGGCCTG	CCCTTTGGGTTACGGGGTTT	142
SREBP-1	<i>Srebf1</i>	NM_001313979.1	GTCACCAGCTTCAGTCCAGG	GACCTGAGCAGCCTGCGGCC	102
SREBP-2	<i>Srebf2</i>	NM_033218.1	ACCCCTTGACTTCCTTGCTG	CAGCCACAGGAGGAGAGTTG	146

2.2.3.3. Sodium dodecyl sulfate-polyacrylamide gel electrophoresis (SDS-PAGE) analysis of proteins

2.2.3.3.1. Sample preparation

Samples were prepared with x 5 sample/loading buffer (reducing buffer). Sodium dodecyl sulfate-polyacrylamide gel electrophoresis (SDS-PAGE) sample buffer (Laemmli buffer) contained 0.312 M Tris-HCl, pH 6.8, 10% (v/v) sodium dodecyl sulfate (SDS), 25% (v/v) β -mercaptoethanol, 50% (v/v) glycerol and 0.05% (v/v) bromophenol blue. The ratios between reducing sample buffer (x 5): diluted sample was 1:5. The required volume of protein extract was diluted with water to obtain x 1 final sample buffer concentration with **10 and 20 μ g of protein/25 μ L total sample volume/lane**. Samples were then vortexed, heat denatured at 95°C for 5 min and then resolved by SDS-PAGE as described below.

2.2.3.3.2. Gel preparation and electrophoresis

SDS-PAGE gels have two components, the resolving and stacking components. The stacking gel (5% acrylamide) was prepared with 30% (v/v) bio acryl-P 37.5:1 (Alfa-Aesar, Cat. No: J61505), 1 M Tris-HCl pH 6.8, 10% (w/v) ammonium persulfate (Fisher Scientific, Cat. No: A/P470/46), 10% (w/v) sodium dodecyl sulfate (SDS, Fisher Scientific, Cat. No: BP 166-500), 0.1% (v/v) N', N', N', N'-tetramethyl ethylenediamine (TEMED, Thermofisher Scientific, Cat. No: 110-18-9) and Milli-Q H₂O. The resolving phase was a 10% acrylamide gel (unless otherwise stated) prepared from 30% (v/v) bio acryl-P 37.5:1 (Alfa-Aesar, Cat. No: J61505), 1.5 M Tris-HCl pH 8.8, 10% (w/v) ammonium persulfate (Fisher Scientific, Cat. No: A/P470/46), 10% (w/v) SDS (Fisher Scientific), 0.04% (v/v) TEMED (Thermofisher Scientific, Cat. No: 110-18-9) and Milli-Q H₂O. Both gel components were prepared in a Novex gel cassette (1 mm, Life Technologies, Cat. No: NC2010).

Samples (25 μ L; 10 or 20 μ g of protein/25 μ L total sample volume/lane) were loaded into the gels using gel loading pipet tips (Fisher Scientific, Cat. No: 02-707-181) and a PAGE ruler plus pre-stained protein ladder (5 μ L, Thermo Scientific, Cat. No: 26619). SDS-PAGE gel electrophoresis was performed in running buffer containing 200 mM glycine, 25 mM Tris-HCl, 0.1% (w/v) SDS, pH 8.8, at 80 V for 30 min and 100 V for 1.5 h or until desired migration of the samples. Proteins were visualized by staining with Coomassie blue stain containing, 0.25% (w/v) Coomassie brilliant blue R-250, 10% (v/v) acetic acid and 50% (v/v) methanol.

2.2.3.4. Western blotting

After SDS-PAGE, transfer of proteins from the SDS-PAGE to nitrocellulose blotting membranes (0.45 μ m NC, GE healthcare, Cat. No: 10600003) was performed using wet transfer conditions. A sandwich with stacks was prepared whereby the bottom and top layers of the stacks were a sheet of Whatman filter paper (3 mm, GE healthcare, Cat. No: 1001-917) and in the middle of the sandwich the SDS-PAGE gel was placed in direct contact with the nitrocellulose blotting membrane. The layered sandwiched was inserted into a transfer tank cassette containing transfer buffer; 100 mM glycine, 12.5

mM Tris-HCl, 0.1 % (w/v) SDS, 20% (v/v) methanol. The electro transfer of protein to the membrane was undertaken at 4°C for 1 h at constant 0.75 A and at 250 V.

If necessary, ponceau staining (1% (w/v) ponceau stain, Sigma, Cat. No: P3504 and 3% (w/v) trichloroacetic acid, Sigma, Cat. No: 76-03-9) was carried out to observe proteins on membranes post transfer before the antibody-mediated detection. After transfer, the nitrocellulose membrane was removed from the transfer cassette and placed in a clean blotting box protein side up. The membrane was covered with ponceau stain (1 mL) and shaken gently for 3 minutes. Ponceau stain was removed and the membrane washed with water. After visualization of transferred protein bands, the blotting membrane was washed with T-TBS (150 mM NaCl, 2.5 mM KCl, 25 mM Tris-HCl, 0.1% (v/v) Tween 20 (Sigma, Cat. No: 9005-64-5), pH 7.6) to remove the reversible stain. To prevent antibodies from binding to the membrane non-specifically and to reduce the background, a blocking step was carried out by incubating the membrane with 5% (w/v) non-fat dried skimmed milk powder (Oxoid, Cat. No: LP0031) diluted in TBS (150 mM NaCl, 2.5 mM KCl, 25 mM Tris-HCl, pH 7.6) at room temperature for 30 min. After blocking, the membrane was washed three times with T-TBS (150 mM NaCl, 2.5 mM KCl, 25 mM Tris-HCl, 0.1% (v/v) Tween 20, Sigma, Cat. No: 9005-64-5), pH 7.6 for 10 min on a shaker. An indirect method was used to identify the protein of interest on the membrane. The antibodies for western blot analysis were sourced as detailed in **Table 2.2.2**.

and with the working dilutions described. To detect the protein of interest, primary antibody incubation was undertaken overnight at 4°C in a 10 mL dilution of the appropriate primary antibody prepared in 3% (w/v) bovine serum albumin (BSA, Sigma, Cat. No: A7906) in TBS (150 mM NaCl, 2.5 mM KCl, 25 mM Tris-HCl, 0.1% (v/v), pH 7.6) on a blot rocker (IKA, England). The following day, sequential four washing steps were performed on the primary antibody probed blot at room temperature for 5 min on a blot shaker with T-TBS (150 mM NaCl, 2.5 mM KCl, 25 mM Tris-HCl, 0.1% (v/v) Tween 20 (Sigma, Cat. No: 9005-64-5), pH 7.6). For detecting the target antigen, the blot was probed with an appropriate secondary antibody conjugated to Horseradish peroxidase containing 5% (w/v) non-fat dried skimmed milk powder (Oxoid, Cat. No: LP0031) diluted in T-TBS at room temperature for 1 h on a blot shaker.

Blots were then washed again 4 times with T-TBS for 5 min. For the detection step, the probed blots were incubated for 5 min in home-made enhanced chemiluminescence (ECL) western blotting detection reagent, 5 mL of each solution (solution A containing, 1 M Tris-HCl, pH 8.5, 90 mM p-coumaric acid (Sigma, Cat. No:9008), 250 mM 3-aminophthalhydrazide (Luminol, Sigma, Cat. No: A-8511) and solution B containing 1 M Tris-HCl, pH 8.5, 30% (w/v) H₂O₂) was used. If necessary, commercially available Pierce™ ECL western blotting substrate (Thermo Fisher Scientific, Cat. No: 32106) was used by following the instructions provided with the reagents by the manufacturer to reduce the background issue on the blots, which was caused by some antibodies which were purchased from different companies. Finally, the blots were exposed to Amersham Hyperfilm™ ECL film (GE healthcare, Cat.

No: 28906837), which was subsequently processed using an Optimax 2010 film processor (PROTEC GmbH & Co, Germany).

2.2.3.5. Densitometry analysis

Densitometry of bands on SDS-PAGE and Western blots was undertaken using the open software package ImageJ (National Institutes for Health (NIH), USA). The relative protein expression of a protein of interest in the samples were normalized to the house-keeping β -actin protein.

Table 2.2.2. List of antibodies used and sourced from different companies for Western blotting.

Target protein	UniProt ID	Molecular weight (kDa)	Type	Dilution	Host species	Source company	Catalog No
Anti-ACC-1	Q5SWU9	265	Primary	1:1000	Rabbit	GeneTex	GTX132081
Anti-ACC-1-P (Ser79)	Q5SWU9	265	Primary	1:1000	Rabbit	GeneTex	GTX133974
Anti-AMPK	Q5EG47	62	Primary	1:1000	Rabbit	Cell Signaling	2532
Anti-AMPK-P (Thr172)	Q5EG47	62	Primary	1:500	Rabbit	Cell Signaling	2535
Anti- β -actin	P60710	42	Primary	1:1000	Mouse	Sigma	A5441
Anti-CPT-1A	P97742	88	Primary	1:1000	Rabbit	GeneTex	GTX114337
Anti-eEF2	P58252	95	Primary	1:1000	Rabbit	Cell Signaling	2332
Anti-eEF2-P (Thr56)	P58252	95	Primary	1:1000	Rabbit	Cell Signaling	2331
Anti-eIF2	Q6ZWX6	36	Primary	1:1000	Rabbit	abcam	ab26197
Anti-eIF2-P (S51)	Q6ZWX6	36	Primary	1:1000	Rabbit	abcam	ab32157
Anti-HMGCR	Q01237	97	Primary	1:1000	Rabbit	GeneTex	GTX54088
Anti-mTOR	Q9JLN9	289	Primary	1:1000	Rabbit	GeneTex	GTX101557
Anti-SREBP-1	Q9WTN3	120	Primary	1:1000	Mouse	Fisher	11384493
Anti-SREBP-2	Q3U1N2	122	Primary	1:1000	Rabbit	abcam	ab30682
Anti-mouse IgG-Peroxidase	-	-	Secondary	1:5000	Goat	Sigma	A4416
Anti-rabbit IgG-Peroxidase	-	-	Secondary	1:5000	Goat	Sigma	A6154

2.2.4. Nitric oxide /Nitrite measurement by Griess Assay

2.2.4.1. Preparation of sulphanilamide and N-(1-naphthyl)-ethylenediamine dihydrochloride (NED) solution

Sulphanilamide and NED solution were prepared freshly as follows.

0.1% (w/v) sulphanilamide in 5% (v/v) phosphoric acid: Sulphanilamide (0.02 g) (Sigma, Cat. No: S9251) was dissolved in 20 mL of 5% (v/v) phosphoric acid.

0.1% (w/v) solution of NED: NED (0.02 g) (Sigma, Cat. No: N5889) was dissolved in 20 mL of water.

2.2.4.2. Preparation of Samples

Frozen cell culture media (2 mL), collected from L-arginine additions to BNL CL2 and 3T3 L1 cells, were used for nitrite assay. Samples were vortexed and then centrifuged for 10 min at 1500 rpm and the supernatant without cell pellet was collected. Cell culture supernatant (50 μ L) was used in the assay.

2.2.4.3. Griess assay

A key molecule of the L-arginine metabolic pathway is nitric oxide (NO) (Wu and Morris, 2008). Accumulation of NO in the cell culture media was analysed indirectly by quantifying one of the oxidation products, nitrite (NO₂⁻). Nitrite accumulation in cell culture supernatants after L-Arg supplementation was determined by Griess assay (Griess, 1879; the principle of this reaction is shown in **Fig 2.2.2**) using sodium nitrite as a standard. In brief, nitrite standard solutions were prepared from a stock sodium nitrite solution (0.1 M) with concentrations ranging from 0 to 25 μ M (0, 1.25, 2.5, 5, 10, 15, 20 and 25 μ M) in L-arginine deficient SILAC media for DMEM and dispensed into a 96-well-plate in triplicate (50 μ L/well). Samples of cell culture supernatants with or without L-Arg additions and the control complete media addition (50 μ L) were also dispensed into the 96-well-plate in triplicate. 1% (w/v) sulphanilamide solution in 5% (v/v) phosphoric acid (50 μ L) was added to both sample and nitrite standard wells. After a 10 min incubation at room temperature in the dark, a 0.1% (w/v) solution of NED (50 μ L) was added to each well followed by a 10 min incubation at room temperature in the dark (total volume/well = 150 μ L). Absorbance at 540 nm was then measured using a FLUOstar omega microplate reader (BMG Labtech, Germany). Absorbance was measured within 15 min of last incubation to avoid fading of colour of the product. The data was averaged and the average of the blank standard (0 μ M) was subtracted from all other data. A standard curve relating absorbance to known nitrite concentration was generated and a linear line was fitted using a linear regression. Calculation of nitrite concentration in unknown experimental samples was obtained using the equation of the line fitted for the standard samples.

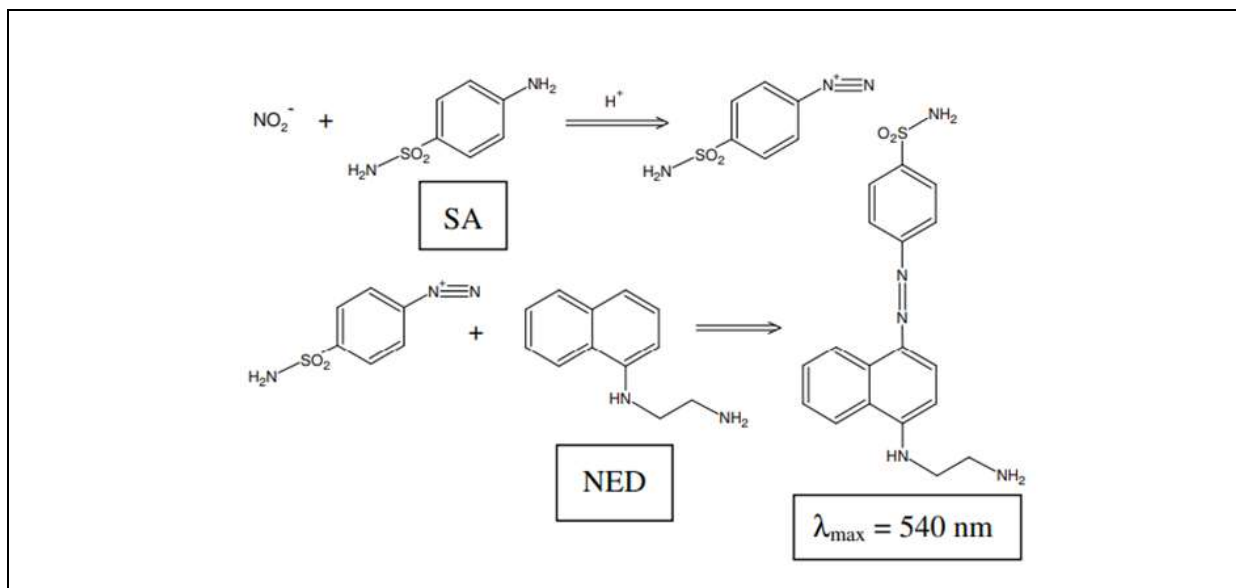


Figure 2.2.2. Principle of nitrite quantitation using the Griess reaction

In this assay, nitrite is first reacted with a diazotizing reagent, sulfanilamide (SA), in acidic media to form an intermediate transient diazonium salt, which is then allowed to react with a coupling reagent, N-naphthylethylenediamine (NED), to form a stable azo compound, an intense purple coloured product, detected at 540 nm (Sun *et al.*, 2003).

2.2.5. Analysis of L-arginine, L-ornithine and L-citrulline by HPLC

2.2.5.1. Processing of biological samples

Samples were collected as described in 2.2.1.3, then vortexed and centrifuged at 1500 rpm for 10 min to obtain the cell free culture supernatant for HPLC analysis.

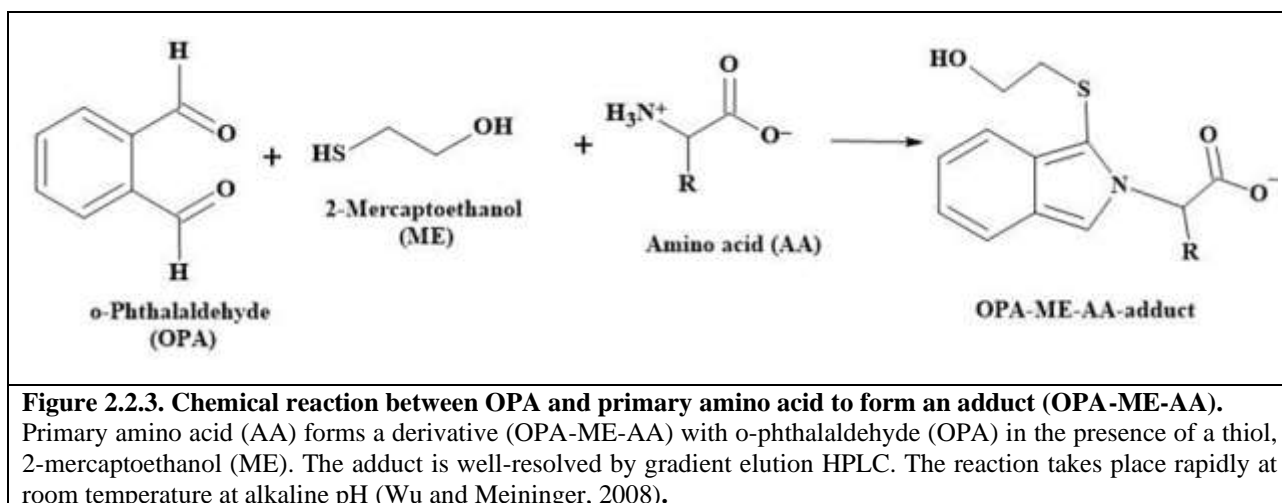
2.2.5.2. Deproteinization of samples for amino acid analysis

Samples were deproteinised (cell culture serum samples contain protein, a potential source of amino acids after protein degradation, therefore protein in serum samples should be prevented by deproteinisation) using a modified protocol of that described by Yang *et al.* (2014). To remove FBS and cellular proteins from the supernatant of the cell culture media, 100% (v/v) ice-cold ethanol (400 μL) was added to the cell culture supernatant (100 μL) followed by vortexing vigorously for 15 min at room temperature. Samples were then centrifuged at 17000 g for 15 min at 0°C. The supernatant (approximately 500 μL) was then transferred to a fresh microcentrifuge tube and the solvent and media removed by vacuum centrifugation in a SpeedVac-Plus SC110A concentrator centrifuge (Savant, USA) for 1.25 h at 45°C. The vacuum dried supernatant residue was then reconstituted in 80% (v/v) ethanol (100 μL) and vigorously vortexed for 5 min and then centrifuged again at 17000 g for 15 min at 0°C to collect the supernatant. To remove ethanol completely (to obtain high resolution of the amino acids and increase binding to the column in the HPLC experiment), the supernatant of resuspended sample (100 μL) was then further vacuum centrifuged by SpeedVac-Plus SC110A concentrator centrifuge (Savant, USA) for 30 min at 45°C and then 100 μL of water added.

2.2.5.3. HPLC amino acid analysis

2.2.5.3.1. Pre-column derivatization

Amino acids were derivatized at room temperature using a pre-column derivatisation method. O-phthalaldehyde (OPA) reagent complete solution (Sigma, Cat. No: P0532) consisting of OPA (1 mg/mL), Brij^R 35 (for optimum separation of citrulline from threonine and of ornithine from lysine (Wu and Meininger, 2008)), methanol, 2-mercaptoethanol, potassium hydroxide and boric acid, pH 10.4, was used as a pre-column derivatization agent, specially formulated for primary amines and amino acids at alkaline pH. OPA reacts with primary amino acids in the presence of a thiol (2-mercaptoethanol) to form adducts (OPA-ME-AA) (**Fig 2.2.3**), which are well-resolved by HPLC with appropriate gradient conditions and mobile phases with organic modifiers (Walker and Mills, 1995).



2.2.5.3.2. Mobile phase buffers

Mobile phase A (0.1 M sodium acetate, pH 7.2) was prepared as described by Wu & Meininger (2008). In brief, sodium acetate (0.1 M) (Sigma, 99.0%, Cat. No: S7545), 9% methanol, and 0.5% tetrahydrofuran (ACROS Organics, 99.5%, Cat. No: 10292182), adjusted to pH 7.2 by HCl, was prepared and mixed after each addition before being filtered through a 0.2 µm nylon membrane filter (MERCK, Cat. No GNWP04700) prior to use in HPLC analysis. The mobile phase B was 100% (v/v) methanol.

2.2.5.3.3. Preparation of amino acid standards

A standard amino acid mixture (6 mM), consisting of the essential 20 amino acids, was a gift from Dr Andrew Lawrence, School of Biosciences, University of Kent, and was prepared as outlined previously (Moore *et al.*, 2018). In brief, the standard amino acid powder mixture (20 L-amino acids and glycine, Sigma, Cat. No: 09416-1EA) was dissolved at an alkaline pH to formulate a stock solution of standard amino acid mixture (6 mM) and then diluted to obtain a working amino acid standard (0.6 mM for each amino acid). Additionally, L-citrulline

(Sigma, Cat. No: C7629) and L-ornithine monohydrochloride (Sigma, Cat. No: O2375) (0.6 mM of each) were added to the standard amino acid mixture from respective stock solution of L-citrulline and L-ornithine (6 mM of each) to form an extended amino acid standard solution.

2.2.5.3.4. Amino acid HPLC analysis

An Agilent 1100 HPLC (Agilent Technologies, Germany) equipped with a diode-array detector (DAD) was used. HPLC experimental conditions were optimised (OPA derivatisation method, column, detection parameters and DAD detector) to obtain well-resolved peaks for the intended amino acids. Samples were injected (25 μ L) onto an ACE HPLC column; RP-C18, dimensions 125 \times 4.6 mm, 5 μ m (Cat. No: ACE 126-1246). The column was operated with a flow rate of 1.1 mL/min using organic modifiers; 0.1 M sodium acetate, pH 7.2 as mobile phase A and 100% methanol as mobile phase B. Before running the sample set, the column was fluxed sequentially with water and methanol for 5 min and then equilibrated with mobile phase A for 10 min at a flow rate of 1.1 mL/min at 30°C.

To a dark glass vial (1.5 mL), an extended amino acid standard mixture (0.6 mM each) or test cell culture sample solution (100 μ L) was added. The autosampler was automated to mix 25 μ L of a standard or sample solution with 25 μ L of the OPA reagent solution and allowed for incubation for 1 min in a reaction loop. The derivatized solution was then immediately delivered into the HPLC column without any delay as the amino acid derivatives are very unstable, with short half-lives (2.3-72.3 min) (Walker and Mills, 1995). This problem was overcome by automating the derivatization and replacing the OPA micro vial often. Amino acids were separated with linear gradient as described in the **Table 2.2.3** with a total running time of 49 min; flow rate, 1.1 mL/min. The detector, DAD, was programmed to switch to 338 nm, 10 nm bandwidth, and reference wavelength 390 nm, 20 nm bandwidth. The molar absorptivity of each derivatized amino acid was detected at 338 nm (λ_{max}).

Table 2.2.3. HPLC gradient program for separation of L-Arg, L-Cit and L-Orn at flow rate 1.1 mL/min.

Mobile Phase (%)	Time (min)										
	0	15	20	24	26	34	38	40	42	42.1	49
A	86	86	70	65	53	50	30	0	0	86	86
B	14	14	30	35	47	50	70	100	100	14	14

2.2.5.3.5. Standard curve generation for L-arginine, L-citrulline and L-ornithine

Stock solutions of L-arginine, L-citrulline and L-ornithine (20 mM, 10 mL each and 1000 μ M, 50 mL each) were diluted to give a range of concentrations of each amino acid standard (10, 20, 30, 40, 50, 100, 250, 500, 750 and 1000 μ M). The range of standard solutions were run with OPA on the HPLC. Peaks in the HPLC chromatogram were integrated using the software provided by the manufacture (Agilent Technologies,

Germany) to obtain the area of the peaks and from these a standard curve was plotted with the area of the signals (mAU x Sec) against concentration to obtain best fit standard curves for each amino acid.

2.2.5.3.6. HPLC data analysis

Identification of particular amino acid signals was based on the comparison between the retention time of the extended amino acid standard mixture and the amino acids of interest from analysis of samples. Quantitation was based on the standard curve method using a linear curve fitted by linear regression analysis. The unknown concentration of each amino acid in experimental samples was calculated using the equation of the line fitted for the standard curves of amino acids.

2.2.6. Analysis of L-arginine, L-citrulline and L-ornithine adducts with OPA derivatising agent by liquid chromatography– mass spectrometry (LC–MS)

LC-MS (UltiMate 3000 HPLC and UHPLC Systems, Thermo Fisher) was carried out to confirm the molecular mass of the L-arginine, L-citrulline and L-ornithine adducts after derivatisation with the derivatisation agent o-phthalaldehyde (OPA) containing β -mercaptoethanol. Mobile phase modifiers were 0.1% (v/v) formic acid and H₂O (mobile phase A) and 0.1% (v/v) formic acid and methanol (mobile phase B). An autosampler was programmed to inject a sample volume 20 μ L into the analytical column (C18; 4.6 mm x 150 mm, 5 μ m, from Zorbax Eclipse), guarded with SecurityGuard™ ULTRA Cartridges UHPLC column (C18; 2 mm, 2.1 mm). Before running a sample, the column was washed sequentially with 2% mobile phase B and then equilibrated with 2% mobile phase B for 13 min before the first sample at a flow rate of 1.5 mL/min and constant column temperature of 40°C. The amino acid adducts were resolved with the gradient described in **Table 2.2.4**. The signals were detected at a wavelength of 340 nm. Mass spectrometry was undertaken in positive mode [MH]⁺ (L-arginine) and negative mode [M-H]⁻ (L-arginine, L-citrulline and L-ornithine) to confirm the presence of the expected adducts.

Table 2.2.4. LC-MS gradient used to identify the derivatisation adducts of amino acids (OPA-ME-AA) at a flow rate 1.5 mL/min.

Time (min)	1	> 8	2.5	2.5
Gradient Mobile Phase B %	2	2-100	100	2

2.2.7. Statistical analysis

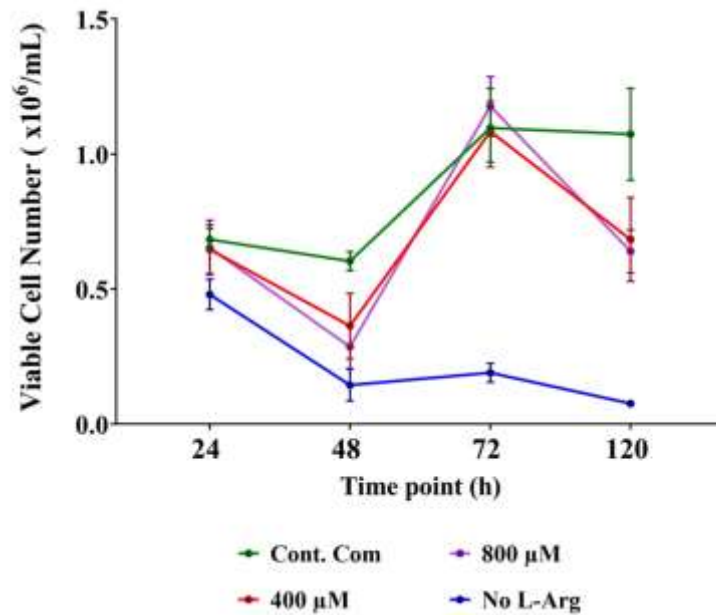
Statistical analysis was undertaken using GraphPad Prism 9.4.1 software and Microsoft Excel. Samples were analysed in triplicate biological replicates. Data interpreted of means and standard deviation were analysed using two-way ANOVA. The Tukey's multiple comparison method was used to determine differences among the means of the treatment groups (0, 400 and 800 μ M L-Arg) with the control complete DMEM media addition and untreated samples at T=0 across the time points 24 and 72 h. Probability values ≤ 0.05 were

considered to indicate statistical significance. The stars approach intended to flag levels of significance were followed (American Psychological Association style, New England Journal of Medicine) as ns = $P > 0.05$, * = $P \leq 0.05$, ** = $P \leq 0.01$, *** = $P \leq 0.001$ and **** = $P \leq 0.0001$.

2.3. Results

2.3.1. Impact of L-Arg addition on culture viability and viable cell numbers in BNL CL2 cells

Establishment of cell culture models for investigating cell fitness (cell culture growth and viability parameters) is described in **2.2.1.3**. Samples were collected at 24, 48, 72 and 120 h time points for cell growth analysis of BNL CL2 cells. All cell samples were analysed with biological triplicate cultures. The viable number of cells was compared between the control complete DMEM medium and the no L-arginine SILAC DMEM media (0 μM L-arginine) and when SILAC DMEM had 400 and 800 μM L-arginine added. **Figure 2.3.1** shows that there was a decline in BNL CL2 cell numbers from 24 to 48 h in all samples and conditions. After this time the proliferation of cells increased for the control and the 400 and 800 μM L-arginine supplemented cell samples from 48 to 72 h. However, the cell number continued to decrease in the no L-Arg (0 μM) cell samples across this time period. Cell number declined in the 400 and 800 μM L-Arg supplemented cell samples between 72 and 120 h, whilst there was a plateau in the growth of the cell samples grown in control complete DMEM. Overall, the viable cell number of BNL CL2 cultures was most impacted by an absence of exogenous L-Arg with minor changes with the different concentrations of L-arginine compared to the control. Viable cell number peaked in the control cultures and the 400 and 800 μM L-arginine supplemented cultures after 72 h. The control cell cultures then maintained their viable cell number until 120 h of culture whilst the supplemented cultures decreased. In spite of the similar growth profiles (**Fig 2.3.1**), the effect of L-arginine (0, 400 and 800 μM) compared to the control complete DMEM media was significant (**Fig 2.3.1**) as determined by two-way ANOVA analysis of the means values of the viable cell numbers at the different time points followed by a Tukey multiple comparison test.



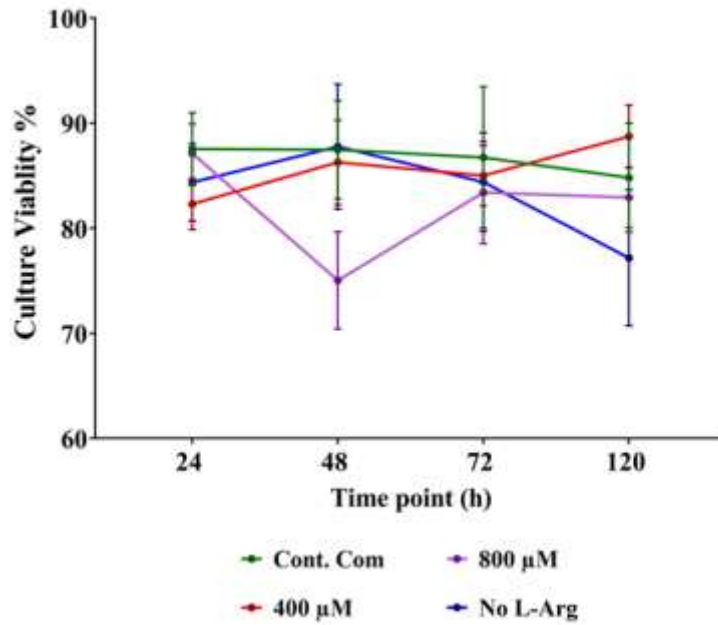
Source of Variation	P value	P value summary	Significant?
Interaction	<0.0001	****	Yes
Time point	<0.0001	****	Yes
L-Arg +/- and Control (Com)	<0.0001	****	Yes

Tukey's multiple comparisons test	Viable cell number			
	24 h	48 h	72 h	120 h
Cont. Com vs. 400 μM	ns	*	ns	***
Cont. Com vs. 800 μM	ns	**	ns	****
Cont. Com vs. No L-Arg	ns	****	****	****
400 μM vs. 800μM	ns	ns	ns	ns
400 μM vs. No L-Arg	ns	*	****	****
800 μM vs. No L-Arg	ns	ns	****	****

Figure 2.3.1. Cell growth profile of BNL CL2 cells with different concentrations of L-arginine and the control. Cell growth/viable cell number profiles of BNL CL2 cells with different concentrations of L-arginine (0, 400 and 800 μM) and the control complete DMEM media at 24, 48, 72 and 120 h. Data points represent the mean ± SD of each culture sample. Error bars represent the standard deviation from the mean (n = 3). The tables summarise two-way ANOVA followed by a Tukey multiple comparison test using GraphPad Prism 9.4.1. The stars flag the levels of significance; ns = P > 0.05, * = P ≤ 0.05, ** = P ≤ 0.01, *** = P ≤ 0.001 and **** = P ≤ 0.0001.

Figure 2.3.2 reports the culture viability of cultures grown in either control complete DMEM or L-arginine supplemented samples (400 and 800 μM) and no L-arginine SILAC DMEM at 24, 48, 72 and 120 h. Culture viability was generally maintained between 80-90% across the 120 h. Noticeably the largest difference was a drop in viability of the cultures with 800 μM L-Arg addition from 24 to 48 h time period, after which the

viability then increased again from 48 to 72 h and then remained steady. Overall, the viability of the BNL CL2 cultures was not significantly impacted by the different L-Arg conditions except for a few timepoints and conditions as outlined in **Fig 2.3.2**. As described above, the cultures with the highest concentration of L-arginine (800 μ M) had a large drop in viability at 48 h and at 120 h the no L-Arg cultures had decreased culture viability compared to other culture conditions.



Source of Variation	P value	P value summary	Significant?
Interaction	0.0225	*	Yes
Time point	0.7313	ns	No
L-Arg +/- and Control (Com)	0.0766	ns	No

Tukey's multiple comparisons test	Culture viability			
	24 h	48 h	72 h	120 h
Cont. Com vs. 400 μ M	ns	ns	ns	ns
Cont. Com vs. 800 μ M	ns	**	ns	ns
Cont. Com vs. No L-Arg	ns	ns	ns	ns
400 μ M vs. 800 μ M	ns	*	ns	ns
400 μ M vs. No L-Arg	ns	ns	ns	*
800 μ M vs. No L-Arg	ns	**	ns	ns

Figure 2.3.2. Culture viability profile of BNL CL2 cells grown in different concentrations of L-arginine and the control.

Culture viability profile of BNL CL2 cells grown in different concentrations of L-Arg (0, 400 and 800 μ M) and the control complete DMEM media at 24, 48, 72 and 120 h. Culture viability is expressed as % of viable cells. Data points represent the mean \pm SD of each sample. Error bars represent the standard deviation from the mean (n = 3). Tables

summarise two-way ANOVA followed by a Tukey multiple comparison test using GraphPad Prism 9.4.1. The stars indicate the levels of significance; ns = $P > 0.05$, * = $P \leq 0.05$, ** = $P \leq 0.01$, *** = $P \leq 0.001$ and **** = $P \leq 0.0001$.

2.3.2. qRT-PCR analysis of target genes and assays upon culturing of BNL CL2 cells in different exogenous L-arginine concentrations

Cells were grown as described in section 2.2.1.3 and 2.2.2 and sampled for transcriptional mRNA level analysis by qRT-PCR. RNA samples were control complete DMEM media, no L-arginine SILAC DMEM media and 400 and 800 μM L-arginine addition to BNL CL2 cells. Cell samples were collected at T=0, 24 and 72 h and RNA extraction, DNAase treatment and qRT-PCR analysis were undertaken as described in section 2.2.2. Relative gene expression analysis ($\Delta\Delta\text{Ct}$) was used to quantify target gene mRNA expression normalised to a reference gene, β -actin. The target gene expression was normalized to β -actin to obtain the ΔCt and then the relative difference (ΔCt) between target and β -actin was normalized to the ΔCt value of the control no L-arginine added sample at the 24 h culture time point to obtain the $\Delta\Delta\text{Ct}$ value. The target genes investigated were AMPK, ACC-1, CPT-1, HMG-CoA reductase, SREBP-1 and SREBP-2 as these genes are potentially modulated in response to changes in L-arginine through signalling pathways discussed elsewhere in this thesis. The relative expression of each gene (as opposed to absolute expression that was not determined and absolute quantification determines expression levels in absolute numbers of mRNA copies) was denoted as RE. Here target gene expression was explained relative to one of the controls; 0 μM L-Arg at 24 h and housekeeping gene; β -actin.

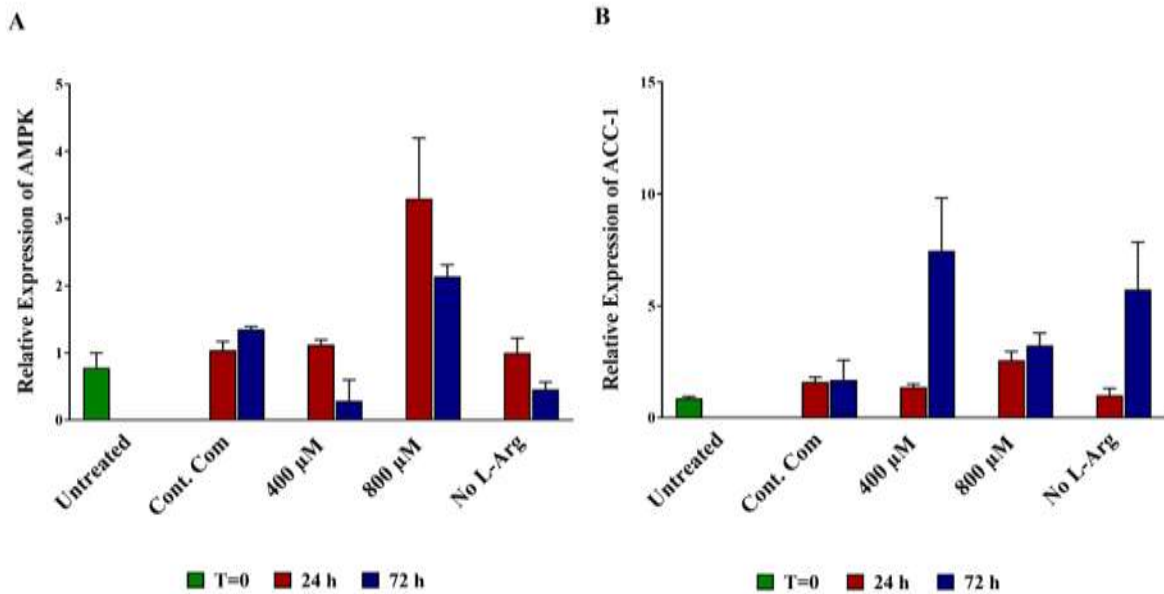
The first transcript investigated was the mRNA levels of the key regulator gene involved in the oxidation of energy substrates, AMPK (Cantó and Auwerx, 2013). AMPK was regulated in response to L-arginine addition with increasing extracellular concentrations increasing the observed AMPK mRNA expression in the BNL CL2 cells (**Fig 2.3.3A**). From qRT-PCR data, *AMPK* gene expression was increased ($P < 0.0001$) in 800 μM L-Arg addition cultures at 24 (RE 3.29) and 72 h (RE 2.14) when compared to the control complete DMEM media cultures.

The mRNA levels of the key lipogenic enzyme, ACC1, was decreased ($P < 0.0001$) in cultures with arginine at 400 μM (RE 1.4) compared to the control (RE 1.6) but increased ($P < 0.0001$) at 72 h (RE 7.46) compared to the control complete DMEM media cultures (RE 1.69) (**Fig 2.3.3B**).

Very similar CPT-1A gene expression was observed in all culture conditions (**Fig 2.3.4A**). The highest relative expressions among the samples was 1.2 for control complete DMEM addition at 72 h, 1.03 for 800 μM L-Arg at 24 h and 1.36 for no L-Arg media at 72 h. It is therefore clear that *CPT-1A* gene expression did not differ much between the control and L-Arg supplemented cultures, reflecting little impact of L-Arg supplementation on *CPT-1A* gene expression at the transcript level.

A further gene investigated was HMG CoA reductase (HMGCR), responsible for cholesterol synthesis and a gene controlled itself by sterol regulatory element binding protein-2 (SREBP-2), a key regulator and transcription factor in cholesterol metabolism (Wong et al., 2015; Tao et al., 2013). HMGCR ($P < 0.0001$) and SREBP-2 ($P < 0.0001$) were decreased in mRNA expression compared to the DMEM control in response to 800 μM L-Arg addition at 24 h (RE-HMGCR 2.59 and RE-SREBP-2 1.29 respectively compared to RE 2.98 and RE 1.66 of control) (**Fig 2.3.4B** and **Fig 2.3.5B**) while the mRNA levels for AMPK increased ($P < 0.0001$) in 800 μM L-Arg addition at same time point (RE 3.29) when compared to the complete DMEM control RE of AMPK 1.04. Under these conditions, reduced SREBP-2 expression could potentially reduce the expression of HMGCR leading to reduce cholesterol biosynthesis.

A further SREBP transcription factor, sterol regulatory element-binding protein-1 (SREBP-1), that regulates genes involved the *de novo* lipogenesis and glycolysis pathways (Ruiz *et al.*, 2014) decreased in expression ($P < 0.0001$) in 800 μM L-Arg cultures at 72 h (RE 1.60) when compared to the control complete DMEM addition (RE 2.49) at the same time point (**Fig 2.3.5A**). Among all the genes investigated in BNL CL2 cells, lipogenic genes ACC-1 (RE 7.46) and SREBP-1 (RE 6.76) increased the most in mRNA expression, whereas AMPK gene expression was lowest in 400 μM L-Arg addition at 72 h (RE 0.29).



Source of Variation	AMPK		ACC-1	
	P value	Significant?	P value	Significant?
Interaction	****	Yes	****	Yes
Time point	****	Yes	****	Yes
L-Arg +/- and control (Com)	****	Yes	****	Yes

Tukey's multiple comparisons test	AMPK			ACC-1		
	T=0	24 h	72 h	T=0	24 h	72 h
Untreated vs. Cont. Com	**	***	****	ns	ns	ns
Untreated vs. 400 μM	**	***	ns	ns	ns	****
Untreated vs. 800 μM	**	****	****	ns	**	***
Untreated vs. No L-Arg	**	***	ns	ns	ns	****
Cont. Com vs. 400 μM	ns	ns	***	ns	ns	****
Cont. Com vs. 800 μM	ns	****	**	ns	ns	ns
Cont. Com vs. No L-Arg	ns	ns	**	ns	ns	****
400 μM vs. 800 μM	ns	****	****	ns	ns	****
400 μM vs. No L-Arg	ns	ns	ns	ns	ns	ns
800 μM vs. No L-Arg	ns	****	****	ns	ns	*

Figure 2.3.3. Relative mRNA expression of AMPK and ACC-1 in BNL CL2 cells cultured in different concentrations of L-arginine and the control.

Relative mRNA transcript expression ($\Delta\Delta Ct$) of AMPK (A) and ACC-1 (B) in BNL CL2 cells cultured in medium of different L-arginine concentrations (0, 400 and 800 μM) and control complete DMEM media 24 and 72 h after addition. Untreated cultures at T=0. Data points represent the mean \pm SD of each sample. Error bars represent the standard deviation from the mean (n =3). Tables summarise two-way ANOVA followed by a Tukey multiple comparison test using GraphPad Prism 9.4.1. The stars indicate the levels of significance; ns = P > 0.05, * = P \leq 0.05, ** = P \leq 0.01, *** = P \leq 0.001 and **** = P \leq 0.0001.

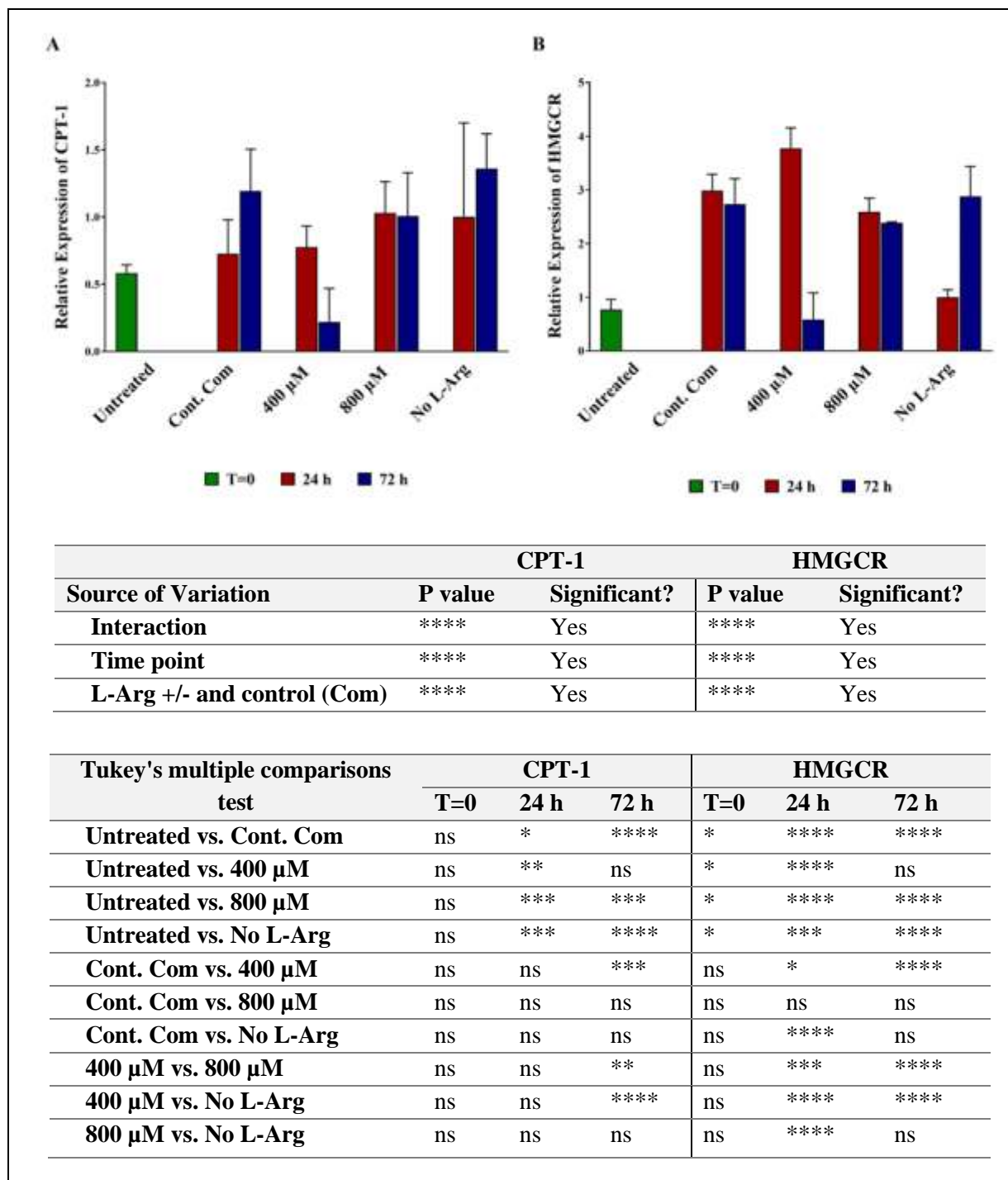
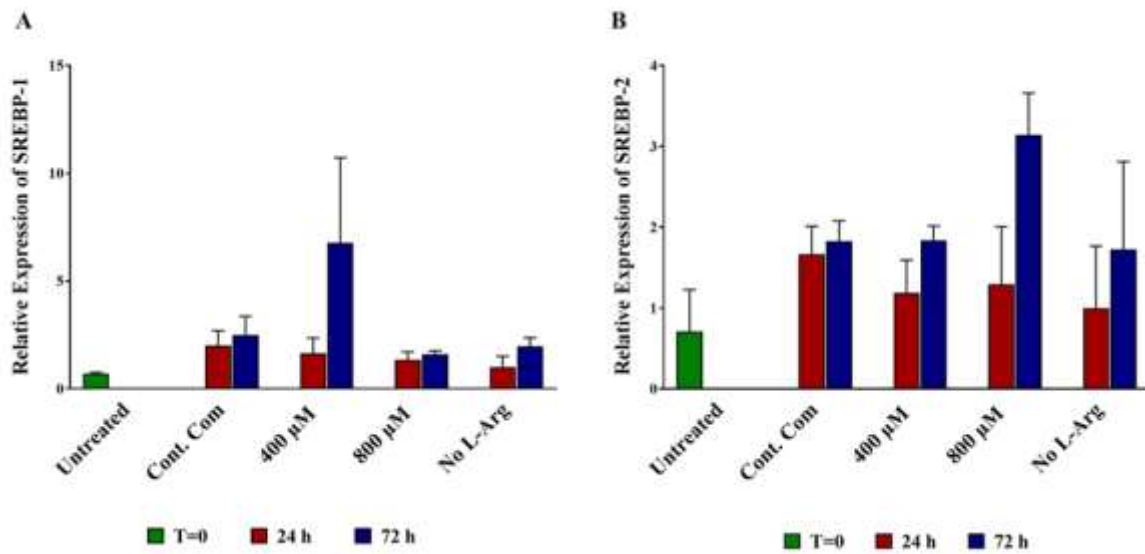


Figure 2.3.4. Relative mRNA expression of CPT-1 and HMGCR in BNL CL2 cells cultured in different concentrations of L-arginine and the control.

Relative mRNA transcript expression ($\Delta\Delta Ct$) of CPT-1 (A) and HMGCR (B) in BNL CL2 cells cultured in medium of different L-arginine concentrations (0, 400 and 800 μM) and control complete DMEM media 24 and 72 h after addition. Untreated cultures at T=0. Data points represent the mean \pm SD of each sample. Error bars represent the standard deviation from the mean (n = 3). Tables summarise two-way ANOVA followed by a Tukey multiple comparison test using GraphPad Prism 9.4.1. The indicate the levels of significance; ns = P > 0.05, * = P \leq 0.05, ** = P \leq 0.01, *** = P \leq 0.001 and **** = P \leq 0.0001.



Source of Variation	SREBP-1		SREBP-2	
	P value	Significant?	P value	Significant?
Interaction	***	Yes	***	Yes
Time point	****	Yes	****	Yes
L-Arg +/- and control (Com)	***	Yes	***	Yes

Tukey's multiple comparisons test	SREBP-1			SREBP-2		
	T=0	24 h	72 h	T=0	24 h	72 h
Untreated vs. Cont. Com	ns	ns	ns	ns	**	***
Untreated vs. 400 µM	ns	ns	****	ns	*	***
Untreated vs. 800 µM	ns	ns	ns	ns	*	****
Untreated vs. No L-Arg	ns	ns	ns	ns	ns	***
Cont. Com vs. 400 µM	ns	ns	***	ns	ns	ns
Cont. Com vs. 800 µM	ns	ns	ns	ns	ns	*
Cont. Com vs. No L-Arg	ns	ns	ns	ns	ns	ns
400 µM vs. 800 µM	ns	ns	****	ns	ns	*
400 µM vs. No L-Arg	ns	ns	****	ns	ns	ns
800 µM vs. No L-Arg	ns	ns	ns	ns	ns	**

Figure 2.3.5. Relative mRNA expression of SREBP-1 and SREBP-2 in BNL CL2 cells cultured in different concentrations of L-arginine and the control.

Relative mRNA transcript expression ($\Delta\Delta\text{Ct}$) of SREBP-1 (A) and SREBP-2 (B) in BNL CL2 cells cultured in medium of different L-arginine concentrations (0, 400 and 800 μM) and control complete DMEM media 24 and 72 h after addition. Untreated samples at T=0. Data points represent the mean \pm SD of each sample. Error bars represent the standard deviation from the mean (n = 3). Tables summarise two-way ANOVA followed by a Tukey multiple comparison test using GraphPad Prism 9.4.1. The stars indicate the levels of significance; ns = $P > 0.05$, * = $P \leq 0.05$, ** = $P \leq 0.01$, *** = $P \leq 0.001$ and **** = $P \leq 0.0001$.

2.3.3. Monitoring protein and post-translational phosphorylation expression in response to L-Arg supplementation

Western blotting for all target proteins was undertaken in protein samples of BNL CL2 cells in three biological replicates as described in sections 2.2.1.3 and 2.2.3. The samples were L-arginine test concentrations (0, 400 and 800 μ M) and the controls complete DMEM media addition at 24 and 72 h timepoints and untreated samples at T=0. Two combinations of gels were used to allow (a) comparison within a concentration with changing culture time (Figs 2.3.6-2.3.12) and (b) comparison across concentrations at a specific culture time point (Figs 2.3.13-2.3.20). Target protein expression was normalized to β -actin protein to obtain relative differences between target and β -actin proteins. All data was normalized to the value of no L-Arg added samples (0 μ M L-arginine) at 24 h culture time point to obtain the final relative-normalised data, this was denoted as RE in the following sections.

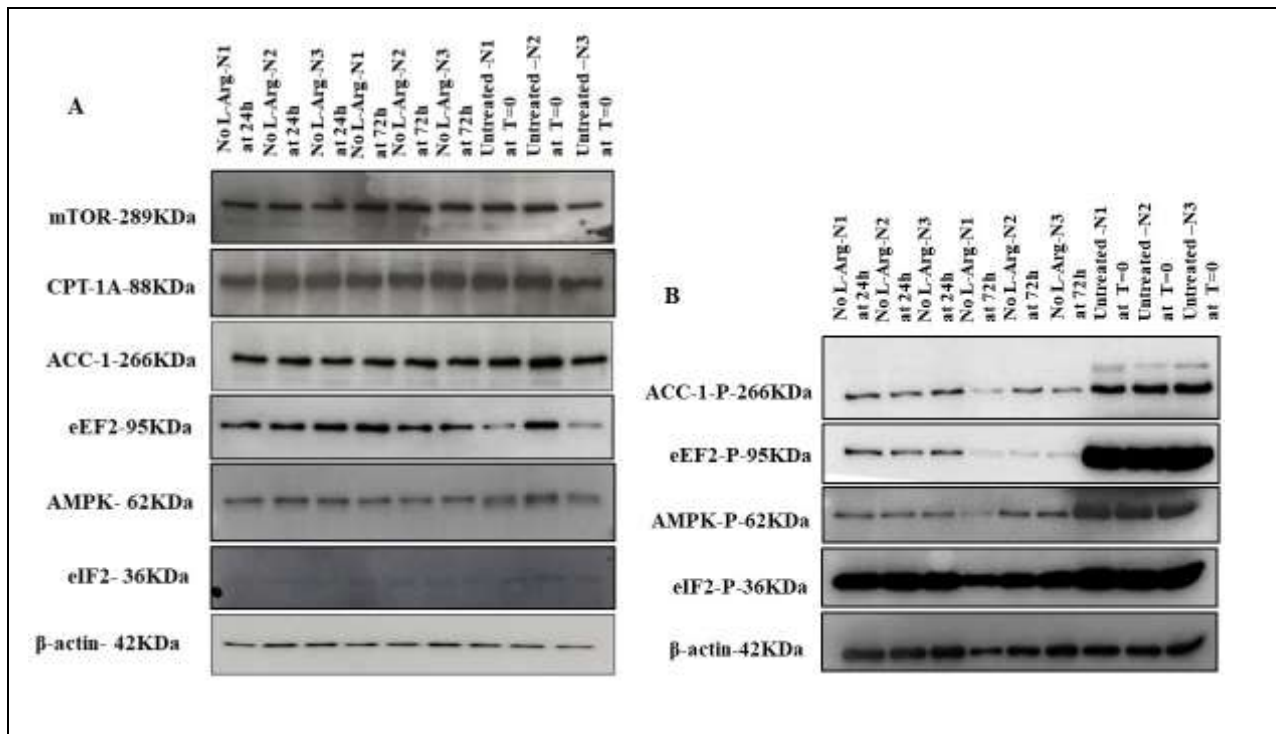


Figure 2.3.6. Western blot comparison for target proteins and phosphorylated proteins expression in BNL CL2 cells cultured at 0 μ M L-Arg concentration for 24 and 72 h and untreated at T=0.

Western blot comparison of (A) the expression of key proteins involved in L-arginine/NO metabolic pathway signalling, and (B) the amount of phospho-protein of key targets in cultured BNL CL2 cells cultured in no L-arginine SILAC DMEM media for 24 and 72 h and in one of the control, untreated culture samples at T=0. β -actin is used as a loading control. The same amount of protein (10 μ g) from different treatment groups was loaded from biological triplicate cultures into 10% SDS-polyacrylamide gels for the separation of target proteins.

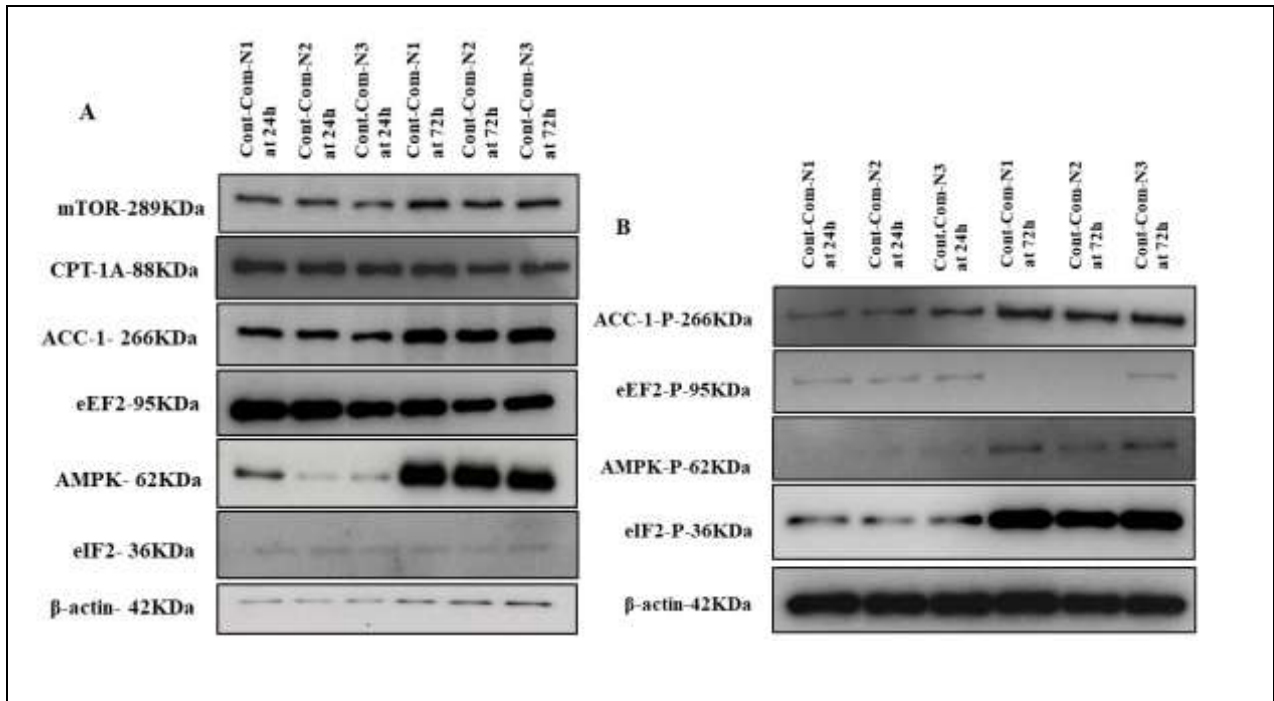


Figure 2.3.7. Western blot comparison for target proteins and phosphorylated proteins expression in BNL CL2 cells cultured at the control complete DMEM for 24 and 72 h.

Western blot comparison of (A) the expression of key proteins involved in L-arginine/NO metabolic pathway signalling, and (B) the amount of phosphor-protein of key targets in cultured BNL CL2 cells cultured in control complete DMEM media for 24 and 72 h. β-actin is used as a loading control. The same amount of protein (10 μg) from different treatment groups was loaded from biological triplicate cultures into 10% SDS–polyacrylamide gels for the separation of target proteins.

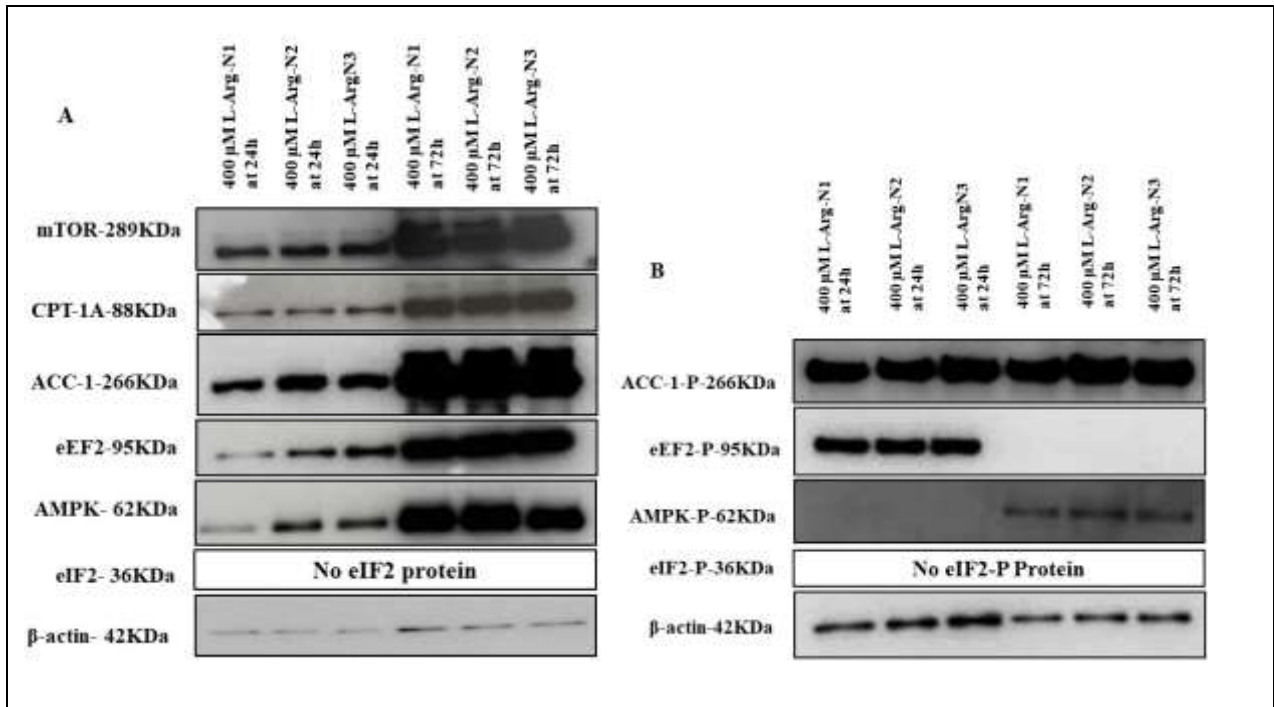


Figure 2.3.8. Western blot comparison for target proteins and phosphorylated proteins expression in BNL CL2 cells cultured at 400 μM L-Arg concentration for 24 and 72 h.

Western blot comparison of (A) the expression of key proteins involved in L-arginine/NO metabolic pathway signalling, and (B) the amount of phospho-protein of key targets in cultured BNL CL2 cells cultured in 400 μM L-arginine in L-arginine free SILAC DMEM media for 24 and 72 h. β-actin is used as a loading control. The same amount of protein (10 μg) from different treatment groups was loaded from biological triplicate cultures into 10% SDS-polyacrylamide gels for the separation of target proteins. No eIF2 protein means, eIF2 protein was not detected in the prepared protein samples.

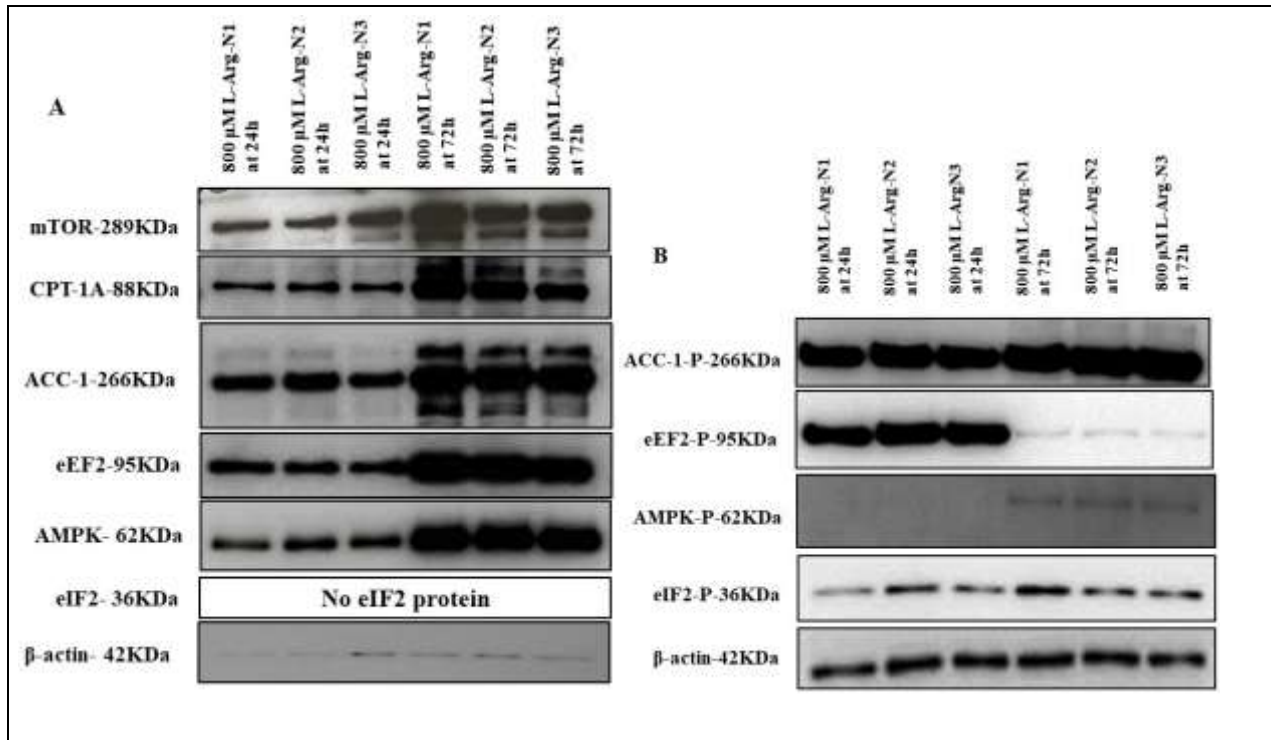


Figure 2.3.9. Western blot comparison for target proteins and phosphorylated proteins expression in BNL CL2 cells cultured at 800 μ M L-Arg concentration for 24 and 72 h.

Western blot comparison of (A) the expression of key proteins involved in L-arginine/NO metabolic pathway signalling, and (B) the amount of phospho-protein of key targets in cultured BNL CL2 cells cultured in 800 μ M L-arginine in L-arginine free SILAC DMEM media for 24 and 72 h. β -actin is used as a loading control. The same amount of protein (10 μ g) from different treatment groups was loaded from biological triplicate cultures into 10% SDS–polyacrylamide gels for the separation of target proteins. No eIF2 protein means, eIF2 protein was not detected in the prepared protein samples.

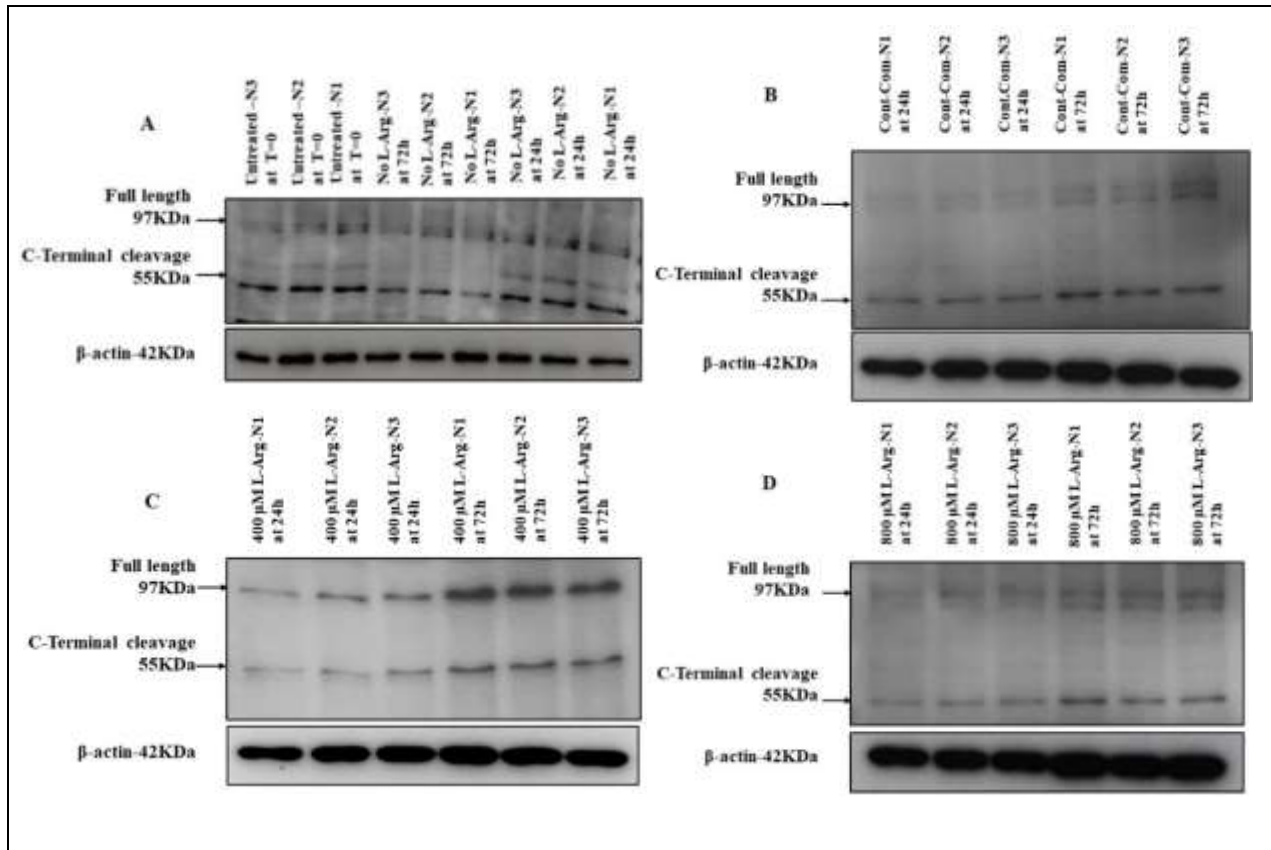


Figure 2.3.10. Western blot comparison for HMGCR expression in BNL CL2 cells cultured at 0, 400 and 800 μM L-Arg concentration and the control for 24 and 72 h and untreated at T=0.

Western blot comparison of lipogenic protein levels of HMGCR precursor form (upper band) and HMGCR mature form (lower band) in BNL CL2 cells cultured in customized media containing (A) no L-arginine SILAC DMEM and untreated cell samples at T=0, (B) complete DMEM, (C) 400 μM L-arginine, and (D) 800 μM L-arginine for 24 and 72 h. β-actin is used as a loading control. The same amount of protein (20 μg) from different treatment groups was loaded from biological triplicate cultures into 10% SDS-polyacrylamide gels for the separation of target proteins.

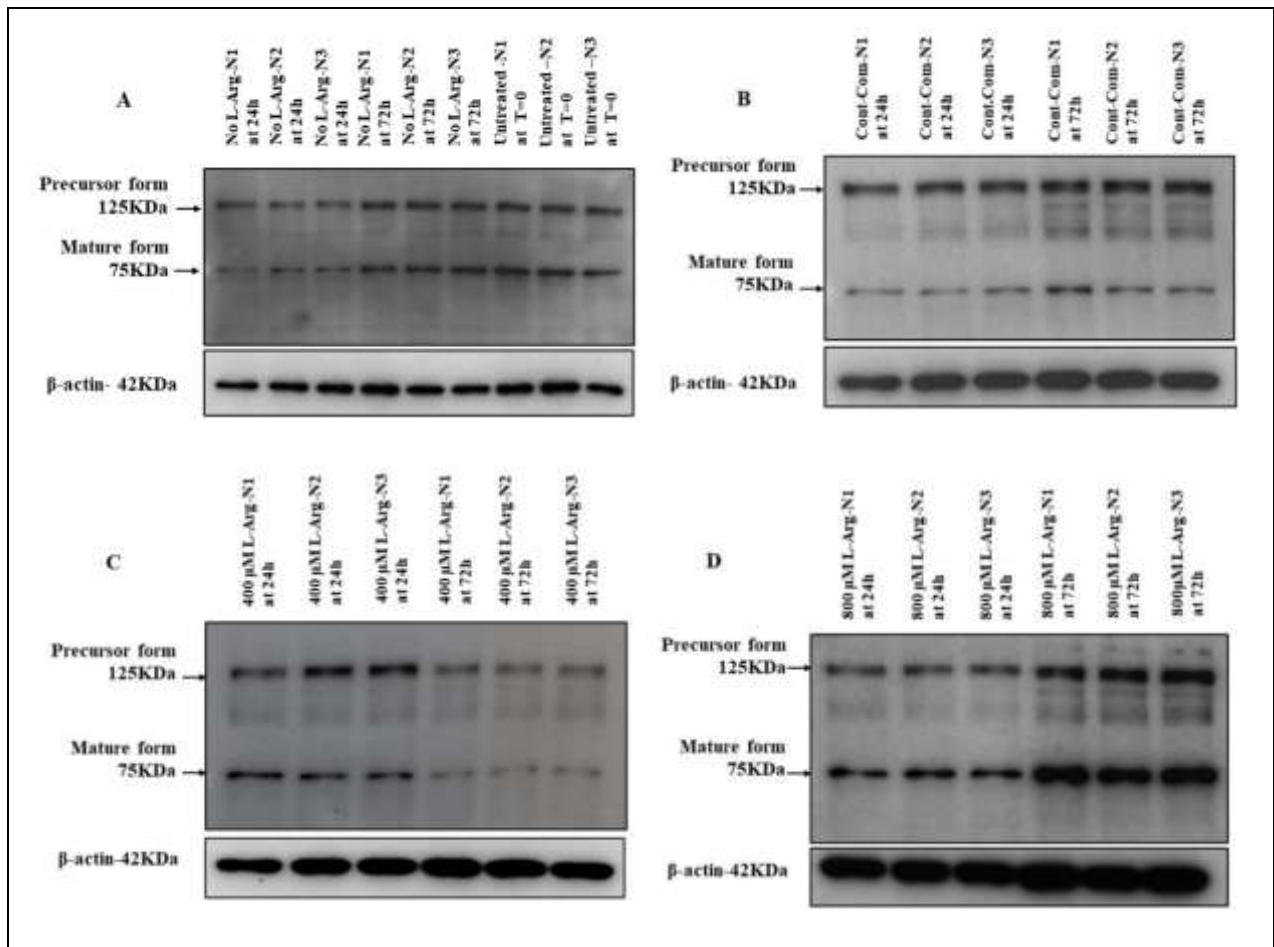


Figure 2.3.11. Western blot comparison for SREBP-1 expression in BNL CL2 cells cultured at 0, 400 and 800 μ M L-Arg concentration and the control for 24 and 72 h and untreated at T=0.

Western blot comparison of lipogenic protein levels of SREBP-1 precursor form (upper band) and SREBP-1 mature form (lower band) in BNL CL2 cells cultured in customized media containing (A) no L-arginine SILAC DMEM and untreated cell samples at T=0, (B) complete DMEM, (C) 400 μ M L-arginine, and (D) 800 μ M L-arginine for 24 and 72 h. β -actin is used as a loading control. The same amount of protein (20 μ g) from different treatment groups was loaded from biological triplicate cultures into 10% SDS-polyacrylamide gels for the separation of target proteins.

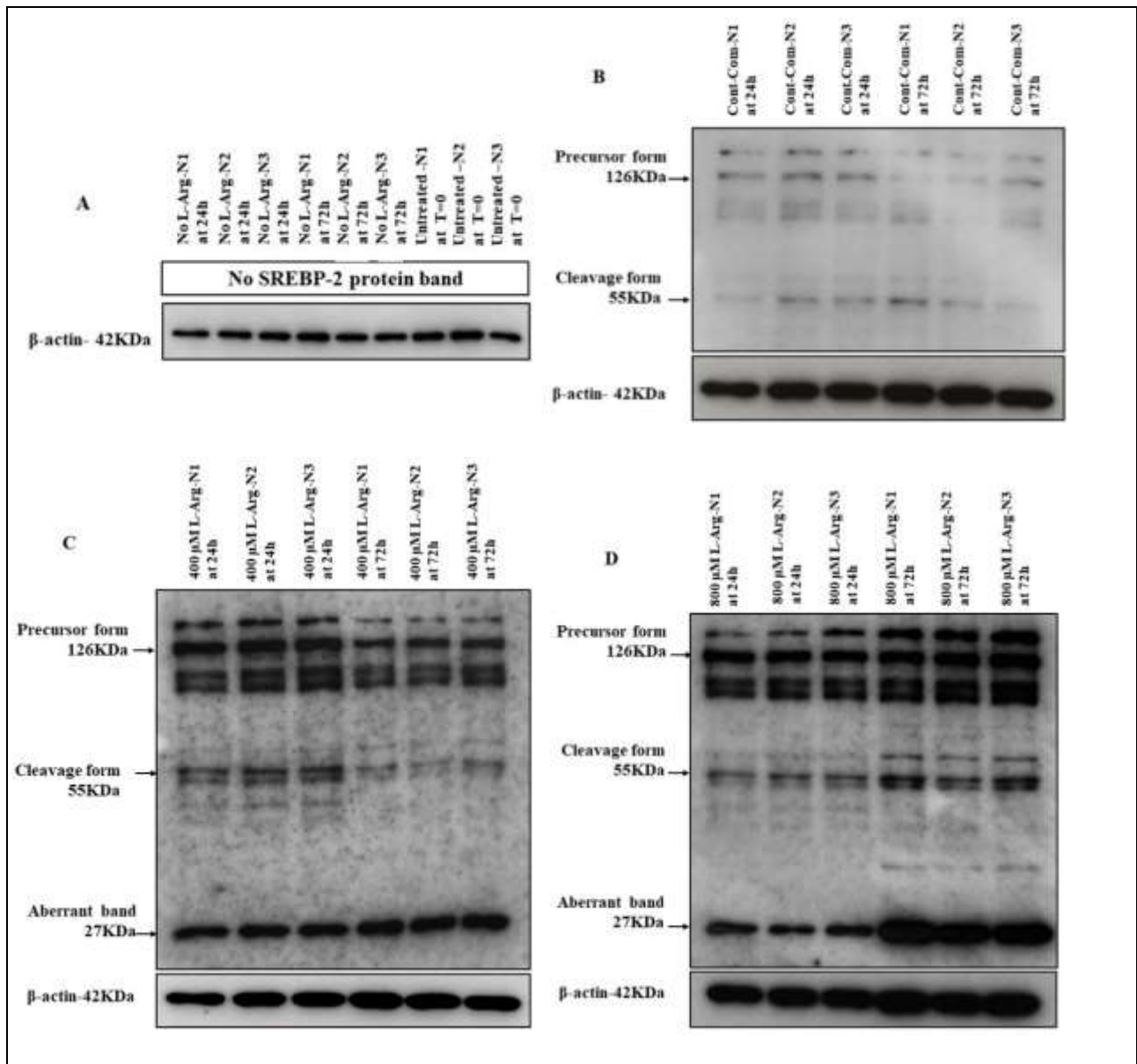


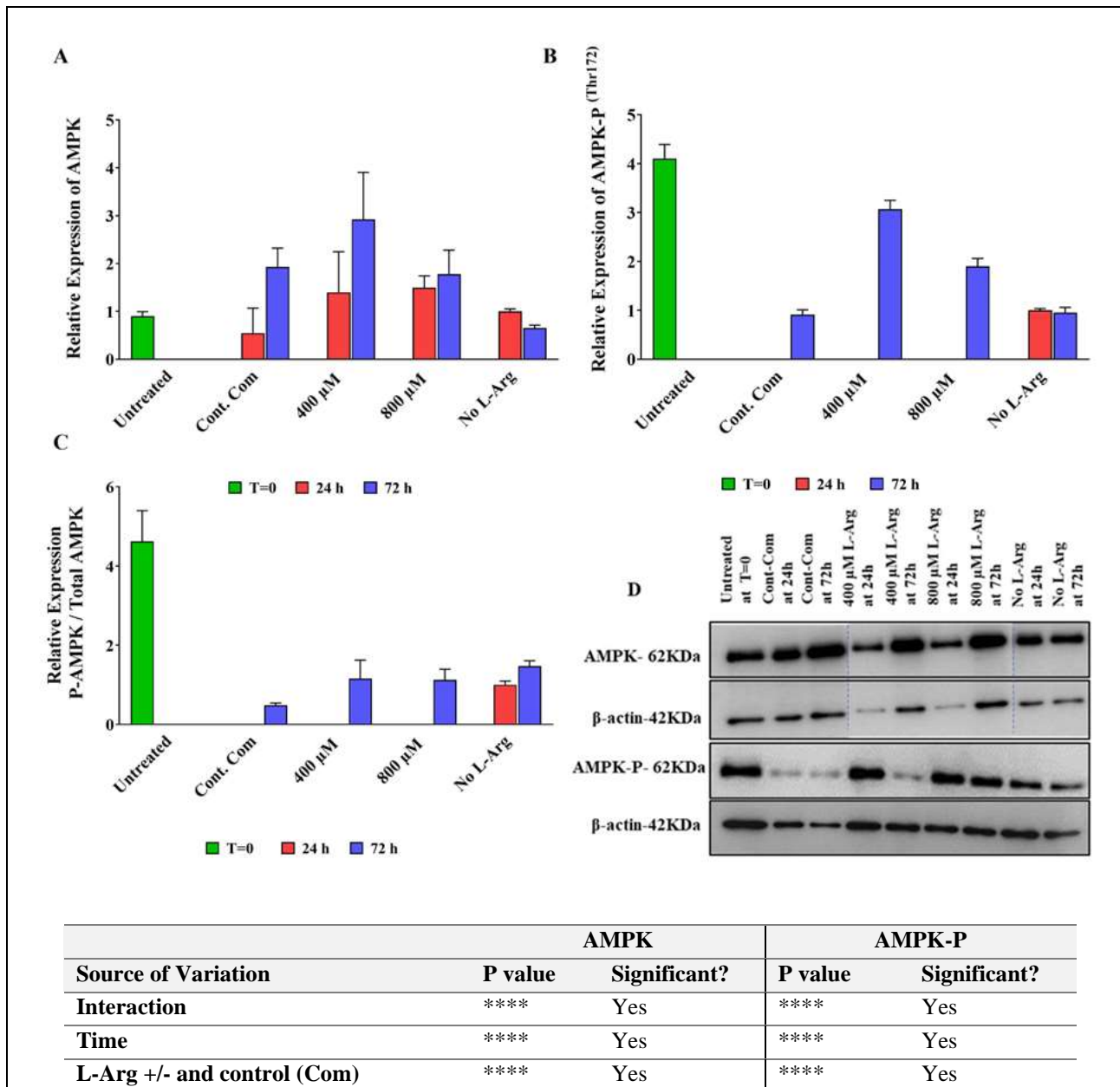
Figure 2.3.12. Western blot comparison for SREBP-2 expression in BNL CL2 cells cultured at 0, 400 and 800 μ M L-Arg concentration and the control for 24 and 72 h and untreated at T=0.

Western blot comparison of lipogenic protein levels of SREBP-2 precursor form (upper band) and SREBP-2 mature form (lower band) in BNL CL2 cells cultured in customized media containing (A) no L-arginine SILAC DMEM and untreated cell samples at T=0, (B) complete DMEM, (C) 400 μ M L-arginine, and (D) 800 μ M L-arginine for 24 and 72 h. β -actin is used as a loading control. The same amount of protein (20 μ g) from different treatment groups was loaded from biological triplicate cultures into 10% SDS–polyacrylamide gels for separation of target proteins. The aberrant band (27KDa) appears in the blots may be cleavage products of SREBP-2 during post-translational modification.

A comparison across L-arginine concentrations with culture time of total and phosphorylated levels of AMPK in BNL CL2 cells is presented in **Fig 2.3.13**. The AMPK protein that plays a role in cellular energy homeostasis showed increased expression ($P < 0.0001$) when cultured in 400 (2.6-fold) and 800 μ M (2.75-fold) L-arginine compared to the control complete media samples at 24 h. AMPK protein expression peaked (1.52-fold) in 400

μM cultured samples at 72 h. AMPK protein expression in no L-arginine media samples at 24 h was decreased ($P < 0.0001$) (0.3-fold).

When phosphorylation of AMPK was investigated, in 400 (0.7-fold) and 800 μM (0.46-fold) L-Arg cultured samples phosphorylation was decreased ($P < 0.0001$) when compared to untreated samples at T=0 (RE 4.1). There were no differences ($P < 0.0001$) in total or phosphorylated AMPK protein in no L-Arg media samples. Increasing L-arginine concentrations from 400 to 800 μM resulted in increased ($P < 0.0001$) phosphorylated AMPK levels at 72 h. A summary of the impact of L-arginine concentration on AMPK protein expression and phosphorylation with culture time is reported in detail in **Figure 2.3.13** below.



Tukey's multiple comparisons test	AMPK			AMPK-P		
	T=0	24 h	72 h	T=0	24 h	72 h
Untreated vs. Cont. Com	ns	ns	****	****	ns	****
Untreated vs. 400 μ M	ns	**	****	****	ns	****
Untreated vs. 800 μ M	ns	***	****	****	ns	****
Untreated vs. No L-Arg	ns	*	ns	****	****	****
Cont. Com vs. 400 μ M	ns	ns	*	ns	ns	****
Cont. Com vs. 800 μ M	ns	ns	ns	ns	ns	****
Cont. Com vs. No L-Arg	ns	ns	**	ns	****	ns
400 μ M vs. 800 μ M	ns	ns	*	ns	ns	****
400 μ M vs. No L-Arg	ns	ns	****	ns	****	****
800 μ M vs. No L-Arg	ns	ns	*	ns	****	****

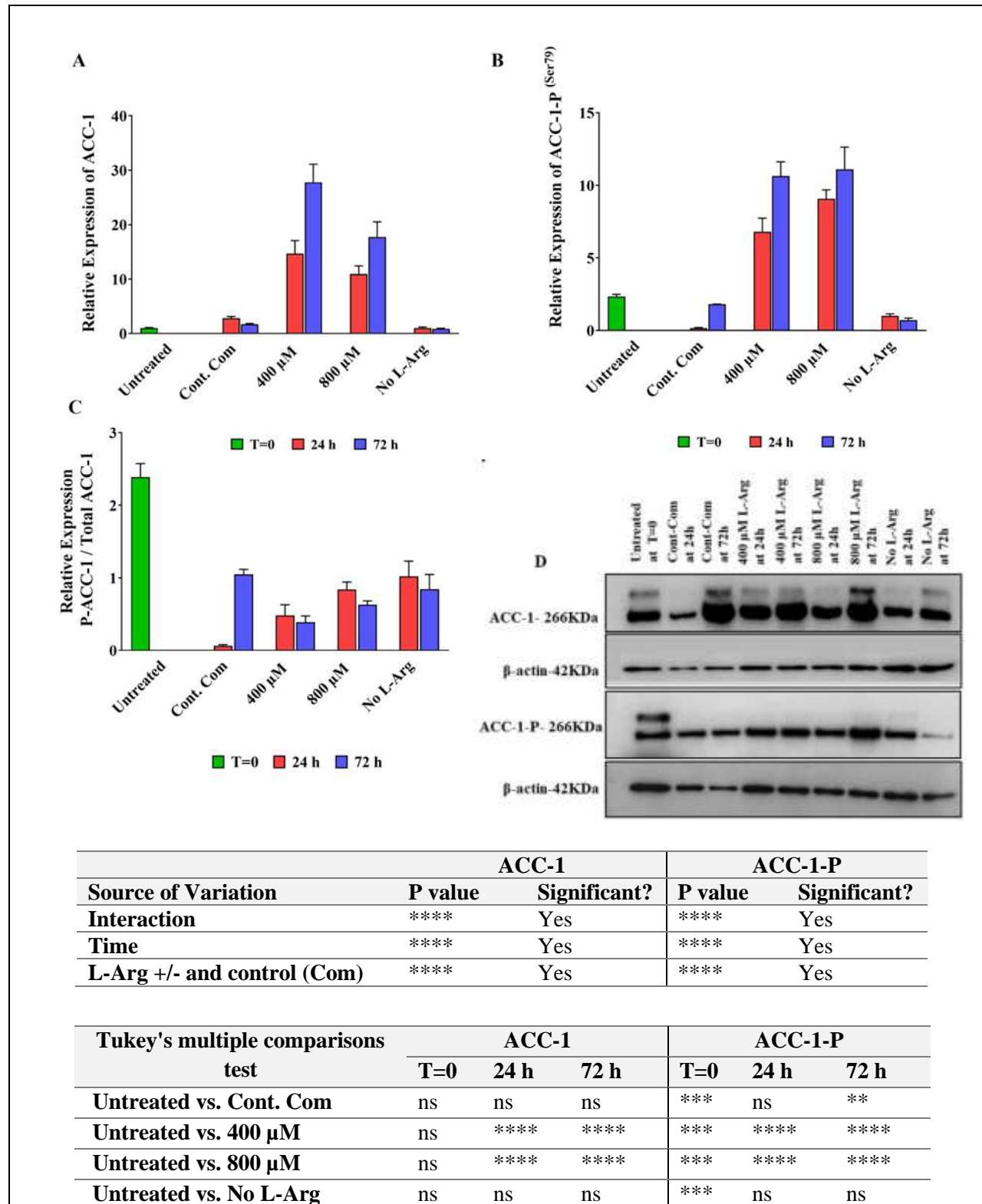
Figure 2.3.13. Relative protein expression and a western blot across concentration with time for AMPK α protein and AMPK α -P in BNL CL2 cells.

Relative protein amounts for total AMPK α (A), phosphorylated AMPK α at Thr172 (AMPK α -P) (B) and the ratio of AMPK α -P to total AMPK α in BNL CL2 cells (C). An example blot image of AMPK α and AMPK α -P across concentrations with culture time is shown in (D). Cells were cultured for 24 or 72 h in customized media containing 0, 400 and 800 μ M L-arginine. Controls were addition of complete DMEM or untreated cultures at T=0. The same amount of total protein (10 μ g) from different culture conditions was loaded into 10% SDS–polyacrylamide gels for the separation of AMPK α and phosphorylated AMPK α proteins and two representative blots from each treatment group are shown with the respective to the house-keeping-protein, β -actin (D). Bands in the blots were quantified using ImageJ software and the data are normalised to β -actin and then expressed as relative to the no L-arginine SILAC DMEM (0 μ M L-arginine) control at 24 h. Data points represent the mean \pm SD. Error bars represent the standard deviation from the mean (n = 3). The tables summarise two-way ANOVA followed by a Tukey multiple comparison test using GraphPad Prism 9.4.1. The stars indicate the levels of significance; ns = P > 0.05, * = P \leq 0.05, ** = P \leq 0.01, *** = P \leq 0.001 and **** = P \leq 0.0001.

Total and phosphorylated levels of ACC-1 protein in BNL CL2 cells under different L-arginine culture conditions are presented in **Fig 2.3.14**. The expression of this regulator of fatty acid metabolism, ACC-1, increased (P<0.0001) in both total ACC-1 protein and phosphorylated ACC-1 in cells cultured in L-arginine at 400 and 800 μ M. Total ACC-1 protein was increased in 400 (5-fold) and 800 μ M (4-fold) L-arginine cultures (P<0.0001) compared to the control complete DMEM addition cultures at 24 h. After 72 h of culture time the increase in expression was further elevated in 400 and 800 μ M L-arginine cultures (P<0.0001) with total ACC-1 amounts increased by 16-fold and 10-fold, respectively, in comparison with control complete DMEM cultures. Total ACC-1 protein was decreased (P<0.0001) in the untreated sample at T=0 (RE-0.98) and no L-Arg added samples had the lowest relative expression of ACC-1 at 72 h (RE 0.8) among all samples.

When phosphorylation of ACC-1 was investigated, this was much higher (P<0.0001) in 400 (39-fold) and 800 μ M (52.5-fold) L-arginine cultured cells at 24 h compared to the control complete media cultures, although the increase was less at 72 h (6-fold) in both 400 and 800 μ M samples in comparison with the control. As a result, the ratio of phosphorylated ACC-1 to total ACC-1 was massively increased (P<0.0001) at 24 h after addition

of the L-arginine (Fig 2.3.14B and C). A summary of the impact of L-arginine concentration on ACC-1 protein expression and phosphorylation with culture time is reported in detail in Figure 2.3.14 below.



Cont. Com vs. 400 μM	ns	****	****	ns	****	****
Cont. Com vs. 800 μM	ns	****	****	ns	****	****
Cont. Com vs. No L-Arg	ns	ns	ns	ns	ns	ns
400 μM vs. 800 μM	ns	*	****	ns	***	ns
400 μM vs. No L-Arg	ns	****	****	ns	****	****
800 μM vs. No L-Arg	ns	****	****	ns	****	****

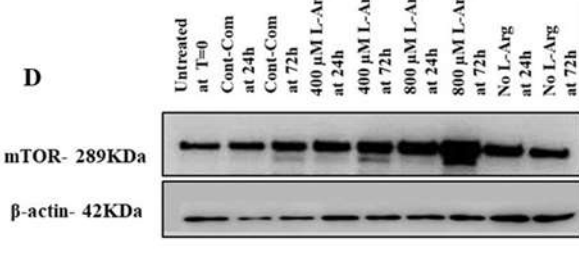
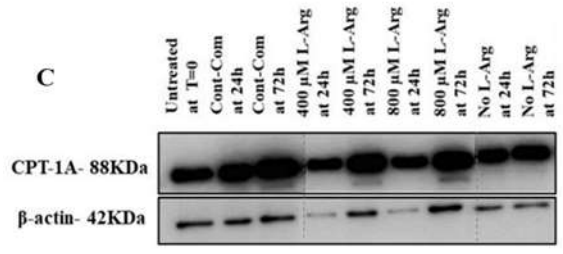
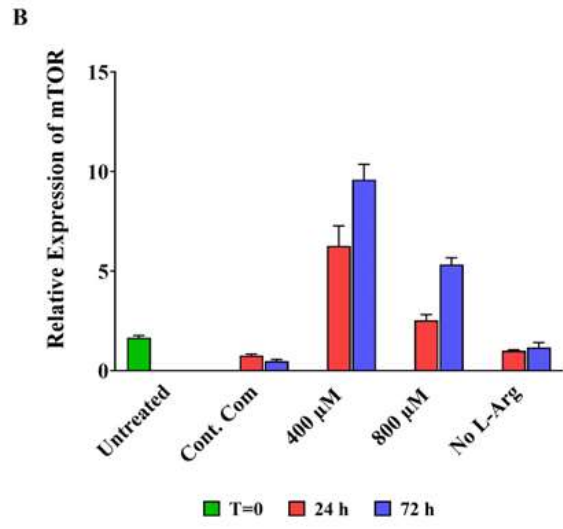
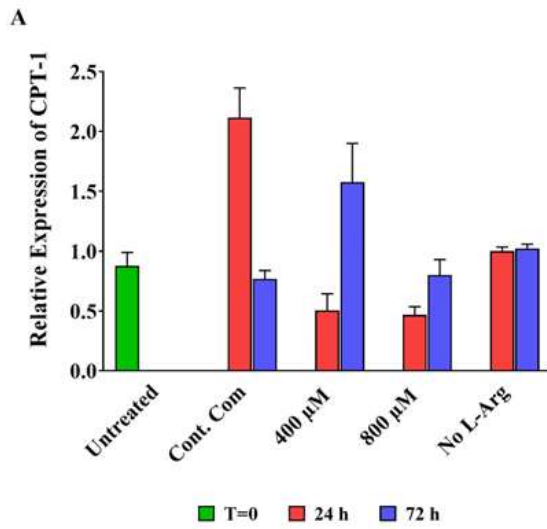
Figure 2.3.14. Relative protein expression and a western blot across concentration with time for ACC-1 protein and ACC-1-P in BNL CL2 cells.

Relative protein amounts for total ACC-1 (A), phosphorylated ACC-1 at Ser79 (AMPK α -P) (B), and the ratio of ACC-1-P to total ACC-1 in BNL CL2 cells (C). An example blot image of ACC-1 and ACC-1-P across concentrations with time is shown in (D). Cells were cultured for 24 or 72 h in customized media containing 0, 400 and 800 μ M L-arginine. Controls were addition of complete DMEM or untreated samples at T=0. The same amount of total protein (10 μ g) from different culture conditions was loaded into 10% SDS–polyacrylamide gels for the separation of ACC-1 and phosphorylated ACC-1 proteins and two representative blots from each treatment group are shown with the respective to the house-keeping protein, β -actin (D). Bands in the blots were quantified by using ImageJ software and the data are normalised to β -actin and then expressed as relative to the no L-arginine SILAC DMEM (0 μ M L-arginine) control at 24 h time point. Data points represent the mean \pm SD. Error bars represent the standard deviation from the mean (n = 3). The tables summarise two-way ANOVA followed by a Tukey multiple comparison test using GraphPad Prism 9.4.1. The stars indicate the levels of significance; ns = P > 0.05, * = P \leq 0.05, ** = P \leq 0.01, *** = P \leq 0.001 and **** = P \leq 0.0001.

Analysis of carnitine palmitoyl transferase I (CPT-1) protein was also undertaken and is reported in **Fig 2.3.15A**. CPT-1 has an important role in fatty acid metabolism that makes this protein important in many metabolic disorders (Schreurs, Kuipers and Van Der Leij, 2010). Cultures with 400 and 800 μ M L-arginine had decreased amount (0.2-fold) (P<0.0001) CPT-1A expression at 24 h compared with the control complete DMEM addition cultures. However, at 72 h cultures grown in 400 μ M L-arginine had increased (P<0.0001) levels of CPT-1A protein (2-fold) in comparison to the control. CPT-1A protein expression in complete media addition cultures at 24 h were increased (RE 2.11, P<0.0001) compared to the untreated at T=0 (RE 0.9). A summary of the impact of L-arginine concentration on CPT-1A protein expression with culture time is reported in detail in **Figure 2.3.15** below.

Analysis of the expression of the mammalian target of rapamycin (mTOR) protein, which is considered a master regulator in the cell as it regulates multiple different cellular processes (Saxton and Sabatini, 2017), with changing L-arginine culture concentrations is shown in **Fig 2.3.15B**. L-arginine at 400 (8.2-fold) and 800 μ M (3.3-fold) increased (P<0.0001) mTOR protein expression at 24 h, and the levels progressively increased (P<0.0001) in 400 (19.7-fold) and 800 μ M (10.9-fold) with culture time at 72 h compared to the control complete DMEM addition cultures. Relative expression of mTOR protein in complete DMEM addition at 24 h (RE 0.76) was decreased (P<0.0001) compared to the untreated sample at T=0 (RE 1.66). There was no change (P<0.0001) in mTOR protein expression (RE 1.0) in no L-arginine cultures at 24 and 72 h time points

compared to the control. A summary of the impact of L-arginine concentration on mTOR protein expression with culture time is reported in detail in **Figure 2.3.15** below.



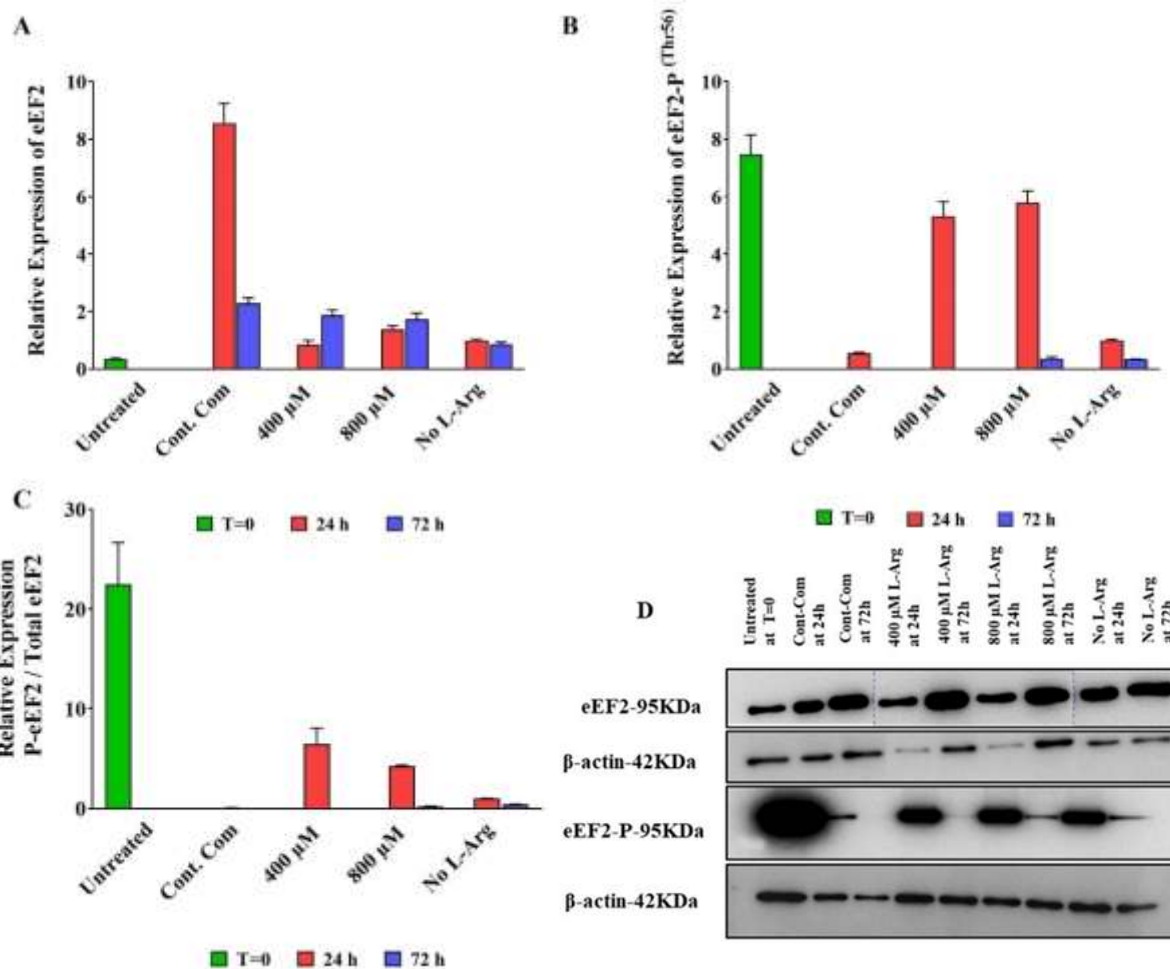
Source of Variation	CPT-1		mTOR	
	P value	Significant?	P value	Significant?
Interaction	****	Yes	****	Yes
Time	****	Yes	****	Yes
L-Arg +/- and Control (Com)	****	Yes	****	Yes

Tukey's multiple comparisons test	CPT-1			mTOR		
	T=0	24 h	72 h	T=0	24 h	72 h
Untreated vs. Cont. Com	****	****	****	****	ns	Ns
Untreated vs. 400 µM	****	***	****	****	****	****
Untreated vs. 800 µM	****	***	****	****	****	****
Untreated vs. No L-Arg	****	****	****	****	*	**
Cont. Com vs. 400 µM	ns	****	****	ns	****	****
Cont. Com vs. 800 µM	ns	****	ns	ns	****	****
Cont. Com vs. No L-Arg	ns	****	ns	ns	ns	ns
400 µM vs. 800 µM	ns	ns	****	ns	****	****
400 µM vs. No L-Arg	ns	***	****	ns	****	****
800 µM vs. No L-Arg	ns	****	ns	ns	****	****

Figure 2.3.15. Relative protein expression and western blots across concentration with time for CPT-1 protein and mTOR in BNL CL2 cells.

Relative protein amounts for CPT-1 (A) and mTOR (B) in BNL CL2 cells and representative blot images for CPT-1 (C) and mTOR (D) across L-arginine concentrations with culture time. Cells were cultured for 24 or 72 h in customized media containing 0, 400 and 800 μ M L-arginine. Controls were addition of complete DMEM or untreated cultures at T=0. The same amount of total protein (10 μ g) from different culture conditions was loaded into 10% SDS-polyacrylamide gels for the separation of CPT-1 and mTOR proteins and two representative blots from each treatment group are shown with the house-keeping protein, β -actin (C and D). Bands on blots were quantified by using ImageJ software and the data are normalised to the house-keeping protein, β -actin and then expressed relative to the no L-arginine SILAC DMEM (0 μ M L-arginine) cultures at 24 h. Data points represent the mean \pm SD. Error bars represent the standard deviation from the mean (n = 3). The tables summarise two-way ANOVA followed by a Tukey multiple comparison test using GraphPad Prism 9.4.1. The stars indicate the levels of significance; ns = P > 0.05, * = P \leq 0.05, ** = P \leq 0.01, *** = P \leq 0.001 and **** = P \leq 0.0001.

Western blot analysis of the eukaryotic elongation factor 2 (eEF2) protein, an essential factor for protein synthesis, and its phosphorylated levels, was also undertaken and is shown in **Fig 2.3.16**. Phosphorylation results in reduced activity of eEF2 and slowed protein synthesis. Increasing extracellular concentrations of L-arginine from 400 to 800 μ M had an effect on total eEF2 levels in BNL CL2 cells. Total eEF2 protein expression was decreased (P<0.0001) in cells cultured in L-arginine at 400 and 800 μ M at 24 h (0.1-fold and 0.2-fold, respectively) and 72 h (0.8-fold and 0.75-fold, respectively), in comparison with the control complete DMEM cultures at the same time points. On-the-other-hand, eEF2 phosphorylation progressively increased (P<0.0001) when cells were cultured in in 400 and 800 μ M L-arginine (by 9.7-fold and 10.6-fold, respectively) at 24 h. As a result, the ratio of phosphorylated eEF2 to total eEF2 increased (P<0.0001) by 100.5-fold and 66-fold, respectively when compared the value of the control (Fig 2.3.16B and C). Whilst there was a large amount of phosphorylated eEF2 present at 24 h, there was no detectable phosphorylated eEF2 protein in 400 and 800 μ M L-arginine cultures, or the control complete DMEM media cultures at 72 h. Total eEF2 protein expression was significantly higher (P<0.0001) in complete DMEM media controls at 24 h (RE 7.55) compared to the untreated cultures at T=0 (0.33), however, the phosphorylated eEF2 protein expression showed the opposite profile (P<0.0001). Relative protein expression of eEF2 did not change (P<0.0001) in the no L-arginine cultures at 72 h (RE around 1.0) but phosphorylated eEF2 was increased (P<0.0001) at 24 h (RE 1.0) compared to that at 72 h (RE 0.33). A summary of the impact of L-arginine concentration on eEF2 protein expression and phosphorylation with culture time is reported in detail in **Figure 2.3.16** below.



Source of Variation	eEF2		eEF2-P	
	P value	Significant?	P value	Significant?
Interaction	****	Yes	****	Yes
Time	****	Yes	****	Yes
L-Arg +/- and control (Com)	****	Yes	****	Yes

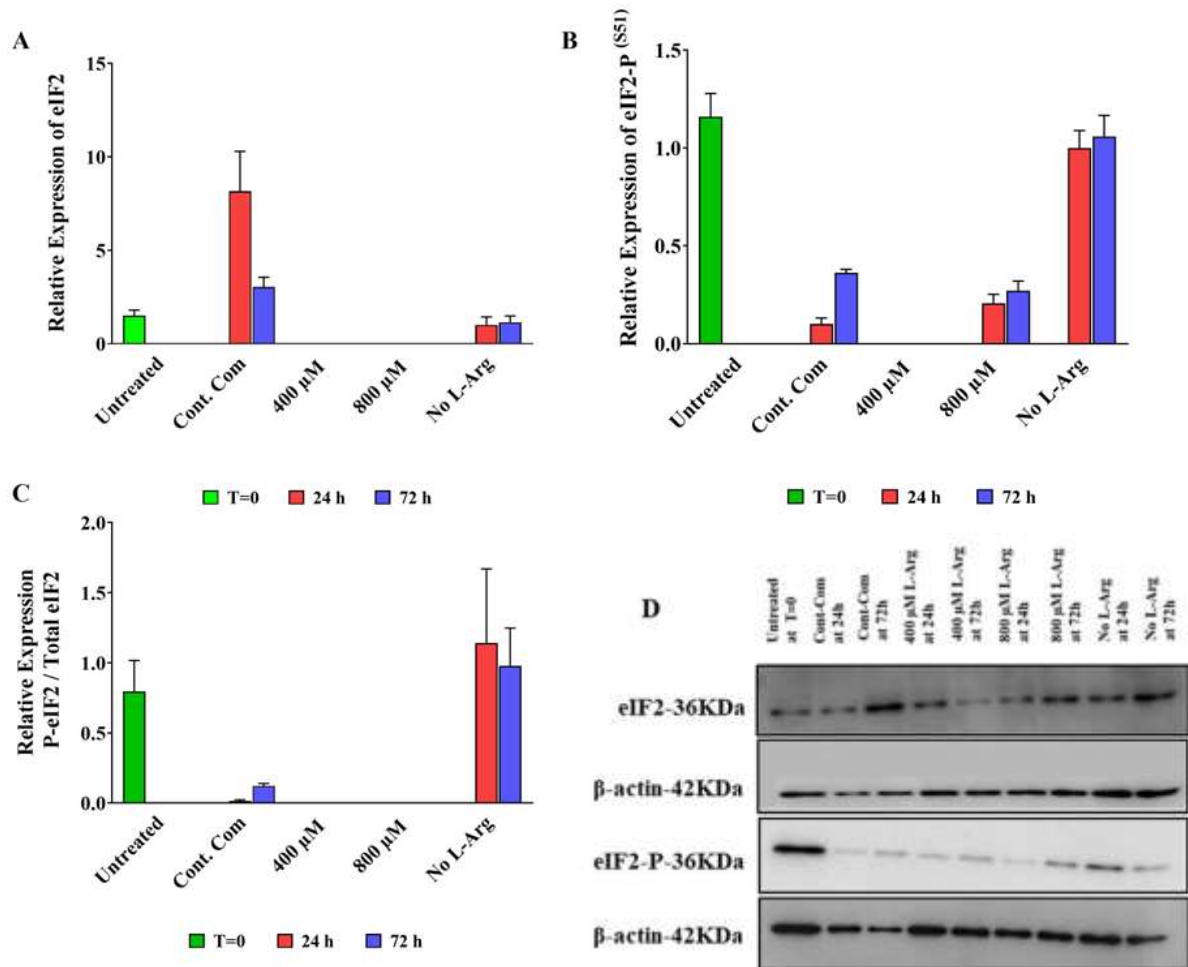
Tukey's multiple comparisons test	eEF2			eEF2-P		
	T=0	24 h	72 h	T=0	24 h	72 h
Untreated vs. Cont. Com	ns	****	****	****	ns	ns
Untreated vs. 400 μ M	ns	***	****	****	****	ns
Untreated vs. 800 μ M	ns	****	****	****	****	ns
Untreated vs. No L-Arg	ns	****	***	****	***	ns
Cont. Com vs. 400 μ M	ns	****	ns	ns	****	ns
Cont. Com vs. 800 μ M	ns	****	*	ns	****	ns
Cont. Com vs. No L-Arg	ns	****	****	ns	ns	ns
400 μ M vs. 800 μ M	ns	*	ns	ns	ns	ns

400 μM vs. No L-Arg	ns	ns	****	ns	****	ns
800 μM vs. No L-Arg	ns	ns	****	ns	****	ns

Figure 2.3.16. Relative protein expression and a western blot across concentration with time for eEF2 protein and eEF2-P in BNL CL2 cells.

Relative protein amounts for total eEF2 (A), phosphorylated eEF2 at Thr56 (eEF2-P) (B) and the ratio of eEF2-P to total eEF2 in BNL CL2 cells (C). A representative blot image of eEF2 and eEF2-P across L-arginine concentrations with culture time is shown (D). Cells were cultured for 24 and 72 h in customized media containing 0, 400 and 800 μ M L-arginine. Controls were addition of complete DMEM and untreated samples at T=0. The same amount of total protein (10 μ g) from different culture conditions was loaded into 10% SDS–polyacrylamide gels for the separation of eEF2 and phosphorylated eEF2 proteins and two representative blots from each treatment group are shown with the respective to the house-keeping protein, β -actin (D). Bands in blots were quantified using ImageJ software and the data are normalised to the house-keeping protein, β -actin and then expressed as relative values to the cells cultured with no L-arginine SILAC DMEM (0 μ M L-arginine) at 24 h. Data points represent the mean \pm SD. Error bars represent the standard deviation from the mean (n = 3). The tables summarise two-way ANOVA followed by a Tukey multiple comparison test using GraphPad Prism 9.4.1. The stars indicate the levels of significance; ns = $P > 0.05$, * = $P \leq 0.05$, ** = $P \leq 0.01$, *** = $P \leq 0.001$ and **** = $P \leq 0.0001$.

As well as monitoring the impact of L-arginine culture concentration on translation elongation factor eEF2, the impact on the translation initiation factor eukaryotic initiation factor 2a (eIF2 α) protein was investigated. eIF2 is required for most forms of eukaryotic translation initiation and its activity is controlled by phosphorylation of the eIF2 α subunit. The expression and phosphorylation of eIF2 α with culture time in different L-arginine concentrations are presented in **Fig 2.3.17**. Increasing extracellular concentrations of L-arginine from 400 to 800 μ M did not affect total eIF2 α but increased ($P < 0.0001$) phosphorylated eIF2 α levels in 800 μ M (2-fold) cultured cells at 24 h in comparison with the control. In contrast, protein expression of total and phosphorylated eIF2 α were increased in 0 μ M L-arginine at 72 h (RE 1.1) and untreated samples at T=0 (RE 1.5). A summary of the impact of L-arginine concentration on eIF2 α protein expression and phosphorylation with culture time is reported in detail in **Figure 2.3.17** below.



Source of Variation	eIF2		eIF2-P	
	P value	Significant?	P value	Significant?
Interaction	****	Yes	****	Yes
Time	****	Yes	ns	No
L-Arg +/- and control (Com)	****	Yes	****	Yes

Tukey's multiple comparisons test	eIF2			eIF2-P		
	T=0	24 h	72 h	T=0	24 h	72 h
Untreated vs. Cont. Com	*	****	****	****	ns	****
Untreated vs. 400 μ M	*	ns	ns	****	ns	ns
Untreated vs. 800 μ M	*	ns	ns	****	***	****
Untreated vs. No L-Arg	*	ns	ns	****	****	****
Cont. Com vs. 400 μ M	ns	****	****	ns	ns	****
Cont. Com vs. 800 μ M	ns	****	****	ns	ns	ns
Cont. Com vs. No L-Arg	ns	****	**	ns	****	****
400 μ M vs. 800 μ M	ns	ns	ns	ns	***	****

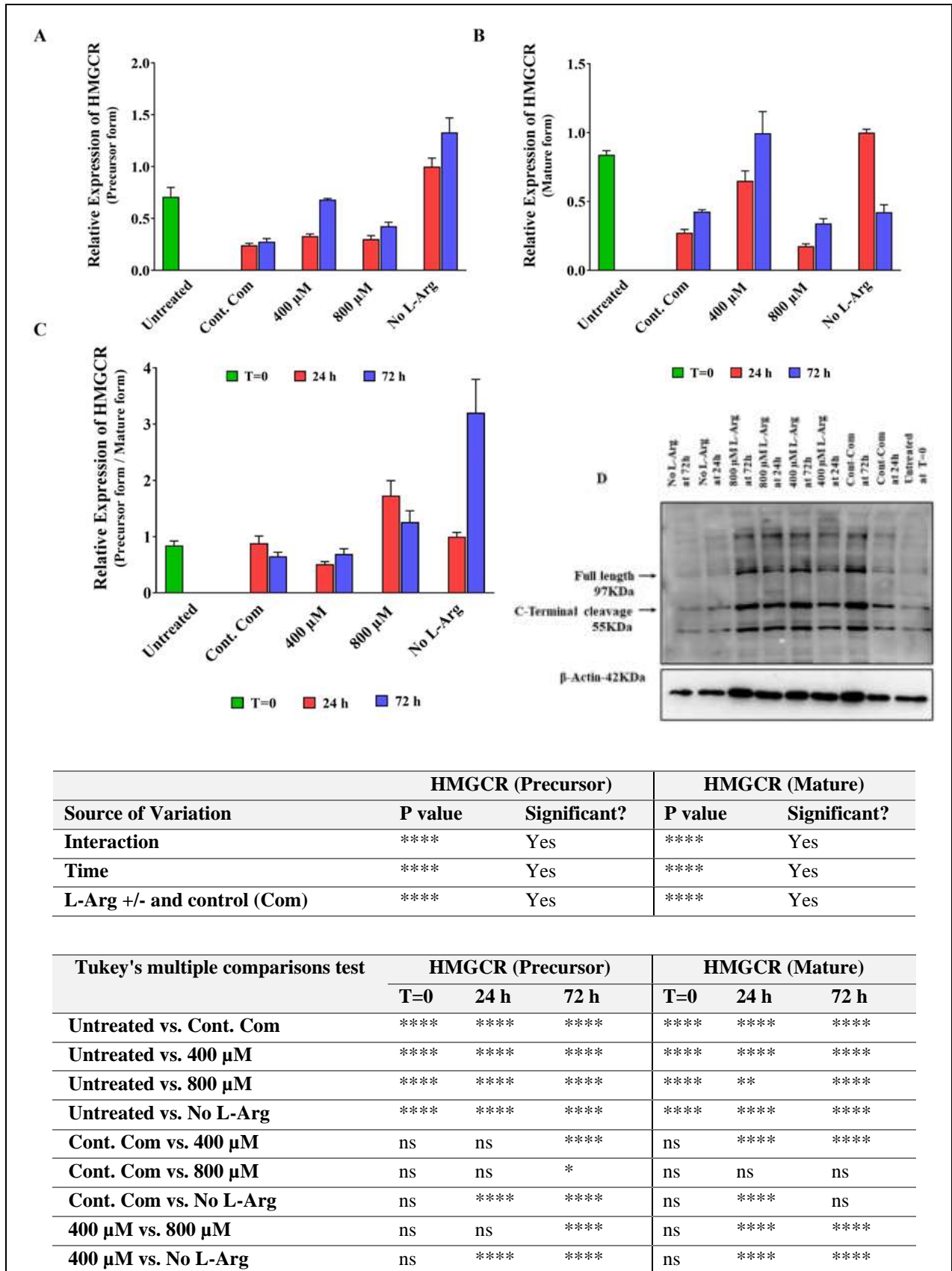
400 μM vs. No L-Arg	ns	ns	ns	ns	****	****
800 μM vs. No L-Arg	ns	ns	ns	ns	****	****

Figure 2.3.17. Relative protein expression and a western blot across concentration with time for eIF α protein and eIF α -P in BNL CL2 cells.

Relative protein amounts for total eIF2 α (A), phosphorylated eIF2 α at S51 (eIF2 α -P) (B) and the ratio of eIF2 α -P to total eIF2 α in BNL CL2 cells (C). A representative blot image of eIF2 α and eIF2 α -P across L-arginine concentrations with culture time is shown (D). Cells were cultured for 24 and 72 h in customized media containing 0, 400 and 800 μ M L-arginine. Controls were addition of complete DMEM and untreated samples at T=0. The same amount of total protein (10 μ g) from different culture conditions was loaded into 10% SDS–polyacrylamide gels for the separation of eIF2 α and phosphorylated eIF2 α proteins and two representative blots from each treatment group are shown with the house-keeping protein, β -actin (D). Bands in the blots were quantified using ImageJ software and the data are normalised to the house-keeping protein, β -actin and then expressed as relative values to cells cultured with no L-arginine SILAC DMEM (0 μ M L-arginine) at 24 h. Data points represent the mean \pm SD. Error bars represent the standard deviation from the mean (n = 3). The tables summarise two-way ANOVA followed by a Tukey multiple comparison test using GraphPad Prism 9.4.1. The stars indicate the levels of significance; ns = P > 0.05, * = P \leq 0.05, ** = P \leq 0.01, *** = P \leq 0.001 and **** = P \leq 0.0001.

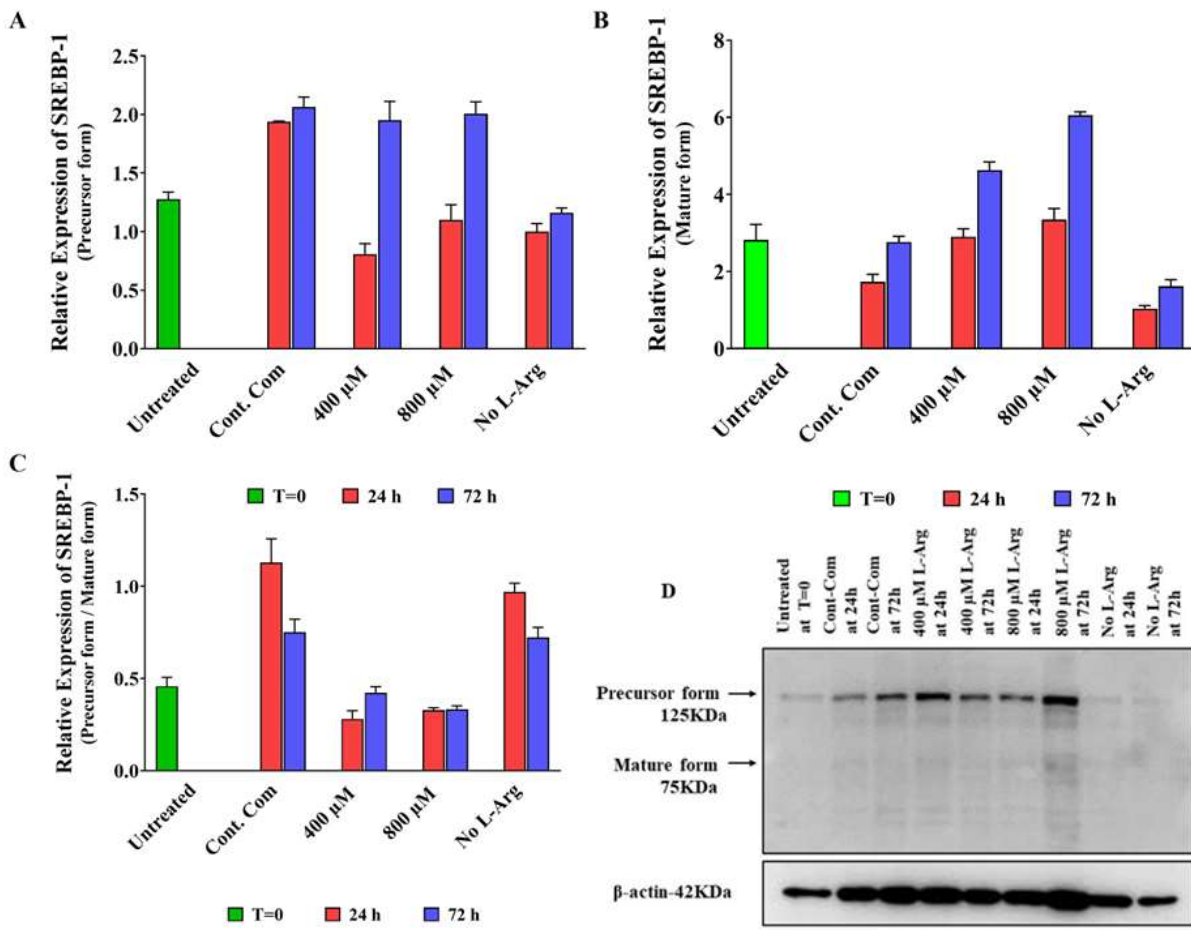
A number of further key protein targets were investigated in the BNL CL2 cells involved in signalling pathways that respond to L-arginine availability. The first of these was HMG-CoA reductase (3-hydroxy-3-methylglutaryl-coenzyme A reductase; HMGCR), the rate-controlling enzyme that regulates biosynthesis of cholesterol. Analysis of the expression of this protein in the cultures with different L-arginine concentrations is shown in **Fig 2.3.18**. The amounts of the N-terminal membrane domain of HMGCR increased (P<0.0001) in 400 (24 h; 1.3-fold and 72 h; 2.4-fold) and 800 μ M (24 h; 1.2-fold and 72 h; 1.5-fold) L-arginine samples when compared to the control complete DMEM addition cultures. In cells cultured in L-arginine at 400 μ M the amount of the C-terminal catalytic domain of HMGCR at 24 h (2.37-fold, P<0.0001) and 72 h (2.34-fold, P<0.0001) was also increased. Interestingly, and perhaps strangely, the amount of the active site located in the long carboxyl terminal domain in the cytosol was decreased (P<0.0001) in the samples from cultures grown in high L-arginine (800 μ M) at 24 (0.64-fold) and 72 h (0.8-fold).

The precursor and mature forms of HMGCR were decreased in amounts (P<0.0001) in complete DMEM cultures at 24 h (RE 0.24) compared to the untreated at T=0 (RE-0.7). The expression of the HMGCR precursor form was increased in no L-arginine cultures at 72 h (RE1.33) but the mature form was decreased at the same time point. The ratio of N-terminal precursor form to catalytically active C-terminal cleavage form was decreased (P<0.0001) in cultures grown in L-arginine at 400 μ M at 24 h. By contrast, the ratio was increased (P<0.0001) in 800 μ M L-arginine cultures at 24 and 72 h in comparison with the control complete DMEM cultures. A summary of the impact of L-arginine concentration on HMGCR protein expression with culture time is reported in detail in **Figure 2.3.18** below.



800 μ M vs. No L-Arg	ns	****	****	ns	****	ns
<p>Figure 2.3.18. Relative protein expression and a western blot across concentration with time for precursor and mature of HMGCR in BNL CL2 cells.</p> <p>Relative hepatic lipogenic protein levels of HMGCR precursor form (upper band) (A), and HMGCR mature form (lower band) (B), and the ratio of N-terminal precursor form to catalytically active C-terminal cleavage form of HMGCR (C) in BNL CL2 cells. A representative blot image of HMGCR across concentrations with time is shown (D). Cells were cultured for 24 and 72 h in customized media containing 0, 400 and 800 μM L-arginine. Controls were addition of control complete DMEM and untreated samples at T=0. The same amount of total proteins (20 μg) from different culture conditions was loaded into 10% SDS–polyacrylamide gels for the separation of HMGCR and a representative blot from each treatment group is shown with the house-keeping protein, β-actin (D). Bands in blots were quantified using ImageJ software and the data are normalised to the house-keeping protein, β-actin and then expressed as relative values to the cells cultured with no L-arginine SILAC DMEM (0 μM L-arginine) at 24 h. Data points represent the mean \pm SD. Error bars represent the standard deviation from the mean (n = 3). The tables summarise two-way ANOVA followed by a Tukey multiple comparison test using GraphPad Prism 9.4.1. The stars indicate the levels of significance; ns = P > 0.05, * = P \leq 0.05, ** = P \leq 0.01, *** = P \leq 0.001 and **** = P \leq 0.0001.</p>						

Additional proteins involved in sterol biosynthesis were also investigated, including SREBP-1 and SREBP-2. Sterol regulatory element-binding proteins (SREBPs) are transcription factors that regulate the synthesis of enzymes involved in sterol biosynthesis and their analysis here is presented in **Fig 2.3.19** and **2.3.20**. When investigating SREBP-1, its catalytically inactive precursor form was decreased in amounts (P<0.0001) in cultures with 400 (0.4-fold) and 800 μ M (0.6-fold) L-arginine when compared to the control DMEM cultures at 24 h. However, expression of the precursor form at 72 h was more or less the same between these samples. When monitoring the catalytically active C-terminal mature form of SREBP-1, expression was increased (P<0.0001) in comparison to the control (1.7-fold) in 400 μ M L-arginine cultures at 24 and 72 h. The amount of the mature form of SREBP-1 increased further (P<0.0001) in cultures grown in the presence of L-arginine at 800 μ M at 24 (1.9-fold) and 72 h (2.2-fold). The precursor form of SREBP-1 was also increased (P<0.0001) in complete DMEM control samples (RE 1.93) compared to the untreated at T=0 (RE 1.3) but the mature form of SREBP-1 was decreased in complete DMEM cultures at 24 h (RE 1.7) compared to the untreated control at T=0 (2.8). The ratio of the catalytically inactive precursor to catalytically active mature form was decreased (P<0.0001) in 400 and 800 μ M L-arginine cultured cells at 24 and 72 h in comparison to the control (meaning there was more mature form in these samples). The ratio was increased (P<0.0001) in complete DMEM control cultures at 24 h compared to the untreated T=0 cultures. A summary of the impact of L-arginine concentration on SREBP-1 protein expression with culture time is reported in detail in **Figure 2.3.19** below (β -actin does not show even band across the blot in **Figure 2.3.19D**. However, this uneven band was not significantly impacted the data analysis, as the target protein was normalised to housekeeping protein; β -actin in each sample).



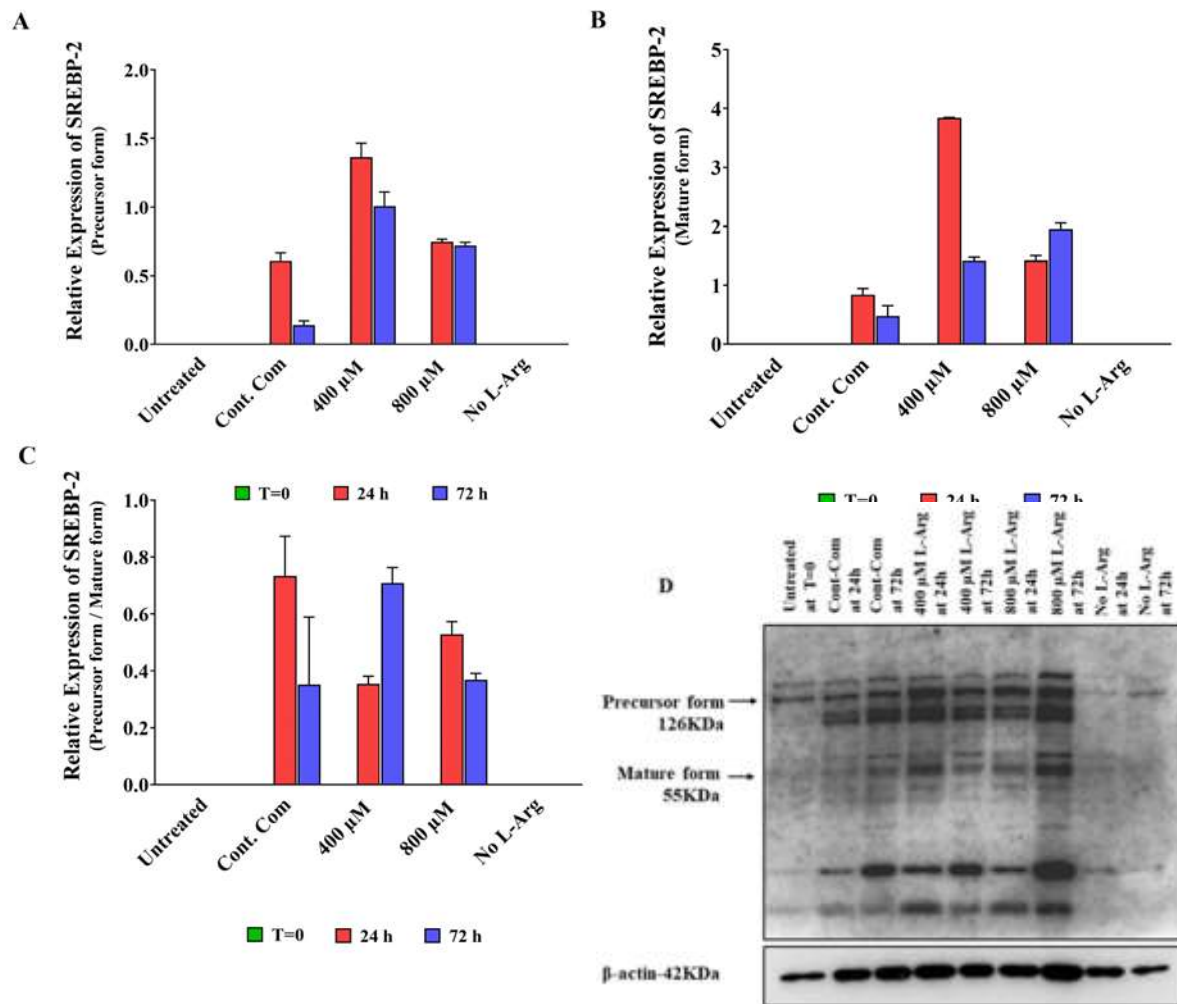
Source of Variation	SREBP-1 (Precursor)		SREBP-1 (Mature)	
	P value	Significant?	P value	Significant?
Interaction	****	Yes	****	Yes
Time	****	Yes	****	Yes
L-Arg +/- and control (Com)	****	Yes	****	Yes

Tukey's multiple comparisons test	SREBP-1 (Precursor)			SREBP-1 (Mature)		
	T=0	24 h	72 h	T=0	24 h	72 h
Untreated vs. Cont. Com	****	****	****	****	****	****
Untreated vs. 400 μ M	****	****	****	****	****	****
Untreated vs. 800 μ M	****	****	****	****	****	****
Untreated vs. No L-Arg	****	****	****	****	****	****
Cont. Com vs. 400 μ M	ns	****	ns	ns	****	****
Cont. Com vs. 800 μ M	ns	****	ns	ns	****	****
Cont. Com vs. No L-Arg	ns	****	****	ns	***	****
400 μ M vs. 800 μ M	ns	***	ns	ns	*	****
400 μ M vs. No L-Arg	ns	*	****	ns	****	****
800 μ M vs. No L-Arg	ns	ns	****	ns	****	****

Figure 2.3.19. Relative protein expression and a western blot across concentration with time for precursor and mature of SREBP-1 in BNL CL2 cells.

Relative hepatic lipogenic protein levels of precursor SREBP-1 (upper band) (A), mature SREBP-1 (lower band) (B), and the ratio of catalytically inactive precursor to catalytically active mature form of SREBP-1 (C) in BNL CL2 cells. A representative blot image of SREBP-1 across L-arginine concentrations with time is shown (D). Cells were cultured for 24 and 72 h in customized media containing 0, 400 and 800 μ M L-arginine. Controls were addition of complete DMEM and untreated samples at T=0. The same amount of total protein (20 μ g) from different culture conditions was loaded into 10% SDS–polyacrylamide gels for the separation of SREBP-1 and a representative blot from each treatment group is shown with the house-keeping protein, β -actin (D). Bands in blots were quantified using ImageJ software and the data are normalised to the house-keeping protein, β -actin and then expressed as relative values to the cells cultured with no L-arginine SILAC DMEM (0 μ M L-arginine) at 24 h. Data points represent the mean \pm SD. Error bars represent the standard deviation from the mean (n = 3). The tables summarise two-way ANOVA followed by a Tukey multiple comparison test using GraphPad Prism 9.4.1. The stars indicate the levels of significance; ns = P > 0.05, * = P \leq 0.05, ** = P \leq 0.01, *** = P \leq 0.001 and **** = P \leq 0.0001.

The other SREBP family protein investigated was SREBP-2 (**Fig 2.3.20**). SREBP-2 protein expression was increased (P<0.0001) in its precursor and catalytic forms in additional L-arginine supplemented samples at 24 and 72 h compared to control complete DMEM cultured samples. L-arginine at 400 μ M increased (P<0.0001) the precursor form of SREBP-2 at 24 (2.2-fold) and 72 h (7.2-fold). Interestingly, increasing extracellular concentrations of L-arginine to 800 μ M showed a progressive increase (P<0.0001) in the precursor form by 1.2-fold and 5.1-fold at 24 and 72 h, respectively. The amount of the catalytically active mature form was decreased at 72 h when compared to 24 h in 400 μ M L-arginine cultured samples. In contrast, the expression of the mature form increased in 800 μ M L-arginine cultured cells from 24 (1.7-fold) to 72 h (4.0-fold). The ratio of catalytically inactive precursor from to catalytically active form increased by 2.4-fold and 1.25-fold in 400 and 800 μ M L-arginine cultured cells respectively at 72 h (**Fig 2.3.20B** and **C**) compared to the control, but was decreased at 24 h. Noticeably, there was no detectable SREBP-2 protein expression, neither precursor form nor mature form, in the samples from cultures with no L-arginine addition at 24 and 72 h and untreated at T=0. A summary of the impact of L-arginine concentration on SREBP-2 protein expression with culture time is reported in detail in **Figure 2.3.20** below.



Source of Variation	SREBP-2 (Precursor)		SREBP-2 (Mature)	
	P value	Significant?	P value	Significant?
Interaction	****	Yes	****	Yes
Time	****	Yes	****	Yes
L-Arg +/- and control (Com)	****	Yes	****	Yes

Tukey's multiple comparisons test	SREBP-2 (Precursor)			SREBP-2 (Mature)		
	T=0	24 h	72 h	T=0	24 h	72 h
Untreated vs. Cont. Com	ns	****	**	ns	****	****
Untreated vs. 400 μM	ns	****	****	ns	****	****
Untreated vs. 800 μM	ns	****	****	ns	****	****
Untreated vs. No L-Arg	ns	ns	ns	ns	ns	ns
Cont. Com vs. 400 μM	ns	****	****	ns	****	****
Cont. Com vs. 800 μM	ns	**	****	ns	****	****
Cont. Com vs. No L-Arg	ns	****	**	ns	****	****

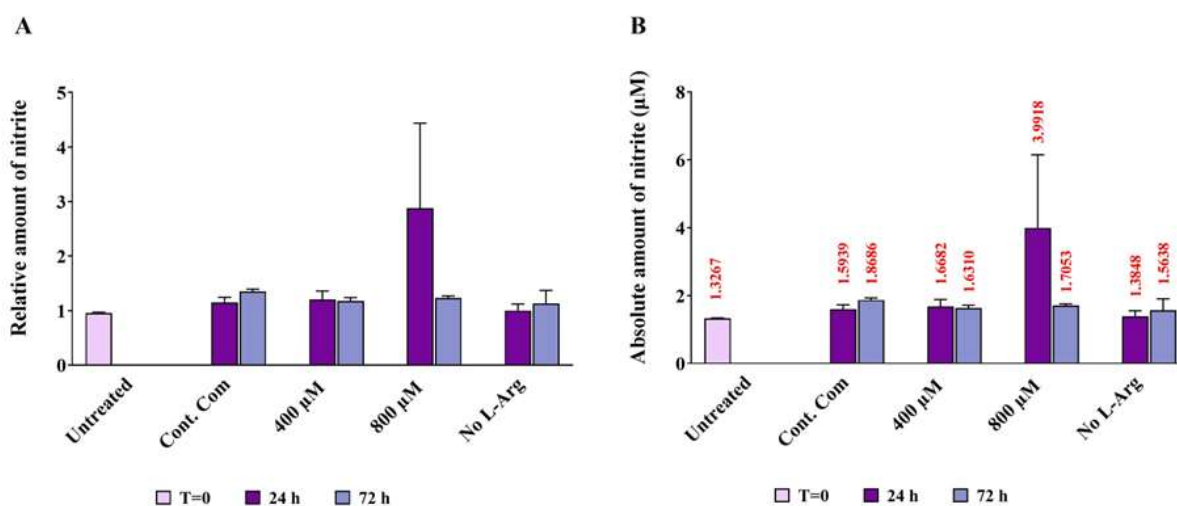
400 μM vs. 800 μM	ns	****	****	ns	****	****
400 μM vs. No L-Arg	ns	****	****	ns	****	****
800 μM vs. No L-Arg	ns	****	****	ns	****	****

Figure 2.3.20. Relative protein expression and a western blot across concentration with time for precursor and mature of SREBP-2 in BNL CL2 cells.

Relative hepatic lipogenic protein levels of precursor SREBP-2 (upper band) (A), mature SREBP-2 (lower band) (B), and the ratio of catalytically inactive precursor to catalytically active mature form of SREBP-2 (C) in BNL CL2 cells. A representative blot image for a comparison of SREBP-2 across L-arginine concentrations with time is shown in (D). Cells were cultured for 24 and 72 h in customized media containing 0, 400 and 800 μ M L-arginine. Controls were addition of complete DMEM and untreated samples at T=0. The same amount of total protein (20 μ g) from different culture conditions was loaded into 10% SDS–polyacrylamide gels for the separation of SREBP-2 and a representative blot from each treatment group is shown with the house-keeping protein, β -actin. Bands in the blots were quantified using ImageJ software and the data are normalised to the house-keeping protein, β -actin and then expressed as relative values to the cells cultured with no L-arginine SILAC DMEM (0 μ M L-arginine) at 24 h. Data points represent the mean \pm SD. Error bars represent the standard deviation from the mean (n = 3). The tables summarise two-way ANOVA followed by a Tukey multiple comparison test using GraphPad Prism 9.4.1. The stars indicate the levels of significance; ns = P > 0.05, * = P \leq 0.05, ** = P \leq 0.01, *** = P \leq 0.001 and **** = P \leq 0.0001.

2.3.4. Determination of nitric oxide/nitrite measurements by Griess Assay in BNL CL2 cells grown in different concentrations of exogenous L-arginine

It is known that excess exogenous L-arginine causes NO-mediated biological effects in spite of saturated amounts of L-arginine, a substrate of nitric oxide synthase isoforms, in a phenomenon known as the “L-arginine paradox” (Rajapakse and Mattson, 2009). Such observations have been reported in a study on the cellular activation of endothelial nitric oxide synthase (eNOS) in human endothelial cells (Shin, Mohan and Fung, 2011). Even when the level of L-arginine in the intracellular pool significantly exceeds the Km of NO synthase for L-arginine in a normal physiological state, the synthesis of endogenous NO is dependent on the extracellular L-arginine concentration (Rajapakse and Mattson, 2009). The major metabolic pathway of endogenously produced NO is that it is metabolized to an oxidised form of NO; nitrite (NO₂⁻), which is then subsequently converted to nitrate (NO₃⁻) semi quantitatively based on oxygen availability (Wennmalm et al., 1993; Weitzberg et al., 2010). In this study the amount of nitrite, the metabolized downstream reactive product of NO, present in the cell culture samples was quantified by using Griess assay as NO is known to accumulate in cell culture. Calculated nitrite concentration in unknown experimental samples was achieved using the equation of the line fitted for the standard samples (Fig 2.3.21B). The concentration of nitrite in each sample was then normalized to the concentration of nitrite present in no L-Arg added sample at 24 h to obtain the relative nitrite concentration (Fig 2.3.21A).



Source of Variation	P value	P value summary	Significant?
Interaction	<0.0001	****	Yes
Time	<0.0001	****	Yes
L-Arg +/- and Control (Com)	0.0002	***	Yes

Tukey's multiple comparisons test	Amount of Nitrite		
	T=0	24 h	72 h
Untreated vs. Cont. Com	ns	*	**
Untreated vs. 400 µM	ns	**	*
Untreated vs. 800 µM	ns	****	**
Untreated vs. No L-Arg	ns	*	*
Cont. Com vs. 400 µM	ns	ns	ns
Cont. Com vs. 800 µM	ns	***	ns
Cont. Com vs. No L-Arg	ns	ns	ns
400 µM vs. 800 µM	ns	***	ns
400 µM vs. No L-Arg	ns	ns	ns
800 µM vs. No L-Arg	ns	****	ns

Figure 2.3.21. The effect of exogenous L-arginine concentration on nitrite production in BNL CL2 cells.

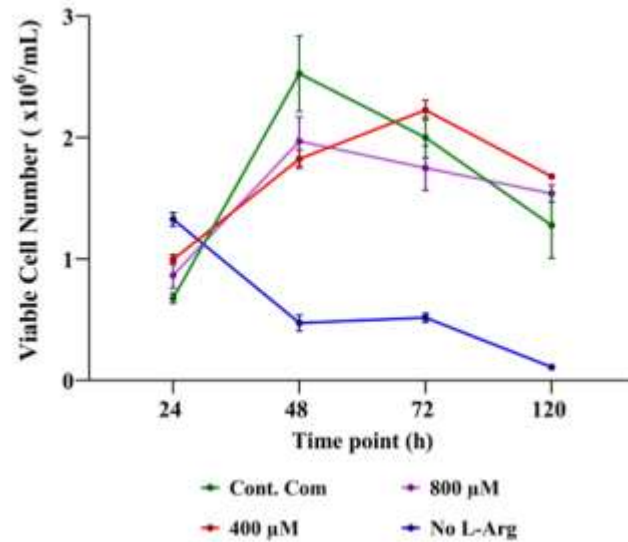
Cell culture supernatant was obtained from cultured BNL CL2 cells grown in the presence of 0, 400 or 800 µM L-arginine for 24 or 72 h. Controls were complete DMEM addition and untreated cell samples at T=0 as described in section 2.2.2. Cell culture supernatant (50 µL) was incubated at room temperature in the dark for 10 min sequentially with sulphanilamide solution (1% sulphanilamide in 5% phosphoric acid), which reacts with nitrite ion to form diazonium salt, which was then coupled with 0.1% (w/v) solution of NED. Finally, the coloured product was measured using a spectrometer at 540 nm to determine the nitrite concentration quantitatively. The concentration of nitrite from experimental samples was obtained using the equation of the line fitted to standard samples. The data are expressed as relative (A) and absolute (B) values. Quantified nitrite was normalised to the nitrite amount presence in cultures with no L-arginine SILAC DMEM (0 µM L-arginine) at 24 h. Data points represent the mean ± SD. Error bars represent the standard deviation from the mean (n = 3). The tables summarise two-way ANOVA followed by a Tukey multiple comparison test using GraphPad Prism 9.4.1. The stars indicate the levels of significance; ns = P > 0.05, * = P ≤ 0.05, ** = P ≤ 0.01, *** = P ≤ 0.001 and **** = P ≤ 0.0001.

Interestingly, increasing extracellular concentrations of L-arginine to 800 μM increased NO synthesis in BNL CL2 cells (**Fig 2.3.21**). This is consistent with a reported study where cultured primary rat hepatocytes cells were incubated with or without L-arginine medium (L-arginine content 50 mg/L, 287 μM) and increased NO formation via the NO/cyclicGMP pathway was reported in the L-arginine cultured samples (Testsuo *et al.*, 1992). The amount of NO_2^- present in 800 μM L-Arg samples was high ($P < 0.0001$) at 24 h (2.5-fold) compared to the control complete DMEM cultured samples at the same time point in BNL CL2 cells. However, the amount of nitrite presents in untreated samples at T=0 and in 0, 400 μM L-arginine and complete DMEM cultured samples was low regardless of the time point investigated. It is noted that in regard to these findings, the transcript analysis described earlier in this chapter shows that the relative gene expression of AMPK was increased in cells cultured in 800 μM L-arginine at 24 h when the amount of nitrite present in the samples was high. A summary of the impact of L-arginine concentration on the amount of nitrite present (absolute concentration (**A**) and relative concentration (**B**) in the cell culture media with culture time is reported in **Figure 2.3.21** above.

2.3.5. Impact of L-Arg addition on culture viability and viable cell numbers in 3T3 L1 cells

Establishment of cell culture models for investigating cell fitness (cell culture growth and viability parameters) is described in **2.2.1.3**. Samples were collected at 24, 48, 72 and 120 h time points for cell growth analysis. All cell samples were analysed with biological triplicate cultures. The viable number of cells was compared between the control complete DMEM medium and the no L-arginine SILAC DMEM media (0 μM L-arginine) and when SILAC DMEM had 400 and 800 μM L-arginine added. **Figure 2.3.22** shows that there was an increase in 3T3 L1 cell numbers from 24 to 48 h except in the no L-arginine supplemented cell samples. However, thereafter there was a decline in 3T3 L1 cell numbers from 48 to 120 h in all samples and conditions except the 400 μM L-arginine supplemented cell samples. The proliferation of cells increased for the control complete DMEM addition and 800 μM L-arginine supplemented cell samples from 24 to 48 h and then there was a decline in cell numbers for both samples between 48 and 120 h timepoints. The viable cell numbers of the control and 800 μM L-arginine supplemented samples reached 1.3×10^6 and 1.54×10^6 viable cells/mL, respectively. Interestingly, the viable number of cells gradually increased in 400 μM L-arginine supplemented cultures from 24 to 72 h and then there was a decline. Overall, in comparison to the control, an absence of exogenous L-arginine decreased the viability of 3T3 L1 cultures. Viable cell number peaked in the control cultures at 2.52×10^6 cells/mL at 48 h and the 400 μM L-arginine supplemented cultures had a peak viable number of 2.23×10^6 cells/mL at 48 h and 800 μM L-arginine supplemented culture peaked at 1.97×10^6 cells/mL at 72 h. Regardless of the growth profiles (**Fig 2.3.22**), the effect of L-arginine (0, 400 and 800 μM) compared to the control complete DMEM media was significant (**Fig 2.3.22**) as determined by two-way

ANOVA analysis of the means values of the viable cell numbers at the different time points followed by a Tukey multiple comparison test.



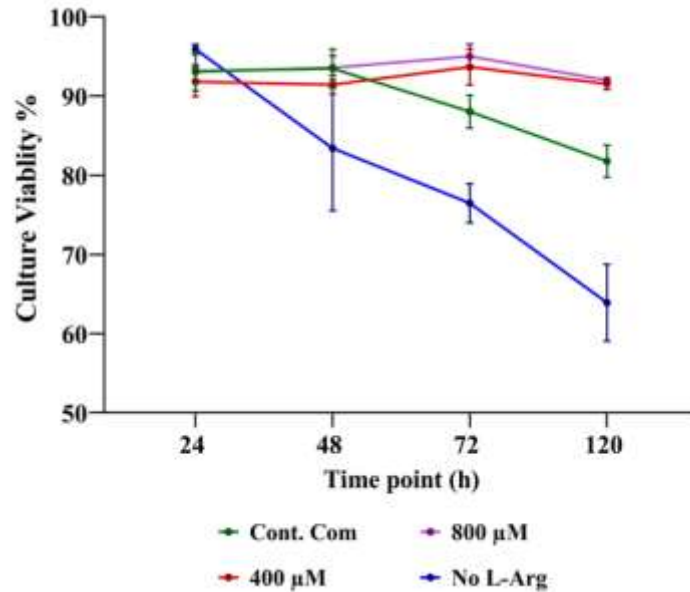
Source of Variation	P value	P value summary	Significant?
Interaction	<0.0001	****	Yes
Time point	<0.0001	****	Yes
L-Arg +/- and Control (Com)	<0.0001	****	Yes

Tukey's multiple comparisons test	Viable cell number			
	24 h	48 h	72 h	120 h
Cont. Com vs. 400 μM	*	****	ns	**
Cont. Com vs. 800 μM	ns	***	ns	ns
Cont. Com vs. No L-Arg	****	****	****	****
400 μM vs. 800 μM	ns	ns	**	ns
400 μM vs. No L-Arg	*	****	****	****
800 μM vs. No L-Arg	**	****	****	****

Figure 2.3.22. Cell growth profile of 3T3 L1 cells with different concentrations of L-arginine and the control. Cell growth/viable cell number profiles of 3T3 L1 cells with different concentrations of L-arginine (0, 400 and 800 μM) and the control complete DMEM media at 24, 48, 72 and 120 h. Data points represent the mean ± SD of each culture sample. Error bars represent the standard deviation from the mean (n = 3). The tables summarise two-way ANOVA followed by a Tukey multiple comparison test using GraphPad Prism 9.4.1. The stars flag the levels of significance; ns = P > 0.05, * = P ≤ 0.05, ** = P ≤ 0.01, *** = P ≤ 0.001 and **** = P ≤ 0.0001.

Figure 2.3.23 reports the culture viability of cultures grown in either control complete DMEM or L-arginine supplemented samples (400 and 800 μM) and no L-arginine SILAC DMEM at 24, 48, 72 and 120 h. Culture viability of the samples and conditions was generally maintained between 80-95% across the 120 h except no-L-arginine SILAC DMEM (0 μM) cultures. Culture viability of the control complete DMEM addition

showed a constant level from 24 to 48 h time period and thereafter there was a decline in viability. Culture viability of 400 and 800 μM L-arginine supplemented cultures was also quite constant across the 24 to 72 h time period after which the viability decreased from 72 to 120 h to 91.5% and 92% respectively.



Source of Variation	P value	P value summary	Significant?
Interaction	<0.0001	****	Yes
Time point	<0.0001	****	Yes
L-Arg +/- and Control (Com)	<0.0001	****	Yes

Tukey's multiple comparisons test	Culture viability			
	24 h	48 h	72 h	120 h
Cont. Com vs. 400 μM	ns	ns	ns	**
Cont. Com vs. 800 μM	ns	ns	*	***
Cont. Com vs. No L-Arg	ns	***	***	****
400 μM vs. 800μM	ns	ns	ns	ns
400 μM vs. No L-Arg	ns	**	****	****
800 μM vs. No L-Arg	ns	***	****	****

Figure 2.3.23. Culture viability profile of 3T3 L1 cells grown in different concentrations of L-arginine and the control.

Culture viability profile of 3T3 L1 cells grown in different concentrations of L-Arg (0, 400 and 800 μM) and the control complete DMEM media at 24, 48, 72 and 120 h. Culture viability is expressed as % of viable cells. Data points represent the mean \pm SD of each sample. Error bars represent the standard deviation from the mean ($n = 3$). Tables summarise two-way ANOVA followed by a Tukey multiple comparison test using GraphPad Prism 9.4.1. The stars indicate the levels of significance; ns = $P > 0.05$, * = $P \leq 0.05$, ** = $P \leq 0.01$, *** = $P \leq 0.001$ and **** = $P \leq 0.0001$.

The viability of the cultures with 0 μ M L-Arg addition dropped significantly from 24 to 120 h time period, reaching a low of 64%. It is interesting to note that the culture viability of 400 and 800 μ M L-arginine cultures followed the same pattern. In comparison to other culture conditions, cultures with the lowest concentration of L-arginine (0 μ M) decreased in culture viability rapidly. The presence of excess L-arginine (400 and 800 μ M) compared to the control complete DMEM media was significant (**Fig 2.3.23**) as determined by two-way ANOVA analysis of the means values of the culture viability at the different time points followed by a Tukey multiple comparison test.

2.3.6. qRT-PCR analysis of targets genes upon culturing of 3T3 L1 cells in different exogenous L-arginine concentrations

Cells were grown as described in section 2.2.1.3 and 2.2.2 and sampled for transcriptional mRNA level analysis by qRT-PCR. Data analysis and normalisation of the data of qRT PCR were followed as described in section 2.3.2. RNA samples were control complete DMEM media, no L-arginine SILAC DMEM media and 400 and 800 μ M L-arginine addition to 3T3 L1 cells and collected at T=0, 24 and 72 h. The target transcripts AMPK, ACC-1, CPT-1, HMG-CoA reductase, SREBP-1 and SREBP-2, which are hypothetically modulated by changes in L-arginine through signalling pathways, were investigated. The relative expression of each gene was determined and denoted as RE.

L-arginine concentration-related regulation of the AMPK gene, a key regulator of energy substrate oxidation (Cantó and Auwerx, 2013), was observed in the 3T3 L1 cells (**Fig 2.3.24A**). From the qRT-PCR data, AMPK gene expression was increased ($P < 0.0001$) in 400 μ M L-Arg addition cultures at 24 (RE 3.26) and 72 h (RE 1.49) when compared to the control complete DMEM media cultures. AMPK mRNA expression also increased ($P < 0.0001$) in 800 μ M L-arginine cultures (RE 1.91) at 24 h in comparison to the control (RE 0.28), however, the AMPK expression in both 800 μ M and the control samples was more or less the same at 72 h. AMPK mRNA expression was more-or-less unchanged in no L-arginine added samples at 24 and 72 h time points.

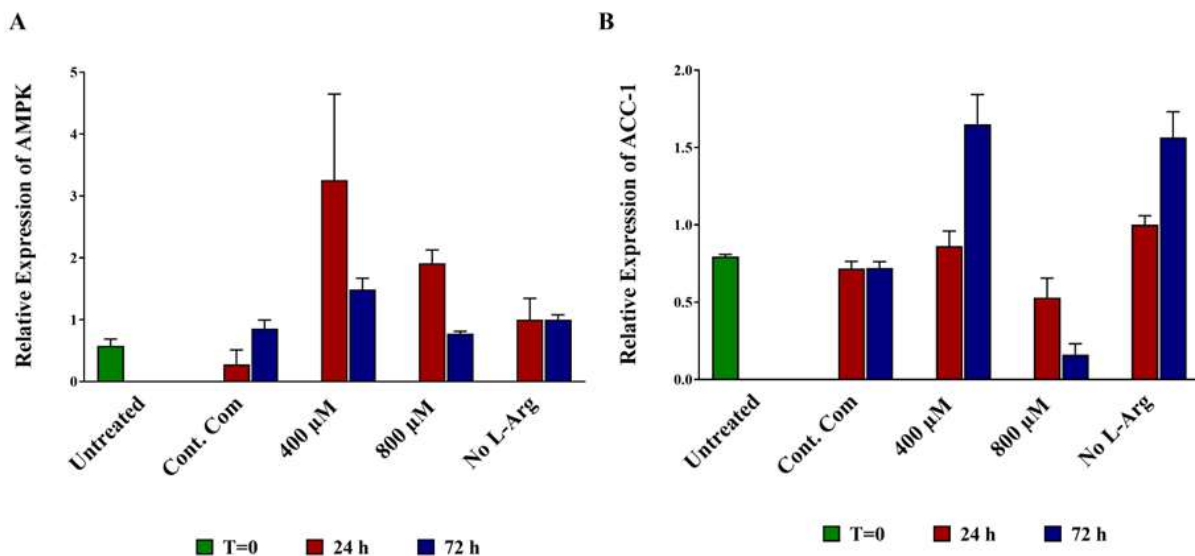
The mRNA levels of the key lipogenic enzyme, ACC-1, was slightly increased ($P < 0.0001$) in cultures with arginine at 400 μ M (RE 0.86) compared to the control (RE 0.72) and increased ($P < 0.0001$) at 72 h (RE 1.65) compared to the control complete DMEM media cultures (RE 0.72) (**Fig 2.3.24B**). Noticeably, there was no difference in ACC-1 mRNA expression within the time points 24 (RE 0.72) and 72 h (RE 0.72) in the control complete DMEM. ACC-1 gene expression was decreased ($P < 0.0001$) in 800 μ M L-arginine cultures at 24 (RE 0.53) and 72 h (RE 0.16) in comparison to the control (at 24 and 72 h; RE 0.72) and no L-arginine added samples (at 24; RE 1 and 72 h; RE 1.56).

The key regulator gene for the fatty acid oxidation, CPT-1A showed an overall increase in L-arginine added culture conditions when compared to the control (**Fig 2.3.25A**). The highest relative expressions among the

samples were 7.09 for 800 μ M L-arginine addition at 72 h compared to the control (RE 3.62) and 3.35 at 24 h in comparison to the control (RE 2.32). The 400 μ M L-Arg culture also showed increased ($P < 0.0001$) CPT-1A mRNA expression at 24 (RE 2.77) and 72 h (RE 4.48) in comparison to the control at 24 (RE 2.32) and 72 h. (RE 3.62). It is therefore clear that in 3T3 L1 cells, L-Arg supplementation has an impact on transcription of the *CPT-1A* gene, as evidenced by the difference in gene expression between the control and L-Arg-supplemented cultures.

The transcript amounts of the key players in cholesterol metabolism, HMGCR and SREBP-2 were also investigated and in general increased ($P < 0.0001$) in 400 and 800 μ M L-arginine cultures compared to the control at 24 and 72 h. HMGCR ($P < 0.0001$) and SREBP-2 ($P < 0.0001$) were increased in mRNA expression compared to the DMEM control in response to 400 μ M L-Arg addition at 72 h (RE-HMGCR 5.28 and RE-SREBP-2 4.48, respectively compared to RE 2.86 and RE 3.62 of control) (**Fig 2.3.25B** and **Fig 2.3.26B**). Noticeably, SREBP-2 mRNA expression peaked in 800 μ M L-arginine added samples at 72 h (RE 7.08) in comparison to the control (RE 3.62).

An additional SREBP transcription factor and the regulator of *de novo* lipogenesis and glycolysis pathways (Ruiz *et al.*, 2014), SREBP-1 decreased ($P < 0.0001$) and was similar in expression in 400 and 800 μ M L-Arg cultures at 24 h (RE 0.88) compared to the control complete DMEM addition (RE 0.99) at the same time point (**Fig 2.3.26A**). However, SREBP-1 transcript expression was increased in 400 μ M L-arginine added sample at 72 h (RE 1.19) compared to the control (RE 1.04). Among all the samples investigated, the relative expression of SREBP-1 peaked in no L-arginine added cultures at 72 h (RE 1.72) compared to the control (RE 1.04).

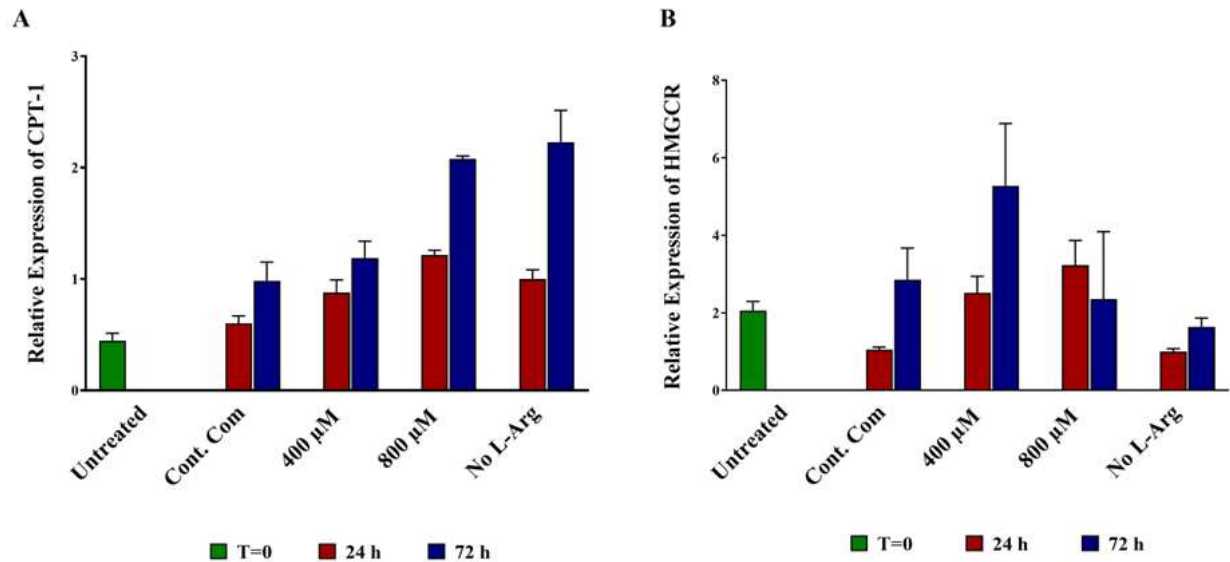


Source of Variation	AMPK		ACC-1	
	P value	Significant?	P value	Significant?
Interaction	****	Yes	****	Yes
Time point	****	Yes	****	Yes
L-Arg +/- and control (Com)	****	Yes	****	Yes

Tukey's multiple comparisons test	AMPK			ACC-1		
	T=0	24 h	72 h	T=0	24 h	72 h
Untreated vs. Cont. Com	ns	ns	ns	****	****	****
Untreated vs. 400 µM	ns	****	***	****	****	****
Untreated vs. 800 µM	ns	****	ns	****	****	ns
Untreated vs. No L-Arg	ns	*	*	****	****	****
Cont. Com vs. 400 µM	ns	****	ns	ns	ns	****
Cont. Com vs. 800 µM	ns	***	ns	ns	ns	****
Cont. Com vs. No L-Arg	ns	ns	ns	ns	**	****
400 µM vs. 800 µM	ns	**	ns	ns	***	****
400 µM vs. No L-Arg	ns	****	ns	ns	ns	ns
800 µM vs. No L-Arg	ns	*	ns	ns	****	****

Figure 2.3.24. Relative mRNA expression of AMPK and ACC-1 in 3T3 L1 cells cultured in different concentrations of L-arginine and the control.

Relative mRNA transcript expression ($\Delta\Delta C_t$) of AMPK (A) and ACC-1 (B) in 3T3 L1 cells cultured in medium of different L-arginine concentrations (0, 400 and 800 μM) and control complete DMEM media 24 and 72 h after addition. Untreated cultures at T=0. Data points represent the mean \pm SD of each sample. Error bars represent the standard deviation from the mean (n =3). Tables summarise two-way ANOVA followed by a Tukey multiple comparison test using GraphPad Prism 9.4.1. The stars indicate the levels of significance; ns = $P > 0.05$, * = $P \leq 0.05$, ** = $P \leq 0.01$, *** = $P \leq 0.001$ and **** = $P \leq 0.0001$.



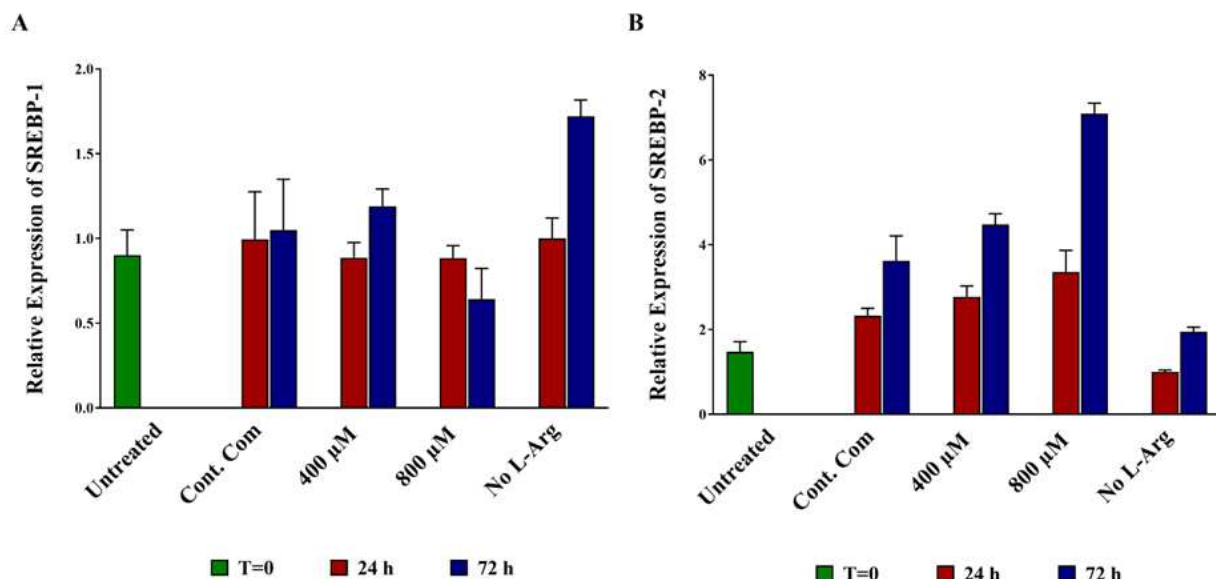
Source of Variation	CPT-1		HMGCR	
	P value	Significant?	P value	Significant?
Interaction	****	Yes	****	Yes
Time point	****	Yes	****	Yes
L-Arg +/- and control (Com)	****	Yes	****	Yes

Tukey's multiple comparisons test	CPT-1			HMGCR		
	T=0	24 h	72 h	T=0	24 h	72 h
Untreated vs. Cont. Com	***	****	****	**	ns	***
Untreated vs. 400 µM	***	****	****	**	***	****
Untreated vs. 800 µM	***	****	****	**	****	**
Untreated vs. No L-Arg	***	****	****	**	ns	*
Cont. Com vs. 400 µM	ns	*	ns	ns	ns	**
Cont. Com vs. 800 µM	ns	****	****	ns	**	ns
Cont. Com vs. No L-Arg	ns	***	****	ns	ns	ns
400 µM vs. 800 µM	ns	**	****	ns	ns	***
400 µM vs. No L-Arg	ns	ns	****	ns	ns	****
800 µM vs. No L-Arg	ns	ns	ns	ns	**	ns

Figure 2.3.25. Relative mRNA expression of CPT-1 and HMGCR in 3T3 L1 cells cultured in different concentrations of L-arginine and the control.

Relative mRNA transcript expression ($\Delta\Delta C_t$) of CPT-1 (A) and HMGCR (B) in 3T3 L1 cells cultured in medium of different L-arginine concentrations (0, 400 and 800 μM) and control complete DMEM media 24 and 72 h after addition. Untreated cultures at T=0. Data points represent the mean \pm SD of each sample. Error bars represent the standard deviation from the mean (n = 3). Tables summarise two-way ANOVA followed by a Tukey multiple comparison test

using GraphPad Prism 9.4.1. The indicate the levels of significance; ns = $P > 0.05$, * = $P \leq 0.05$, ** = $P \leq 0.01$, *** = $P \leq 0.001$ and **** = $P \leq 0.0001$.



Source of Variation	SREBP-1		SREBP-2	
	P value	Significant?	P value	Significant?
Interaction	***	Yes	***	Yes
Time point	****	Yes	****	Yes
L-Arg +/- and control (Com)	***	Yes	***	Yes

Tukey's multiple comparisons test	SREBP-1			SREBP-2		
	T=0	24 h	72 h	T=0	24 h	72 h
Untreated vs. Cont. Com	****	****	****	****	****	****
Untreated vs. 400 µM	****	****	****	****	****	****
Untreated vs. 800 µM	****	****	****	****	****	****
Untreated vs. No L-Arg	****	****	****	****	***	****
Cont. Com vs. 400 µM	ns	ns	ns	ns	ns	**
Cont. Com vs. 800 µM	ns	ns	**	ns	***	****
Cont. Com vs. No L-Arg	ns	ns	****	ns	****	****
400 µM vs. 800 µM	ns	ns	***	ns	*	****
400 µM vs. No L-Arg	ns	ns	***	ns	****	****
800 µM vs. No L-Arg	ns	ns	****	ns	****	****

Figure 2.3.26. Relative mRNA expression of SREBP-1 and SREBP-2 in 3T3 L1 cells cultured in different concentrations of L-arginine and the control.

Relative mRNA transcript expression ($\Delta\Delta Ct$) of SREBP-1 (A) and SREBP-2 (B) in 3T3 L1 cells cultured in medium of different L-arginine concentrations (0, 400 and 800 μM) and control complete DMEM media 24 and 72 h after addition. Untreated samples at T=0. Data points represent the mean \pm SD of each sample. Error bars represent the standard deviation from the mean (n = 3). Tables summarise two-way ANOVA followed by a Tukey multiple comparison test using GraphPad Prism 9.4.1. The stars indicate the levels of significance; ns = P > 0.05, * = P \leq 0.05, ** = P \leq 0.01, *** = P \leq 0.001 and **** = P \leq 0.0001.

2.3.7. Monitoring protein and post-translational phosphorylation expression in response to L-Arg supplementation

Western blotting for all target proteins was undertaken in protein samples of 3T3 L1 cells in three biological replicates as described in sections 2.2.1.3 and 2.2.3. The samples were L-arginine test concentrations (0, 400 and 800 μ M) and the controls complete DMEM media addition at 24 and 72 h timepoints and untreated samples at T=0. Two combinations of gels were used to allow (a) comparison within a concentration with changing culture time (Figs 2.3.27-2.3.33) and (b) comparison across concentrations at a specific culture time point (Figs 2.3.34-2.3.41). Target protein expression was normalized to β -actin protein. All data was then normalized to the value of no L-Arg added samples (0 μ M L-arginine) at 24 h culture time point, denoted as RE in the following sections.

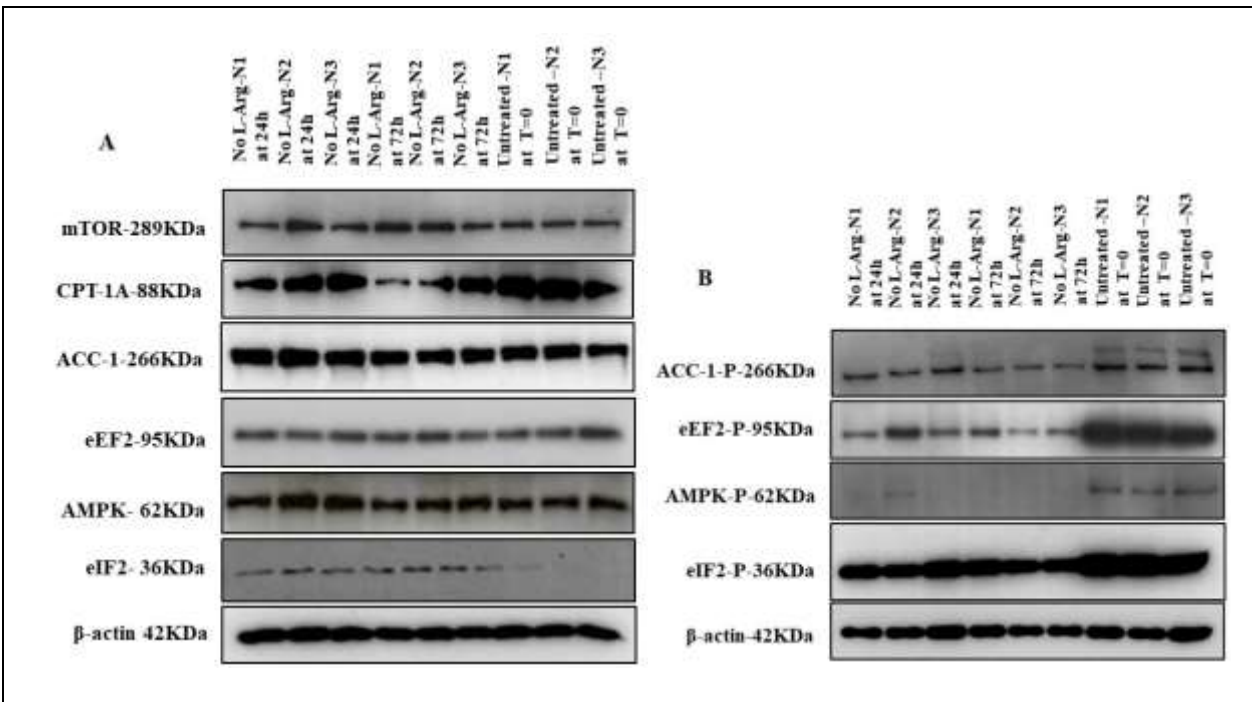


Figure 2.3.27. Western blot comparison for target proteins and phosphorylated proteins expression in 3T3 L1 cells cultured at 0 μ M L-Arg concentration for 24 and 72 h and untreated at T=0.

Western blot comparison of (A) the expression of key proteins involved in L-arginine/NO metabolic pathway signalling, and (B) the amount of phospho-protein of key targets in cultured 3T3 L1 cells cultured in no L-arginine SILAC DMEM media for 24 and 72 h and in one of the control, untreated culture samples at T=0. β -actin is used as a loading control. The same amount of protein (10 μ g) from different treatment groups was loaded from biological triplicate cultures into 10% SDS-polyacrylamide gels for the separation of target proteins.

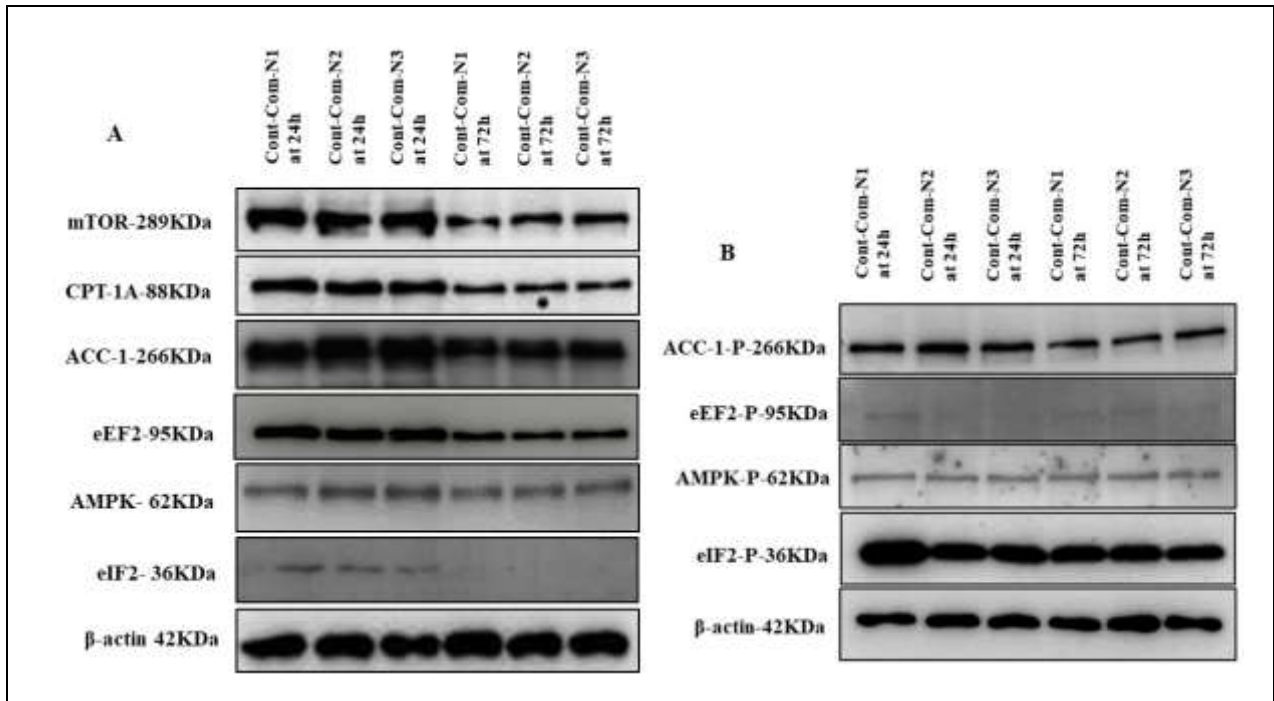


Figure 2.3.28. Western blot comparison for target proteins and phosphorylated proteins expression in 3T3 L1 cells cultured at the control complete DMEM for 24 and 72 h.

Western blot comparison of (A) the expression of key proteins involved in L-arginine/NO metabolic pathway signalling, and (B) the amount of phospho-protein of key targets in cultured 3T3 L1 cells cultured in control complete DMEM media for 24 and 72 h. β-actin is used as a loading control. The same amount of protein (10 μg) from different treatment groups was loaded from biological triplicate cultures into 10% SDS–polyacrylamide gels for the separation of target proteins.

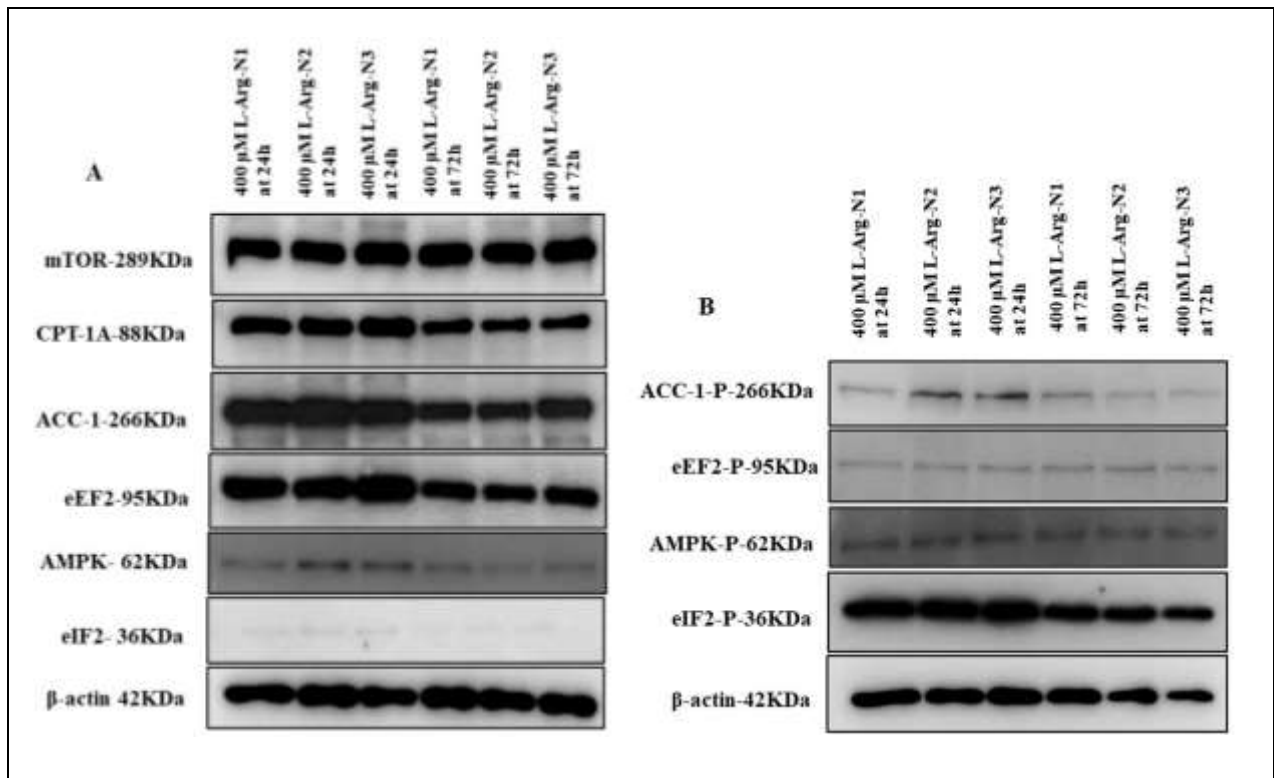


Figure 2.3.29. Western blot comparison for target proteins and phosphorylated proteins expression in 3T3 L1 cells cultured at 400 μ M L-Arg concentration for 24 and 72 h.

Western blot comparison of (A) the expression of key proteins involved in L-arginine/NO metabolic pathway signalling, and (B) the amount of phospho-protein of key targets in cultured 3T3 L1 cells cultured in 400 μ M L-arginine in L-arginine free SILAC DMEM media for 24 and 72 h. β -actin is used as a loading control. The same amount of protein (10 μ g) from different treatment groups was loaded from biological triplicate cultures into 10% SDS-polyacrylamide gels for the separation of target proteins.

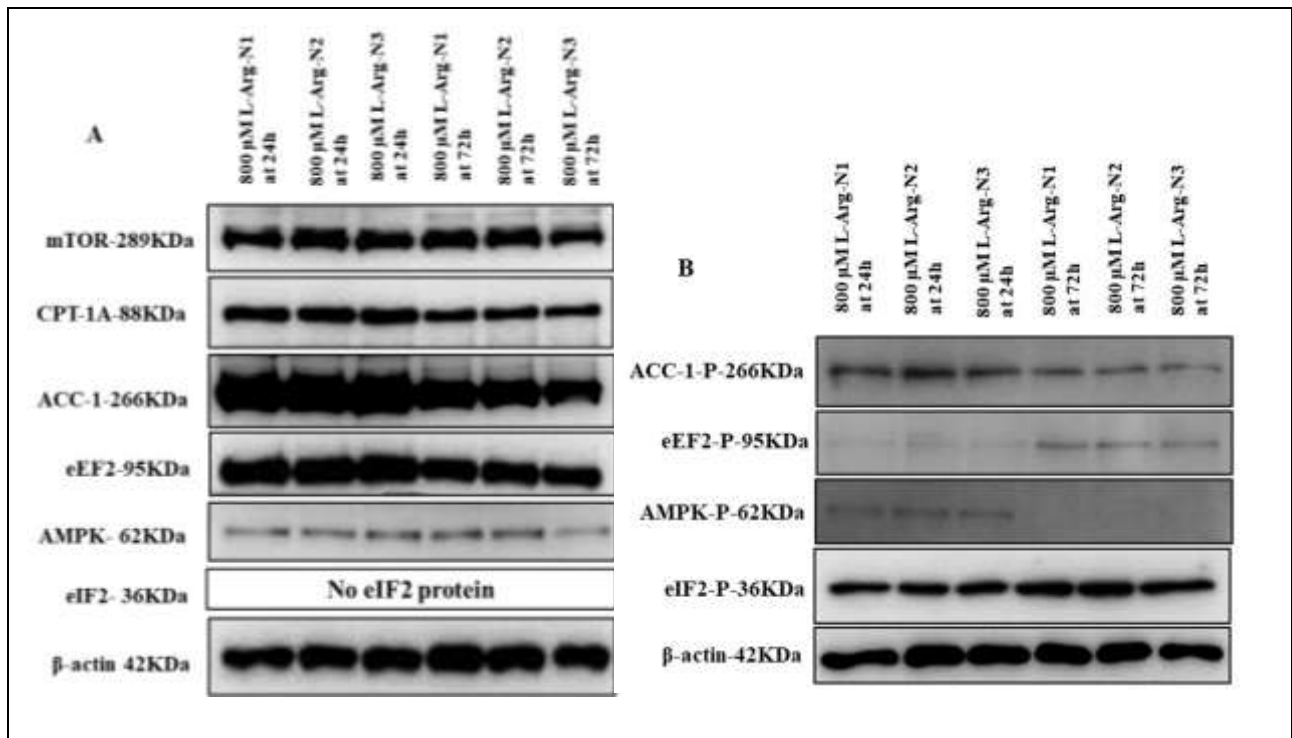


Figure 2.3.30. Western blot comparison for target proteins and phosphorylated proteins expression in 3T3 L1 cells cultured at 800 μM L-Arg concentration for 24 and 72 h.

Western blot comparison of (A) the expression of key proteins involved in L-arginine/NO metabolic pathway signalling, and (B) the amount of phospho-protein of key targets in cultured 3T3 L1 cells cultured in 800 μM L-arginine in L-arginine free SILAC DMEM media for 24 and 72 h. β-actin is used as a loading control. The same amount of protein (10 μg) from different treatment groups was loaded from biological triplicate cultures into 10% SDS-polyacrylamide gels for the separation of target proteins. No eIF2 protein means, eIF2 protein was not detected in the prepared protein samples.

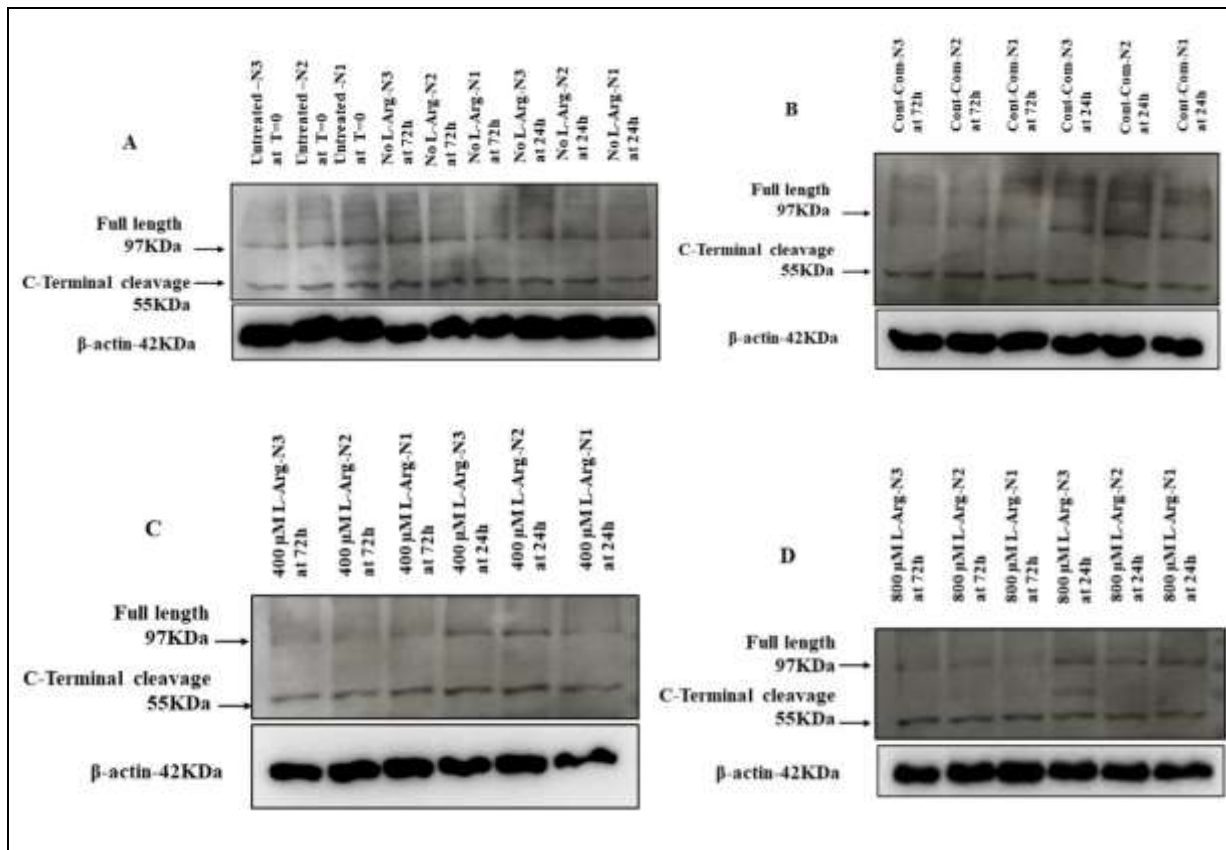


Figure 2.3.31. Western blot comparison for HMGCR expression in 3T3 L1 cells cultured at 0, 400 and 800 μM L-Arg concentration and the control for 24 and 72 h and untreated at T=0.

Western blot comparison of lipogenic protein levels of HMGCR precursor form (upper band) and HMGCR mature form (lower band) in 3T3 L1 cells cultured in customized media containing (A) no L-arginine SILAC DMEM and untreated cell samples at T=0, (B) complete DMEM, (C) 400 μM L-arginine, and (D) 800 μM L-arginine for 24 and 72 h. β-actin is used as a loading control. The same amount of protein (20 μg) from different treatment groups was loaded from biological triplicate cultures into 10% SDS–polyacrylamide gels for the separation of target proteins.

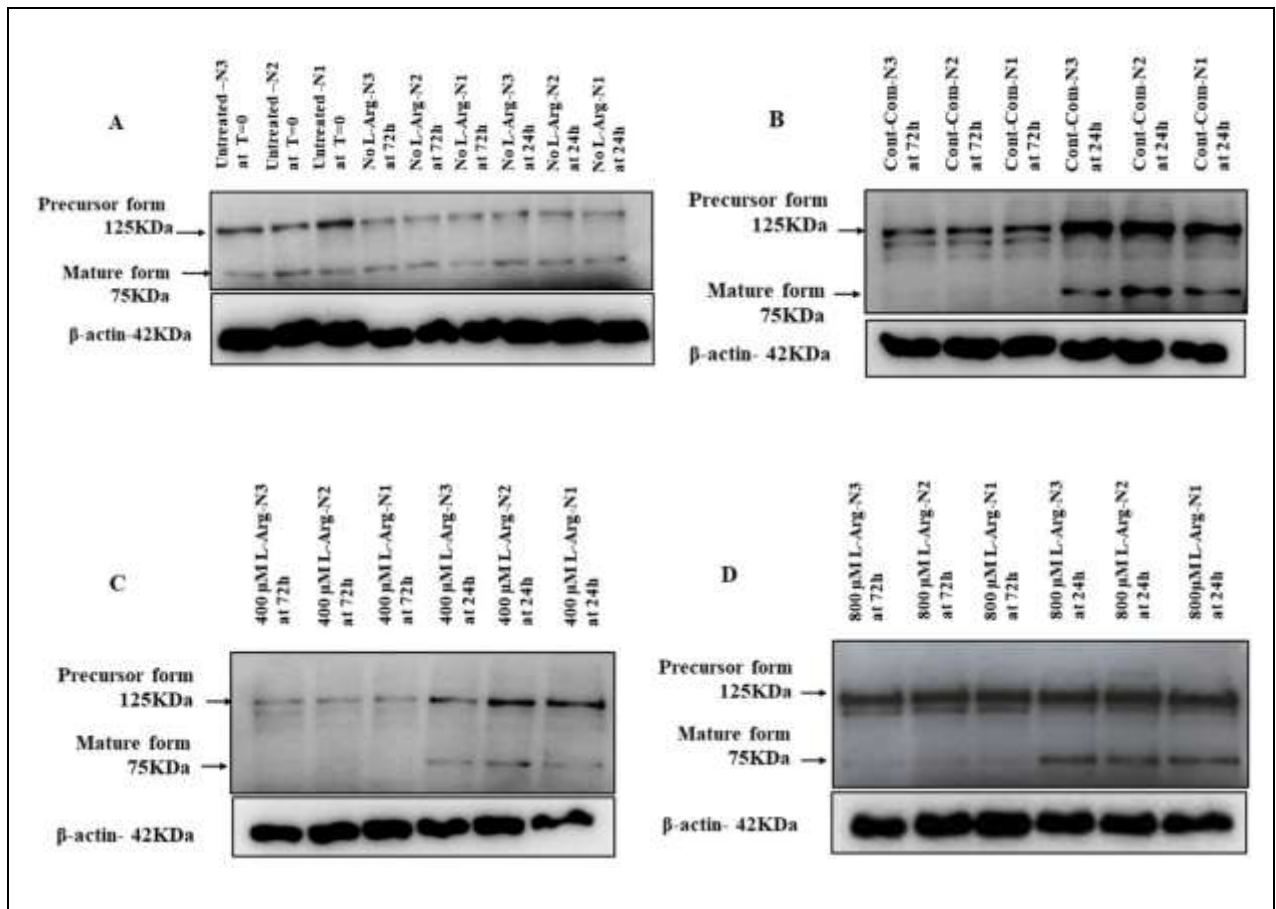


Figure 2.3.32. Western blot comparison for SREBP-1 protein expression in 3T3 L1 cells cultured at 0, 400 and 800 μM L-Arg concentration and the control for 24 and 72 h and untreated at T=0.

Western blot comparison of lipogenic protein levels of SREBP-1 precursor form (upper band) and SREBP-1 mature form (lower band) in 3T3 L1 cells cultured in customized media containing (A) no L-arginine SILAC DMEM and untreated cell samples at T=0, (B) complete DMEM, (C) 400 μM L-arginine, and (D) 800 μM L-arginine for 24 and 72 h. β -actin is used as a loading control. The same amount of protein (20 μg) from different treatment groups was loaded from biological triplicate cultures into 10% SDS–polyacrylamide gels for the separation of target proteins.

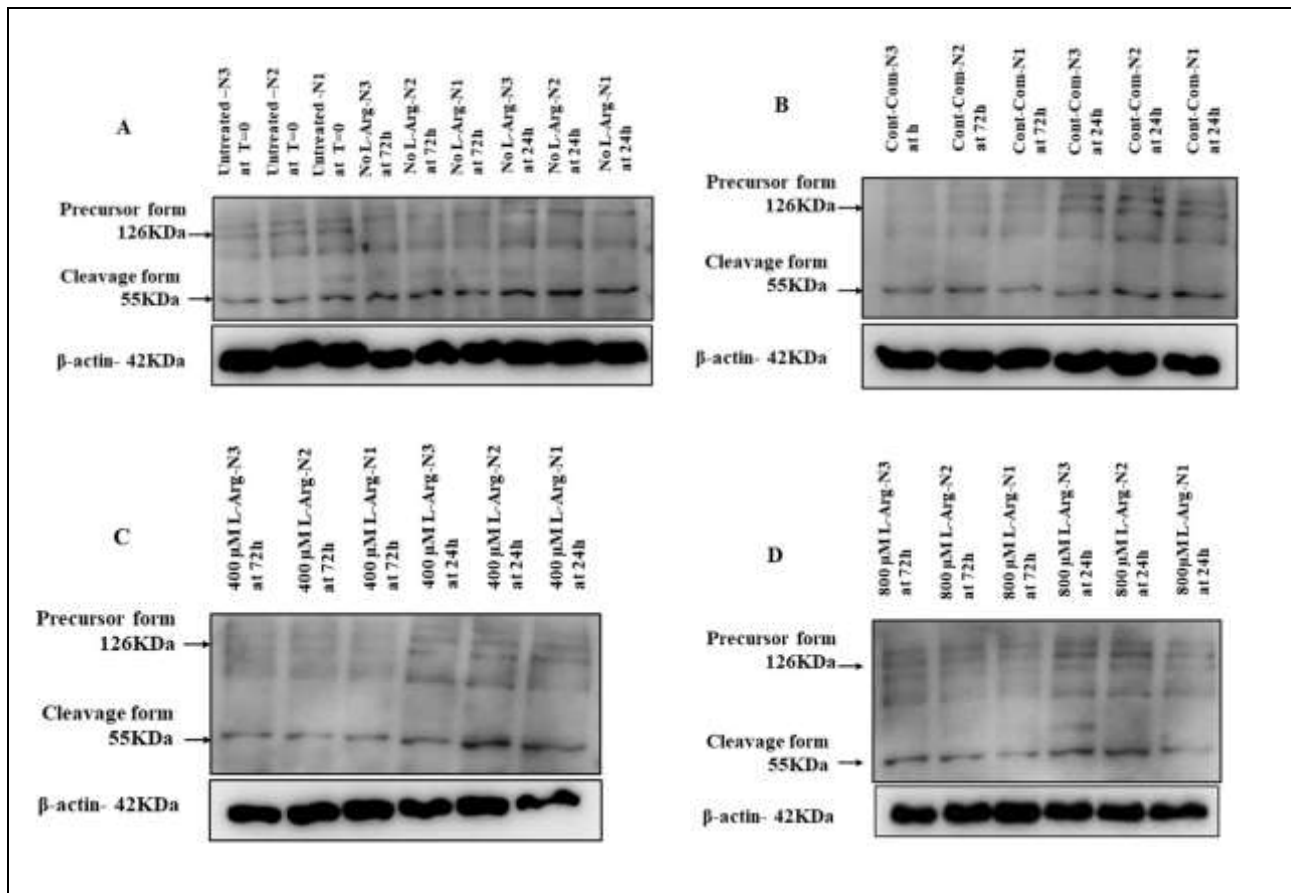


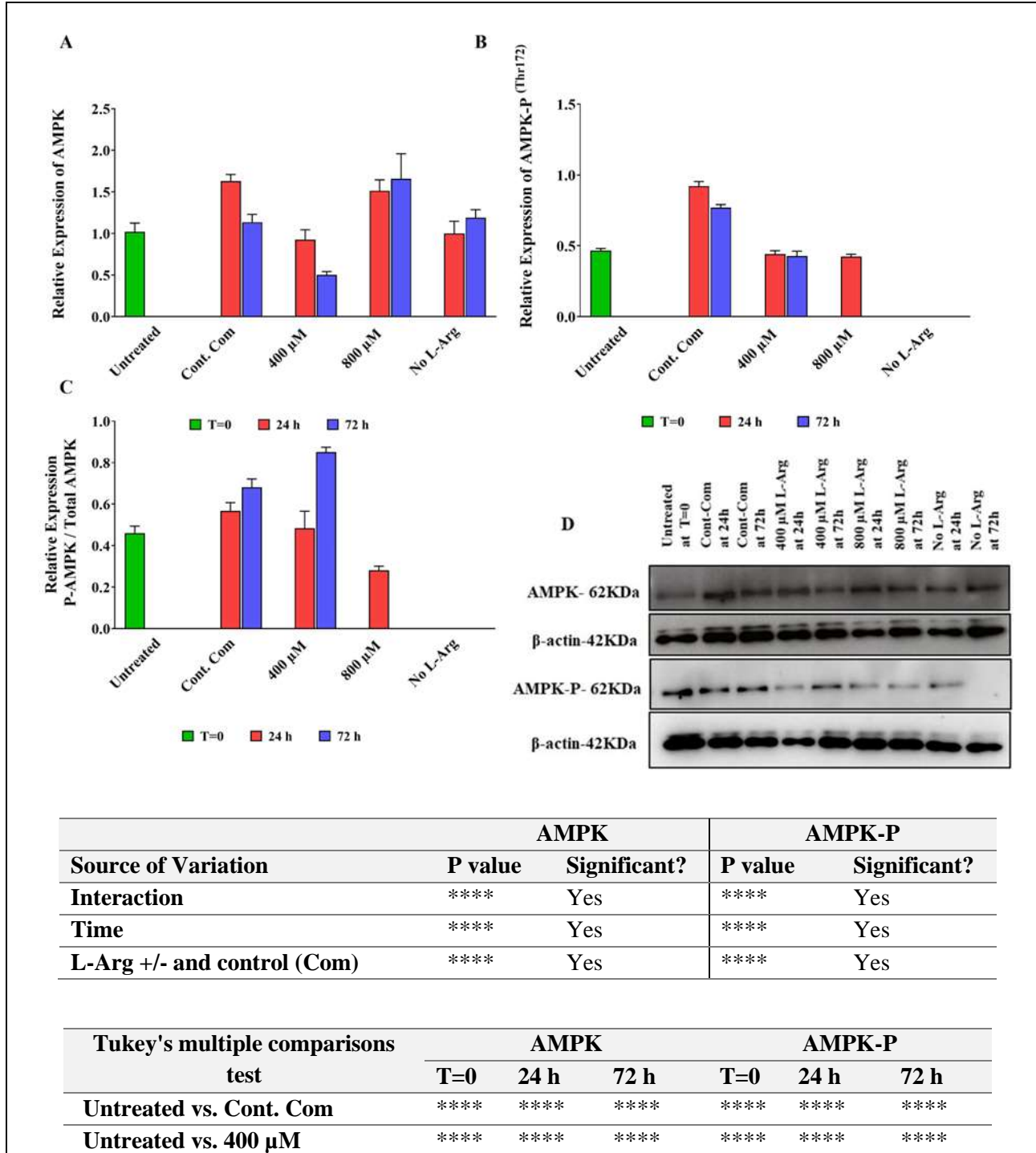
Figure 2.3.33. Western blot comparison for SREBP-2 protein expression in 3T3 L1 cells cultured at 0, 400 and 800 μM L-Arg concentration and the control for 24 and 72 h and untreated at T=0.

Western blot comparison of lipogenic protein levels of SREBP-2 precursor form (upper band) and SREBP-2 mature form (lower band) in 3T3 L1 cells cultured in customized media containing (A) no L-arginine SILAC DMEM and untreated cell samples at T=0, (B) complete DMEM, (C) 400 μM L-arginine, and (D) 800 μM L-arginine for 24 and 72 h. β -actin is used as a loading control. The same amount of protein (20 μg) from different treatment groups was loaded from biological triplicate cultures into 10% SDS–polyacrylamide gels for the separation of target proteins.

A comparison across L-arginine concentrations with culture time of total and phosphorylated levels of AMPK in 3T3 L1 cells is presented in **Fig 2.3.34**. The AMPK protein expression showed increased and peaked expression ($P < 0.0001$) when cultured in 800 μM (1.5-fold) L-arginine after 72 h compared to the control complete media samples at 72 h. AMPK protein expression was decreased ($P < 0.0001$) when cultured in 400 μM at 24 (RE 0.93) and 72 h (RE 0.50) compared to the control complete DMEM media additions at 24 (RE 1.63) and 72 h (RE 1.13). AMPK protein expression in no L-arginine media samples at 72 h (RE 1.19) was more-or-less the same as the control at 72 h.

When investigating the phosphorylation of AMPK, in 400 μM L-Arg cultured samples phosphorylation was very similar ($P < 0.0001$) at 24 (RE 0.52) and 72 h (RE 0.53) and more or less the same when compared to untreated samples at T=0 (RE 0.58). There was no ($P < 0.0001$) detectable phosphorylated AMPK protein in no L-Arg media samples. Increasing L-arginine concentrations to 800 μM resulted in decreased ($P < 0.0001$)

phosphorylated AMPK levels at 24 (RE 0.52) and 72 h (RE 0) in comparison to the control at 24 (RE 1.14) and 72 h (RE 0.95). When comparing phosphorylated AMPK protein to total AMPK protein, the ratio was increased in 400 μ M L-arginine (1.25-fold) cultures at 72 h in comparison to the control at the same time point. A summary of the impact of L-arginine concentration on AMPK protein expression and phosphorylation with culture time is reported in **Figure 2.3.34** below.



Untreated vs. 800 μM	****	****	****	****	****	ns
Untreated vs. No L-Arg	****	****	****	****	ns	ns
Cont. Com vs. 400 μM	ns	****	****	ns	****	****
Cont. Com vs. 800 μM	ns	ns	****	ns	****	****
Cont. Com vs. No L-Arg	ns	****	ns	ns	****	****
400 μM vs. 800 μM	ns	****	****	ns	ns	****
400 μM vs. No L-Arg	ns	ns	****	ns	****	****
800 μM vs. No L-Arg	ns	****	***	ns	****	ns

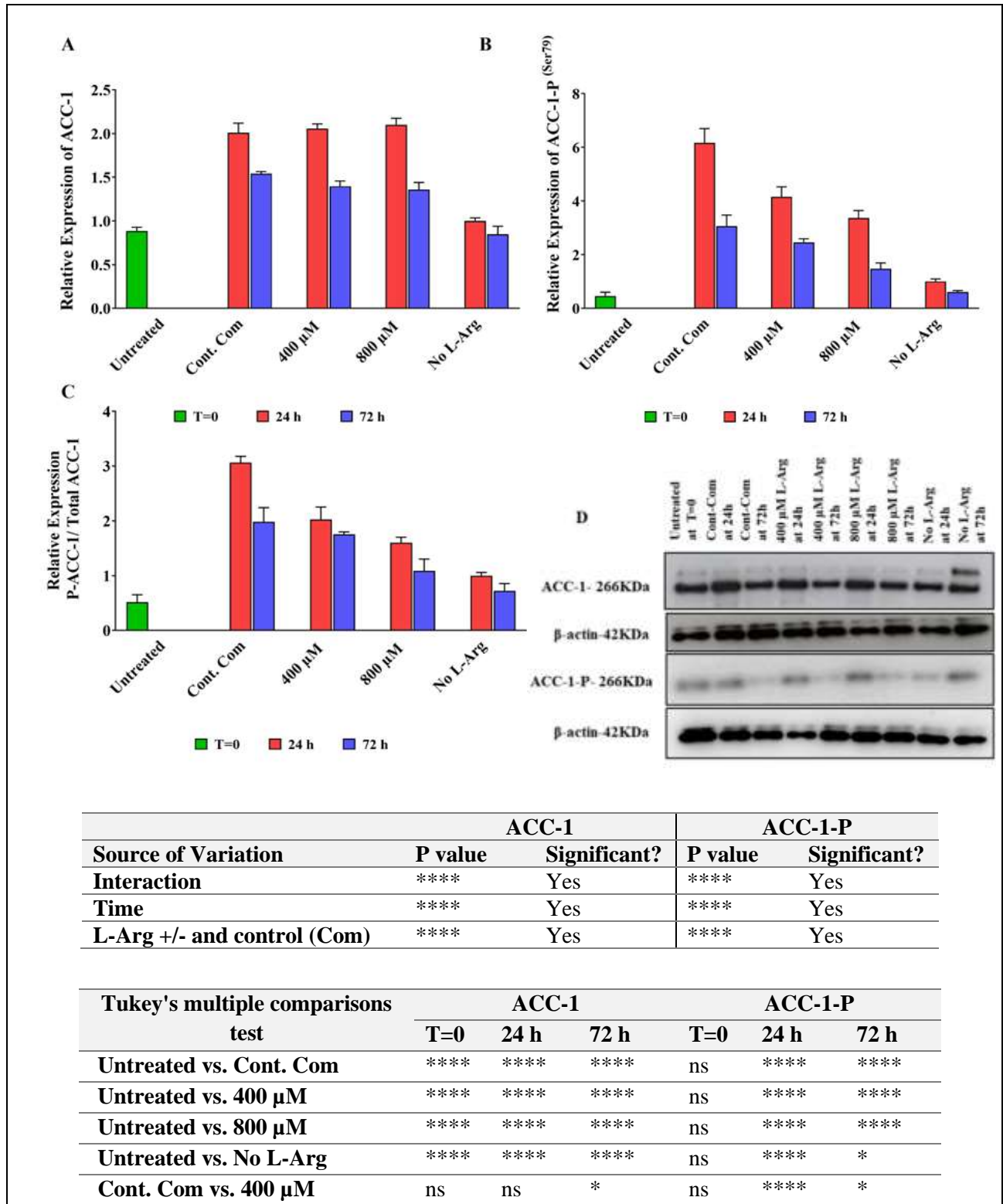
Figure 2.3.34. Relative protein expression and a western blot across concentration with time for AMPK α protein and AMPK α -P in 3T3 L1 cells.

Relative protein amounts for total AMPK α (A), phosphorylated AMPK α at Thr172 (AMPK α -P) (B) and the ratio of AMPK α -P to total AMPK α in 3T3 L1 cells (C). An example blot image of AMPK α and AMPK α -P across concentrations with culture time is shown in (D). Cells were cultured for 24 or 72 h in customized media containing 0, 400 and 800 μ M L-arginine. Controls were addition of complete DMEM or untreated cultures at T=0. The same amount of total protein (10 μ g) from different culture conditions was loaded into 10% SDS–polyacrylamide gels for the separation of AMPK α and phosphorylated AMPK α proteins and two representative blots from each treatment group are shown with the respective to the house-keeping-protein, β -actin (D). Bands in the blots were quantified using ImageJ software and the data are normalised to β -actin and then expressed as relative to the no L-arginine SILAC DMEM (0 μ M L-arginine) control at 24 h. Data points represent the mean \pm SD. Error bars represent the standard deviation from the mean (n = 3). The tables summarise two-way ANOVA followed by a Tukey multiple comparison test using GraphPad Prism 9.4.1. The stars indicate the levels of significance; ns = P > 0.05, * = P \leq 0.05, ** = P \leq 0.01, *** = P \leq 0.001 and **** = P \leq 0.0001.

Total and phosphorylated levels of ACC-1 protein in 3T3 L1 cells under different L-arginine culture conditions are presented in **Fig 2.3.35**. The expression of this regulator of fatty acid metabolism decreased (P<0.0001) with the time in cells cultured in L-arginine at 400 and 800 μ M and in the control. Relative ACC-1 protein expression in the control, 400 and 800 μ M L-arginine cultures (P<0.0001) at 24 h was 2.0, 2.0 and 2.10 respectively, whereas the relative ACC-1 protein expression for these samples at 72 h was decreased (P<0.0001) as 1.54, 1.4 and 1.36. After 72 h of culture time total ACC-1 amounts in the untreated sample at T=0 (RE-0.88) and no L-Arg added samples (RE 0.85) had similar and the lowest relative expression of ACC-1 among all samples.

When phosphorylation of ACC-1 was investigated, this was almost halved from its level at 24 h to 72h. The relative expression of phosphorylated ACC-1 in the control, 400 and 800 μ M L-Arg cultures at 24 h were 6.16, 4.15 and 3.36 and at 72 h were 3.06, 2.45 and 1.47 respectively. Among all samples, expression of phosphorylated ACC-1 was higher in the control (RE 6.16) at 24 h and the amounts of phosphorylated ACC-1 was increased (P<0.0001) (2-fold) in comparison to the 800 μ M L-arginine added samples at 24 and 72 h time points. Phosphorylated ACC-1 amounts in the untreated sample at T=0 (RE 0.46) and no L-Arg cultures (RE 0.60) were the lowest relative expression of phosphorylated ACC-1 among all samples. The ratio of phosphorylated ACC-1 to total ACC-1 was increased (P<0.0001) in the control at 24 (1.9-fold) and 72 h (1.82-fold) compared to the additions of 800 μ M L-arginine at the same time points (**Fig 2.3.35B** and C). A summary

of the impact of L-arginine concentration on ACC-1 protein expression and phosphorylation with culture time is reported in **Figure 2.3.35** below.



Cont. Com vs. 800 μM	ns	ns	**	ns	****	****
Cont. Com vs. No L-Arg	ns	****	****	ns	****	****
400 μM vs. 800 μM	ns	ns	ns	ns	**	****
400 μM vs. No L-Arg	ns	****	****	ns	****	****
800 μM vs. No L-Arg	ns	****	****	ns	****	***

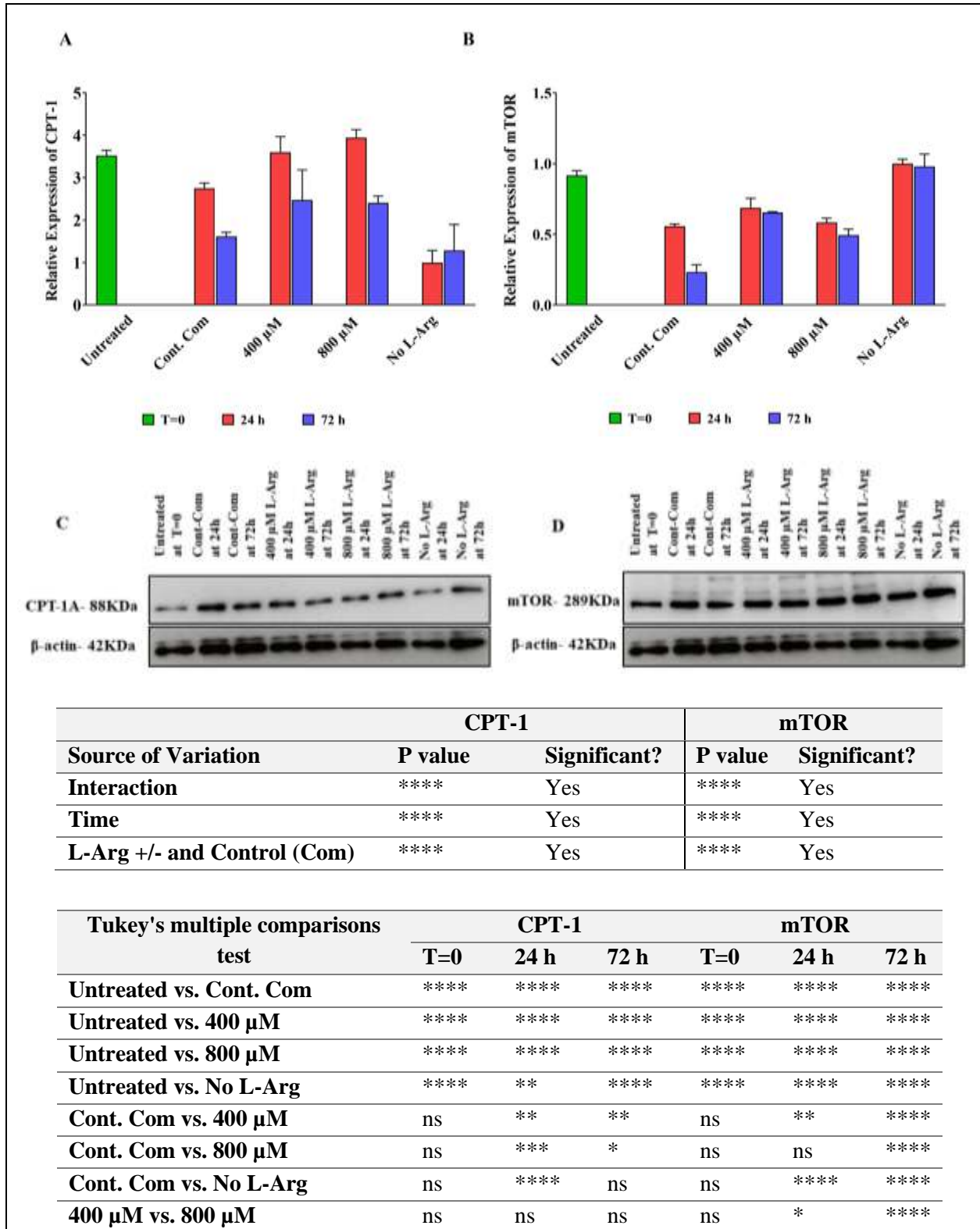
Figure 2.3.35. Relative protein expression and a western blot across concentration with time for ACC-1 protein and ACC-1-P in 3T3 L1 cells.

Relative protein amounts for total ACC-1 (A), phosphorylated ACC-1 at Ser79 (AMPK α -P) (B), and the ratio of ACC-1-P to total ACC-1 in 3T3 L1 cells (C). An example blot image of ACC-1 and ACC-1-P across concentrations with time is shown in (D). Cells were cultured for 24 or 72 h in customized media containing 0, 400 and 800 μ M L-arginine. Controls were addition of complete DMEM or untreated samples at T=0. The same amount of total protein (10 μ g) from different culture conditions was loaded into 10% SDS–polyacrylamide gels for the separation of ACC-1 and phosphorylated ACC-1 proteins and two representative blots from each treatment group are shown with the respective to the house-keeping protein, β -actin (D). Bands in the blots were quantified by using ImageJ software and the data are normalised to β -actin and then expressed as relative to the no L-arginine SILAC DMEM (0 μ M L-arginine) control at 24 h time point. Data points represent the mean \pm SD. Error bars represent the standard deviation from the mean (n = 3). The tables summarise two-way ANOVA followed by a Tukey multiple comparison test using GraphPad Prism 9.4.1. The stars indicate the levels of significance; ns = P > 0.05, * = P \leq 0.05, ** = P \leq 0.01, *** = P \leq 0.001 and **** = P \leq 0.0001.

Investigation of carnitine palmitoyl transferase I (CPT-1) protein was also undertaken and is reported in **Fig 2.3.36A**. The protein CPT-1A, that has key role in fatty acid metabolism, was increased in L-arginine added samples compared to the control. Cultures with 400 (1.31-fold) and 800 μ M L-arginine (1.43-fold) had increased amounts (P<0.0001) CPT-1A expression at 24 h compared with the control complete DMEM cultures and after 72 h cultures grown in 400 (1.43-fold) and 800 μ M L-arginine (1.5-fold) also had increased (P<0.0001) levels of CPT-1A protein in comparison to the control. CPT-1A protein expression in complete media addition cultures were lowest at 24 (RE 2.75) and 72 h (RE 1.61) compared to the L-arginine treated samples. A summary of the impact of L-arginine concentration on CPT-1A protein expression with culture time is reported in **Figure 2.3.36A** below.

Analysis of the expression of the mammalian target of rapamycin (mTOR) protein, which is considered a master regulator and has multi-faceted roles in the cell, with changing L-arginine culture concentrations is shown in **Fig 2.3.36B**. mTOR protein expression in samples with L-arginine at 400 and 800 μ M showed little change across the time period (P<0.0001). Relative expression of mTOR protein in 400 μ M L-arginine cultures at 24 (RE 0.68) and 72 h (RE 0.65) increased (P<0.0001) compared to the control complete DMEM addition cultures at 24 (RE 0.56) and 72 h (RE 0.23). Protein expression of mTOR increased (P<0.0001) in L-arginine cultures with 400 (2.8-fold) and 800 μ M (2.1-fold) at 72 h compared to the control complete DMEM addition at 72 h. There was a noticeable change (P<0.0001) in mTOR protein expression in no L-arginine cultures at 24 (RE 1.0) and 72 h (RE 0.98) and untreated sample at T=0 (RE 0.92) time points compared to the control at 24

(RE 0.56) and 72 h (RE 0.23). A summary of the impact of L-arginine concentration on mTOR protein expression with culture time is reported in **Figure 2.3.36B** below.



400 μM vs. No L-Arg	ns	****	***	ns	****	****
800 μM vs. No L-Arg	ns	****	***	ns	****	****

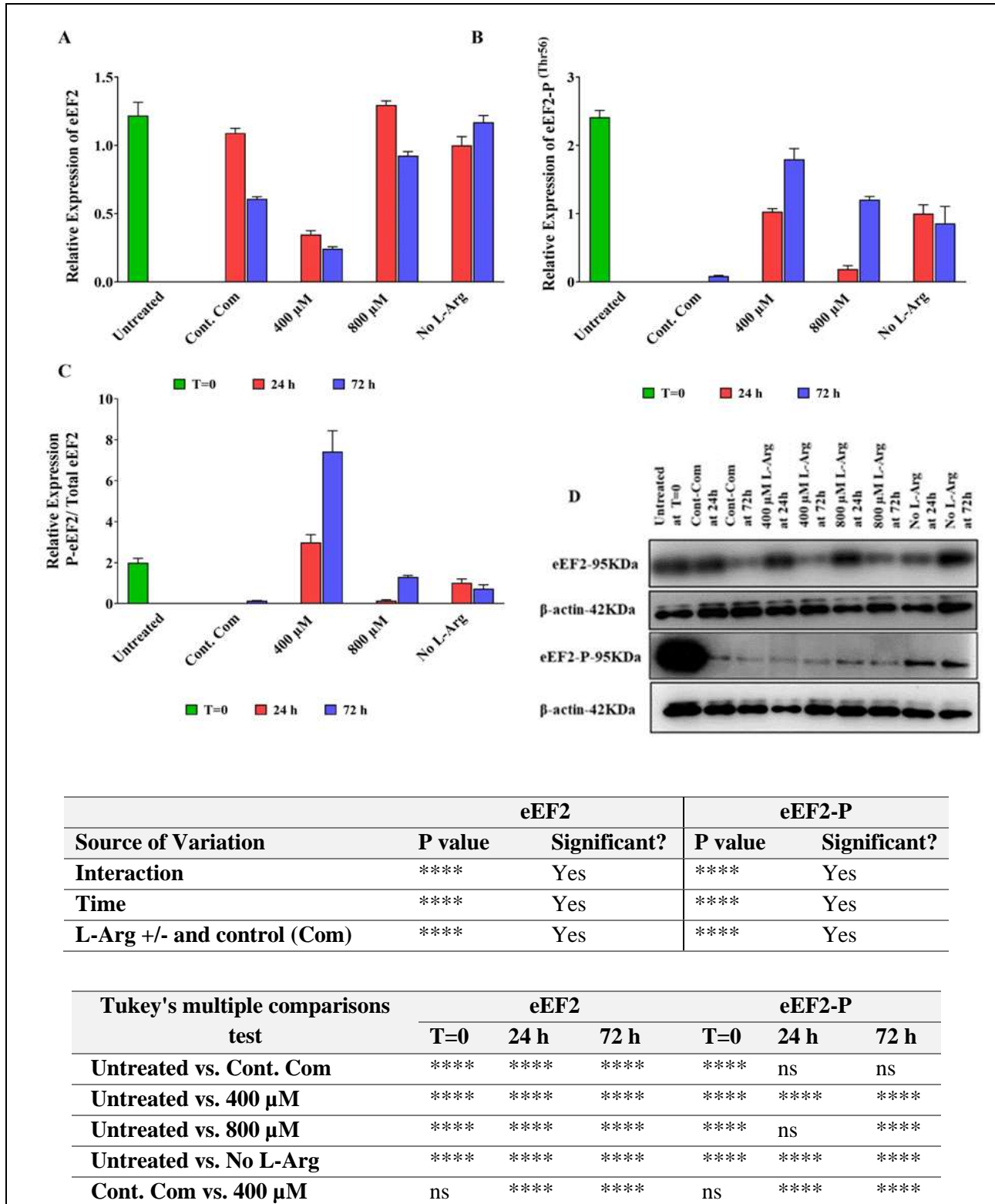
Figure 2.3.36. Relative protein expression and western blots across concentration with time for CPT-1 protein and mTOR in 3T3 L1 cells.

Relative protein amounts for CPT-1A (**A**) and mTOR (**B**) in 3T3 L1 cells and representative blot images for CPT-1A (**C**) and mTOR (**D**) across L-arginine concentrations with culture time. Cells were cultured for 24 or 72 h in customized media containing 0, 400 and 800 μ M L-arginine. Controls were addition of complete DMEM or untreated cultures at T=0. The same amount of total protein (10 μ g) from different culture conditions was loaded into 10% SDS–polyacrylamide gels for the separation of CPT-1A and mTOR proteins and two representative blots from each treatment group are shown with the house-keeping protein, β -actin (**C** and **D**). Bands on blots were quantified by using ImageJ software and the data are normalised to the house-keeping protein, β -actin and then expressed relative to the no L-arginine SILAC DMEM (0 μ M L-arginine) cultures at 24 h. Data points represent the mean \pm SD. Error bars represent the standard deviation from the mean (n = 3). The tables summarise two-way ANOVA followed by a Tukey multiple comparison test using GraphPad Prism 9.4.1. The stars indicate the levels of significance; ns = $P > 0.05$, * = $P \leq 0.05$, ** = $P \leq 0.01$, *** = $P \leq 0.001$ and **** = $P \leq 0.0001$.

Western blot analysis of the eukaryotic elongation factor 2 (eEF2) protein, an essential factor for protein synthesis, and its phosphorylated levels, was also undertaken and is shown in **Fig 2.3.37**. Increasing extracellular concentrations of L-arginine from 400 to 800 μ M had an effect on total eEF2 levels in 3T3 L1 cells. Total eEF2 protein expression was increased ($P < 0.0001$) in cells cultured in L-arginine at 800 μ M at 24 (1.2-fold) and 72 h (1.52-fold), in comparison with the control complete DMEM cultures. However, L-arginine at 400 μ M had decreased ($P < 0.0001$) protein expression of eEF2 at 24 (RE 0.35) and 72 h (RE 0.24) compared to the control at 24 (RE 1.09) and 72 h (RE 0.61) timepoints. The activity of eEF2 is reduced by phosphorylation; eEF2 phosphorylation progressively increased ($P < 0.0001$) when cells were cultured in 400 and 800 μ M L-arginine (by 21-fold and 14.1-fold, respectively) at 72 h compared to the control complete DMEM addition at the same time point. Whilst there was no detectable phosphorylated eEF2 protein in the control at 24 h time point, the phosphorylated eEF2 protein in 400 and 800 μ M L-arginine cultures at 24 h was increased (1.03-fold and 0.19-fold, respectively) in comparison to the control complete DMEM media culture at 24 h. Phosphorylated eEF2 protein level peaked ($P < 0.0001$) in untreated samples at T=0 (RE 2.4) among all samples. Phosphorylated eEF2 was increased ($P < 0.0001$) in no L-arginine added sample at 72 h (RE 0.86) in comparison to the control at 72 h (RE 0.08).

The ratio of phosphorylated eEF2 to total eEF2 increased ($P < 0.0001$) in L-arginine treated samples, 400 and 800 μ M at 72 h by 53-fold and 9.3-fold, respectively when compared to the control (**Fig 2.3.37B** and **C**). Total eEF2 protein expression and the phosphorylated eEF2 protein expression showed the opposite profile in their expression in a time dependant manner. Relative protein expression of eEF2 in L-arginine treated samples (400 and 800 μ M) was decreased with increasing culture time, whereas the phosphorylated eEF2 levels was increased. As a result, notably the ratio of phosphorylated eEF2 to total eEF2 increased ($P < 0.0001$) in arginine at 400 μ M at 24 (ratio-2.98) and 72 h (ratio-7.42) compared to the control at 24 (ratio 0) and 72 h (ratio 0.14).

A summary of the impact of L-arginine concentration on eEF2 protein expression and phosphorylation with culture time is reported in **Figure 2.3.37** below.



	eEF2		eEF2-P	
Source of Variation	P value	Significant?	P value	Significant?
Interaction	****	Yes	****	Yes
Time	****	Yes	****	Yes
L-Arg +/- and control (Com)	****	Yes	****	Yes

Tukey's multiple comparisons test	eEF2			eEF2-P		
	T=0	24 h	72 h	T=0	24 h	72 h
Untreated vs. Cont. Com	****	****	****	****	ns	ns
Untreated vs. 400 μ M	****	****	****	****	****	****
Untreated vs. 800 μ M	****	****	****	****	ns	****
Untreated vs. No L-Arg	****	****	****	****	****	****
Cont. Com vs. 400 μ M	ns	****	****	ns	****	****

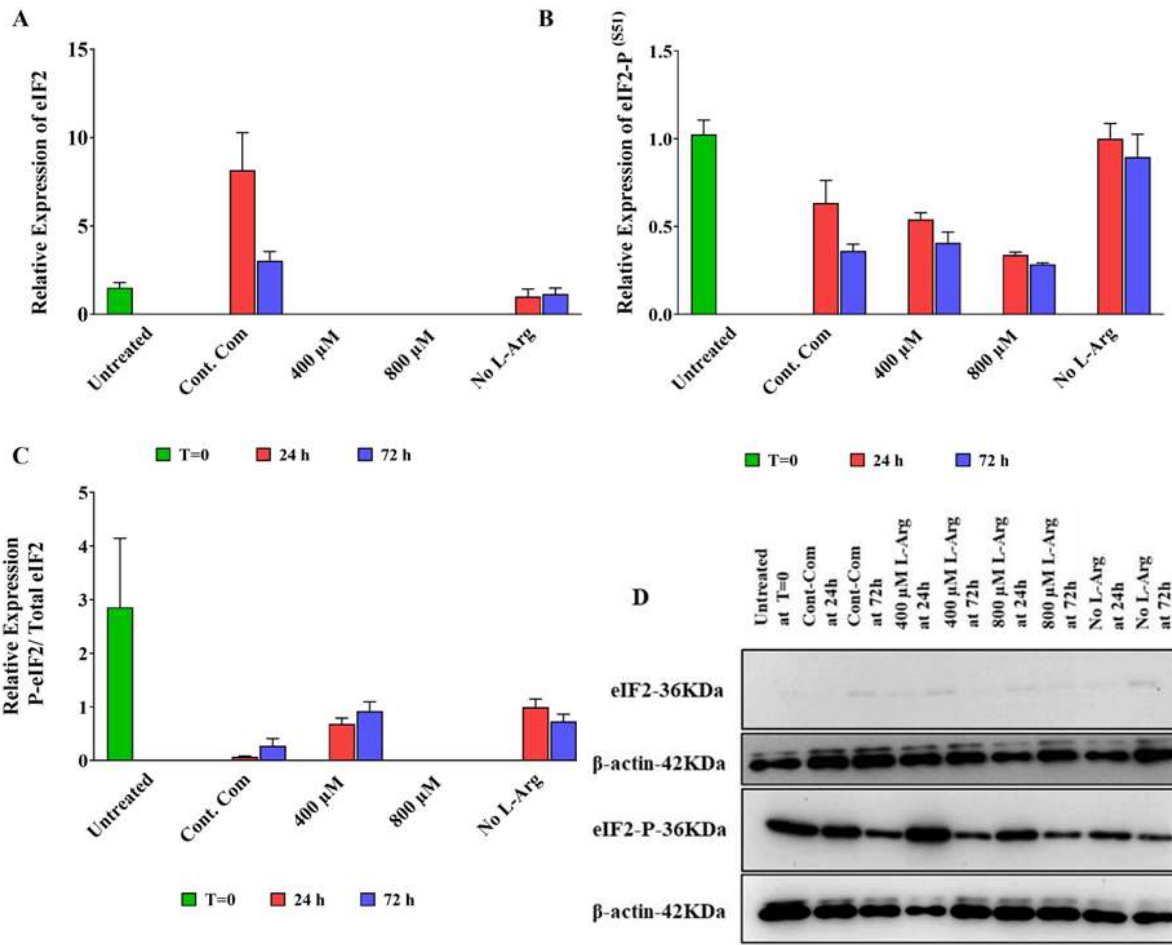
Cont. Com vs. 800 μM	ns	****	****	ns	ns	****
Cont. Com vs. No L-Arg	ns	*	****	ns	****	****
400 μM vs. 800 μM	ns	****	****	ns	****	****
400 μM vs. No L-Arg	ns	****	****	ns	ns	****
800 μM vs. No L-Arg	ns	****	****	ns	****	**

Figure 2.3.37. Relative protein expression and a western blot across concentration with time for eEF2 protein and eEF2-P in 3T3 L1 cells.

Relative protein amounts for total eEF2 (A), phosphorylated eEF2 at Thr56 (eEF2-P) (B) and the ratio of eEF2-P to total eEF2 in 3T3 L1 cells (C). A representative blot image of eEF2 and eEF2-P across L-arginine concentrations with culture time is shown (D). Cells were cultured for 24 and 72 h in customized media containing 0, 400 and 800 μ M L-arginine. Controls were addition of complete DMEM and untreated samples at T=0. The same amount of total protein (10 μ g) from different culture conditions was loaded into 10% SDS-polyacrylamide gels for the separation of eEF2 and phosphorylated eEF2 proteins and two representative blots from each treatment group are shown with the respective to the house-keeping protein, β -actin (D). Bands in blots were quantified using ImageJ software and the data are normalised to the house-keeping protein, β -actin and then expressed as relative values to the cells cultured with no L-arginine SILAC DMEM (0 μ M L-arginine) at 24 h. Data points represent the mean \pm SD. Error bars represent the standard deviation from the mean (n = 3). The tables summarise two-way ANOVA followed by a Tukey multiple comparison test using GraphPad Prism 9.4.1. The stars indicate the levels of significance; ns = P > 0.05, * = P \leq 0.05, ** = P \leq 0.01, *** = P \leq 0.001 and **** = P \leq 0.0001.

The impact of L-arginine additions on the eukaryotic translation initiation factor eukaryotic initiation factor 2 α (eIF2 α) protein was also analysed. The expression and phosphorylation of eIF2 α with culture time in different L-arginine concentrations are presented in **Fig 2.3.38**. Surprisingly and perhaps strangely, there was no detectable eIF2 α protein expression (P<0.0001) in 800 μ M L-arginine cultures at 24 and 72 h. However, the eIF2 α protein expression was observed in L-arginine at 400 μ M at 24 (RE 0.80) and 72 h (RE 0.44), but the expression was lower (P<0.0001) in comparison to the control culture at 24 (RE 9.08) and 72 h (RE 1.71).

Upon phosphorylation of the eIF2 α subunit, global translation is attenuated. At 24 h, eIF2 α protein expression in 400 (RE 0.54) and 800 μ M L-arginine (RE 0.34) cultures was lower compared to the control at 24 h (RE 0.63). Increasing extracellular concentrations of L-arginine to 800 μ M did not impact phosphorylated eIF2 α at 24 (RE 0.34) and 72 h (RE 0.28) compared to the control at 24 (RE 0.63) and 72 h (RE 0.36). However, phosphorylated eIF2 α levels increased (P<0.0001) in 400 μ M (1.13-fold) cultured cells at 72 h in comparison with the control. In contrast, protein expression of phosphorylated eIF2 α were increased (P<0.0001) and higher in 0 μ M L-arginine at 72 h (RE 0.9) and untreated samples at T=0 (RE 1.02). The ratio of phosphorylated eIF2 α to total eIF2 α protein was increased (P<0.0001) in 400 μ M L-arginine cultures at 24 (9.70-fold) and 72 h (3.36-fold) in comparison to the control. Further, the ratio between phosphorylated eIF2 α and total eIF2 α was much higher in untreated sample at T=0 (ratio-2.86) compared to the control. No L-Arg added sample at 72 h had increased (P<0.0001) ratio (2.66-fold) in comparison to the control. A summary of the impact of L-arginine concentration on eIF2 α protein expression and phosphorylation with culture time is reported in **Figure 2.3.38** below.



Source of Variation	eIF2		eIF2-P	
	P value	Significant?	P value	Significant?
Interaction	****	Yes	****	Yes
Time	****	Yes	ns	No
L-Arg +/- and control (Com)	****	Yes	****	Yes

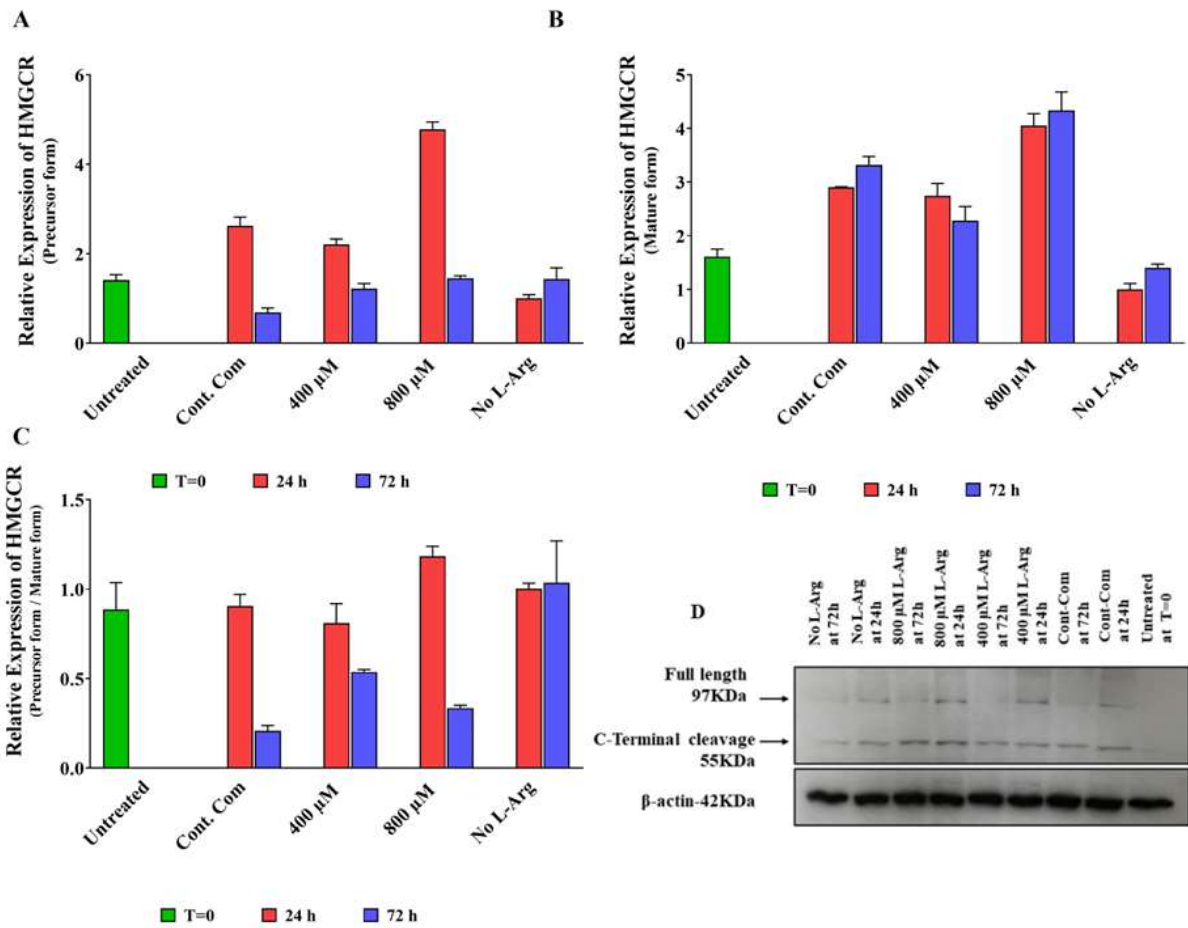
Tukey's multiple comparisons test	eIF2			eIF2-P		
	T=0	24 h	72 h	T=0	24 h	72 h
Untreated vs. Cont. Com	*	****	****	****	****	****
Untreated vs. 400 μM	*	ns	ns	****	****	****
Untreated vs. 800 μM	*	ns	ns	****	****	****
Untreated vs. No L-Arg	*	ns	ns	****	****	****
Cont. Com vs. 400 μM	ns	****	****	ns	ns	ns
Cont. Com vs. 800 μM	ns	****	****	ns	****	ns
Cont. Com vs. No L-Arg	ns	****	**	ns	****	****
400 μM vs. 800 μM	ns	ns	ns	ns	**	ns

400 μM vs. No L-Arg	ns	ns	ns	ns	****	****
800 μM vs. No L-Arg	ns	ns	ns	ns	****	****

Figure 2.3.38. Relative protein expression and a western blot across concentration with time for eIF2 α protein and eIF2 α -P in 3T3 L1 cells.

Relative protein amounts for total eIF2 α (A), phosphorylated eIF2 α at S51 (eIF2 α -P) (B) and the ratio of eIF2 α -P to total eIF2 α in 3T3 L1 cells (C). A representative blot image of eIF2 α and eIF2 α -P across L-arginine concentrations with culture time is shown (D). Cells were cultured for 24 and 72 h in customized media containing 0, 400 and 800 μ M L-arginine. Controls were addition of complete DMEM and untreated samples at T=0. The same amount of total protein (10 μ g) from different culture conditions was loaded into 10% SDS–polyacrylamide gels for the separation of eIF2 α and phosphorylated eIF2 α proteins and two representative blots from each treatment group are shown with the house-keeping protein, β -actin (D). Bands in the blots were quantified using ImageJ software and the data are normalised to the house-keeping protein, β -actin and then expressed as relative values to cells cultured with no L-arginine SILAC DMEM (0 μ M L-arginine) at 24 h. Data points represent the mean \pm SD. Error bars represent the standard deviation from the mean (n = 3). The tables summarise two-way ANOVA followed by a Tukey multiple comparison test using GraphPad Prism 9.4.1. The stars indicate the levels of significance; ns = P > 0.05, * = P \leq 0.05, ** = P \leq 0.01, *** = P \leq 0.001 and **** = P \leq 0.0001.

L-arginine regulated signalling pathways in the 3T3 L1 cells were investigated by analysing a further key and cholesterol synthesis regulator protein, HMG-CoA reductase (HMGCR). Analysis of the expression of this protein in the cultures with different L-arginine concentrations is shown in **Fig 2.3.39**. The amounts of the N-terminal membrane domain of HMGCR increased (P<0.0001) in 800 μ M (24 h; 1.8-fold and 72 h; 2.1-fold) L-arginine samples when compared to the control complete DMEM addition cultures. In cells cultured in L-arginine at 400 μ M the amount of the N-terminal membrane domain of HMGCR at 72 h (1.77-fold, P<0.0001) was also increased. The C-terminal catalytic domain of HMGCR in L-arginine at 800 μ M (24 h; 1.4-fold and 72 h; 1.3-fold) had increased (P<0.0001) expression when compared to the control complete DMEM addition cultures. However, the expression of the mature form of HMGCR was decreased in 400 μ M (24 h; RE 2.74 and 72 h; RE 2.28) in comparison to the control (24 h; RE 2.9 and 72 h; RE 3.3). Interestingly, the ratio to the precursor domain to the mature domain was increased (P<0.0001) in the samples from cultures grown in high L-arginine (800 μ M) at 24 (1.3-fold) and 72 h (1.61-fold) compared to the control. Beside these, samples cultured in 400 μ M had increased (2.58-fold, P<0.0001) ratio to the N-terminal precursor form to catalytically active C-terminal of HMGCR protein. A summary of the impact of L-arginine concentration on HMGCR protein expression with culture time is reported in **Figure 2.3.39** below.



Source of Variation	HMGCRCR (Precursor)		HMGCRCR (Mature)	
	P value	Significant?	P value	Significant?
Interaction	****	Yes	****	Yes
Time	****	Yes	****	Yes
L-Arg +/- and control (Com)	****	Yes	****	Yes

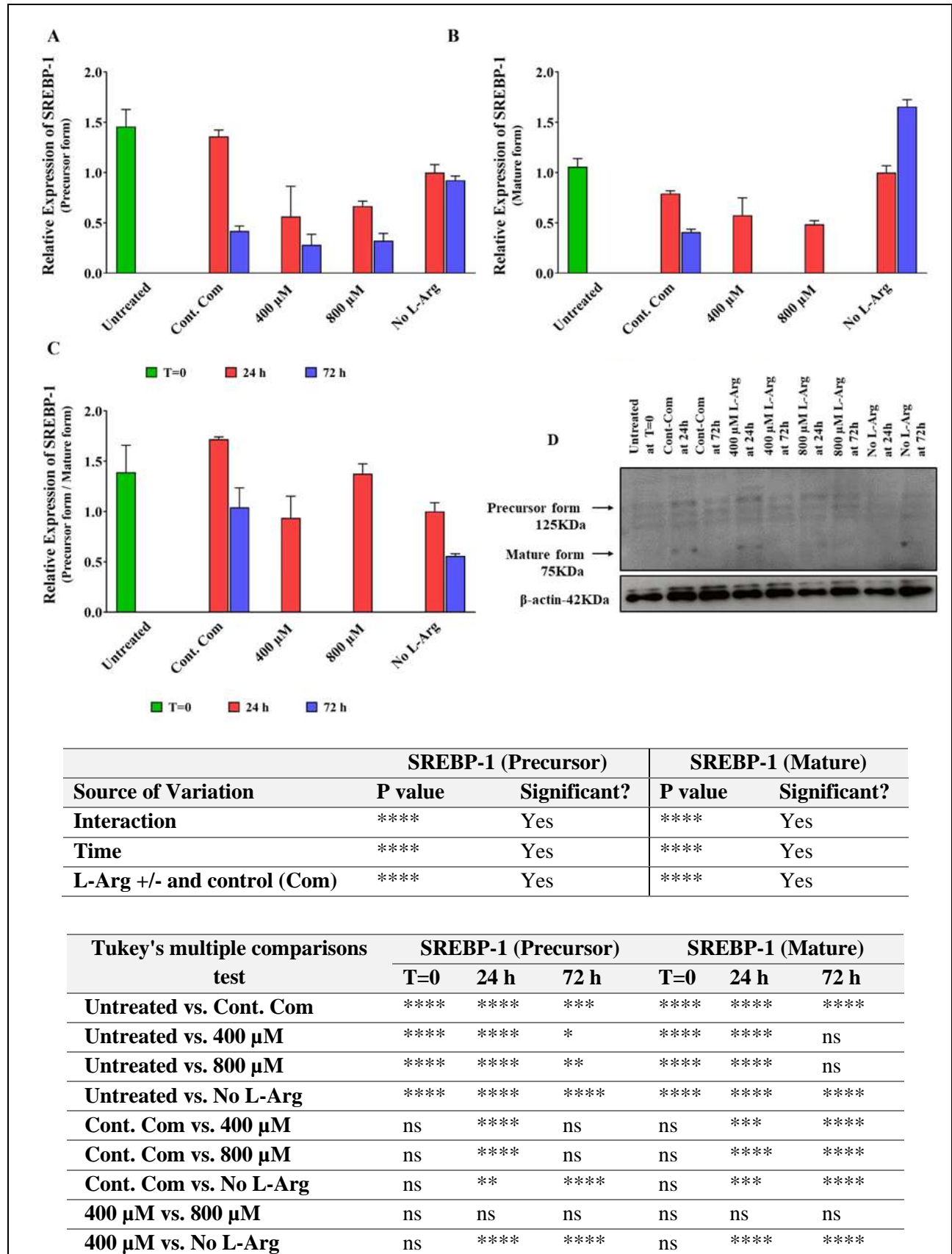
Tukey's multiple comparisons test	HMGCRCR (Precursor)			HMGCRCR (Mature)		
	T=0	24 h	72 h	T=0	24 h	72 h
Untreated vs. Cont. Com	****	****	****	****	****	****
Untreated vs. 400 μM	****	****	****	****	****	****
Untreated vs. 800 μM	****	****	****	****	****	****
Untreated vs. No L-Arg	****	****	****	****	****	****
Cont. Com vs. 400 μM	ns	***	****	ns	ns	****
Cont. Com vs. 800 μM	ns	****	****	ns	****	****
Cont. Com vs. No L-Arg	ns	****	****	ns	****	****
400 μM vs. 800 μM	ns	****	ns	ns	****	****

400 μM vs. No L-Arg	ns	****	ns	ns	****	****
800 μM vs. No L-Arg	ns	****	ns	ns	****	****

Figure 2.3.39. Relative protein expression and a western blot across concentration with time for precursor and mature of HMGCR in 3T3 L1 cells.

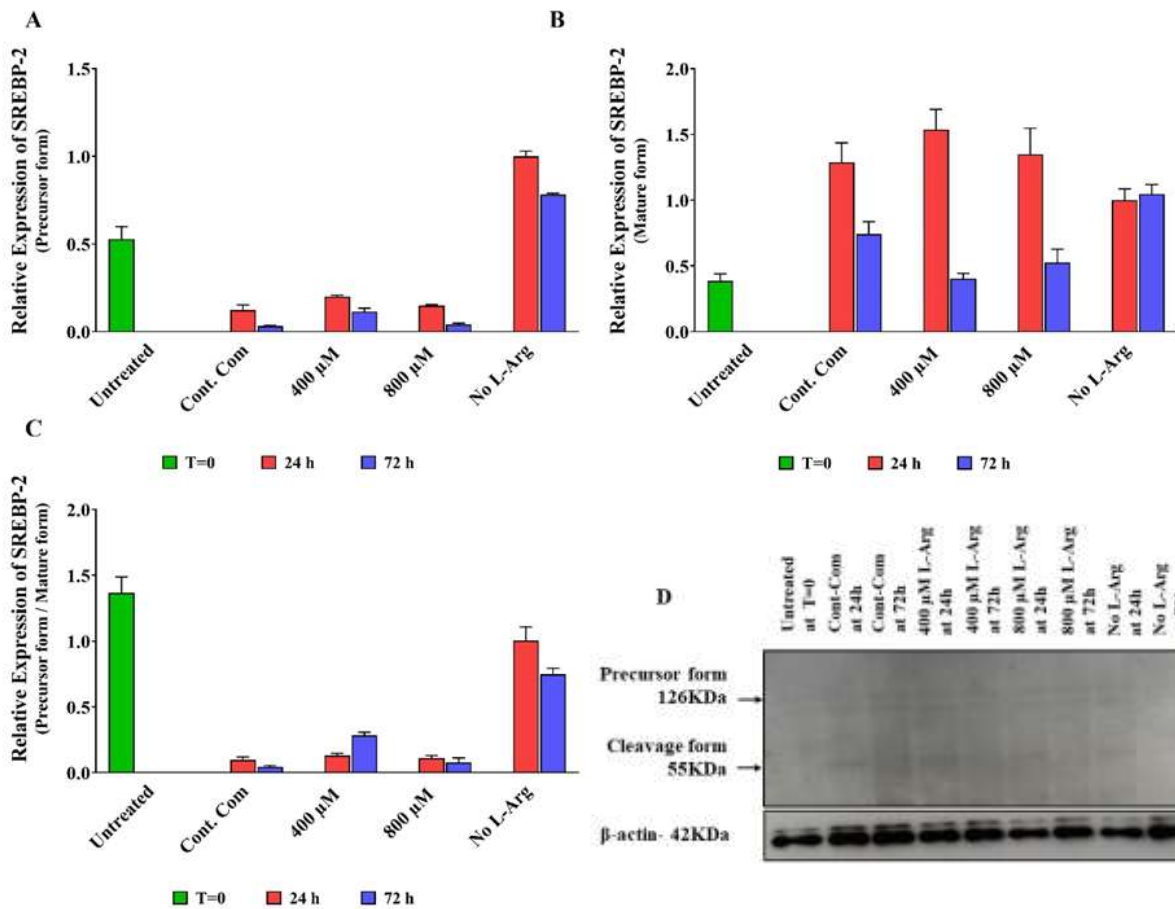
Relative hepatic lipogenic protein levels of HMGCR precursor form (upper band) (A), and HMGCR mature form (lower band) (B), and the ratio of N-terminal precursor form to catalytically active C-terminal cleavage form of HMGCR (C) in 3T3 L1 cells. A representative blot image of HMGCR across concentrations with time is shown (D). Cells were cultured for 24 and 72 h in customized media containing 0, 400 and 800 μ M L-arginine. Controls were addition of control complete DMEM and untreated samples at T=0. The same amount of total proteins (20 μ g) from different culture conditions was loaded into 10% SDS–polyacrylamide gels for the separation of HMGCR and a representative blot from each treatment group is shown with the house-keeping protein, β -actin (D). Bands in blots were quantified using ImageJ software and the data are normalised to the house-keeping protein, β -actin and then expressed as relative values to the cells cultured with no L-arginine SILAC DMEM (0 μ M L-arginine) at 24 h. Data points represent the mean \pm SD. Error bars represent the standard deviation from the mean (n = 3). The tables summarise two-way ANOVA followed by a Tukey multiple comparison test using GraphPad Prism 9.4.1. The stars indicate the levels of significance; ns = $P > 0.05$, * = $P \leq 0.05$, ** = $P \leq 0.01$, *** = $P \leq 0.001$ and **** = $P \leq 0.0001$.

Transcription factors that regulate the sterol biosynthesis; sterol regulatory element-binding proteins (SREBPs; SREBP-1 and SREBP-2) were also investigated and their analysis here is presented in **Fig 2.3.40** and **2.3.41**. When analysing catalytically inactive precursor form SREBP-1, expression was decreased ($P < 0.0001$) in cultures with 400 (24 h; 0.41-fold and 72 h; 0.67-fold) and 800 μ M (24 h; 0.49-fold and 72 h; 0.77-fold) L-arginine when compared to the control DMEM cultures at 24 and 72 h. However, expression of the precursor form at 72 h was higher in untreated sample at T=0. Samples cultured in no L-Arg showed increased (RE 0.92, $P < 0.0001$) expression of mature SREBP-1 compared to the L-Arg treated samples (400 and 800 μ M). When monitoring the catalytically active C-terminal mature form of SREBP-1, expression was decreased ($P < 0.0001$) in 400 (0.73-fold) and 800 μ M (0.61-fold) L-arginine cultures at 24 in comparison to the control at 24 h. Interestingly, the amount of the mature form of SREBP-1 decreased (almost RE 0, $P < 0.0001$) in cultures grown in the presence of L-arginine at 400 and 800 μ M at 72 h. However, the mature SREBP-1 expression was higher in untreated sample at T=0 (RE 1.06) and no L-Arg added sample at 72 h (RE 1.66). The precursor and mature forms of SREBP-1 was increased ($P < 0.0001$) in complete DMEM control samples and as a result the ratio of the catalytically inactive precursor to catalytically active mature form was also increased ($P < 0.0001$) in the control compared to 400 (1.76-fold) and 800 μ M (1.25-fold) L-arginine cultured cells leading to accumulate more precursor form in the control compared to other samples. The ratio was also higher (1.72-ratio, $P < 0.0001$) in complete DMEM control cultures at 24 h compared to the untreated T=0 cultures (1.38-raio). A summary of the impact of L-arginine concentration on SREBP-1 protein expression with culture time is reported in **Figure 2.3.40** below.



800 μ M vs. No L-Arg	ns	**	****	ns	****	****
<p>Figure 2.3.40. Relative protein expression and a western blot across concentration with time for precursor and mature of SREBP-1 in 3T3 L1 cells.</p> <p>Relative hepatic lipogenic protein levels of precursor SREBP-1 (upper band) (A), mature SREBP-1 (lower band) (B), and the ratio of catalytically inactive precursor to catalytically active mature form of SREBP-1 (C) in 3T3 L1 cells. A representative blot image of SREBP-1 across L-arginine concentrations with time is shown (D). Cells were cultured for 24 and 72 h in customized media containing 0, 400 and 800 μM L-arginine. Controls were addition of complete DMEM and untreated samples at T=0. The same amount of total protein (20 μg) from different culture conditions was loaded into 10% SDS–polyacrylamide gels for the separation of SREBP-1 and a representative blot from each treatment group is shown with the house-keeping protein, β-actin (D). Bands in blots were quantified using ImageJ software and the data are normalised to the house-keeping protein, β-actin and then expressed as relative values to the cells cultured with no L-arginine SILAC DMEM (0 μM L-arginine) at 24 h. Data points represent the mean \pm SD. Error bars represent the standard deviation from the mean (n = 3). The tables summarise two-way ANOVA followed by a Tukey multiple comparison test using GraphPad Prism 9.4.1. The stars indicate the levels of significance; ns = P > 0.05, * = P \leq 0.05, ** = P \leq 0.01, *** = P \leq 0.001 and **** = P \leq 0.0001.</p>						

The other SREBP family protein investigated was SREBP-2 (**Fig 2.3.41**). SREBP-2 protein expression was increased (P<0.0001) in its precursor and catalytic forms in additional L-arginine supplemented samples at 24 h compared to control complete DMEM cultured samples. Catalytically inactive precursor form of SREBP-2 was increased in 400 (24 h; 1.61-fold and 72 h; 3.45-fold) and 800 μ M (24 h; 1.2-fold and 72 h; 1.2-fold) L-arginine cultured samples compared to the control. When the catalytically active form of SREBP-2 was investigated, there was a change in its expression in a time dependant manner. Expression of mature form of SREBP-2 was increased (P<0.0001) in L-arginine cultures (400; 1.2-fold and 800 μ M; 1.05-fold) at 24 h, whereas decreased (P<0.0001) at 72 h (400; 0.54-fold and 800 μ M; 0.70-fold) compared to the control. Untreated sample at T=0 (RE 0.39) showed lower expression of the mature form of SREBP-2. Interestingly, the ratio of catalytically inactive precursor from to catalytically active form increased in 400 (24 h; 1.35-fold and 72 h; 6.37-fold) and 800 μ M (24 h; 1.14-fold and 72 h; 1.7-fold) L-arginine cultured cells (**Fig 2.3.41B** and **C**) compared to the control at the same time points. Noticeably, there was a higher ratio (16.7-fold) in the samples from cultures with no L-arginine addition at 72 h compared to the control at 72 h and untreated at T=0 (ratio 1.36). A summary of the impact of L-arginine concentration on SREBP-2 protein expression with culture time is reported in **Figure 2.3.41** below.



Source of Variation	SREBP-2 (Precursor)		SREBP-2 (Mature)	
	P value	Significant?	P value	Significant?
Interaction	****	Yes	****	Yes
Time	****	Yes	****	Yes
L-Arg +/- and control (Com)	****	Yes	****	Yes

Tukey's multiple comparisons test	SREBP-2 (Precursor)			SREBP-2 (Mature)		
	T=0	24 h	72 h	T=0	24 h	72 h
Untreated vs. Cont. Com	****	****	ns	****	****	****
Untreated vs. 400 μM	****	****	****	****	****	****
Untreated vs. 800 μM	****	****	ns	****	****	****
Untreated vs. No L-Arg	****	****	****	****	****	****
Cont. Com vs. 400 μM	ns	**	***	ns	*	***
Cont. Com vs. 800 μM	ns	ns	ns	ns	ns	*
Cont. Com vs. No L-Arg	ns	****	****	ns	**	**
400 μM vs. 800 μM	ns	ns	**	ns	ns	ns
400 μM vs. No L-Arg	ns	****	****	ns	****	****

800 μ M vs. No L-Arg	ns	****	****	ns	***	****
<p>Figure 2.3.41. Relative protein expression and a western blot across concentration with time for precursor and mature of SREBP-2 in 3T3 L1 cells.</p> <p>Relative hepatic lipogenic protein levels of precursor SREBP-2 (upper band) (A), mature SREBP-2 (lower band) (B), and the ratio of catalytically inactive precursor to catalytically active mature form of SREBP-2 (C) in 3T3 L1 cells. A representative blot image for a comparison of SREBP-2 across L-arginine concentrations with time is shown in (D). Cells were cultured for 24 and 72 h in customized media containing 0, 400 and 800 μM L-arginine. Controls were addition of complete DMEM and untreated samples at T=0. The same amount of total protein (20 μg) from different culture conditions was loaded into 10% SDS–polyacrylamide gels for the separation of SREBP-2 and a representative blot from each treatment group is shown with the house-keeping protein, β-actin. Bands in the blots were quantified using ImageJ software and the data are normalised to the house-keeping protein, β-actin and then expressed as relative values to the cells cultured with no L-arginine SILAC DMEM (0 μM L-arginine) at 24 h. Data points represent the mean \pm SD. Error bars represent the standard deviation from the mean (n = 3). The tables summarise two-way ANOVA followed by a Tukey multiple comparison test using GraphPad Prism 9.4.1. The stars indicate the levels of significance; ns = P > 0.05, * = P \leq 0.05, ** = P \leq 0.01, *** = P \leq 0.001 and **** = P \leq 0.0001.</p>						

2.3.8. Determination of nitric oxide / nitrite measurements by Griess Assay in 3T3 L1 cells grown in different concentrations of exogenous L-arginine

In this study the amount of nitrite, the metabolized downstream reactive product of NO accumulated in cell culture was quantified by using Griess assay. Interestingly, excess exogenous L-arginine addition increased (P<0.0001) NO synthesis in 3T3 L1 cells (**Fig 2.3.42**). The amount of NO₂⁻ present in 400 (1.4-fold) and 800 μ M (2.1-fold) L-Arg samples was high (P<0.0001) at 24 h compared to the control complete DMEM cultured samples at the same time point in 3T3 L1 cells. At 72 h, the amount of nitrite present in 400 μ M L-arginine cultured samples was increased (NO₂⁻; 4.70 μ M, 1.54-fold), whereas in 800 μ M was decreased (NO₂⁻; 1.91 μ M, 0.62-fold) in comparison to the control complete DMEM cultured sample at 72 h (NO₂⁻; 3.05 μ M). However, the amount of nitrite present in untreated samples at T=0 (NO₂⁻; 0.48 μ M) and in 0 μ M (24 h; NO₂⁻; 1.45 μ M and 72 h; NO₂⁻; 1.50 μ M) cultured samples was low regardless of the time point. It is noted that in regard to these overall findings, the amount of nitrite present in the samples was higher in L-Arg treated samples. A summary of the impact of L-arginine concentration on the amount of nitrite present (absolute concentration (A) and relative concentration (B) in the cell culture media with culture time is reported in **Figure 2.3.42**.

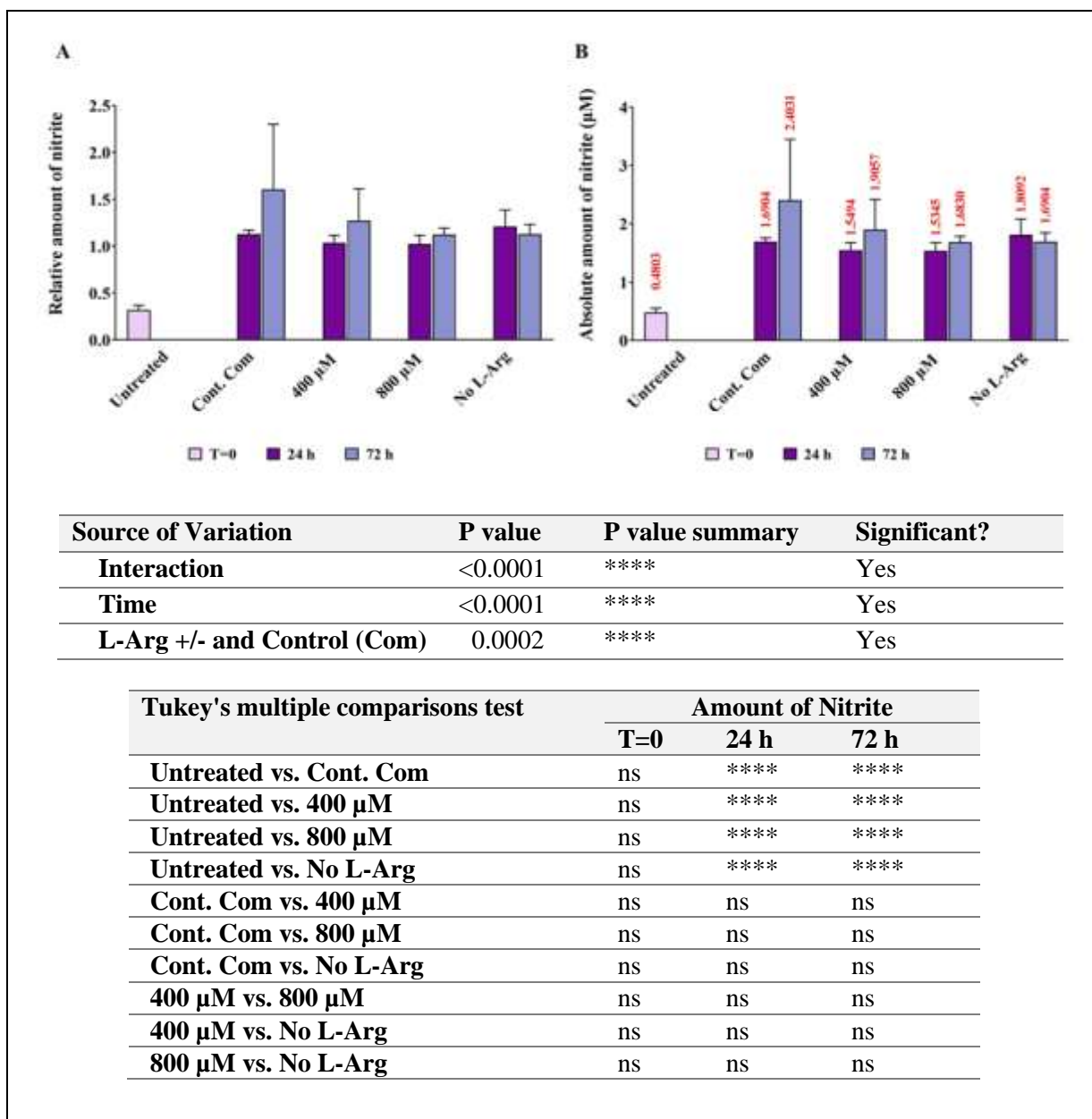


Figure 2.3.42. The effect of exogenous L-arginine concentration on nitrite production in 3T3 L1 cells.

Cell culture supernatant was obtained from cultured 3T3 L1 cells grown in the presence of 0, 400 or 800 µM L-arginine for 24 or 72 h. Controls were complete DMEM addition and untreated cell samples at T=0 as described in section 2.2.2. Cell culture supernatant (50 µL) was incubated at room temperature in the dark for 10 min sequentially with sulphanilamide solution (1% sulphanilamide in 5% phosphoric acid), which reacts with nitrite ion to form diazonium salt, which was then coupled with 0.1% (w/v) solution of NED. Finally, the coloured product was measured using a spectrometer at 540 nm to determine the nitrite concentration quantitatively. The concentration of nitrite from experimental samples was obtained using the equation of the line fitted to standard samples. The data are expressed as relative (A) and absolute (B) values. Quantified nitrite was normalised to the nitrite amount presence in cultures with no L-arginine SILAC DMEM (0 µM L-arginine) at 24 h. Data points represent the mean ± SD. Error bars represent the standard deviation from the mean (n = 3). The tables summarise two-way ANOVA followed by a Tukey multiple comparison test using GraphPad Prism 9.4.1. The stars indicate the levels of significance; ns = P > 0.05, * = P ≤ 0.05, ** = P ≤ 0.01, *** = P ≤ 0.001 and **** = P ≤ 0.0001.

2.3.9. Confirmation of the formation of the expected L-arginine, L-ornithine and L-citrulline adducts for amino acid analysis by liquid chromatography–mass spectrometry (LC-MS)

Before undertaking the amino acid analysis by HPLC, mass spectrometry was undertaken to ensure that the expected adducts were formed and detected for analysis. Primary amines in the amino acids are reacted with o-phthalaldehyde (OPA) and β -mercaptoethanol (ME) to form amino acid adducts that are then detected after separation by HPLC to determine amino acid concentrations. The expected mass and the experimental mass measured of the OPA-ME-amino acid adducts are described in **Table 2.3.1**.

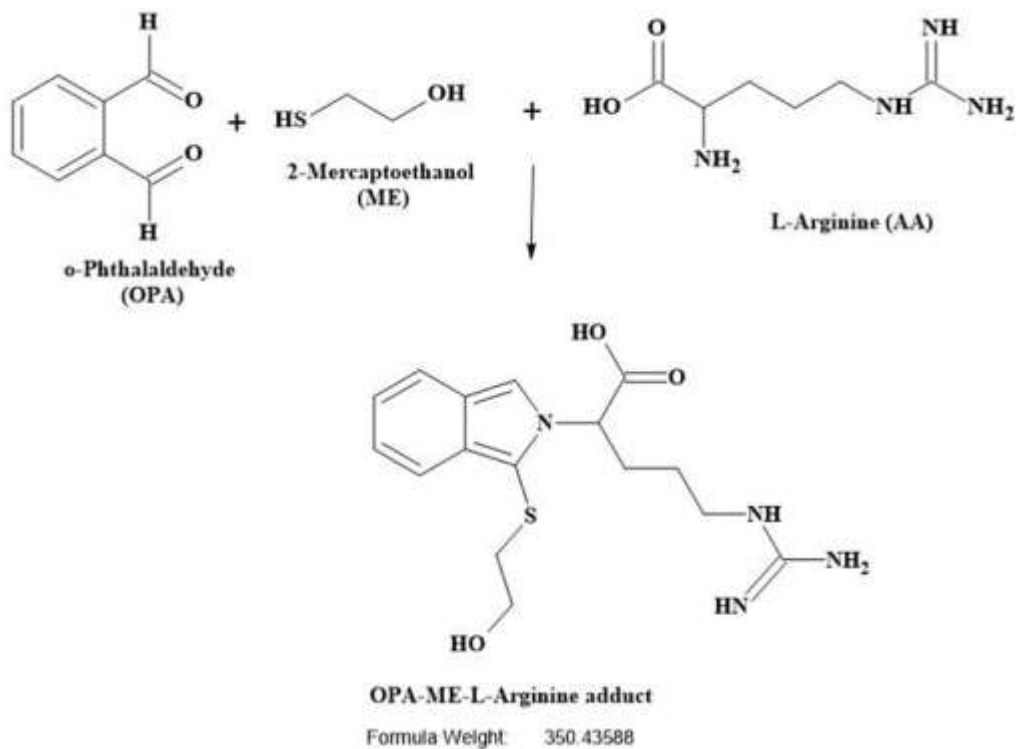
Table 2.3.1. Comparison of expected mass of the adducts with the experimental mass

Adducts	Expected mass of the adducts	Experimental mass measured in positive polarity [MH] ⁺	Experimental mass measured in negative polarity [M-H] ⁻
OPA-ME-L-arginine	350.16	351.44	349.00
OPA-ME-L-citrulline	351.19	351.40	Not determined
OPA-ME-L-ornithine	308.12	309.40	Not determined

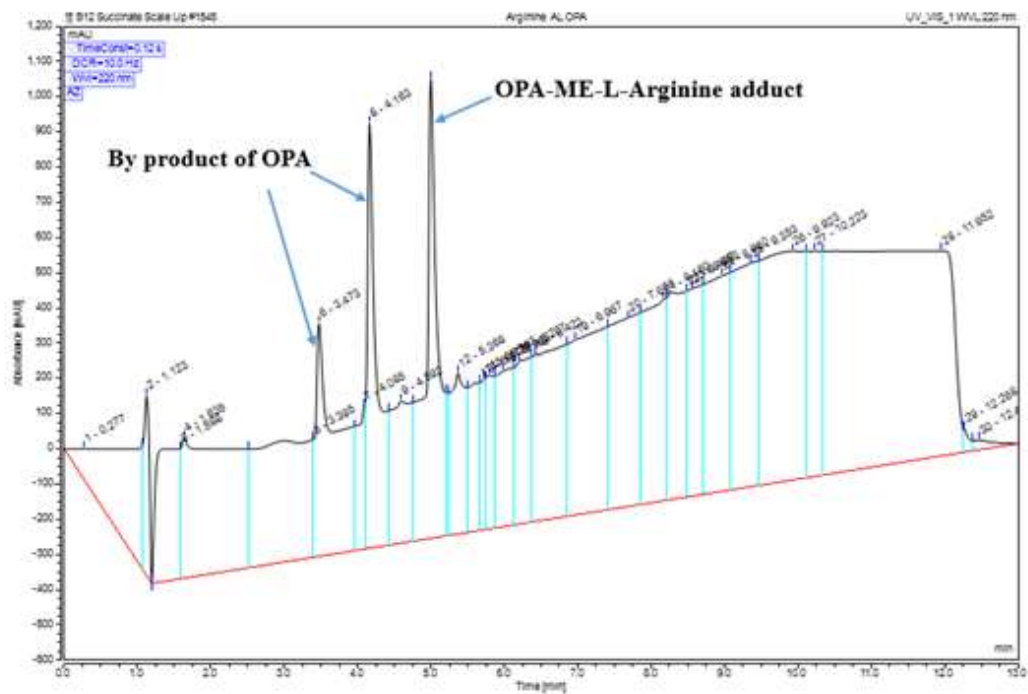
The formation of the correct L-arginine adduct was confirmed by LC-MS. In the liquid chromatography chromatogram, there were three signals observed for L-Arg and OPA; two peaks on the left (retention times 3.5 and 4.25 min) due to the OPA and by products and combination products of OPA and a signal on the right (retention time 5 min) is for the OPA-ME-L-arginine adduct (**Fig 2.3.43B**). The single peak on the right was confirmed as the formation of the expected L-arginine adduct (OPA-ME-L-Arg) by mass spectrometry (expected mass m/z 351.44 in positive polarity, **Fig 2.2.43C** and m/z 349.0 in negative polarity, **Fig 2.3.44D**).

Switching of polarity between positive polarity [MH]⁺ (**Fig 2.3.43C**, **Fig 2.3.45** and **Fig 2.3.47**) and negative polarity [M-H]⁻ (**Fig 2.3.43D**) further confirmed that the L-arginine adduct (OPA-ME-L-Arg) was formed during the pre-column-derivatization process. The formation of OPA-ME-amino acid adduct in positive polarity [MH]⁺ was confirmed for the other amino acids of interest too, L-ornithine (**Fig 2.3.44** and **Fig 2.3.45**) and L-citrulline (**Fig 2.3.44** and **Fig 2.3.47**) by LC-MS.

A



B



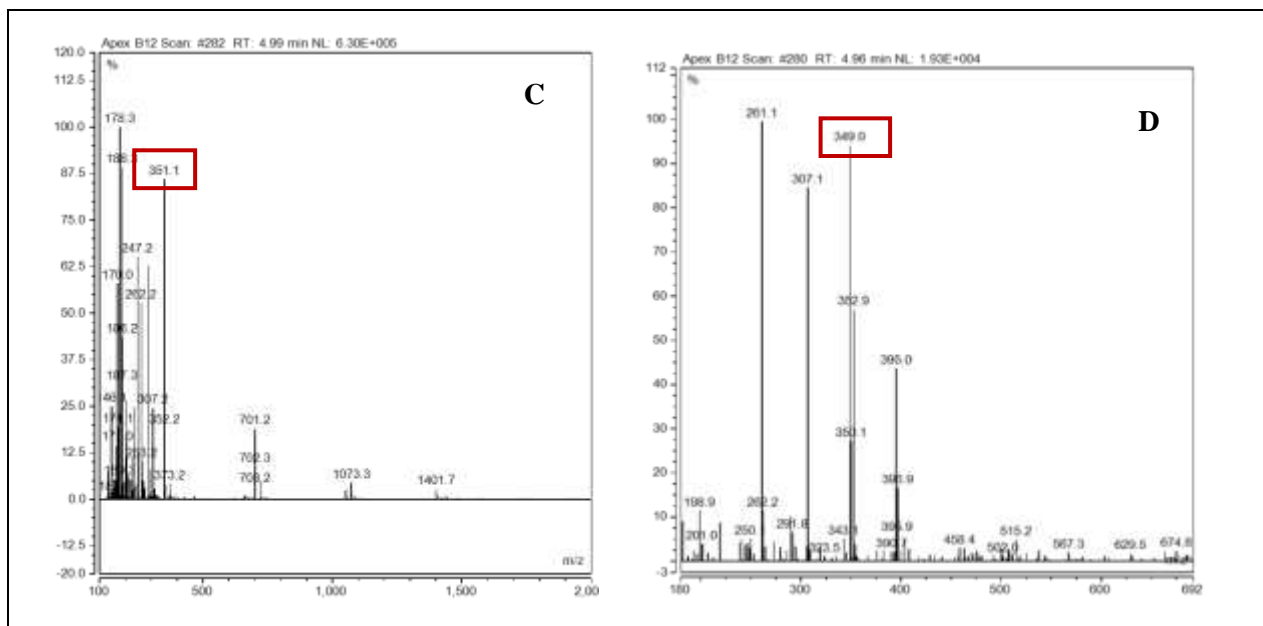


Figure 2.3.43. Schematic reaction mechanism and mass spectrum for formation of L-arginine adduct in positive polarity and negative polarity.

(A) Reaction schematic for formation of L-arginine adduct (isoindole derivative) and expected mass by reacting with the derivatizing agent OPA containing ME. (B) LC chromatogram with the signals observed for L-arginine with OPA absorbance at 220 nm. The two peaks on the left are derived from OPA and other products of OPA and the single peak on the right is for the expected OPA-ME-L-arginine adduct. (C) Mass spectra with a protonated molecule (with positive polarity $[MH]^+$) detected at a base peak at m/z 351.1 for the diagnostic fragment ion for the OPA-ME-L-arginine adduct. (D) Mass spectra with an ionized molecule (with negative polarity $[M-H]^-$) detected at a base peak at m/z 349.0 for the diagnostic fragment ion for the OPA-ME-L-arginine adduct.

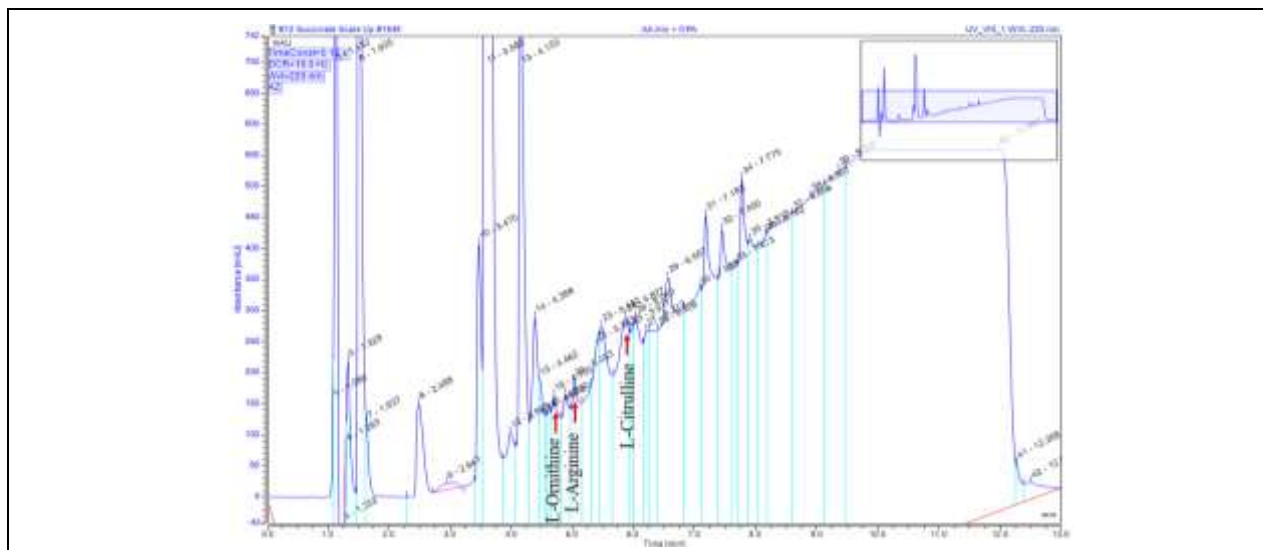


Figure 2.3.44. Liquid chromatogram for standard amino acids mix.

Liquid chromatography trace showing components present in a sample consisting of the standard amino acids mix after derivatization with OPA, and the retention time (min) and absorbance (mAU) of each peak. Mass spectra of the target amino acid adducts labelled in this LC-chromatogram are shown in the figures below.

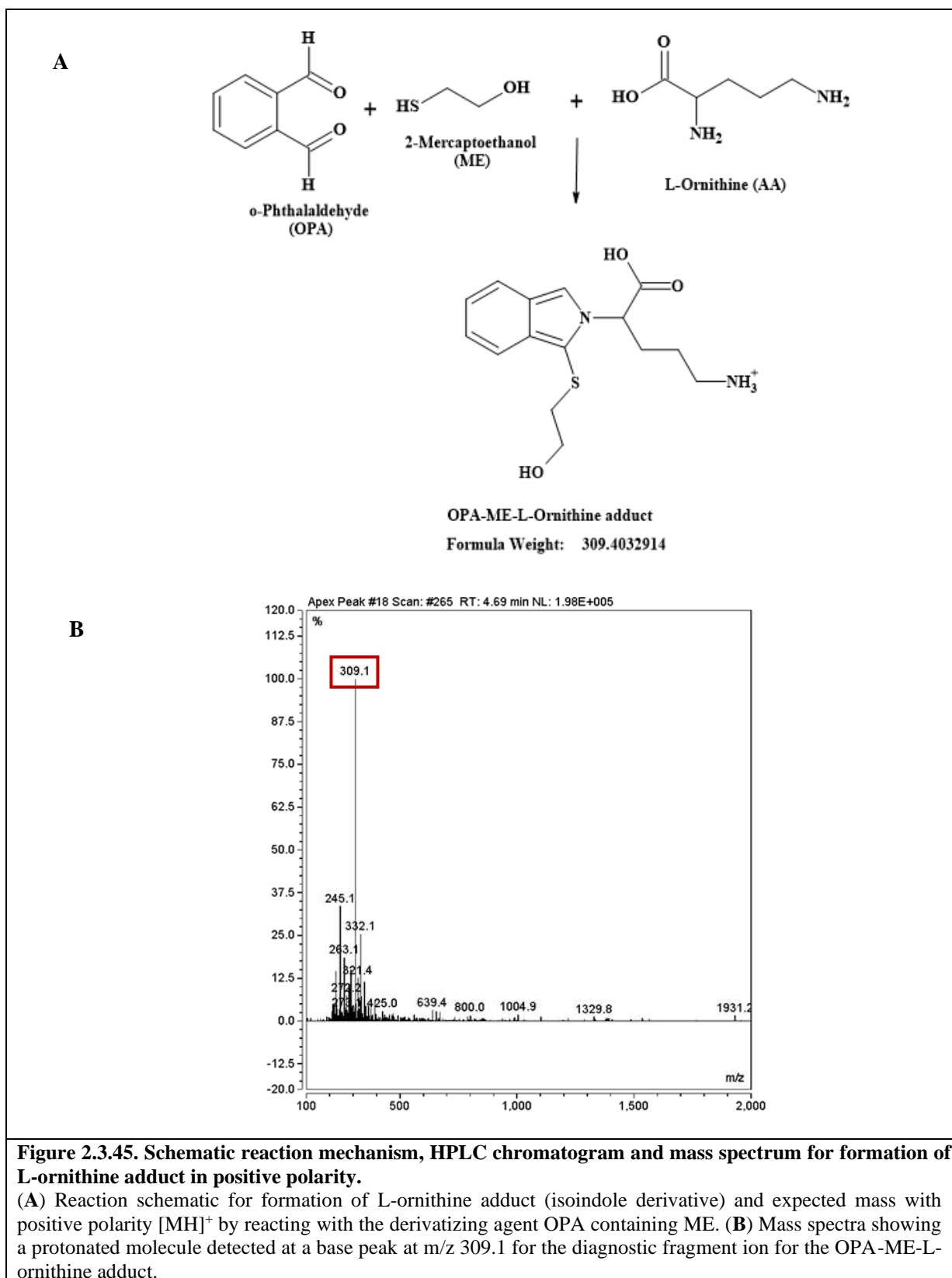


Figure 2.3.45. Schematic reaction mechanism, HPLC chromatogram and mass spectrum for formation of L-ornithine adduct in positive polarity.

(A) Reaction schematic for formation of L-ornithine adduct (isoindole derivative) and expected mass with positive polarity $[MH]^+$ by reacting with the derivatizing agent OPA containing ME. (B) Mass spectra showing a protonated molecule detected at a base peak at m/z 309.1 for the diagnostic fragment ion for the OPA-ME-L-ornithine adduct.

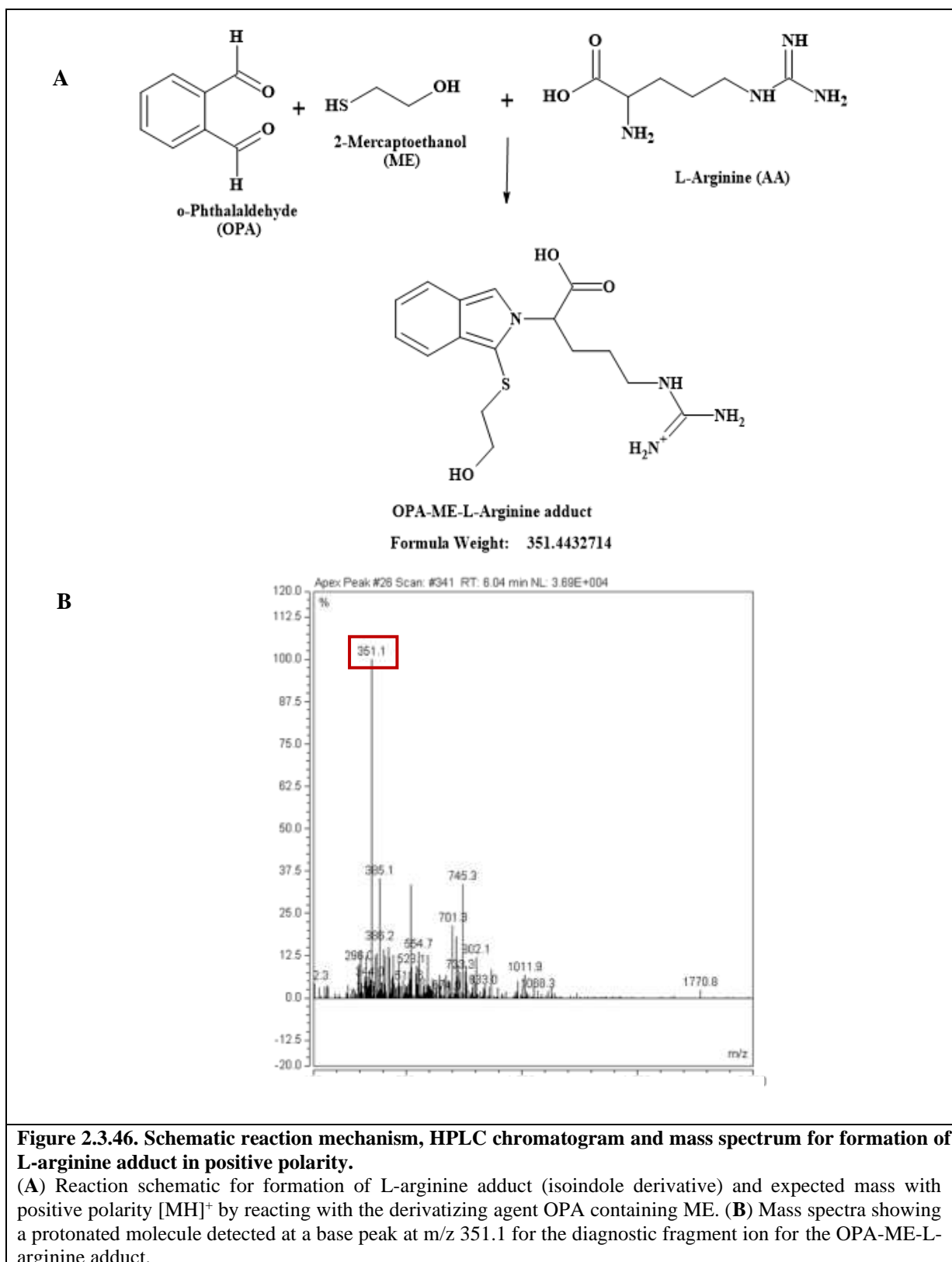


Figure 2.3.46. Schematic reaction mechanism, HPLC chromatogram and mass spectrum for formation of L-arginine adduct in positive polarity.

(A) Reaction schematic for formation of L-arginine adduct (isoindole derivative) and expected mass with positive polarity $[MH]^+$ by reacting with the derivatizing agent OPA containing ME. (B) Mass spectra showing a protonated molecule detected at a base peak at m/z 351.1 for the diagnostic fragment ion for the OPA-ME-L-arginine adduct.

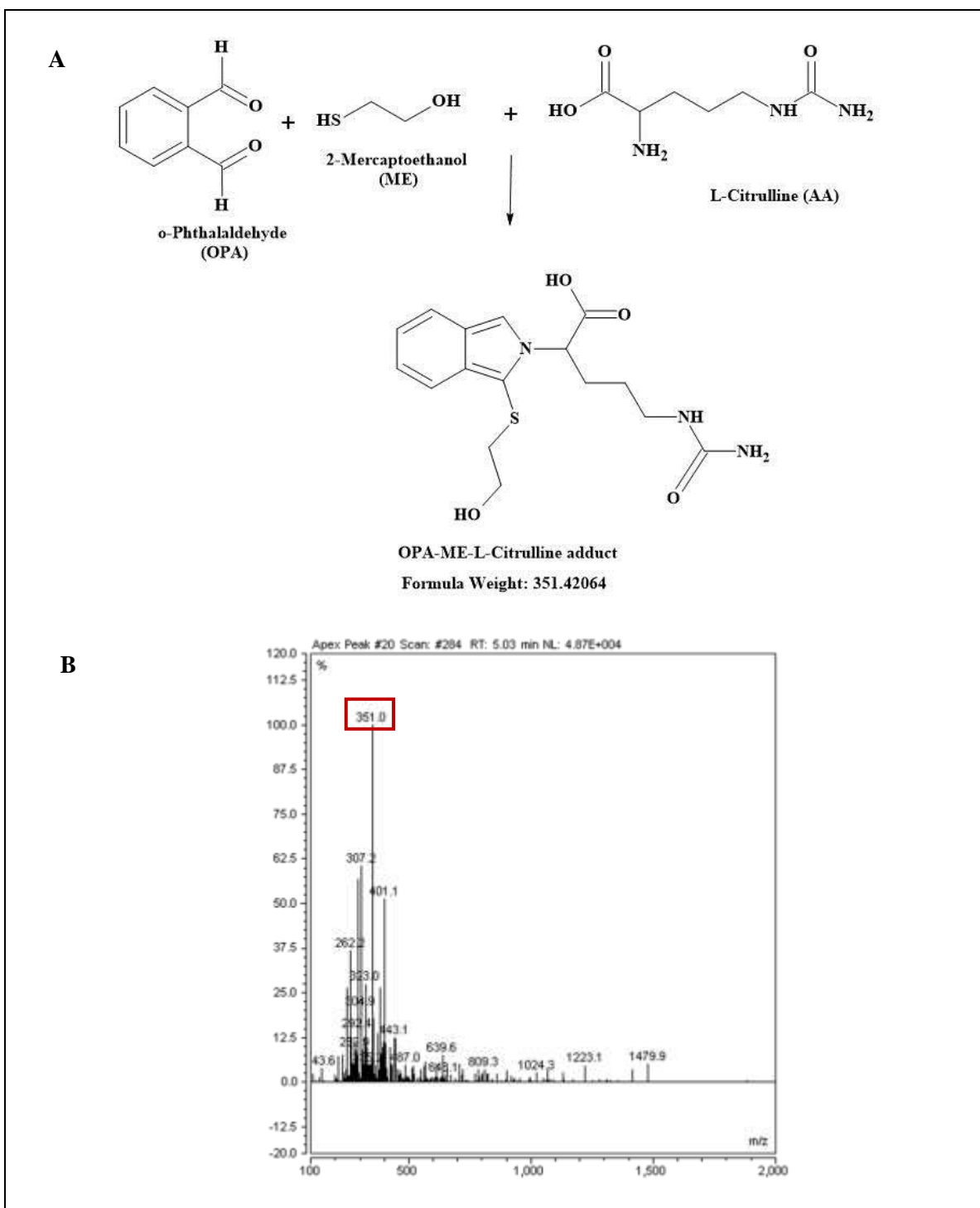


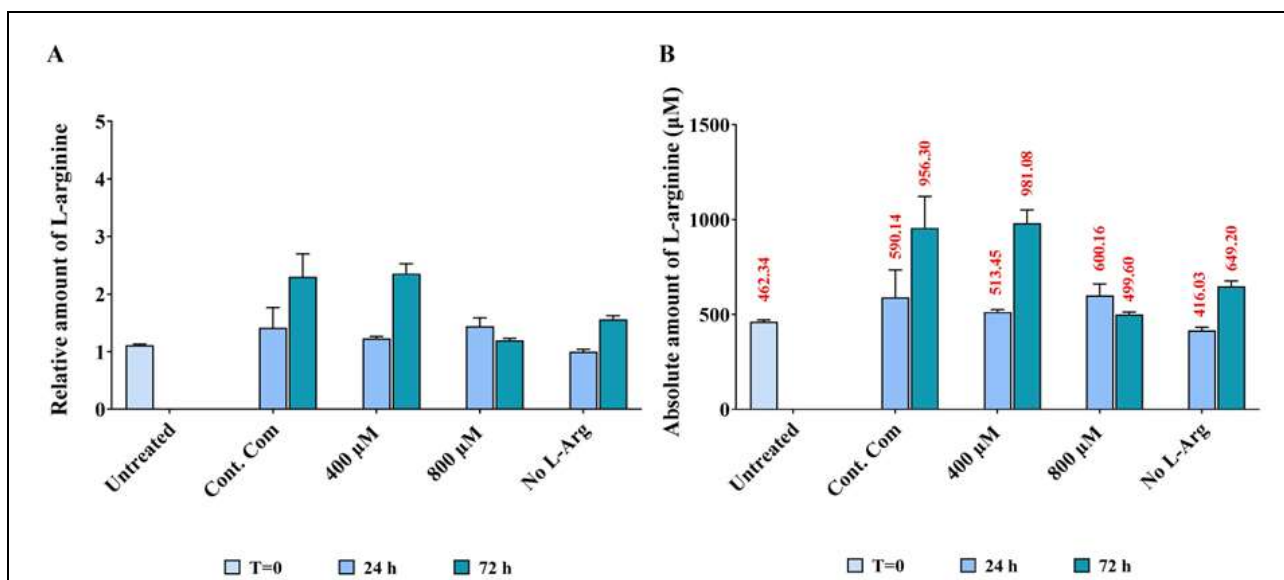
Figure 2.3.47. Schematic reaction mechanism, HPLC chromatogram and mass spectrum for formation of L-citrulline adduct in positive polarity.

(A) Reaction schematic for formation of L-citrulline adduct (isoindole derivative) and expected mass with positive polarity $[MH]^+$ by reacting with the derivatizing agent OPA containing ME. (B) Mass spectra showing a protonated molecule detected at a base peak at m/z 351.0 for the diagnostic fragment ion for the OPA-ME-L-citrulline adduct.

2.3.10. HPLC analysis of residue L-arginine, L-ornithine and L-citrulline in the cell culture media of BNL CL2 cells cultured in different initial L-arginine concentrations by HPLC

As described in the introduction chapter, L-arginine is oxidised and produces L-citrulline and NO, this pathway is catalysed by NOS. Calculated residual concentration of selected amino acids, L-Arg, L-Cit and L-Orn in experimental samples was undertaken using the equation of the line fitted for standard amino acid samples to give the absolute concentration of L-Arg, L-Cit and L-Orn (**Fig 2.3.48B, Fig 2.3.49B and Fig 2.3.50B**, respectively) present in the samples. The absolute concentration of each amino acid was then normalized to the absolute concentration of the respective amino acid present in no L-Arg cultures at 24 h to obtain the relative concentration of selected amino acids L-Arg, L-Cit and L-Orn (**Fig 2.3.48A, Fig 2.3.49A and Fig 2.3.50A**, respectively).

When investigating L-arginine present in the cultured serum samples (**Fig 2.3.48**) the amount of L-arginine increased ($P < 0.0001$) in the samples cultured in control complete DMEM (956.3 μM) and 400 μM L-arginine (981.1 μM) at 72 h time point. Cell samples cultured in no L-arginine at 72 h also showed high ($P < 0.0001$) amounts of L-arginine (649.19 μM). Arginine at 400 μM had decreased (0.87-fold, $P < 0.0001$) amount of L-arginine at 24 h but the amount was increased (1.025-fold, $P < 0.0001$) at 72 h in comparison to the control. The opposite profile was observed in samples cultured in 800 μM L-arginine, which was increased (1.017-fold, $P < 0.0001$) in the amount of L-arginine at 24 h after which this was decreased (0.52-fold, $P < 0.0001$) at 72 h compared to the control.



Source of Variation	P value	P value summary	Significant?
Interaction	<0.0001	****	Yes
Time	<0.0001	****	Yes
L-Arg +/- and Control (Com)	<0.0001	****	Yes

Tukey's multiple comparisons test	Amount of L-arginine		
	T=0	24 h	72 h
Untreated vs. Cont. Com	****	****	****
Untreated vs. 400 μM	****	****	****
Untreated vs. 800 μM	****	****	****
Untreated vs. No L-Arg	****	****	****
Cont. Com vs. 400 μM	ns	ns	ns
Cont. Com vs. 800 μM	ns	ns	****
Cont. Com vs. No L-Arg	ns	*	****
400 μM vs. 800 μM	ns	ns	****
400 μM vs. No L-Arg	ns	ns	****
800 μM vs. No L-Arg	ns	**	*

Figure 2.3.48. Relative and absolute quantification of residual serum L-Arg in BNL CL2 cells cultured in different L-Arg concentrations and the control for 24 and 72 h.

Relative (A) and absolute (B) residue amount of L-Arg analysed in plasma samples of BNL CL2 cells cultured in different amount of L-Arg (0, 400 and 800 μM) and the control complete DMEM media after 24 and 72 h. Untreated cultures at T=0. Data points represent the mean ± SD of each sample. Error bars represent the standard deviation from the mean (n=3). Tables summarise two-way ANOVA followed by a Tukey multiple comparison test using GraphPad Prism 9.4.1. The stars indicate the levels of significance; ns = P > 0.05, * = P ≤ 0.05, ** = P ≤ 0.01, *** = P ≤ 0.001 and **** = P ≤ 0.0001.

When analysing L-citrulline present in the different cultured conditions (Fig 2.3.49), surprisingly, untreated sample at T=0 showed the highest amount of L- citrulline (85.96 μM) (P<0.0001) among all samples. The

second highest amount of L-citrulline was in samples cultured in control complete DMEM at 24 h (4.74 μM) and no L-arginine added at 72 h (4.73 μM). More or less the same amount of L-citrulline ($P < 0.0001$) was present in 400 and 800 μM L-arginine samples across culture. The control had a high amount of L-citrulline ($P < 0.0001$) compared to the L-Arg treated samples cultured in 400 and 800 μM at 24 (0.79-fold and 0.62-fold, respectively) and 72 h (0.97-fold and 0.74-fold, respectively).

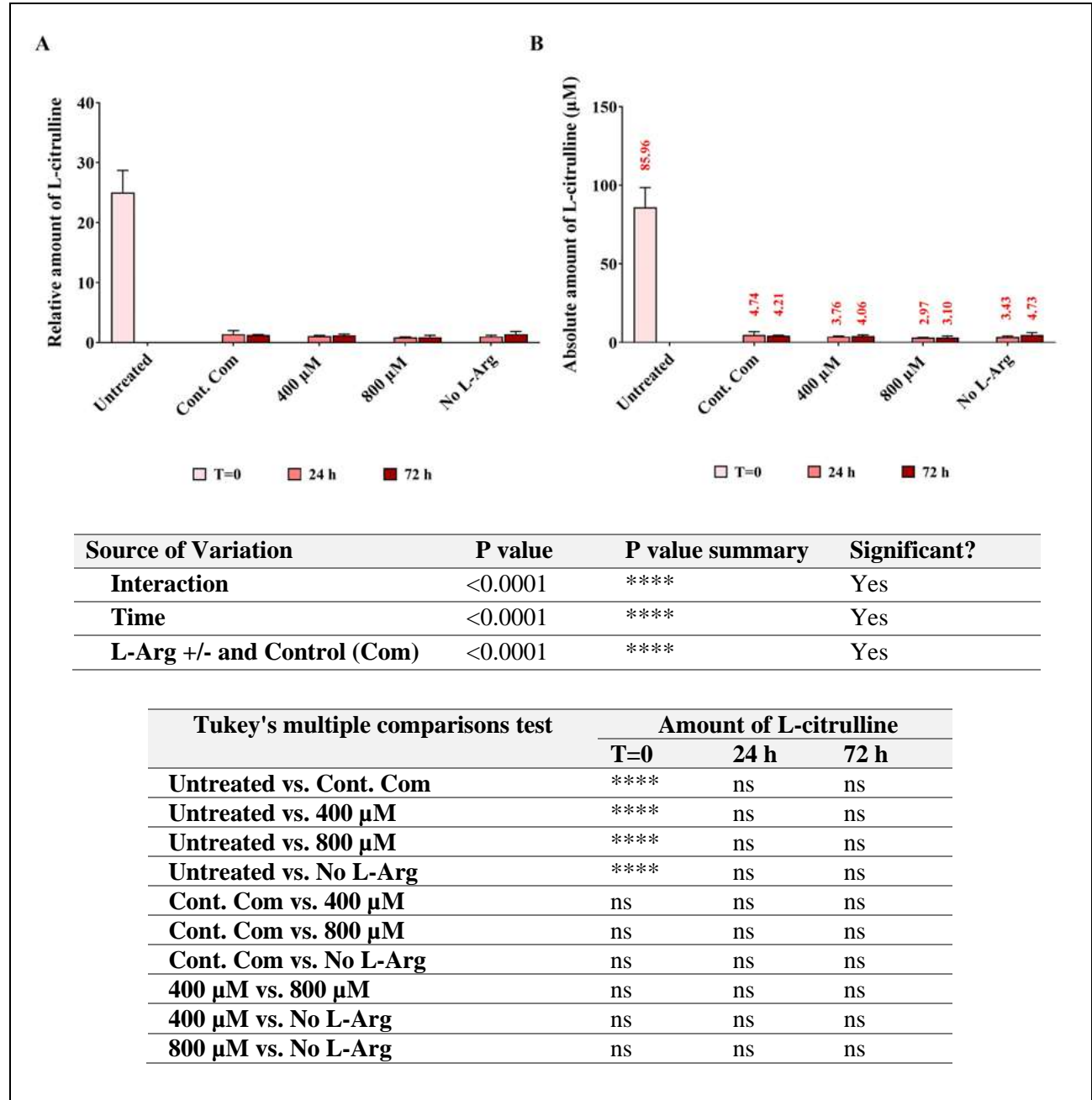
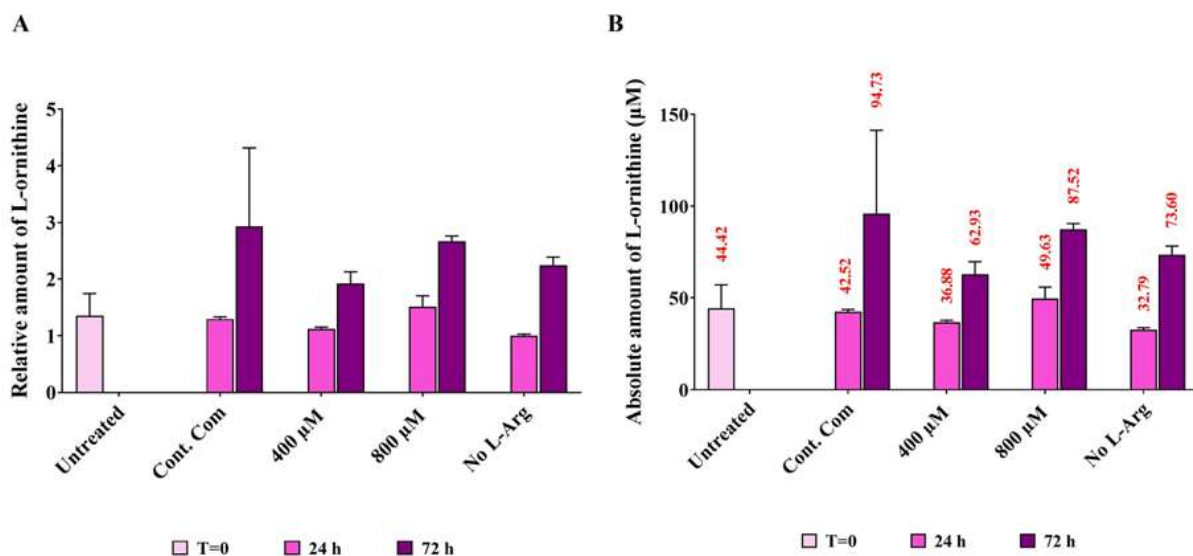


Figure 2.3.49. Relative and absolute quantification of residual serum L-Cit in BNL CL2 cells cultured in different L-Arg concentrations and the control for 24 and 72 h.

Relative (A) and absolute (B) residue amount of L-Cit analysed in plasma samples of BNL CL2 cells cultured in different amount of L-Arg (0, 400 and 800 μ M) and the control complete DMEM media after 24 and 72 h. Untreated cultures at T=0. Data points represent the mean \pm SD of each sample. Error bars represent the standard deviation from the mean (n =3). Tables summarise two-way ANOVA followed by a Tukey multiple comparison test using GraphPad Prism 9.4.1. The stars indicate the levels of significance; ns = $P > 0.05$, * = $P \leq 0.05$, ** = $P \leq 0.01$, *** = $P \leq 0.001$ and **** = $P \leq 0.0001$.

When investigating the amount of L-ornithine present in the cultured samples (**Fig 2.3.50**), there was an overall increase ($P < 0.0001$) in the amount of L-ornithine across the time points in all samples. However, the control samples cultured in complete DMEM had the highest amount of L-ornithine (44.52 μ M) ($P < 0.0001$) compared to all the samples except L-Arg at 800 μ M (24 h; 49.63 μ M) and untreated at T=0 (44.42 μ M). Samples cultured in L-arginine at 400 μ M contained decreased ($P < 0.0001$) amounts of L-ornithine at 24 (0.87-fold) and 72 h (0.655-fold). However, in samples cultured in L-Arg at 800 μ M there was increased ($P < 0.0001$) amounts of L-ornithine present at 24 (1.17-fold) and 72 h (0.91-fold). Very similar fold change (0.77-fold) was observed in the samples cultured in 0 μ M L-arginine at 24 and 72 h compared to the control at the same time points.



Source of Variation	P value	P value summary	Significant?
Interaction	<0.0001	****	Yes
Time	<0.0001	****	Yes
L-Arg +/- and Control (Com)	<0.0001	****	Yes

Tukey's multiple comparisons test	Amount of L-ornithine		
	T=0	24 h	72 h
Untreated vs. Cont. Com	**	**	****
Untreated vs. 400 µM	**	**	****
Untreated vs. 800 µM	**	***	****
Untreated vs. No L-Arg	**	*	****
Cont. Com vs. 400 µM	ns	ns	*
Cont. Com vs. 800 µM	ns	ns	ns
Cont. Com vs. No L-Arg	ns	ns	ns
400 µM vs. 800 µM	ns	ns	ns
400 µM vs. No L-Arg	ns	ns	ns
800 µM vs. No L-Arg	ns	ns	ns

Figure 2.3.50. Relative and absolute quantification of residual serum L-Orn in BNL CL2 cells cultured in different L-Arg concentrations and the control for 24 and 72 h.

Relative (A) and absolute (B) residue amount of L-Orn analysed in plasma samples of BNL CL2 cells cultured in different amount of L-Arg (0, 400 and 800 µM) and the control complete DMEM media after 24 and 72 h. Untreated cultures at T=0. Data points represent the mean ± SD of each sample. Error bars represent the standard deviation from the mean (n =3). Tables summarise two-way ANOVA followed by a Tukey multiple comparison test using GraphPad Prism 9.4.1. The stars indicate the levels of significance; ns = P > 0.05, * = P ≤ 0.05, ** = P ≤ 0.01, *** = P ≤ 0.001 and **** = P ≤ 0.0001.

2.3.11. HPLC analysis of residue L-arginine, and L-ornithine and L-citrulline in the cell culture media of 3T3 L1 cells cultured in different initial L-arginine concentrations by HPLC

The amount of L-arginine in cultured 3T3 L1 samples was also investigated by HPLC (Fig 2.3.51). L-arginine was not detectable in samples cultured in the control complete DMEM at 24 h. The amount of L-arginine decreased with culture time in 400 and 800 μM L-arginine at 24 (287.27 μM and 243.14 μM , respectively) and 72 h (159.29 μM and 206.99 μM , respectively). At 72 h, L-arginine at 400 (0.74-fold) and 800 μM (0.96-fold) had decreased in comparison to the control at 72 h. However, at time point 72 h, samples cultured with no L-Arg had increased amount of L-Arg (1.09-fold) compared to the control at 72 h.

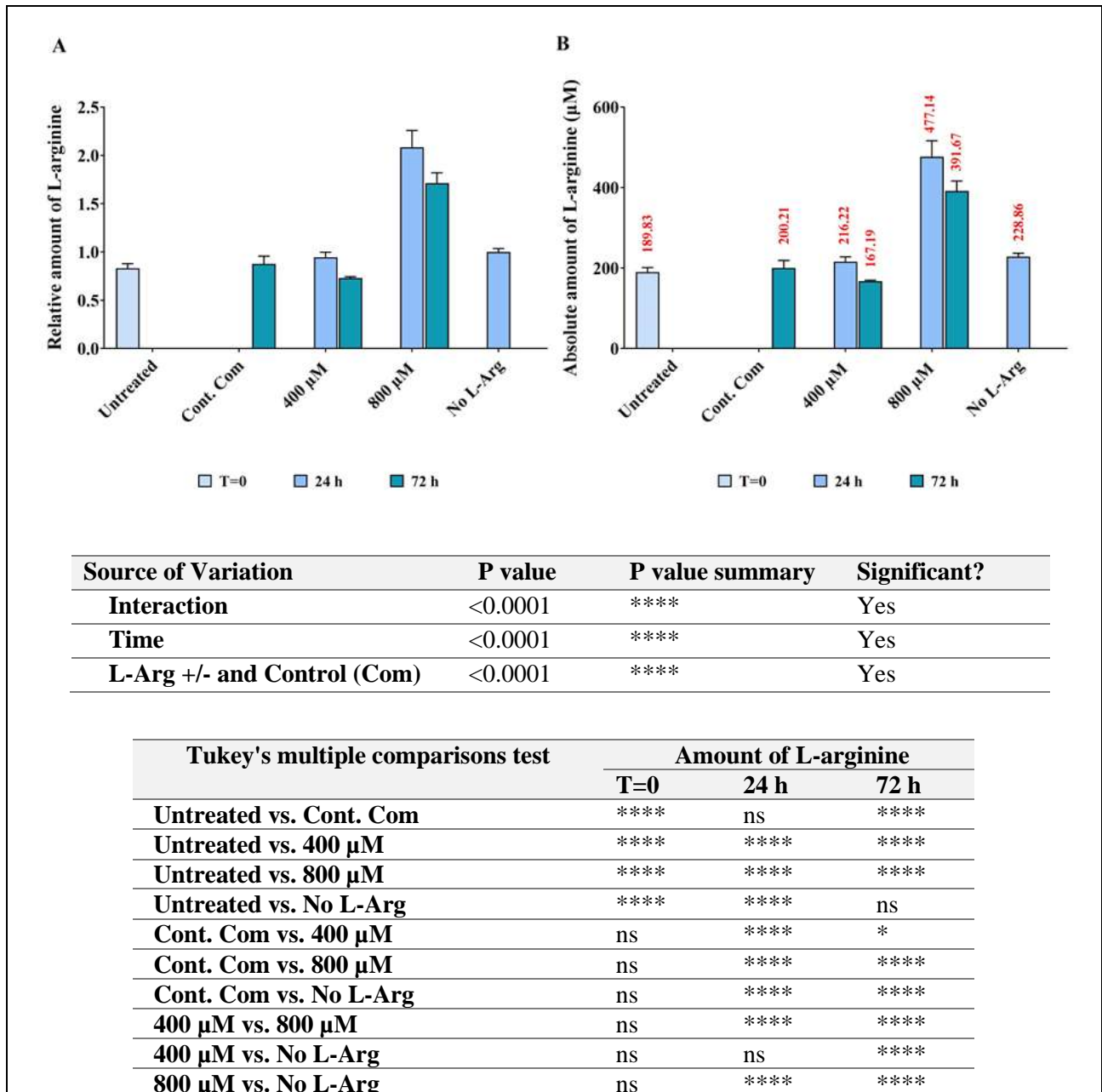


Figure 2.3.51. Relative and absolute quantification of residual serum L-Arg in 3T3 L1 cells cultured in different L-Arg concentrations and the control for 24 and 72 h.

Relative (A) and absolute (B) residue amount of L-Arg analysed in plasma samples of 3T3 L1 cells cultured in different amount of L-Arg (0, 400 and 800 μM) and the control complete DMEM media after 24 and 72 h. Untreated cultures at T=0. Data points represent the mean \pm SD of each sample. Error bars represent the standard deviation from the mean (n =3). Tables summarise two-way ANOVA followed by a Tukey multiple comparison test using GraphPad Prism 9.4.1. The stars indicate the levels of significance; ns = $P > 0.05$, * = $P \leq 0.05$, ** = $P \leq 0.01$, *** = $P \leq 0.001$ and **** = $P \leq 0.0001$.

In the investigation of L-citrulline (**Fig 2.3.52**), untreated samples at T=0 had the highest amount of L-citrulline (37.49 μM) among all samples. There was no detectable amount of L-citrulline present in some cultured samples. The amount of L-citrulline present in 800 μM L-arginine was higher (1.13-fold) compared to the control. At 24 h, there was no detectable amount of L-citrulline present in the cultured samples except for samples cultured in no L-Arg (0.26 μM).

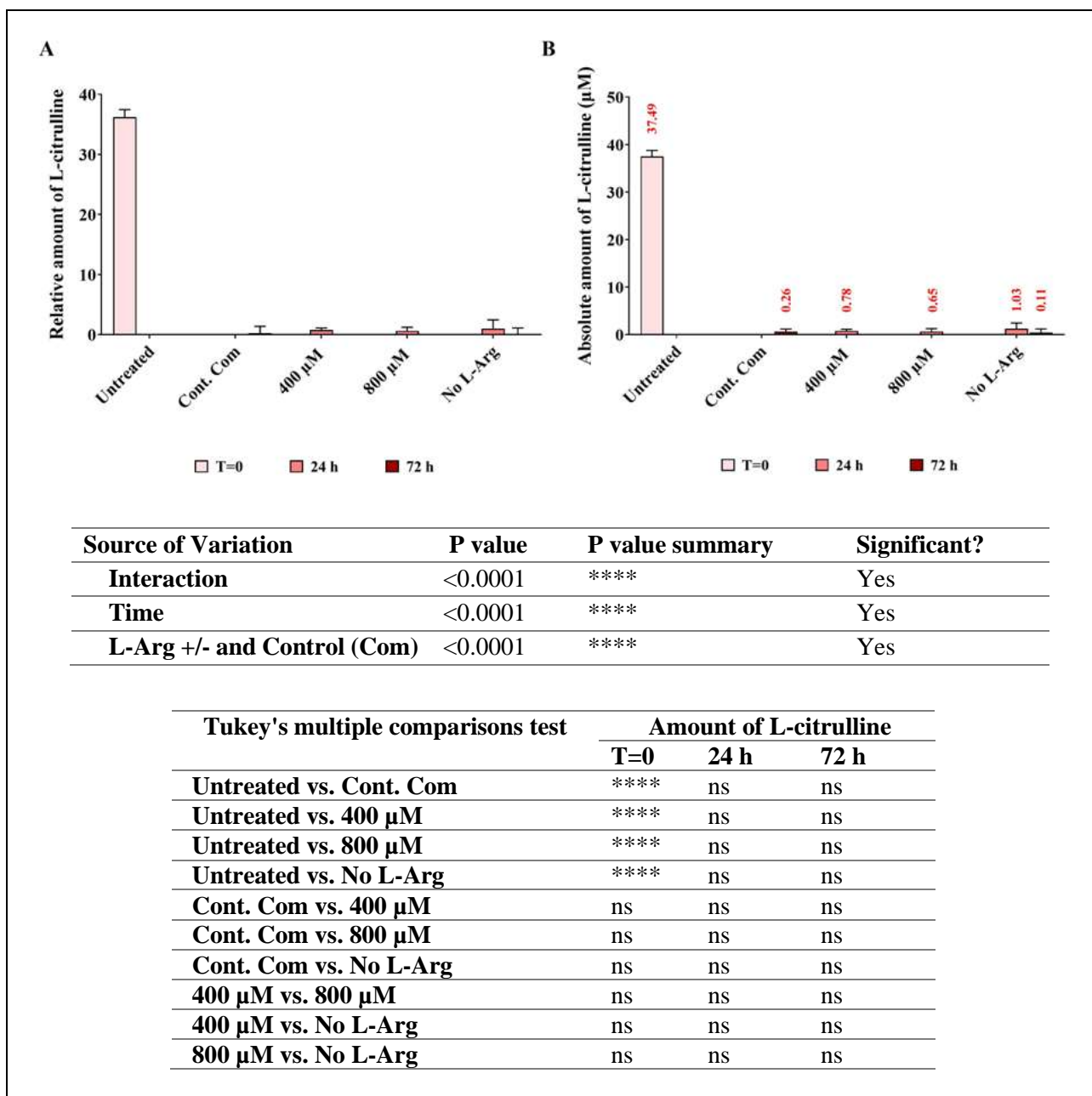


Figure 2.3.52. Relative and absolute quantification of residual serum L-Cit in 3T3 L1 cells cultured in different L-Arg concentrations and the control for 24 and 72 h.

Relative (A) and absolute (B) residue amount of L-Cit analysed in plasma samples of 3T3 L1 cells cultured in different amount of L-Arg (0, 400 and 800 µM) and the control complete DMEM media after 24 and 72 h. Untreated cultures at T=0. Data points represent the mean ± SD of each sample. Error bars represent the standard deviation from the mean (n =3). Tables summarise two-way ANOVA followed by a Tukey multiple comparison test using GraphPad Prism 9.4.1. The stars indicate the levels of significance; ns = P > 0.05, * = P ≤ 0.05, ** = P ≤ 0.01, *** = P ≤ 0.001 and **** = P ≤ 0.0001.

For the analysis of L-ornithine (Fig 2.3.53), samples cultured in 0 µM L-Arg had the highest amount of L-ornithine (49.86 µM) among all samples. The amount of L-ornithine was increased in samples cultured in L-arginine (400 and 800 µM) and the control complete DMEM across the time points. However, L-arginine at

400 (24 h; 0.27-fold and 72 h 0.76-fold) and 800 μM (24 h; 0.76-fold and 72 h 0.52-fold) contained less L-ornithine compared to the control samples cultured in complete DMEM at 24 and 72 h time points.

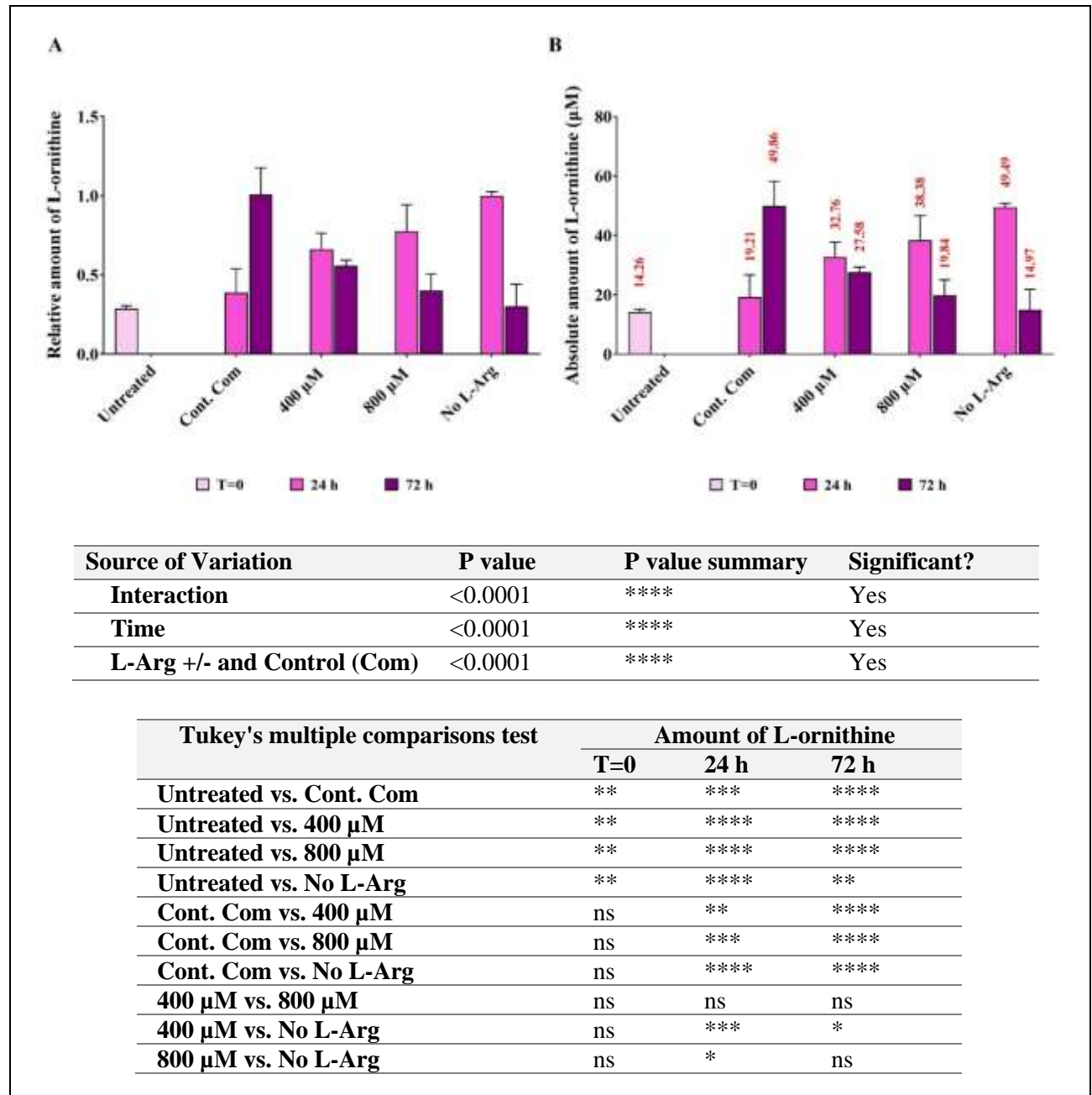


Figure 2.3.53. Relative and absolute quantification of residual serum L-Orn in 3T3 L1 cells cultured in different L-Arg concentrations and the control for 24 and 72 h.

Relative (A) and absolute (B) residue amount of L-Orn analysed in plasma samples of 3T3 L1 cells cultured in different amount of L-Arg (0, 400 and 800 μM) and the control complete DMEM media after 24 and 72 h. Untreated cultures at T=0. Data points represent the mean \pm SD of each sample. Error bars represent the standard deviation from the mean (n =3). Tables summarise two-way ANOVA followed by a Tukey multiple comparison test using GraphPad Prism 9.4.1. The stars indicate the levels of significance; ns = P > 0.05, * = P \leq 0.05, ** = P \leq 0.01, *** = P \leq 0.001 and **** = P \leq 0.0001.

2.4. Discussion

2.4.1. The impact of exogenous L-arginine supplementation on BNL CL2 cells

2.4.1.1. Impact of exogenous L-arginine on target transcripts and proteins

The L-arginine metabolic pathway and the signalling molecules involved and subsequent cellular processes impacted is detailed in the introduction chapter (**Fig 1.6.1**). In this chapter the cellular response of BNL CL2 cells to growth in different exogenous L-arginine concentrations has been evaluated. BNL CL2 cells are derived from a mouse liver and are thus an *in-vitro* cell culture model to investigate how liver cells respond to differing exogenous L-arginine concentrations. The liver plays an important role in the metabolism of L-arginine (Nijveldt *et al.*, 2004). Previous studies have reported that the ‘average’ plasma concentration of L-arginine in fed-rats is 175 μM (Wu and Morris, 2008) and therefore the initial concentrations investigated here were at a similar and higher range. Other studies have indicated that there are no adverse effects in experimental adult rats chronically administered, via enteral diets, large amounts of L-arginine (2.14 g/kg body weight⁻¹ d⁻¹) (Wu *et al.*, 2007). However, a recent review article suggests that L-arginine supplementation to different cell models within the range of 100 μM – 100 mM reflects the impact of L-arginine in the treatment of carbohydrate and lipid metabolism disorders (Szlas, Kurek and Krejpcio, 2022). Therefore, the concentrations of arginine used in this study (400 to 800 μM) are relevant to the physiological ranges found in mammals and to the nutritional and clinical concentrations impacting health and disease in mammals. It is important to note that in most cases the most prevalent impacts were observed with 800 μM culturing. The DMEM control was measured to be 250 μM . Thus, the addition of 400 μM concentrations represents a 1.6-fold increase in exogenous L-arginine whilst the addition 800 μM represents a 3.2-fold increase above the control.

Exogenous L-arginine is transported into cells. The cationic amino acid transporters y⁺L, one of the cationic amino acid transporter proteins distributed in the basolateral plasma membrane of mammalian cells, facilitates the transport of cationic amino acids such as L-arginine across the membrane. The imported L-arginine is then used as a source for protein synthesis and other catabolic reactions of L-arginine, such as the synthesis of nitric oxide (NO), urea, creatine and agmatine from arginine (Closs *et al.*, 2006). Studies have shown that increasing extracellular concentrations of L-arginine results in an increase in the intracellular concentration of L-arginine

in a dose dependent manner. For example, an *in-vitro* study in bovine aortic endothelial cells cultured in varying extracellular concentrations of arginine (0.1 to 10 mM) confirmed that increasing extracellular L-arginine produced a dose-dependent increase in intracellular arginine (Arnal *et al.*, 1995). In line with these findings, I hypothesised that exogenous L-arginine supplementation (400 and 800 μ M) of BNL CL2 cultured cells would impact intracellular signalling of L-arginine responsive pathways. To determine if this was correct, gene and protein expression of L-arginine responsive pathways were examined to explore the molecular mechanisms and cellular responses in BNL CL2 cells as a model.

In order to determine the impact of different exogenous L-arginine concentrations on the liver derived BNL CL2 cell line, target mRNA, protein and protein post-translational modifications were monitored in L-arginine responsive pathways. The key downstream target of the L-arginine/NO metabolic pathway, AMPK, increased at the transcript level (RE 3.29; $P < 0.0001$) when cells were cultured in L-arginine concentrations of 800 μ M compared to that observed in control complete DMEM media cultured samples at 24 h. The expression of AMPK is known to have specificity to tissue and localization within cells (Afinanisa, Cho and Seong, 2021). However, exposure of human umbilical vein endothelial cells (HUVEC) to elevated L-arginine (100 μ M for 2 h) has been shown to be sufficient to increase overall AMPK expression by 25% when compared to controls (Mohan *et al.*, 2013). Interestingly, the profile of the impact of additional exogenous L-arginine concentrations on AMPK expression at the transcript (mRNA) and protein level was generally similar but not the same with large difference at 400 μ M after 72 h and 800 μ M at 24 h (**Fig 2.4.1**). This may reflect a time dependent link between changes in transcription before changes in protein synthesis are observed and the fact that there are a number of metabolic signalling pathways that converge and cross-talk with AMPK to coordinate responses to nutritional and hormonal signalling of the cells (Garcia and Shaw, 2017). With regard to time dependent changes, it would be interesting in future studies to determine if the drop in transcript amounts in 400 μ M cultures at 72 h resulted in a drop in protein amounts at a later time point for example. Further, in this study AMPK transcript expression was analysed by monitoring one of the catalytic subunits of AMPK isoforms; AMPK α 1. However, in protein analysis, the primary antibody for anti-AMPK detects both isoforms of AMPK α (AMPK α 1 and AMPK α 2) but does not distinguish the isoforms present in the samples. This may also account for differences between the protein and transcript data.

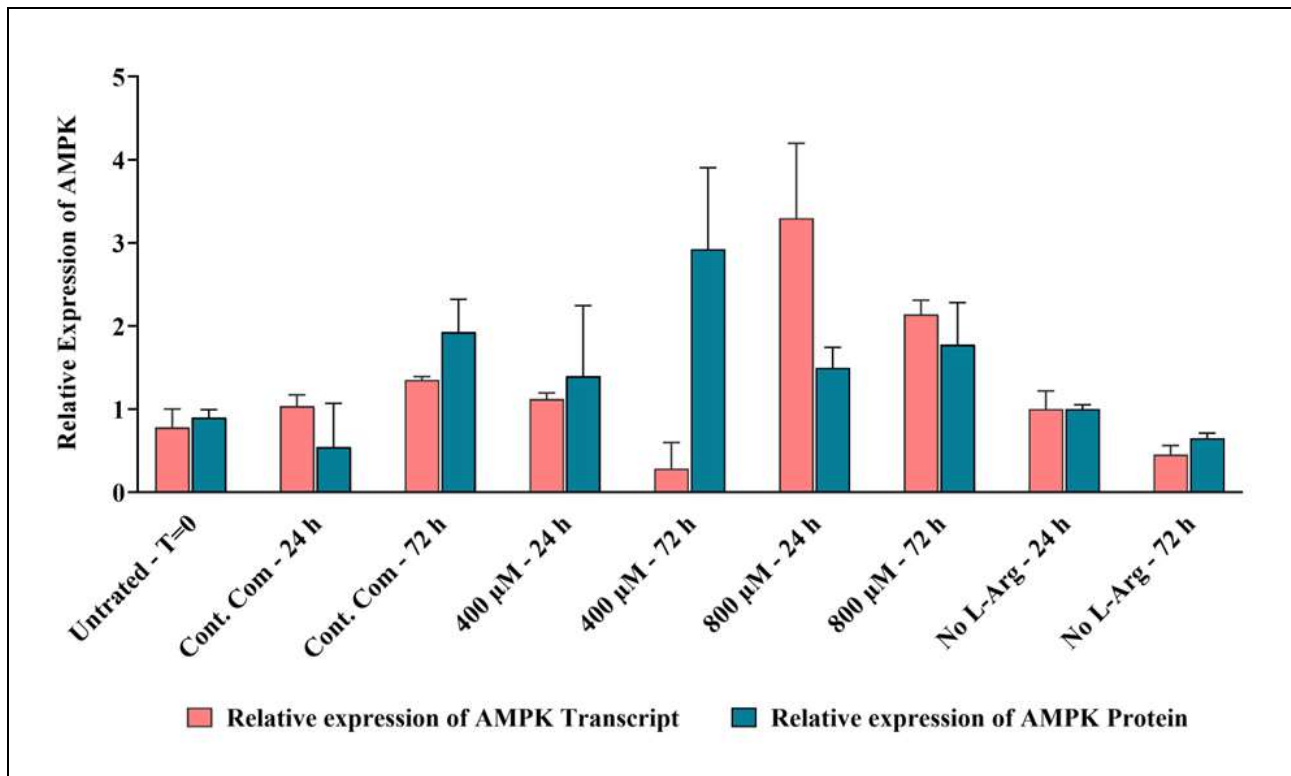


Figure 2.4.1. Comparison of relative AMPK mRNA and protein expression in BNL CL2 cells cultured in different exogenous L-arginine amounts for different times.

Relative transcript expression was maximum when culturing at 800 µM L-arginine for 24 h, whereas the relative protein expression was maximal at 400 µM L-arginine after 72 h when compared to the control complete DMEM culture time points.

In addition to AMPK protein amounts, phosphorylation was also investigated. Phosphorylated AMPK levels were increased in response to increased extracellular concentrations of L-arginine from 0 to 400 and 800 µM in a culture time dependent manner. Phosphorylation of AMPK activates AMPK and the phosphorylation status thus controls overall cellular lipid metabolism (Willows *et al.*, 2017). Activated AMPK phosphorylates its downstream target ACC-1 (Su *et al.*, 2014) and in this study the levels of phosphorylated ACC-1 in 800 µM L-arginine cultured samples at 72 h were increased by 6-fold over that of the control complete media DMEM. Phosphorylation of ACC-1 inactivates this enzyme and suppresses fatty acid synthesis. If this was the case it would be expected that the inactivation of ACC-1 via its phosphorylation would lead to an increase in the activity of CPT-1, facilitating the transport of long-chain fatty acids from the cytosol to the mitochondria for oxidation (Viollet *et al.*, 2006; Schmidt & Herpin, 1998). However, in the BNL CL2 cells, the concentrations of L-arginine investigated did not affect *CPT-1* gene expression at the mRNA transcript level and consequently there was no difference in CPT-1A protein expression in 800 µM L-arginine cultures at 72 h compared with the control (**Fig 2.4.2**). However, perhaps unexpectedly, in L-arginine cultures at 400 µM at 72 h there was an increased level of CPT-1A protein (2-fold) in comparison to the control complete DMEM cultures.

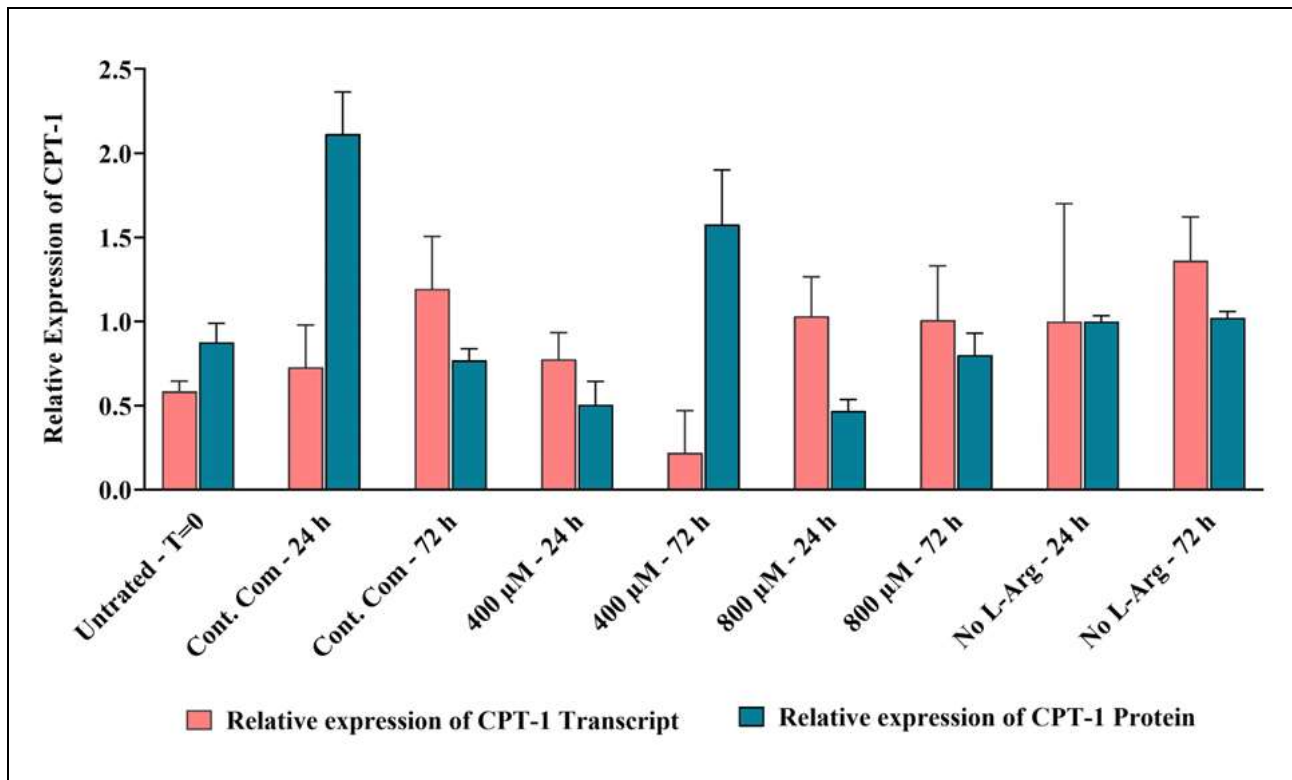


Figure 2.4.2. Comparison of relative CPT-1 mRNA and protein expression in BNL CL2 cells cultured in different exogenous L-arginine amounts for different times.

Relative transcript expression of CPT-1 was maximum when culturing at 400 and 800 μ M for 24 h in comparison to the control complete DMEM after 24 h, whereas the relative CPT-1A protein expression was maximal at 400 μ M L-arginine after 72 h over to the control after 72 h.

When the lipogenic genes ACC-1 (RE 7.46) and SREBP-1 (RE 6.76) were investigated the expression increased at the mRNA level, whereas the AMPK mRNA was lowest, in cells cultured in 400 mM L-Arg for 72 h in comparison with the complete DMEM control. The highest mRNA amounts of these lipogenic mRNAs was accompanied by increases in the respective proteins at the same time point; ACC-1 protein expression was 16-fold higher than the control and the catalytically active form of SREBP-1 was increased (1.7-fold) at the same time point (**Fig 2.4.3** and **Fig 2.4.4**). This suggests an inverse relationship between AMPK and expression of these proteins responsible for the induction of lipogenesis by the liver.

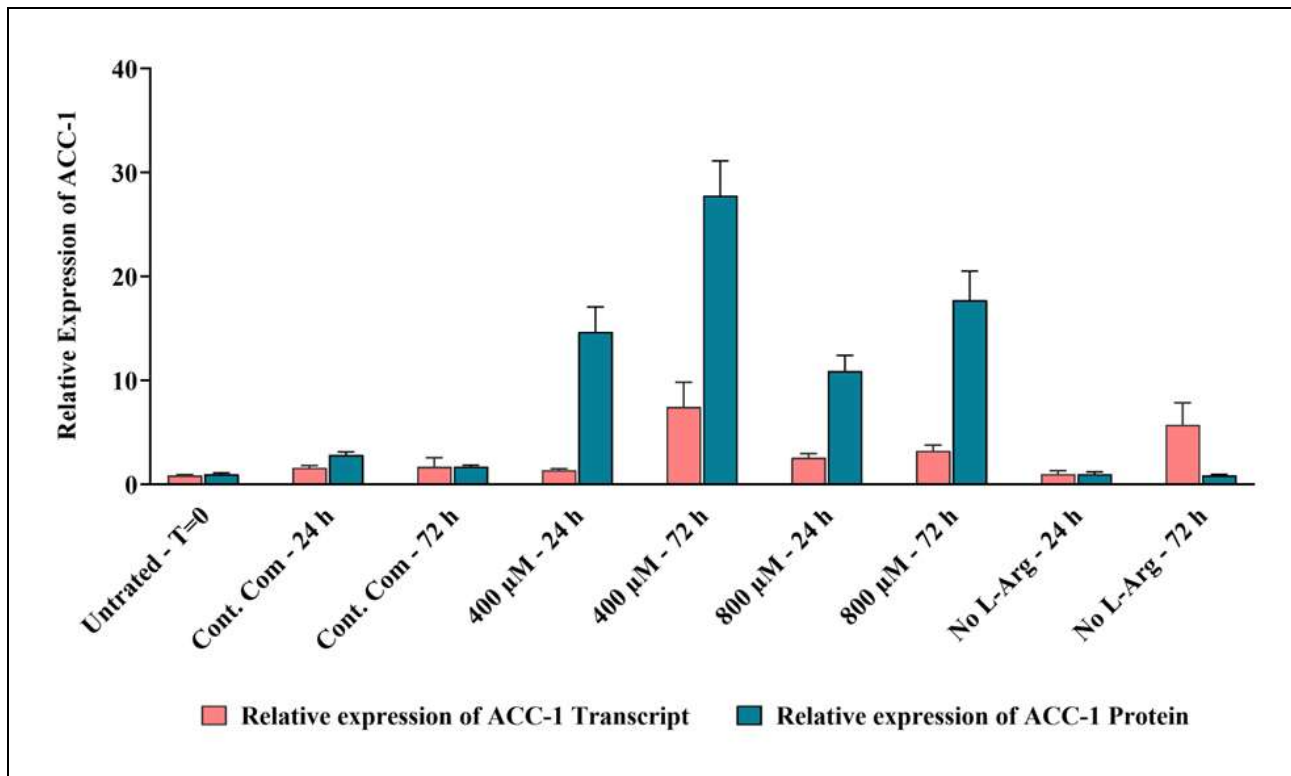


Figure 2.4.3. Comparison of relative ACC-1 mRNA and protein expression in BNL CL2 cells cultured in different exogenous L-arginine amounts for different times.

Relative transcript and protein expression of ACC-1 was maximum when culturing at 400 μ M L-arginine for 72 h, when compared to the control complete DMEM culture after 72 h.

Further investigation of the SREBP-1 mRNA expression showed that this was decreased in 800 μ M L-Arg cultures at 72 h (RE 1.60) compared to the control complete DMEM cultures (RE 2.49). On-the-other-hand, at the protein level expression of the precursor form of SREBP-1 was more or less the same as the control complete DMEM samples while the catalytically active mature form of SREBP-1 was increased (2.2-fold) over that of the control. Thus, the ratio of precursor to mature form was decreased (0.4-fold) compared to the control and there was more active mature form in the 800 μ M samples. This result suggests a post-translational mechanism explaining how the key transcription factor, SREBP-1, can rapidly control genes in the *de-novo* lipogenesis and glycolysis pathways upon perception of excess exogenous (and presumably intracellular) L-arginine. The immature SREBP-1 protein is inactive until activated by cleavage to generate the active mature transcription factor, presumably in response to elevated L-arginine amounts. Interestingly, the transcript and full length of SREBP-1 protein amounts followed the same trend in all culture conditions (Fig 2.4.4) and thus it is this post-translational processing event that is used to respond to changes in L-arginine concentrations and modulate subsequent gene expression.

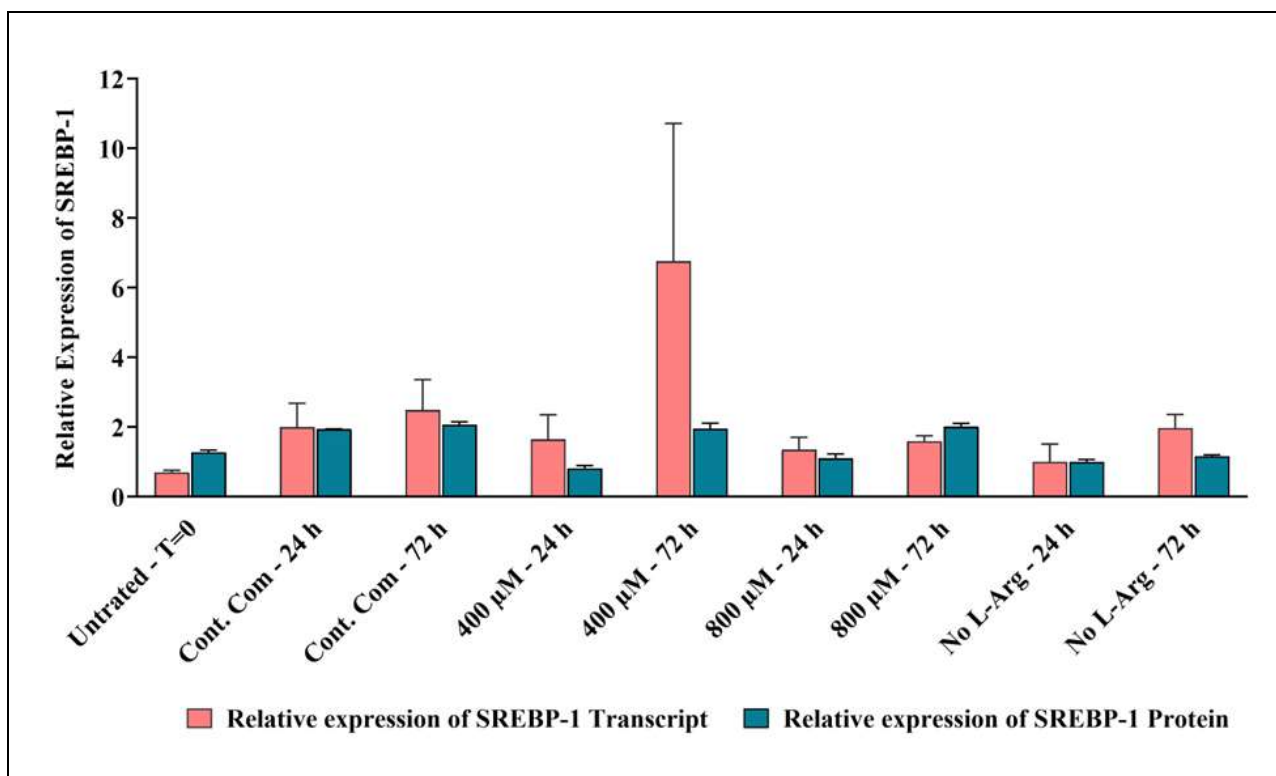


Figure 2.4.4. Comparison of relative SREBP-1 mRNA and protein expression in BNL CL2 cells cultured in different exogenous L-arginine amounts for different times.

Relative transcript expression of SREBP-1 was maximum when culturing at 400 μ M L-arginine for 72 h, whereas the relative protein expression was very similar at 400 μ M L-arginine after 72 h when compared to the control complete DMEM culture time points but SREBP-1 protein was less at 400 μ M after 24 h.

HMGCR and SREBP-2 mRNA expression decreased in response to 800 μ M L-Arg culturing after 24 h compared to the control complete DMEM culture samples while mRNA levels for AMPK, increased in 800 μ M L-Arg addition cultures at the same time point (RE 3.29) compared to the control. At the protein level, the precursor and mature form of SREBP-2 was increased (1.2-fold and 1.7-fold, respectively) in 800 μ M L-Arg cultures at 24 h compared to the control complete DMEM media at the same time point. Thus, like SREBP-1, the ratio of precursor to mature form was decreased (0.7-fold) compared to the control and more active mature protein was present. Under this same experimental condition, the amount of the N-terminal domain and catalytically active C-terminal domain of HMGCR was decreased (0.2-fold and 0.64-fold, respectively), therefore, the ratio of the N-domain to C-domain was increased (1.95-fold) in comparison to the ratio between the forms of HMGCR in the control. This ratio of SREBP-2 (and SREBP-1) forms to HMGCR forms likely balances the re-programming of lipid and sterol synthesis in the cell in response to elevated L-arginine. There was no common relationship between the transcript and protein expression of HMGCR (Fig 2.4.5) or SREBP-2 (Fig 2.4.6).

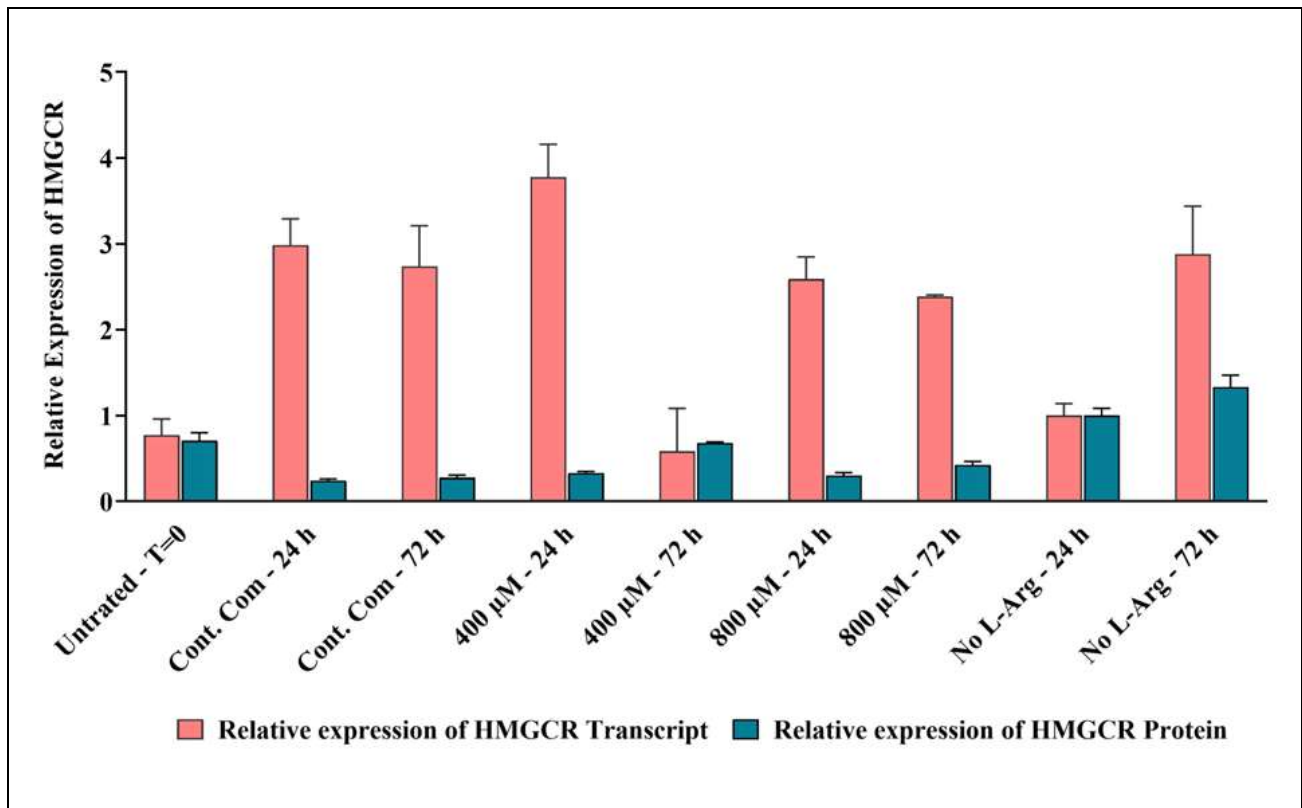


Figure 2.4.5. Comparison of relative HMGCR mRNA and protein expression in BNL CL2 cells cultured in different exogenous L-arginine amounts for different times.

Relative transcript expression of HMGCR was maximum when culturing at 400 μ M L-arginine for 24 h, whereas the relative HMGCR protein expression was maximal at 0 μ M L-arginine after 72 h when compared to the control complete DMEM culture time points. Overall, higher transcript expression of HMGCR did not involve in high translation level of HMGCR protein, the figure shows L-Arg at 400 μ M after 24 h had shown highest transcript level for HMGCR but translational level of HMGCR was lowest at 24 h.

Relative expression of the master regulator of cell growth and metabolism, mTOR protein, was decreased at 800 μ M L-arginine culture conditions at 24 h when compared to the control, whereas AMPK gene and protein expression were increased in 800 μ M L-arginine cultures at 24 and 72 h respectively. The reduction in mTOR could reflect responses to slow growth and proliferation due to high L-arginine concentrations. Further evidence of a slowing of translation and general protein synthesis is observed in the increased phosphorylation of eIF2 α (2-fold) at 72 h compared to the control complete DMEM added sample and the increase in phosphorylation of eukaryotic elongation factor-2 (a downstream target of AMPK (Yamada *et al.*, 2019) which will slow elongation (Knight *et al.*, 2015). In this study, upon phosphorylation, the activated AMPK at 800 μ M at 72 h downregulates the activity of the translation elongation factor by increasing the phosphorylation of eEF2 at Thr-56 in 800 μ M L-arginine cultured samples at 72 h.

eEF2 is modulated through the mTOR/eEF2K/eEF2 signalling pathway (Browne *et al.*, 2004; Yamada *et al.*, 2019). mTOR protein expression was actually increased in 400 (19.8-fold) and 800 μ M (10.9-fold) L-arginine

cultures at 72 h, and at this time phosphorylation of eEF2 was decreased, the opposite to that observed at 24 h. The explanation for this is that upon initial culturing in high exogenous L-arginine conditions mTOR is decreased and eIF2 α and eEF2 are phosphorylated to reduce protein synthesis and presumably cell growth and proliferation. However, after the cells have responded to this increase, this response is reversed to renew protein synthesis and allow new protein synthesis, cell growth and proliferation to proceed at ‘normal’ pace. This is thus presumably an important response and cellular mechanism to ensure large changes in L-arginine concentration are not detrimental to cell health.

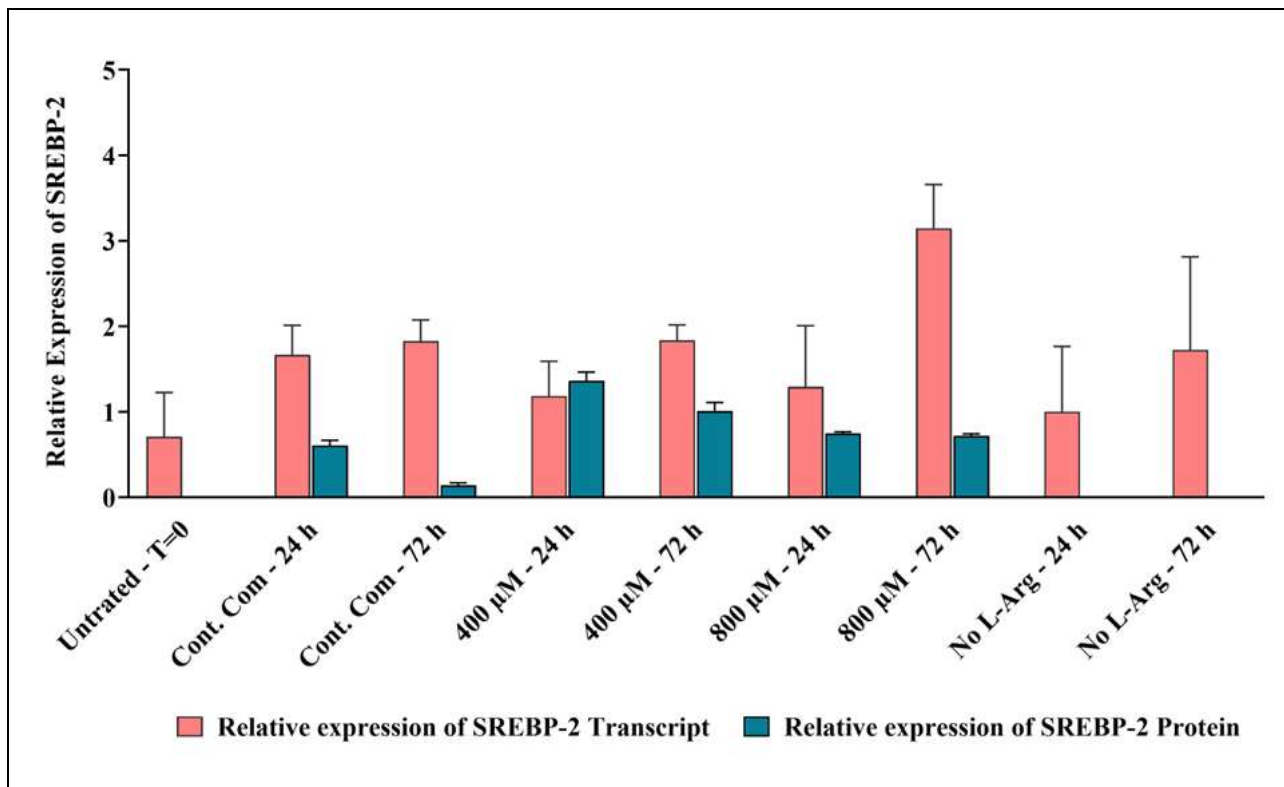


Figure 2.4.6. Comparison of relative SREBP-2 mRNA and protein expression in BNL CL2 cells cultured in different exogenous L-arginine amounts for different times.

Relative transcript expression of SREBP-2 was maximum when culturing at 800 μ M L-arginine for 72 h, whereas the relative protein expression was maximal at 400 μ M L-arginine after 24 h when compared to the control complete DMEM culture time points.

2.4.1.2. Nitrite response in BNL CL2 cells to exogenous L-arginine

A previous study with a neuronal cell line (CAD cells) that produces NO by nNOS enzymatic activity, has shown that NO synthesis is mainly depended on the extracellular arginine concentration and the study further confirmed that changing the membrane potential and physiological factors regulated the intake of L-arginine from extracellular pools (Bae *et al.*, 2005). The optimum amount of NO produced by other two isoforms of NOS; eNOS and iNOS, in rat superior mesenteric artery rings, is reportedly also depend on the extracellular L-arginine concentration and sensing of L-arginine to synthesis NO is subject to the impairment of endothelial

cells or induction of iNOS (MacKenzie and Wadsworth, 2003). One further previous study undertaken with isotopic ^3H -L-arginine reported that extracellular L-arginine contributed to the endothelium-dependent vasodilation in human umbilical vein endothelial cells (HUVECs) by regulating small (SKCa) conductance Ca^{2+} -activated potassium channels (Simonsen *et al.*, 2019). These studies collectively show that NO is produced from exogenous L-arginine, and responds to exogenous L-arginine concentrations, regardless of the NOS isoforms present in the specific tissues. In the BNL CL2 hepatocyte cells, the amount of NO_2^- present in the cell samples was high when grown in exogenous 800 μM L-arginine after 24 h compared to the control complete DMEM cultures at the same time point. The production of nitrite via the L-arginine/ NO pathway impacts the control and expression of AMPK, where the *AMPK* gene expression was also elevated in 800 μM L-arginine cultures at 24 h. At lower exogenous L-arginine conditions elevated NO_2^- was not observed and thus only at the highest concentration of L-arginine was an impact on NO and hence AMPK expression observed.

2.4.1.3. HPLC analysis of amino acids in BNL CL2 cell culture

Metabolism of arginine occurs in the liver to produce urea (Nijveldt *et al.*, 2004). Arginase activity is high in liver to facilitate the urea cycle, therefore to maintain the nutritional status of arginine (bioavailability of arginine in the human body) by dietary intake, there is an arginine-citrulline-arginine cycle within the major organs or systems; intestine, liver and kidneys. The amino acid content in liver cells is thus mainly regulated by the urea cycle (Fig 2.4.7).

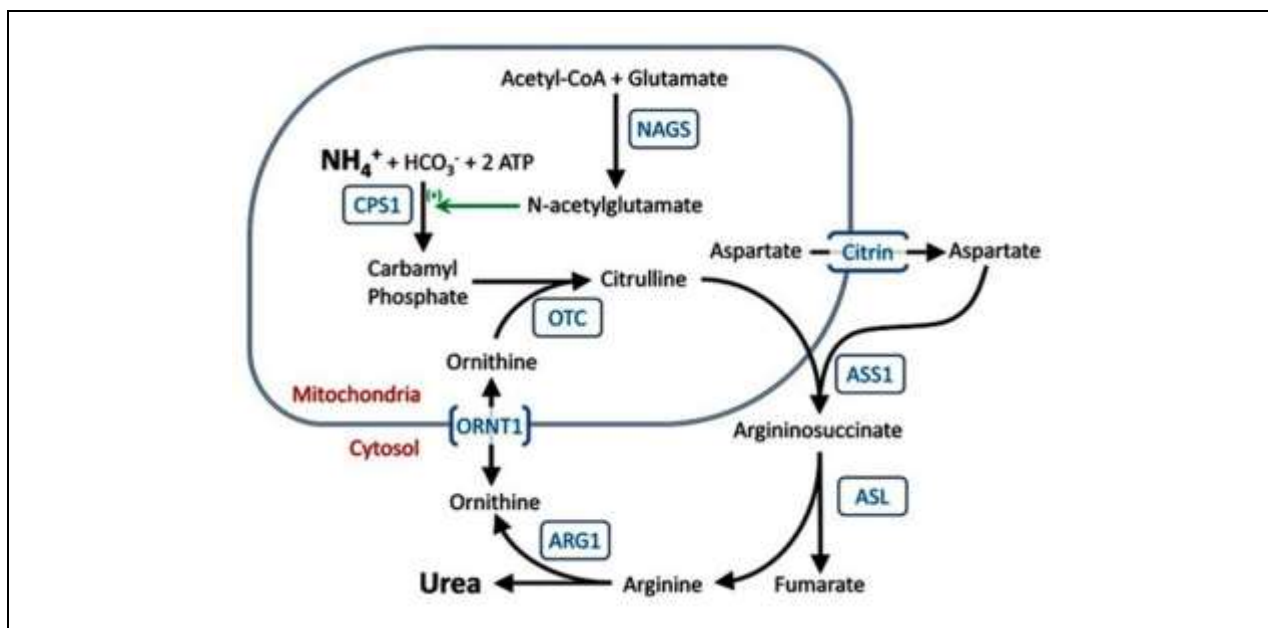


Figure 2.4.7. Comprised urea cycle pathway.

Fate of selected 3 amino acids in the urea cycle in liver cells are depicted in the diagram. There are five catalytic enzymes involved in this pathway, they are carbamoylphosphatase I (CPS1), ornithine transcarbamylase (OTC), argininosuccinic acid synthetase (ASS1), argininosuccinic acid lyase (ASL) and arginase (ARG1). One cofactor-producing enzyme is N-acetyl glutamate synthetase (NAGS). Ornithine translocase (ORNT1) and Citrin are two amino acid transporters (Mew *et al.*, 2018).

In this study we used two different culture media (complete DMEM and No L-Arg SILAC DMEM) that consisted of different concentrations of amino acids (**Appendix II**) and FBS (10% v/v). FBS itself contains protein and amino acids (**Appendix II**) to facilitate the growth of the cells. Therefore, baseline content of selected amino acids in the control complete DMEM media with 10% FBS and no L-Arg SILAC DMEM media with 10% FBS was analysed in three biological replicates by HPLC (**Table 2.4.1**). The HPLC data confirmed that the concentration of L-Arg in no L-Arg was 0 μM and the concentration of L-Arg in the control complete DMEM was 250.26 μM .

Table 2.4.1. Selected amino acids concentration in growth media with 10 % FBS

Samples	Concentration		
	L-Arginine (μM)	L-Citrulline (μM)	L-Ornithine (μM)
Control complete DMEM media with 10%FBS	250.256	45.213	11.909
No L-Arg SILAC DMEM media with 10%FBS	0.000	55.712	14.978

Arginine is synthesized from citrulline in almost all cell types (Tan, 2012). Amino acid homeostasis including amino acid uptake, *de-novo* synthesis and recycling impacts the availability of each amino acid in the serum samples. It was expected that over time the fate of amino acids such as depletion at different rates, oxidation, release from dying cells and synthesise and release/secretion of some amino acids will impact the concentration of amino acids in the plasma (Bröer and Bröer, 2017). L-glutamine and L-arginine are both conditionally essential amino acids. In *de-novo* synthesis of amino acids, for example, glutamine is an amino acid that can be used as a precursor to synthesis L-citrulline (Marini *et al.*, 2010). The culture media used in this study contained high glutamine concentrations (**Appendix II**; L-glutamine in complete DMEM; 3972.6 μM and no L-arginine SILAC DMEM; 3995.9 μM) compared to other amino acids presented. Therefore, we analysed the residual amounts of selected amino acids presented in the cultures serum samples and compared it to the initial amounts or compared it across the time period.

When sample L-Arg was analysed by the HPLC, the L-arginine amount was high in 400 μM at 72 h (981.1 μM) and 800 μM at 24 h (600.16 μM) compared to the control complete DMEM cultures at 24 (590.14 μM) and 72 h (956.3 μM). Therefore, excess L-Arg addition to the BNL CL2 cells impacted the amount of L-Arg present in the cultures in a time dependent manner. L-citrulline was high in untreated at T=0 (85.96 μM) compared to all other samples. This may reflect that the culture growth media contained very much high concentrations of glutamine, which could be used as a precursor to synthesis L-citrulline at T=0 (**Appendix II**) although how this would occur at T=0 is unknown. It was noted that the amount of L-citrulline present in the L-arginine treated samples was independent of culture time, but dependent on the amount of exogenously

added L-arginine, because the levels of L-citrulline in L-arginine at 400 and 800 μM after 24 (400 μM ; 3.76 μM and 800 μM ; 2.97 μM) and 72 h (400 μM ; 4.1 μM and 800 μM ; 3.1 μM) were more or less the same.

2.4.2. The impact of exogenous L-arginine supplementation on 3T3 L1 cells

2.4.2.1. Impact of exogenous L-arginine on target transcripts and proteins

After 24 h, in 3T3 L1 cells cultures with additional 400 μM L-arginine concentration, the transcript levels of AMPK increased (RE 3.26; $P < 0.0001$) compared to the control samples cultured in complete DMEM media. The results indicated that elevated L-arginine concentrations had an effect on AMPK expression, consistent with the BNL CL2 findings and other reported findings that arginine increases the expression and activity of AMPK, thereby modulating lipid metabolism and energy balance (Tan, 2012). There was not a similar pattern for protein and transcript expression of AMPK in response to exogenous L-arginine concentrations (**Fig 2.4.8**). Changes in AMPK transcription before changes in protein synthesis are observed in many cultured conditions; this may reflect a time dependent link between the transcription and translation processes. As reported above, this was also observed in BNL CL2 cells and reflects the multifaceted cell signalling pathways that converge and cross-talk with AMPK to coordinate responses to nutritional and hormonal signalling of the cells (Garcia and Shaw, 2017).

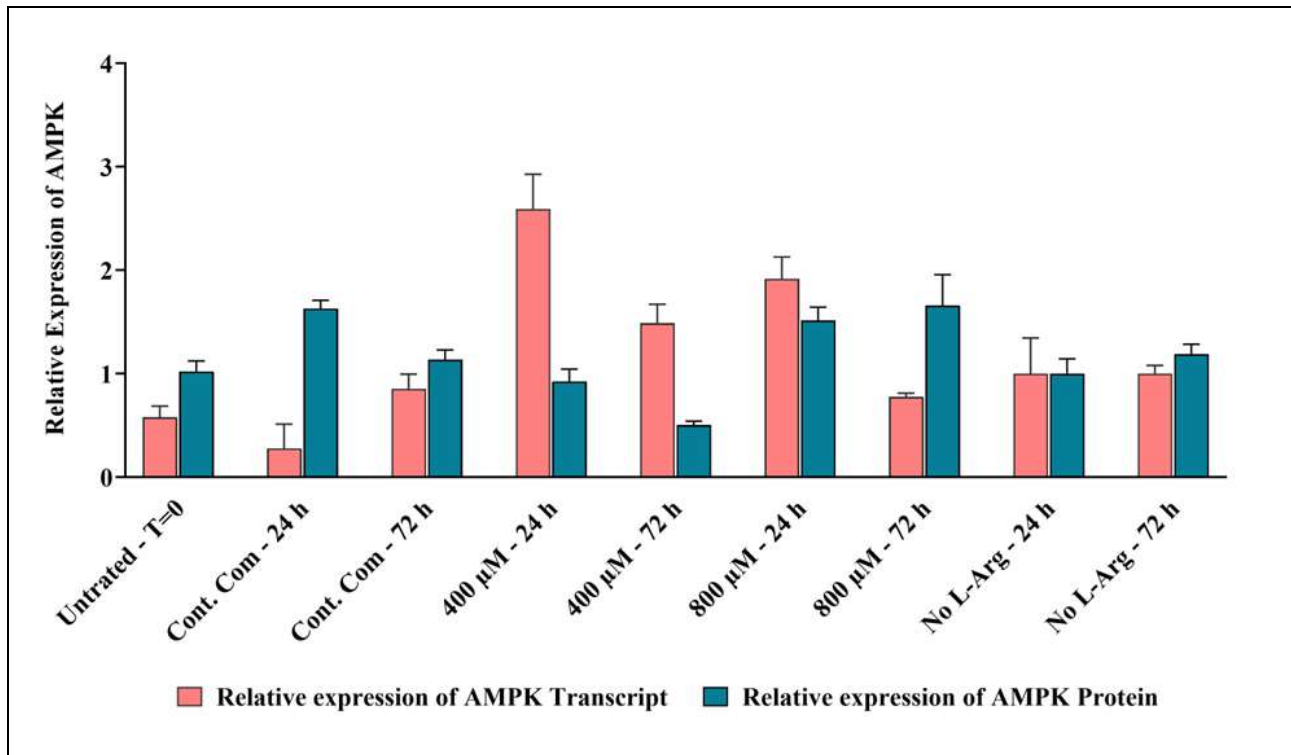


Figure 2.4.8. Comparison of relative AMPK mRNA and protein expression in 3T3 L1 cells cultured in different exogenous L-arginine amounts for different times.

Relative transcript expression of AMPK was maximum when culturing at 400 and 800 μM L-arginine for 24 h when compared to the control complete DMEM culture time point, whereas the relative protein expression was maximal and more or less same in 800 μM L-arginine after 24 and 72 h and the control after 24 h.

When investigated phosphorylated AMPK protein, it is noted from the profiles (**Fig 2.3.34** and **Fig 2.3.35**) that phosphorylated AMPK and phosphorylated ACC-1 levels in the control complete DMEM media were 2.07 and 1.48-fold higher respectively compared to the samples cultured in 400 μ M L-arginine at time point 24 h. As a consequence, ACC-1 (**Fig 2.4.9**) could be inactivated through its phosphorylation, allowing CPT-1 to act in its role in the transport of long-chain fatty acids to the mitochondria for oxidation (Viollet et al., 2006; Schmidt & Herpin, 1998). In this scenario, in 3T3 L1 cells, perhaps unexpectedly, CPT-1A protein expression decreased in the control complete DMEM samples (**Fig 2.4.10**) in comparison to the L-Arg cultures. However, CPT-1 mRNA expression did not show significant increases or decreases among cultures whilst the samples cultured in 400 and 800 μ M L-arginine had a peak expression of CPT-1A protein after 24 h. Interestingly, the effects of arginine on lipogenesis in adipocytes was reported in a study using 9-week-old male Zucker diabetic fatty rats, when rats were pair-fed with a specified diet and fed with drinking water containing arginine-HCl (1.51%) or alanine (2.55%, isonitrogenous control) for 10 weeks. The results indicated that the expression of major genes accountable for fatty acid oxidation in adipose tissue (e.g. AMPK and CPT-2) were increased by arginine supplementation (Fu *et al.*, 2005).

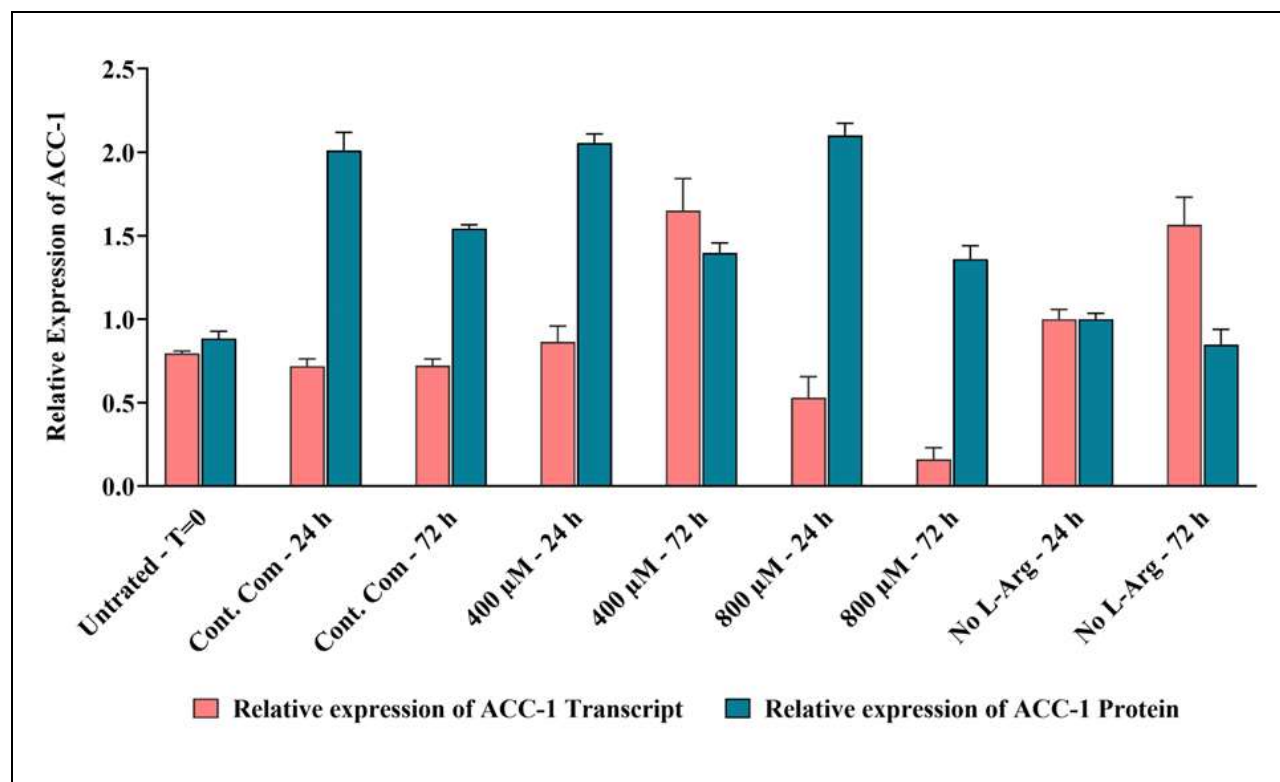


Figure 2.4.9. Comparison of relative ACC-1 mRNA and protein expression in 3T3 L1 cells cultured in different exogenous L-arginine amounts for different times.

Relative transcript expression of ACC-1 was maximum when culturing at 0 and 400 μ M L-arginine for 72 h when compared to the control complete DMEM culture time point, whereas the relative ACC-1 protein expression was maximal and more or less same at 400 and 800 μ M L-arginine and the control after 24 h.

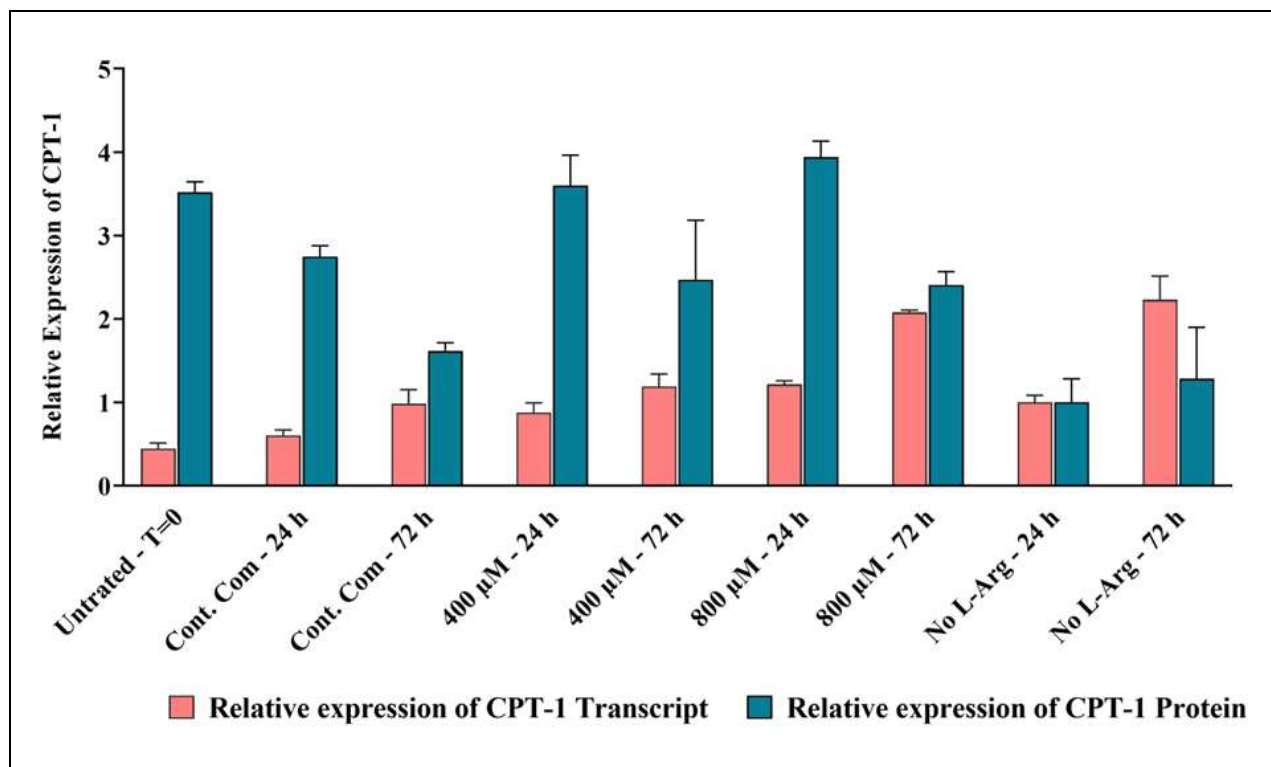


Figure 2.4.10. Comparison of relative CPT-1 mRNA and protein expression in 3T3 L1 cells cultured in different exogenous L-arginine amounts for different times.

Relative transcript expression of CPT-1 was maximum when culturing at 400 and 800 µM L-arginine for 24 and 72 h when compared to the control complete DMEM culture time points, whereas the relative CPT-1A protein expression was maximal at 400 and 800 µM L-arginine after 24 h over to the control after 24 h.

Investigations of transcript and protein levels of lipogenic SREBP-1 revealed that there were opposite profiles between the mRNA and the protein level of SREBP-1 in samples cultured in 400 µM L-arginine. Overall, SREBP-1 mRNA expression was higher than protein expression in L-Arg treated samples after 24 h in comparison to the control after 24 h (**Fig 2.4.11**). It was noted from the lipogenic ACC-1 and CPT-1A (**Fig 2.4.9 - Fig 2.4.10**) and cholesterol synthesis regulators HMGCR, SREBP-1 and 2 (**Fig 2.4.12, Fig 2.4.11** and **Fig 2.4.13**) profiles that the highest mRNA amounts of these transcripts were not accompanied by increases in the respective proteins in the cultured samples at the same time point. This suggests that there may be an inverse relationship between expression of these transcripts and proteins in a time dependent manner (slow protein synthesis) in 3T3 L1 cells.

Further investigation of the SREBP-1 mRNA expression showed that this was decreased in 400 (RE 0.88) and 800 µM L-Arg (RE 0.88) cultures at 24 h compared to the control complete DMEM cultures (RE 0.99). Moreover, at the protein level, expression of the precursor and catalytically active mature forms of SREBP-1 were decreased over that of the control. As a result of this, the ratio of precursor to mature form was also

decreased in 400 (0.56-fold) and 800 μM (0.8-fold) cultures compared to the control at 24 h and thereby there was more active mature form in the L-Arg treated samples (400 and 800 μM). It was noted from these ratios of post-translational mechanism that the catalytically active mature form of SREBP-1 decreases with increasing exogenous L-arginine supplementation. Besides these, the levels of mature form of SREBP-1 present in L-Arg treated samples (400 and 800 μM) at 72 h were not in detectable amount (RE 0) (**Fig 2.3.40C**). This further suggests that the expression of SREBP-1 presumably modulates in response to elevated exogenous L-arginine amounts and depend on the time point.

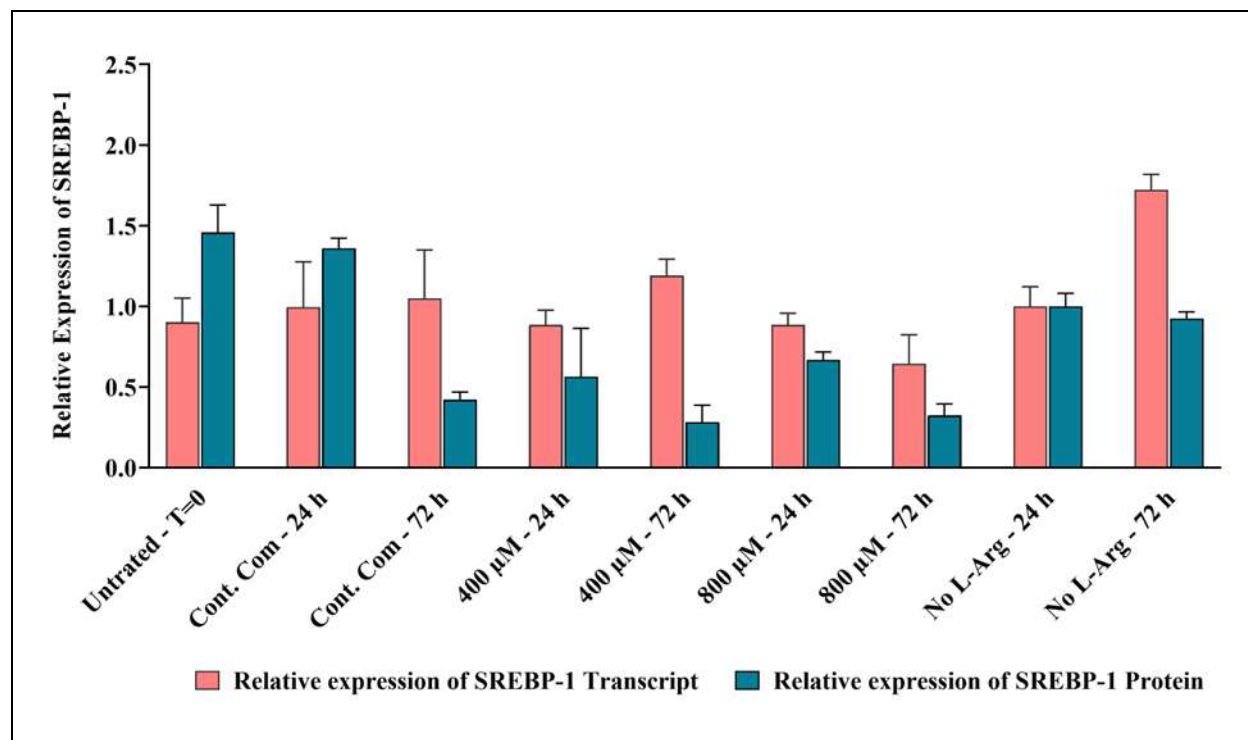


Figure 2.4.11. Comparison of relative SREBP-1 mRNA and protein expression in 3T3 L1 cells cultured in different exogenous L-arginine amounts for different times.

Relative transcript expression of SREBP-1 was maximum when culturing at 0 and 400 μM L-Arg for 72 h when compared to the control complete DMEM culture time point, whereas the relative SREBP-1 protein expression was maximal at untreated sample at T=0 and in the control after 24 h compared to the L-Arg treated samples at 24 and 72 h.

There was no common relationship between the transcript (lowest) and protein expression of HMGCR (**Fig 2.4.12**) or SREBP-2 (**Fig 2.4.13**). In post-translational modification of HMGCR, the ratio of the N-domain to catalytically active C-domain was increased (2.5-fold) in 400 μM at 72 h and also increasing L-arginine concentration to 800 μM increased the ratio of N-domain to C-domain at 24 (1.3-fold) and 72 h (1.61-fold) in comparison to the ratio in the control. Interestingly, like post-translational modification of HMGCR, the ratio of precursor to mature form of SREBP-2 was increased in 400 and 800 μM L-Arg cultures at 24 (1.35-fold and 1.14-fold, respectively) and 72 h (6.37-fold and 1.7-fold, respectively) compared to the control complete

DMEM media at the same time points. This suggests that there are more catalytically inactive precursor proteins (HMGCR and SREBP-2) present in the L-Arg treated cell samples compared to the control.

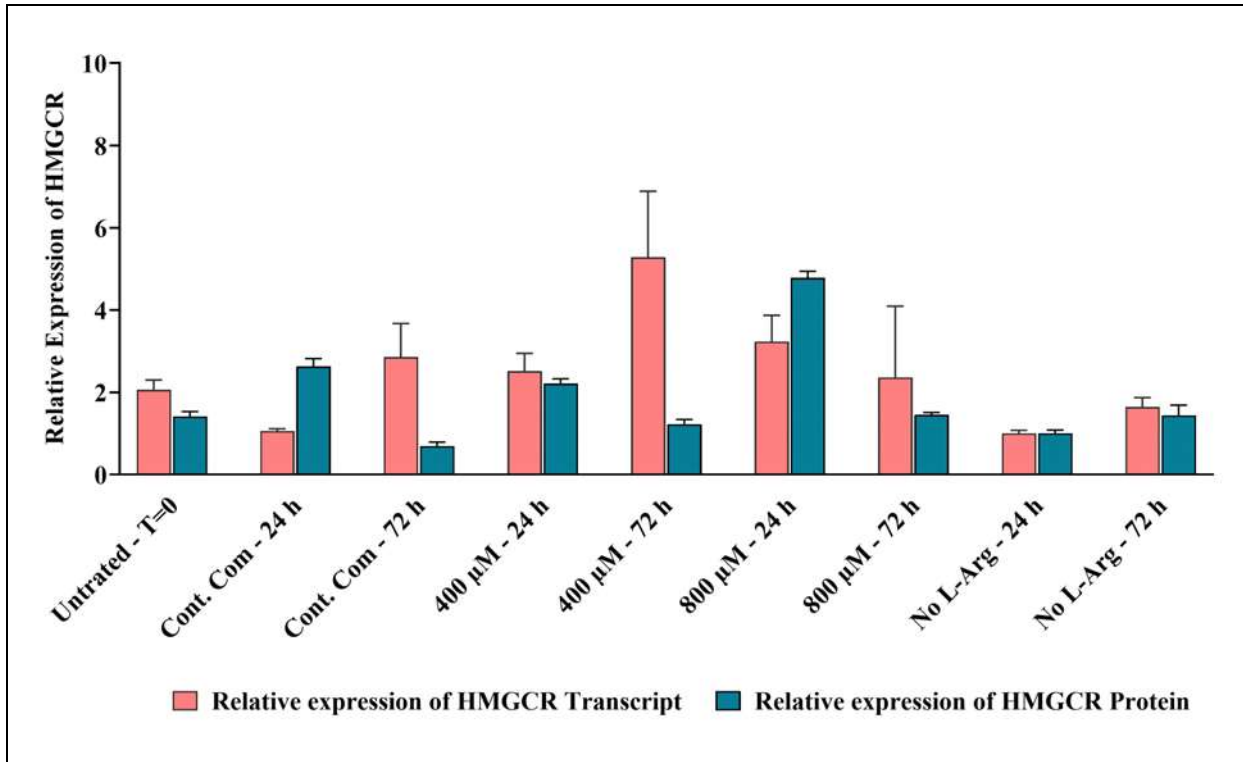


Figure 2.4.12. Comparison of relative HMGCR mRNA and protein expression in 3T3 L1 cells cultured in different exogenous L-arginine amounts for different times.

Relative transcript expression of HMGCR was maximum when culturing at 400 μM for 24 and 72 h and 800 μM for 24 h when compared to the control complete DMEM culture time points, whereas the relative HMGCR protein expression was maximal at 800 μM L-arginine after 24 h over to the control after 24 h.

Cell growth and metabolism are regulated by a master regulator, mTOR protein. At the relative protein expression level, there was increased mTOR at 400 and 800 μM L-arginine culture conditions at 24 and 72 h when compared to the control. This increasing expression of mTOR could reflect responses to increase the growth and proliferation of the 3T3 L1 cells due to elevated exogenous L-arginine concentrations. Further evidence for this is provided in that the viable 3T3 L1 cells number in 400 μM cultured conditions was gradually increased from 24 (1.0×10^6 viable cells/mL, 1.5-fold) to 72 h (2.23×10^6 viable cells/mL, 1.12-fold) compared to the control.

Increased phosphorylation of eIF2α (1.13-fold) was observed in 400 μM L-Arg at 72 h compared to the control complete DMEM added sample, potentially indicating a slowing of translation and general protein synthesis in the 3T3 L1 cells. The increase in phosphorylation of eukaryotic elongation factor-2, (a downstream target

of AMPK, Yamada *et al.*, 2019) also slows elongation (Knight *et al.*, 2015) and was observed with translation elongation factor phosphorylation increasing (21-fold) in 400 μM L-arginine cultured samples at 72 h.

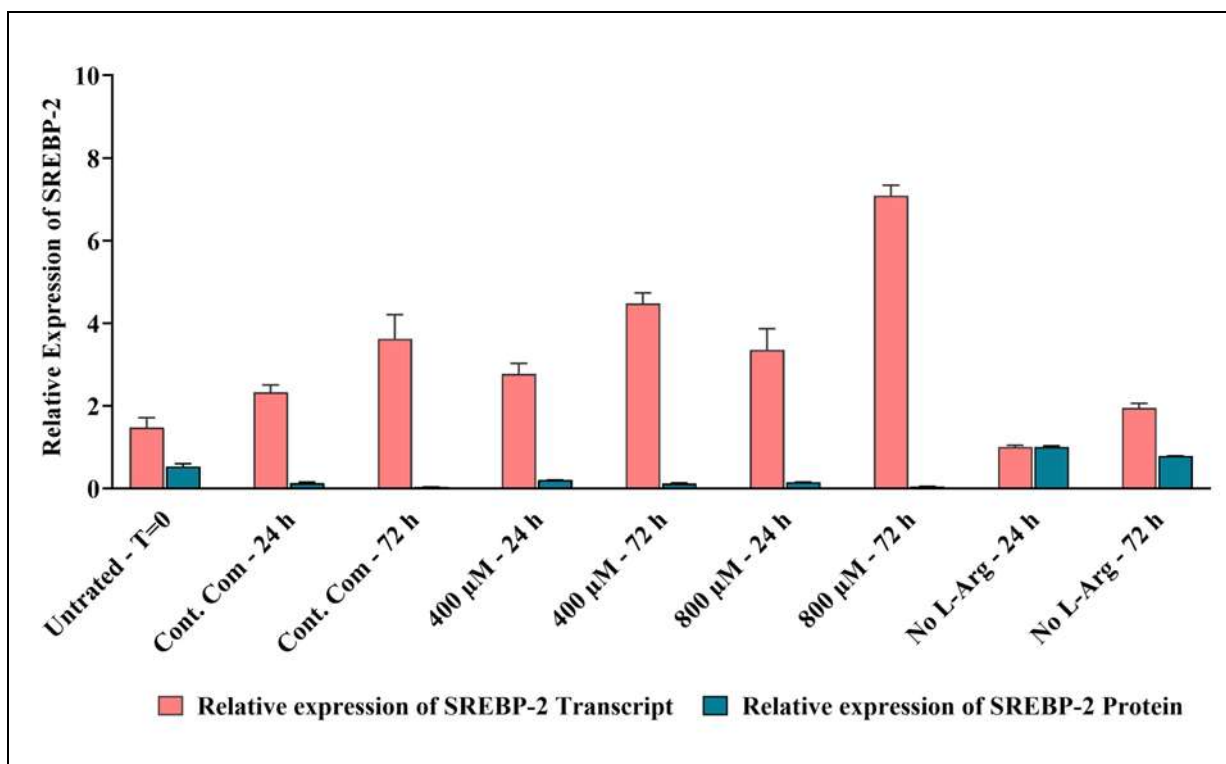


Figure 2.4.13. Comparison of relative SREBP-2 mRNA and protein expression in 3T3 L1 cells cultured in different exogenous L-arginine amounts for different times.

Relative transcript expression of SREBP-2 was maximum when culturing at 400 and 800 μM L-arginine for 72 h when compared to the control complete DMEM culture time point, whereas the relative SREBP-2 protein expression was maximal at 0 μM L-arginine after 24 and 72 h over to the control culture time points.

2.4.2.2. Nitrite response in 3T3 L1 cells to exogenous L-arginine

In the 3T3 L1 adipocyte cells, the amount of NO_2^- present in the cell samples was high (2.1-fold) when grown in exogenous 800 μM L-arginine after 24 h compared to the control complete DMEM cultures, as in BNL CL2. However, the amount was decreased at 72 h of culture. At 400 μM there was an increased amount of nitrite at 24 (1.4-fold) and 72 h (1.54-fold) over the control samples. The production of nitrite via the L-arginine/ NO pathway impacts the expression of AMPK. At lower exogenous L-arginine conditions elevated NO_2^- was not observed (untreated at T=0, 0.48 μM , lowest) and thus only at the excess exogenous concentrations of L-arginine was there a potential impact on NO and hence AMPK expression as observed at 400 μM at 72 h.

2.4.2.3. HPLC analysis of amino acids in 3T3 L1 cells

Large amounts of branched chain amino acids (BCAAs) are metabolised in adipose tissue (Herman *et al.*, 2010). An isotopic labelled study reported that in adipose tissue insulin and the amount of glucose in the medium play a role in the integration of glycine, L-proline and histidine (Carruthers and Winegrad, 1962). The

role of white adipose tissue (WAT) in amino acid metabolism has been described and these studies predict that WAT consists of a completely functional urea cycle (Arriarán *et al.*, 2016) (**Fig 2.4.14**).

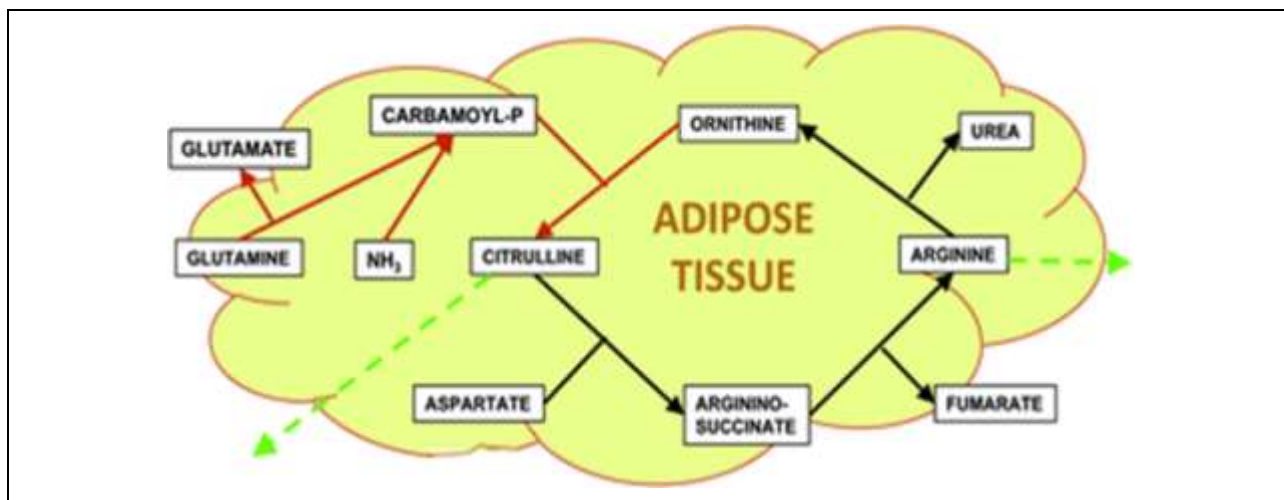


Figure 2.4.14. The urea cycle of rat white adipose tissue.

In this remarkable pathway L-arginine, L-ornithine and L-citrulline are involved in urea cycle of white adipose tissue (Arriarán *et al.*, 2016).

In this study, in 3T3 L1 cultured cell supernatants L-Arg was high in L-Arg treated cell samples after 24 h compared to the control, but decreased after 72 h. From the urea cycle outlined in **Fig 2.4.14**, it is proposed from the data that exogenously added excess L-Arg might not be used for the synthesis of L-Orn but rather be utilised by enzymes involved in L-Arg metabolism. L-Arg is a substrate for nitric oxide synthase and arginase enzyme which produces L-Cit and L-Orn, respectively (Cao *et al.*, 2020). It has been reported that Km values for arginine of arginase I and II (around 10 mmol/L) are significantly higher than that of iNOS (around 5 μ mol/L) (Mori, 2007). This reflects that arginase needs a lot of L-Arg substrate to actively involve in the synthesis of L-Orn. It is suggested that when excess L-Arg (400 and 800 μ M) was added to 3T3 L1 cells, the substrate L-Arg concentration was higher than the enzymatic activity of arginase therefore 3T3 L1 cells cultured in excess L-Arg did not show high cell culture supernatant L-Orn concentrations. This also assumes that L-Orn could be secreted and thus investigating intracellular amounts would be interesting in the future.

2.4.3. Overall conclusions from the work presented in this chapter

The work presented in this chapter shows that addition of higher concentrations of L-arginine to the culture medium of BNL CL2 and 3T3 L1 cells does impact subsequent cell signalling in a concentration and time dependent manner. The absence of L-arginine also resulted in a rapid drop in culture viability and decreased growth as expected, confirming the presence is required for growth of these cells. Further, the key enzyme AMPK was activated in both cell types in response to L-arginine addition at both a transcript and protein level whilst changes in phosphorylation were also observed in the BNL CL2 cell model. As discussed in the

introduction chapter of this thesis, the overall effect of AMPK activation is to switch off ATP-consuming pathways (including lipogenesis and gluconeogenesis), while turning on ATP-producing pathways (including fatty acid and glucose oxidation). Activated AMPK phosphorylated its downstream target ACC-1, the rate-controlling enzyme for the synthesis of malonyl-CoA, a precursor for de novo fatty acid synthesis. In arginine-supplemented BNL CL2 cells, the increased expression of subsequent lipogenic genes (SREPB-1) is expected to increase the synthesis of fatty acids and triglycerides in the liver. On-the-other-hand, for 3T3 L1 adipose cells these store lipid but also release free fatty acids as an energy source for other tissues, such as liver and skeletal muscles (Frayn *et al.*, 2003). In 3T3 L1 cells, ACC-1 phosphorylation was high in the control samples compared to L-Arg treated samples. Therefore, L-Arg treatment may increase free fatty acids availability in adipose tissue by reducing ACC-1 phosphorylation. However, the results presented in this work also show that, in contrast to the liver cells, L-arginine increased the expression of CPT-1 indicating a potent effect of L-arginine on inhibiting adipose tissue fatty acid synthesis.

In summary, additional L-arginine supplementation increased expression of key enzymes for fatty acid oxidation in the liver and additionally increased the expression of CPT-1 in adipose tissue cells, while decreasing hepatic expression of key enzymes for lipogenesis and cholesterol synthesis. These coordinated changes in gene and protein expression (summarized in final discussion **Figs 5.1.1** and **5.1.2**) among insulin-sensitive tissues may partially provide a molecular mechanism for the fat mass deposition during obesity and how that would be overcome by L-Arg supplementation.

Chapter-3 AMPK and ACC-1 cell signalling upon addition of exogenous L-arginine and NOS inhibitors, co-factors and NO donors to BNL CL2 and 3T3 L1 cells

3.1. Introduction

L-arginine metabolism in the cell can give rise to nitric oxide and citrulline production via nitric oxide synthase (NOS) or urea production and ornithine via arginase activity as described in the main introduction and Chapter 2 of this thesis. NO is an important cellular signalling molecule that produces nitrite, a regulator of gene expression. Synthesis of NO requires a number of co-factors including tetrahydrobiopterin (BH₄). The biological availability of NO is affected by the iNOS inhibitor N^G-nitro-L-arginine methyl ester (L-NAME) and the NO donor S-nitroso-N-acetyl-DL-penicillamine (SNAP). The work undertaken in this chapter was conducted to test the hypothesis that L-arginine supplementation regulates expression of AMPK and ACC-1 and possibly other key metabolites involved in the L-Arg metabolism of in insulin-sensitive tissues, specifically investigating the impact of cofactors and inhibitors of the NO pathways that are impacted by L-arginine concentrations. The work shows that NO, produced as a result of L-Arg addition and the factors L-NAME, BH₄ and SNAP that regulate NO bioavailability, impacted BNL CL2 and 3T3 L1 cells NO/AMPK/ACC-1 signalling pathways via regulating mRNA expression and subsequently protein expression and concomitant changes in the cell culture concentrations of L-Arg, L-Cit and L-Orn.

3.2. Materials and Methods

3.2.1. Preparation of stock solutions of L-arginine, N^o-nitro-L-arginine methyl ester hydrochloride (L-NAME), 5,6,7,8-tetrahydrobiopterin (BH₄) and S-nitroso-N-acetyl-DL-penicillamine (SNAP) solution

3.2.1.1. Preparation of stock solutions of L-arginine

Preparation of stock solutions of L-arginine, and growth medium with varying L-arginine concentrations, were undertaken as described in section 2.2.1.2.

3.2.1.2. Preparation of L-NAME stock solution

L-NAME (Sigma-Aldrich, Cat. No: N5751) was used to inhibit NOS activity in cell culture samples. The solubility of L-NAME in water is 50 mg/mL. A working stock solution (12.5 mg/mL) was prepared by dissolving 0.125 g of L-NAME either in 10 mL complete DMEM or in 10 mL SILAC L-Arg deficient DMEM media for adding to cell culture samples with or without L-Arg deficient media addition. L-NAME (4 mM) was added to 2 x 10⁵ viable cells in 2 mL of culture media containing different concentrations of L-arginine (0, 400 and 800 μM) and the control complete DMEM.

3.2.1.3. Preparation of BH₄ stock solution

BH₄ (Fisher, Cat.No:15743447) was used as a co-factor of NOS to facilitate the NOS/L-arginine metabolic pathway. The solubility of BH₄ in water is >20 mg/ml. A working stock solution (5 mg/mL) was prepared by dissolving 50 mg of BH₄ either in 10 mL complete DMEM or in 10 mL SILAC L-Arg deficient DMEM media. BH₄ (40 μM) was then added to 2 x 10⁵ viable cells in 2 mL of culture media containing different concentrations of L-arginine (0, 400 and 800 μM) and the control complete DMEM.

3.2.1.4. Preparation of SNAP stock solution

SNAP (Sigma-Aldrich, Cat. No: N3398) was used as an external NO donor to investigate how the external NO addition impacted the L-arginine/NO pathway. The solubility of SNAP in water is ≥ 2 mg/mL but in dimethyl sulfoxide (DMSO) is ≥ 20 mg/mL, therefore DMSO was used as a solvent. A working stock solution of SNAP (4 mg/mL) was prepared by dissolving 0.04 g of SNAP in 10 mL DMSO, then the solution was sonicated to obtain a clear faint green colour solution. SNAP (100 μM) was added to 2x 10⁵ cells in 2 mL of culture media containing different concentrations of L-arg (0, 400 and 800 μM) and control complete DMEM.

3.2.2. Establishment of cell culture models for investigating AMPK and ACC-1 cell signalling upon addition of exogenous L-Arg and L-NAME; BH₄; co-factor and SNAP to BNL CL2 and 3T3 L1 cells

BNL CL2 cells or 3T3 L1 cells were seeded into 6-well tissue culture plates (Greiner Bio-One) at 2x10⁵ viable cells/well in 2 mL of complete DMEM media as described in section 2.2.1.3. The cells were then incubated in a static incubator (Thermo Forma, Thermo Fisher) for 24 h at 37°C, 5% CO₂. After 24 h, the media was replaced with media with different concentrations of L-arginine (0, 400 and 800 μM) or the control complete DMEM with 10% (v/v) FBS (2 mL/ well) with additions of either L-NAME (a NOS inhibitor, 4 mM) or BH₄ (a NOS co-factor, 40 μM) and cells and cell culture supernatant then harvested at two time points; after this addition, 24 and 72 h post addition (**Fig 3.2.1 and Fig 3.2.2**). In another set of experiments, after 24 h the media was replaced with media of different concentrations of L-arginine (0, 400 and 800 μM) or the control complete DMEM with 10% (v/v) FBS (2 mL/ well) with addition of SNAP (a NO donor, 100 μM) (**Fig 3.2.3**) and cells and cell culture supernatant harvested 6 and 24 h post addition. Subsequently samples were differently lysed for mRNA and protein work as described below. The cell culture media (2 mL) from addition experiments was also collected from the cell cultures and frozen at -20°C.

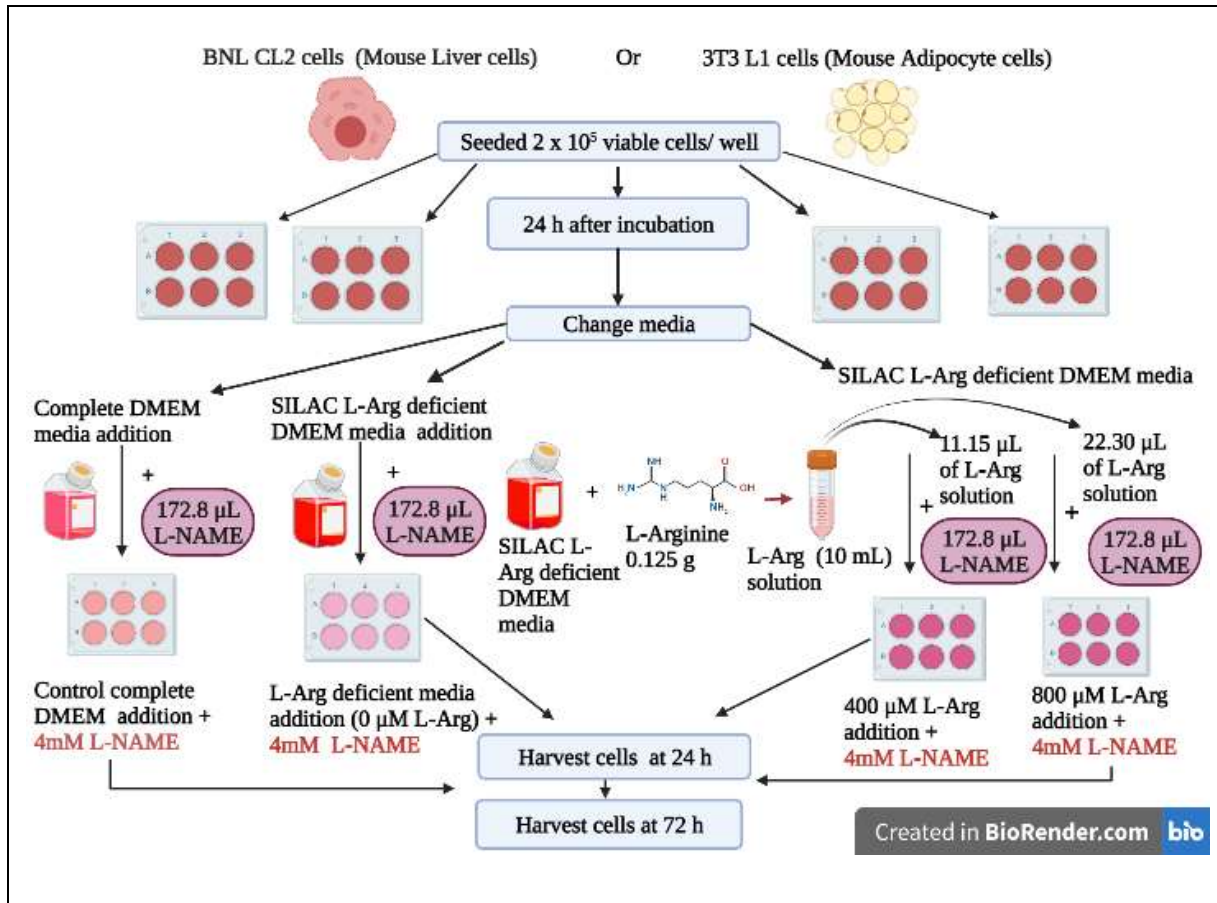


Figure 3.2.1. Schematic diagram outlining L-arginine and L-NAME (4 mM) supplementation of medium into BNL CL2 or 3T3 L1 cell cultures.

Cells were maintained with different extracellular concentrations of L-arginine (0, 400 and 800 μ M) in SILAC L-Arg deficient media or the control complete DMEM with 10% FBS (2 mL/ well) with L-NAME (4 mM). Samples were collected 24 and 72 h post addition of L-arginine for analysis.

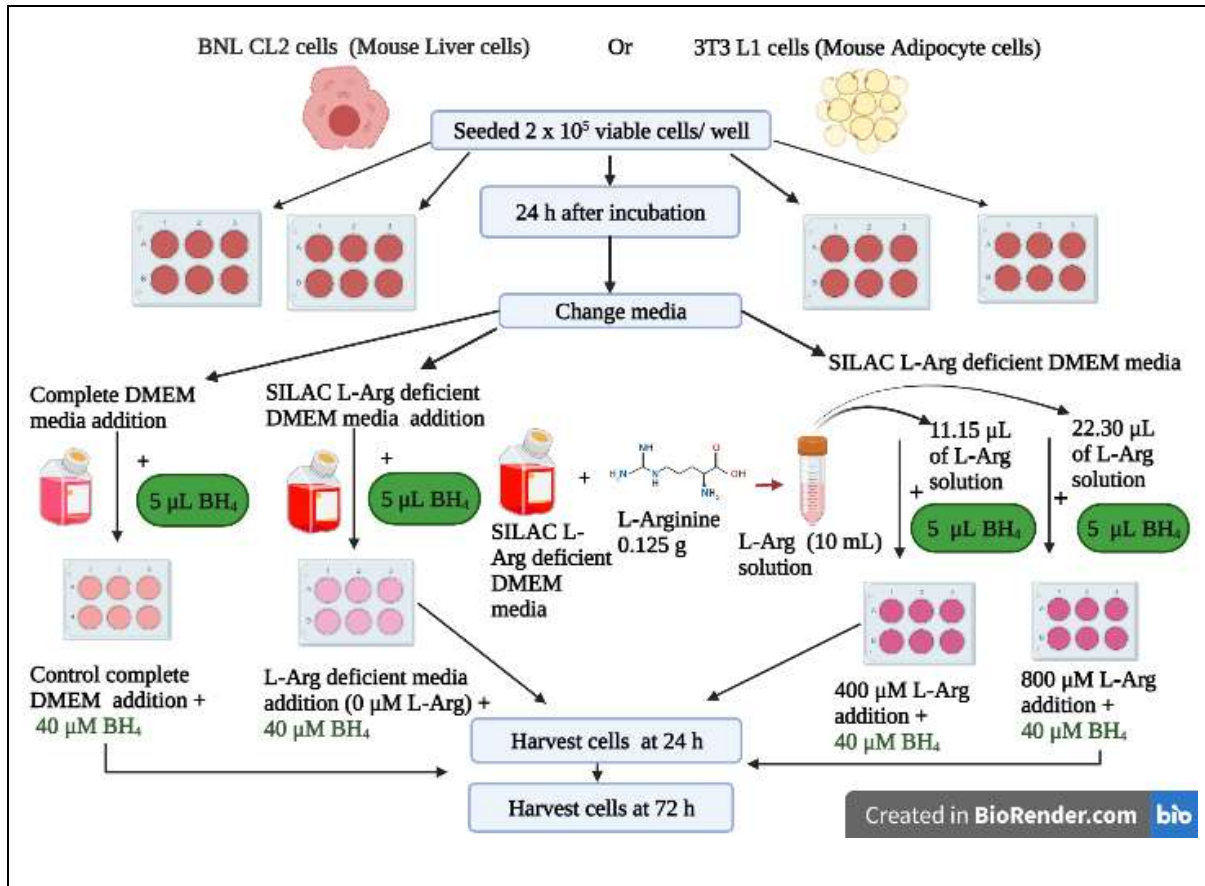


Figure 3.2.2. Schematic diagram outlining L-arginine and BH_4 (40 μ M) supplementation into medium for BNL CL2 or 3T3 L1 cell cultures.

Cells were maintained with different extracellular concentrations of L-arginine (0, 400 and 800 μ M) in SILAC L-Arg deficient media or the control complete DMEM with 10% FBS (2 mL/ well) with BH_4 (40 μ M). Samples were collected 24 and 72 h post addition of L-arginine for analysis.

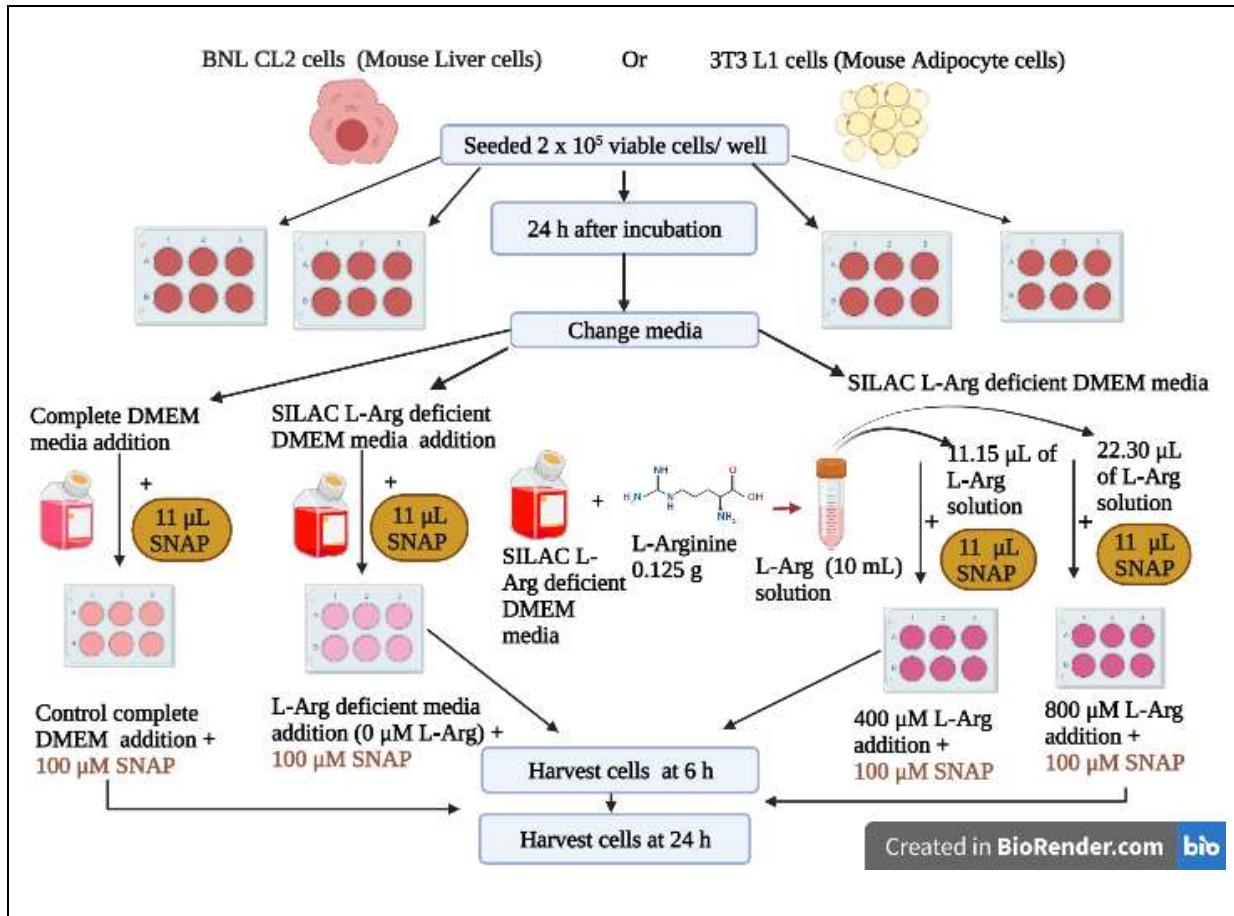


Figure 3.2.3. Schematic diagram outlining L-arginine and SNAP (100 μ M) supplementation into medium for BNL CL2 or 3T3 L1 cell cultures.

Cells were maintained with different extracellular concentrations of L-arginine (0, 400 and 800 μ M) in SILAC L-Arg deficient media or the control complete DMEM with 10% FBS (2 mL/ well) with SNAP (100 μ M). Samples were collected 6 and 24 h post addition of L-arginine for analysis.

3.2.3. RNA extraction and quantitative real-time PCR (qRT-PCR) for transcript mRNA analysis

Cells grown as described in section 3.2.2 were harvested at the respective time points and washed with pre-warmed PBS (2 mL/well) followed by lysis using RLT lysis buffer (350 μ L, Qiagen) and total RNA lysates were scraped off into Eppendorf tubes (1.5 mL) and snap frozen in dry-ice and stored at -80°C or immediately further processed. RNA extraction from collected RNA lysates and quantitative real-time PCR (qRT-PCR) for transcript mRNA analysis was followed as described in section 2.2.2.

3.2.3.1. qRT-PCR methods

Primers designed for PCR amplification of target genes of interest AMPK and ACC-1 are described in **Table 2.3.1**. qRT-PCR amplification of target sequences was undertaken using the commercially available iTaqTM Universal SYBR Green One-Step Kit (Bio-Rad, Cat. No: 1725151). qRT-PCR methods were followed as described in section 2.2.2.1.

3.2.4. Protein and post-translational modification (phosphorylation) analysis

3.2.4.1. Total protein extraction

Samples for protein analysis were generated by culturing cells as described in section 3.2.2 and collected either 24 and 72 h (L-NAME or BH₄) or 6 and 24 h (SNAP) after L-arginine supplementation. Samples for analysis were collected by removing the media and then washing the cells twice with chilled PBS (2 mL/well). Plates were then kept on ice and modified radioimmunoprecipitation (RIPA) lysis buffer added to the cells. The modified RIPA lysis buffer consisted of ice-cold 20 mM HEPES-NaOH, pH 7.2, containing 100 mM NaCl, 1% (w/v) Triton X-100 (Sigma, Cat. No: 9002-93-1), cOmplete™ mini protease inhibitor cocktail (Roche, Cat. No 11836153001, 1 tablet/10 mL lysis buffer) with 10 mM sodium β-glycerophosphate, 50 mM NaF, 1 mM activated sodium orthovanadate (Na₃VO₄), 0.2 mM phenylmethylsulfonyl fluoride (PMSF), 10 µg/ml leupeptin and 2 µg/mL pepstatin added. During harvesting, lysis buffer (200 µL/well) was added and after 10 min on ice the cells were dislodged from the flask using a cell scraper and the cell lysates (approximately 200 µL) obtained. The cell lysates were centrifuged at 17,000 g for 10 min and then the collected protein extract kept at -80°C until required for analysis.

3.2.4.2. Bradford assay to determine protein concentration in samples

Bradford assay to determine the protein concentration in different concentrations of L-Arg with L-NAME (4 mM), BH₄ (40 µM) and SNAP (100 µM) was undertaken as described in section 2.2.3.2.

3.2.4.3. Sodium dodecyl sulphate-polyacrylamide gel electrophoresis (SDS-PAGE) analysis of proteins

3.2.4.3.1. Sample preparation

10 µg of protein/25 µL total sample volume/lane samples were prepared as described in section 2.2.3.3.1.

3.2.4.3.2. Gel preparation and electrophoresis

SDS-PAGE gels were prepared as detailed in section 2.2.3.3.2.

3.2.4.4. Western blotting

Western blotting was undertaken as described in section 2.2.3.4. The AMPK and ACC-1 antibodies for western blot analysis were sourced as detailed in Table 2.3.2 and with the working dilutions described.

3.2.4.5. Densitometry analysis

Densitometry of bands on SDS-PAGE and western blots was undertaken using the open software package ImageJ (National Institutes for Health (NIH), USA). The relative protein expression of a protein of interest in the samples were normalized to the house-keeping β-actin protein.

3.2.5. Nitric oxide /Nitrite measurement by Griess Assay

0.1% (w/v) sulphanilamide in 5% (v/v) phosphoric acid and 0.1% (w/v) N-(1-naphthyl)-ethylenediamine dihydrochloride (NED) solution were freshly prepared as described in section 2.2.4.1.

3.2.5.1. Preparation of samples for analysis

Cell culture media (2 mL) were collected from L-arginine and either L-NAME or BH₄ or SNAP additions to BNL CL2 and 3T3 L1 cells as described in 3.2.2 and used for nitrite assay as detailed in section 2.2.4.2.

3.2.5.2. Griess assay

Accumulation of NO in the cell culture media was analysed indirectly by quantifying nitrite (NO₂⁻) present in the media using Griess assay detailed in section 2.2.4.3.

3.2.6. Analysis of L-arginine, L-ornithine and L-citrulline by HPLC

3.2.6.1. Processing of biological samples

Samples were collected from L-arginine with either L-NAME or BH₄ or SNAP additions to BNL CL2 and 3T3 L1 cells as described in 3.2.2, then vortexed and centrifuged at 1500 rpm for 10 min to obtain the cell free culture supernatant for the HPLC analysis.

3.2.6.2. Deproteinization of samples for amino acid analysis

Samples were deproteinised using 100% (v/v) ice-cold ethanol method, a modified protocol of that described in section 2.2.5.2.

3.2.6.3. HPLC amino acid analysis

Pre-column derivatization using a O-phthaldialdehyde (OPA) complete solution reagent, preparation of mobile phase buffers (mobile phase A; 0.1 M sodium acetate, pH 7.2 and mobile phase B; 100% methanol), preparation of amino acid standards (0.6 mM for each amino acid), amino acid HPLC analysis using a reverse phase-C18 column with a flow rate of 1.1 mL/min, detection of molar absorptivity of each derivatized amino acid at 338 nm with a diode-array detector (DAD), standard curve generation for L-arginine, L-citrulline and L-ornithine plotted with the area of the signals (mAU x Sec) against concentration for each amino acid and HPLC data analysis were followed as described in section 2.2.5.3.

3.2.7. Statistical analysis

Statistical analysis was undertaken using GraphPad Prism 9.4.1 software and Microsoft Excel. Samples were analysed in triplicate biological replicates. Statistically significant differences between sample means and standard deviation were analysed using two-way ANOVA. The Tukey's multiple comparison method was used to determine differences among the means of the treatment groups (0, 400 and 800 μM L-Arg) with the control complete DMEM media addition with either L-NAME or BH₄ or SNAP in BNL CL2 or 3T3 L1 cells

across the time points either 24 and 72 h or 6 and 24 h. Probability values ≤ 0.05 were considered to indicate statistical significance. The stars approach intended to flag levels of significance were followed (American Psychological Association style, New England Journal of Medicine) as ns = $P > 0.05$, * = $P \leq 0.05$, ** = $P \leq 0.01$, *** = $P \leq 0.001$ and **** = $P \leq 0.0001$.

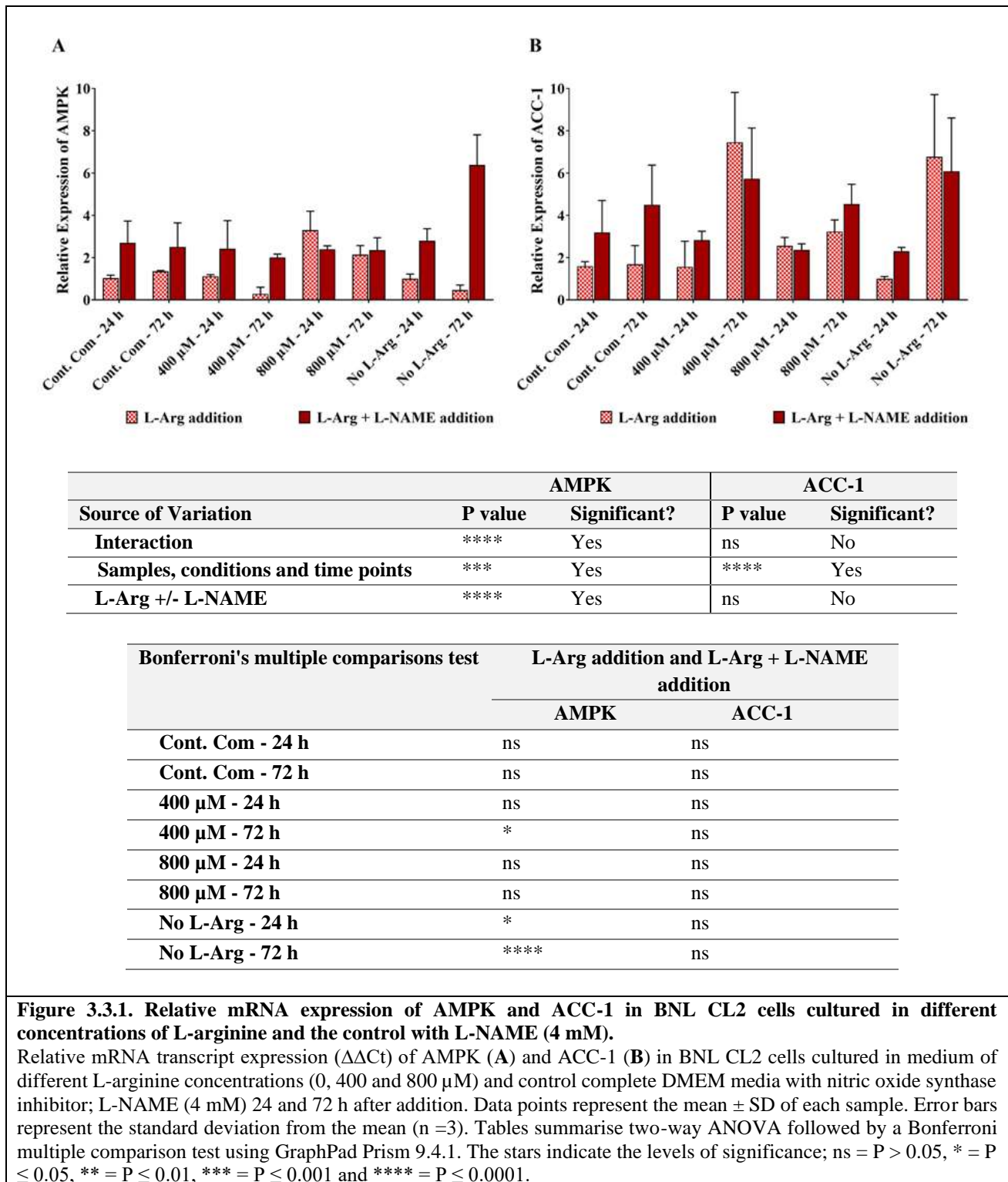
3.3. Results

3.3.1. qRT-PCR analysis of targets genes (AMPK and ACC-1) upon culturing of BNL CL2 cells in different exogenous L-Arg concentrations and L-NAME (4 mM), BH₄ (40 μ M) and SNAP (100 μ M)

Cells were grown as described in section 3.2.2 and sampled for transcriptional mRNA level analysis by qRT-PCR. RNA samples were control complete DMEM media, no L-arginine SILAC DMEM media and 400 and 800 μ M L-arginine with or without either L-NAME (NOS inhibitor, 4 mM), BH₄ (NOS co-factor, 40 μ M) or SNAP (NO donor, 100 μ M) addition. Cells cultured in different L-Arg concentrations with or without either L-NAME or BH₄ addition to BNL CL2 cells were collected at 24 and 72 h and samples cultured in different L-Arg concentrations with SNAP were collected at 6 and 24 h. Relative gene expression analysis ($\Delta\Delta$ Ct) was used to quantify target gene mRNA expression normalised to a reference gene, β -actin. The target gene expression was normalized to β -actin to obtain the Δ Ct and then the relative difference (Δ Ct) between target and β -actin was normalized to the Δ Ct value of the control no L-arginine added sample at the 24 h culture time point to obtain the $\Delta\Delta$ Ct value. The target genes investigated were AMPK, the key downstream target of L-Arginine/NO metabolic pathway and ACC-1, downstream target of AMPK and lipogenic gene involved in fatty acid synthesis. The relative expression of each gene was denoted as RE.

3.3.1.1. AMPK and ACC-1 transcript analysis upon L-NAME (4 mM) addition to BNL CL2 cells

The impact of L-NAME (NOS inhibitor) on AMPK gene expression in the cultured BNL CL2 cells with different L-Arg additions with or without L-NAME (4 mM) is presented in **Fig 3.3.1A**. The expression of AMPK mRNA was high ($P < 0.0001$) in samples cultured in no L-Arg with L-NAME at 72 h (2.5-fold compared to the control with L-NAME at 72 h) among all samples with or without L-NAME. It was shown in chapter 2 that when cells were treated with 800 μ M L-Arg, AMPK gene expression was highest at 24 h (RE 3.3). However, when cells were cultured in 800 μ M L-Arg with L-NAME, the AMPK expression was decreased ($P < 0.0001$) at 24 h (RE 2.4) in the presence of NOS inhibitor L-NAME, but increased ($P < 0.0001$) in 800 μ M L-Arg with L-NAME at 72 h (RE 2.35) compared to arginine at 800 μ M at 72 h (RE 2.14). Except for L-Arg at 800 μ M with L-NAME at 24 h, all samples with L-NAME showed increased ($P < 0.0001$) AMPK gene expression compared to the control samples and the samples treated with different concentrations of L-Arginine (0, 400 and 800 μ M). AMPK mRNA expression also decreased ($P < 0.0001$) with the time of culture when the cells grown in L-Arg and L-NAME, except at 0 μ M with L-NAME.



The impact of L-NAME on *ACC-1* gene expression is presented in **Fig 3.3.1B**. When comparing the difference of *ACC-1* gene expression between L-Arg treated, and L-Arg and L-NAME treated samples, *ACC-1* gene expression was increased ($P < 0.0001$) in L-arginine at 800 μ M with L-NAME at 72 h (RE 4.53) compared to

the ACC-1 expression in the samples cultured in 800 μ M L-Arg (RE 3.23). Interestingly, across the time points ACC-1 expression was increased ($P<0.0001$) in L-Arg and L-NAME treated samples, this was highest in the samples cultured in 0 μ M L-Arg and L-NAME (24h; RE 2.3 and 72 h; RE 6.07). The highest ACC-1 gene expression was in 0 μ M L-Arg and L-NAME samples at 72 h (1.35-fold) compared to the control sample cultured in complete DMEM with L-NAME.

3.3.1.2. AMPK and ACC-1 transcript analysis upon BH₄ (40 μ M) addition to BNL CL2 cells

The impact of BH₄ (co-factor of NOS, 40 μ M) addition to BNL CL2 cells in different exogenous L-arginine concentrations on AMPK mRNA is presented in **Fig 3.3.2A**. Upon BH₄ addition to the cells with excess exogenous L-Arg, the AMPK mRNA expression was high ($P<0.0001$) in samples cultured in 400 μ M L-Arg with BH₄ at 24 (1.5-fold) and 72 h (5.8-fold) compared to the samples cultured in 400 μ M L-Arg only. Arginine at 800 μ M with BH₄ showed decreased ($P<0.0001$) AMPK expression at 24 h (0.64-fold) whereas the expression was increased ($P<0.0001$) at 72 h (1.55-fold) compared to 800 μ M L-Arg. AMPK expression was also increased ($P<0.0001$) in samples cultured at 0 μ M L-Arg with BH₄ at 72 h (1.67-fold) compared to the 0 μ M L-Arg. Interestingly, samples cultured with different amounts of L-Arg and BH₄ increased ($P<0.0001$) the AMPK mRNA levels compared to the L-Arg only treated samples, except the control complete DMEM with BH₄, where the AMPK expression decreased with time at 24 (RE 3.0) and 72 h (RE 1.45).

The impact of BH₄ on ACC-1 mRNA is presented in **Fig 3.3.2B**. Among all samples, ACC-1 gene expression was decreased ($P<0.0001$) in the samples cultured with 400 μ M L-Arg and BH₄ at 72 h compared to the 400 μ M L-Arg at 72 h. Noticeably, ACC-1 mRNA levels were increased ($P<0.0001$) with culture time in samples cultured in different concentrations of L-Arg (0, 400 and 800 μ M) with BH₄ except the control with BH₄. The samples cultured in L-arginine with BH₄ had increased ($P<0.0001$) expression of ACC-1 mRNA after 24 h (the control complete DMEM + BH₄; 3.34-fold, 400 μ M + BH₄; 1.72-fold, 800 μ M + BH₄; 1.4-fold and 0 μ M + BH₄; 2.42-fold) in comparison to the control and L-arginine treated samples without BH₄. After 72 h, the ACC-1 mRNA expression was low ($P<0.0001$) in samples cultured in 400 (RE 6.00) and high in 800 μ M L-Arg (RE 7.56) with BH₄ in comparison to the samples cultured without BH₄ (400 μ M; RE 7.46 and 800 μ M; RE 3.23)

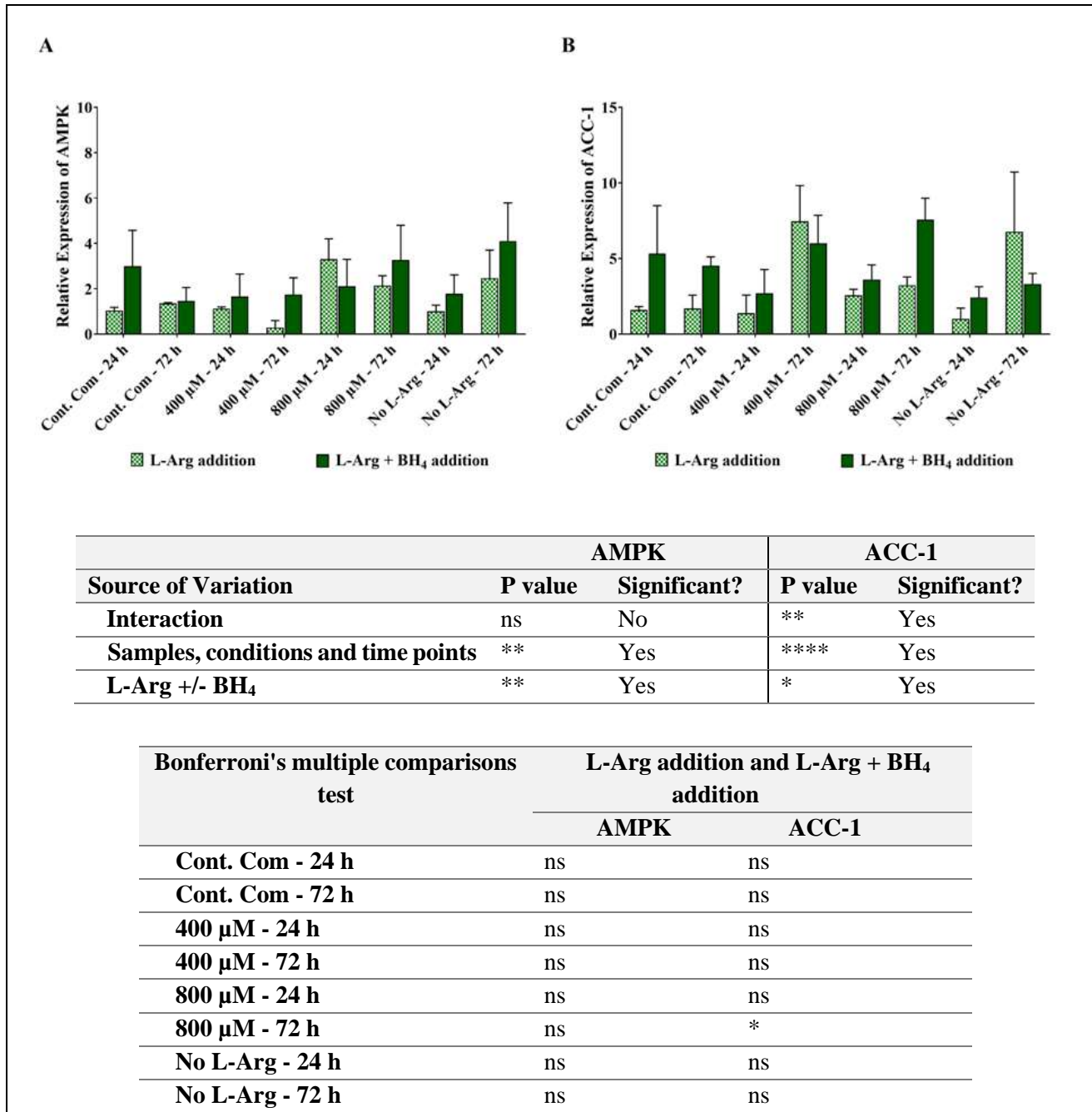


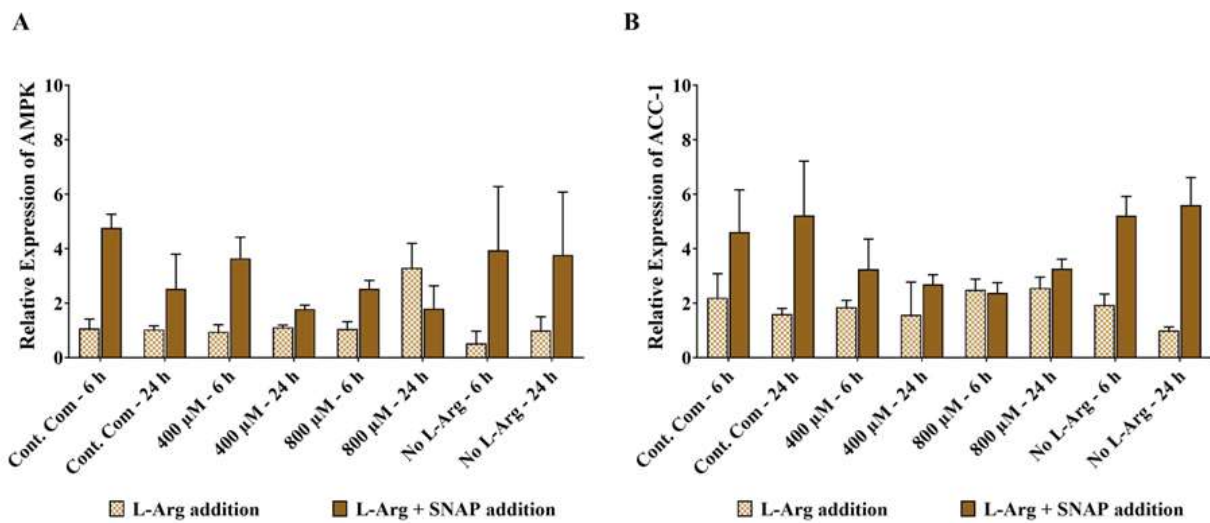
Figure 3.3.2. Relative mRNA expression of AMPK and ACC-1 in BNL CL2 cells cultured in different concentrations of L-arginine and the control with BH₄ (40 μM).

Relative mRNA transcript expression ($\Delta\Delta C_t$) of AMPK (A) and ACC-1 (B) in BNL CL2 cells cultured in medium of different L-arginine concentrations (0, 400 and 800 μM) and control complete DMEM media with the co-factor of nitric oxide synthase inhibitor; BH₄ (40 μM) 24 and 72 h after addition. Data points represent the mean \pm SD of each sample. Error bars represent the standard deviation from the mean (n = 3). Tables summarise two-way ANOVA followed by a Bonferroni multiple comparison test using GraphPad Prism 9.4.1. The stars indicate the levels of significance; ns = P > 0.05, * = P \leq 0.05, ** = P \leq 0.01, *** = P \leq 0.001 and **** = P \leq 0.0001.

3.3.1.3. AMPK and ACC-1 transcript analysis upon SNAP (100 μ M) addition to BNL CL2 cells

AMPK mRNA expression was evaluated in excess exogenous L-arginine with or without SNAP (NO donor; 100 μ M) addition and the relative expression is presented in **Fig 3.3.3A**. Overall, the samples cultured in L-Arg and SNAP had increased ($P < 0.0001$) expression of AMPK at 6 and 24 h compared to the samples cultured in L-Arg without SNAP at the same time points. However, AMPK mRNA levels decreased ($P < 0.0001$) at 800 μ M with SNAP at 24 h (0.54-fold) in comparison to the 800 μ M L-Arg. After 6 h, when compared with and without SNAP addition, there was increased ($P < 0.0001$) AMPK mRNA expression in the samples cultured with NO donor SNAP (the control complete DMEM + SNAP; 4.34-fold, 400 μ M + SNAP; 3.84-fold, 800 μ M + SNAP; 2.4-fold and 0 μ M + SNAP; 7.43-fold). Noticeably, this increase was highest in 0 μ M L-Arg (7.43-fold) among all the samples at 6 h.

ACC-1 mRNA expression is presented in **Fig 3.3.3B**. Overall, SNAP addition increased the expression of ACC-1 mRNA in L-Arg treated hepatocytes cells at 6 and 24 h in comparison to the samples cultured in different concentrations of L-Arg and the control complete DMEM. However, after 6 h L-arginine at 800 μ M with SNAP (0.95-fold) showed decreased ($P < 0.0001$) ACC-1 transcript expression over the 800 μ M L-Arg at 6 h. Comparison of ACC-1 mRNA expression in the presence and absence of SNAP in the L-Arg treated BNL CL2 cells showed that there was an increase ($P < 0.0001$) between the samples cultured with SNAP compared to the samples without SNAP at 6 h (the control complete DMEM + SNAP; 2.1-fold, 400 μ M + SNAP; 1.76-fold and 0 μ M + SNAP; 2.69-fold), except in 800 μ M and SNAP (0.95-fold). Samples cultured with SNAP and L-Arg had increased ($P < 0.0001$) ACC-1 mRNA expression with culture time, except at 400 μ M L-Arg with SNAP ($P < 0.0001$) (6 h; RE 3.25 and 24 h; RE 2.7).



Source of Variation	AMPK		ACC-1	
	P value	Significant?	P value	Significant?
Interaction	**	Yes	***	Yes
Samples, conditions and time points	ns	No	ns	No
L-Arg +/- SNAP	****	Yes	****	Yes

Bonferroni's multiple comparisons test	L-Arg addition and L-Arg + SNAP addition	
	AMPK	ACC-1
Cont. Com - 6 h	***	*
Cont. Com - 24 h	ns	***
400 μM - 6 h	*	ns
400 μM - 24 h	ns	ns
800 μM - 6 h	ns	ns
800 μM - 24 h	ns	ns
No L-Arg - 6 h	**	***
No L-Arg - 24 h	*	****

Figure 3.3.3. Relative mRNA expression of AMPK and ACC-1 in BNL CL2 cells cultured in different concentrations of L-arginine and the control with SNAP (100 μM).

Relative mRNA transcript expression ($\Delta\Delta Ct$) of AMPK (A) and ACC-1 (B) in BNL CL2 cells cultured in medium of different L-arginine concentrations (0, 400 and 800 μM) and control complete DMEM media with nitric oxide donor; SNAP (100 μM) 6 and 24 h after addition. Data points represent the mean \pm SD of each sample. Error bars represent the standard deviation from the mean (n = 3). Tables summarise two-way ANOVA followed by a Bonferroni multiple comparison test using GraphPad Prism 9.4.1. The stars indicate the levels of significance; ns = P > 0.05, * = P \leq 0.05, ** = P \leq 0.01, *** = P \leq 0.001 and **** = P \leq 0.0001.

3.3.2. Monitoring protein expression (AMPK and ACC-1) in response to L-Arg supplementation to BNL CL2 cells with L-NAME (4 mM), BH₄ (40 μM) and SNAP (100 μM) additions

Cells were grown as described in section 3.2.4 and sampled for protein analysis by western blotting. The samples were control complete DMEM media, no L-arginine SILAC DMEM media and 400 and 800 μM L-arginine with or without either L-NAME (NOS inhibitor, 4 mM), BH₄ (NOS co-factor, 40 μM) or SNAP (NO donor, 100 μM) addition and samples were collected at either 6, 24 or 72 h. Two combinations of gels were used to allow (a) comparison within a concentration with changing culture time (Figs 3.3.4, 3.3.7 and 3.3.10) and (b) comparison across concentrations at a specific culture time point (Figs 3.3.5 - 3.3.6, 3.3.8 - 3.3.9 and 3.3.11 - 3.3.12). Target protein expression was normalized to β-actin as a loading control. All data was then normalized to the value of no L-Arg added samples (0 μM L-arginine) at 24 h culture time point to obtain the final relative-normalised data, this was denoted as RE in the following sections.

3.3.2.1. AMPK and ACC-1 protein expressions upon L-NAME (4 mM) addition to BNL CL2 cells

Fig 3.3.5 presents the relative protein expression of AMPK upon L-NAME addition to BNL CL2 cells in different exogenous L-arginine concentrations. Interestingly, AMPK protein expression was decreased ($P < 0.0001$) in the samples cultured in L-NAME and L-arginine (400 and 800 μM) at 24 (0.26-fold and 0.31-fold, respectively) and 72 h (0.13-fold and 0.24-fold, respectively) compared to the arginine at 400 and 800 μM samples. Noticeably, the relative AMPK protein expression in the samples cultured in L-NAME and excess exogenous L-Arginine (400 and 800 μM) was more or less the same irrespective of the time points (for 400 μM + L-NAME at 24; RE 0.36 and 72 h; RE 0.37 and for 800 μM + L-NAME at 24; RE 0.46 and 72 h; RE 0.42). After 24 h, the samples cultured in L-NAME and L-Arg showed decreased ($P < 0.0001$) AMPK protein expression (400 μM + L-NAME; 0.26-fold and 800 μM + L-NAME; 0.31-fold) compared to the L-Arg at 400 and 800 μM at 24 h, whereas after 24 h the AMPK protein expression was increased ($P < 0.0001$) in the samples cultured in complete DMEM with L-NAME (1.33-fold) compared to the control complete DMEM.

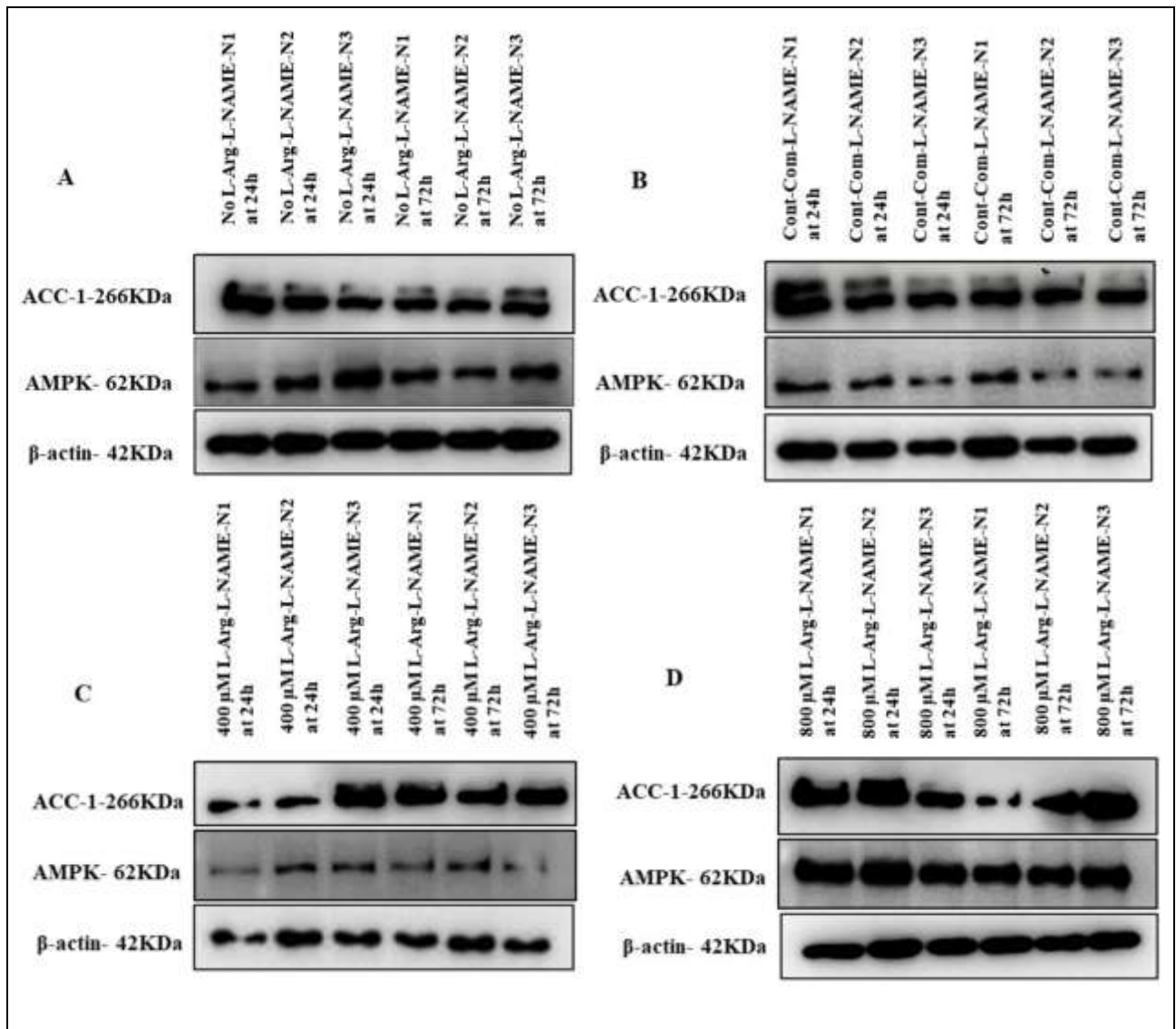
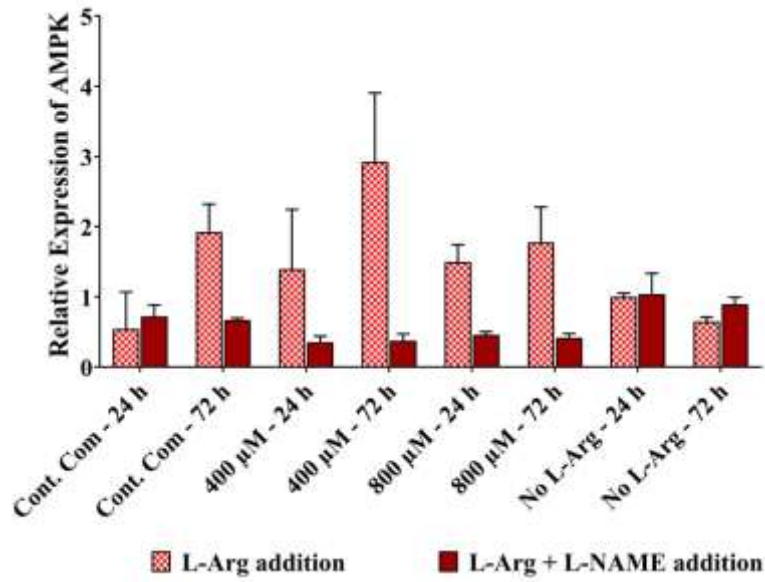


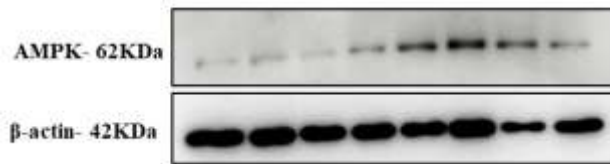
Figure 3.3.4. Western blot comparison for AMPK and ACC-1 protein expressions in BNL CL2 cells cultured in different concentrations of L-arginine and the control with L-NAME (4 mM).

Western blot comparison of the expression of key protein; AMPK and lipogenic ACC-1 protein levels investigated in L-arginine/NO metabolic pathway signalling in BNL CL2 cells cultured in customized media containing (A) no L-arginine SILAC DMEM and L-NAME (4 mM) (B) complete DMEM and L-NAME (4 mM), (C) 400 μM L-arginine and L-NAME (4 mM), and (D) 800 μM L-arginine and L-NAME (4 mM) for 24 and 72 h. β-actin is used as a loading control. The same amount of protein (10 μg) from different treatment groups was loaded from biological triplicate cultures into 10% SDS–polyacrylamide gels for the separation of target proteins.



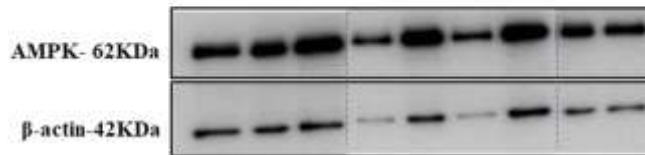
B

Cont-Com-L-NAME at 24h
 Cont-Com-L-NAME at 72h
 400 μM L-Arg-L-NAME at 24h
 400 μM L-Arg-L-NAME at 72h
 800 μM L-Arg-L-NAME at 24h
 800 μM L-Arg-L-NAME at 72h
 No L-Arg-L-NAME at 24h
 No L-Arg-L-NAME at 72h



C

Untreated at T=0
 Cont-Com at 24h
 Cont-Com at 72h
 400 μM L-Arg at 24h
 400 μM L-Arg at 72h
 800 μM L-Arg at 24h
 800 μM L-Arg at 72h
 No L-Arg at 24h
 No L-Arg at 72h



AMPK			
Source of Variation	P value	P value summary	Significant?
Interaction	<0.0001	****	Yes
Samples, conditions and time points	0.0044	**	Yes
L-Arg +/- L-NAME	<0.0001	****	Yes

Bonferroni's multiple comparisons test

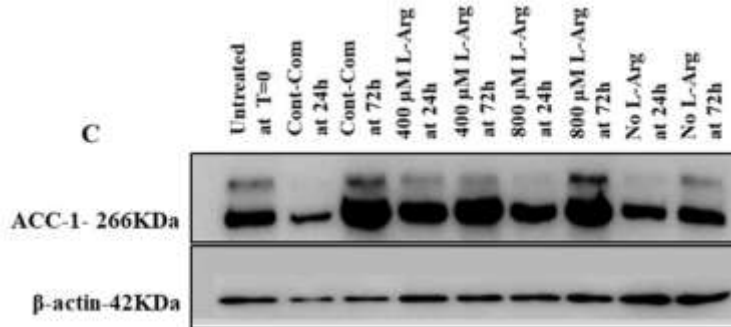
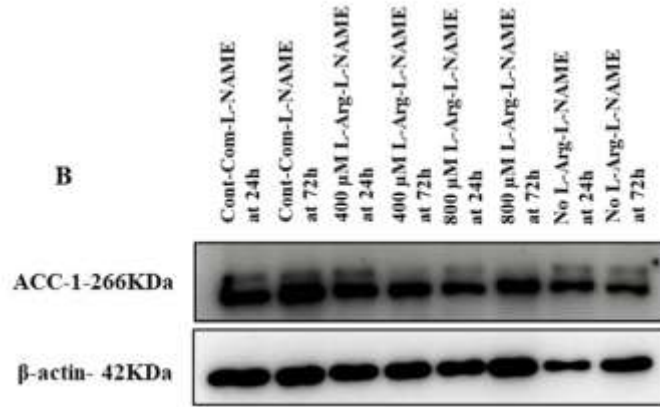
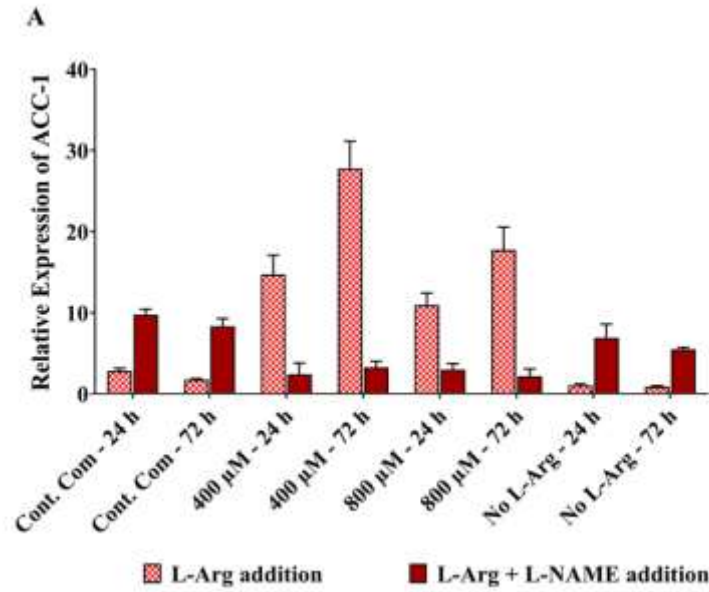
L-Arg addition and L-Arg + L-NAME addition

	AMPK
Cont. Com - 24 h	ns
Cont. Com - 72 h	**
400 μ M - 24 h	*
400 μ M - 72 h	****
800 μ M - 24 h	*
800 μ M - 72 h	**
No L-Arg - 24 h	ns
No L-Arg - 72 h	ns

Figure 3.3.5. Relative protein expression and western blot comparisons (with or without L-NAME) for AMPK protein in BNL CL2 cells cultured in different concentrations of L-arginine and the control with L-NAME (4 mM).

Relative protein expression of AMPK (A), western blot comparison of the expression of key protein, AMPK involved in L-arginine/NO metabolic pathway signalling investigated in BNL CL2 cells cultured with L-NAME (4 mM) in no L-arginine SILAC DMEM, complete DMEM, 400 μ M L-arginine and 800 μ M L-arginine for 24 and 72 h (B) and the amount of AMPK in cultured BNL CL2 cells without L-NAME for 24 and 72 h (C). The same amount of protein (10 μ g) from different treatment groups was loaded from biological triplicate cultures into 10% SDS–polyacrylamide gels for the separation of target proteins. Two representative blots from each treatment group are shown with the respective to the house-keeping-protein, β -actin. Bands in the blots were quantified using ImageJ software and the data are normalised to β -actin and then expressed as relative to the no L-arginine SILAC DMEM (0 μ M L-arginine) control at 24 h. Data points represent the mean \pm SD. Error bars represent the standard deviation from the mean (n = 3). The tables summarise two-way ANOVA followed by a Bonferroni multiple comparison test using GraphPad Prism 9.4.1. The stars indicate the levels of significance; ns = $P > 0.05$, * = $P \leq 0.05$, ** = $P \leq 0.01$, *** = $P \leq 0.001$ and **** = $P \leq 0.0001$.

Fig 3.3.6 presents the relative protein expression of ACC-1 upon L-NAME addition. As discussed in the results section in chapter 2, relative ACC-1 protein expression was unexpectedly increased to the highest levels in the samples cultured in L-Arg at 24 (400 μ M; 5.1-fold and 800 μ M; 3.8-fold) and 72 h (400 μ M; 16.1-fold and 800 μ M; 10.3-fold) compared to the control complete DMEM. However, when the NOS inhibitor L-NAME was added to these samples the relative ACC-1 expression was decreased ($P < 0.0001$) to the lowest levels at 24 (400 μ M; 0.24-fold and 800 μ M; 0.3-fold) and 72 h (400 μ M; 0.4-fold and 800 μ M; 0.25-fold) compared to the L-NAME added to the control complete DMEM. Like complete DMEM with L-NAME at 24 and 72 h, the samples cultured in 0 μ M L-Arg showed increased ($P < 0.0001$) ACC-1 protein expression at 24 (RE 6.89) and 72 h (RE 5.44) compared to the L-Arg (400 and 800 μ M) and L-NAME samples at the same time points. Overall, L-NAME addition to the samples cultured in L-Arg had decreased ($P < 0.0001$) relative ACC-1 protein expression, whereas L-NAME addition to the control complete DMEM and no L-Arg had increased ($P < 0.0001$) relative ACC-1 protein expression.



ACC-1			
Source of Variation	P value	P value summary	Significant?
Interaction	<0.0001	****	Yes
Samples, conditions and time points	<0.0001	****	Yes
L-Arg +/- L-NAME	<0.0001	****	Yes

Bonferroni's multiple comparisons test	L-Arg addition and L-Arg + L-NAME addition ACC-1
Cont. Com - 24 h	****
Cont. Com - 72 h	****
400 μ M - 24 h	****
400 μ M - 72 h	****
800 μ M - 24 h	****
800 μ M - 72 h	****
No L-Arg - 24 h	***
No L-Arg - 72 h	**

Figure 3.3.6. Relative protein expression and western blot comparisons (with or without L-NAME) for ACC-1 protein in BNL CL2 cells cultured in different concentrations of L-arginine and the control with L-NAME (4 mM).

Relative protein expression of ACC-1 (A), western blot comparison of the expression of lipogenic protein, ACC-1 involved in L-arginine/NO metabolic pathway signalling investigated in BNL CL2 cells cultured with L-NAME (4 mM) in no L-arginine SILAC DMEM, complete DMEM, 400 μ M L-arginine and 800 μ M L-arginine for 24 and 72 h (B) and the amount of ACC-1 in cultured BNL CL2 cells without L-NAME for 24 and 72 h (C). The same amount of protein (10 μ g) from different treatment groups was loaded from biological triplicate cultures into 10% SDS–polyacrylamide gels for the separation of target proteins. Two representative blots from each treatment group are shown with the respective to the house-keeping-protein, β -actin. Bands in the blots were quantified using ImageJ software and the data are normalised to β -actin and then expressed as relative to the no L-arginine SILAC DMEM (0 μ M L-arginine) control at 24 h. Data points represent the mean \pm SD. Error bars represent the standard deviation from the mean (n = 3). The tables summarise two-way ANOVA followed by a Bonferroni multiple comparison test using GraphPad Prism 9.4.1. The stars indicate the levels of significance; ns = P > 0.05, * = P \leq 0.05, ** = P \leq 0.01, *** = P \leq 0.001 and **** = P \leq 0.0001.

3.3.2.2. AMPK and ACC-1 protein expression upon BH₄ (40 μ M) addition to BNL CL2 cells

The impact of BH₄ addition on AMPK protein expression in BNL CL2 cells cultured in different exogenous L-arginine concentrations and BH₄ is presented in **Fig 3.3.8**. Overall, the relative AMPK protein expression was decreased (P<0.0001) among all the samples cultured in BH₄ compared to the samples without BH₄. However, AMPK protein expression was increased (P<0.0001) across culture time when the cells were treated with BH₄ (after 72 h, the control + BH₄; 4-fold, 400 μ M + BH₄; 1.25-fold and 800 μ M + BH₄; 1.3-fold) except for the samples cultured in 0 μ M L-Arg and BH₄ (at 24; RE 0.76 and 72 h; RE 0.55). Arginine at 800 μ M with BH₄ at 24 (5.42-fold) and 72 h (1.75-fold) had the highest AMPK protein expression (P<0.0001) compared to the control complete DMEM with BH₄.

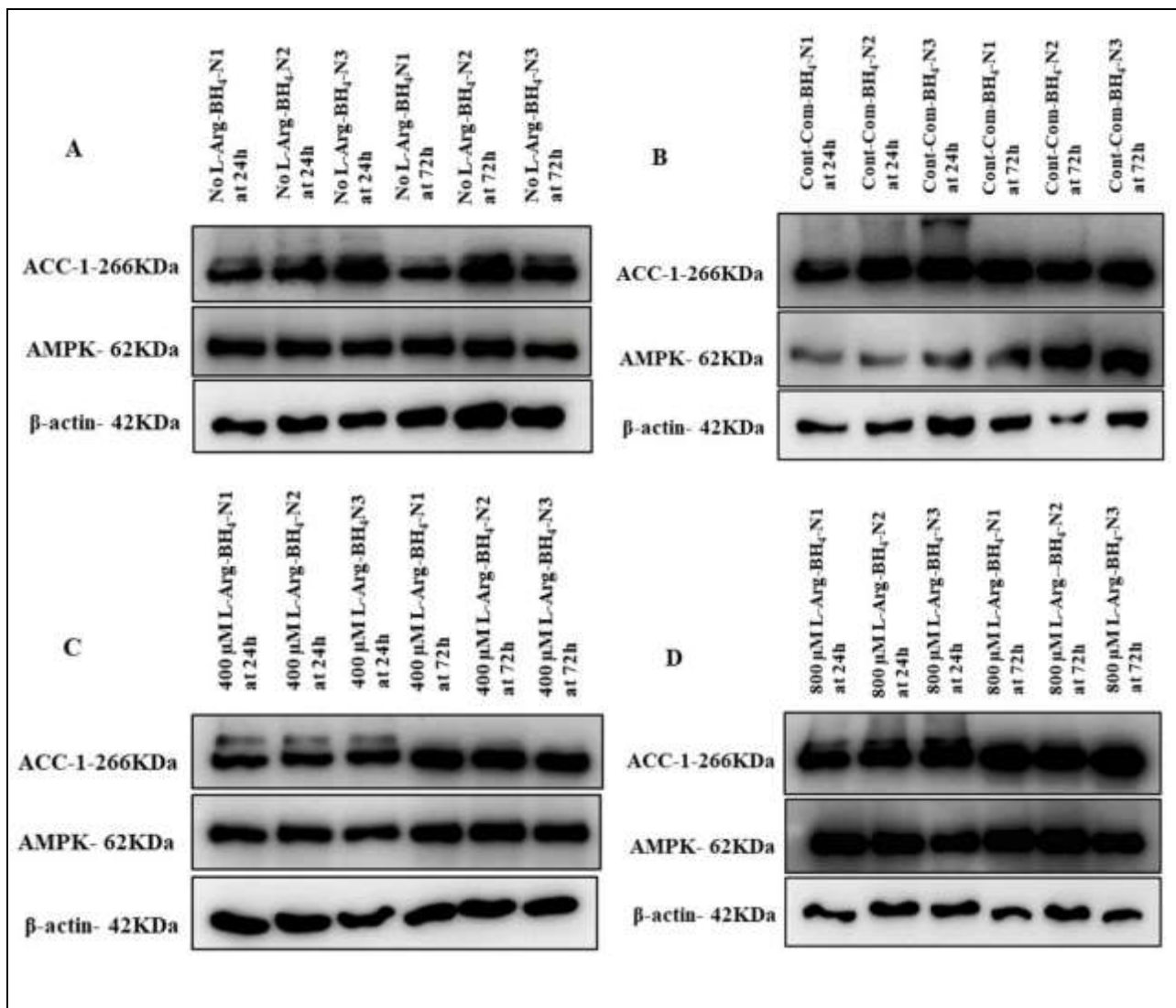
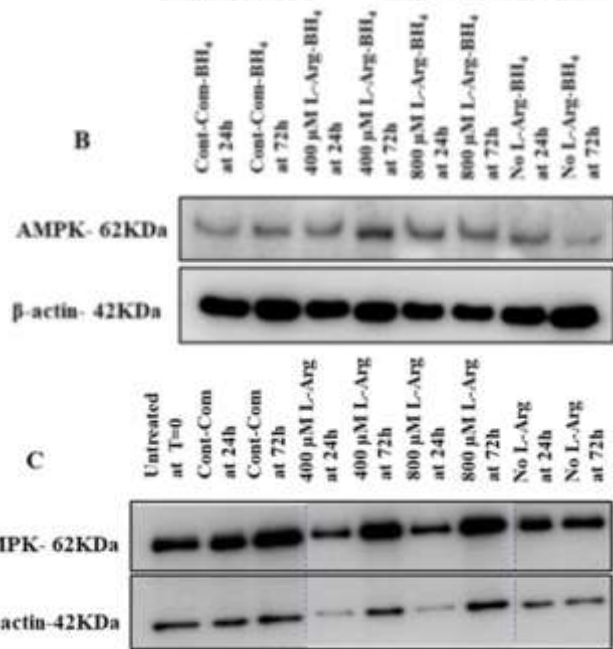
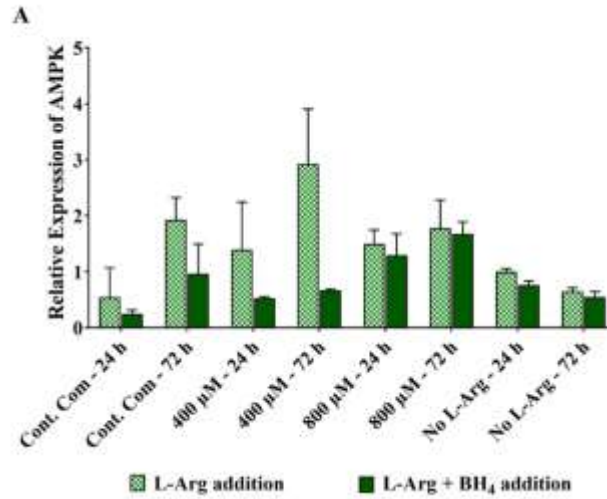


Figure 3.3.7. Western blot comparison for AMPK and ACC-1 protein expressions in BNL CL2 cells cultured in different concentrations of L-arginine and the control with BH4 (40 μM).

Western blot comparison of the expression of key protein; AMPK and ACC-1 protein levels investigated in L-arginine/NO metabolic pathway signalling in BNL CL2 cells cultured in customized media containing (A) no L-arginine SILAC DMEM and BH₄ (40 μM) (B) complete DMEM and BH₄ (40 μM), (C) 400 μM L-arginine and BH₄ (40 μM), and (D) 800 μM L-arginine and BH₄ (40 μM) for 24 and 72 h. β-actin is used as a loading control. The same amount of protein (10 μg) from different treatment groups was loaded from biological triplicate cultures into 10% SDS–polyacrylamide gels for the separation of target proteins.



AMPK			
Source of Variation	P value	P value summary	Significant?
Interaction	0.0014	**	Yes
Samples, conditions and time points	<0.0001	****	Yes
L-Arg +/- BH ₄	<0.0001	****	Yes

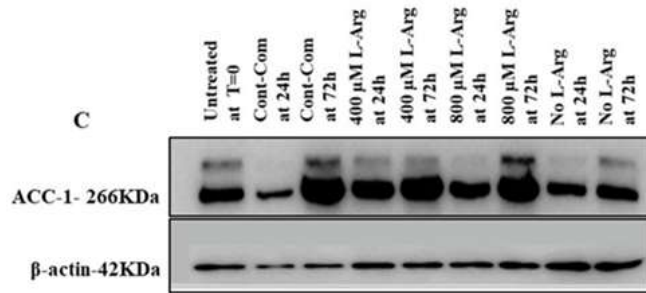
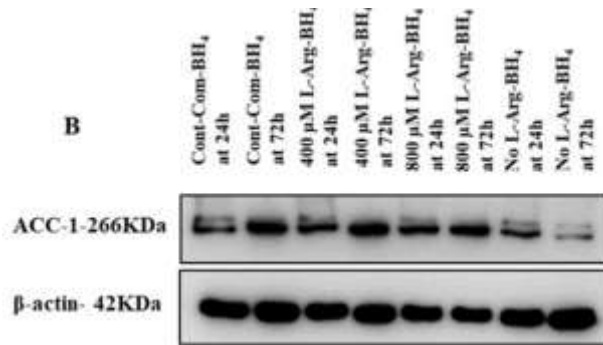
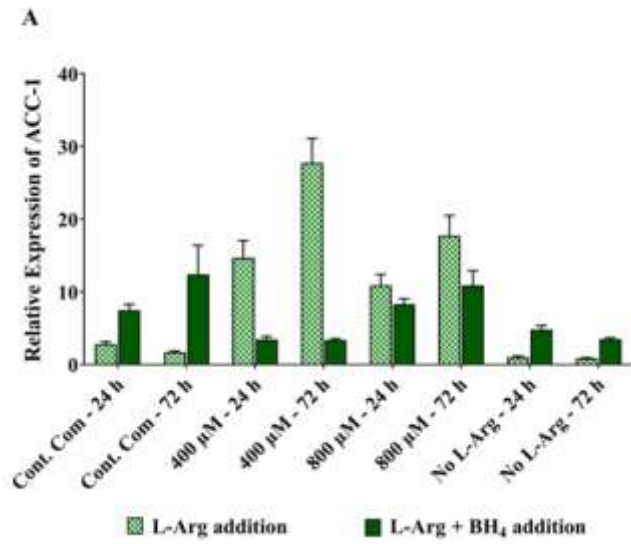
Bonferroni's multiple comparisons test	L-Arg addition and L-Arg + BH ₄ addition
	AMPK
Cont. Com - 24 h	ns
Cont. Com - 72 h	ns
400 μM - 24 h	ns
400 μM - 72 h	****

800 µM - 24 h	ns
800 µM - 72 h	ns
No L-Arg - 24 h	ns
No L-Arg - 72 h	ns

Figure 3.3.8. Relative protein expression and western blot comparisons (with or without BH₄) for AMPK protein in BNL CL2 cells cultured in different concentrations of L-arginine and the control with BH₄ (40 µM).

Relative protein expression of AMPK (A), western blot comparison of the expression of key protein, AMPK involved in L-arginine/NO metabolic pathway signalling investigated in BNL CL2 cells cultured with BH₄ (40 µM) in no L-arginine SILAC DMEM, complete DMEM, 400 µM L-arginine and 800 µM L-arginine for 24 and 72 h (B) and the amount of AMPK in cultured BNL CL2 cells without BH₄ for 24 and 72 h (C). The same amount of protein (10 µg) from different treatment groups was loaded from biological triplicate cultures into 10% SDS–polyacrylamide gels for the separation of target proteins. Two representative blots from each treatment group are shown with the respective to the house-keeping-protein, β-actin. Bands in the blots were quantified using ImageJ software and the data are normalised to β-actin and then expressed as relative to the no L-arginine SILAC DMEM (0 µM L-arginine) control at 24 h. Data points represent the mean ± SD. Error bars represent the standard deviation from the mean (n = 3). The tables summarise two-way ANOVA followed by a Bonferroni multiple comparison test using GraphPad Prism 9.4.1. The stars indicate the levels of significance; ns = P > 0.05, * = P ≤ 0.05, ** = P ≤ 0.01, *** = P ≤ 0.001 and **** = P ≤ 0.0001.

The impact of BH₄ addition on ACC-1 protein expression in BNL CL2 cells cultured in different exogenous L-arginine concentrations and BH₄ is presented in **Fig 3.3.9**. The relative ACC-1 protein expression was decreased (P<0.0001) in the samples cultured in 400 and 800 µM L-Arg and BH₄ at 24 (0.23-fold and 0.76-fold, respectively) and 72 h (0.76-fold and 0.61-fold, respectively) compared to the samples cultured in 400 and 800 µM L-Arg without BH₄ at the same time points. Among BH₄ treated samples, after 24 h ACC-1 protein expression decreased (P<0.0001) in arginine at 400 µM and BH₄ (0.46-fold) whereas this was increased in arginine at 800 µM and BH₄ (1.11-fold) in comparison to the control complete DMEM with BH₄. However, after 72 h there was decreased (P<0.0001) ACC-1 protein expression observed in 400 (0.27-fold) and 800 µM L-Arg with BH₄ (0.88-fold) compared to the control with BH₄ after 72 h.



		ACC-1	
Source of Variation	P value	P value summary	Significant?
Interaction	<0.0001	****	Yes
Samples, conditions and time points	<0.0001	****	Yes
L-Arg +/- BH ₄	<0.0001	****	Yes

Bonferroni's multiple comparisons test	L-Arg addition and L-Arg + BH ₄ addition
	ACC-1

Cont. Com - 24 h *

Cont. Com - 72 h	****
400 μM - 24 h	****
400 μM - 72 h	****
800 μM - 24 h	ns
800 μM - 72 h	***
No L-Arg - 24 h	ns
No L-Arg - 72 h	ns

Figure 3.3.9. Relative protein expression and western blot comparisons (with or without BH₄) for ACC-1 protein in BNL CL2 cells cultured in different concentrations of L-arginine and the control with BH₄ (40 μ M).

Relative protein expression of ACC-1 (A), western blot comparison of the expression of lipogenic protein, ACC-1 involved in L-arginine/NO metabolic pathway signalling investigated in BNL CL2 cells cultured with BH₄ (40 μ M) in no L-arginine SILAC DMEM, complete DMEM, 400 μ M L-arginine and 800 μ M L-arginine for 24 and 72 h (B) and the amount of ACC-1 in cultured BNL CL2 cells without BH₄ for 24 and 72 h (C). The same amount of protein (10 μ g) from different treatment groups was loaded from biological triplicate cultures into 10% SDS–polyacrylamide gels for the separation of target proteins. Two representative blots from each treatment group are shown with the respective to the house-keeping-protein, β -actin. Bands in the blots were quantified using ImageJ software and the data are normalised to β -actin and then expressed as relative to the no L-arginine SILAC DMEM (0 μ M L-arginine) control at 24 h. Data points represent the mean \pm SD. Error bars represent the standard deviation from the mean (n = 3). The tables summarise two-way ANOVA followed by a Bonferroni multiple comparison test using GraphPad Prism 9.4.1. The stars indicate the levels of significance; ns = P > 0.05, * = P \leq 0.05, ** = P \leq 0.01, *** = P \leq 0.001 and **** = P \leq 0.0001.

3.3.2.3. AMPK and ACC-1 protein expressions upon SNAP (100 μ M) addition to BNL CL2 cells

Relative AMPK protein expression in BNL CL2 cells cultured with exogenous L-Arg and SNAP at 6 and 24 h time points is presented in **Fig 3.3.11**. After 24 h, AMPK protein expression was decreased (P<0.0001) in the samples cultured with SNAP (the control + SNAP 0.41-fold, 400 μ M + SNAP; 0.2-fold and 800 μ M 0.23-fold) compared to the samples cultured without SNAP. The samples cultured with 0 μ M L-Arg and SNAP had the lowest AMPK expression at 24 h.

Relative ACC-1 protein expression in BNL CL2 cells cultured with exogenous L-Arg and SNAP at 6 and 24 h time points is presented in **Fig 3.3.12**. Like AMPK expression, after 24 h, the ACC-1 protein expression was decreased (P<0.0001) in samples cultured with SNAP (the control + SNAP 0.68-fold, 400 μ M + SNAP; 0.085-fold and 800 μ M 0.1-fold) compared to the samples cultured without SNAP. There was a large decrease (P<0.0001) in ACC-1 protein expression in the samples cultured in 400 and 800 μ M with SNAP. The samples cultured with 0 μ M L-Arg and SNAP had highest (P<0.0001) ACC-1 expression at 24 h (RE 3.0) among the SNAP treated samples.

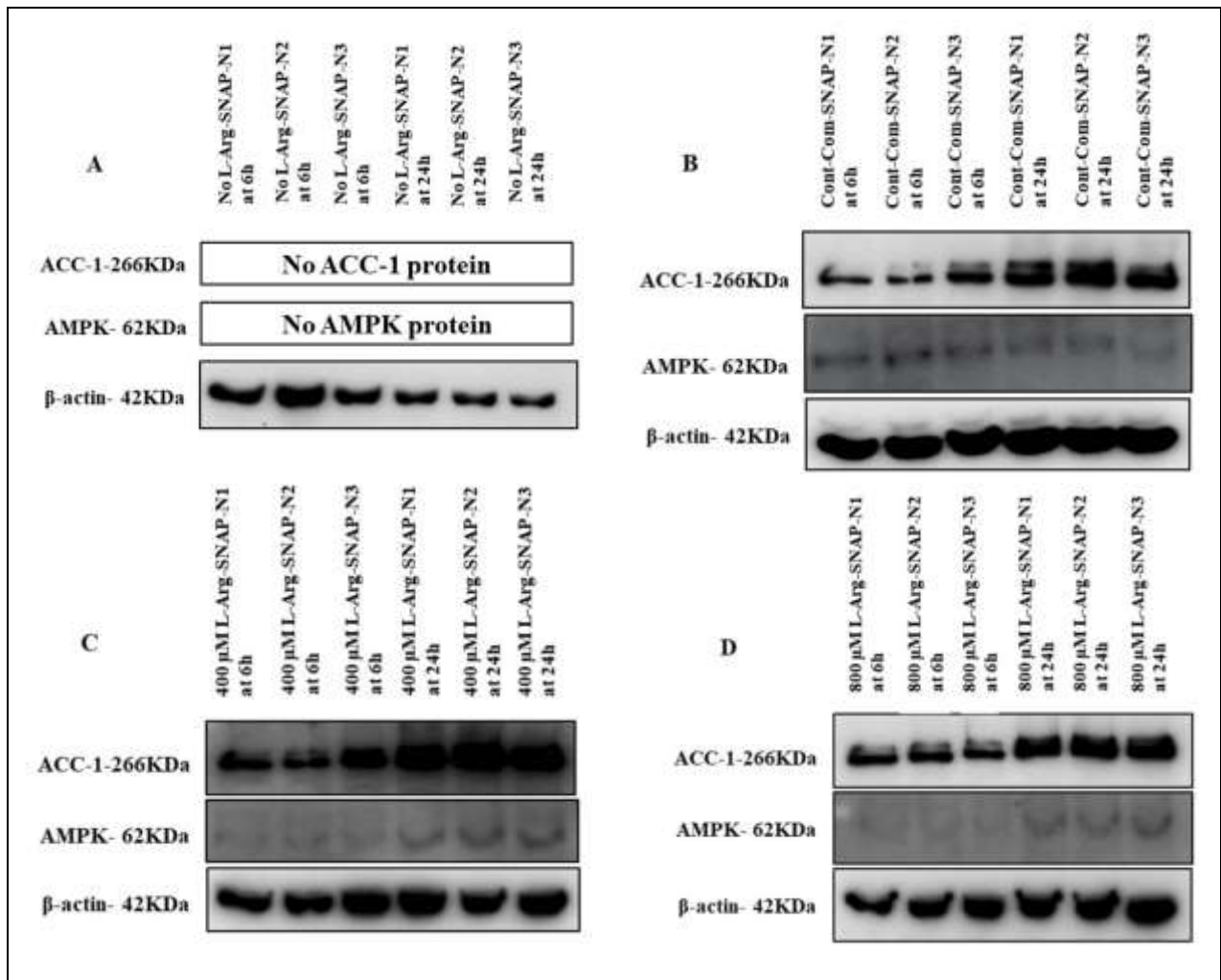


Figure 3.3.10. Western blot comparison for AMPK and ACC-1 protein expressions in BNL CL2 cells cultured in different concentrations of L-arginine and the control with SNAP (100 μM).

Western blot comparison of the expression of key protein; AMPK and lipogenic ACC-1 protein levels investigated in L-arginine/NO metabolic pathway signalling in BNL CL2 cells cultured in customized media containing (A) no L-arginine SILAC DMEM and SNAP (100 μM) (B) complete DMEM and SNAP (100 μM), (C) 400 μM L-arginine and SNAP (100 μM), and (D) 800 μM L-arginine and SNAP (100 μM) for 6 and 24 h. β-actin is used as a loading control. The same amount of protein (10 μg) from different treatment groups was loaded from biological triplicate cultures into 10% SDS-polyacrylamide gels for the separation of target proteins.

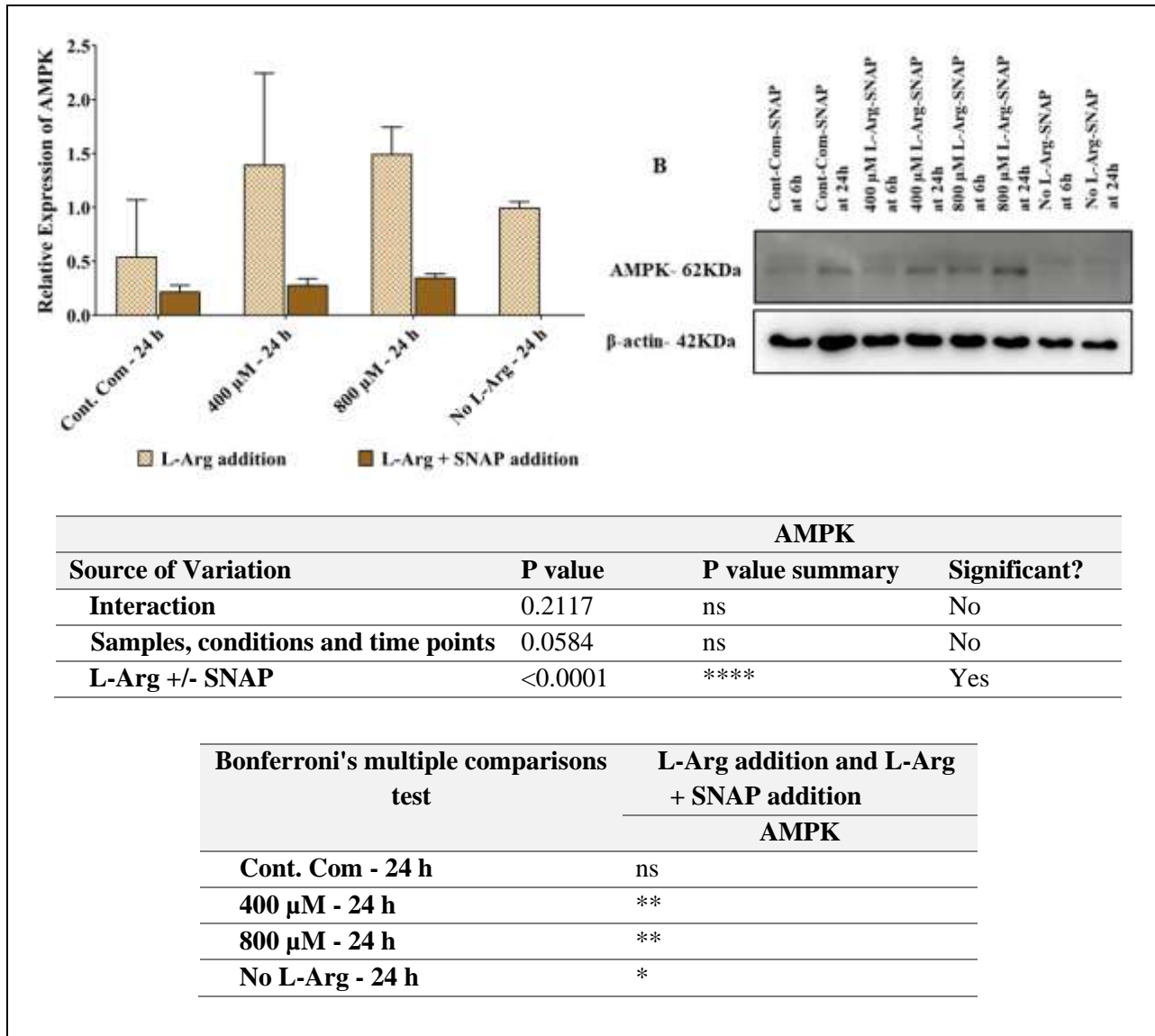


Figure 3.3.11. Relative protein expression and western blot comparisons for AMPK protein in BNL CL2 cells cultured in different concentrations of L-arginine and the control with SNAP (100 μ M).

Relative protein expression of AMPK (A), western blot comparison of the expression of key protein, AMPK involved in L-arginine/NO metabolic pathway signalling investigated in BNL CL2 cells cultured with SNAP (100 μ M) in no L-arginine SILAC DMEM, complete DMEM, 400 μ M L-arginine and 800 μ M L-arginine for 6 and 24 h (B). The same amount of protein (10 μ g) from different treatment groups was loaded from biological triplicate cultures into 10% SDS-polyacrylamide gels for the separation of target proteins. The representative blot from the treatment group is shown with the respective to the house-keeping-protein, β -actin. Bands in the blots were quantified using ImageJ software and the data are normalised to β -actin and then expressed as relative to the no L-arginine SILAC DMEM (0 μ M L-arginine) control at 24 h. Data points represent the mean \pm SD. Error bars represent the standard deviation from the mean (n = 3). The tables summarise two-way ANOVA followed by a Bonferroni multiple comparison test using GraphPad Prism 9.4.1. The stars indicate the levels of significance; ns = P > 0.05, * = P \leq 0.05, ** = P \leq 0.01, *** = P \leq 0.001 and **** = P \leq 0.0001.

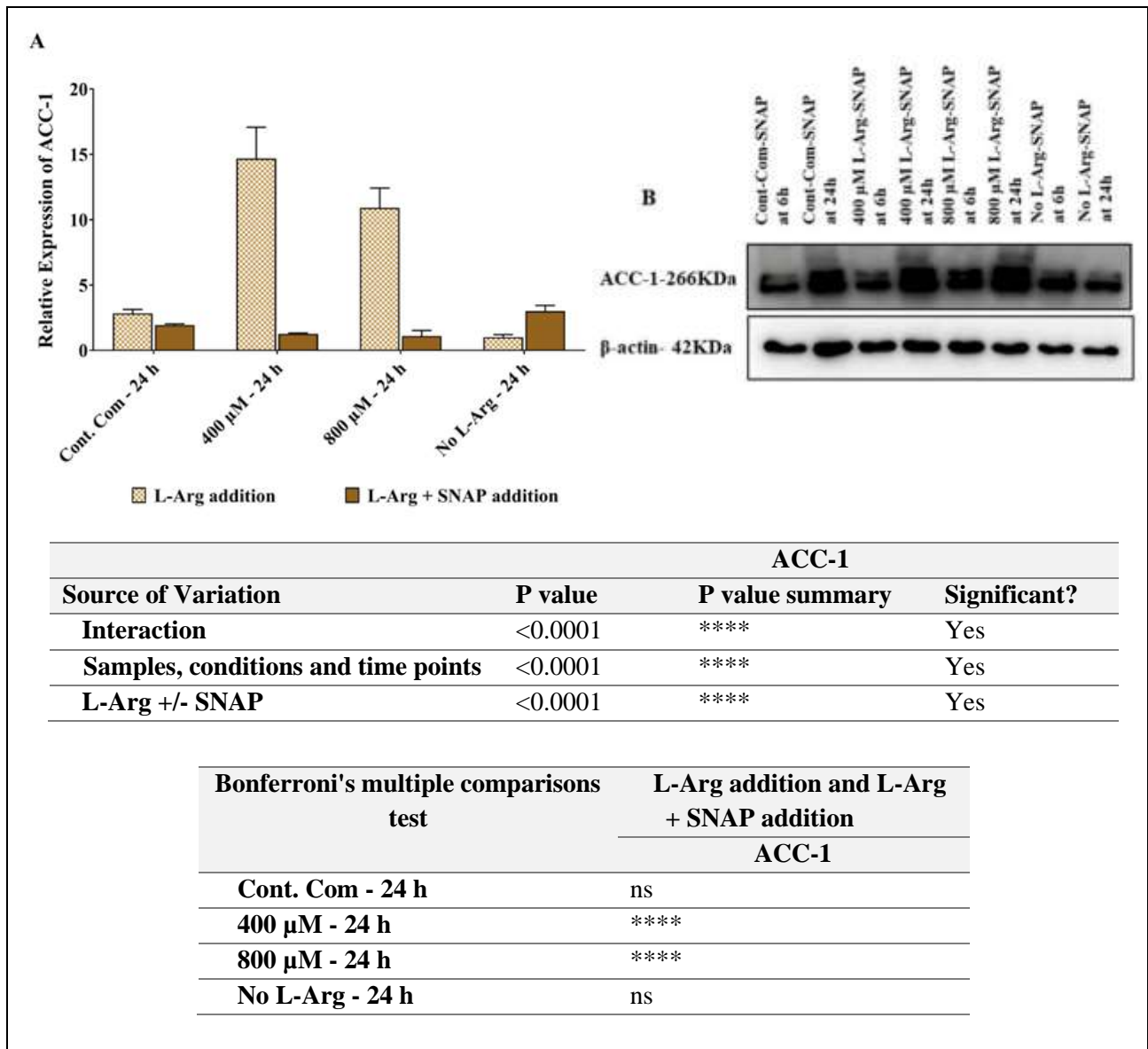


Figure 3.3.12. Relative protein expression and western blot comparisons for ACC-1 protein in BNL CL2 cells cultured in different concentrations of L-arginine and the control with SNAP (100 μM).

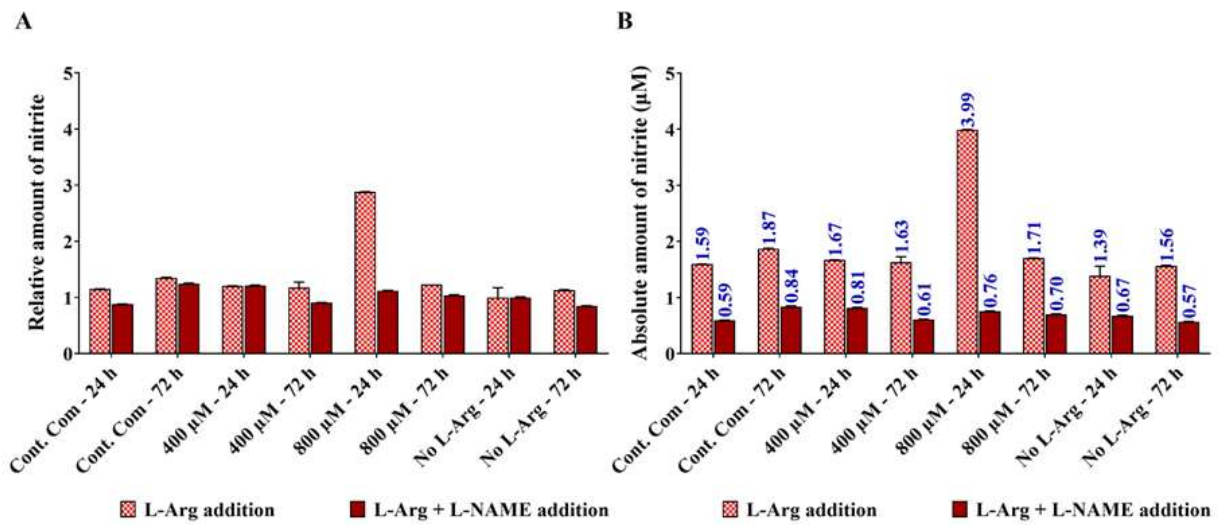
Relative protein expression of ACC-1 (A), western blot comparison of the expression of lipogenic protein, ACC-1 involved in L-arginine/NO metabolic pathway signalling investigated in BNL CL2 cells cultured with SNAP (100 μM) in no L-arginine SILAC DMEM, complete DMEM, 400 μM L-arginine and 800 μM L-arginine for 6 and 24 h (B). The same amount of protein (10 μg) from different treatment groups was loaded from biological triplicate cultures into 10% SDS-polyacrylamide gels for the separation of target proteins. The representative blot from the treatment group is shown with the respective to the house-keeping-protein, β-actin. Bands in the blots were quantified using ImageJ software and the data are normalised to β-actin and then expressed as relative to the no L-arginine SILAC DMEM (0 μM L-arginine) control at 24 h. Data points represent the mean ± SD. Error bars represent the standard deviation from the mean (n = 3). The tables summarise two-way ANOVA followed by a Bonferroni multiple comparison test using GraphPad Prism 9.4.1. The stars indicate the levels of significance; ns = P > 0.05, * = P ≤ 0.05, ** = P ≤ 0.01, *** = P ≤ 0.001 and **** = P ≤ 0.0001.

3.3.3. Determination of nitric oxide / nitrite measurements by Griess Assay in BNL CL2 cells in different concentrations of exogenous L-arginine with L-NAME (4 mM), BH₄ (40 μM) and SNAP (100 μM)

The amount of nitrite presents in the serum samples of the BNL CL2 cells cultured in different concentrations of L-Arg and the control complete DMEM were analysed with or without either L-NAME, BH₄ or SNAP. The amount of nitrite present in the samples was normalised to the amount of nitrite present in the no L-Arg (0 μM) cell samples at 24 h and then the relative (**A**) and the absolute (**B**) amount of nitrite present in the cell serum samples are presented in the **Figs 3.3.13-15** compared to cell samples cultured without L-NAME, BH₄ or SNAP.

When L-NAME (4 mM) was added to the BNL CL2 cells cultured in L-Arg (0, 400 and 800 μM) and the control complete DMEM, the amount of nitrite present is reported in **Fig 3.3.13**. The amount of signalling molecule, NO involved in L-arginine/NO pathway decreased ($P < 0.0001$) in the samples cultured with L-NAME after 24 (the control + L-NAME; 0.37-fold, 400 μM + L-NAME; 0.49-fold, 800 μM + L-NAME; 0.19-fold and 0 μM + L-NAME; 0.49-fold) and 72 h (the control + L-NAME; 0.44-fold, 400 μM + L-NAME; 0.37-fold, 800 μM + L-NAME; 0.41-fold and 0 μM + L-NAME; 0.36-fold) compared to the samples cultured without L-NAME. Interestingly, a large decrease ($P < 0.0001$) in the amount of nitrite was observed in the samples cultured at highest L-Arg 800 μM with L-NAME (0.54 μM nitrite) in comparison to the samples cultured without L-NAME (2.88 μM nitrite) after 24 h. Over culture time the amount of nitrite decreased ($P < 0.0001$) in cells treated with L-NAME (400 μM + L-NAME; 0.75-fold, 800 μM + L-NAME; 0.93-fold and 0 μM L-Arg + L-NAME; 0.84-fold) except the control with L-NAME after 72 h (1.4-fold). The concentration of nitrite was increased ($P < 0.0001$) in the samples cultured with excess L-Arg (400 and 800 μM) with L-NAME at 24 h (400 μM + L-NAME; 0.81 μM and 800 μM + L-NAME; 0.76 μM) compared to the control with L-NAME after 24 h (0.59 μM), whereas after 72 h the amount of nitrite was decreased ($P < 0.0001$) in the former samples (400 μM + L-NAME; 0.61 μM and 800 μM + L-NAME; 0.70 μM) compared to the later samples (the control + L-NAME; 0.84 μM).

When the co-factor of NOS, BH₄ (40 μM) was added to the cells cultured in L-Arg (0, 400 and 800 μM) and the control complete DMEM, the amount of nitrite present in the cell samples were analysed and are shown in **Fig 3.3.14**. Generally, the addition of BH₄ increased ($P < 0.0001$) the amount of nitrite present in the cell samples at 24 (the control + BH₄; 22.88-fold, 400 μM + BH₄; 17.13, 800 μM + BH₄; 11.95-fold and 0 μM + BH₄; 10.88-fold) and 72 h (the control + BH₄; 20.69-fold, 400 μM + BH₄; 24.14, 800 μM + BH₄; 22.66-fold and 0 μM + BH₄; 0.99-fold). Among all BH₄ treated cell samples, the highest amount of nitrite was observed in the samples at 800 μM L-Arg with BH₄ after 24 h (47.72 μM nitrite) compared to the samples cultured at 800 μM L-Arg without BH₄ at 24 h (2.88 μM nitrite). The largest decrease was observed in 0 μM L-Arg with BH₄ over the culture period (at 24 h nitrite amount; 15.09 μM and after 72 h nitrite amount; 1.56 μM).

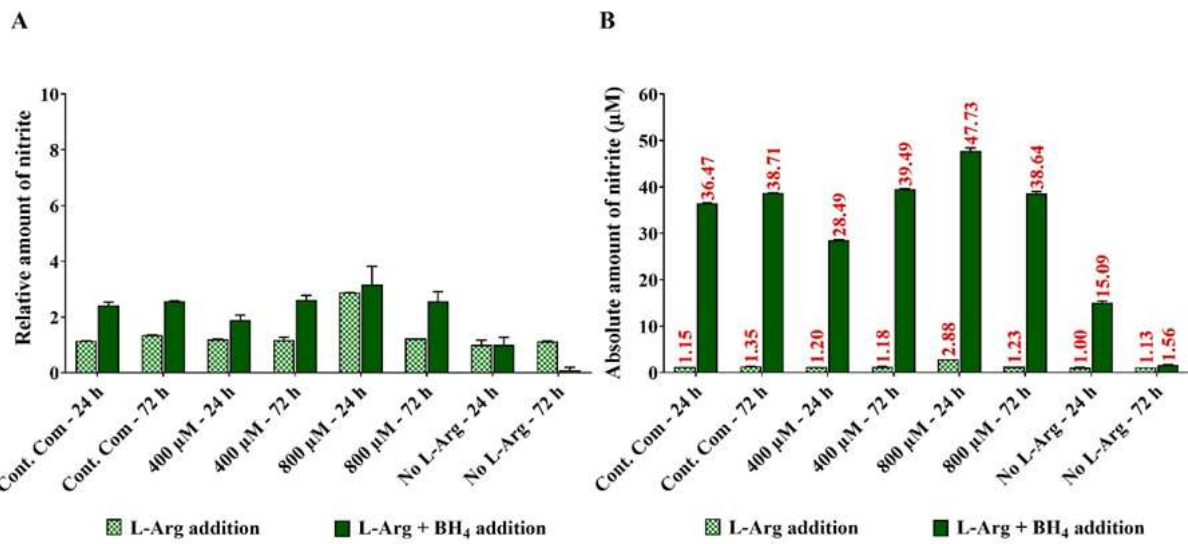


Source of Variation	P value	Amount of Nitrite	
		P value summary	Significant?
Interaction	<0.0001	****	Yes
Samples, conditions and time points	<0.0001	****	Yes
L-Arg +/- L-NAME	<0.0001	****	Yes

Bonferroni's multiple comparisons test	L-Arg addition and L-Arg + L-NAME addition
	Amount of Nitrite
Cont. Com - 24 h	****
Cont. Com - 72 h	ns
400 µM - 24 h	ns
400 µM - 72 h	****
800 µM - 24 h	****
800 µM - 72 h	***
No L-Arg - 24 h	ns
No L-Arg - 72 h	****

Figure 3.3.13. The effect of exogenous L-arginine concentration and iNOS inhibitor, L-NAME addition on nitrite production in BNL CL2 cells.

Cell culture supernatant was obtained from cultured BNL CL2 cells grown in the presence of L-NAME (4 mM) in 0, 400 or 800 µM L-arginine and the control complete DMEM for 24 or 72 h. The concentration of nitrite from experimental samples was obtained using the equation of the line fitted to standard samples. The data are expressed as relative (A) and absolute (B) values. To obtain relative value, quantified nitrite was normalised to the nitrite amount presence in cultures with no L-arginine SILAC DMEM (0 µM L-arginine) at 24 h. Data points represent the mean ± SD. Error bars represent the standard deviation from the mean (n = 3). The tables summarise two-way ANOVA followed by a Bonferroni multiple comparison test using GraphPad Prism 9.4.1. The stars indicate the levels of significance; ns = P > 0.05, * = P ≤ 0.05, ** = P ≤ 0.01, *** = P ≤ 0.001 and **** = P ≤ 0.0001.



		Amount of Nitrite	
Source of Variation	P value	P value summary	Significant?
Interaction	<0.0001	****	Yes
Samples, conditions and time points	<0.0001	****	Yes
L-Arg +/- BH ₄	<0.0001	****	Yes

Bonferroni's multiple comparisons test	L-Arg addition and L-Arg + BH ₄ addition
	Amount of Nitrite
Cont. Com - 24 h	****
Cont. Com - 72 h	****
400 µM - 24 h	**
400 µM - 72 h	****
800 µM - 24 h	ns
800 µM - 72 h	****
No L-Arg - 24 h	ns
No L-Arg - 72 h	****

Figure 3.3.14. The effect of exogenous L-arginine concentration and co-factor of iNOS, BH₄ addition on nitrite production in BNL CL2 cells.

Cell culture supernatant was obtained from cultured BNL CL2 cells grown in the presence of BH₄ (40 µM) in 0, 400 or 800 µM L-arginine and the control complete DMEM for 24 or 72 h. The concentration of nitrite from experimental samples was obtained using the equation of the line fitted to standard samples. The data are expressed as relative (A) and absolute (B) values. To obtain relative value, quantified nitrite was normalised to the nitrite amount presence in cultures with no L-arginine SILAC DMEM (0 µM L-arginine) at 24 h. Data points represent the mean ± SD. Error bars represent the standard deviation from the mean (n = 3). The tables summarise two-way ANOVA followed by a Bonferroni multiple comparison test using GraphPad Prism 9.4.1. The stars indicate the levels of significance; ns = P > 0.05, * = P ≤ 0.05, ** = P ≤ 0.01, *** = P ≤ 0.001 and **** = P ≤ 0.0001.

When SNAP (100 μM) was added, the amount of nitrite present in the cell samples is shown in **Fig 3.3.15**. Overall, upon addition of the NO donor to cells cultured in L-Arg (0, 400 and 800 μM) and the control complete DMEM there was a large increase ($P < 0.0001$) in the nitrite amount at 6 (the control + SNAP; 623.51-fold, 400 μM + SNAP; 571.52-fold; 800 μM + SNAP; 180.58-fold and 0 μM + SNAP; 542.25-fold) and 24 h (the control + SNAP; 16.02-fold, 400 μM + SNAP; 32.08-fold; 800 μM + SNAP; 8.60-fold and 0 μM + SNAP; 19.44-fold) compared to the cell samples cultured without NO donor at the same timepoints. The highest amount of nitrite present in the samples was that of the L-arginine at 400 μM with SNAP (53.36 μM) compared to the 400 μM L-Arg without SNAP at 24 h (1.67 μM).

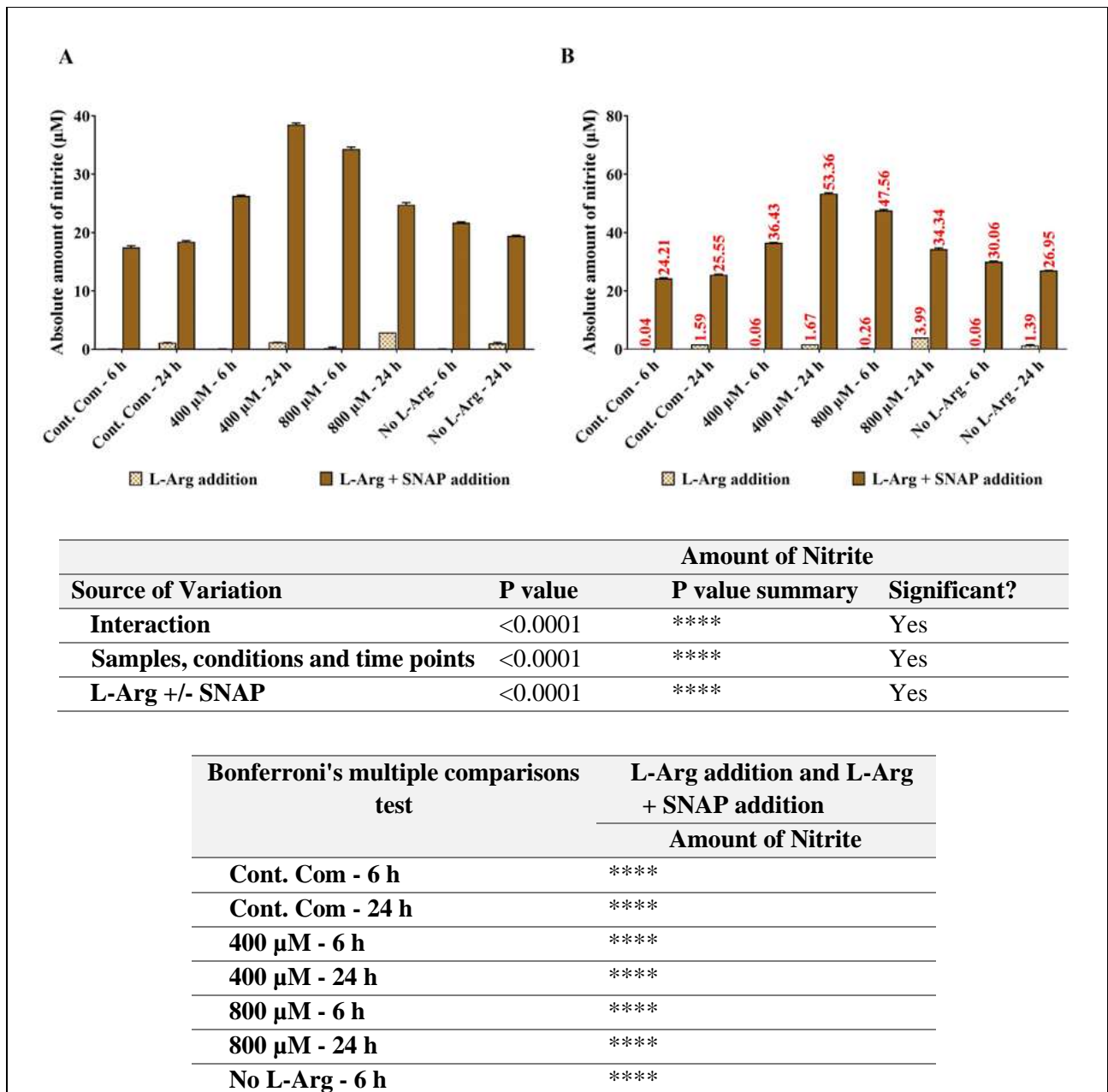


Figure 3.3.15. The effect of exogenous L-arginine concentration and external NO donor, SNAP addition on nitrite production in BNL CL2 cells.

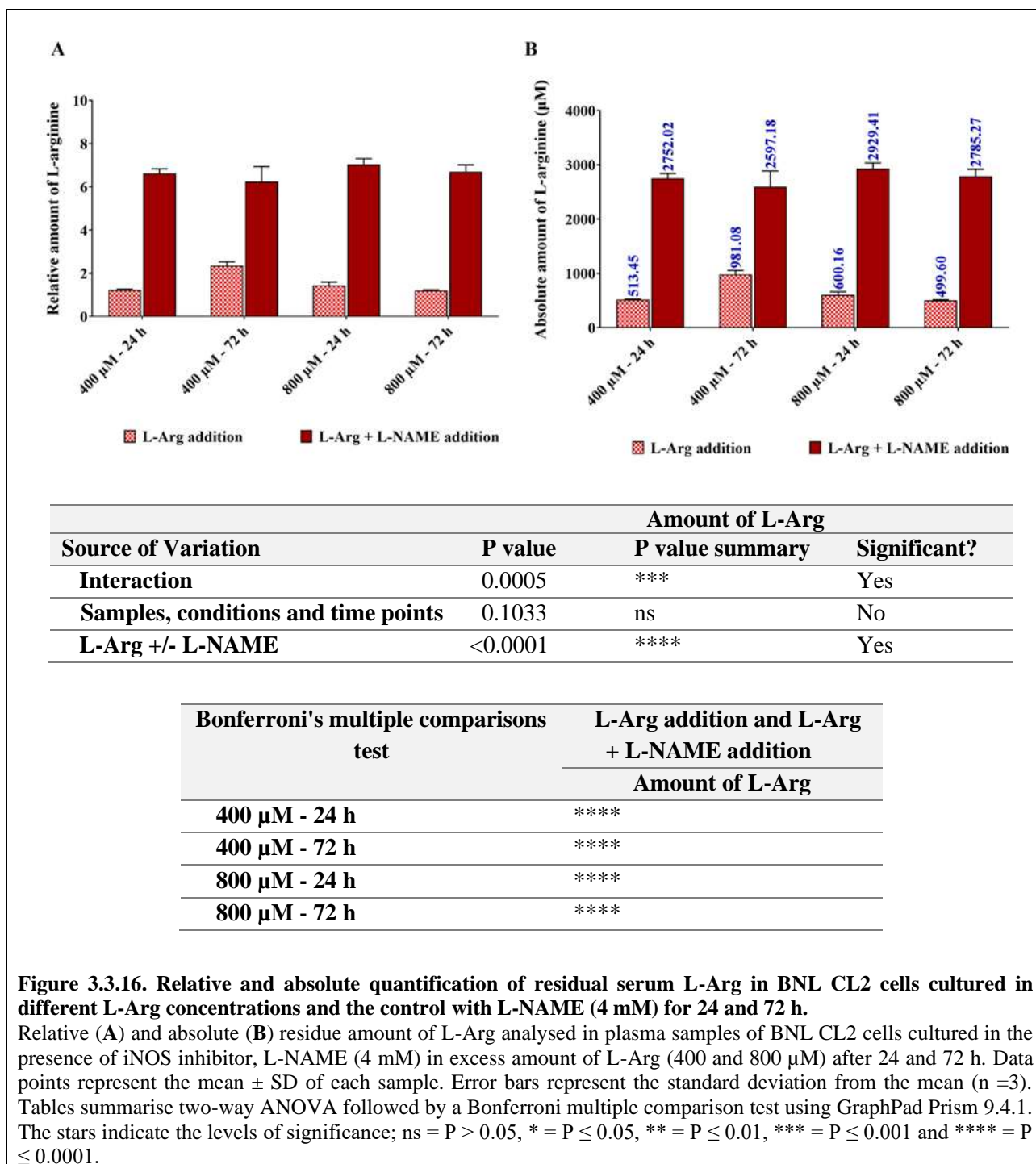
Cell culture supernatant was obtained from cultured BNL CL2 cells grown in the presence of SNAP (100 μ M) in 0, 400 or 800 μ M L-arginine and the control complete DMEM for 6 or 24 h. The concentration of nitrite from experimental samples was obtained using the equation of the line fitted to standard samples. The data are expressed as relative (**A**) and absolute (**B**) values. To obtain relative value, quantified nitrite was normalised to the nitrite amount presence in cultures with no L-arginine SILAC DMEM (0 μ M L-arginine) at 24 h. Data points represent the mean \pm SD. Error bars represent the standard deviation from the mean (n = 3). The tables summarise two-way ANOVA followed by a Bonferroni multiple comparison test using GraphPad Prism 9.4.1. The stars indicate the levels of significance; ns = P > 0.05, * = P \leq 0.05, ** = P \leq 0.01, *** = P \leq 0.001 and **** = P \leq 0.0001.

3.3.4. HPLC analysis of residue L-arginine, and L-ornithine and L-citrulline in the cell culture media of BNL CL2 cells cultured in different initial L-arginine concentrations with L-NAME (4 mM), BH₄ (40 μ M) and SNAP (100 μ M)

The amount of L-arginine and the catabolic products or precursor of L-arginine; L-citrulline and L-ornithine present in the cell culture samples of the BNL CL2 cells cultured in different concentrations of L-Arg and the control complete DMEM were analysed with or without either nitric oxide synthase inhibitor; L-NAME, co-factor of nitric oxide synthase; BH₄ or external NO donor; SNAP. The amount of each target amino acid present in the samples was normalised to the amount of particular amino acid present in the no L-Arg (0 μ M) cell samples at 24 h and then the relative (**A**, denoted as RA) and the absolute amount (**B**) of target amino acid present in the cell samples are presented in the **Figs 3.3.16-3.3.24** compared to the BNL CL2 cell samples cultured without either L-NAME, BH₄ or SNAP.

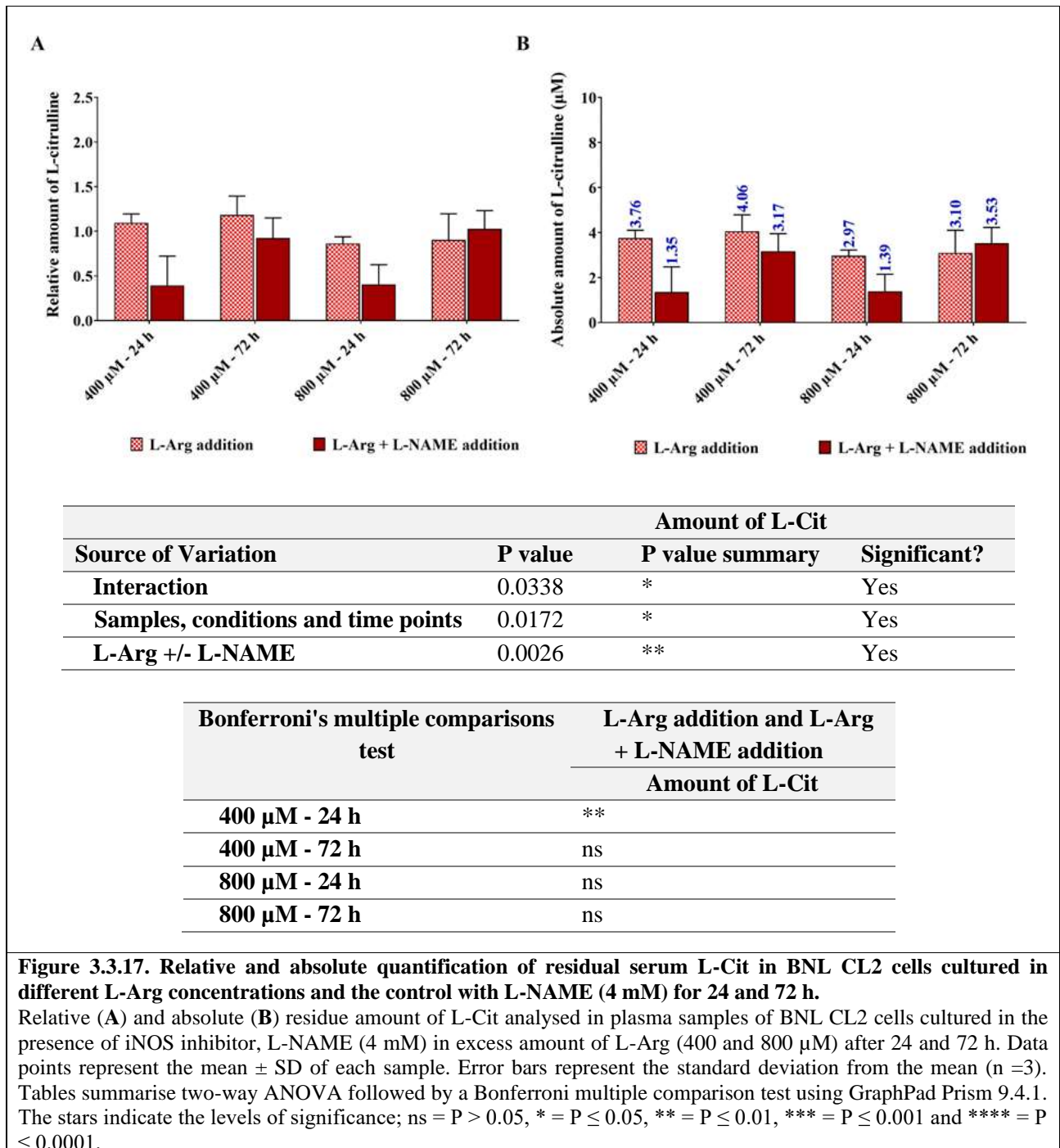
3.3.4.1. HPLC analysis upon NOS inhibitor L-NAME (4 mM) addition to BNL CL2 cells

L-arginine present in the cell culture samples (**Fig 3.3.16**) collected from cells cultured in 400 and 800 μ M L-Arg with L-NAME after 24 (5.37-fold and 4.89-fold, respectively) and 72 h (2.64-fold and 5.58-fold, respectively) was high (P<0.0001) compared to the samples cultured without L-NAME at the same time points. Across the culture the amount of L-Arg decreased (P > 0.05) in the samples cultured with excess L-Arg at 400 and 800 μ M with L-NAME (after 72 h; 0.94-fold and 0.95-fold, respectively). After 24 h, L-Arg at 400 μ M had decreased (P<0.0001) amount of L-Arg (0.87-fold), however when L-NAME was added to the samples the amount of L-Arg present was increased (P<0.0001) (4.65-fold) compared to the control sample.



The amino acid synthesised via the L-Arg/NOS metabolic pathway, L-citrulline was analysed in the cell culture supernatant and is shown in **Fig 3.3.17**. The amount of L-citrulline was decreased (P<0.01) in the samples cultured in L-Arg (400 and 800 μM) and L-NAME (0.36-fold and 0.47-fold, respectively) compared to the samples without L-NAME at 24 h, however, after 72 h the amount of L-citrulline decreased (P<0.01) in L-Arg

at 400 μM with L-NAME (0.78-fold), while increased ($P < 0.01$) in L-Arg at 800 μM with L-NAME (1.14-fold) over samples cultured without L-NAME.



The amino acid synthesised via L-Arg/Arginase pathway, L-ornithine (**Fig 3.3.18**) had decreased ($P > 0.05$) in the samples cultured with 400 μM L-Arg and L-NAME (0.96-fold), whereas it had increased ($P > 0.05$) with 800 μM L-Arg with L-NAME (1.36-fold) compared to the samples cultured without L-NAME at the same

time point. Interestingly, the amount of culture supernatant L-ornithine was increased ($P < 0.001$) with culture time when the cells in 400 (1.32-fold) and 800 μM L-Arg (1.21-fold) were treated with L-NAME.

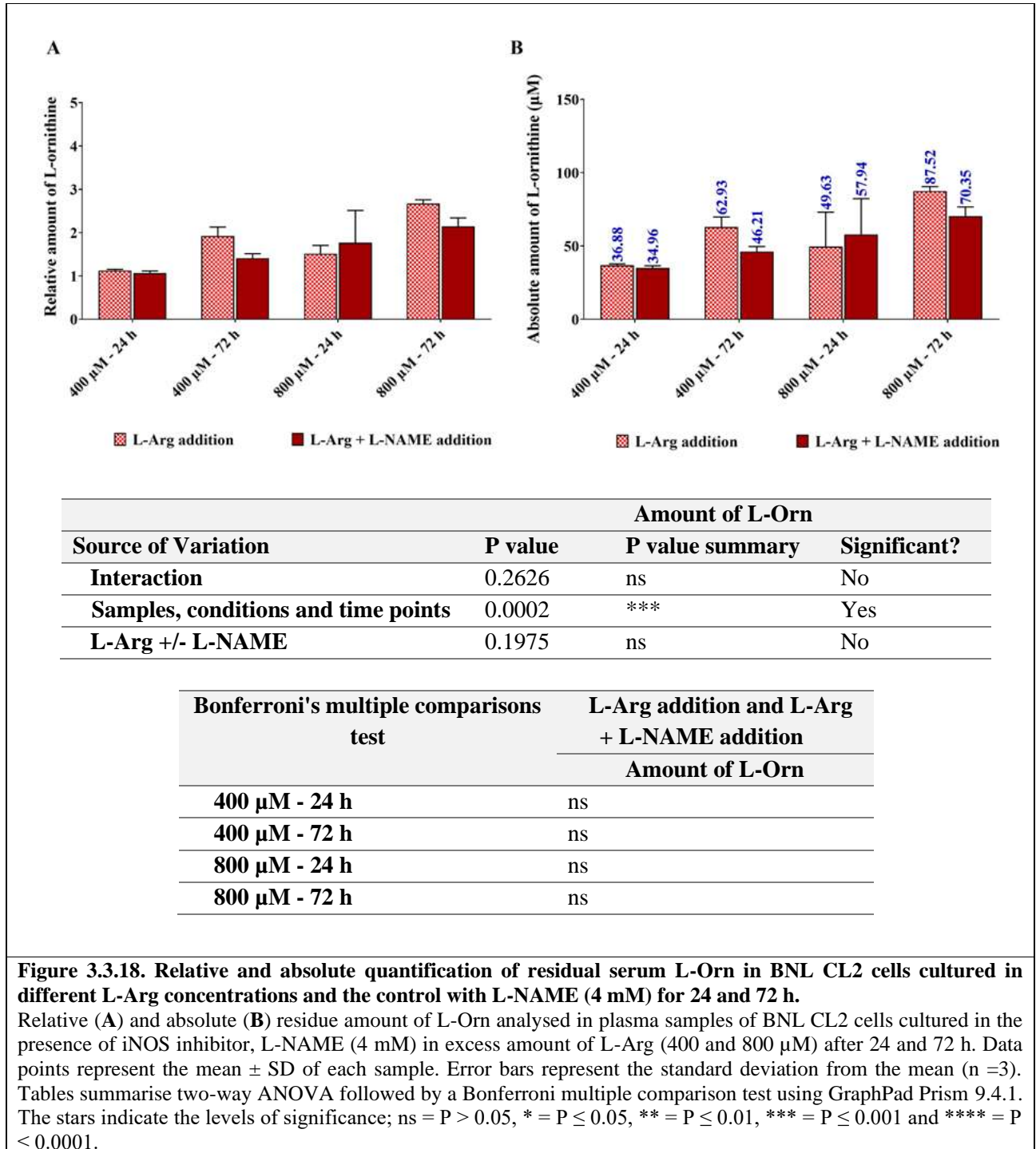


Figure 3.3.18. Relative and absolute quantification of residual serum L-Orn in BNL CL2 cells cultured in different L-Arg concentrations and the control with L-NAME (4 mM) for 24 and 72 h.

Relative (A) and absolute (B) residue amount of L-Orn analysed in plasma samples of BNL CL2 cells cultured in the presence of iNOS inhibitor, L-NAME (4 mM) in excess amount of L-Arg (400 and 800 μM) after 24 and 72 h. Data points represent the mean \pm SD of each sample. Error bars represent the standard deviation from the mean ($n = 3$). Tables summarise two-way ANOVA followed by a Bonferroni multiple comparison test using GraphPad Prism 9.4.1. The stars indicate the levels of significance; ns = $P > 0.05$, * = $P \leq 0.05$, ** = $P \leq 0.01$, *** = $P \leq 0.001$ and **** = $P \leq 0.0001$.

3.3.4.2. HPLC analysis upon NOS co-factor, BH₄ (40 μM) addition to BNL CL2 cells

When the co-factor of NOS was added the amount of L-arginine present in the cell culture supernatant samples were analysed and are presented in **Fig 3.3.19**. Addition of BH₄ to the cell samples cultured in L-Arg (400 and 800 μM) reduced the amount of L-Arg presented in the supernatant samples at 24 (400 μM+ BH₄; 0.48-fold and 800 μM + BH₄; 0.91-fold) and 72 h (400 μM+ BH₄; 0.14-fold and 800 μM + BH₄; 0.98-fold) compared to the samples without BH₄ at the same time points.

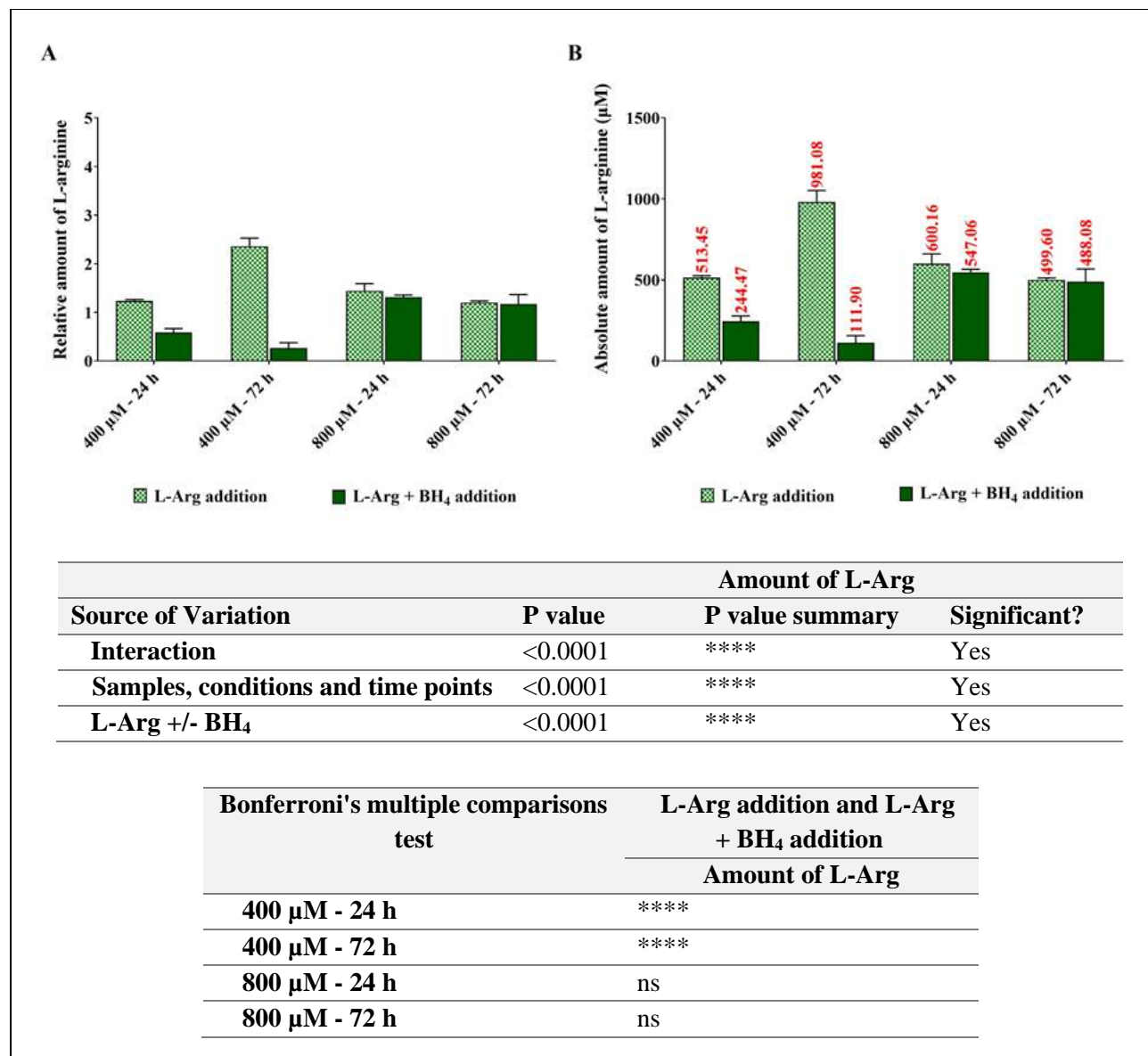


Figure 3.3.19. Relative and absolute quantification of residual serum L-Arg in BNL CL2 cells cultured in different L-Arg concentrations and the control with BH₄ (40 μM) for 24 and 72 h.

Relative (A) and absolute (B) residue amount of L-Arg analysed in plasma samples of BNL CL2 cells cultured in the presence of co-factor of iNOS, BH₄ (40 μM) in excess amount of L-Arg (400 and 800 μM) after 24 and 72 h. Data points represent the mean ± SD of each sample. Error bars represent the standard deviation from the mean (n =3).

Tables summarise two-way ANOVA followed by a Bonferroni multiple comparison test using GraphPad Prism 9.4.1. The stars indicate the levels of significance; ns = $P > 0.05$, * = $P \leq 0.05$, ** = $P \leq 0.01$, *** = $P \leq 0.001$ and **** = $P \leq 0.0001$.

L-citrulline, being a precursor to L-arginine, was investigated in the cell culture supernatant samples and the results are shown in **Fig 3.3.20**. After 24 h the addition of BH₄ to the cells had decreased ($P < 0.01$) the amount of L-citrulline present in the samples cultured in L-Arg and BH₄ (400 μ M+ BH₄; 0.049-fold and 800 μ M + BH₄; 0.42-fold), whereas L-citrulline levels were increased ($P < 0.01$) after 72 h (400 μ M+ BH₄; 1.06-fold and 800 μ M + BH₄; 1.26-fold) compared to the samples cultured without BH₄ at 24 and 72 h.

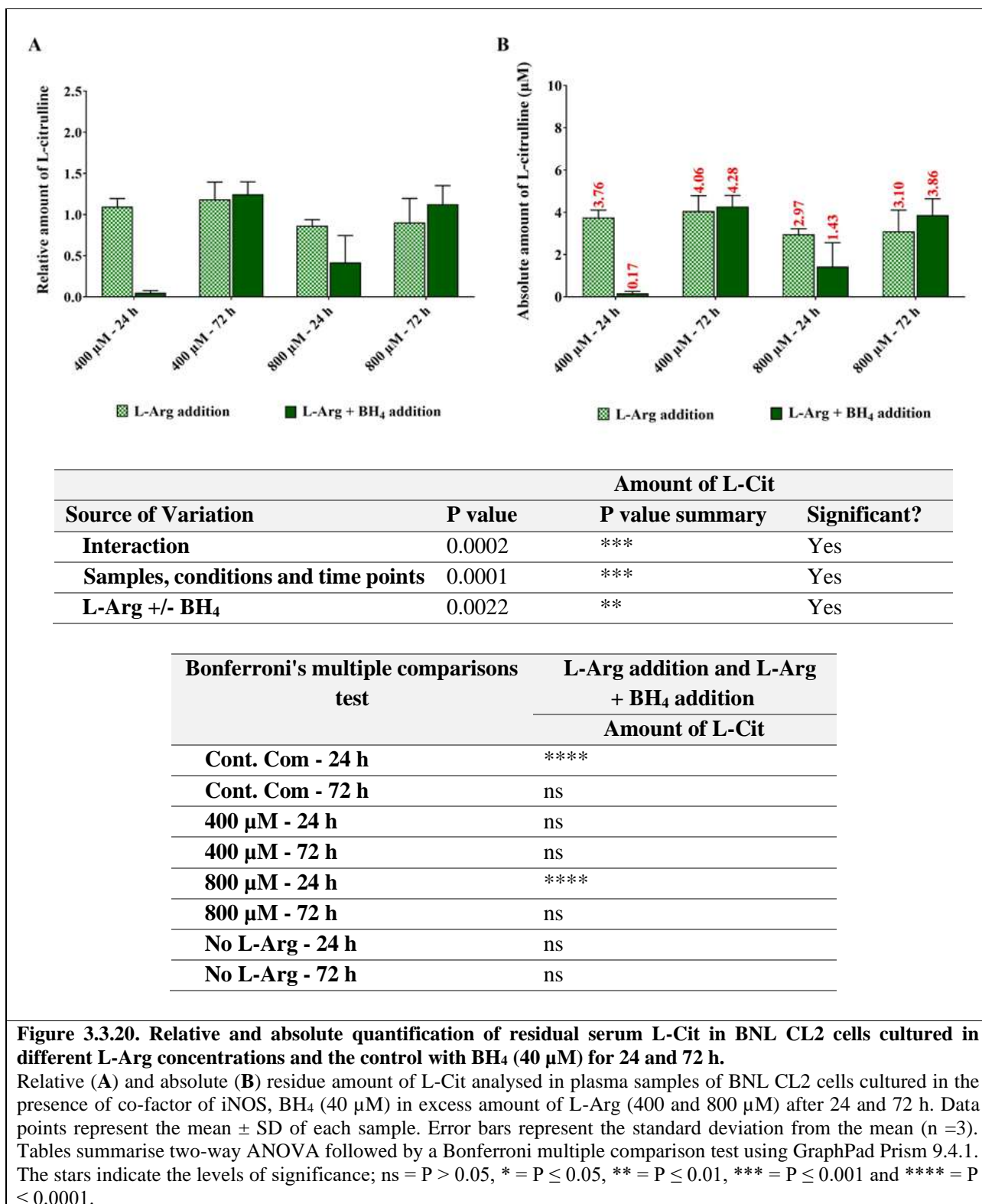


Figure 3.3.20. Relative and absolute quantification of residual serum L-Cit in BNL CL2 cells cultured in different L-Arg concentrations and the control with BH₄ (40 µM) for 24 and 72 h.

Relative (A) and absolute (B) residue amount of L-Cit analysed in plasma samples of BNL CL2 cells cultured in the presence of co-factor of iNOS, BH₄ (40 µM) in excess amount of L-Arg (400 and 800 µM) after 24 and 72 h. Data points represent the mean ± SD of each sample. Error bars represent the standard deviation from the mean (n =3). Tables summarise two-way ANOVA followed by a Bonferroni multiple comparison test using GraphPad Prism 9.4.1. The stars indicate the levels of significance; ns = P > 0.05, * = P ≤ 0.05, ** = P ≤ 0.01, *** = P ≤ 0.001 and **** = P ≤ 0.0001.

L-ornithine was also analysed in the cell culture supernatant samples of the cells cultured in BH₄ and is presented in **Fig 3.3.21**. Addition of BH₄ to cells grown in L-Arg (400 µM) decreased (P<0.01) the amount of

L-ornithine at 24 (0.96-fold) and 72 h (0.54-fold) compared to the cells grown without BH₄ at the same time points. Arginine at high concentration, 800 μM increased (P<0.01) the amount of L-ornithine at 24 h (1.05-fold), whereas there was decreased (P<0.01) concentrations at 72 h (0.78-fold) compared to cells grown without BH₄.

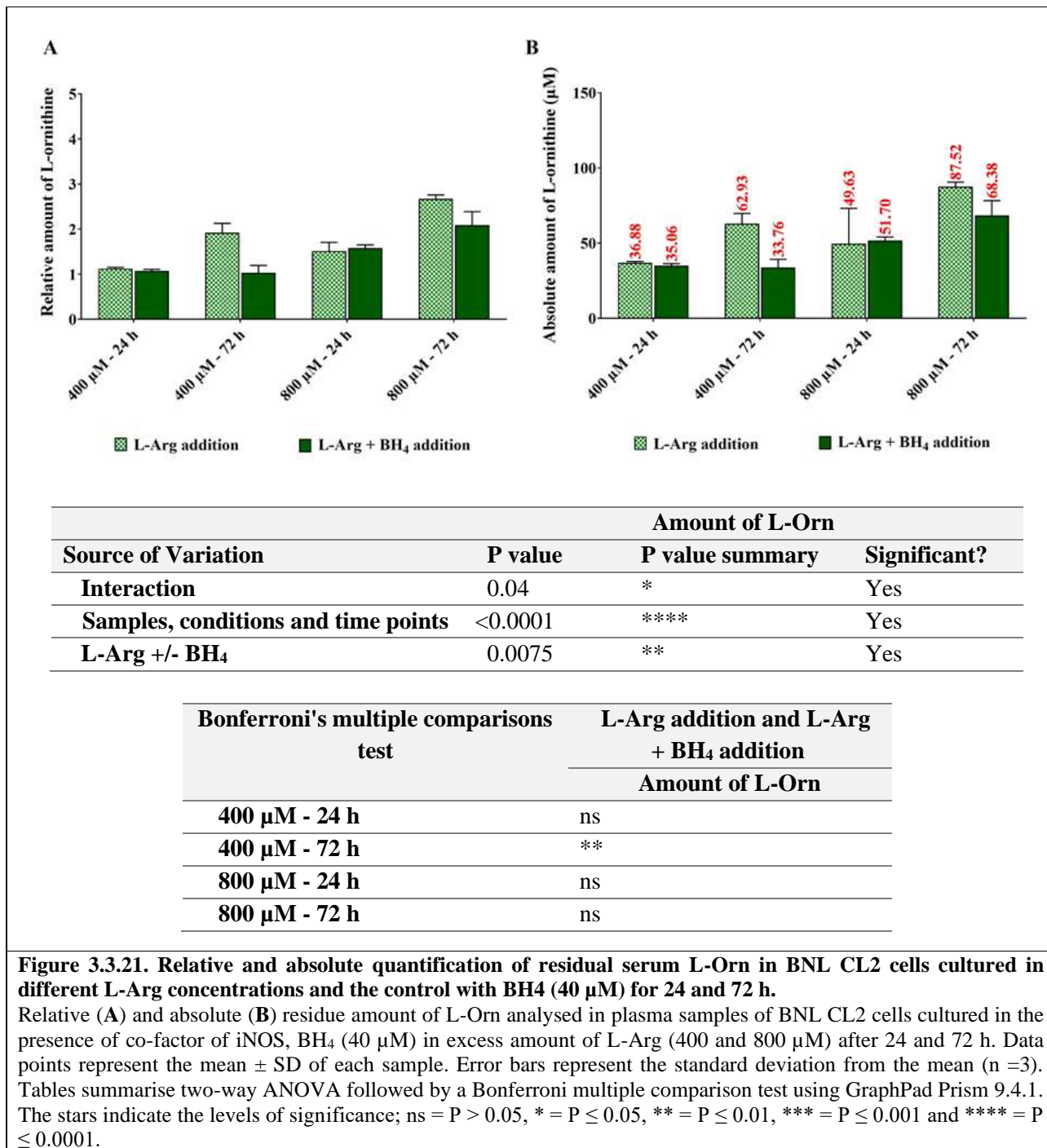


Figure 3.3.21. Relative and absolute quantification of residual serum L-Orn in BNL CL2 cells cultured in different L-Arg concentrations and the control with BH₄ (40 μM) for 24 and 72 h.

Relative (A) and absolute (B) residue amount of L-Orn analysed in plasma samples of BNL CL2 cells cultured in the presence of co-factor of iNOS, BH₄ (40 μM) in excess amount of L-Arg (400 and 800 μM) after 24 and 72 h. Data points represent the mean ± SD of each sample. Error bars represent the standard deviation from the mean (n =3). Tables summarise two-way ANOVA followed by a Bonferroni multiple comparison test using GraphPad Prism 9.4.1. The stars indicate the levels of significance; ns = P > 0.05, * = P ≤ 0.05, ** = P ≤ 0.01, *** = P ≤ 0.001 and **** = P ≤ 0.0001.

3.3.4.3. HPLC analysis upon external NO donor, SNAP (100 μM) addition to BNL CL2 cells

The amount of L-Arg present in the samples with SNAP was investigated and is presented in **Fig 3.3.22**. The level of cell culture supernatant L-Arg in the samples cultured in excess exogenous L-Arg (400 and 800 μM) and treated with SNAP was decreased ($P < 0.0001$) after 6 (400 μM + SNAP; 0.84-fold and 800 μM + SNAP; 0.72-fold) and 24 h (400 μM + SNAP; 0.41-fold and 800 μM + SNAP; 0.82-fold) compared to the samples without SNAP at the same time points.

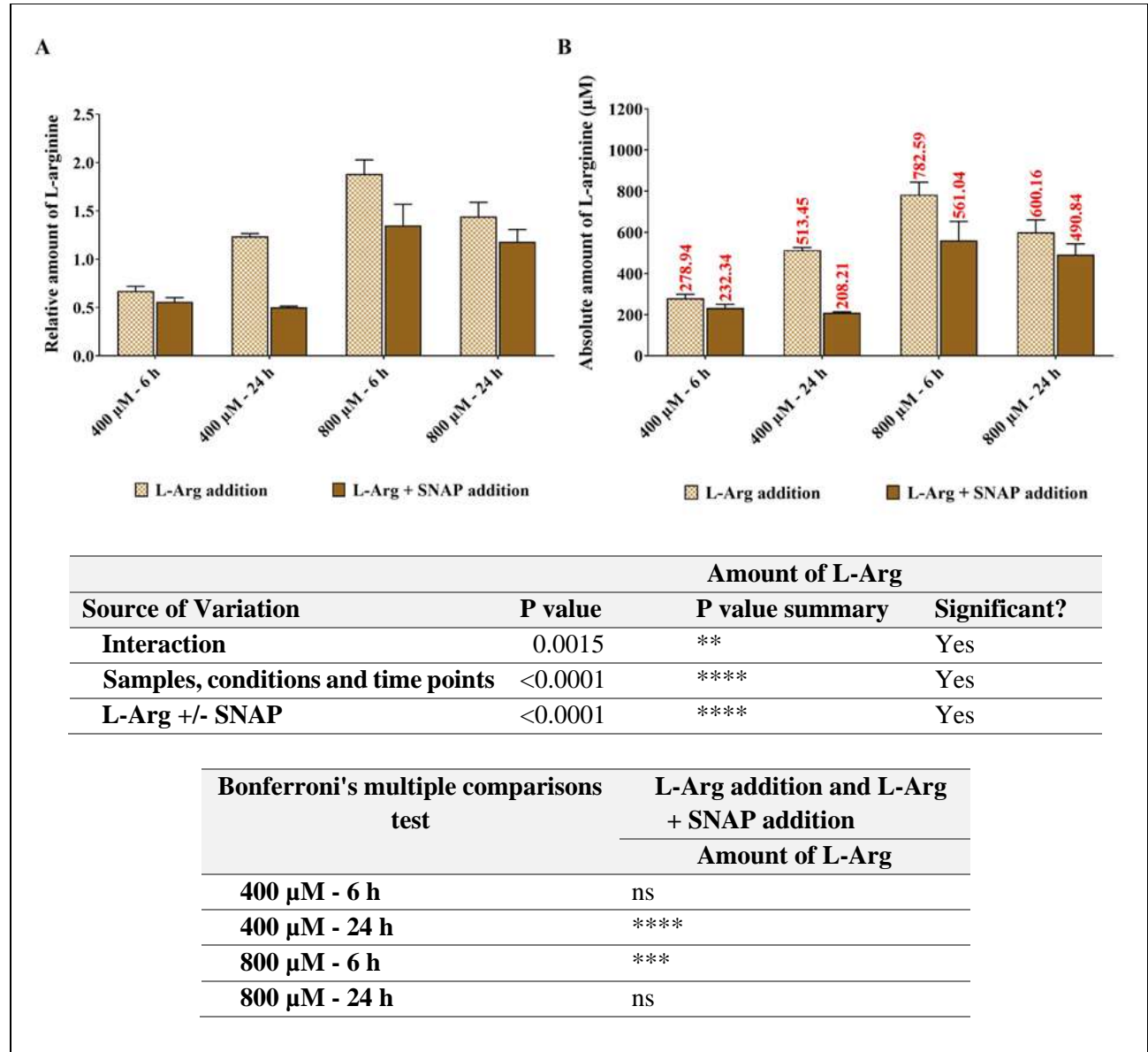


Figure 3.3.22. Relative and absolute quantification of residual serum L-Arg in BNL CL2 cells cultured in different L-Arg concentrations and the control with SNAP (100 μM) for 6 and 24 h.

Relative (A) and absolute (B) residue amount of L-Arg analysed in plasma samples of BNL CL2 cells cultured in the presence of external NO donor, SNAP (100 μM) in excess amount of L-Arg (400 and 800 μM) after 6 and 24 h. Data points represent the mean \pm SD of each sample. Error bars represent the standard deviation from the mean ($n = 3$). Tables summarise two-way ANOVA followed by a Bonferroni multiple comparison test using GraphPad Prism 9.4.1. The stars indicate the levels of significance; ns = $P > 0.05$, * = $P \leq 0.05$, ** = $P \leq 0.01$, *** = $P \leq 0.001$ and **** = $P \leq 0.0001$.

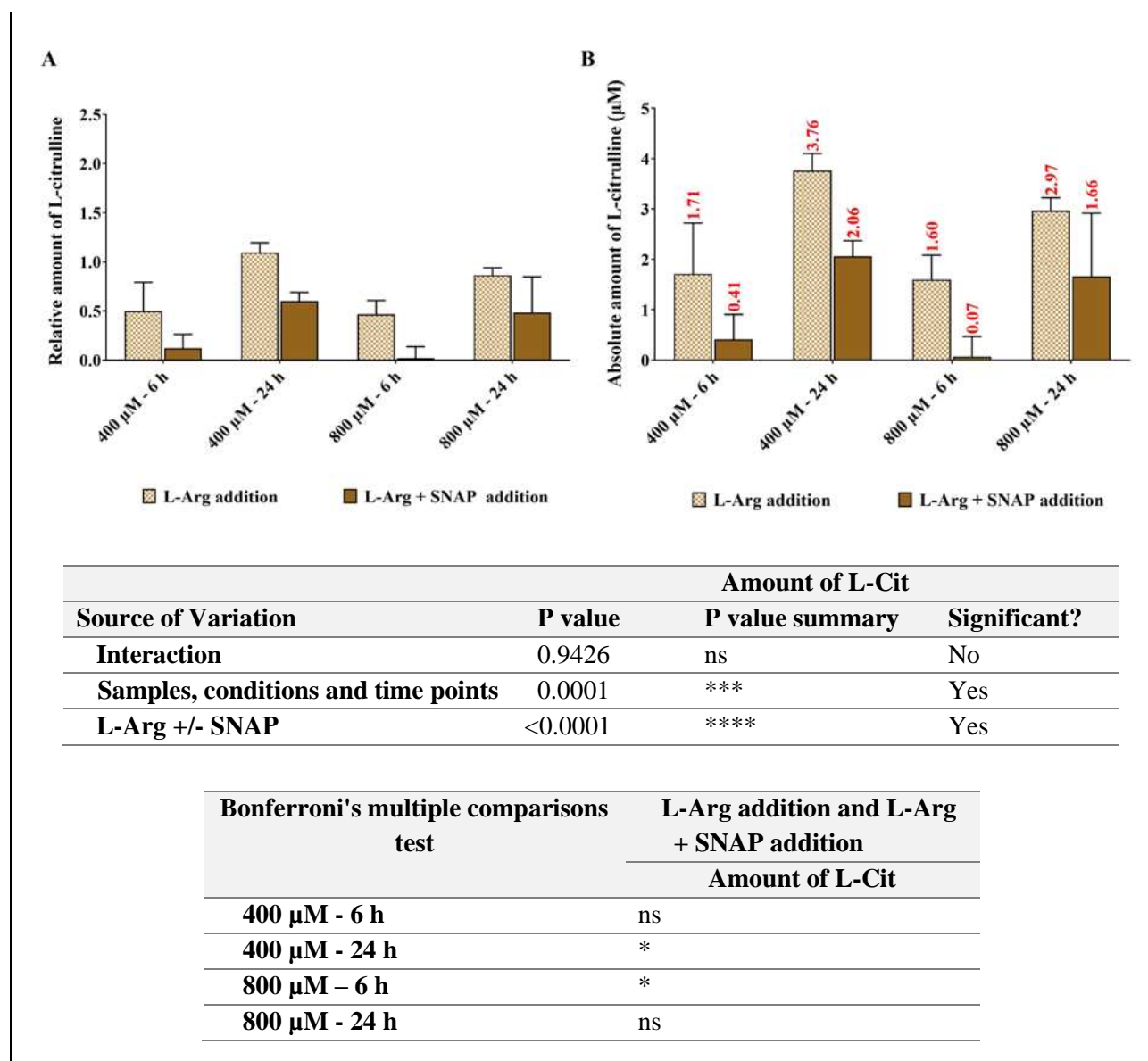


Figure 3.3.23. Relative and absolute quantification of residual serum L-Cit in BNL CL2 cells cultured in different L-Arg concentrations and the control with SNAP (100 µM) for 6 and 24 h.

Relative (A) and absolute (B) residue amount of L-Cit analysed in plasma samples of BNL CL2 cells cultured in the presence of external NO donor, SNAP (100 µM) in excess amount of L-Arg (400 and 800 µM) after 6 and 24 h. Data points represent the mean \pm SD of each sample. Error bars represent the standard deviation from the mean (n =3). Tables summarise two-way ANOVA followed by a Bonferroni multiple comparison test using GraphPad Prism 9.4.1. The stars indicate the levels of significance; ns = P > 0.05, * = P \leq 0.05, ** = P \leq 0.01, *** = P \leq 0.001 and **** = P \leq 0.0001.

L-citrulline concentrations upon SNAP addition is also shown in the **Fig 3.3.23**. SNAP addition to cells cultured in L-arginine (400 and 800 µM) reduced (P<0.0001) the level of L-citrulline present after 6 (400 µM + SNAP; 0.24-fold and 800 µM + SNAP; 0.043-fold) and 24 h (400 µM + SNAP; 0.55-fold and 800 µM + SNAP; 0.56-fold) compared to the samples cultured without SNAP at the same time points. SNAP addition to

the cells grown in 400 (P=0.0001, 5-fold) and 800 μM (P=0.0001, 24-fold) L-Arg increased the amount of L-citrulline across culture.

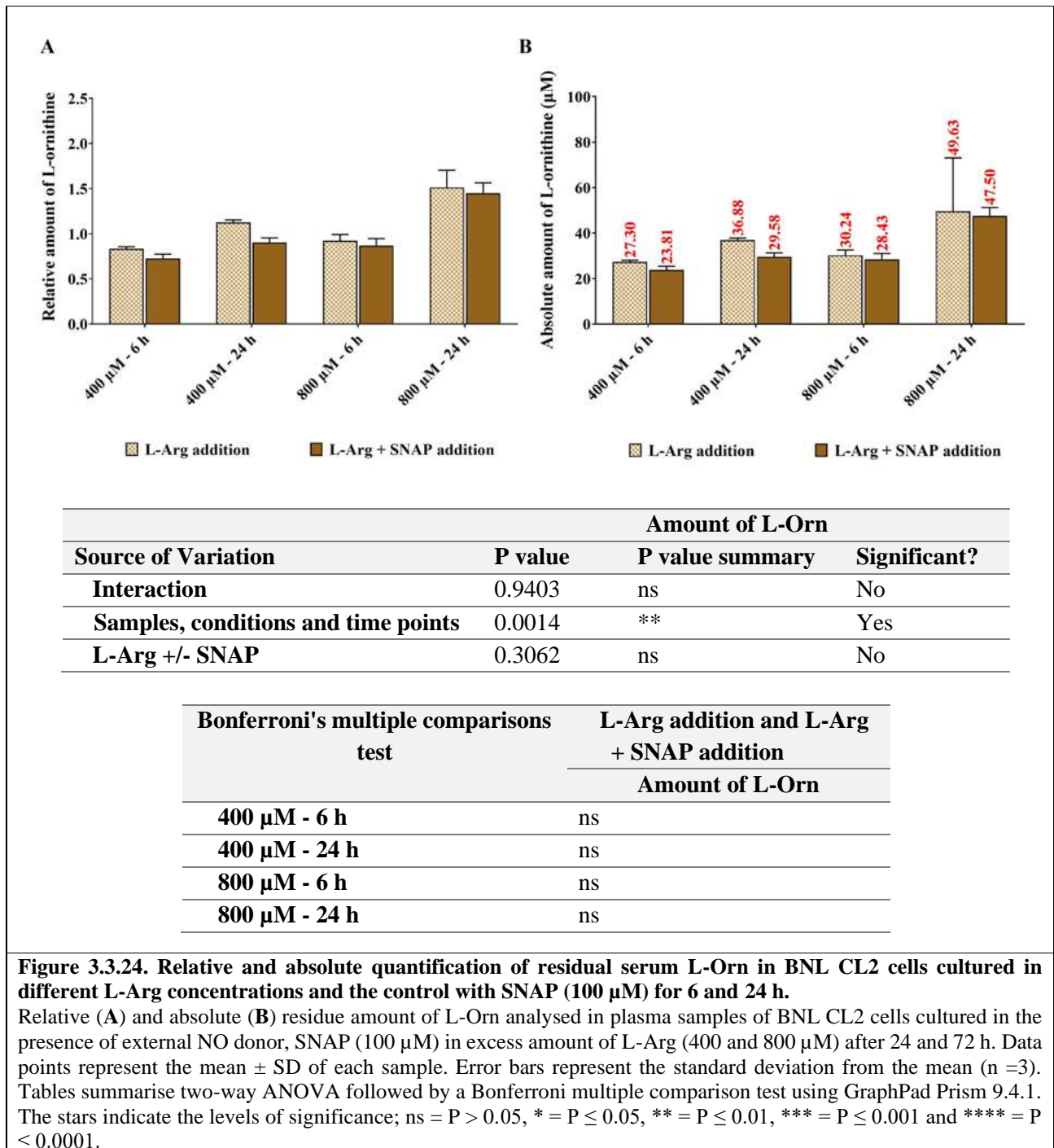


Figure 3.3.24. Relative and absolute quantification of residual serum L-Orn in BNL CL2 cells cultured in different L-Arg concentrations and the control with SNAP (100 μM) for 6 and 24 h.

Relative (A) and absolute (B) residue amount of L-Orn analysed in plasma samples of BNL CL2 cells cultured in the presence of external NO donor, SNAP (100 μM) in excess amount of L-Arg (400 and 800 μM) after 24 and 72 h. Data points represent the mean \pm SD of each sample. Error bars represent the standard deviation from the mean (n =3). Tables summarise two-way ANOVA followed by a Bonferroni multiple comparison test using GraphPad Prism 9.4.1. The stars indicate the levels of significance; ns = P > 0.05, * = P \leq 0.05, ** = P \leq 0.01, *** = P \leq 0.001 and **** = P \leq 0.0001.

Finally, the amount of L-ornithine in the cell culture supernatant samples cultured with L-Arg and SNAP was analysed and is presented in **Fig 3.3.24**. As with the other amino acids monitored, L-Arg and L-Cit, overall,

the amount of L-ornithine was decreased in the samples cultured with SNAP but not to a significant amount ($P=0.3062$).

3.3.5. qRT-PCR analysis of targets genes (AMPK and ACC-1) upon culturing of 3T3 L1 cells in different exogenous L-arginine concentrations and L-NAME (4 mM), BH₄ (40 μM) and SNAP (100 μM)

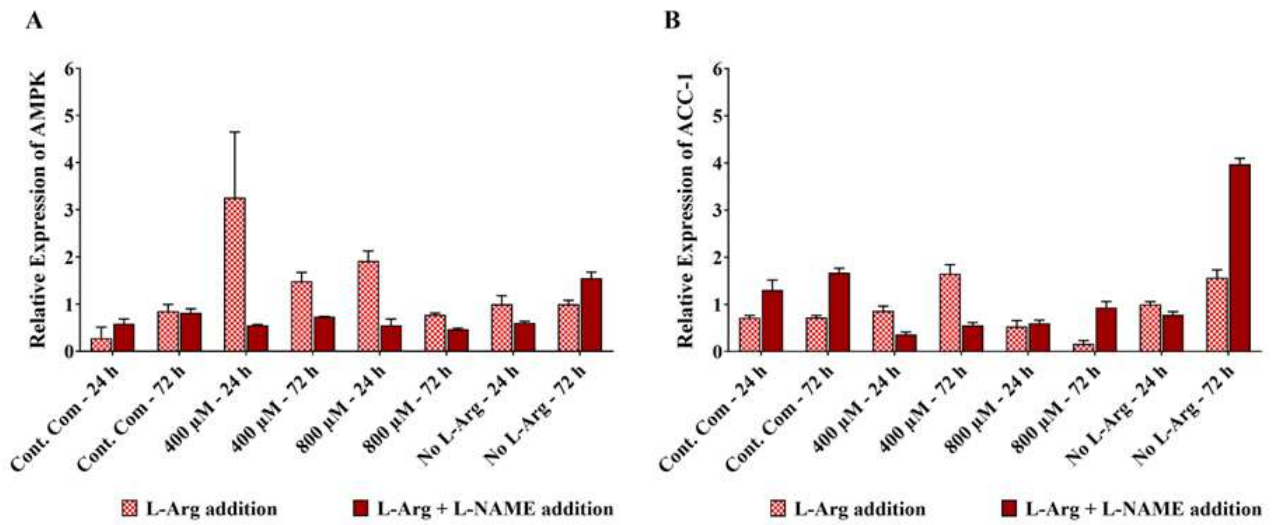
As for the BNL CL2 cells, the impact of adding L-NAME, BH₄ and SNAP on target gene, protein and amino acid expression and concentrations was evaluated.

3.3.5.1. AMPK and ACC-1 transcript analysis upon L-NAME (4 mM) addition to 3T3 L1 cells

Fig 3.3.25A shows the impact of L-NAME addition on AMPK mRNA levels in 3T3 L1 cells in different exogenous L-arginine concentrations. Overall, L-NAME treated samples cultured with excess exogenous L-Arg (400 and 800 μM) showed decreased ($P<0.0001$) AMPK gene expression for 24 and 72 h in comparison to the control samples. **Fig 3.3.25B** shows the impact of L-NAME addition on ACC-1 mRNA levels in 3T3 L1 cells. The mRNA levels of ACC-1 were increased ($P<0.0001$) in arginine at highest concentration (800 μM) with L-NAME (24 h; 1.13-fold and 72 h; 5.81-fold) and the control complete DMEM with L-NAME (24 h; 1.81-fold and 72 h; 2.32-fold).

3.3.5.2. AMPK and ACC-1 transcripts analysis upon BH₄ (40 μM) addition to 3T3 L1 cells

AMPK mRNA expression was investigated in 3T3 L1 cells cultured with BH₄ and is presented in **Fig 3.3.26A**. Addition of BH₄ to the cells decreased ($P<0.0001$) AMPK mRNA expression in the samples cultured in excess L-Arg (400 and 800 μM) at time points 24 (400 μM + BH₄; 0.19-fold and 800 μM + BH₄; 0.23-fold) and 72 h (400 μM + BH₄; 0.59-fold and 800 μM + BH₄; 0.54-fold), while increased ($P<0.0001$) the expression of AMPK gene in the control complete DMEM with BH₄ at time points 24 (2.68-fold) and 72 h (1.18-fold) compared to the respective samples cultured without BH₄. ACC-1 mRNA expression was also analysed in 3T3 L1 cells cultured with BH₄ and the results presented in **Fig 3.3.26B**. Relative expression of ACC-1 was decreased ($P<0.0001$) in the samples cultured in 400 μM L-Arg and BH₄ after 24 (0.84-fold) and 72 h (0.77-fold) compared to the samples cultured without BH₄. However, ACC-1 transcript level was increased ($P<0.0001$) in arginine at the highest concentration (800 μM) with BH₄ and the control complete DMEM with BH₄ at 24 (1.38-fold and 1.74-fold, respectively) and 72 h (4.69-fold and 2.4-fold, respectively) in comparison to the respective samples without BH₄.

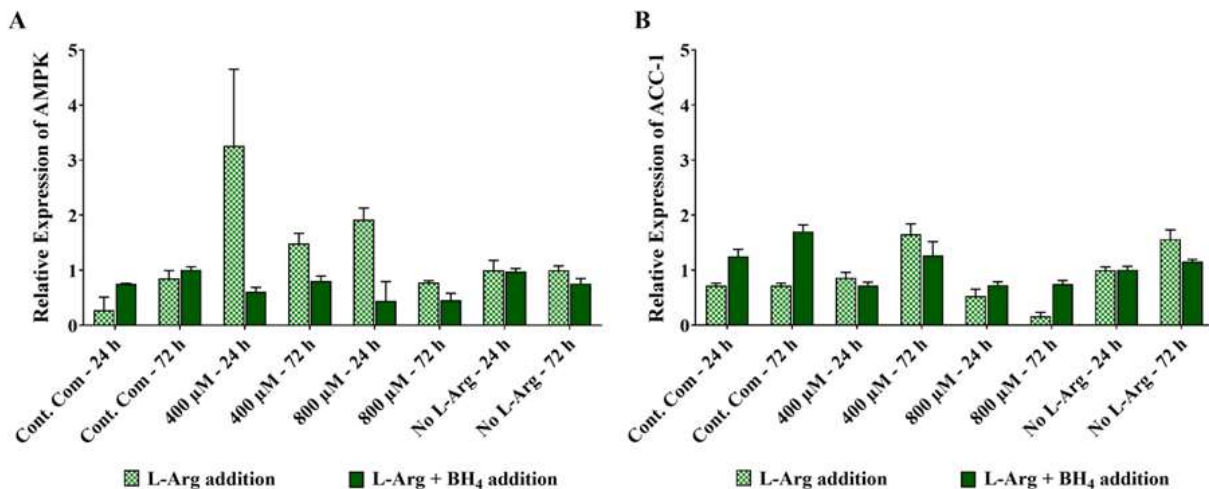


Source of Variation	AMPK		ACC-1	
	P value	Significant?	P value	Significant?
Interaction	****	Yes	****	Yes
Samples, conditions and time points	****	Yes	****	Yes
L-Arg +/- L-NAME	****	Yes	****	Yes

Bonferroni's multiple comparisons test	L-Arg addition and L-Arg + L-NAME addition	
	AMPK	ACC-1
Cont. Com - 24 h	ns	****
Cont. Com - 72 h	ns	****
400 μM - 24 h	****	****
400 μM - 72 h	ns	****
800 μM - 24 h	***	ns
800 μM - 72 h	ns	****
No L-Arg - 24 h	ns	ns
No L-Arg - 72 h	ns	****

Figure 3.3.25. Relative mRNA expression of AMPK and ACC-1 in 3T3 L1 cells cultured in different concentrations of L-arginine and the control with L-NAME (4 mM).

Relative mRNA transcript expression ($\Delta\Delta Ct$) of AMPK (A) and ACC-1 (B) in 3T3 L1 cells cultured in medium of different L-arginine concentrations (0, 400 and 800 μM) and control complete DMEM media with nitric oxide synthase inhibitor; L-NAME (4 mM) 24 and 72 h after addition. Data points represent the mean \pm SD of each sample. Error bars represent the standard deviation from the mean (n = 3). The tables summarise two-way ANOVA followed by a Tukey multiple comparison test using GraphPad Prism 9.4.1. The stars indicate the levels of significance; ns = $P > 0.05$, * = $P \leq 0.05$, ** = $P \leq 0.01$, *** = $P \leq 0.001$ and **** = $P \leq 0.0001$.



Source of Variation	AMPK		ACC-1	
	P value	Significant?	P value	Significant?
Interaction	****	Yes	****	Yes
Samples, conditions and time points	****	Yes	****	Yes
L-Arg +/- BH ₄	****	Yes	****	Yes

Bonferroni's multiple comparisons test	L-Arg addition and L-Arg + BH ₄ addition	
	AMPK	ACC-1
Cont. Com - 24 h	ns	****
Cont. Com - 72 h	ns	****
400 μM - 24 h	****	ns
400 μM - 72 h	ns	**
800 μM - 24 h	***	ns
800 μM - 72 h	ns	****
No L-Arg - 24 h	ns	ns
No L-Arg - 72 h	ns	**

Figure 3.3.26. Relative mRNA expression of AMPK and ACC-1 in 3T3 L1 cells cultured in different concentrations of L-arginine and the control with BH₄ (40 μM).

Relative mRNA transcript expression ($\Delta\Delta Ct$) of AMPK (A) and ACC-1 (B) in 3T3 L1 cells cultured in medium of different L-arginine concentrations (0, 400 and 800 μM) and control complete DMEM media with the co factor of nitric oxide synthase inhibitor; BH₄ (40 μM) 24 and 72 h after addition. Data points represent the mean \pm SD of each sample. Error bars represent the standard deviation from the mean (n =3). The tables summarise two-way ANOVA followed by a Tukey multiple comparison test using GraphPad Prism 9.4.1. The stars indicate the levels of significance; ns = P > 0.05, * = P \leq 0.05, ** = P \leq 0.01, *** = P \leq 0.001 and **** = P \leq 0.0001.

3.3.5.3. AMPK and ACC-1 transcripts analysis upon SNAP (100 μM) addition to 3T3 L1 cells

SNAP (100 μ M) was added to the 3T3 L1 cells cultured in different L-Arg concentrations and the relative expression of AMPK mRNA was investigated and presented in **Fig 3.3.27A**. There was no significant difference ($P=0.1835$) in the expression of AMPK mRNA between the samples cultured with or without SNAP. The mRNA amounts for ACC-1 was also investigated when SNAP (100 μ M) was added and the relative expression is presented in **Fig 3.3.27B**. Overall comparison between the samples cultured with SNAP and without SNAP revealed that there was an increase ($P<0.0001$) in ACC-1 mRNA in the samples treated with SNAP.

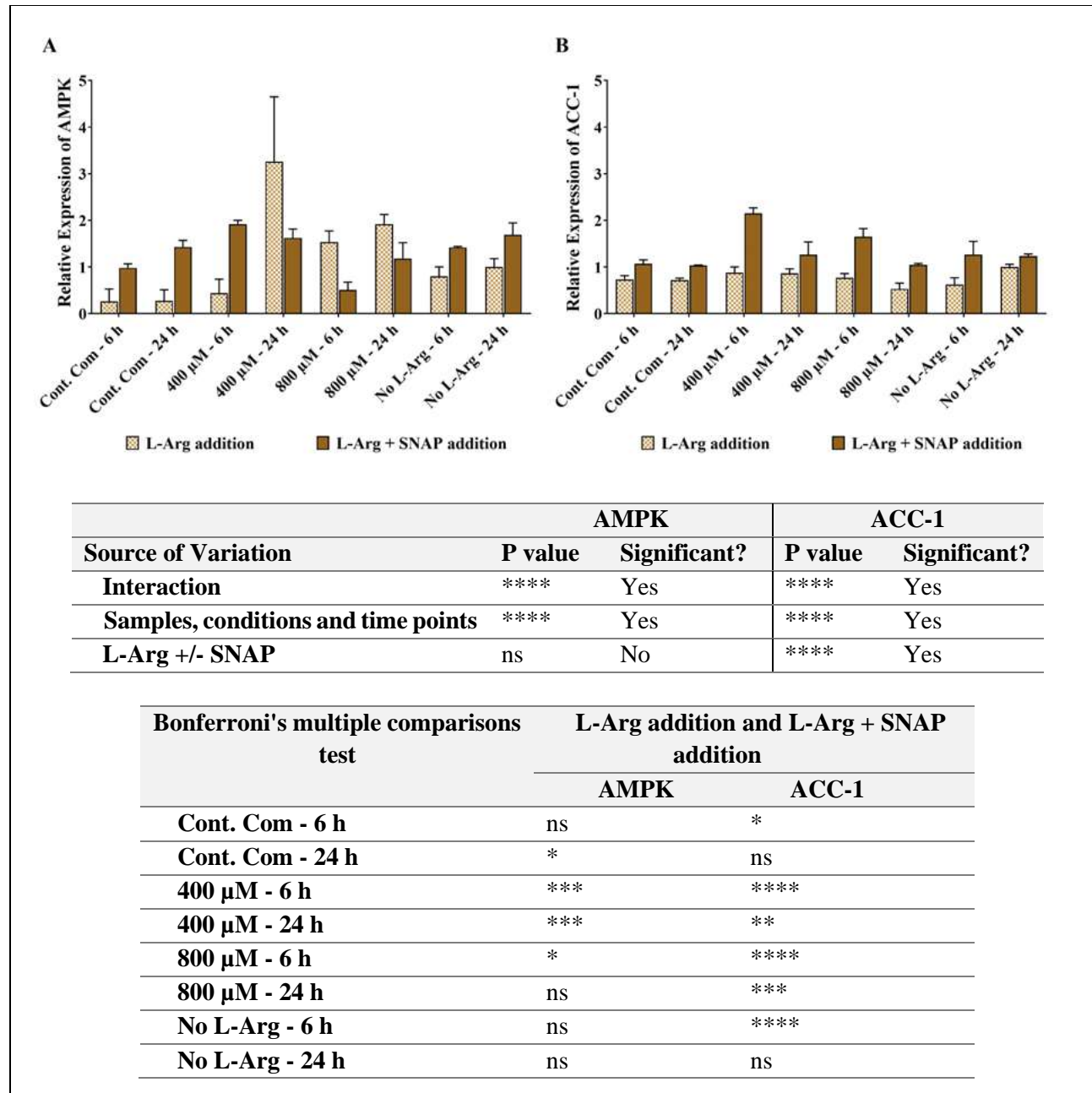


Figure 3.3.27. Relative mRNA expression of AMPK and ACC-1 in 3T3 L1 cells cultured in different concentrations of L-arginine and the control with SNAP (100 µM).

Relative mRNA transcript expression ($\Delta\Delta C_t$) of AMPK (A) and ACC-1 (B) in 3T3 L1 cells cultured in medium of different L-arginine concentrations (0, 400 and 800 µM) and control complete DMEM media with nitric oxide donor; SNAP (100 µM) 6 and 24 h after addition. Data points represent the mean \pm SD of each sample. Error bars represent the standard deviation from the mean (n =3). Tables summarise two-way ANOVA followed by a Tukey multiple comparison test using GraphPad Prism 9.4.1. The stars indicate the levels of significance; ns = $P > 0.05$, * = $P \leq 0.05$, ** = $P \leq 0.01$, *** = $P \leq 0.001$ and **** = $P \leq 0.0001$.

3.3.6. Monitoring protein expression (AMPK and ACC-1) in response to L-Arg supplementation to 3T3 L1 cells with L-NAME (4 mM), BH₄ (40 µM) and SNAP (100 µM)

3.3.6.1. AMPK and ACC-1 protein expression upon L-NAME (4 mM) addition to 3T3 L1 cells

As for the BNL CL2 cells, protein expression (AMPK and ACC-1) was also investigated (**Fig 3.3.28**). The relative protein expression of AMPK upon L-NAME addition to different exogenous L-arginine concentrations is presented in **Fig 3.3.29**. Overall, the addition of L-NAME reduced ($P < 0.0001$) the AMPK protein expression. The relative protein expression of ACC-1 upon L-NAME addition is presented in **Fig 3.3.30**. Like AMPK protein expression, overall, L-NAME addition to the 3T3 L1 cells decreased ($P < 0.0001$) the ACC-1 protein expression in all the cell samples treated with L-NAME at 24 (the control + L-NAME; 0.23-fold, 400 µM +L-NAME; 0.22-fold, 800 µM + L-NAME; 0.25-fold and 0 µM + L-NAME; 0) and 72 h (the control + L-NAME; 0.46-fold, 400 µM +L-NAME; 0.36-fold, 800 µM + L-NAME; 0.41-fold and 0 µM + L-NAME; 0.91-fold) compared to the samples without L-NAME.

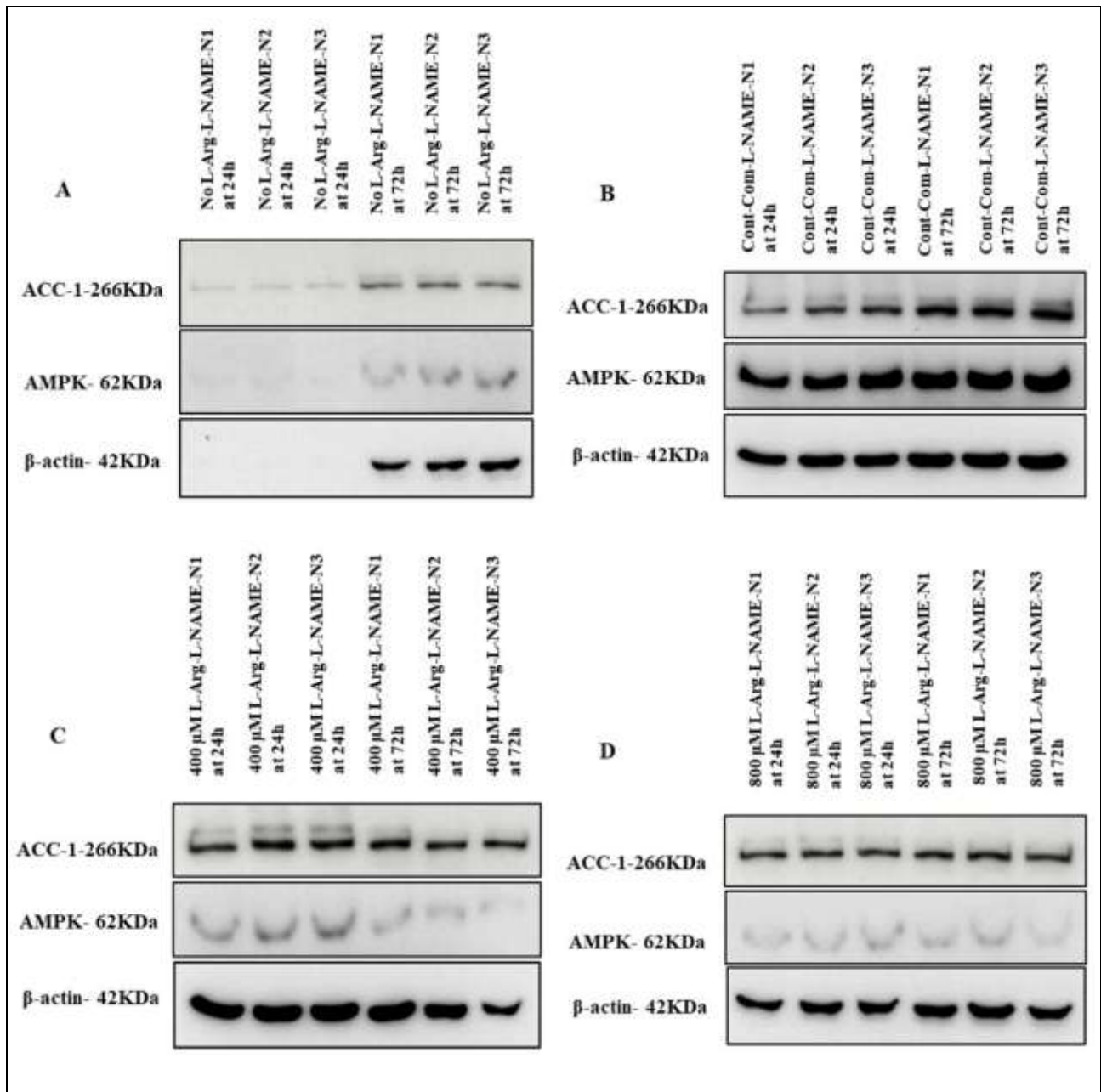
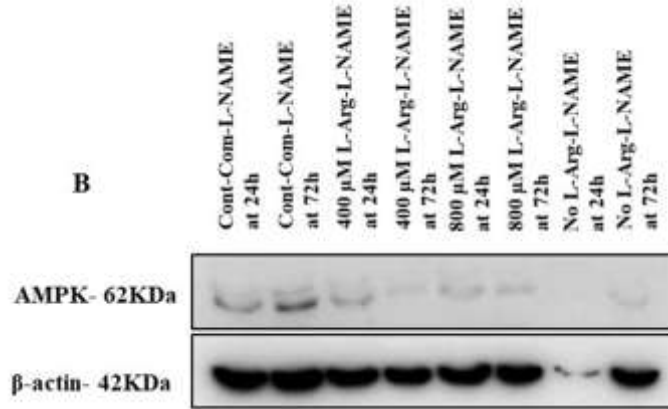
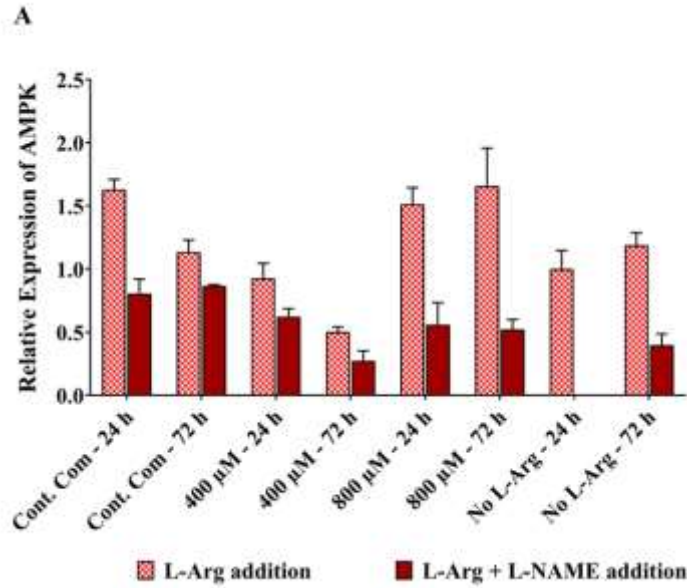


Figure 3.3.28. Western blot comparison for AMPK and ACC-1 protein expressions in 3T3 L1 cells cultured in different concentrations of L-arginine and the control with L-NAME (4 mM).

Western blot comparison of the expression of key protein; AMPK and lipogenic ACC-1 protein levels investigated in L-arginine/NO metabolic pathway signalling in 3T3 L1 cells cultured in customized media containing (A) no L-arginine SILAC DMEM and L-NAME (4 mM) (B) complete DMEM and L-NAME (4 mM), (C) 400 μM L-arginine and L-NAME (4 mM), and (D) 800 μM L-arginine and L-NAME (4 mM) for 24 and 72 h. β-actin is used as a loading control. The same amount of protein (10 μg) from different treatment groups was loaded from biological triplicate cultures into 10% SDS–polyacrylamide gels for the separation of target proteins.

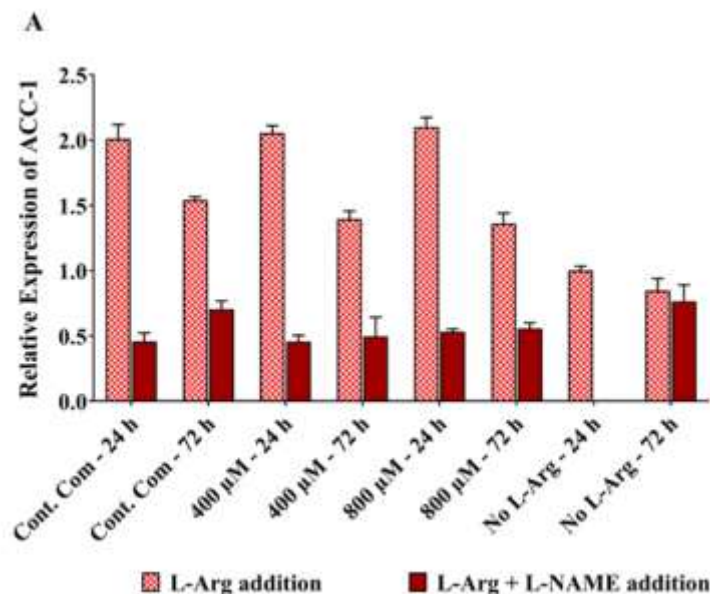


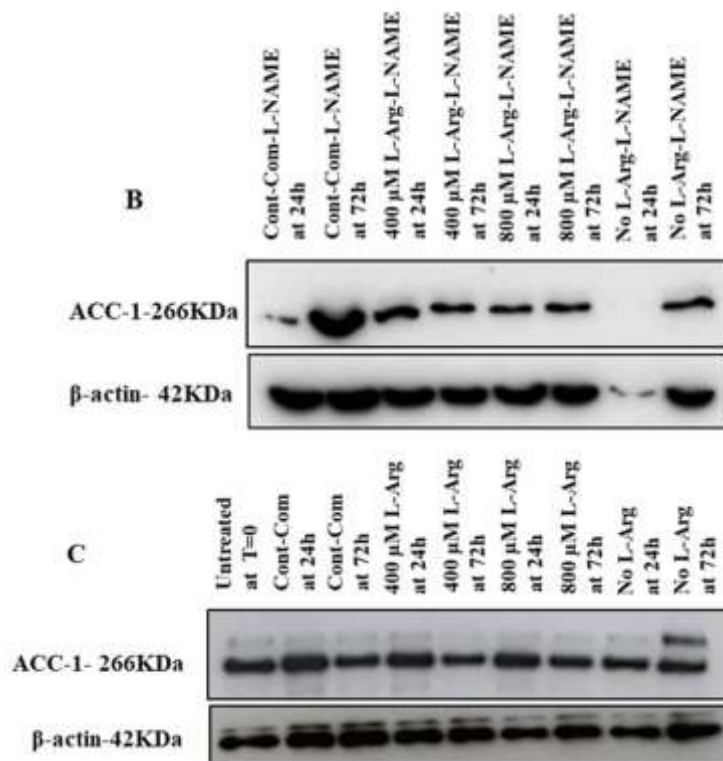
AMPK			
Source of Variation	P value	P value summary	Significant?
Interaction	<0.0001	****	Yes
Samples, conditions and time points	<0.0001	****	Yes
L-Arg +/- L-NAME	<0.0001	****	Yes

Bonferroni's multiple comparisons test L-Arg addition and L-Arg + L-NAME addition

AMPK	
Cont. Com - 24 h	****
Cont. Com - 72 h	ns
400 μ M - 24 h	*
400 μ M - 72 h	ns
800 μ M - 24 h	****
800 μ M - 72 h	****
No L-Arg - 24 h	****
No L-Arg - 72 h	****

Figure 3.3.29. Relative protein expression and western blot comparisons (with or without L-NAME) for AMPK protein in 3T3 L1 cells cultured in different concentrations of L-arginine and the control with L-NAME (4 mM). Relative protein expression of AMPK (A), western blot comparison of the expression of key protein, AMPK involved in L-arginine/NO metabolic pathway signalling investigated in 3T3 L1 cells cultured with L-NAME (4 mM) in no L-arginine SILAC DMEM, complete DMEM, 400 μ M L-arginine and 800 μ M L-arginine for 24 and 72 h (B) and the amount of AMPK in cultured 3T3 L1 cells without L-NAME for 24 and 72 h (C). The same amount of protein (10 μ g) from different treatment groups was loaded from biological triplicate cultures into 10% SDS–polyacrylamide gels for the separation of target proteins. Two representative blots from each treatment group are shown with the respective to the house-keeping-protein, β -actin. Bands in the blots were quantified using ImageJ software and the data are normalised to β -actin and then expressed as relative to the no L-arginine SILAC DMEM (0 μ M L-arginine) control at 24 h. Data points represent the mean \pm SD. Error bars represent the standard deviation from the mean (n = 3). The tables summarise two-way ANOVA followed by a Bonferroni multiple comparison test using GraphPad Prism 9.4.1. The stars indicate the levels of significance; ns = $P > 0.05$, * = $P \leq 0.05$, ** = $P \leq 0.01$, *** = $P \leq 0.001$ and **** = $P \leq 0.0001$.





ACC-1			
Source of Variation	P value	P value summary	Significant?
Interaction	<0.0001	****	Yes
Samples, conditions and time points	<0.0001	****	Yes
L-Arg +/- L-NAME	<0.0001	****	Yes

Bonferroni's multiple comparisons test	L-Arg addition and L-Arg + L-NAME addition
	ACC-1
Cont. Com - 24 h	****
Cont. Com - 72 h	****
400 μM - 24 h	****
400 μM - 72 h	****
800 μM - 24 h	****
800 μM - 72 h	****
No L-Arg - 24 h	****
No L-Arg - 72 h	ns

Figure 3.3.30. Relative protein expression and western blot comparisons (with or without L-NAME) for ACC-1 protein in 3T3 L1 cells cultured in different concentrations of L-arginine and the control with L-NAME (4 mM).

Relative protein expression of ACC-1 (A), western blot comparison of the expression of lipogenic protein, ACC-1 involved in L-arginine/NO metabolic pathway signalling investigated in 3T3 L1 cells cultured with L-NAME (4 mM) in no L-arginine SILAC DMEM, complete DMEM, 400 μM L-arginine and 800 μM L-arginine for 24 and 72 h (B) and the amount of ACC-1 in cultured 3T3 L1 cells without L-NAME for 24 and 72 h (C). The same amount of

protein (10 µg) from different treatment groups was loaded from biological triplicate cultures into 10% SDS–polyacrylamide gels for the separation of target proteins. Two representative blots from each treatment group are shown with the respective to the house-keeping-protein, β-actin. Bands in the blots were quantified using ImageJ software and the data are normalised to β-actin and then expressed as relative to the no L-arginine SILAC DMEM (0 µM L-arginine) control at 24 h. Data points represent the mean ± SD. Error bars represent the standard deviation from the mean (n = 3). The tables summarise two-way ANOVA followed by a Bonferroni multiple comparison test using GraphPad Prism 9.4.1. The stars indicate the levels of significance; ns = P > 0.05, * = P ≤ 0.05, ** = P ≤ 0.01, *** = P ≤ 0.001 and **** = P ≤ 0.0001.

3.3.6.2. AMPK and ACC-1 protein expression upon BH₄ (40 µM) addition to 3T3 L1 cells

The impact of addition of BH₄ on relative AMPK and ACC-1 protein expressions in the 3T3 L1 cells cultured in L-Arg and the control complete DMEM was evaluated and presented in (**Fig 3.3.31**). Generally, addition of BH₄ to the 3T3 L1 cells had decreased (P<0.0001) the expression of AMPK protein after 24 (the control + BH₄; 0.10-fold, 400 µM + BH₄; 0.3-fold, 800 µM + BH₄; 0.2-fold) and 72 h (the control + BH₄; 0.12-fold, 400 µM + BH₄; 0.38-fold, 800 µM + BH₄; 0.46-fold) compared to the cell samples cultured without BH₄ **Fig 3.3.32**.

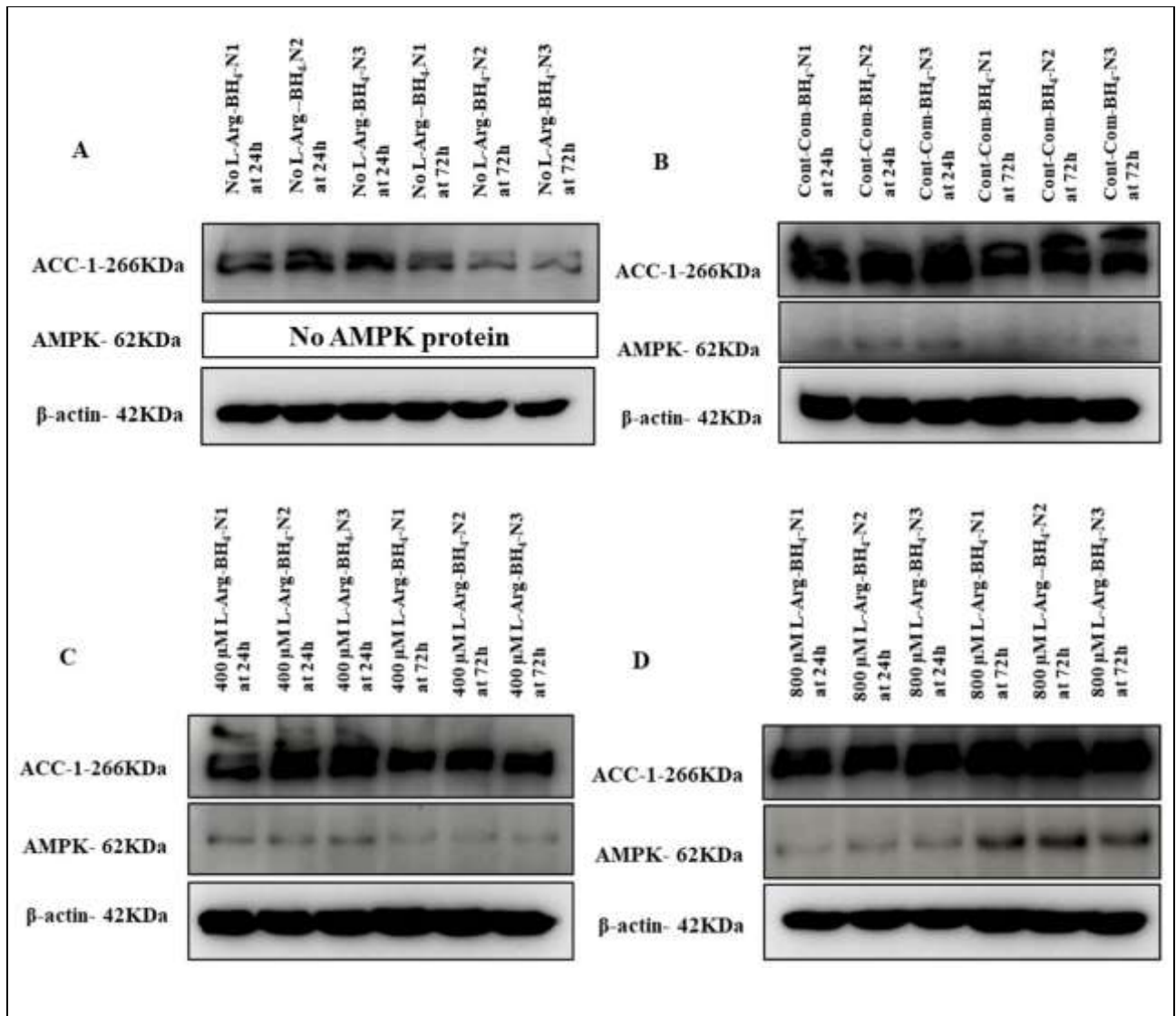
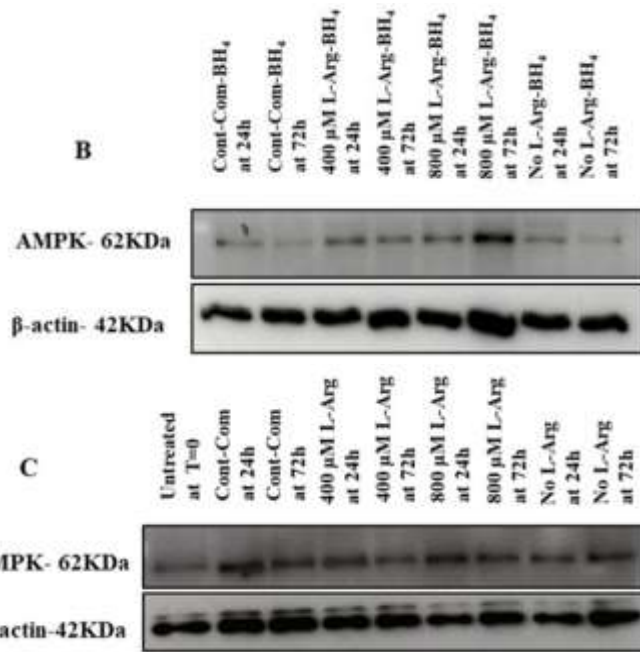
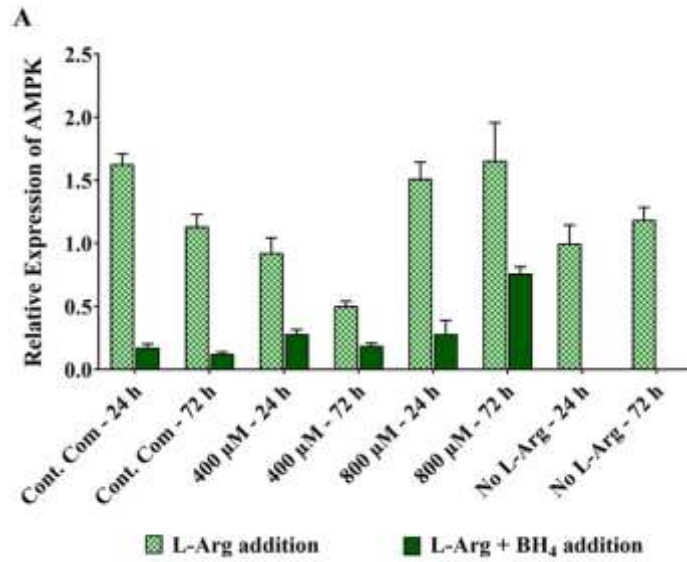


Figure 3.3.31. Western blot comparison for AMPK and ACC-1 protein expressions in 3T3 L1 cells cultured in different concentrations of L-arginine and the control with BH₄ (40 μM).

Western blot comparison of the expression of key protein; AMPK and lipogenic ACC-1 protein levels investigated in L-arginine/NO metabolic pathway signalling in 3T3 L1 cells cultured in customized media containing (A) no L-arginine SILAC DMEM and BH₄ (40 μM) (B) complete DMEM and BH₄ (40 μM), (C) 400 μM L-arginine and BH₄ (40 μM), and (D) 800 μM L-arginine and BH₄ (40 μM) for 24 and 72 h. β-actin is used as a loading control. The same amount of protein (10 μg) from different treatment groups was loaded from biological triplicate cultures into 10% SDS-polyacrylamide gels for the separation of target proteins. No AMPK protein means, AMPK protein did not detect in the prepared protein samples.



	AMPK		
Source of Variation	P value	P value summary	Significant?
Interaction	**	Yes	**
Samples, conditions and time points	****	Yes	****
L-Arg +/- BH ₄	****	Yes	****

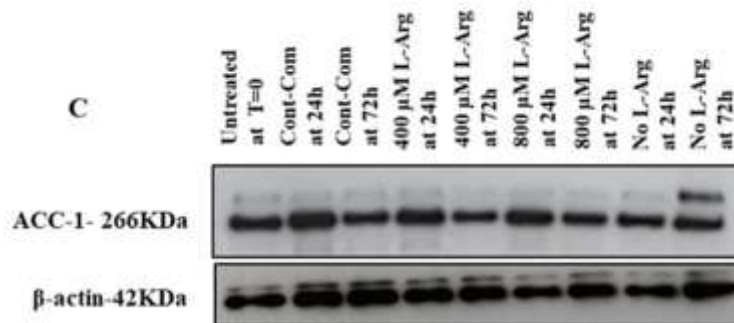
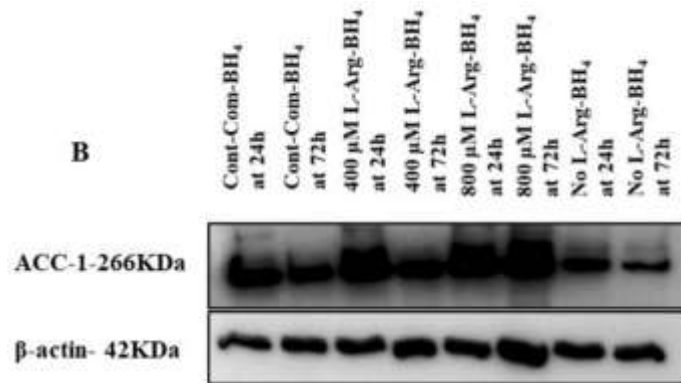
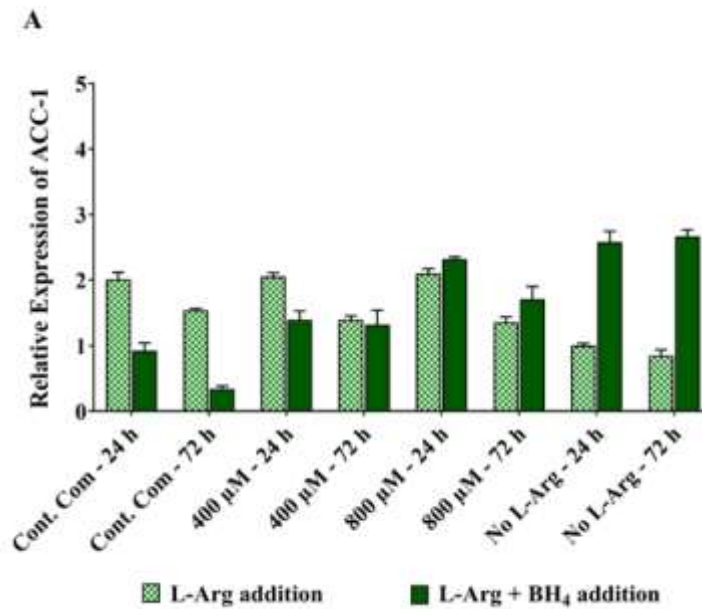
Bonferroni's multiple comparisons test	L-Arg addition and L-Arg + BH ₄ addition
AMPK	
Cont. Com - 24 h	ns

Cont. Com - 72 h	ns
400 μM - 24 h	ns
400 μM - 72 h	****
800 μM - 24 h	ns
800 μM - 72 h	ns
No L-Arg - 24 h	ns
No L-Arg - 72 h	ns

Figure 3.3.32. Relative protein expression and western blot comparisons (with or without BH₄) for AMPK protein in 3T3 L1 cells cultured in different concentrations of L-arginine and the control with BH₄ (40 μ M).

Relative protein expression of AMPK (A), western blot comparison of the expression of key protein, AMPK involved in L-arginine/NO metabolic pathway signalling investigated in 3T3 L1 cells cultured with BH₄ (40 μ M) in no L-arginine SILAC DMEM, complete DMEM, 400 μ M L-arginine and 800 μ M L-arginine for 24 and 72 h (B) and the amount of AMPK in cultured 3T3 L1 cells without BH₄ for 24 and 72 h (C). The same amount of protein (10 μ g) from different treatment groups was loaded from biological triplicate cultures into 10% SDS–polyacrylamide gels for the separation of target proteins. Two representative blots from each treatment group are shown with the respective to the house-keeping-protein, β -actin. Bands in the blots were quantified using ImageJ software and the data are normalised to β -actin and then expressed as relative to the no L-arginine SILAC DMEM (0 μ M L-arginine) control at 24 h. Data points represent the mean \pm SD. Error bars represent the standard deviation from the mean (n = 3). The tables summarise two-way ANOVA followed by a Bonferroni multiple comparison test using GraphPad Prism 9.4.1. The stars indicate the levels of significance; ns = P > 0.05, * = P \leq 0.05, ** = P \leq 0.01, *** = P \leq 0.001 and **** = P \leq 0.0001.

The impact of addition of BH₄ on relative ACC-1 protein expression is presented in **Fig 3.3.33**. BH₄ addition to the cells cultured at 400 μ M L-Arg and the control decreased (P<0.0001) the expression of ACC-1 after 24 (400 μ M + BH₄; 0.68-fold and the control + BH₄; 0.46-fold) and 72 h (400 μ M + BH₄; 0.94-fold and the control + BH₄; 0.22-fold) compared to the cell samples without BH₄ at the same time points. However, the ACC-1 protein expression was increased (P<0.0001) at the highest and lowest concentrations (800 and 0 μ M, respectively) of L-Arg treated samples with BH₄ at 24 (800 μ M + BH₄; 1.1-fold and 0 μ M + BH₄; 2.58-fold) and 72 h (800 μ M + BH₄; 1.26-fold and 0 μ M + BH₄; 3.14-fold) compared to the samples without co-factor BH₄ at the same time points.



		ACC-1	
Source of Variation	P value	P value summary	Significant?
Interaction	<0.0001	****	Yes
Samples, conditions and time points	<0.0001	****	Yes
L-Arg +/- BH ₄	<0.0001	****	Yes

Bonferroni's multiple comparisons test	L-Arg addition and L-Arg + BH ₄ addition
	ACC-1
Cont. Com - 24 h	*
Cont. Com - 72 h	****
400 μM - 24 h	****
400 μM - 72 h	****
800 μM - 24 h	ns
800 μM - 72 h	***
No L-Arg - 24 h	ns
No L-Arg - 72 h	ns

Figure 3.3.33. Relative protein expression and western blot comparisons (with or without BH₄) for ACC-1 protein in 3T3 L1 cells cultured in different concentrations of L-arginine and the control with BH₄ (40 μM).

Relative protein expression of ACC-1 (A), western blot comparison of the expression of lipogenic protein, ACC-1 involved in L-arginine/NO metabolic pathway signalling investigated in 3T3 L1 cells cultured with BH₄ (40 μM) in no L-arginine SILAC DMEM, complete DMEM, 400 μM L-arginine and 800 μM L-arginine for 24 and 72 h (B) and the amount of ACC-1 in cultured 3T3 L1 cells without BH₄ for 24 and 72 h (C). The same amount of protein (10 μg) from different treatment groups was loaded from biological triplicate cultures into 10% SDS–polyacrylamide gels for the separation of target proteins. Two representative blots from each treatment group are shown with the respective to the house-keeping-protein, β-actin. Bands in the blots were quantified using ImageJ software and the data are normalised to β-actin and then expressed as relative to the no L-arginine SILAC DMEM (0 μM L-arginine) control at 24 h. Data points represent the mean ± SD. Error bars represent the standard deviation from the mean (n = 3). The tables summarise two-way ANOVA followed by a Bonferroni multiple comparison test using GraphPad Prism 9.4.1. The stars indicate the levels of significance; ns = P > 0.05, * = P ≤ 0.05, ** = P ≤ 0.01, *** = P ≤ 0.001 and **** = P ≤ 0.0001.

3.3.6.3. AMPK and ACC-1 protein expression upon SNAP (100 μM) addition to 3T3 L1 cells

The changes in AMPK and ACC-1 protein expression upon SNAP addition to the 3T3 L1 cells cultured in different concentrations of L-Arg and the control complete DMEM was investigated and is shown in (Fig 3.3.34). AMPK protein expression did not change significantly (P=0.0908) between samples with and without SNAP addition Fig 3.3.35.

The changes in ACC-1 protein expression upon SNAP addition are shown in Fig 3.3.36. There was a large decrease (P<0.0001) in ACC-1 protein expression in the samples cultured in different concentrations of L-Arg (0, 400 and 800 μM) and the control complete DMEM followed by SNAP addition at 24 h (the control + SNAP; 0.2-fold, 400 μM + SNAP; 0.21-fold, 800 μM + SNAP; 0.18-fold and 0 μM + SNAP; 0.33-fold) compared to the cell samples cultured without SNAP. Across the culture time the relative expression of ACC-1 protein was increased (P<0.0001) in L-Arg with SNAP (400; 2.1-fold and 800 μM; 1.85-fold) whereas, decreased (P<0.0001) in the control (0.3-fold) and no L-Arg (0.63-fold) cell samples treated with SNAP.

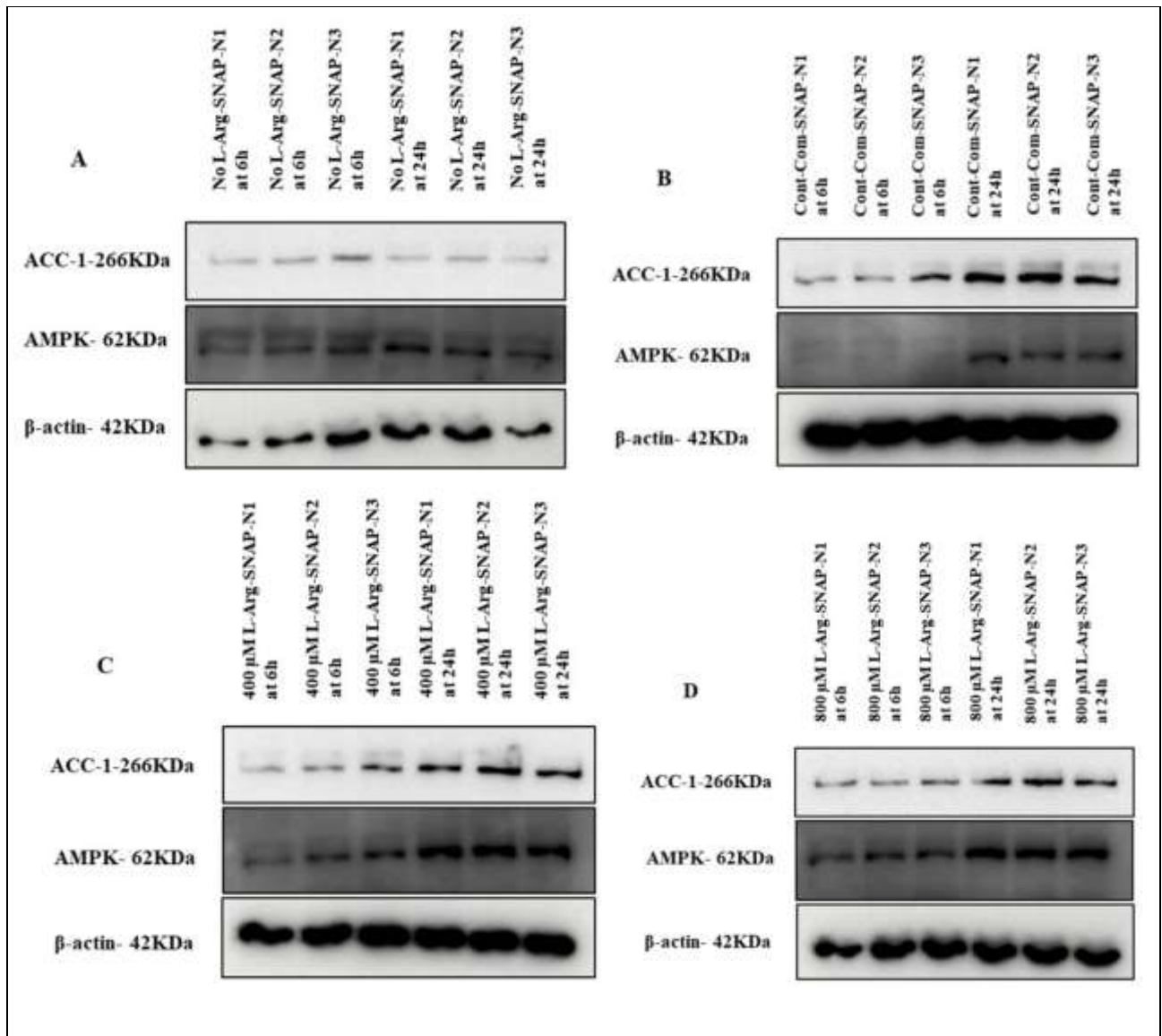


Figure 3.3.34. Western blot comparison for AMPK and ACC-1 protein expressions in 3T3 L1 cells cultured in different concentrations of L-arginine and the control with SNAP (100 μ M).

Western blot comparison of the expression of key protein; AMPK and lipogenic ACC-1 protein levels investigated in L-arginine/NO metabolic pathway signalling in 3T3 L1 cells cultured in customized media containing (A) no L-arginine SILAC DMEM and SNAP (100 μ M) (B) complete DMEM and SNAP (100 μ M), (C) 400 μ M L-arginine and SNAP (100 μ M), and (D) 800 μ M L-arginine and SNAP (100 μ M) for 6 and 24 h. β -actin is used as a loading control. The same amount of protein (10 μ g) from different treatment groups was loaded from biological triplicate cultures into 10% SDS-polyacrylamide gels for the separation of target proteins.

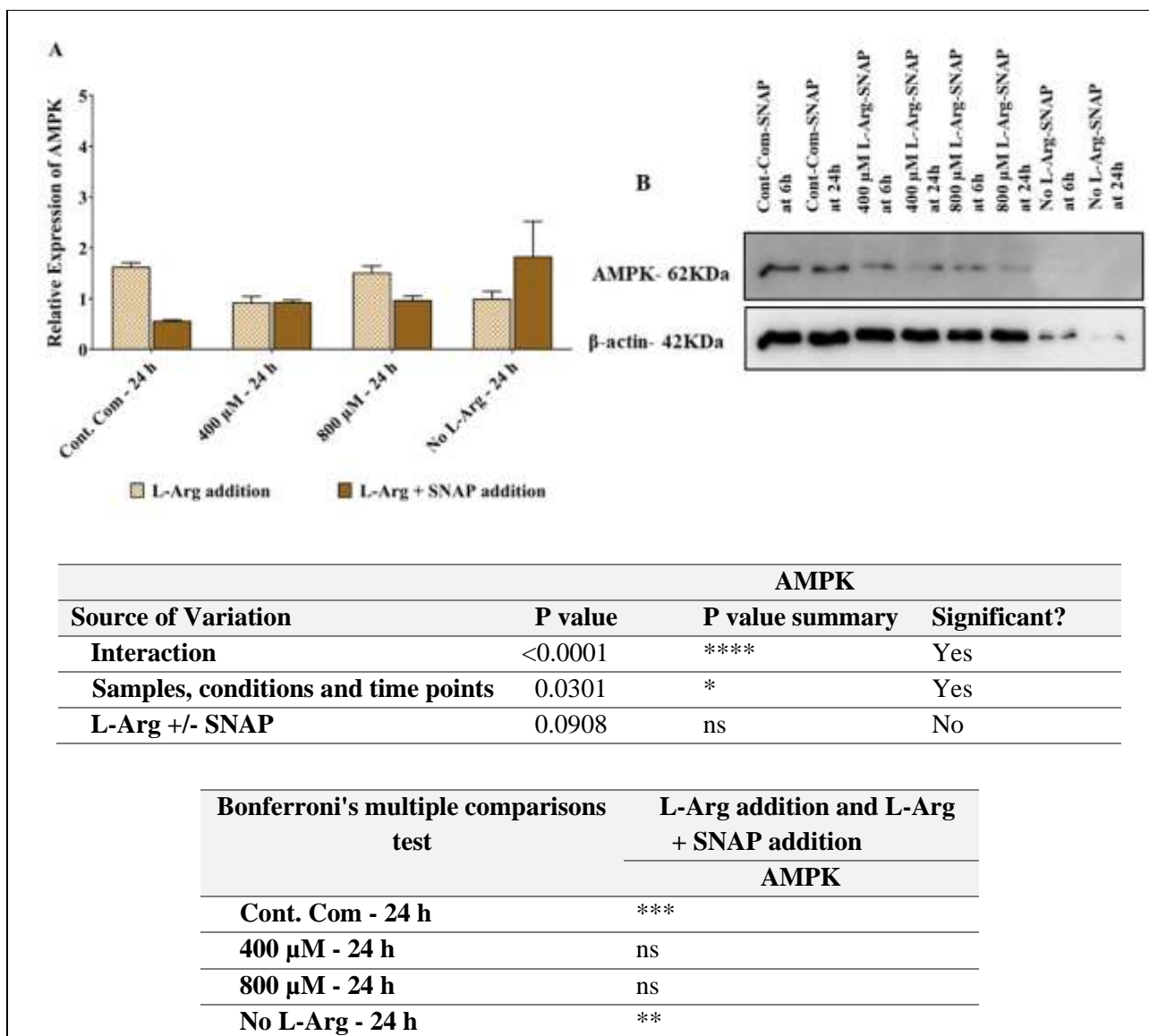


Figure 3.3.35. Relative protein expression and western blot comparison for AMPK protein in 3T3 L1 cells cultured in different concentrations of L-arginine and the control with SNAP (100 μM).

Relative protein expression of AMPK (A), western blot comparison of the expression of key protein, AMPK involved in L-arginine/NO metabolic pathway signalling investigated in 3T3 L1 cells cultured with SNAP (100 μM) in no L-arginine SILAC DMEM, complete DMEM, 400 μM L-arginine and 800 μM L-arginine for 6 and 24 h (B). The same amount of protein (10 μg) from different treatment groups was loaded from biological triplicate cultures into 10% SDS–polyacrylamide gels for the separation of target proteins. The representative blot from the treatment group is shown with the respective to the house-keeping-protein, β-actin. Bands in the blots were quantified using ImageJ software and the data are normalised to β-actin and then expressed as relative to the no L-arginine SILAC DMEM (0 μM L-arginine) control at 24 h. Data points represent the mean ± SD. Error bars represent the standard deviation from the mean (n = 3). The tables summarise two-way ANOVA followed by a Bonferroni multiple comparison test using GraphPad Prism 9.4.1. The stars indicate the levels of significance; ns = P > 0.05, * = P ≤ 0.05, ** = P ≤ 0.01, *** = P < 0.001 and **** = P < 0.0001.

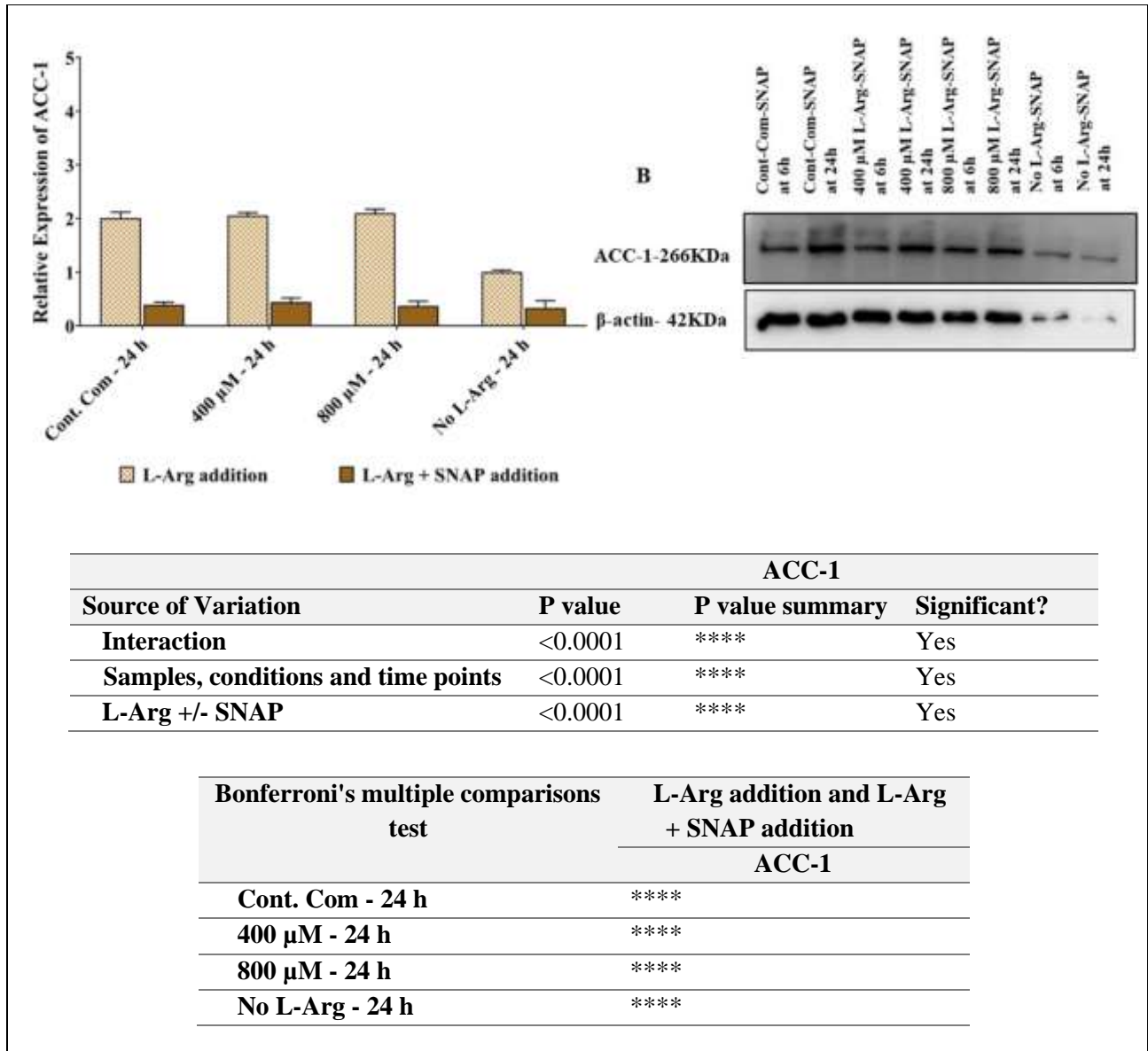


Figure 3.3.36. Relative protein expression and western blot comparison for ACC-1 protein in 3T3 L1 cells cultured in different concentrations of L-arginine and the control with SNAP (100 μ M).

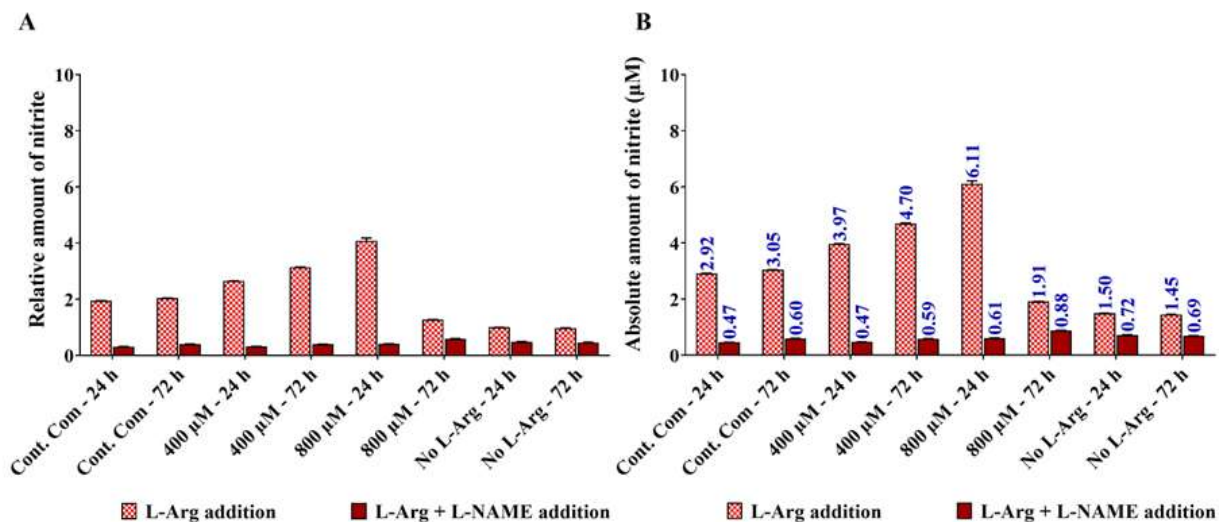
Relative protein expression of ACC-1 (A), western blot comparison of the expression of lipogenic protein, ACC-1 involved in L-arginine/NO metabolic pathway signalling investigated in 3T3 L1 cells cultured with SNAP (100 μ M) in no L-arginine SILAC DMEM, complete DMEM, 400 μ M L-arginine and 800 μ M L-arginine for 6 and 24 h (B). The same amount of protein (10 μ g) from different treatment groups was loaded from biological triplicate cultures into 10% SDS-polyacrylamide gels for the separation of target proteins. The representative blot from the treatment group is shown with the respective to the house-keeping-protein, β -actin. Bands in the blots were quantified using ImageJ software and the data are normalised to β -actin and then expressed as relative to the no L-arginine SILAC DMEM (0 μ M L-arginine) control at 24 h. Data points represent the mean \pm SD. Error bars represent the standard deviation from the mean (n = 3). The tables summarise two-way ANOVA followed by a Bonferroni multiple comparison test using GraphPad Prism 9.4.1. The stars indicate the levels of significance; ns = P > 0.05, * = P \leq 0.05, ** = P \leq 0.01, *** = P \leq 0.001 and **** = P \leq 0.0001.

3.3.7. Determination of nitric oxide /nitrite by Griess Assay in 3T3 L1 cells grown in different concentrations of exogenous L-arginine with L-NAME (4 mM), BH₄ (40 μM) and SNAP (100 μM)

The effect of NOS inhibition by L-NAME, NOS facilitation by co-factor BH₄ or addition of external NO donor SNAP on nitrite synthesis upon culturing of the cells in different concentrations of L-Arg and the control complete DMEM was investigated and the results presented in the **Figs 3.3.37-3.3.39**. The amount of nitrite present in the samples was normalised to the amount of nitrite present in the no L-Arg (0 μM) cell samples at 24 h and then the relative (**A**) and the absolute (**B**) amount of nitrite present in the cell samples are presented. For the analysis of L-NAME (4 mM) addition to the 3T3 L1 cells cultured in L-Arg (0, 400 and 800 μM) and the control complete DMEM, the amount of nitrite present in the cell samples is presented in **Fig 3.3.37**. The amount of NO decreased ($P < 0.0001$) in the samples cultured with L-NAME after 24 (the control + L-NAME; 0.16-fold, 400 μM + L-NAME; 0.12-fold, 800 μM + L-NAME; 0.10-fold and 0 μM + L-NAME; 0.48-fold) and 72 h (the control + L-NAME; 0.2-fold, 400 μM + L-NAME; 0.13-fold, 800 μM + L-NAME; 0.45-fold and 0 μM + L-NAME; 0.47-fold) compared to the samples cultured without L-NAME. Interestingly, a large drop ($P < 0.0001$) in the amount of nitrite was observed in the samples cultured in excess L-Arg 400 and 800 μM with L-NAME (0.47 and 0.61 μM nitrite, respectively) in comparison to the samples cultured without L-NAME (400; 3.97 and 800 μM L-Arg; 6.11 μM nitrite) after 24 h.

When the co-factor of NOS, BH₄ (40 μM) was added the amount of nitrite present in the cell culture supernatant samples were analysed and the results shown in **Fig 3.3.38**. Generally, the addition of BH₄ resulted in an increase ($P < 0.0001$) in the amount of nitrite present in the cell culture supernatant samples at 24 (the control + BH₄; 18.2-fold, 400 μM + BH₄; 13.9, 800 μM + BH₄; 7.36-fold and 0 μM + BH₄; 15.15-fold) and 72 h (the control + BH₄; 17.34-fold, 400 μM + BH₄; 10.7, 800 μM + BH₄; 26.4-fold and 0 μM + BH₄; 41.88-fold) over samples cultured without BH₄.

When the external NO donor, SNAP (100 μM) was added to the 3T3 L1 cells cultured in L-Arg (0, 400 and 800 μM) and the control complete DMEM the amount of nitrite present in the cell culture samples were analysed and the results shown in **Fig 3.3.39**. Overall, upon addition of SNAP to 3T3 L1 cells cultured in L-Arg (0, 400 and 800 μM) there was a large increase ($P < 0.0001$) in the nitrite amount at 6 (the control + SNAP; 305.26-fold, 400 μM + SNAP; 40.66-fold; 800 μM + SNAP; 116.39-fold and 0 μM + SNAP; 28.02-fold) and 24 h (the control + SNAP; 14.46-fold, 400 μM + SNAP; 6.8-fold; 800 μM + SNAP; 6.75-fold and 0 μM + SNAP; 42.2-fold) compared to the cell samples cultured without NO donor at the same timepoints.



		Amount of Nitrite	
Source of Variation	P value	P value summary	Significant?
Interaction	<0.0001	****	Yes
Samples, conditions and time points	<0.0001	****	Yes
L-Arg +/- L-NAME	<0.0001	****	Yes

Bonferroni's multiple comparisons test	L-Arg addition and L-Arg + L-NAME addition
	Amount of Nitrite
Cont. Com - 24 h	****
Cont. Com - 72 h	****
400 µM - 24 h	****
400 µM - 72 h	****
800 µM - 24 h	****
800 µM - 72 h	****
No L-Arg - 24 h	****
No L-Arg - 72 h	****

Figure 3.3.37. The effect of exogenous L-arginine concentration and iNOS inhibitor, L-NAME addition on nitrite production in 3T3 L1 cells.

Cell culture supernatant was obtained from cultured 3T3 L1 cells grown in the presence of L-NAME (4 mM) in 0, 400 or 800 µM L-arginine and the control complete DMEM for 24 or 72 h. The concentration of nitrite from experimental samples was obtained using the equation of the line fitted to standard samples. The data are expressed as relative (A) and absolute (B) values. To obtain relative value, quantified nitrite was normalised to the nitrite amount presence in cultures with no L-arginine SILAC DMEM (0 µM L-arginine) at 24 h. Data points represent the mean ± SD. Error bars represent the standard deviation from the mean (n = 3). The tables summarise two-way ANOVA followed by a Bonferroni multiple comparison test using GraphPad Prism 9.4.1. The stars indicate the levels of significance; ns = P > 0.05, * = P ≤ 0.05, ** = P ≤ 0.01, *** = P ≤ 0.001 and **** = P ≤ 0.0001.

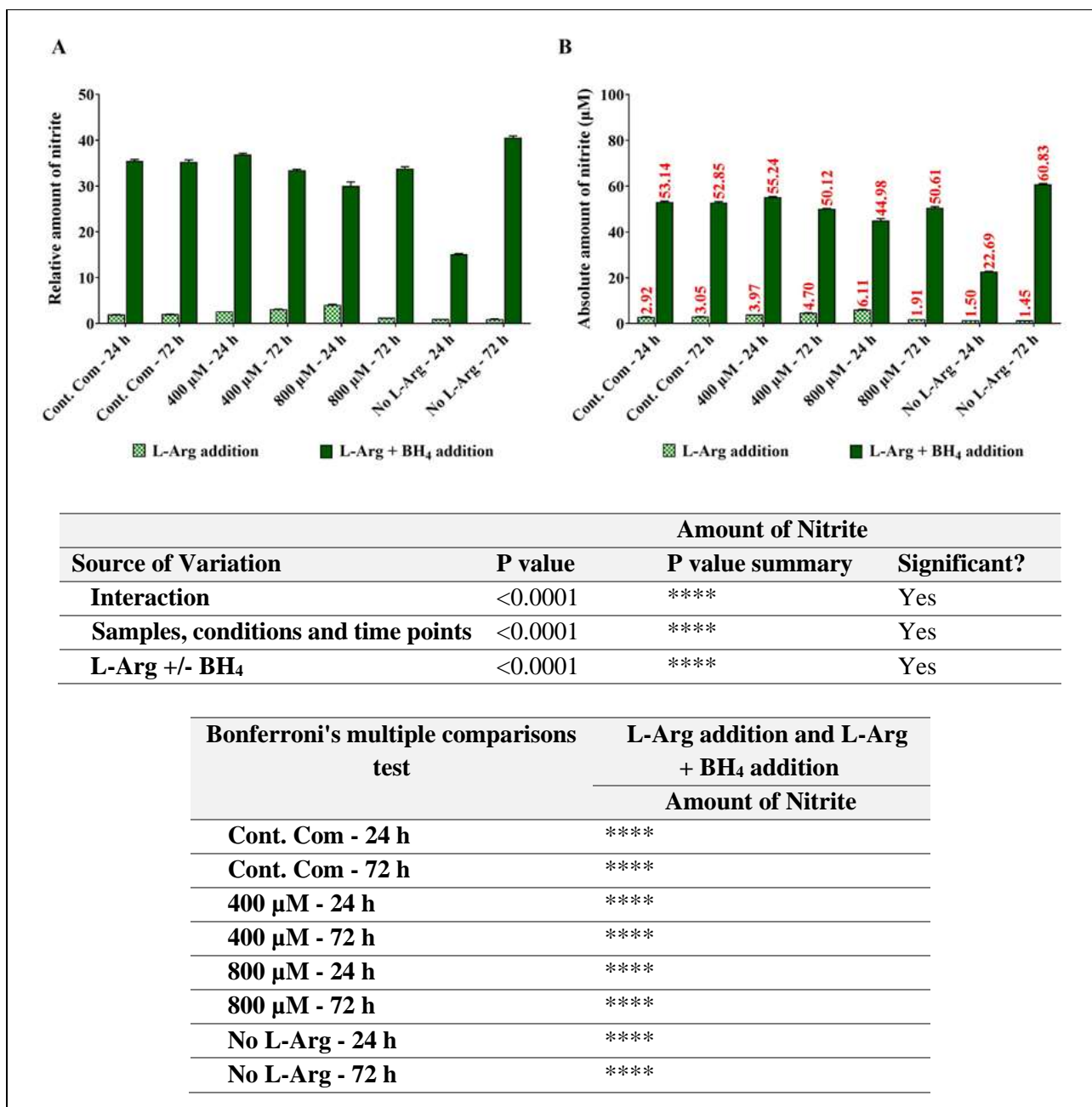


Figure 3.3.38. The effect of exogenous L-arginine concentration and co-factor of iNOS, BH₄ addition on nitrite production in 3T3 L1 cells.

Cell culture supernatant was obtained from cultured 3T3 L1 cells grown in the presence of BH₄ (40 µM) in 0, 400 or 800 µM L-arginine and the control complete DMEM for 24 or 72 h. The concentration of nitrite from experimental samples was obtained using the equation of the line fitted to standard samples. The data are expressed as relative (A) and absolute (B) values. To obtain relative value, quantified nitrite was normalised to the nitrite amount presence in cultures with no L-arginine SILAC DMEM (0 µM L-arginine) at 24 h. Data points represent the mean ± SD. Error bars represent the standard deviation from the mean (n = 3). The tables summarise two-way ANOVA followed by a Bonferroni multiple comparison test using GraphPad Prism 9.4.1. The stars indicate the levels of significance; ns = P > 0.05, * = P ≤ 0.05, ** = P ≤ 0.01, *** = P ≤ 0.001 and **** = P ≤ 0.0001.

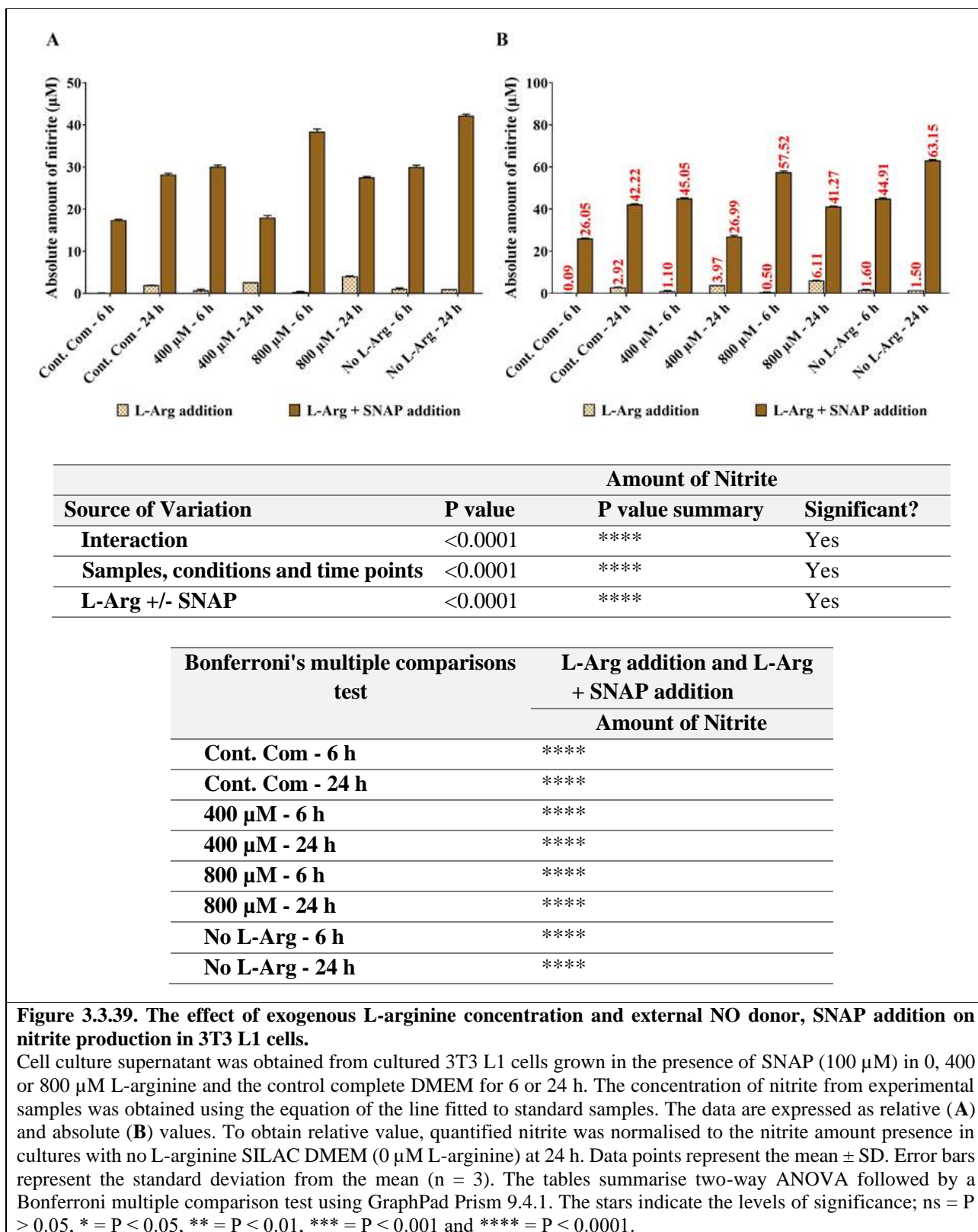


Figure 3.3.39. The effect of exogenous L-arginine concentration and external NO donor, SNAP addition on nitrite production in 3T3 L1 cells.

Cell culture supernatant was obtained from cultured 3T3 L1 cells grown in the presence of SNAP (100 μ M) in 0, 400 or 800 μ M L-arginine and the control complete DMEM for 6 or 24 h. The concentration of nitrite from experimental samples was obtained using the equation of the line fitted to standard samples. The data are expressed as relative (A) and absolute (B) values. To obtain relative value, quantified nitrite was normalised to the nitrite amount presence in cultures with no L-arginine SILAC DMEM (0 μ M L-arginine) at 24 h. Data points represent the mean \pm SD. Error bars represent the standard deviation from the mean (n = 3). The tables summarise two-way ANOVA followed by a Bonferroni multiple comparison test using GraphPad Prism 9.4.1. The stars indicate the levels of significance; ns = P > 0.05, * = P \leq 0.05, ** = P \leq 0.01, *** = P \leq 0.001 and **** = P \leq 0.0001.

3.3.8. HPLC analysis of residue L-arginine, L-ornithine and L-citrulline in the cell culture media of 3T3 L1 cells cultured in different initial L-arginine with L-NAME (4 mM), BH₄ (40 μM) and SNAP (100 μM)

The amount of L-arginine and the catabolic products or precursor of L-arginine synthesis; L-citrulline and L-ornithine present in the serum samples of the adipocytes 3T3 L1 cells cultured in different concentrations of L-Arg and the control complete DMEM were analysed with or without either nitric oxide synthase inhibitor; L-NAME, co-factor of nitric oxide synthase; BH₄ or external NO donor; SNAP. The amount of each target amino acid present in the samples was normalised to the amount of particular amino acid present in the no L-Arg (0 μM) cell samples at 24 h and then the relative (**A**, denoted as RA) and the absolute (**B**) amount of target amino acids present in the cell samples are presented in the **Figs 3.3.40-3.3.48** compared to the 3T3 L1 cell samples cultured without either L-NAME, BH₄ or SNAP.

3.3.8.1. HPLC analysis upon NOS inhibitor, L-NAME (4 mM) addition to 3T3 L1 cells

L-arginine concentrations in the cell culture supernatant samples (**Fig 3.3.40**) from the cells cultured in 400 and 800 μM L-Arg with L-NAME after 24 (0.74-fold and 0.24-fold, respectively) and 72 h (400 μM + L-NAME; 0.88-fold) was low, although in 400 μM L-Arg with L-NAME after 72 h (2.16-fold) this was increased compared to the samples cultured without L-NAME. **Figure 3.3.40** shows the L-arginine concentration and how this changed with L-arginine and L-NAME addition with culture time.

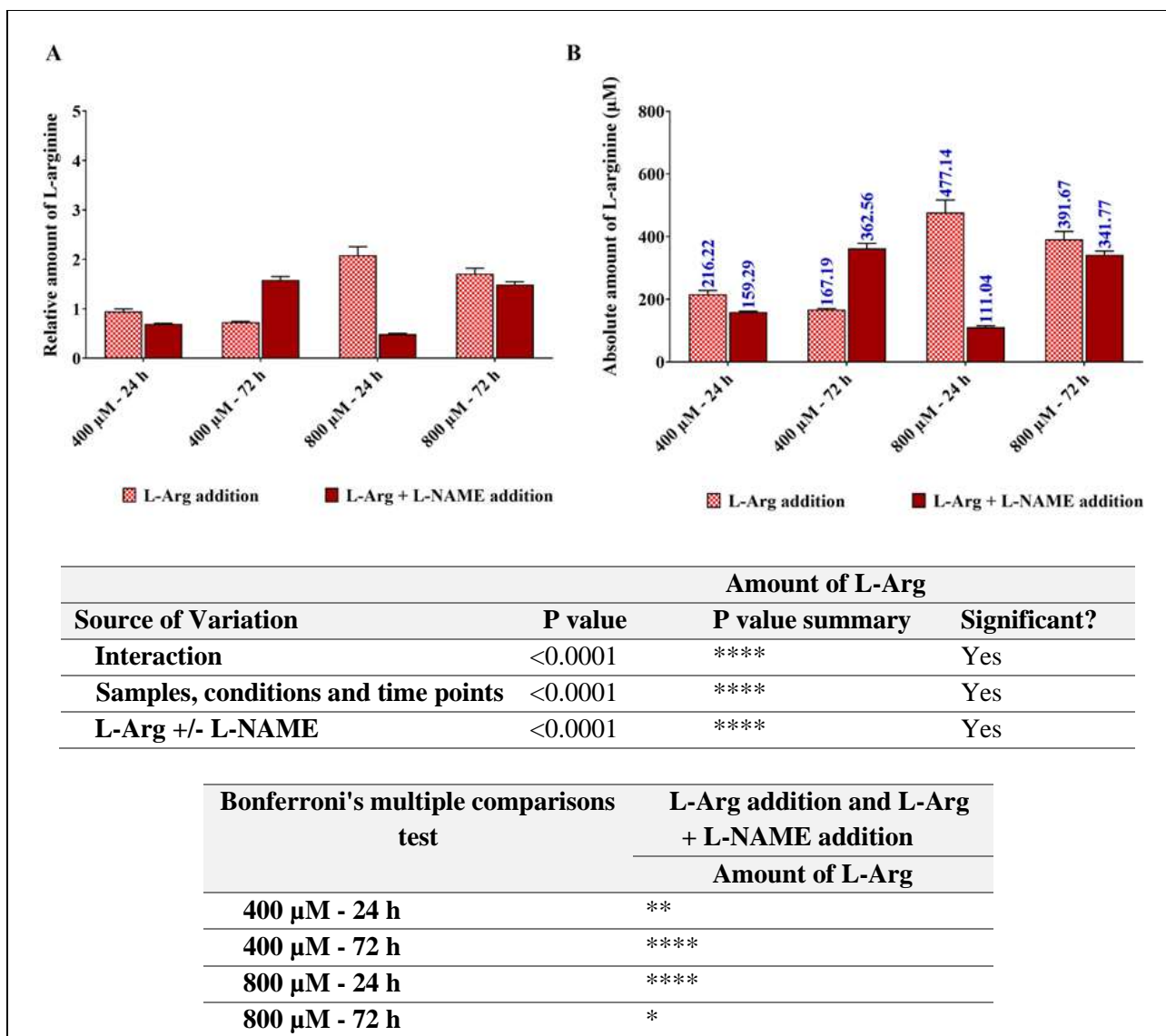


Figure 3.3.40. Relative and absolute quantification of residual serum L-Arg in 3T3 L1 cells cultured in different L-Arg concentrations and the control with L-NAME (4 mM) for 24 and 72 h.

Relative (A) and absolute (B) residue amount of L-Arg analysed in plasma samples of 3T3 L1 cells cultured in the presence of iNOS inhibitor, L-NAME (4 mM) in excess amount of L-Arg (400 and 800 μM) after 24 and 72 h. Data points represent the mean ± SD of each sample. Error bars represent the standard deviation from the mean (n =3). Tables summarise two-way ANOVA followed by a Bonferroni multiple comparison test using GraphPad Prism 9.4.1. The stars indicate the levels of significance; ns = P > 0.05, * = P ≤ 0.05, ** = P ≤ 0.01, *** = P ≤ 0.001 and **** = P ≤ 0.0001.

L-citrulline concentration was also analysed in the cell culture supernatant samples and is shown in **Fig 3.3.41**. L-citrulline was not detected (P<0.001) (RA 0 or negative values) in the samples cultured in L-Arg (400 and 800 μM) and L-NAME.

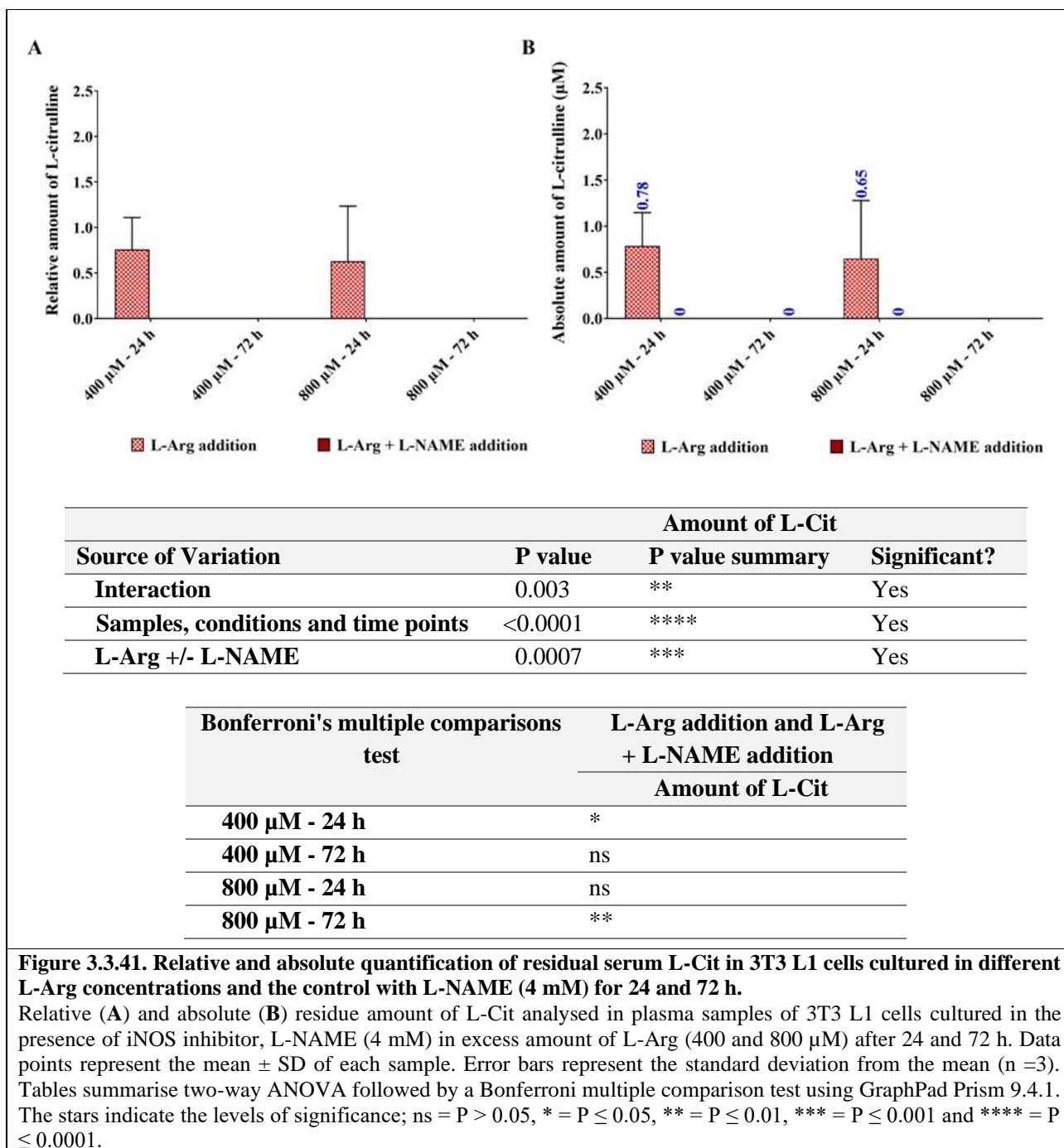


Figure 3.3.41. Relative and absolute quantification of residual serum L-Cit in 3T3 L1 cells cultured in different L-Arg concentrations and the control with L-NAME (4 mM) for 24 and 72 h.

Relative (A) and absolute (B) residue amount of L-Cit analysed in plasma samples of 3T3 L1 cells cultured in the presence of iNOS inhibitor, L-NAME (4 mM) in excess amount of L-Arg (400 and 800 µM) after 24 and 72 h. Data points represent the mean ± SD of each sample. Error bars represent the standard deviation from the mean (n =3). Tables summarise two-way ANOVA followed by a Bonferroni multiple comparison test using GraphPad Prism 9.4.1. The stars indicate the levels of significance; ns = P > 0.05, * = P ≤ 0.05, ** = P ≤ 0.01, *** = P ≤ 0.001 and **** = P ≤ 0.0001.

When L-ornithine concentrations were investigated (Fig 3.3.42) there was no significant changes (P=0.8619) in concentration between samples cultured with and without L-NAME.

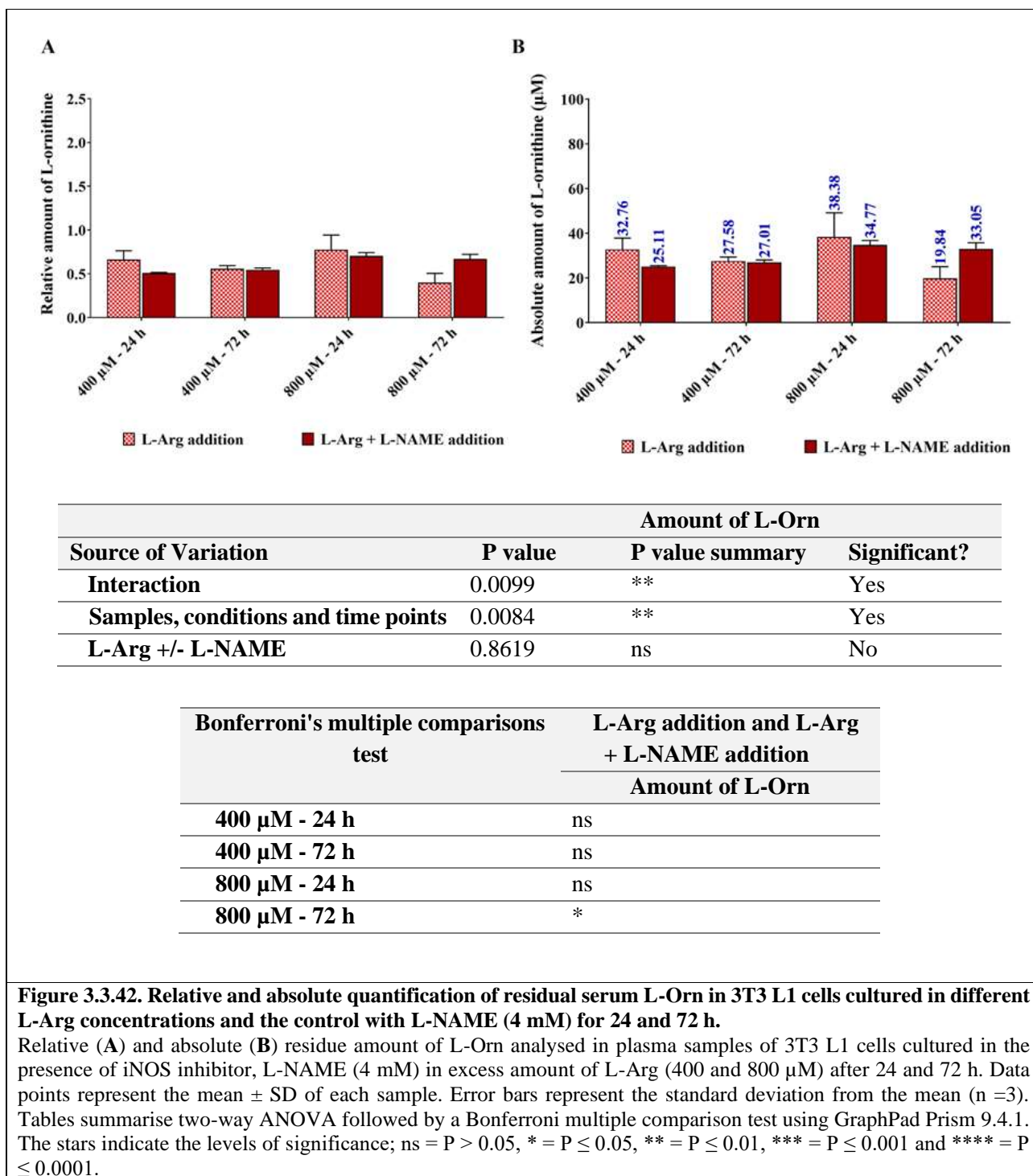


Figure 3.3.42. Relative and absolute quantification of residual serum L-Orn in 3T3 L1 cells cultured in different L-Arg concentrations and the control with L-NAME (4 mM) for 24 and 72 h.

Relative (A) and absolute (B) residue amount of L-Orn analysed in plasma samples of 3T3 L1 cells cultured in the presence of iNOS inhibitor, L-NAME (4 mM) in excess amount of L-Arg (400 and 800 µM) after 24 and 72 h. Data points represent the mean ± SD of each sample. Error bars represent the standard deviation from the mean (n =3). Tables summarise two-way ANOVA followed by a Bonferroni multiple comparison test using GraphPad Prism 9.4.1. The stars indicate the levels of significance; ns = P > 0.05, * = P ≤ 0.05, ** = P ≤ 0.01, *** = P ≤ 0.001 and **** = P ≤ 0.0001.

3.3.8.2. HPLC analysis upon NOS co-factor, BH₄ (40 µM) addition to 3T3 L1 cells

When the cells were grown in the presence and absence of BH₄, the effect of BH₄ on the cell culture supernatant L-Arg concentration was not significant (P=0.0924, **Fig 3.3.43**).

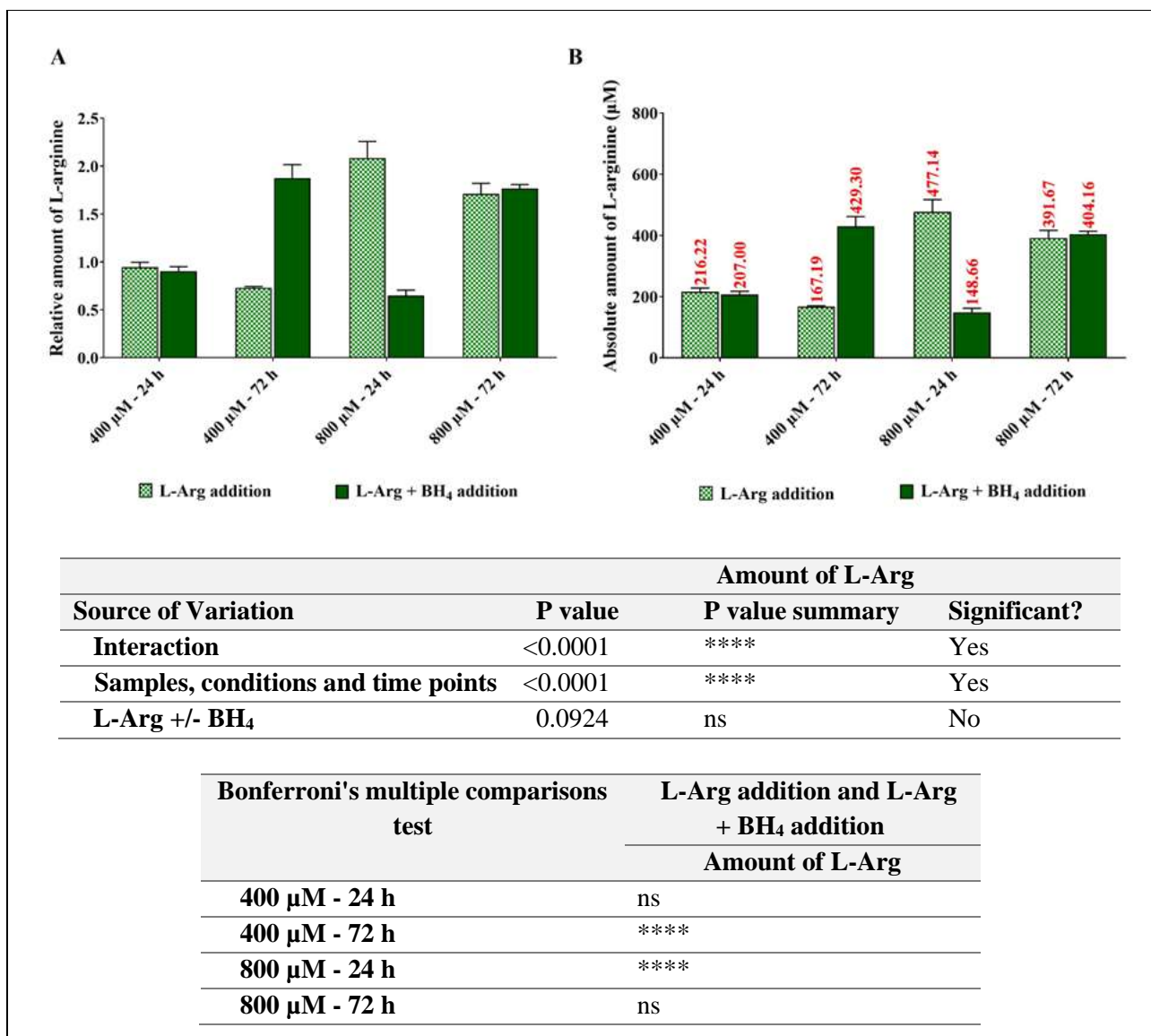


Figure 3.3.43. Relative and absolute quantification of residual serum L-Arg in 3T3 L1 cells cultured in different L-Arg concentrations and the control with BH₄ (40 μM) for 24 and 72 h.

Relative (A) and absolute (B) residue amount of L-Arg analysed in plasma samples of 3T3 L1 cells cultured in the presence of co-factor of iNOS, BH₄ (40 μM) in excess amount of L-Arg (400 and 800 μM) after 24 and 72 h. Data points represent the mean ± SD of each sample. Error bars represent the standard deviation from the mean (n =3). Tables summarise two-way ANOVA followed by a Bonferroni multiple comparison test using GraphPad Prism 9.4.1. The stars indicate the levels of significance; ns = P > 0.05, * = P ≤ 0.05, ** = P ≤ 0.01, *** = P ≤ 0.001 and **** = P ≤ 0.0001.

When L-citrulline was investigated upon BH₄ addition (Fig 3.3.44), most of the cell culture supernatant samples cultured with L-Arg (400 and 800 μM) and BH₄ did not show detectable amounts of L-citrulline.

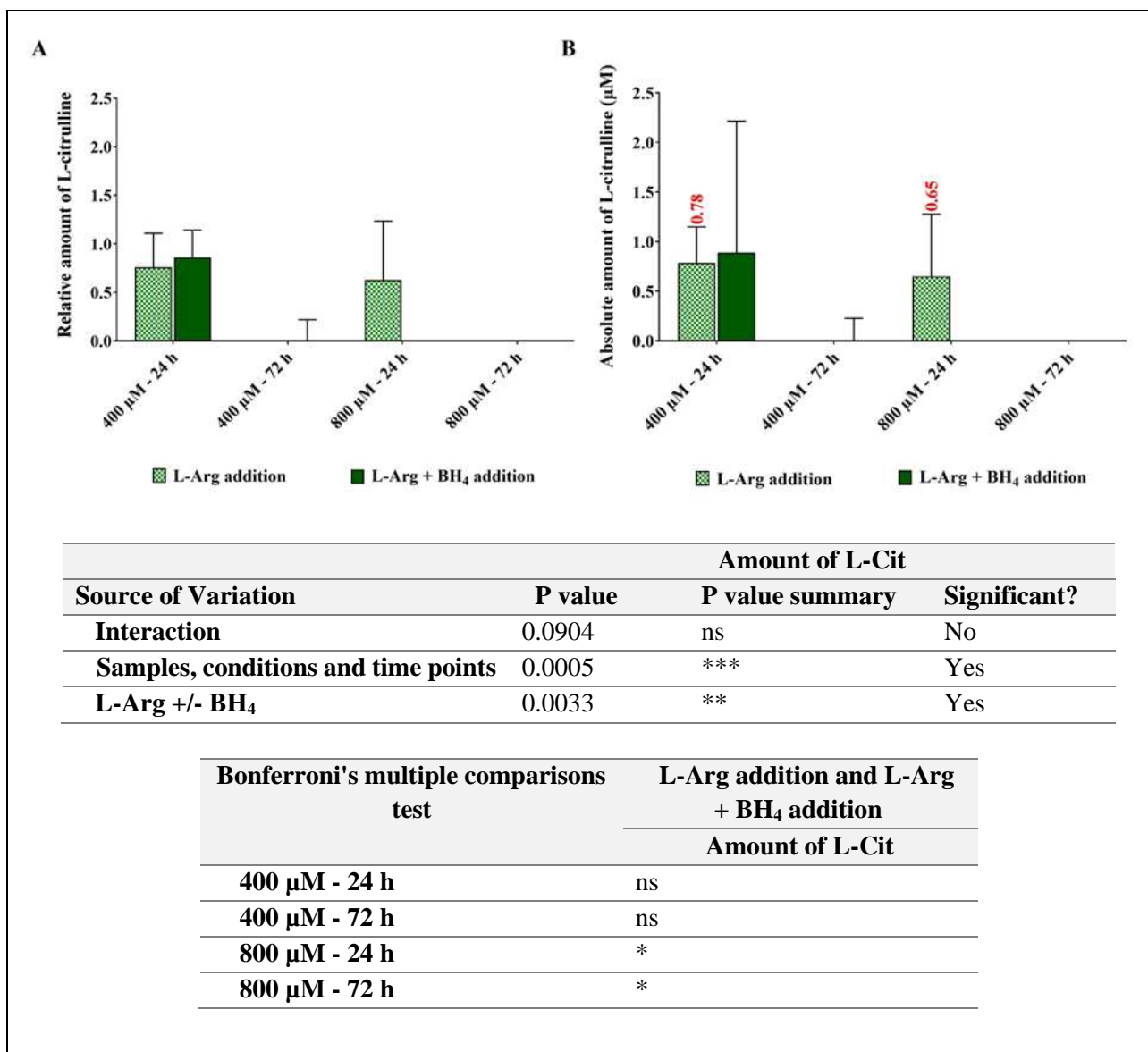


Figure 3.3.44. Relative and absolute quantification of residual serum L-Cit in 3T3 L1 cells cultured in different L-Arg concentrations and the control with BH₄ (40 µM) for 24 and 72 h.

Relative (A) and absolute (B) residue amount of L-Cit analysed in plasma samples of 3T3 L1 cells cultured in the presence of co-factor of iNOS, BH₄ (40 µM) in excess amount of L-Arg (400 and 800 µM) after 24 and 72 h. Data points represent the mean ± SD of each sample. Error bars represent the standard deviation from the mean (n =3). Tables summarise two-way ANOVA followed by a Bonferroni multiple comparison test using GraphPad Prism 9.4.1. The stars indicate the levels of significance; ns = P > 0.05, * = P ≤ 0.05, ** = P ≤ 0.01, *** = P ≤ 0.001 and **** = P ≤ 0.0001.

When L-ornithine was analysed (Fig 3.3.45), this showed that addition of BH₄ to the 3T3 L1 cells in excess L-Arg concentrations (400 and 800 µM) decreased (P<0.0001) the amount of L-Orn at 24 (0.52-fold and 0.36-fold respectively) and 72 h (0.45-fold and 0.60-fold) compared to the cells grown without BH₄ (400 and 800 µM).

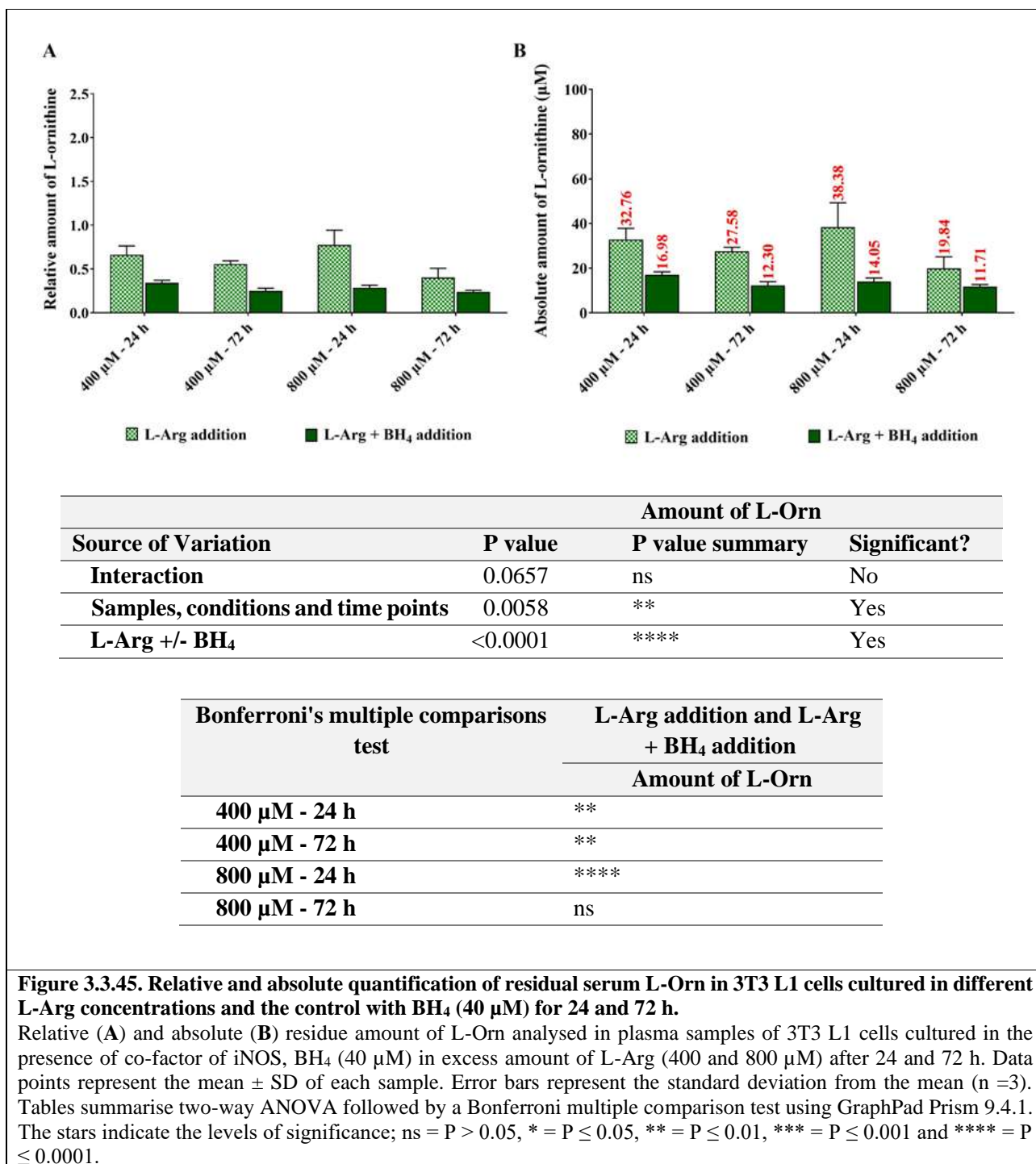


Figure 3.3.45. Relative and absolute quantification of residual serum L-Orn in 3T3 L1 cells cultured in different L-Arg concentrations and the control with BH₄ (40 μM) for 24 and 72 h.

Relative (A) and absolute (B) residue amount of L-Orn analysed in plasma samples of 3T3 L1 cells cultured in the presence of co-factor of iNOS, BH₄ (40 μM) in excess amount of L-Arg (400 and 800 μM) after 24 and 72 h. Data points represent the mean \pm SD of each sample. Error bars represent the standard deviation from the mean (n =3). Tables summarise two-way ANOVA followed by a Bonferroni multiple comparison test using GraphPad Prism 9.4.1. The stars indicate the levels of significance; ns = P > 0.05, * = P \leq 0.05, ** = P \leq 0.01, *** = P \leq 0.001 and **** = P \leq 0.0001.

3.3.8.3. HPLC analysis upon external NO donor, SNAP (100 μM) addition to 3T3 L1 cells

The amount of L-Arg present in the cultured samples with SNAP was analysed and the results are presented in **Fig 3.3.46**. The cell culture supernatant concentration of L-Arg in the samples cultured in L-Arg at 400 μM with SNAP was decreased (P<0.0001) after 6 (400 μM + SNAP; 0.87-fold), but increased (P<0.0001) after 24

h (1.1-fold). **Figure 3.3.46** shows a summary of the L-arginine concentration and how this changed with L-arginine and BH₄ addition with culture time.

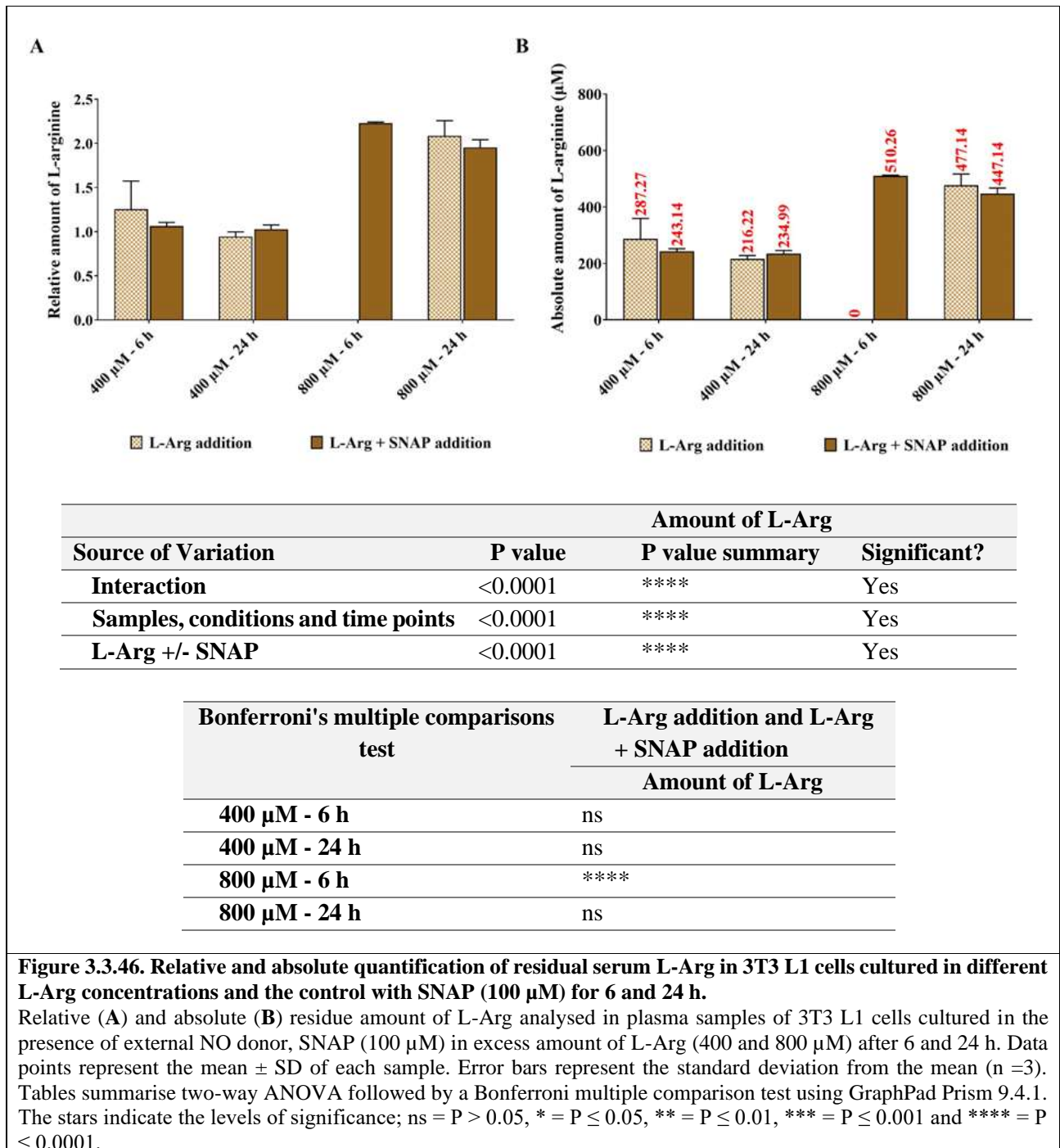


Figure 3.3.46. Relative and absolute quantification of residual serum L-Arg in 3T3 L1 cells cultured in different L-Arg concentrations and the control with SNAP (100 µM) for 6 and 24 h.

Relative (A) and absolute (B) residue amount of L-Arg analysed in plasma samples of 3T3 L1 cells cultured in the presence of external NO donor, SNAP (100 µM) in excess amount of L-Arg (400 and 800 µM) after 6 and 24 h. Data points represent the mean ± SD of each sample. Error bars represent the standard deviation from the mean (n =3). Tables summarise two-way ANOVA followed by a Bonferroni multiple comparison test using GraphPad Prism 9.4.1. The stars indicate the levels of significance; ns = P > 0.05, * = P ≤ 0.05, ** = P ≤ 0.01, *** = P ≤ 0.001 and **** = P ≤ 0.0001.

L-citrulline was not detected with SNAP addition as showed in **Fig 3.3.47**.

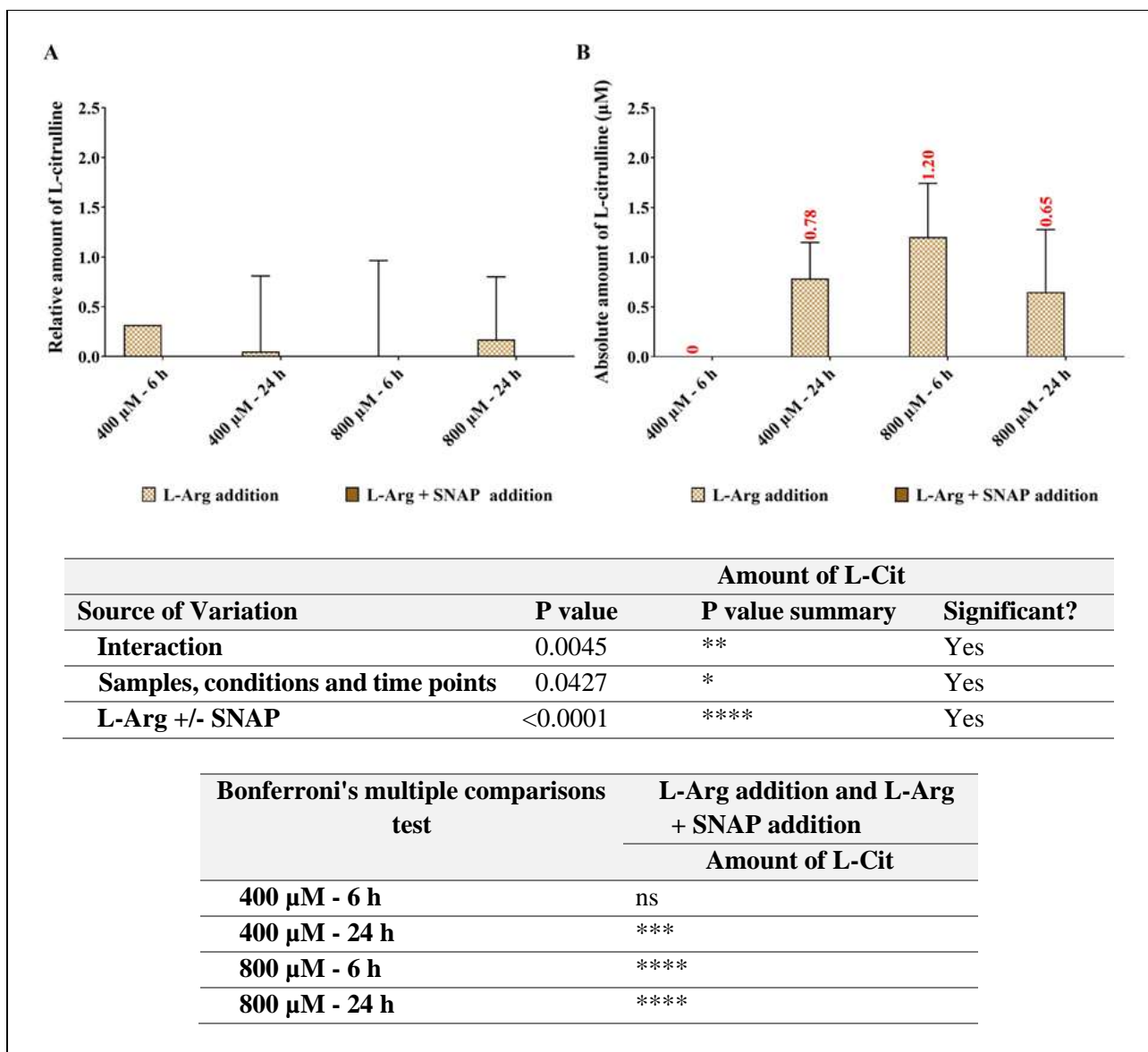


Figure 3.3.47. Relative and absolute quantification of residual serum L-Cit in 3T3 L1 cells cultured in different L-Arg concentrations and the control with SNAP (100 µM) for 6 and 24 h.

Relative (A) and absolute (B) residue amount of L-Cit analysed in plasma samples of 3T3 L1 cells cultured in the presence of external NO donor, SNAP (100 µM) in excess amount of L-Arg (400 and 800 µM) after 6 and 24 h. Data points represent the mean ± SD of each sample. Error bars represent the standard deviation from the mean (n =3). Tables summarise two-way ANOVA followed by a Bonferroni multiple comparison test using GraphPad Prism 9.4.1. The stars indicate the levels of significance; ns = P > 0.05, * = P ≤ 0.05, ** = P ≤ 0.01, *** = P ≤ 0.001 and **** = P ≤ 0.0001.

The amount of L-Orn in samples cultured with L-Arg and SNAP was analysed in 3T3 L1 cells and is presented in **Fig 3.3.48**. The amount of L-ornithine was increased (P<0.05) in the samples cultured with 400 µM L-Arg and SNAP at 6 h (400 µM + SNAP; 3.55-fold), whereas it was decreased (P<0.05) after 24 h (400 µM + SNAP; 0.62-fold) in comparison to samples cultured without SNAP. Arginine at 800 µM had decreased (P<0.05) L-

Orn at 6 h (800 μM + SNAP; 0.94-fold) and 24 h (800 μM + SNAP; 0.5-fold). **Figure 3.3.48** shows a summary of the L-arginine concentration and how this changed with L-arginine and SNAP addition with culture time.

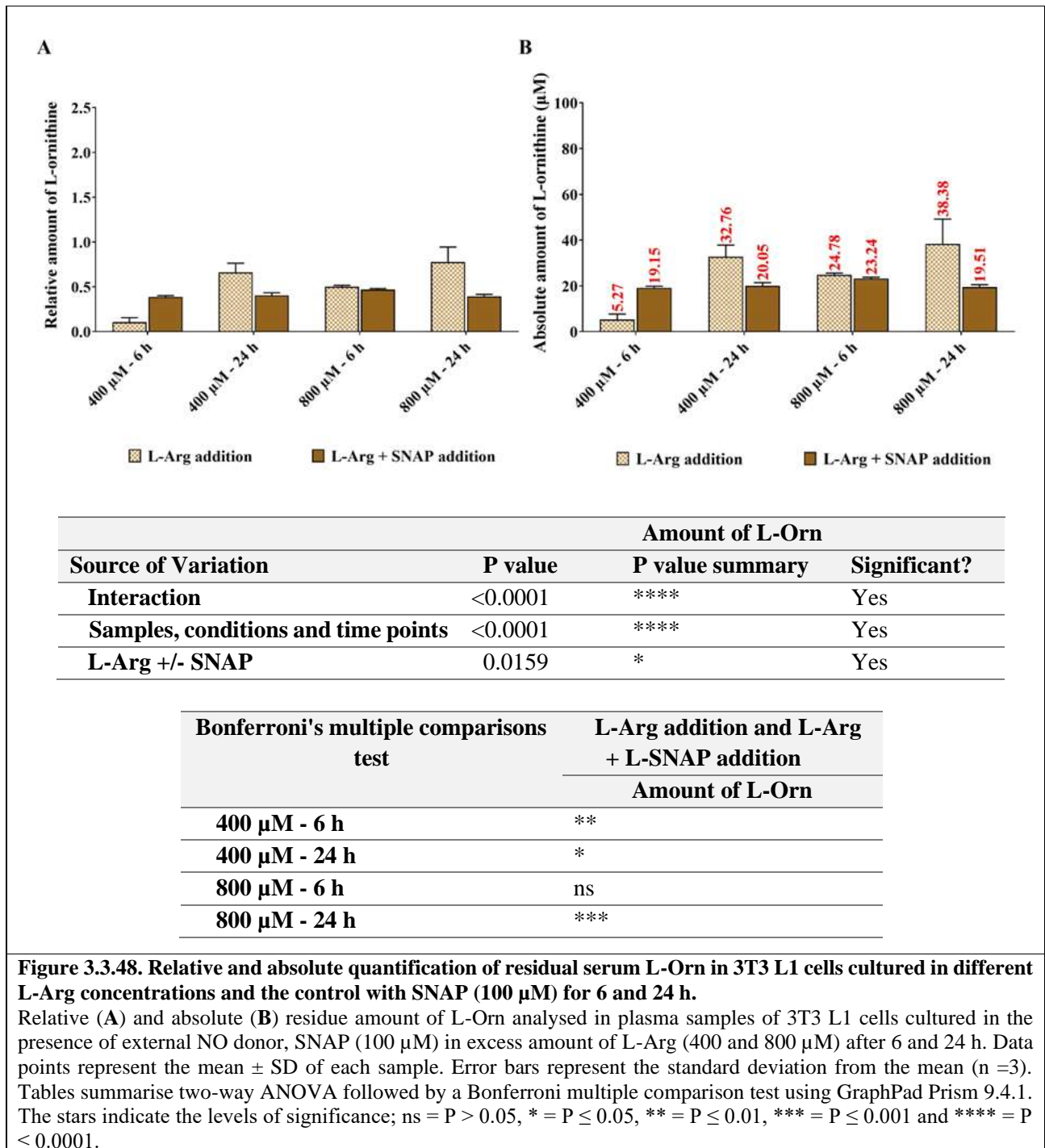


Figure 3.3.48. Relative and absolute quantification of residual serum L-Orn in 3T3 L1 cells cultured in different L-Arg concentrations and the control with SNAP (100 μM) for 6 and 24 h.

Relative (A) and absolute (B) residue amount of L-Orn analysed in plasma samples of 3T3 L1 cells cultured in the presence of external NO donor, SNAP (100 μM) in excess amount of L-Arg (400 and 800 μM) after 6 and 24 h. Data points represent the mean \pm SD of each sample. Error bars represent the standard deviation from the mean (n =3). Tables summarise two-way ANOVA followed by a Bonferroni multiple comparison test using GraphPad Prism 9.4.1. The stars indicate the levels of significance; ns = P > 0.05, * = P \leq 0.05, ** = P \leq 0.01, *** = P \leq 0.001 and **** = P \leq 0.0001.

3.4. Discussion

The SNAP addition in this study required the material to be first dissolved in DMSO, which has a toxic effect on cells and may reduce the proliferation of cells. It is also known that the response of cells to different DMSO concentrations is cell type dependent (De Abreu Costa *et al.*, 2017). For example, a study showed that cell proliferation of HepG2, MDA-MB-231, MCF-7 and VNBRC1 cell lines was impacted by DMSO at concentrations of 10%, 5%, 2.5% and 1.25% (v/v), having a significant toxicity effect on proliferation (Nguyen, Nguyen and Truong, 2020). In this study, a range of DMSO volumes and concentrations in a 2 mL culture volume (2.75 μ L, 0.135 v/v%; 5.5 μ L, 0.27 v/v%; 11 μ L, 0.54 v/v%; 22 μ L, 1.08 v/v%) were investigated and the impact on the viability of BNL CL2 cells determined, showing that 11 μ L (0.27% v/v) DMSO to provide a final concentration of 100 μ M SNAP in 2 mL of culture media had little impact on growth.

3.4.1. BNL CL2 cells grown in different concentrations of exogenous L-arginine with L-NAME (4 mM), BH₄ (40 μ M) and SNAP (100 μ M) additions

It has been reported that L-Arg enhances protein synthesis in a NO-dependent manner in muscle cells when a C2C12 cell model was treated with extra L-arginine supplementation (1 mM) and that addition of L-NAME inhibited NO synthesis and reduced mTOR and p70S6K phosphorylation (Wang *et al.*, 2018). SNP increased NO concentrations, enhanced protein synthesis and increased phosphorylation of mTOR and p70S6K, irrespective of L-NAME treatment in the C2C12 cell model (R. Wang *et al.*, 2018). NO donors can also activate AMPK and increase mitochondrial biogenesis, whereas NOS inhibition diminishes such effects (Baldelli *et al.*, 2014). Therefore, I hypothesised that the L-Arg/NOS/NO pathway regulated by the iNOS inhibitor; L-NAME, co-factor of iNOS; BH₄ and external NO donor; SNAP, which modulation of iNOS enzyme activity would impact the expression of key cell signalling targets in the AMPK-ACC-1 axis via the AMPK/NOS/NO pathway.

qRT-PCR and western blotting were undertaken to investigate the transcript and protein levels of the selected targets AMPK and ACC-1 in the samples cultured in L-NAME (4 mM). In BNL CL2 cells, inhibition of nitric oxide synthase enzymatic activity by L-NAME decreased the L-arginine-stimulated increases of AMPK gene expression in 800 μ M L-Arg at 24 h and upregulates ACC-1 gene expression in 800 μ M L-Arg at 72 h compared with the absence of L-NAME (**Fig 3.4.1**). As expected, the addition of iNOS inhibitor reduced the AMPK and ACC-1 protein expressions in excess L-Arg at 400 and 800 μ M and increased these proteins expression in the control and 0 μ M L-Arg samples over to the samples cultured without L-NAME (**Fig 3.4.1**). This demonstrates that the L-Arg/NOS/NO metabolic pathway and responsive AMPK/ACC-1 cell signalling pathway in the cells were regulated by the iNOS inhibitor L-NAME in relation to the concentration of L-Arg and time dependent manner.

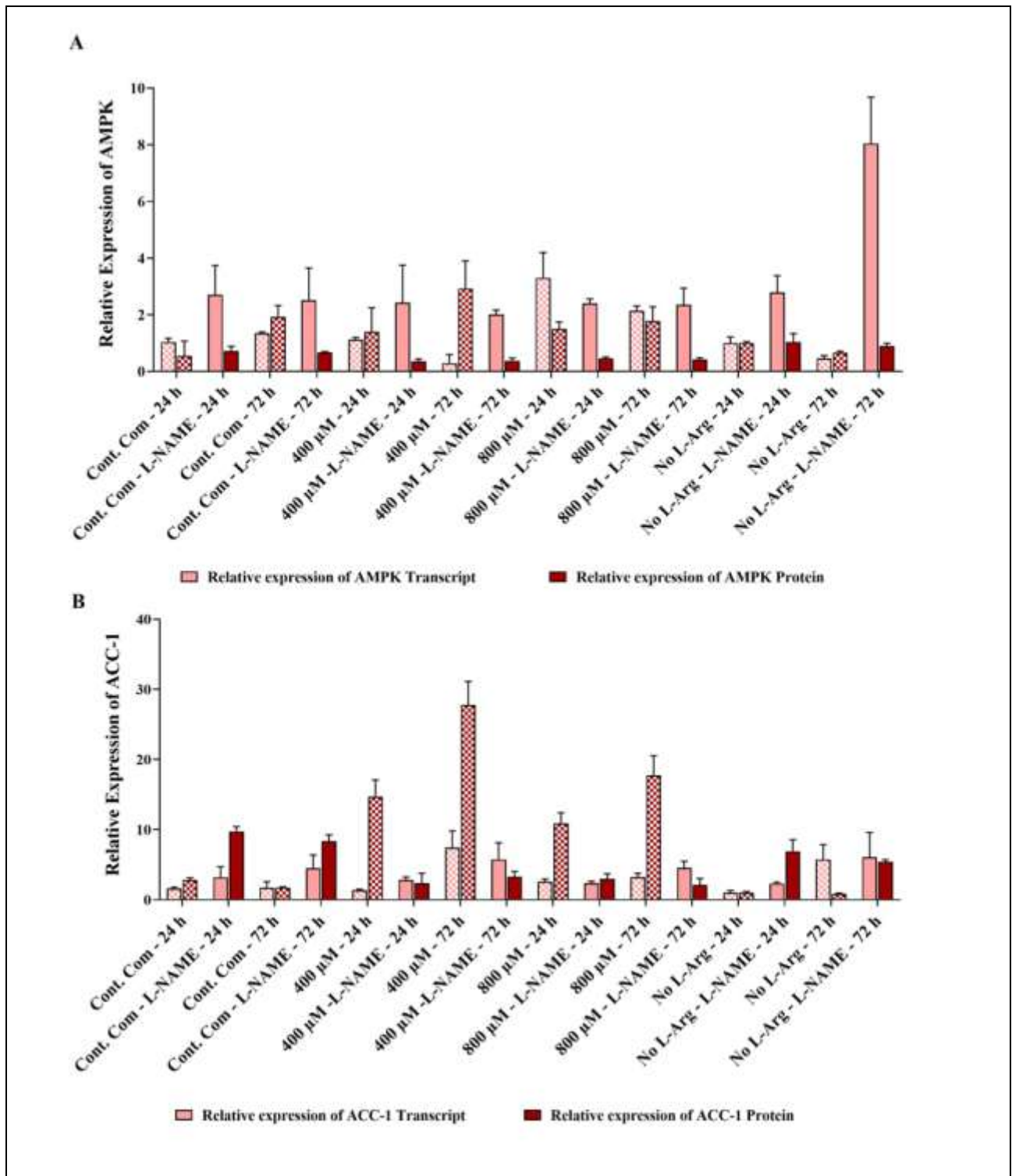


Figure 3.4.1. Comparison of relative AMPK (A) and ACC-1 (B) mRNA and protein expression in BNL CL2 cells cultured in iNOS inhibitor, L-NAME (4 mM) in different exogenous L-arginine amounts for different times.

Relative AMPK transcript expression was lowest when culturing the cells in 800 μ M L-arginine at L-NAME for 24 h, whereas the relative AMPK protein expression was minimal in 400 μ M L-arginine at L-NAME after 72 h when compared to the control complete DMEM and L-NAME culture time points. Relative ACC-1 transcript expression was high in 0 μ M L-Arg and L-NAME for 72 h compared to the control and L-NAME at 72 h and ACC-1 protein expression maximal in the control with L-NAME at 24 h among the samples.

The addition of iNOS co-factor; BH₄ (40 μM) to BNL CL2 cells cultured in excess L-Arg (400 and 800 μM), 0 μM L-Arg and the control complete DMEM, upregulated AMPK gene expression in a time dependent manner (**Fig 3.4.2**). This increasing AMPK gene expression impacts the downstream targets by upregulating ACC-1 transcript levels in L-Arg treated samples. At the protein level, BH₄ addition reduced AMPK protein compared to samples cultured without BH₄. Collectively, these results indicated that AMPK and ACC-1 expression were regulated by BH₄, presence.

Addition of the NO donor, SNAP (100 μM), also impacted on AMPK transcript expression (**Fig 3.4.3**). Noticeably, the addition of SNAP upregulated AMPK and ACC-1 mRNA expressions in the control and 0 μM L-Arg samples over to that of samples cultured in excess exogenous L-Arg. When AMPK and ACC-1 protein expressions were analysed, the samples cultured with SNAP had decreased protein levels in comparison to samples cultured without NO donor (**Fig 3.4.3**). This reflected that the presence of NO either by metabolic pathway of L-Arg or addition of NO by the NO donor to the samples manipulates the transcriptional and translational stages of the targets and NO/AMPK/ACC-1 cell signalling pathway.

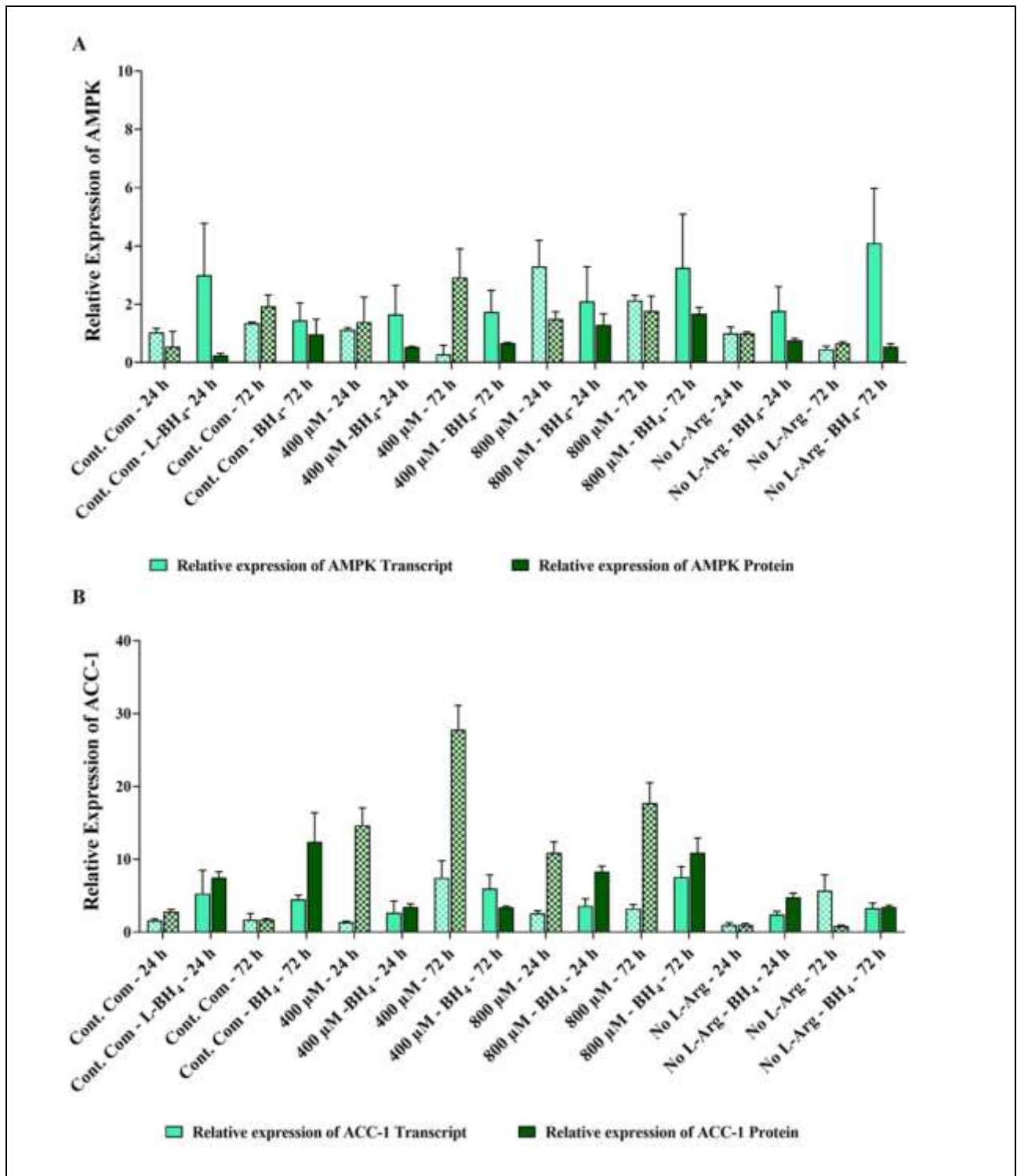


Figure 3.4.2. Comparison of relative AMPK (A) and ACC-1 (B) mRNA and protein expression in BNL CL2 cells cultured in co-factor of iNOS, BH₄ (40 μM) in different exogenous L-arginine amounts for different times.

Relative AMPK transcript expression was maximum when culturing at 0 μM L-arginine and BH₄ for 72 h, whereas the relative AMPK protein expression was maximal at 800 μM L-arginine and BH₄ after 72 h when compared to the control complete DMEM with BH₄ culture time points. Relative ACC-1 transcript expression was maximal at 800 μM L-Arg and BH₄ for 72 h over to the control with BH₄ for 72 h, whereas the relative ACC-1 protein expression was highest in the control with BH₄ at 72 h among the samples.

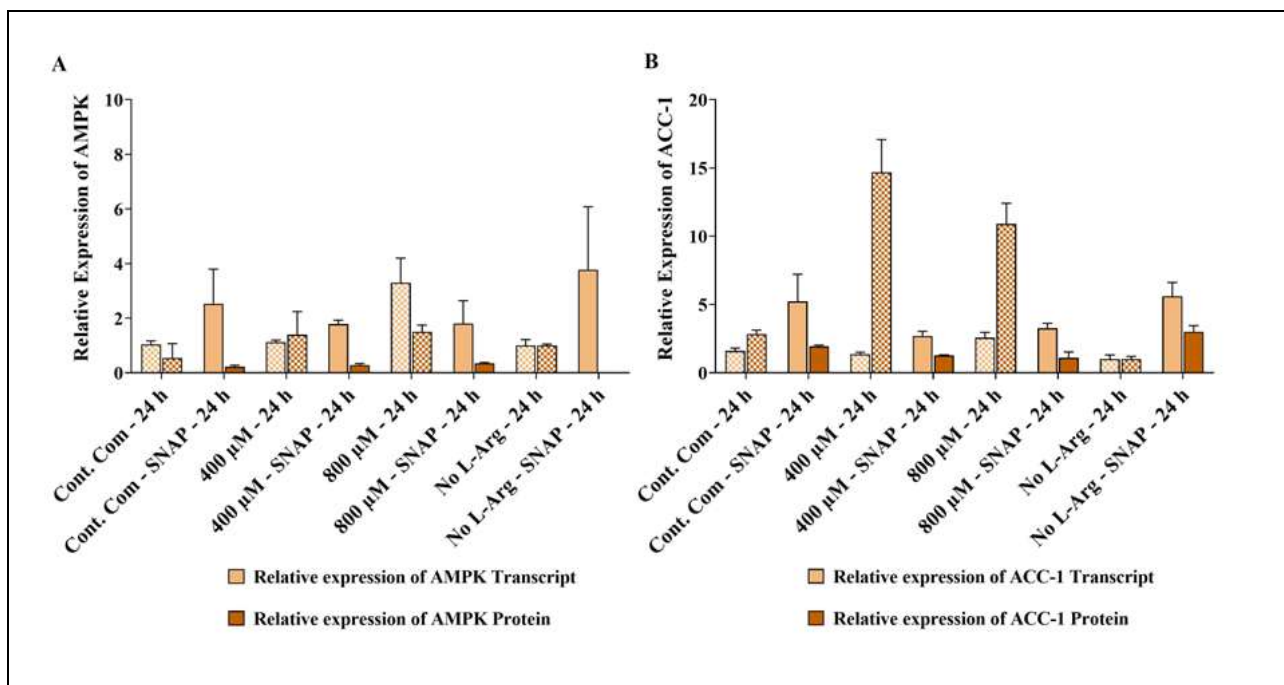


Figure 3.4.3. Comparison of relative AMPK (A) and ACC-1 (B) mRNA and protein expression in BNL CL2 cells cultured in SNAP, as external NO donor (100 μM) in different exogenous L-Arg amounts for different times. Relative AMPK transcript expression was maximum in the control with SNAP at 24 h among all the samples with SNAP, whereas the relative AMPK protein expression was maximal at 800 μM L-arginine in the presence of SNAP after 24 h when compared to the control complete DMEM culture with SNAP for 24 h. Relative ACC-1 transcript and protein expression was high in 0 μM L-Arg with SNAP for 24 h compared to the control with SNAP at 24 h.

3.4.1.1. Nitrite measurements

NO was determined as nitrite amount using a Griess assay. In BNL CL2 cells, the amount of NO_2^- in the samples cultured with iNOS inhibitor, L-NAME, was lowest among all samples. This reduction in NO_2^- negatively effects key transcript expression (AMPK and ACC-1) in BNL CL2 cells cultured in L-Arg and L-NAME (Fig 3.4.1).

The addition of BH_4 co-factor of iNOS increased the production of nitrite in BNL CL2 samples. This demonstrated that the addition of the co-factor BH_4 modulated iNOS enzymatic activity irrespective of the endogenous or exogenous amount of L-Arg within the cell or in the culture media (Fig 3.4.2). Further, when SNAP (NO donor) was added, at 6 h the amount of nitrite in the cell samples was much higher in all samples and conditions (Fig 3.4.3). Interestingly, after 24 h, the amount of nitrite in these cell samples was reduced A previous study undertaken to evaluate the role of NO during prostaglandin E1 protection against D-galactosamine cytotoxicity in cultured hepatocytes using L-NAME (0.5 mM) as inhibitor of iNOS or SNAP (0–750 μM) as NO donor, revealed that different concentrations of NO donor and inhibition of iNOS expression by L-NAME mediated NO-dependent protective effect of pre-administrated prostaglandin E1

against D-galactosamine-induced apoptosis in liver cells (Siendones *et al.*, 2003). Aligned with this study, our results also show that inhibition of iNOS by L-NAME and addition of external NO donor modulated the availability of NO present in the cell samples.

3.4.1.2. HPLC analysis of amino acids

3.4.1.2.1. HPLC analysis for L-NAME addition to BNL CL2 cells

Samples cultured with L-NAME showed much higher amounts of culture supernatant L-Arg compared to samples in its absence and very similar amounts of L-Arg in the samples cultured in excess L-Arg (400 and 800 μ M) with L-NAME at 24 and 72 h (**Fig 3.3.16**). This confirmed that L-NAME competitively inhibits L-arginine metabolism. L-citrulline, produced from L-Arg/iNOS metabolic pathway, was also low in the samples cultured with L-NAME (**Fig 3.3.17**). The amount of L-Cit was increased in L-NAME cultured samples with culture time, possibly due to the decreasing competitive inhibition of L-NAME and its degradation over time. Finally, L-ornithine, produced from L-Arg/arginase, was generally reduced in cultures with L-NAME compared to samples cultured without (**Fig 3.3.18**). It was expected that in liver cells, which are more prone to urea cycle, when NOS inhibitor L-NAME was added the L-Arg/NOS pathway should be inhibited, therefore L-Arg would be fed into the L-Arg/arginase pathway and L-ornithine concentrations increased. But, unexpectedly, the L-ornithine concentration was generally lower in L-NAME treated samples (**Fig 3.3.18**).

3.4.1.2.2. HPLC analysis of BH₄ addition to BNL CL2 cells

When the co-factor of iNOS, BH₄ was added to the cell samples with excess L-Arg, the amount of supernatant L-Arg was low compared to the samples without BH₄ (**Fig 3.3.19**). This suggests that BH₄ addition upregulated iNOS enzyme activity, therefore the available L-Arg was reduced in these samples, this was further confirmed by the nitrite concentration (**Fig 3.3.14**). Further, the production of L-citrulline by the L-Arg/NOS/BH₄ pathway was low in samples cultured in excess L-Arg and BH₄ in comparison to the samples without BH₄ at 24 and 72 h (**Fig 3.3.20**). When the co-factor BH₄ was added, the L-Arg concentration was decreased with culture time, whereas L-Cit and nitrite was increased, demonstrating that the NOS enzymatic reaction mechanism was modulated by addition of co-factor BH₄ (**Fig 3.3.21**). For L-ornithine, the concentration was dependent on the concentration of L-Arg present in the culture media This is explained by the fact that the arginase enzyme, involved in L-ornithine synthesis, has a high Km (around 10 mmol/L, (Mori, 2007)), therefore a large amount of substrate L-Arg is needed in order to saturate the enzyme, which in turn means arginase enzyme has a low affinity for the substrate L-Arg.

3.4.1.2.3. HPLC analysis of SNAP addition to BNL CL2 cells

When external NO donor, SNAP was added cell samples showed a low amount of cell culture supernatant L-Arg compared to the samples cultured without SNAP. Interestingly, the amount of plasma L-Arg decreased across the culture (**Fig 3.3.22**). This might be the result of a limited feedback mechanism of L-Arg/NOS

enzymatic pathway and its products L-Cit and NO. The concentration of L-Cit was low in samples cultured with SNAP (**Fig 3.3.23**) and L-ornithine was also low in the cells grown in the presence of SNAP (**Fig 3.3.24**). Overall, external addition of NO decreased the amount of L-Arg, L-Cit and L-Orn amino acids in the liver cells.

3.4.2. Overall conclusions from the work conducted with BNL CL2 cells

Taken together, when BNL CL2 cells treated with L-NAME, AMPK transcript was decreased but there was increased ACC-1 mRNA expression. Generally, the concentration of L-Arg and the time of culture impacted on transcript levels, while, there was a reduction in the protein levels of AMPK and ACC-1 because of iNOS inhibition.

3.4.3. 3T3 L1 cells grown in different concentrations of exogenous L-arginine with L-NAME (4 mM), BH₄ (40 μM) and SNAP (100 μM) additions

As for the BNL CL2 cells, the impact of the above additions to 3T3 L3 cells was investigated. In 3T3 L1 cells, inhibition of nitric oxide synthase enzyme activity by L-NAME, decreased the L-arginine-stimulated increases of AMPK gene and protein expression in 400 and 800 μM L-Arg at 24 and 72 h. The samples cultured in L-Arg deficient DMEM media and L-NAME showed high relative gene expression for AMPK and ACC-1 after 72 h but decreased protein levels (**Fig 3.4.4**). These results demonstrated that the L-Arg metabolic pathway and the AMPK/ACC-1 cell signalling pathway in the 3T3 L1 cells were regulated by the iNOS inhibitor L-NAME, which overall downregulated the transcript and protein levels of AMPK and ACC-1.

The addition of iNOS co-factor, BH₄, downregulated *AMPK* gene expression in the samples cultured in excess exogenous L-Arg, while upregulated AMPK transcript in the control. However, addition of BH₄ decreased AMPK protein expression in all samples and conditions in comparison to the absence of BH₄, there was no detectable protein in 0 μM L-Arg treated with BH₄ samples (**Fig 3.4.5**). Collectively, these results indicated that transcript and translational levels of AMPK and ACC-1 was modulated by BH₄ in excess exogenous L-Arg grown cells.

It has been reported that both NO donor and the expression of iNOS decreases total protein synthesis non-specifically as a result of the phosphorylation of eIF2 α and inhibition of the 80S initiation complex formation (Kim *et al.*, 1998). Further to this, using NO producers in NT2 neuroepithelial and C2C12 myoblast cells also augment eIF2 α phosphorylation levels (Uma, Yun and Matts, 2001). In this study, external addition of NO via the NO donor, SNAP (100 μM), generally upregulated AMPK transcript amounts. Noticeably, ACC-1 protein expression decreased after 24 h in the presence of SNAP (**Fig 3.4.6**). This likely reflects that the presence of NO either by metabolic pathway of L-Arg or addition of NO by the NO donor to the samples impacts transcriptional and translational expression of AMPK and ACC-1.

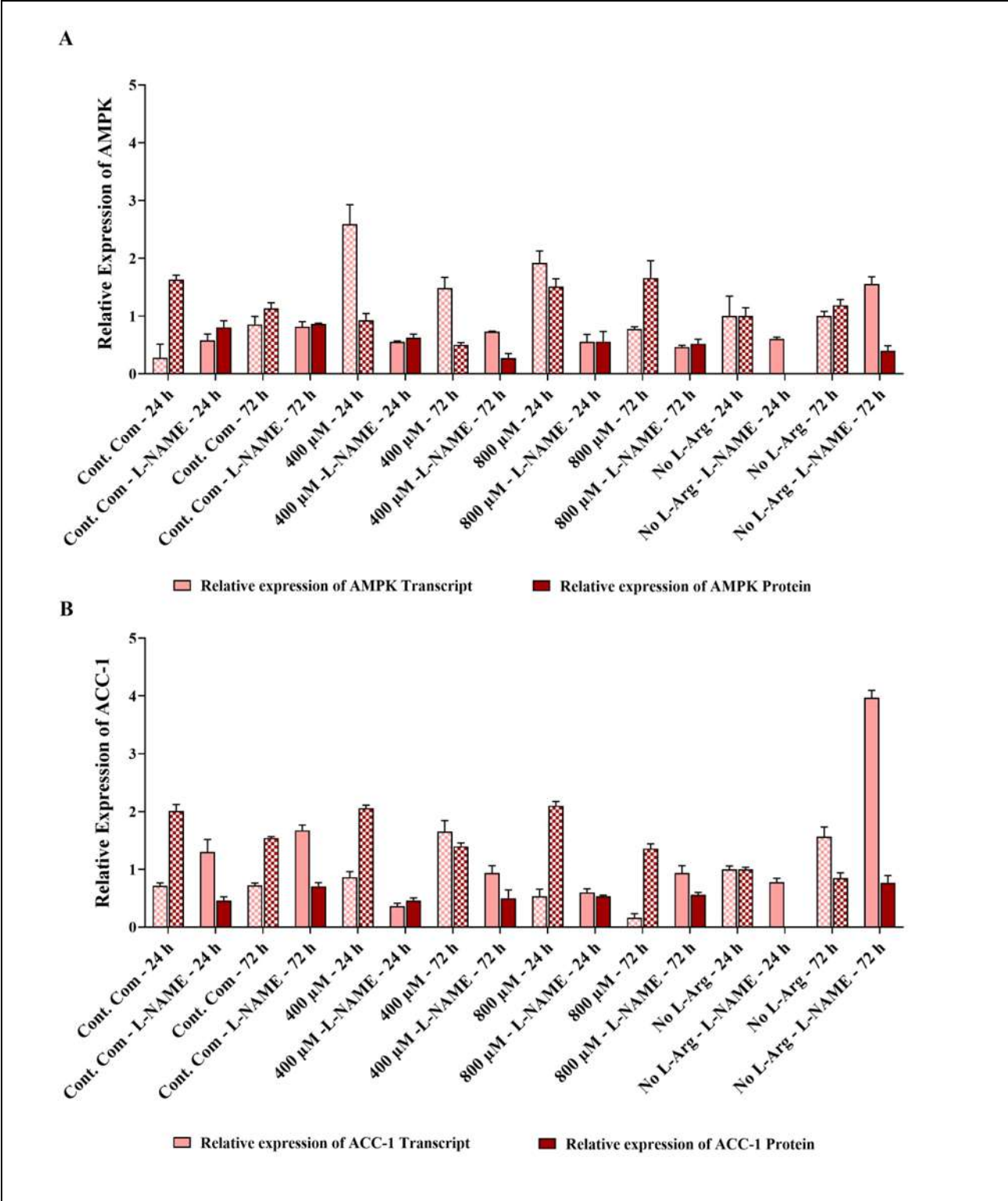


Figure 3.4.4. Comparison of relative AMPK (A) and ACC-1 (B) mRNA and protein expression in 3T3 L1 cells cultured in iNOS inhibitor, L-NAME (4 mM) in different exogenous L-arginine amounts for different times.

Relative AMPK and ACC-1 transcript and ACC-1 protein expressions were maximum when culturing at 0 μM L-arginine with L-NAME for 72 h compared to the control complete DMEM in L-NAME culture time point, whereas the relative AMPK protein expression was maximal at the control with L-NAME for 72 h among all the samples treated with L-NAME.

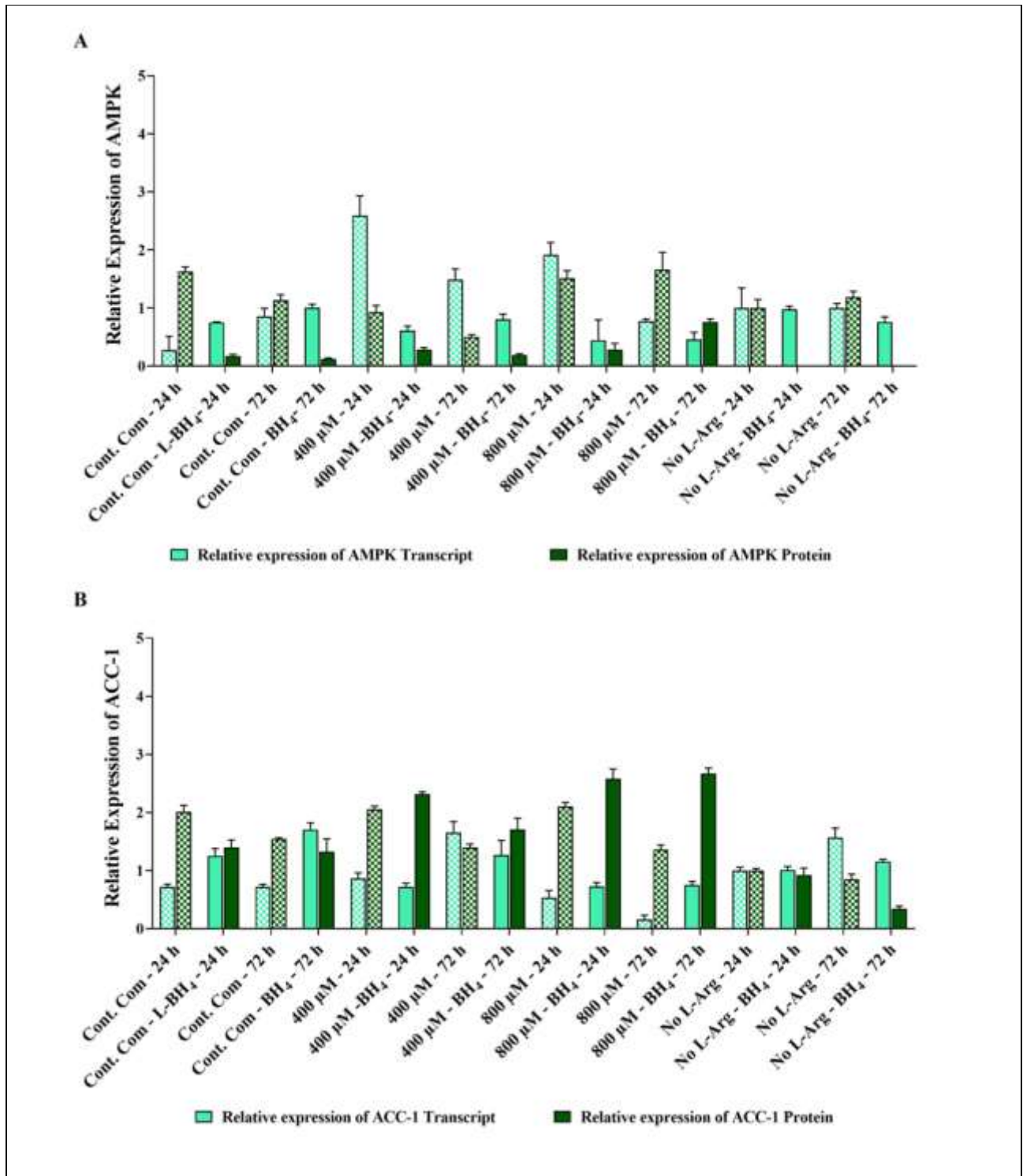


Figure 3.4.5. Comparison of relative AMPK (A) and ACC-1 (B) mRNA and protein expression in 3T3 L1 cells cultured in co-factor of iNOS, BH₄ (40 μM) in different exogenous L-arginine amounts for different times. Relative AMPK and ACC-1 transcript expressions were maximum when culturing at 0 μM L-Arg with BH₄ and the control for 72 h with BH₄, whereas the relative AMPK protein expression was maximal at 800 μM L-arginine treated with BH₄ for 72 h and relative ACC-1 protein was maximal at 0 μM L-Arg with BH₄ after 72 h, when compared to the control complete DMEM culture with BH₄ and the time points.

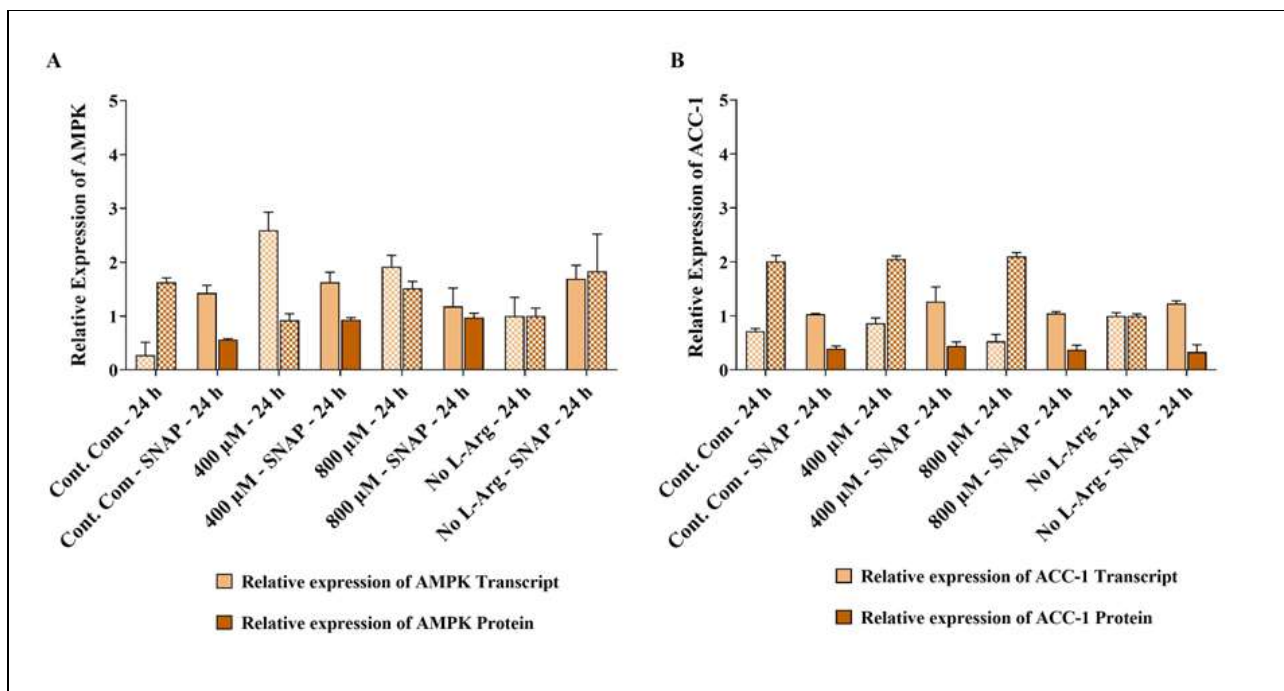


Figure 3.4.6. Comparison of relative AMPK (A) and ACC-1 (B) mRNA and protein expression in 3T3 L1 cells cultured in SNAP, as external NO donor (100 μM) in different exogenous L-arginine amounts for different times. Relative AMPK and ACC-1 transcript expressions were maximum when culturing at 400 μM L-arginine and SNAP for 6 h, whereas the relative AMPK protein expression was maximal at 0 μM L-Arg and SNAP after 6 h when compared to the control complete DMEM culture with SNAP time points. Relative ACC-1 protein expression was maximum at the control with SNAP among all the samples treated with SNAP.

3.4.3.1. Nitrite measurements

In 3T3 L1 cells, like BNL CL2 cells, the amount of NO_2^- in L-NAME added cultures was decreased (**Fig 3.3.37**). This reduction in NO_2^- appeared to negatively impact transcript and protein expression of AMPK and ACC-1 (**Fig 3.4.4**). The addition of BH_4 increased production of nitrite in all samples and conditions in comparison to the absence (**Fig 3.3.38**). This again demonstrates the changes in AMPK and ACC-1 at the transcript and protein levels in the 3T3 L1 cell samples cultured with BH_4 at excess exogenous L-Arg concentrations (**Fig 3.4.5**). The amount of nitrite in the cell culture supernatant samples cultured in SNAP was elevated in all samples (**Fig 3.3.39**). NO donor enhanced nitrite concentrations irrespective of excess L-Arg presence or absence. However, addition of SNAP increased nitrite and impacted the phenotype of the cells for a short period of time, potentially explaining why the samples with high transcript expression did not show high expression of their respective proteins in SNAP treated samples (**Fig 3.4.6**).

3.4.3.2. HPLC analysis of amino acids

3.4.3.2.1. HPLC analysis upon L-NAME addition to 3T3 L1 cells

Culture supernatant concentrations of L-Arg in the samples cultured in L-NAME were generally decreased in comparison to the samples cultured without L-NAME, (**Fig 3.3.40**). It was expected that the availability of L-Arg should increase when the samples were cultured with the iNOS inhibitor, L-NAME, however unexpectedly the L-Arg concentration was decreased in 3T3 L1 cells and there was no detectable amount of L-Cit in the samples cultured with L-NAME (**Fig 3.3.41**). This suggests that in the presence of the iNOS inhibitor, L-NAME the 3T3 L1 cells did not synthesis L-Cit from L-Arg/NOS/NO and L-Cit pathway.

For L-ornithine there was more or less the same amount present in 400 and 800 μ M L-Arg samples after 24 and 72 h (**Fig 3.3.42**). It was expected here as L-NAME inhibited the active binding of L-Arg to the iNOS enzyme, the samples should have L-Arg in high amount that could be used as a substrate for L-Arg/arginase pathway, therefore, the production of L-Orn would increase.

3.4.3.2.2. HPLC analysis upon BH₄ addition to 3T3 L1 cells

When BH₄ was added to the 3T3 L1 cells, the concentration of L-Arg decreased after 24 h but increased after 72 h compared to the samples grown without BH₄. There was in most cases no detectable amount of L-citrulline in the samples cultured in BH₄ (**Fig 3.3.44**) and very similar amounts of L-ornithine (**Fig 3.3.45**).

3.4.3.2.3. HPLC analysis upon SNAP addition to 3T3 L1 cells

When SNAP was added to the cultures, more or less the same amount of L-Arg was observed across the culture in the samples cultured in 400 μ M L-Arg and SNAP while samples grown in higher concentrations of L-Arg, 800 μ M L-Arg with SNAP had decreased L-Arg (**Fig 3.3.46**). There was no detectable amount of plasma L-Cit in all samples and conditions when treated with SNAP (**Fig 3.3.47**), and overall, there was a reduction in the serum L-Orn amount when the cells were cultured in SNAP (**Fig 3.3.48**).

3.4.4. Overall conclusions from the work conducted with 3T3 L1 cells in this chapter

As in BNL CL2 cells, transcript and protein levels of AMPK and ACC-1 were regulated by addition of L-iNOS inhibitor; L-NAME (4 mM), iNOS co-factor; BH₄ (40 μ M) and an external NO donor; SNAP (100 μ M), however the impact of these targets was related to the concentration of L-Arg added to the 3T3 L1 cells and the culture time point of analysis.

Chapter-4 Generation of 3T3 L1 cells stably over-expressing iNOS and the impact upon cell signalling in the presence or absence of elevated exogenous L-arginine

4.1. Introduction

The work in this chapter was conducted to investigate how stably over-expressed iNOS impacts the L-arginine/iNOS/NO pathway and subsequent signalling pathways. The cloning of PCR amplified fragments into a plasmid vector is a routine procedure in recombinant DNA cloning. pBS-iNOS was used as the positive control plasmid for amplification of iNOS, which contained the intact coding sequence as well as the untranslated sequences at the 5' and 3' ends of the transcript. Expression of exogenous iNOS protein was then undertaken.

4.2. Materials and Methods

4.2.1. Establishment of iNOS constructs for iNOS transcript analysis

4.2.1.1. Source of plasmid DNAs and amplification with iNOS primers

The positive control plasmid pBS-iNOS containing the *iNOS* gene was sourced from Addgene (Cat. No: plasmid 19295). pBS-iNOS is 7076 bp in size (bacterial expression vector backbone size is 3000 bp and the iNOS insert size 4110 bp) (**Fig 4.2.1**). The pBS-iNOS plasmid was grown in 10 mL of Lysogeny broth (LB broth) (described in **Table 4.2.1**) with bacterial resistance ampicillin (100 µg/mL). After overnight growth at 37°C with shaking at 200 rpm, plasmid DNA was extracted from 5 mL of the overnight culture and purified using the commercial QIAprep Spin Miniprep Kit (Invitrogen, Cat. No:27104) and the DNA quantified on a Thermo Nano Drop ND 1000 Spectrophotometer (Thermo Scientific, USA) by measuring absorbance at 260 and 280 nm. The iNOS gene was then cloned into the pcDNATM3.1/Hygro (+) (Thermo Fisher Scientific, Cat.No: V87020) a mammalian expression vector **Fig 4.2.2**.

Table 4.2.1. Components for preparing Lysogeny broth

Lysogeny broth components	For 250 mL broth volume (g)
Bactopeptone	2.5
Sodium chloride	2.5
Yeast extract	1.3

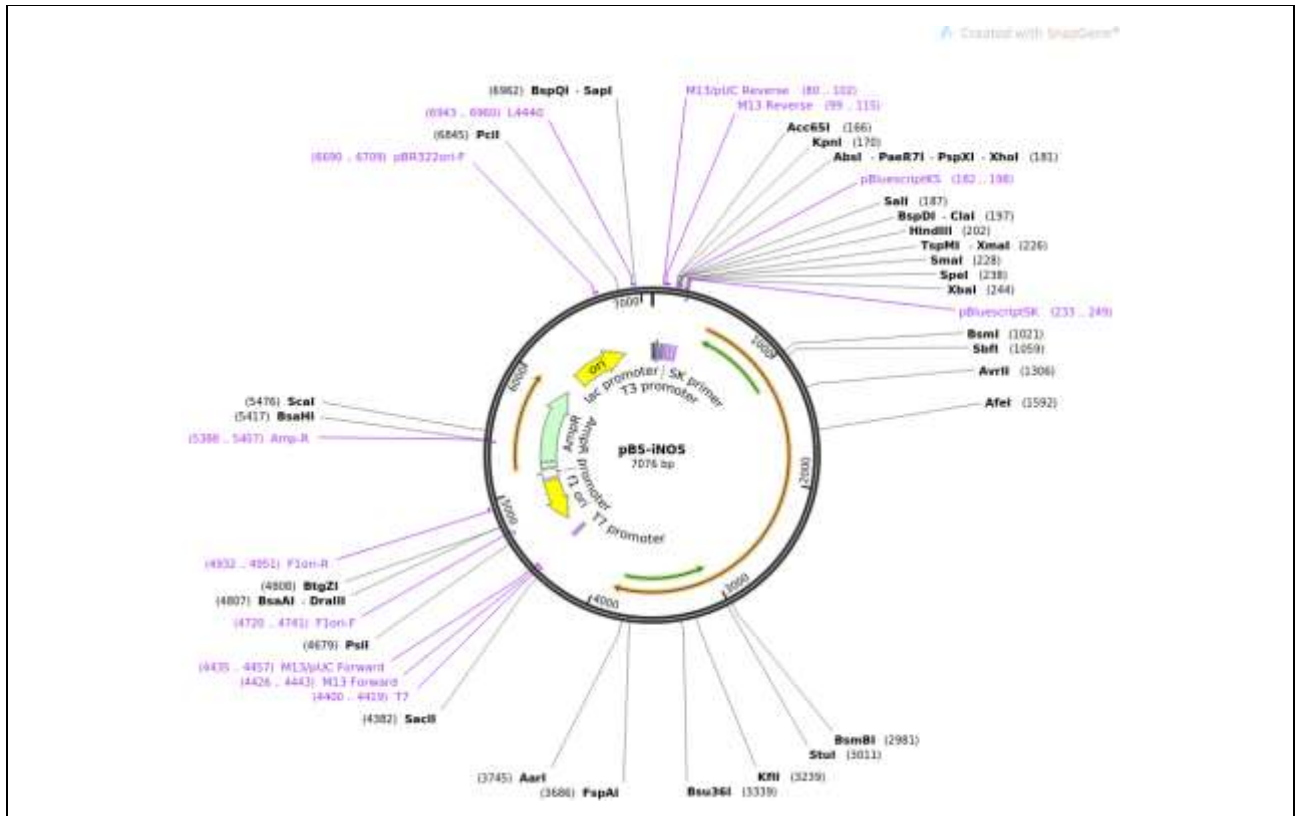


Figure 4.2.1. The positive control plasmid pBS-iNOS sourced from Addgene.

pBS-iNOS consists of 7076 bp (bacterial expression vector backbone size is 3000 bp and the *iNOS* gene insert size is 4110 bp) with the plasmid elements: an origin of replication, antibiotic resistance gene; to ensure the retention of plasmid DNA in bacterial populations, multiple cloning sites (MCS); consisting of restriction enzymes sites to facilitate cloning, promoter region; to drive the transcription of the insert, selectable marker; to select the bacterial populations that have taken up the plasmid for expressing the desired insert and the primer binding site; used as an initiation depot for PCR amplification thereby sequencing primers such as T7 promoter and bovine growth hormone terminator (BGHR) can be used as forward and reverse primers, respectively to verify the sequence of interest.

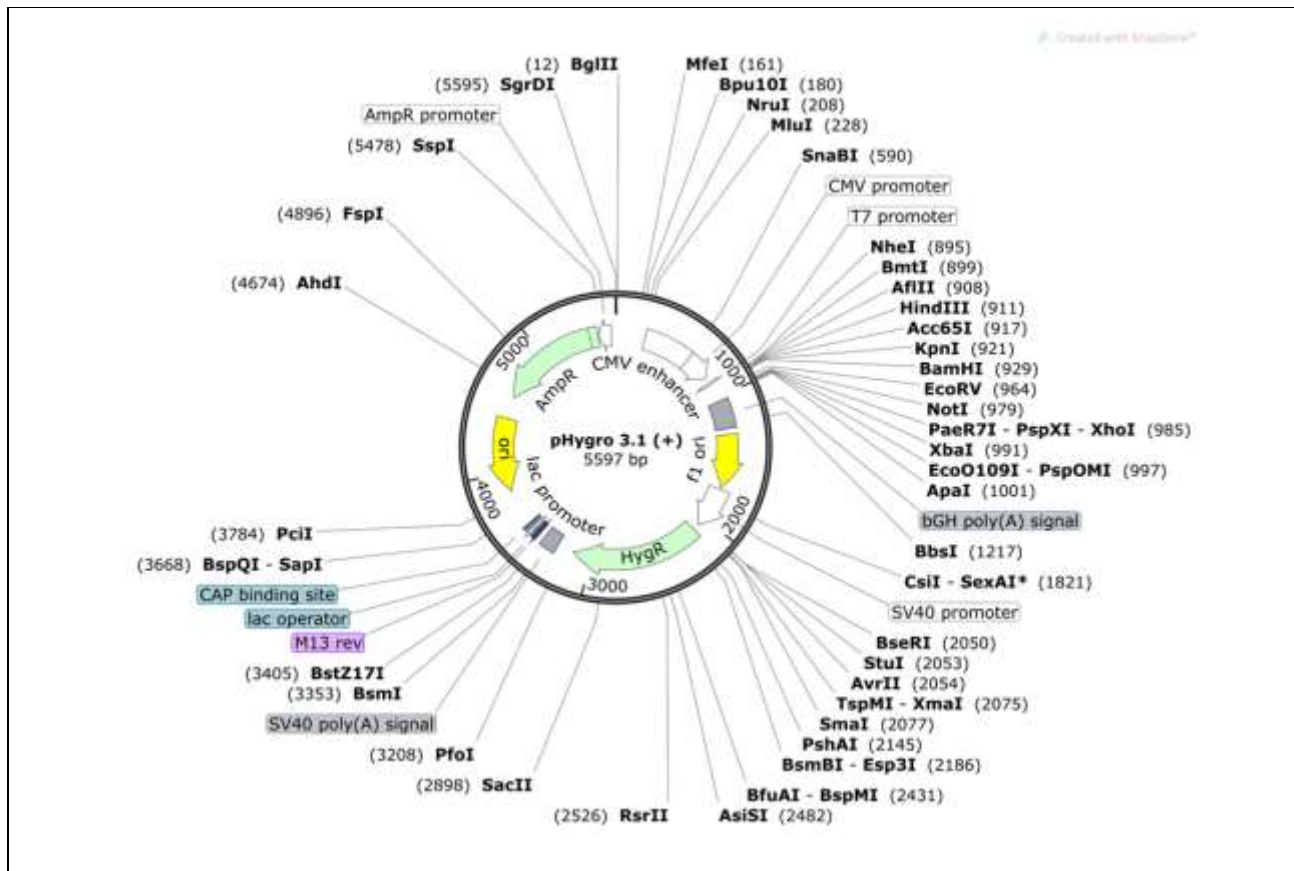


Figure 4.2.2. The mammalian expression vector pcDNA™3.1/Hygro(+).

The plasmid consists of a 5597 bp sequence designed with the plasmid elements: an origin of replication (ori), antibiotic resistance gene, multiple cloning site (MCS); a forward-orientation multiple cloning site, promoter region (CMV promoter), selectable marker (hygromycin) and the primer binding site. It is used for high-level, constitutive expression system in a variety of mammalian cell lines.

4.2.1.2. *iNOS* cloning by PCR

4.2.1.2.1. Designing primers for PCR based cloning

Two sets of primers were designed to amplify two regions of the *iNOS* transcript to ensure that the signal peptide and full open reading frame (ORF) were amplified. One set of primers covered the region that included the untranslated region (UTR) of the *iNOS* transcript and another set cover the region of the ORF of the *iNOS* transcript only (from start codon to stop codon). Both designed PCR primers contained sequence for the restriction site **AAGCTT** and **TCTAGA** for respective restriction enzymes HindIII and XbaI.

Primers for *iNOS*-UTR amplification:

iNOS-UTR-FP-HindIII: 5' **TATAAGCTT**GAGACTCTGGCCCCACG 3' (Tm 61.8°C)

iNOS-UTR-RP-XbaI: 5' CATT TTTATTTTAATCAAAAAAAAAAAGCGGCCG**TCTAGATAT** 3' (Tm 60.3°C)

Primers for *iNOS*-CDS amplification:

iNOS-CDS-ATG-FP-HindIII: 5' TATAAGCTTGACATGGCTTGCCCCTGGAAGTTTC 3' (T_m 64.2°C)

iNOS-CDS-TGA-RP-XbaI: 5' GCCCAAAGCCACGAGGCTCTGATCTAGATAT 3' (T_m 63.9 °C)

4.2.1.2.2. Amplification of target gene sequences

The PCR cloning used overhang regions for the restriction sides of HindIII and XbaI generated with primers as described in section 4.2.1.2.1. Phusion high fidelity DNA polymerase (Thermo scientific, Cat. No: F-580S) was used to amplify specific sequences using the primers designed for amplification of the target *iNOS*. Reaction mixes for PCR of the *iNOS* gene were prepared following the protocol provided with the polymerase and as detailed in Table 4.2.2. Thermal cycling of Phusion PCR conditions for amplification of the target *iNOS* is described below. An agarose gel was performed (section 4.2.1.2.3) to check the amplified products of Phusion high fidelity DNA polymerase PCR reactions.

Phusion PCR conditions:

Denaturation: 98°C, 30 sec.

30 cycles:

Denaturation: 98°C, 10 sec

Annealing: 60°C, 30 sec

Elongation: 72°C, 20 sec/1 kb of DNA

Final elongation: 72°C hold, 10 mins

Hold 20°C

Table 4.2.2. The reaction mixtures components for Phusion high fidelity DNA polymerase PCR

Reaction mixtures components	Volume (µL)
Plasmid DNA diluted to 10 ng/µL	1
5x Phusion HF buffer	20
dNTPs (10 mM)	2
Forward and reverse primers oligos (200 nM)	4
Phusion DNA polymerase	1
Nuclease free water	72
Total PCR reaction volume	100

4.2.1.2.3. Visualising and analysing DNA polymerase PCR product by gel electrophoresis

Agarose gel containing 2% (w/v) agarose was used to resolve the DNA bands of amplified products of Phusion high fidelity DNA polymerase PCR. Agarose (1 g, Melford, Cat. No: A 20090) was dissolved in 50 mL of 1 x Tris-acetate-EDTA (TAE) electrophoresis buffer (50 x TAE buffer; 2 M Tris, 50 mM EDTA, 20 mM glacial acetic acid) by heating in a microwave to yield a clear solution. Once the mixture was cooled down to 'hand-

hot', 3 μ L of DNA-intercalating dye SyBR Green (Invitrogen, Cat. No: S33102) was added to the 50 mL of agarose-TAE solution and casted into an electrophoresis tank. Once the agarose/TAE solidified, the gel tank was filled with 1 x TBE electrophoresis running buffer to a level of around 2 – 3 mm above the gel. Samples (total volume; 8 μ L) were suspended in 6 x blue/orange loading dye (Promega, Cat. No: G210A) to obtain the 1:6 ratios between the sample and the loading dye. DNA marker (100 bp, Promega, Cat. No: G210A) was loaded alongside the samples to determine the sizes of the DNA products. Agarose gel tank was set up and performed electrophoresis at 100 V for 30 - 45 min until the marker dye was around 1 cm from the bottom of the gel. The DNA fragments were visualised under UV light using a Syngene G: Box chemi XT4 (UK).

4.2.1.2.4. Clean-up of PCR products

The Wizard® SV gel and PCR clean-up system (Promega, Cat. No: A9281) was used to clean up the Phusion high fidelity DNA polymerase PCR amplified products (50 μ L) by removing excess dNTPs and primers. Binding of plasmid DNA, washing and elution steps were followed as described in manufacturer protocol. During the elution step, 30 μ L nuclease free water was added to elute the plasmid DNA.

4.2.1.3. Manipulation of plasmid DNA by restriction enzyme cloning method

4.2.1.3.1. Restriction enzyme digestion of PCR products and plasmid DNA

The clean Phusion PCR amplified products and the vector pcDNA3.1/Hygro were digested with the two FastDigest restriction enzymes; HindIII (ThermoFisher, Cat. No: ER0501) and XbaI (ThermoFisher, Cat. No: ER0681) (**Fig 4.2.3**) with universal green buffer that allows any combination of restriction enzymes to work simultaneously in one reaction tube at 37°C for 30 min. Three digestion reaction mixes with plasmid DNAs of iNOS-UTR, iNOS-CDS and vector 3.1/Hygro (approximately 500 ng of vector) were prepared in a total digestion volume of 20 μ L in 3 Eppendorf tubes as described in **Table 4.2.3**. The reaction mixes were mixed gently, centrifuged and incubated at 37°C in a water bath for either 15 min for digestion of PCR inserts or 60 min for the vector.

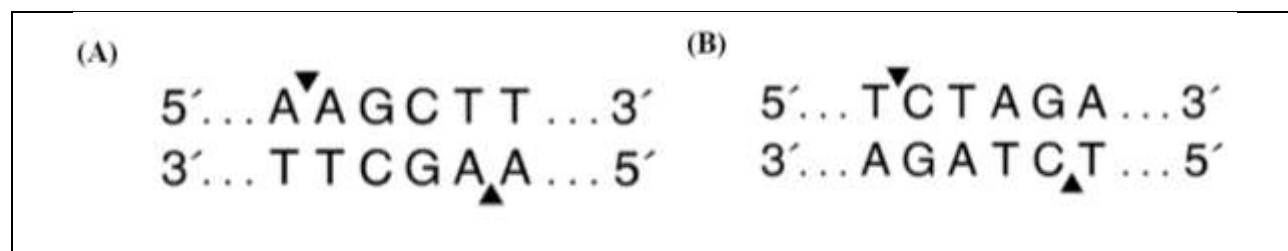


Figure 4.2.3. The FastDigest enzyme cleavage sites.

The arrow indicates where in the restriction site sequence the enzyme cuts. (A) shows the HindIII restriction site A/AGCTT and (B) shows the XbaI restriction site T/CTAGA.

Table 4.2.3. The reaction mix components for double digest of plasmid or PCR product

Reaction mixtures components for double digest	Volume (µL)
Plasmid DNA either CDS or UTR or vector 3.1/Hygro	8
10 x FastDigest Green buffer	2
FastDigest HindIII	1
FastDigest XbaI	1
Nuclease free water	8
Total digestion volume	20

4.2.1.3.2. Agarose gel electrophoresis of restriction enzyme digested product

Agarose/TAE gel (1% w/v) was used to resolve the DNA bands of digested products as detailed in section 4.2.1.2.3. However, to obtain pure digested products by gel extraction, BioRad-certified molecular biology agarose (BioRad, Cat. No: 1613101) was used. Once the agarose gel was run, DNA bands were visualised under a UV light using a Syngene G: Box chemi XT4 (UK) and then the DNA bands were excised and cut into small pieces for DNA purification.

4.2.1.3.3. DNA purification, extraction and quantification

The DNA bands were cut from the agarose gel and then subjected to a gel clean-up and extraction of DNA using the commercially available Wizard® SV gel and PCR clean-up system (Promega, Cat. No: A9281) to recover the DNA for further use. Quantification of DNA was carried out using a Thermo Nano Drop ND 1000 Spectrophotometer (Thermo Scientific, USA) by measuring absorbance at 260 and 280 nm. Additionally, an agarose gel (1% w/v) was performed as described in section 4.2.1.2.3 to confirm the purity and size of the extracted DNA products before and after cleaning of digested products.

4.2.1.3.4. Ligation of DNA

The inserts of either iNOS-UTR or iNOS-CDS with compatible and cohesive-ended configuration ends for XbaI and HindIII were inserted into the 3.1/Hygro vector with compatible ends for HindIII and XbaI by ligation to generate either pcDNA 3.1/Hygro iNOS-CDS (iNOS-CDS) or pcDNA 3.1/Hygro iNOS-UTR (iNOS-UTR) construct. The quantity of vector and the insert was calculated using a ratio of 3:1 (vector: insert = 3:1) using a following equation.

$$\frac{ng\ of\ vector\ X\ kb\ size\ of\ insert}{Kb\ size\ of\ Vector} \times Molar\ ratio\ of\ \frac{Insert}{Vector} = ng\ of\ Insert$$

Preparation of the ligation reaction mix was undertaken using a commercially available T4 DNA ligase (Promega, Cat. No: M1801) following the protocol provided and detailed in **Table 4.2.4**. Ligation was

undertaken at room temperature for 1 h. The ligated products were then transformed into competent *E. coli* cell by the heat shock method.

Table 4.2.4. The reaction mix components for ligation of inserts and vector

Reaction mixtures components for double digest	Volume (µL)
Plasmid DNA of either iNOS-CDS or iNOS-UTR with compatible ends for HindIII and XbaI	3
Plasmid vector 3.1/Hygro DNA with compatible ends for HindIII and XbaI	1
10 x ligase buffer	1
Ligase	1
Nuclease free water	4
Total ligation volume	10

4.2.1.4. Transformation of plasmid DNA into DH5α *Escherichia coli* competent cells

4.2.1.4.1. Generation of DH5α *Escherichia coli* calcium competent cells

To prepare competent DH5α *Escherichia coli* cells, cells were initially streaked onto an LB agar plate (LB broth detailed in **Table 4.2.1** was added with 3.8 g of agar to prepare LB agar plate) and cultured overnight at 37°C. A single colony from the plate was then picked and inoculated into 5 mL of LB starter culture in a 50 mL falcon tube and incubated overnight at 37°C with orbital shaking at 200 rpm. From this overnight starter culture, 1 mL was used to inoculate a 500 mL flask containing 50 mL of liquid LB broth and the flask incubated at 37°C with shaking at 200 rpm and the growth regularly monitored using a spectrophotometer at OD600 nm until an OD600 of between 0.4-0.6 absorbance was obtained. The flask was then immediately chilled on ice and transferred to two chilled 50 mL falcon tubes. The cells were centrifuged at 3500 rpm for 15 min at 4°C and the supernatant discarded. The DH5α cells were then resuspended in 10 mL of filter sterilised 100 mM CaCl₂ and incubated on ice for 30 min. The cells were then pelleted again at 3500 rpm for 15 min at 4°C and then gently resuspended in 2 mL of ice-cold 100 mM CaCl₂ before being incubated on ice for a further 30 min followed by the addition of 1 mL of sterile 80% (v/v) glycerol. By gently pipetting, 100 µl aliquots of the cell suspension were then dispensed into sterile chilled cryo-vials and flash frozen on dry ice. Aliquots of the DH5α *Escherichia coli* competent cells were then stored at -80°C until required.

4.2.1.4.2. Transformation of plasmid DNA into DH5α *Escherichia coli* competent cells

The uptake of plasmid DNA by competent cells was stimulated using a heat shock method. LB agar plates were prepared containing the selection marker ampicillin at 100 mg/mL. Plates were pre-warmed in an incubator before transformation. For transformation, 10 µL of ligated mixes of each iNOS-UTR and iNOS-CDS plasmid and the control plasmid 3.1/Hygro was added to 50 µL of DH5α *Escherichia coli* calcium competent cells and then incubated for 30 min on ice. A heat shock to the cells was delivered at 42°C for 30 sec and the cells were then allowed to recover on ice for 3 min. After heat shocking, 450 µL of LB broth was added to the cells and then incubated with shaking at 200 rpm for 45 min at 37°C. After incubation, 100 µL of

transformation was plated up onto pre-warmed LB-agar-ampicillin plates and incubated in a static incubator at 37°C overnight.

4.2.1.4.3. Screening of transformants

4.2.1.4.3.1. PCR colony screening

Five single white colonies from each plate of iNOS-UTR and iNOS-CDS transformations and a white colony from the control 3.1/Hygro were chosen from the overnight transformation LB-agar-ampicillin plates described in section 4.2.1.4.2. Vector-specific primers were used to screen for the presence of the expected recombinant plasmids; T7 promoter sequencing primer (forward primer) and the bovine growth hormone terminator reverse sequencing primer (BGHR, reverse primer, **Table 4.2.5**). To amplify the recombinant plasmid, Go-Taq DNA polymerase PCR amplification was undertaken using the commercially available Go-Taq DNA polymerase kit (Promega, Cat. No: M3001). Master mixes for Go-Taq DNA polymerase PCR amplification were then prepared following the protocol provided by the manufacturer in a final volume of 15 µL as described in **Table 4.2.6**. 5 µL of transformed bacterial colony solution was prepared by touching the white colony on the agar plate using a pipette tip point and dipping it into a 5 µL nuclease free water and then this colony solution was added to the 15 µL of master mix of Go-Taq DNA polymerase to a total final PCR reaction volume 20 µL. A thermal cycler engine for PCR amplification (Eppendorf, Germany) was used for amplification using the thermal cycling parameters detailed below. Subsequently, 0.3% (w/v) agarose gel analysis was performed as described in section 4.2.1.2.3 by loading 8 µL of the PCR products to check the presence of the expected amplified products.

Go-Taq polymerase thermal cycling conditions for Go-Taq DNA polymerase- mediated PCR amplification:

Initial denaturation: 94°C, 5 min.

25 cycles:

Denaturation: 94°C for 30 sec

Annealing: 50°C for 30 sec

Extension: 72°C, 4 min and 10 sec (1 min/1 kb)

Final extension: 72°C 7 min

Hold 20°C

Table 4.2.5. The sequencing primers used in PCR colony screening

Sequencing Primers	Sequence
T7 promoter, forward primer	TAATACGACTCACTATAGGG
BGH reverse, reverse primer	TAGAAGGCACAGTCGAGG

Table 4.2.6. The reaction mixtures components for Go-Taq DNA polymerase PCR

Reaction mixtures components	Volume (μL)
x 5 GoTaq buffer	4
MgCl ₂ (25 mM)	1.6
dNTPs (10 mM)	0.4
Forward T7 primer oligos (100 nM)	0.8
Reverse BGHR primers oligos (100 nM)	0.8
GoTaq DNA polymerase	0.1
Nuclease free water	7.3
Total PCR reaction volume	15

4.2.1.4.3.2. Plasmid miniprep and restriction digestion

Five well-isolated single white colonies from each plate of iNOS-UTR and iNOS-CDS transformations and a white colony from the control 3.1/Hygro were picked from overnight LB-agar-ampicillin transformation plates, the same colonies that were used for PCR colony screening. While preparing 5 μL of transformed bacterial colony solution of each for PCR colony screening, the pipette tip point was used to streak on a labelled pre-warmed LB-agar-ampicillin plate and incubated in a static incubator at 37°C overnight. The following day, each bacterial colony was used to inoculate a 50 mL falcon tube containing LB broth (5 mL) and ampicillin at 100 $\mu\text{g}/\text{mL}$ and then incubated with shaking a 200 rpm at 37°C overnight. Each overnight culture (5 mL) was used to extract the plasmid DNA using a QIAprep Spin Miniprep Kit (Invitrogen, Cat. No:27104) and then plasmid DNA was quantified using a Thermo Nano Drop ND 1000 Spectrophotometer (Thermo Scientific, USA) by measuring the absorbance at 260 and 280 nm. Once the DNA was purified, the plasmid was screened by restriction digestion. To confirm that the expected inserts were present, the plasmid DNA (500 ng) was digested with ApaI FastDigest enzyme (Thermo Fisher, Cat. No: FD1414). The digestion was undertaken as detailed in section 4.2.1.3.1 and an agarose gel (1% w/v) was used to resolve the DNA bands of digested products as described in section 4.2.1.3.2.

4.2.1.5. Plasmid DNA amplification

Once the expected constructs were confirmed, plasmid DNA was extracted and recovered from selected colonies for each of iNOS-UTR, iNOS-CDS and the control 3.1/Hygro using the commercially available PureLink™ HiPure plasmid filter maxiprep kits (ThermoFisher Scientific, Cat. No: K210016) following the protocols provided and the concentration of the plasmid DNA determined on a nanodrop instrument.

4.2.1.6. DNA sequencing

For sequencing, pre-defined tubes containing sequencing primers; T7 and BGHR and the template plasmid DNA were sequenced using a sequencing service provided by Genewiz, UK Ltd. The plasmid DNA samples were prepared as 20 μL aliquots at 200 ng/ μL .

4.2.1.7. Transient transfection and transient iNOS transcript mRNA analysis

4.2.1.7.1. Transient transfection experiments

BNL CL2 and 3T3 L1 cells were revived and were routinely passaged every 3-4 days. During passaging cells were maintained in vented T25 tissue culture flasks (Sarstedt, Germany) in complete growth medium (10 mL) and incubated in a static incubator (Thermo Forma, Thermo Fisher) at 37°C, 5% CO₂. For experiments, cells were used 2 or 3 days after passage when they were in growth phase. Culture viability (%) and the viable number of cells/mL ($\times 10^6$) were determined using a Vi-CELL analyzer (Beckman Coulter, Life sciences, USA) as detailed in section 2.2.1.3. Cells were seeded into 24-well tissue culture plates (Greiner Bio-One) at 2×10^5 viable cells/well in 2 mL of complete DMEM media. The cells were then incubated in a static incubator (Thermo Forma, Thermo Fisher) for 24 h at 37°C, 5% CO₂. After 24 h, the media was removed and then the cells washed with pre-warmed PBS (2 mL) and replaced with Opti-MEM™, reduced serum medium (1 mL, ThermoFisher, Cat. No: 11058021) and incubated for 1 h at 37°C, 5% CO₂. Transfection reagent; Lipofectamine 2000 (ThermoFisher, Cat. No: 11668027) was used to transfect both BNL CL2 and 3T3 L1 cells. First, 5 µg of plasmid DNA was suspended in 100 µL Opti-MEM™ medium in a 15 mL falcon tube and gently mixed, whilst in a separate 15 mL falcon tube 5 µL of lipofectamine was added to 100 µL of Opti-MEM. Before the contents of each tube were mixed together, they were incubated for 5 min at room temperature and then both tubes mixed gently and incubated for 20 min at room temperature. Finally, 200 µL of the mix was added drop wise to a well and the cells incubated at 37°C, 5% CO₂. The cell culture media was replaced with complete DMEM (1 mL) at 6 h post transfection and cells harvested at 24 h post-transfection.

4.2.1.7.2. RNA extraction and quantitative real-time PCR (qRT-PCR) for transient iNOS transcript mRNA analysis

To analysis the transient expression of exogenous iNOS and endogenous β -actin transcripts RNA extraction from the cells was undertaken as described in section 2.2.2. Extracted total RNA was treated for contaminating DNAase using RQ1 RNase-Free DNase kit (Promega). Diluted RNA (90.91 ng/µL) was then stored at -80°C until required for analysis.

4.2.1.7.3. qRT-PCR analysis methods

Primers (forward and reverse) designed for qRT-PCR analysis of iNOS are detailed in **Table 4.2.7**. qRT-PCR analysis to determine the relative amounts of iNOS mRNA between samples was undertaken using a housekeeping gene; β -actin (primers detailed in **Table 2.3.1**). Primers were diluted to obtain 200 nM stock solutions of each. qRT-PCR amplification of target sequences was undertaken using the commercially available iTaq™ Universal SYBR Green One-Step Kit (Bio-Rad, Cat. No: 1725151). The concentration of RNA of samples was adjusted to 90.91 ng/µL for all reactions. Reaction mixtures for qRT-PCR were then prepared following the protocol provided by the manufacturer for a final reaction volume of 12.5 µL (**Table**

4.2.8). A DNA engine opticon 2 system for real-time PCR detection thermocycler (Bio-Rad) was used for amplification and for producing melt curve profiles of the amplicons using the following parameters. Agarose gel (2%, w/v) analysis was performed to confirm the amplified qRT-PCR products of transient iNOS and housekeeping- β -actin.

qRT-PCR conditions (one-step):

Initial denaturation: 95°C, 1 min.

39 cycles:

Denaturation: 95°C for 10 sec

Annealing and extension: 60°C for 30 sec

Melting profile from 65°C to 95°C read every 0.5°C, hold 2 sec

Table 4.2.7. Primers used for real-time qPCR analysis of the target iNOS gene listed and size of amplicon expected

Target Gene	<i>iNOS</i>
NCBI ID	NM_001313922.1
Forward primer oligo	GCCAACATGCTACTGGAGGT
Reverse primer oligo	TGGAGCACAGCCACATTGAT
Amplicon size (bp)	215

Table 4.2.8. The reaction mixtures components for iTaq™ Universal SYBR Green One-Step qRT-PCR

Reaction mixtures components	Volume (μ L)
RNA diluted to 90.91 ng/ μ L	1
iTaq universal SYBR green reaction mix (2x)	6.3
Forward and reverse primers (200 nM)	2.5
iScript reverse transcriptase	0.15
Nuclease free water	16.6
Total reaction mix volume	12.5

4.2.1.8. Construction of stable iNOS cell pools

4.2.1.8.1. Linearization of Plasmid DNA

Linearisation of the plasmid was undertaken before transfection. The backbone of the plasmid; 3.1/Hygro was cut using PvuI (New England Lab, Cat. No: R0150L) and x 1 NEB buffer 3.1 (New England Lab, Cat. No: B7203S). 50 μ g of each plasmid DNA was digested using 2.5 μ L of PvuI digestive enzyme and x 1 NEB buffer 3.1 in a total reaction volume of 50 μ L at 37°C overnight.

4.2.1.8.2. Plasmid DNA precipitation

50 μ L of water was added to the 50 μ L of digest volume to a total volume 100 μ L and then 10 μ L sodium acetate (3 M, pH 5.2) was added. 250 μ L of 95% (v/v) ice-cold-ethanol was then added and tubes inverted

many times to precipitate the DNA. DNA was then pelleted by centrifugation at 13,000 rpm for 30 min. To prevent contamination, the following steps were undertaken in a cell culture hood. The supernatant was removed and each pellet was washed with 100 μ L of 0.2 μ m filtered 70% (v/v) ethanol. The DNA was pelleted again by centrifugation at 13,000 rpm for 5 minutes and the supernatant removed. The Eppendorf tubes were then allowed to air dry for 15 min. Each DNA pellet was resuspended in 50 μ L of 0.2 μ m filtered x1 Tris-EDTA (TE) buffer and the Eppendorf tubes were left open for 1 h at room temperature and then vortexed thoroughly. Finally, the concentration of linearised soluble DNA was determined using a Thermo Nano Drop ND 1000 Spectrophotometer (Thermo Scientific, USA) by measuring absorbance at 260 and 280 nm.

4.2.1.8.3. Generation of stably expressing iNOS-3T3 L1 cell pools

An iNOS-3T3 L1 stable cell pool was constructed to express iNOS constitutively. Initially, the concentration of hygromycin (200 μ g/mL) to kill cells in the absence of the selection marker from the plasmid was determined. Then, stably expressing iNOS-3T3 L1 cells and the control 3.1/Hygro empty vector were generated using linearised-soluble plasmid DNA and circular plasmid DNAs. The 3T3 L1 cells were therefore transfected as described in section 4.2.1.7.1 with either the linearised or the circular DNA of either the iNOS-CDS or iNOS-UTR or the empty 3.1/Hygro vector. After 6 h, the cell culture media was replaced with complete DMEM with hygromycin at 200 μ g /mL. The stably expressing cells were passaged and samples were collected for mRNA work (as described in section 2.2.2) at each passaging and the stable iNOS pools were cryopreserved at each passaging. Screening of the stable pools was undertaken by qRT-PCR analysis for iNOS and β -actin transcripts to find best pools for L-Arg addition experiment in stably expressing iNOS-3T3 L1 cells.

4.2.1.9. Establishment of cell culture models for analysing culture viability and viable cell numbers in stably expressing iNOS-3T3 L1 cells upon supplementing L-arginine

Cell culture models were established for investigating cell fitness (cell culture growth and viability parameters) in stably expressing iNOS-3T3 L1 cells upon supplementing L-arginine as described in section 2.2.1.3.

4.2.1.10. iNOS and AMPK transcript analysis in stably expressing iNOS-3T3 L1 cells upon supplementing L-arginine

iNOS and downstream target AMPK transcript analysis was undertaken as described in section 2.2.1.3. for the extracted RNA was used for qRT-PCR analysis as described in sections 4.2.1.7.2 and 4.2.1.7.3 for iNOS and AMPK transcripts analysis.

4.2.2. Establishment of iNOS -V5 tagged construct for protein analysis

The expression of iNOS in 3T3 L1 was monitored at the protein level via an affinity tag, V5, at the C-terminus of iNOS. Control V5-tagged empty 3.1/V5-His TOPO™ Hygro vector and enhanced green fluorescent protein (eGFP)-tagged empty 3.1/Hygro vectors were also generated.

4.2.2.1. Source of plasmid DNA and amplification with iNOS primers

The pcDNATM3.1/V5-His TOPOTM (ThermoFisher Scientific, Cat. No: K480001) consisting of the TOPO cloning vector backbone was used as a high-level mammalian expression vector (**Fig 4.2.3**). The plasmid 3.1 Hygro eGFP, (**Fig 4.2.4**), which was constructed with enhanced green fluorescent protein (eGFP) inserted into 3.1 Hygro vector was kindly provided by a colleague, Miss. Laura Dyball. eGFP, is an engineered variant of the original wild-type green fluorescence protein (GFP), was transfected into the BNL CL2 and 3T3 L1 cells to observe GFP protein expression and to demonstrate BNL CL2 and 3T3 L1 cells were being successfully transfected with DNA.

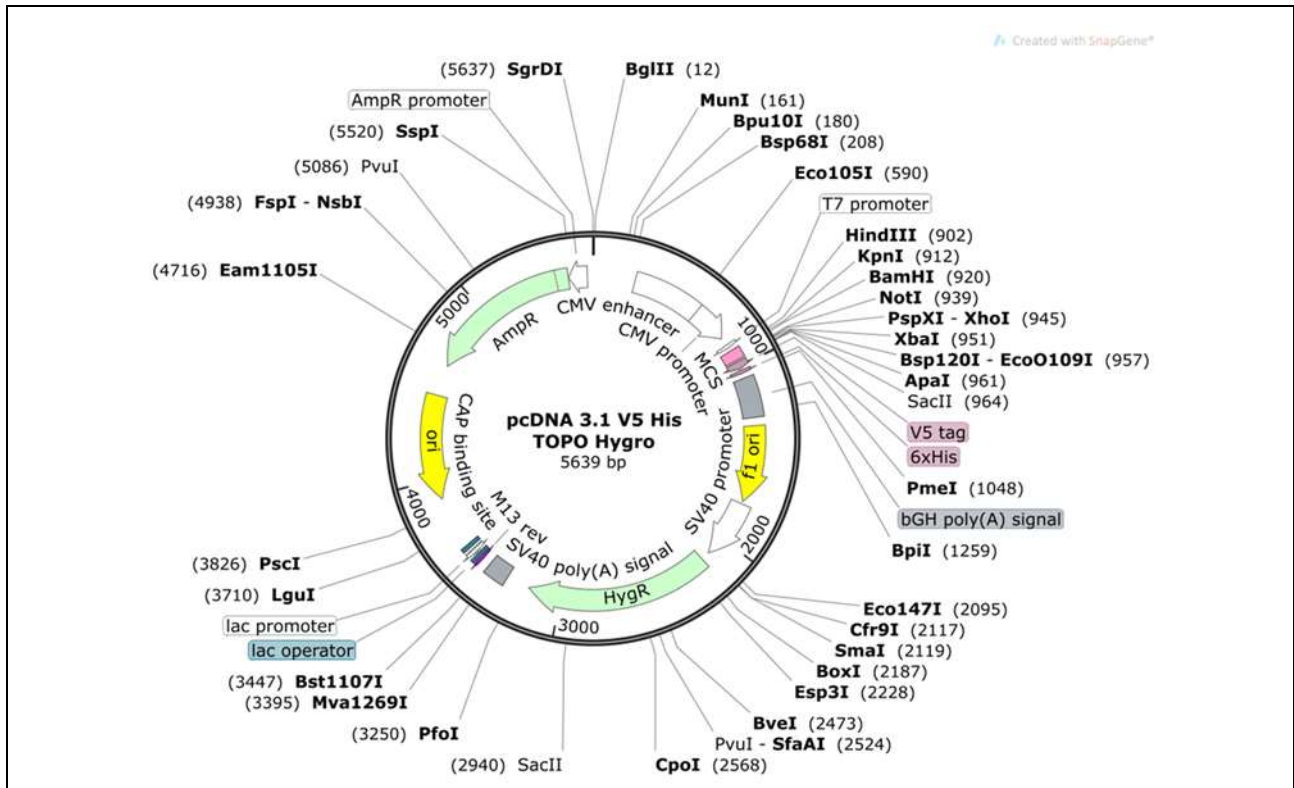


Fig 4.2.3. Diagram of mammalian expression cloning vector; pcDNA 3.1/V5-His TOPOTM Hygro.

This plasmid vector consists of TOPO cloning vector backbone and has 5639 bp sequence designed with the plasmid elements: an origin of replication (ori), antibiotic resistance gene, multiple cloning sites (MCS); a forward-orientation multiple cloning site, strong promoter region (CMV promoter) for high-level and constitutive expression, selectable marker (hygromycin) and the primer binding site. It is used for high-level, constitutive expression system in a variety of mammalian cell lines and used in transfection in TOPO sticky end and restriction enzyme cloning methods. The primer binding site used as an initiation depot for PCR amplification thereby sequencing primers such as T7 promoter and BGHR can be used as forward and reverse primers, respectively to verify the sequence of interest. In addition, the vector infused with 2 protein tags; V5 epitope tag and His tag (6x). C-terminal V5 epitope tag for efficient detection of recombinant proteins with an anti-V5 antibody and contains 42 base pairs and epitope/amino acid sequence is GKPIPNNLLGLDST with molecular mass 1.4 kDa and helps in affinity and antibody-based purification of a protein. Protein sequence of His tag is HHHHHH and DNA sequence is CACCACCACCACCAC and C-terminal polyhistidine (6 x His) sequence is used for purification and detection with an anti-His (C-term) antibody.

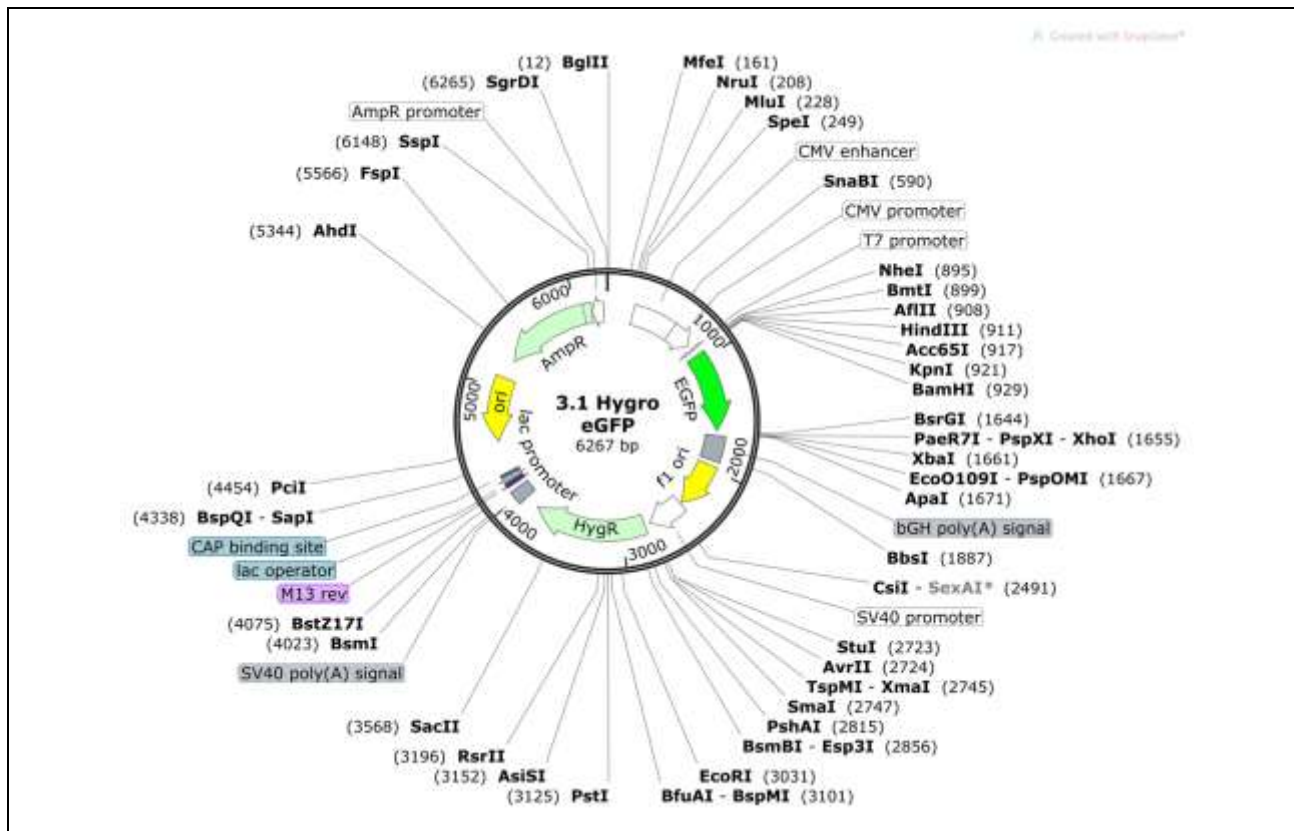


Fig. 4.2.4. eGFP 3.1/Hygro plasmid.

This plasmid DNA contains 6267bp with all plasmid elements along with enhanced green fluorescent protein (eGFP) cloned into the multiple cloning site.

4.2.2.2. PCR-based cloning for the generation of iNOS in-frame with V5 tag plasmid

4.2.2.2.1. Designing primers for iNOS-in frame-V5 PCR-based cloning

A set of primers were designed (described below) to amplify a region of iNOS in the positive control plasmid DNA; pBS-iNOS. The primers were designed with overhang regions for HindIII and XbaI and covered the entire ORF of the iNOS transcript (CDS) and then were used in the cloning of the iNOS into pcDNA 3.1/V5-His-TOPO Hygro vector as described below.

Primers for iNOS-in frame-V5 CDS amplification:

iNOS-CDS-ATG-FP-HindIII: 5' **TATAAGCTTGAC**ATGGCTTGCCCCTGGAAGTTTC 3' (Tm 64.2°C)

iNOS-CDS-TGA-RP-XbaI: 5' GCCCAAAGCCACGAGGCTCTG**TCTAGATAT** 3' (Tm 64°C)

4.2.2.3. Amplification of the iNOS-CDS-in frame with the V5 tag sequence

In order to sub-clone the iNOS-CDS insert from the vector into the cloning vector pcDNA 3.1/V5-His TOPO Hygro, Phusion DNA polymerase PCR was used to generate the amplified products of iNOS-CDS-in frame with V5 tagged with flanking regions for HindIII and XbaI restriction sites as described in 4.2.1.2.2.

4.2.2.4. Digestion of plasmid

The amplified products of Phusion PCR and the pcDNA of 3.1/V5-His-TOPO Hygro vector with HindIII and XbaI restriction sites were digested using a FastDigests; HindIII and XbaI as described in section 4.2.1.3.1. DNA band sizes of the expected digested products were analysed by performing agarose gel electrophoresis and then plasmid DNA was extracted, purified and quantified as detailed in sections 4.2.1.3.2 and 4.2.1.3.3.

4.2.2.5. Ligation of DNA

Ligations were undertaken as described in section 4.2.1.3.4 to generate the iNOS-CDS-in-frame 3.1/V5-His-TOPO Hygro (iNOS-V5 tagged plasmid) plasmid.

4.2.2.6. Transformation of pDNA into competent cells

DH5a *Escherichia coli* competent cells were used for transformation. Either the construct iNOS-V5 tagged plasmid or the control 3.1/V5-His-TOPO Hygro empty vector were transformed into the *E. coli* competent cells by heat shock method as described in section 4.2.1.4.2. Following transformation, colonies containing the insert of interest were confirmed by screening methods for transformants detailed in section 4.2.1.4.3. Restriction digestion of the construct using the FastDigest ApaI was performed as described in 4.2.1.4.3.2. Selected positive colonies were then confirmed by commercially available DNA sequencing (Genewiz, UK).

4.2.2.7. Transient transfection experiments

BNL CL2 and 3T3 L1 cells were transiently transfected with either iNOS-CDS-V5 tagged pcDNA3.1/V5-His-TOPO plasmid, V5-tagged empty pcDNA3.1/V5-His-TOPO vector or eGFP-tagged empty pcDNA3.1/Hygro vector constructs as detailed in section 4.2.1.7.1. Protein samples were collected from the clones to determine transient protein expression of iNOS-V5 24 and 48 h after transfection.

4.2.2.8. Protein extraction and analysis protocols

4.2.2.8.1. Protein extraction and samples preparation

Whole cell lysates were used for protein sample preparation. BNL CL2 and 3T3 L1 cells were cultured in 12-well plates as described in section 4.2.1.7.1 and samples obtained at 24 and 48 h post transfection by washing the cells in 1 mL of pre-warmed PBS. For trypsinisation of cells, pre-warmed 0.05% trypsin-EDTA (0.2 µL) was added and incubated the cells for 5 min at 37°C, 5% CO₂ followed by addition of pre-warmed complete DMEM with 10% (v/v) FBS media (1 mL). The suspension of the cells was then transferred into a sterile 1.5 ml Eppendorf tube and centrifuged 1000 rpm for 5 min to obtain the cell pellets.

Instead of regular protein lysis buffer and modified RIPA lysis buffer that were used previously in chapter 2 (section 2.2.3.1), modified RIPA buffer had 10% (v/v) 1 M dithiothreitol (DTT) and benzonase (Scientific Laboratory Supplies, Cat. No: 1014) added. A Bradford assay was used to find the protein concentration

(sections 2.2.3.2) and protein samples were prepared as detailed in section 2.2.3.3.1 at two different loading protein amounts; 10 and 20 µg of protein /25 µL total protein sample volume/lane. Protein lysate samples for analysis were diluted in x 5 sample buffer to the total loading volume of samples (25 µL) and heat incubated at 95°C for 5 min.

4.2.2.8.2. SDS-PAGE analysis of protein extracts

SDS-PAGE analysis of protein extracts was undertaken as described in section 2.2.3.3.

4.2.2.8.3. Western blot analysis of proteins

Western blot of the protein was followed as detailed in section 2.2.3.4. Blots were then washed in 0.1% TBS-T three times for 10 min per wash, then incubated overnight in a 10 mL, 1 in 5000 dilutions of either V5 primary antibody (Invitrogen, Cat. No:46-0705) or eGFP primary antibody (CRUK, Part No: 3E1) prepared in 3% (w/v) BSA-TBS.

4.2.2.9. Recombinant iNOS-V5 tagged protein detection in 3T3 L1 cells by immunofluorescence

For indirect immunofluorescence staining and imaging of iNOS-V5 epitope tagged recombinant protein and native or endogenous AMPK and ACC-1 proteins, 3T3 L1 cells at 2×10^5 viable cells per well were allowed to attach to sterilised coverslips in 6-well plates for 24 h. Next day, the cells were transiently transfected with a plasmid coding for either iNOS-CDS-V5-tagged 3.1/V5-His-TOPO Hygro or V5-tagged 3.1/V5-His-TOPO Hygro empty vector as described in section 4.2.1.7.1 and incubated for 24 h. Cells were then prepared for immunofluorescence staining and imaging. 24 h after transfection, the culture media was removed from each well and the cells were washed with pre-warmed x1 PBS (2 mL). To fix, immobilize target antigens and permeabilize the cells, precipitating fixative reagent methanol, chilled to -20°C (1 mL/well) was added to the cells and incubated for 5 min on ice before the methanol was removed from each well and the cells dried in air at 4°C. Following fixation, methanol fixed cells were rehydrated with x1 PBS (1mL) and then the PBS was removed. Once the cells were fixed to the cover slides, to block non-specific binding sites on cells before the antibody incubation steps, blocking buffer (250 µL) consisting of 3% (w/v) BSA in x1 PBS was added and incubated for 15 min at room temperature.

An aluminium foiled wrapped box with a square of Parafilm placed on the bottom was assembled in order to spread the antibody solution evenly over the section without air bubbles. Anti-V5 (Invitrogen, Cat. No: 46-0705), anti-AMPK and anti-ACC-1 primary antibody dilutions (1:500) were prepared using 3% BSA in PBS-Tween-20 to visualise specific targets. The cells on the coverslips were probed using appropriate primary antibody droplets (25 µL). The glass cover slips with cells were placed on the antibody droplet with cells side down to contact the antibody solution and then incubated overnight at 4°C. In order to account for background fluorescence, a negative control was also prepared by placing a coverslip on a drop of blocking solution rather

than diluted antibody. Prior to the secondary antibody incubation, PBS with 0.1% (v/v) Tween-20 was pipetted (100 μ L droplets) on 4 sheets of parafilm and the slips were dipped and washed 4 times allowing 5 min on each droplet. The secondary antibody dilutions were prepared with fluorophore-conjugated antibodies; fluorescein isothiocyanate (FITC, 5 μ L, Sigma, Cat. No: F9887) and tetramethylrhodamine isothiocyanate (TRITC, 5 μ L, Sigma, Cat. No: T5393) which were diluted 1:100 in 500 μ L 3% w/v BSA in a light protected tube, centrifuged at 13,000 rpm for 10 min and then 450 μ L of antibody solution transferred to a fresh light protected tube. Secondary antibody solution was dropped (25 μ L) onto parafilm in a damp light protected box and the cover slips placed cells side down (after blotting off any excess wash buffer on slides) and then left to incubate in the dark for 2 h at room temperature. At this stage, the negative control coverslips were placed on a spot of diluted secondary antibodies. After antibody probing, the slips were washed with 100 μ L of PBS with 0.1% (v/v) Tween-20 4 times.

For nuclear staining and anti-fading step, to mount the coverslips on glass slides and to prevent loss of signal during imaging by photo bleaching, 25 μ L of prolongTM gold antifade reagent with 4',6-diamidino-2-phenylindole (DAPI, Invitrogen, Cat. No: P36941, 10 mg/mL) was dropped on a parafilm sheet and the cover slips were placed cell side down for 1 min and unbound DAPI was then removed with PBS washing twice x 10 min. In preparation of imaging, Mowiol (900 μ L) was mixed with phendinediamine (100 μ L) and approximately 5 μ L droplets of this was applied to glass slides and cover slips placed on top cell side down, allowed to dry and then placed at 4°C overnight. The edge around the cover slips was sealed immediately prior to imaging with clear nail varnish. Images were then acquired using a Zeiss confocal microscope (Germany). Two software packages, ZENblue for rendering and processing of 3D images and ZENblack for controlling the microscope and for image acquisition were used.

4.2.3. Nitric oxide /Nitrite measurement by Griess Assay

4.2.3.1. Griess assay

Accumulation of NO in the cell culture media was analysed indirectly by quantifying nitrite (NO_2^-) present in the media using Griess assay as detailed in section 2.2.4.

4.2.4. Analysis of L-arginine, L-ornithine and L-citrulline by HPLC

Analysis of amino acids by HPLC was undertaken as described in section 2.2.5.

4.2.5. Statistical analysis

Statistical analysis was undertaken using GraphPad Prism 9.4.1 software and Microsoft Excel. Samples were analysed in biological triplicates. Data interpreted of means and standard deviation were analysed using two-way ANOVA. The Tukey's multiple comparison method was used to determine differences among the means of the treatment groups (0, 400 and 800 μ M L-Arg) with the control complete DMEM media addition to stably

expressing iNOS-3T3 L1 recombinant cells at time points either at 24 h or 24 and 48 h. Probability values ≤ 0.05 were considered to indicate statistical significance. The stars approach intended to flag levels of significance were followed (American Psychological Association style, New England Journal of Medicine) as ns = $P > 0.05$, * = $P \leq 0.05$, ** = $P \leq 0.01$, *** = $P \leq 0.001$ and **** = $P \leq 0.0001$.

4.3. Results

4.3.1. Generation of iNOS constructs

4.3.1.1. Analysis of Phusion high fidelity DNA polymerase PCR iNOS products by gel electrophoresis

The iNOS gene was amplified from the pBS-iNOS plasmid using primers that would amplify either just the coding region (CDS) or the CDS plus the UTR sequences with the primers that included overhang regions for the restriction enzymes for Hind III and XbaI using a Phusion high fidelity DNA polymerase PCR method. The expected size of the resulting PCR product bands (for iNOS-CDS 3,437 bp and iNOS-UTR 4,118 bp) were observed upon agarose gel electrophoresis analysis (**Fig 4.3.1**).

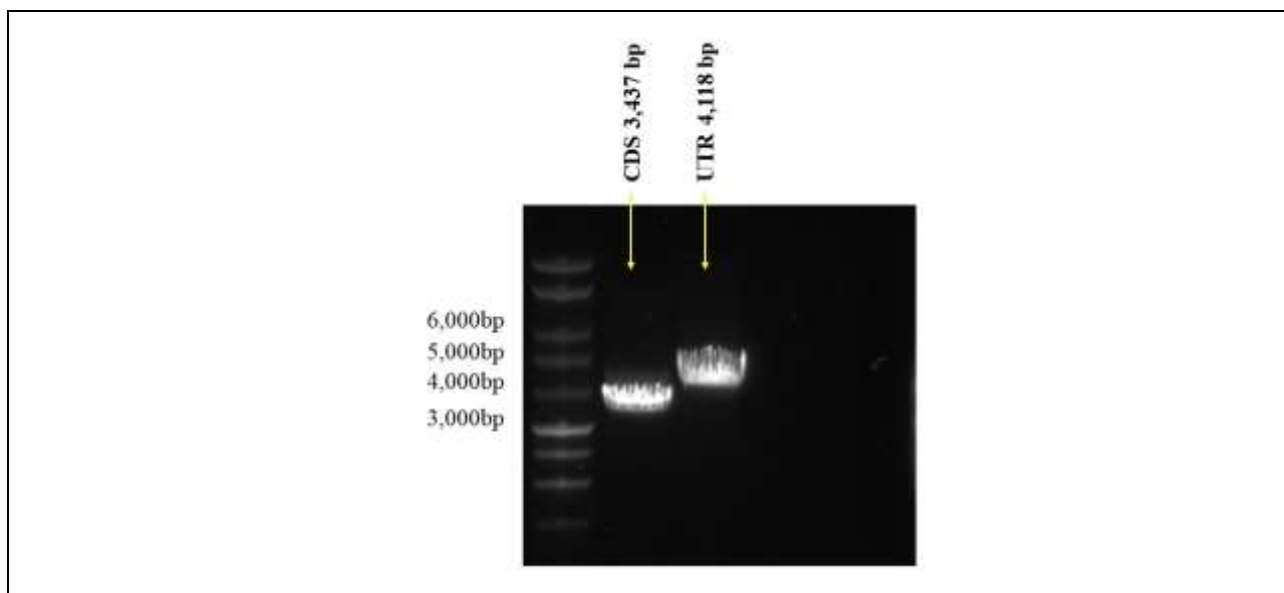


Figure 4.3.1. Agarose gel analysis of the amplified products of Phusion high fidelity DNA polymerase PCR of iNOS gene +/- UTR sequences.

CDS and UTR sequences of iNOS insert were amplified and the products analysed. The amplified product of CDS and UTR sequences of iNOS insert were observed as bands around the expected sizes of 3437 bp and 4118 bp, respectively.

4.3.1.2. Digestion of the iNOS PCR products and pcDNA3.1 hygro plasmid for cloning

The Phusion PCR amplified iNOS-CDS and iNOS-UTR products, and the pcDNA3.1/Hygro mammalian expression vector were digested with the two FastDigest restriction enzymes, HindIII and XbaI ready for ligation. After digestion an agarose gel (1% w/v) was used to resolve the DNA bands of digested products. The digested products of the 3.1/Hygro vector, iNOS-CDS and iNOS-UTR were observed as bands around the expected sizes (expected size 5597 bp, 3437 bp and 4118 bp respectively (**Fig 4.3.2 (A)**). The digested products

were then run on a gel made with BioRad-certified molecular biology agarose to obtain pure clean digested product for ligation (**Fig 4.3.2 (B)**).

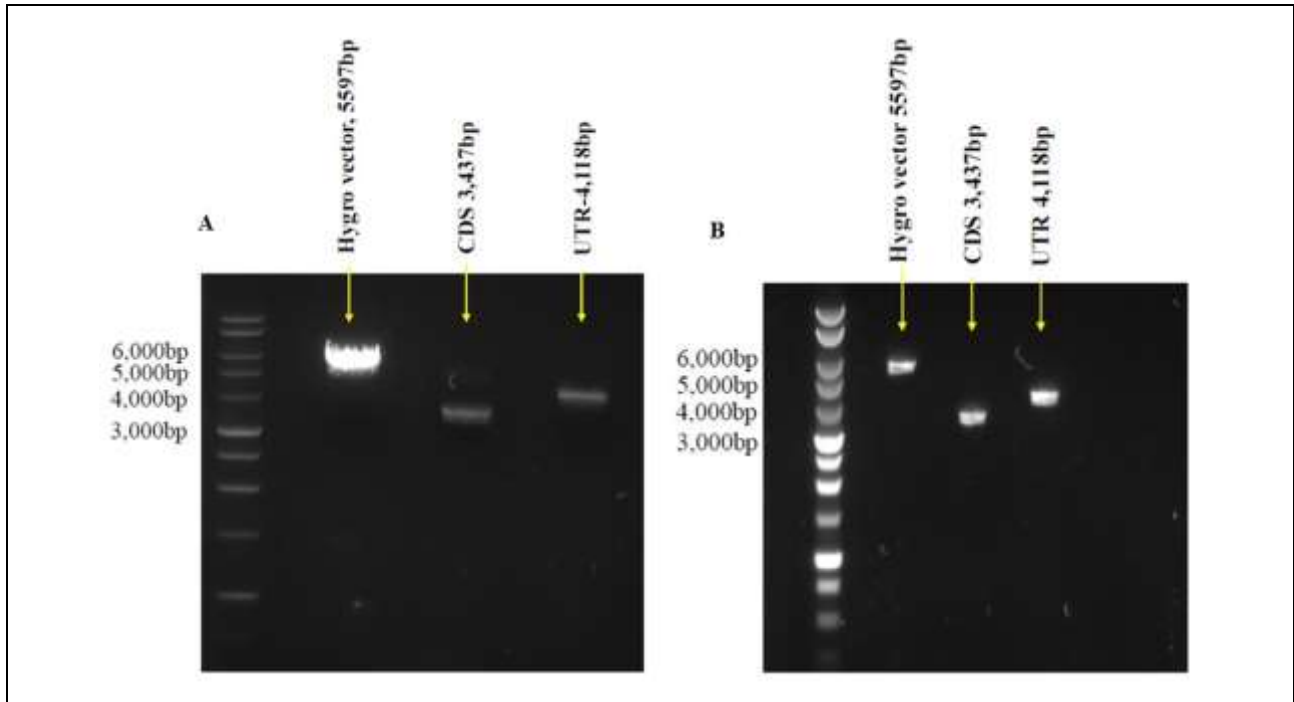


Figure 4.3.2. Agarose gel electrophoresis images of iNOS and pcDNA3.1hygro restriction enzyme digest products.

(A) The digested products of 3.1/Hygro vector, iNOS-CDS and iNOS-UTR were observed as bands around the expected sizes (expected sizes 5,597 bp, 3,437 bp and 4,118 bp respectively) in 1% (w/v) agarose gel. (B) Agarose gel image for the cleaned digested products resolved in the 1% (w/v) agarose gel, prepared using BioRad-certified molecular biology agarose. The agarose image shows the same DNA sizes for the digested products.

4.3.1.3. Ligation of iNOS gene inserts into the pcDNA3.1 vector

The iNOS-CDS or iNOS-UTR inserts with compatible ends for XbaI and HindIII were ligated into the 3.1/Hygro vector with the same compatible ends to generate either pcDNA 3.1 Hygro-iNOS-CDS (**Fig 4.3.3**) or pcDNA 3.1 Hygro-iNOS-UTR (**Fig 4.3.4**).

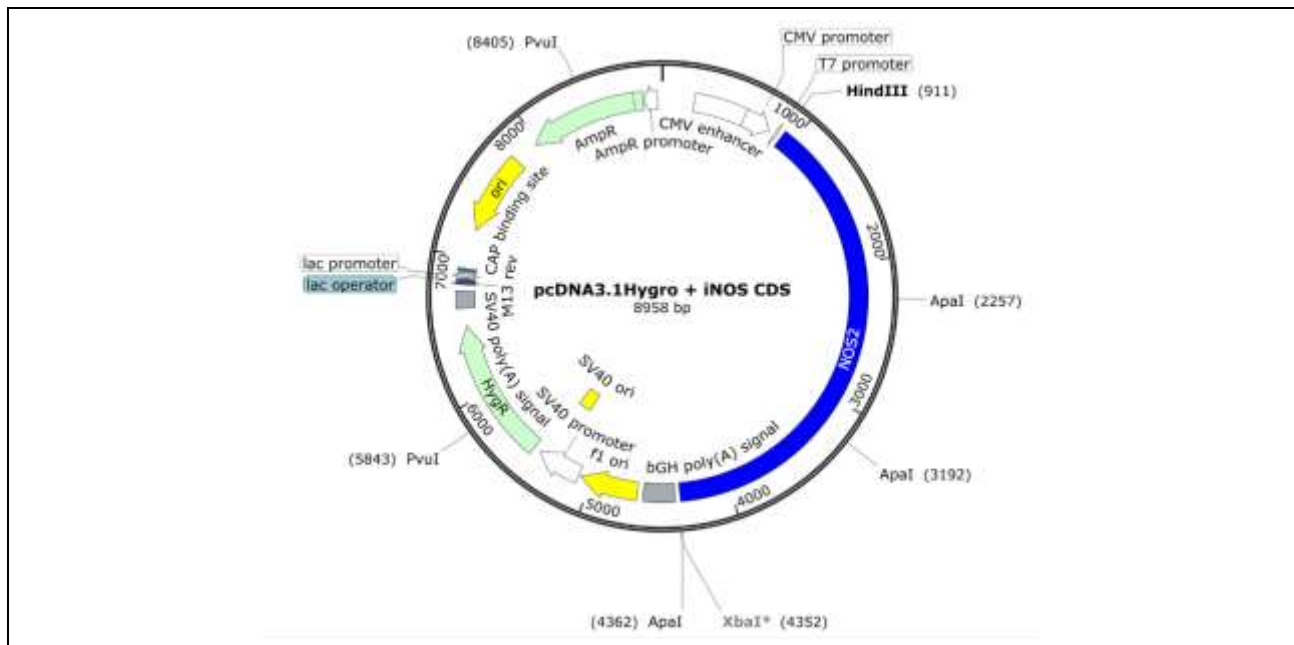


Figure 4.3.3. Generated pcDNA 3.1/ Hygro-iNOS construct with CDS sequence of iNOS.

The coding sequence of iNOS with overhang regions for HindIII and XbaI was inserted into the pcDNA 3.1/Hygro vector to generate pcDNA 3.1/ Hygro-iNOS-CDS plasmid of a size of 8958 bp.

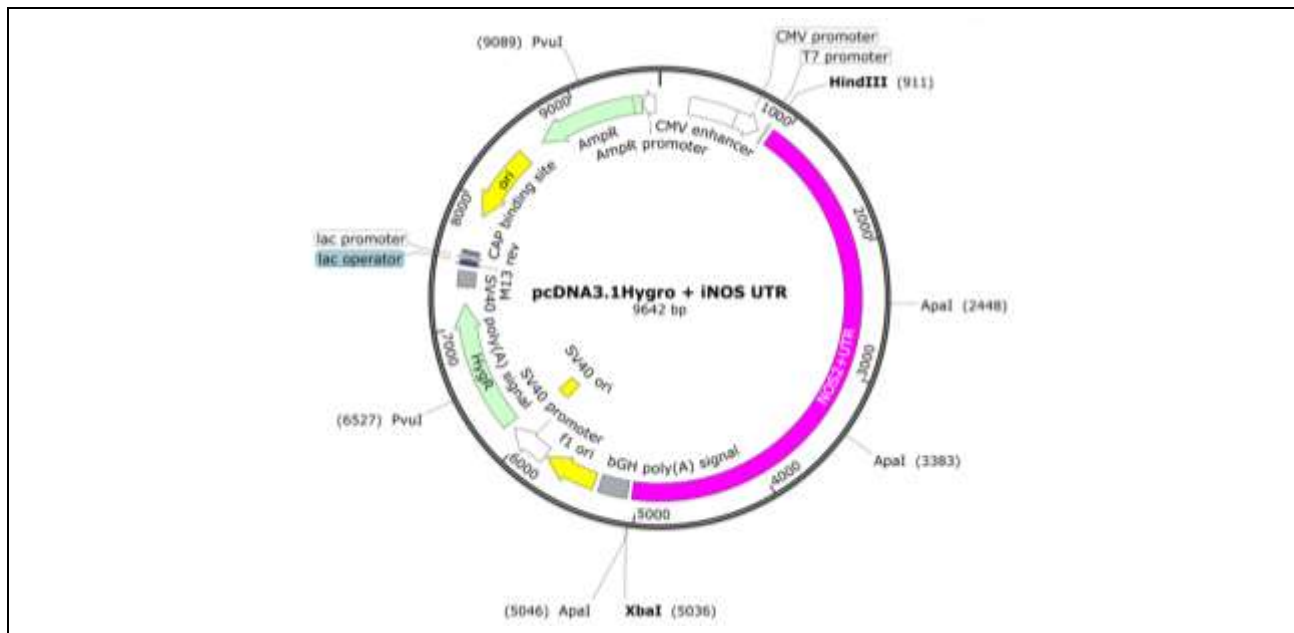


Figure 4.3.4. Generated pcDNA 3.1/ Hygro-iNOS construct including the UTR sequence of iNOS.

The iNOS sequence includes the untranslated regions with overhang regions for HindIII and XbaI and was ligated into the pcDNA 3.1/Hygro vector to construct the pcDNA 3.1/ Hygro-iNOS-UTR plasmid of a size of 9642 bp.

4.3.1.4. Colonies after transformation of ligation reactions into DH5a *Escherichia coli* competent cells

After ligation of pcDNA 3.1 Hygro-iNOS-CDS or pcDNA 3.1 Hygro-iNOS-UTR and the control plasmid, these were transformed to DH5a *Escherichia coli* calcium competent cells and the next day colonies observed for each transformant (**Fig 4.3.5**). Relatively high numbers of colonies were observed for pcDNA 3.1 Hygro-

iNOS-CDS and pcDNA 3.1 Hygro-iNOS-UTR ligation reaction transformants compared to the control 3.1/Hygro transformant (no colonies or very few colonies for the control).

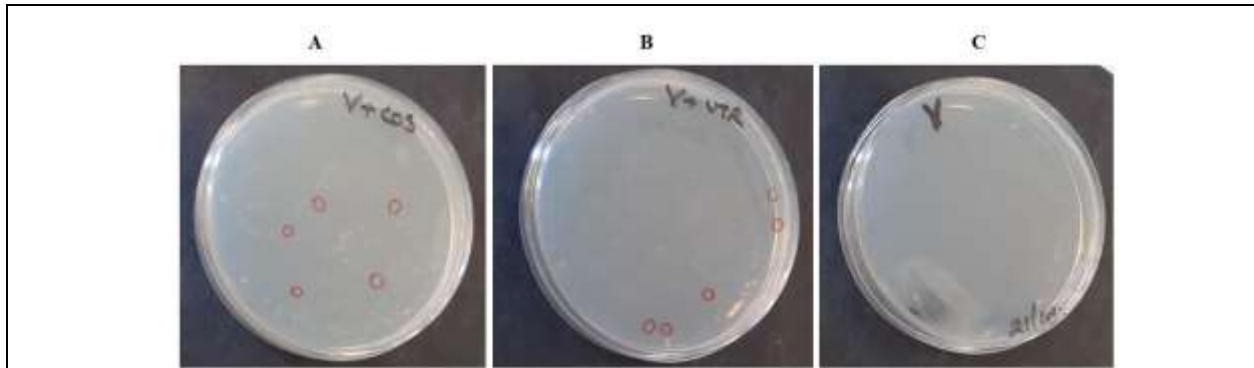


Figure 4.3.5. Colonies for transformation

(A) Colonies for the transformation of 3.1 Hygro-iNOS-CDS ligation. (B) Colonies for the transformation of 3.1 Hygro-iNOS-UTR ligation. (C) Colonies for the transformation of empty vector pcDNA3.1/Hygro.

4.3.1.5. Screening of transformants for presence of desired inserts

4.3.1.5.1. PCR colony screening for transformants

Colony-screening-PCR was undertaken on a single white colony from an LB/agar plate using T7 and BGHR primers and GoTaq DNA polymerase and then 1% (w/v) agarose gel analysis of the PCR products was undertaken to determine if the expected gene insert was present. The expected band sizes for the amplified PCR products were observed with a band for the pcDNA 3.1 Hygro-iNOS-CDS construct observed at approximately 3,437 bp and for pcDNA 3.1 Hygro-iNOS-UTR at approximately 4,118 bp (**Fig 4.3.6**).

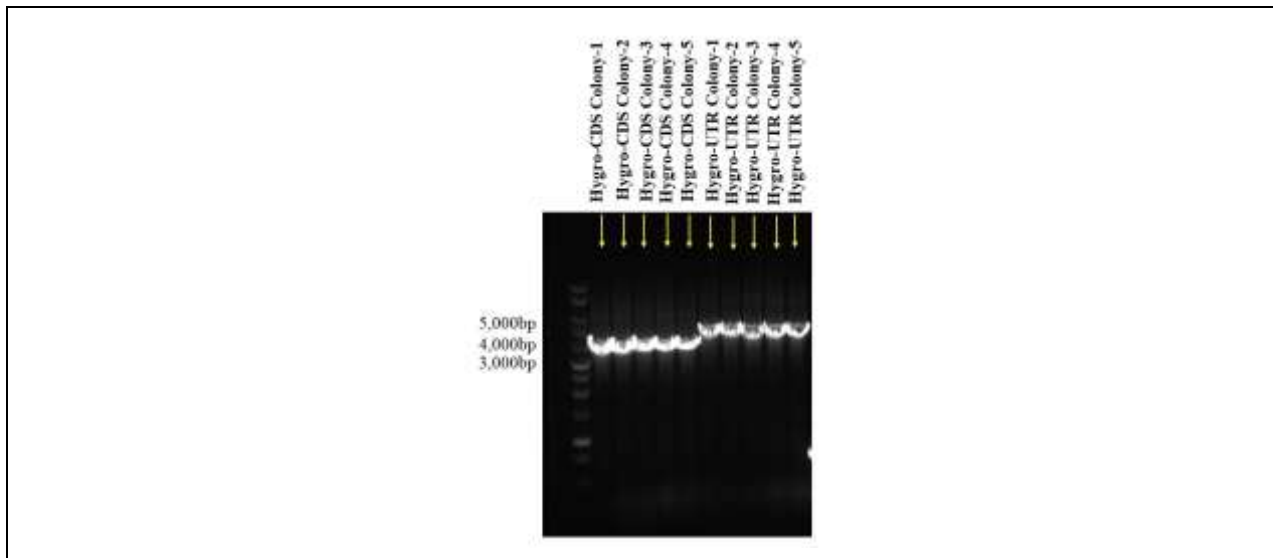


Figure 4.3.6. Agarose gel analysis of PCR products from colony-screening-PCR.

Agarose (1% w/v) gel electrophoresis was performed on colony PCR products generated using T7 and BGHR primers and GoTaq DNA polymerase to amplify the target gene. Expected band sizes for the positive constructs were

observed in the agarose gel with a band for pcDNA 3.1 Hygro-iNOS-CDS construct was observed at approximately 3,437 bp and for pcDNA 3.1 Hygro-iNOS-UTR at approximately 4,118 bp.

4.3.1.5.2. Restriction digests to confirm the presence of the desired insert in pDNA

To confirm ligation of the insert gene into the pcDNA3.1Hygro vector, the pcDNA 3.1 Hygro-iNOS-CDS and pcDNA 3.1 Hygro-iNOS-UTR plasmid DNA was digested with ApaI fast digest enzyme. Three bands were observed at the expected sizes upon agarose gel electrophoresis analysis of the digests. The expected bands for pcDNA 3.1 Hygro-iNOS-CDS were observed, with the theoretical size of the bands being 6796 bp, 1227 bp and 935 bp (**Fig 4.3.7, (A)**) and for pcDNA 3.1 Hygro-iNOS-UTR at 6967 bp, 1720 bp and 955 bp (**Fig 4.3.7, (B)**). A larger amount of each construct was then prepared from a 50 mL culture and recovering the plasmid DNA using a maxi prep kit. The concentration of the constructs from the maxi-prep were pcDNA 3.1/Hygro; 694 ng/ μ L, pcDNA 3.1 Hygro-iNOS-CDS; 2573.8 ng/ μ L and pcDNA 3.1 Hygro-iNOS-UTR; 1622.8 ng/ μ L. The pcDNA obtained from maxi prep was again analysed by restriction digestion using ApaI to obtain the expected bands (**Fig 4.3.7, (C)**), the same as mini prep pcDNA products bands.

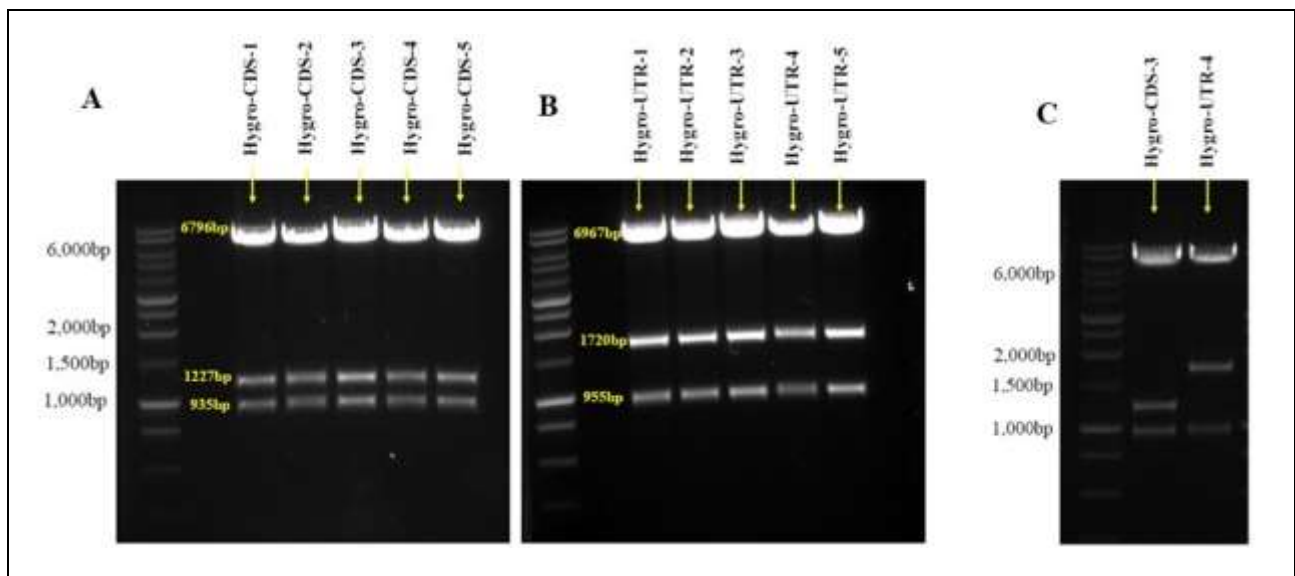


Figure 4.3.7. Agarose gel analysis of ApaI fast digest enzyme digestion of plasmid DNAs.

(A) ApaI digested product bands for the plasmid DNAs pcDNA 3.1 Hygro-iNOS-CDS and (B) pcDNA 3.1 Hygro-iNOS-UTR obtained from mini prep. The expected 3 bands were observed with the expected sizes being 6796 bp, 1227 bp and 935 bp for iNOS-CDS and for iNOS-UTR 6967 bp, 1720 bp and 955 bp. (C) The plasmid DNA obtained from maxiprep also showed the same expected band patterns when digested with ApaI.

4.3.2. Transient transfection of the iNOS constructs and subsequent iNOS transcript analysis

4.3.2.1. qRT-PCR analysis of iNOS transcript amounts upon transient expression in 3T3 L1 and BNL CL2 cells

To analysis the transient expression of the iNOS gene transcript, BNL CL2 and 3T3 L1 cells were grown as described in section 4.2.1.7.1 and samples collected at 24 h after transfection. The target iNOS gene transcript

amounts was then investigated relative to a reference gene, β -actin (Table 4.3.1). At 24 h post transfection, transient iNOS transcript amounts were elevated in iNOS-CDS and iNOS-UTR transfected construct samples compared to the control 3.1/hygro empty vector in BNL CL2 cells. This was confirmed by the amplicon cycle number, with the iNOS C_t of iNOS-CDS and iNOS- UTR being less compared to control. In 3T3 L1 cells, transient iNOS expression was high in iNOS-CDS compared to the control 3.1/hygro (iNOS C_t < β -actin C_t). There was however, little difference between the iNOS- UTR construct and the control 3.1/hygro empty vector (Fig 4.3.8).

Table 4.3.1. Comparison of C_t cycle numbers for the transient expression of iNOS gene transcript and endogenous expression of reference gene β -actin in transfected BNL CL2 and 3T3 L1 cells

Transfected constructs	Ct cycle number of BNL CL2 cells			Ct cycle number of 3T3 L1 cells		
	Empty vector control	iNOS CDS	iNOS CDS	Empty vector control	iNOS CDS	iNOS CDS
iNOS	29.17	18.02	22.01	28.71	18.41	24.45
β -actin	22.05	23.18	25.13	22.29	22.22	25.13

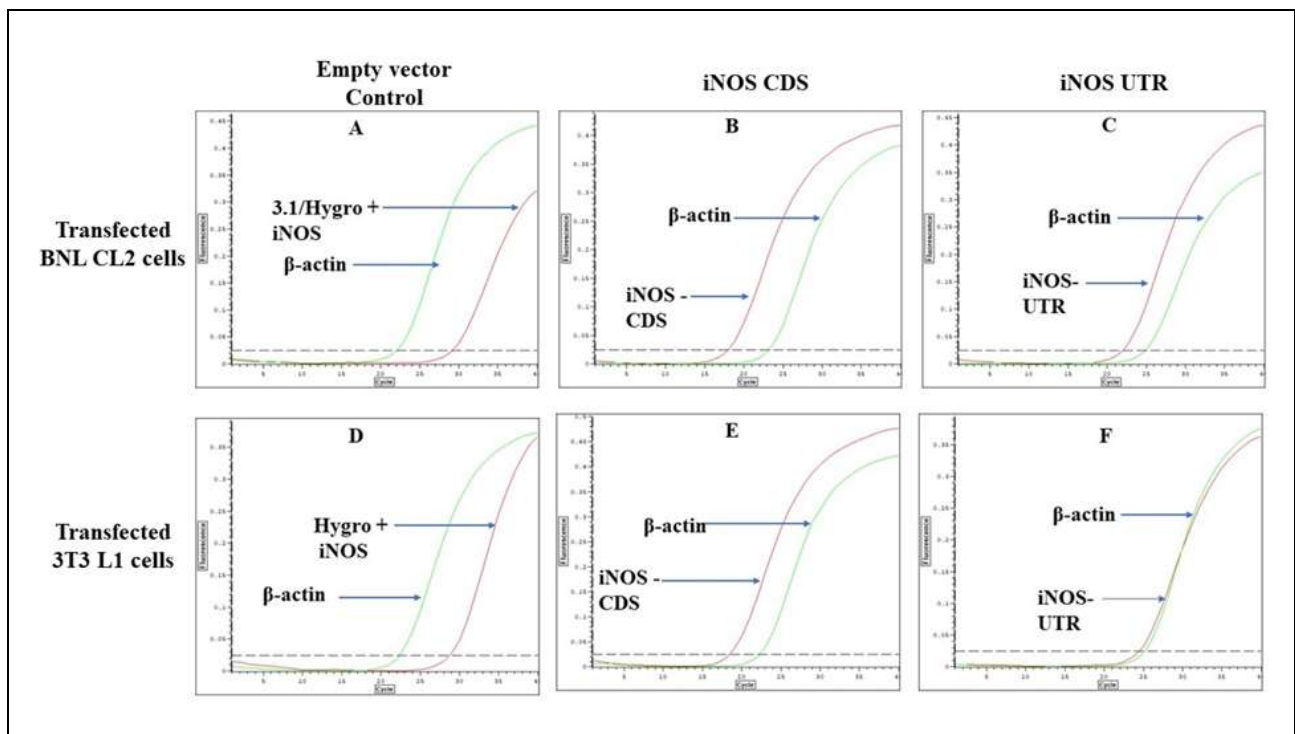


Figure 4.3.8. Relative quantitation of iNOS transcript (Red curve) and reference gene; β -actin transcript (Green curve) amounts.

In cells transfected with either the iNOS constructs or an empty vector control. In the top panel A-C, the results for the transient expression of iNOS-CDS and iNOS-UTR constructs compared to the control 3.1/hygro empty vector in BNL CL2 cells. Amplicon cycle number; iNOS C_t < β -actin C_t in iNOS-CDS and iNOS-UTR constructs, in comparison to the control 3.1/hygro empty vector; iNOS C_t > β -actin C_t . Panels D-F, transient expression of iNOS-CDS and iNOS-UTR constructs compared to the control 3.1/hygro empty vector in 3T3L1 cells where the crossing point threshold cycle

numbers are; $iNOS_{Ct} < \beta\text{-actin}_{Ct}$ in iNOS-CDS construct compared to the control 3.1/hygro empty vector, amplicon cycle numbers were the same for iNOS-UTR construct and the control.

An agarose gel of the qRT-PCR products is shown in **figure 4.3.9**.

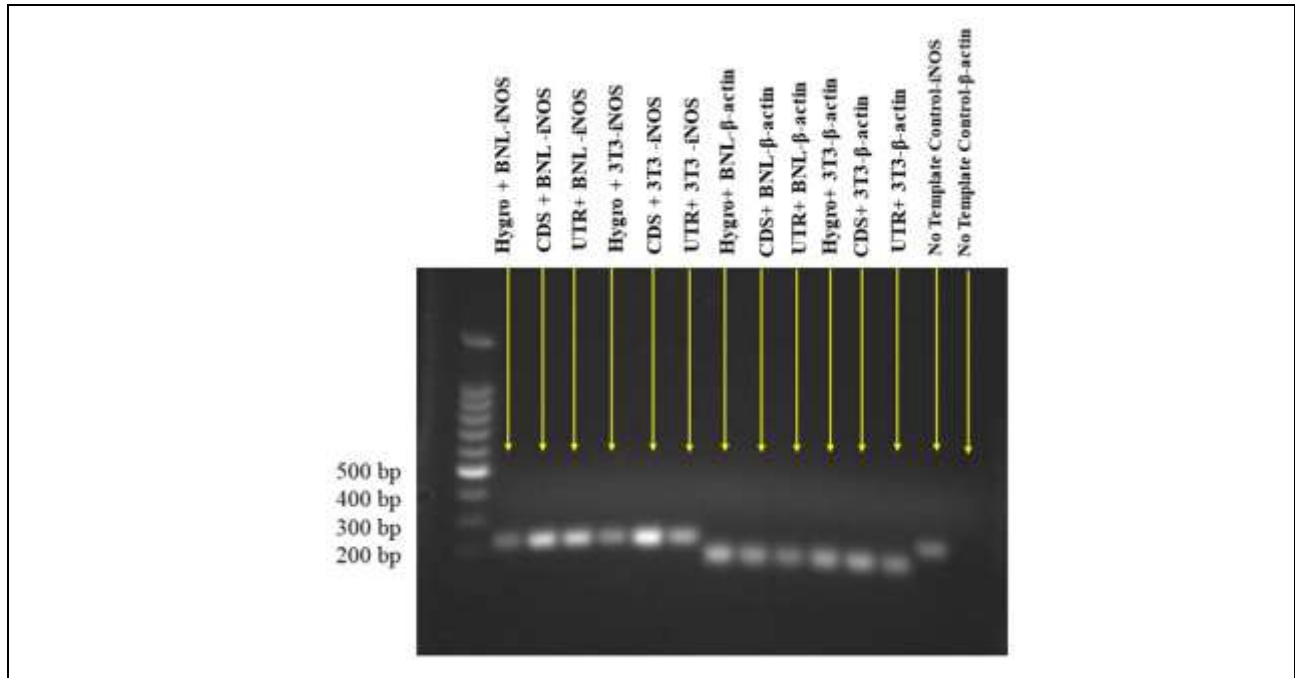


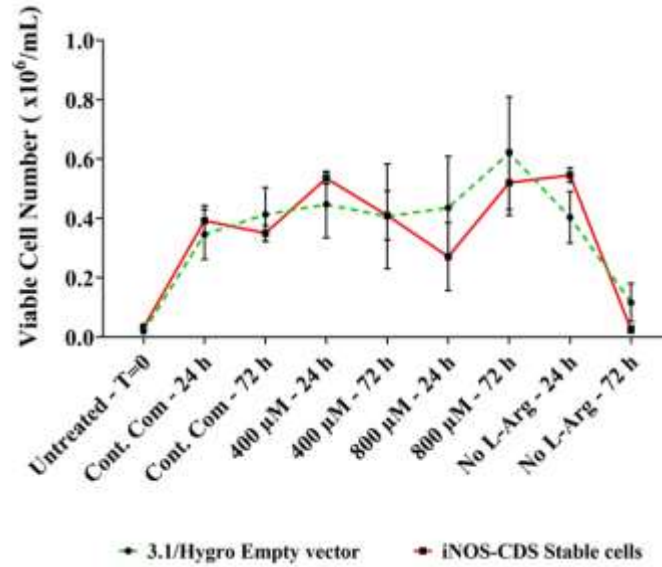
Figure 4.3.9. Agarose gel analysis for the amplicon products of qRT-PCR of iNOS or β -actin transcripts.

Amplicon products of transient iNOS transcript and the reference gene β -actin in iNOS-CDS, iNOS-UTR and the control 3.1/hygro empty vector transfected BNL CL2 and 3T3 L1 cell samples. The band at 215 bp was the expected amplicon of iNOS and the band at approximately 163 bp that for β -actin.

4.3.3. Stable iNOS 3T3 L1 cell pools: The impact of L-Arg addition on culture viability and viable cell numbers

To analysis the cell fitness (cell culture growth and culture viability parameters) in the stably expressing iNOS 3T3 L1 cells upon culturing in excess exogenous L-Arg, cell culture models were established as described in section **4.2.1.7.1** with samples collected at 24 and 72 h time points. A comparison of the viable number of cells and culture viability was investigated between the control complete DMEM medium and the control SILAC DMEM medium containing no L-Arg (0 μ M L-arginine), along with SILAC DMEM containing 400 and 800 μ M L-arginine and untreated cell samples at T=0 either in the control empty vector 3T3 L1 cells or stably expressing iNOS 3T3 L1 cells. **Fig 4.3.10** shows that there was an increase in stable iNOS cell numbers when the stable cells were cultured with 400 μ M L-Arg (1.2-fold), 0 μ M L-Arg (1.38-fold) and the control samples cultured in complete DMEM (1.11-fold) at 24 h, while there was a decline in the stable cells cultured at 800 μ M L-Arg (0.61-fold) after 24 h in comparison to the empty vector 3T3 L1 cells after 24 h. Stable iNOS 3T3 L1 cell numbers were decreased ($P < 0.0001$) from 24 to 72 h in all samples and conditions (control; 0.9-fold, 400 μ M; 0.76-fold, and 0 μ M; 0.05-fold), except at 800 μ M (1.93-fold). Across the time points, the cell

numbers were increased ($P < 0.0001$) in the cells cultured in high concentrations of L-Arg (800 μM) in both stable iNOS (1.93-fold) and empty vector (1.41-fold) 3T3 L1 cells. The growth profiles (**Fig 4.3.10**) show that the effect of L-arginine (0, 400 and 800 μM) compared to the control complete DMEM media in stably expressing iNOS and empty vector 3T3 L1 cells was not significant.



Source of Variation	P value	P value summary	Significant?
Interaction	0.1848	ns	No
Samples, conditions and time points	<0.0001	****	Yes
L-Arg +/- and Cont. Com in 3.1/Hygro Empty vector or iNOS-CDS Stable cells	0.6051	ns	No

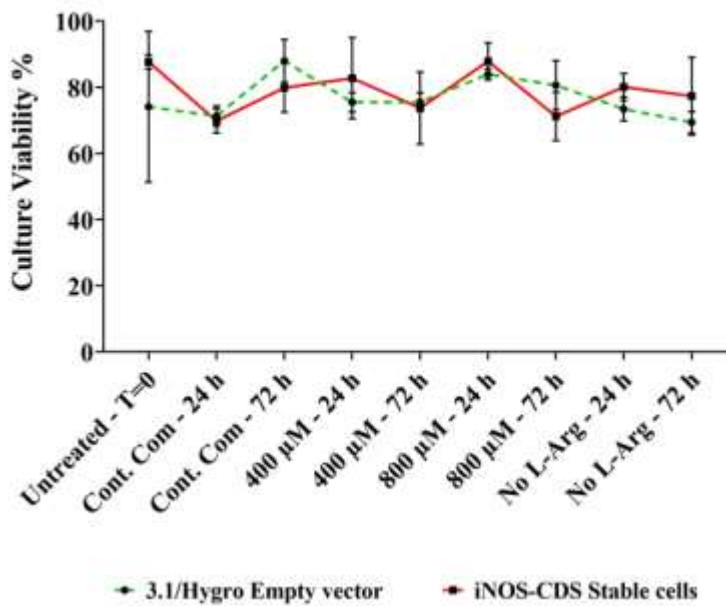
Bonferroni's multiple comparisons test	3.1/Hygro Empty vector - iNOS-CDS Stable cells
	Viable cell number
Untreated - T=0	ns
Cont. Com - 24 h	ns
Cont. Com - 72 h	ns
400 μM - 24 h	ns
400 μM - 72 h	ns
800 μM - 24 h	ns
800 μM - 72 h	ns
No L-Arg - 24 h	ns
No L-Arg - 72 h	ns

Figure 4.3.10. Cell growth profile of stably expressing and empty vector 3T3 L1 cells with different concentrations of L-arginine and the control.

Cell growth/viable cell number profiles of stably expressing iNOS and empty vector 3T3 L1 cells with different concentrations of L-arginine (0, 400 and 800 μM) and the control complete DMEM media at 24 and 72 h. Data

points represent the mean \pm SD of each culture sample. Error bars represent the standard deviation from the mean (n = 3). The tables summarise two-way ANOVA followed by a Bonferroni multiple comparison test using GraphPad Prism 9.4.1. The stars flag the levels of significance; ns = P > 0.05, * = P \leq 0.05, ** = P \leq 0.01, *** = P \leq 0.001 and **** = P \leq 0.0001.

Fig 4.3.11 reports the culture viability of stable and empty vector 3T3 L1 cultures grown in either control complete DMEM or L-arginine supplemented samples (400 and 800 μ M) and no L-arginine SILAC DMEM at 24 and 72 h. Culture viability was generally maintained between 69-90% across the 72 h. There was no significant in the difference was found in the viability of the cultures under the different L-Arg conditions in samples, conditions timepoints as outlined below in **Fig 4.3.11**.



Source of Variation	P value	P value summary	Significant?
Interaction	0.275	ns	No
Samples, conditions and time points	0.0542	ns	No
L-Arg +/- and Cont. Com in 3.1/Hygro Empty vector or iNOS-CDS Stable cells	0.3698	ns	No

Bonferroni's multiple comparisons test	3.1/Hygro Empty vector - iNOS-CDS Stable cells
	Culture viability
Untreated - T=0	ns
Cont. Com - 24 h	ns
Cont. Com - 72 h	ns
400 μ M - 24 h	ns
400 μ M - 72 h	ns

800 μM - 24 h	ns
800 μM - 72 h	ns
No L-Arg - 24 h	ns
No L-Arg - 72 h	ns

Figure 4.3.11. Culture viability profile of stably expressing and empty vector 3T3 L1 cells with different concentrations of L-arginine and the control.

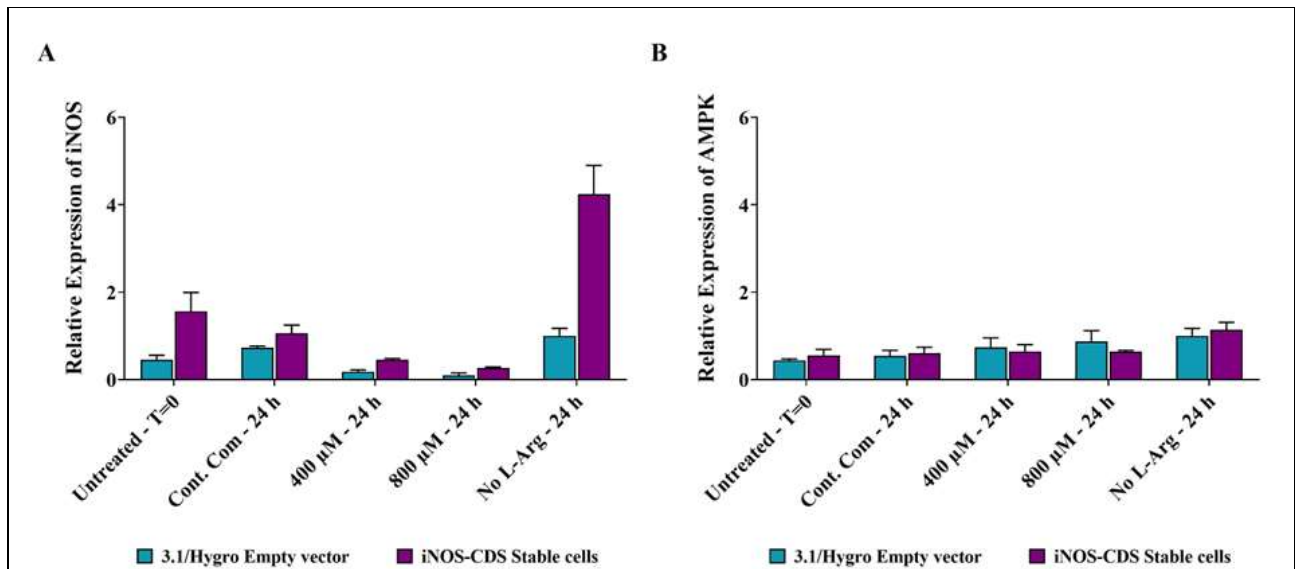
Culture viability profiles of stably expressing iNOS and empty vector 3T3 L1 cells grown in different concentrations of L-Arg (0, 400 and 800 μ M) and the control complete DMEM media at 24 and 72 h. Culture viability is expressed as % of viable cells. Data points represent the mean \pm SD of each sample. Error bars represent the standard deviation from the mean (n = 3). Tables summarise two-way ANOVA followed by a Bonferroni multiple comparison test using GraphPad Prism 9.4.1. The stars indicate the levels of significance; ns = P > 0.05, * = P \leq 0.05, ** = P \leq 0.01, *** = P \leq 0.001 and **** = P \leq 0.0001.

4.3.4. qRT-PCR analysis of iNOS, AMPK and β -actin genes upon culturing of stably expressing iNOS-3T3 L1 cells in different exogenous L-arginine concentrations

Stably expressing iNOS 3T3 L1 cells or empty vector 3T3 L1 cells were grown as described in section 4.2.1.7.1 and sampled for mRNA analysis by qRT-PCR. Relative gene expression analysis ($\Delta\Delta$ Ct) was used to quantify target gene mRNA expression normalised to a reference gene, β -actin (**Fig 4.3.12**). The target genes investigated were iNOS and its downstream target AMPK. The relative expression of each gene was denoted as RE.

4.3.4.1. Relative gene expression of iNOS and AMPK

The factory for the synthesis of NO and L-citrulline from L-arginine is iNOS enzyme, the impact of excess exogenous L-Arg on iNOS transcript expression was investigated as relative expression in the stably expressing iNOS and empty vector 3T3 L1 cells and is shown in **Fig 4.3.12A**. After 24 h, relative iNOS mRNA expression was significantly increased (P<0.0001) in the stable iNOS 3T3 L1 cells (control; 1.45-fold, 400 μ M; 2.5-fold, 800 μ M; 2.71-fold and 0 μ M; 4.24-fold) compared to the empty vector 3T3 L1 cells. Untreated samples grown in stably expressing iNOS at T=0 had also shown high relative iNOS mRNA (3.47-fold) compared to the empty vector 3T3 L1 cells. When AMPK gene expression was analysed in excess L-arginine culture conditions for stably over-expressing iNOS and empty vector 3T3 L1 cells the results generated are presented in **Fig 4.3.12B**. The comparison of relative transcript expression of AMPK in different L-Arg treated conditions and the control between the empty vector and stably expressing iNOS 3T3 L1 was not significant (P=0.9609).



Source of Variation	iNOS		AMPK	
	P value	Significant?	P value	Significant?
Interaction	****	Yes	ns	No
Samples, conditions and time points	****	Yes	****	Yes
L-Arg +/- and Cont. Com in 3.1/Hygro Empty vector or iNOS-CDS Stable cells	****	Yes	ns	No

Bonferroni's multiple comparisons test	3.1/Hygro Empty vector - iNOS-CDS Stable cells	
	iNOS	AMPK
Untreated - T=0	***	ns
Cont. Com - 24 h	ns	ns
400 μM - 24 h	ns	ns
800 μM - 24 h	ns	ns
No L-Arg - 24 h	****	ns

Figure 4.3.12. Relative mRNA expression of iNOS and AMPK in stably expressing iNOS and empty vector 3T3 L1 cells cultured in different concentrations of L-arginine and the control.

Relative mRNA transcript expression ($\Delta\Delta Ct$) of iNOS (A) and AMPK (B) in stably expressing iNOS and empty vector 3T3 L1 cells cultured in medium of different L-arginine concentrations (0, 400 and 800 μM) and control complete DMEM media 24 h after addition. Data points represent the mean \pm SD of each sample. Error bars represent the standard deviation from the mean (n =3). Tables summarise two-way ANOVA followed by a Bonferroni multiple comparison test using GraphPad Prism 9.4.1. The stars indicate the levels of significance; ns = $P > 0.05$, * = $P \leq 0.05$, ** = $P \leq 0.01$, *** = $P \leq 0.001$ and **** = $P \leq 0.0001$.

4.3.5. Generation of iNOS -V5 tagged construct for transient protein analysis

4.3.5.1. Generation of iNOS-V5 construct for iNOS transient and stable protein analysis

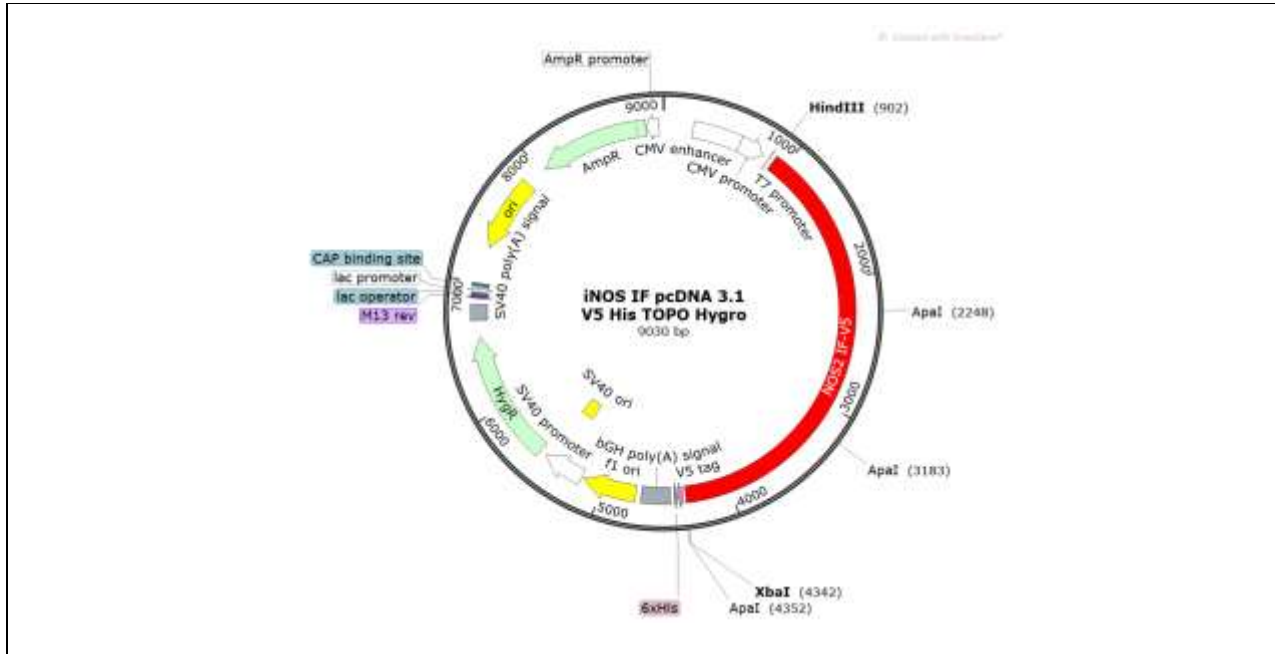


Figure 4.3.13. Generated iNOS-in-frame-3.1/V5-His-TOPO Hygro (iNOS-V5 tagged plasmid) construct. The CDS iNOS gene was cloned in frame with a C-terminal V5 tag epitope using HindIII and XbaI to generate iNOS-in-frame-3.1/V5-His-TOPO Hygro of a size of 9030 bp.

4.3.5.2. Screening for successful iNOS-CDS in-frame with V5 tag plasmid transformants

4.3.5.2.1. PCR colony screening

PCR-based cloning was used to screen for successful iNOS-V5 inserts on single white colonies from an LB/agar plate using T7 and BGHR primers and GoTaq DNA polymerase. A 1% (w/v) agarose gel was then performed to determine presence (or absence) of the expected band at around 6900 bp (**Fig 4.3.14 (A)**).

4.3.5.2.2. Plasmid miniprep and maxiprep restriction digestion to confirm present of iNOS-V5 insert

To confirm ligation of the insert, plasmid DNA was digested with ApaI fast digestive enzyme. Three bands were observed around the expected sizes with the expected bands for iNOS-V5 tagged plasmid being of 6796 bp, 1227 bp and 935 bp in size (**Fig 4.3.14 (B)**). **Fig 4.3.13** showed the generated iNOS-in-frame-3.1/V5-His-TOPO Hygro (iNOS-V5 tagged plasmid) construct.

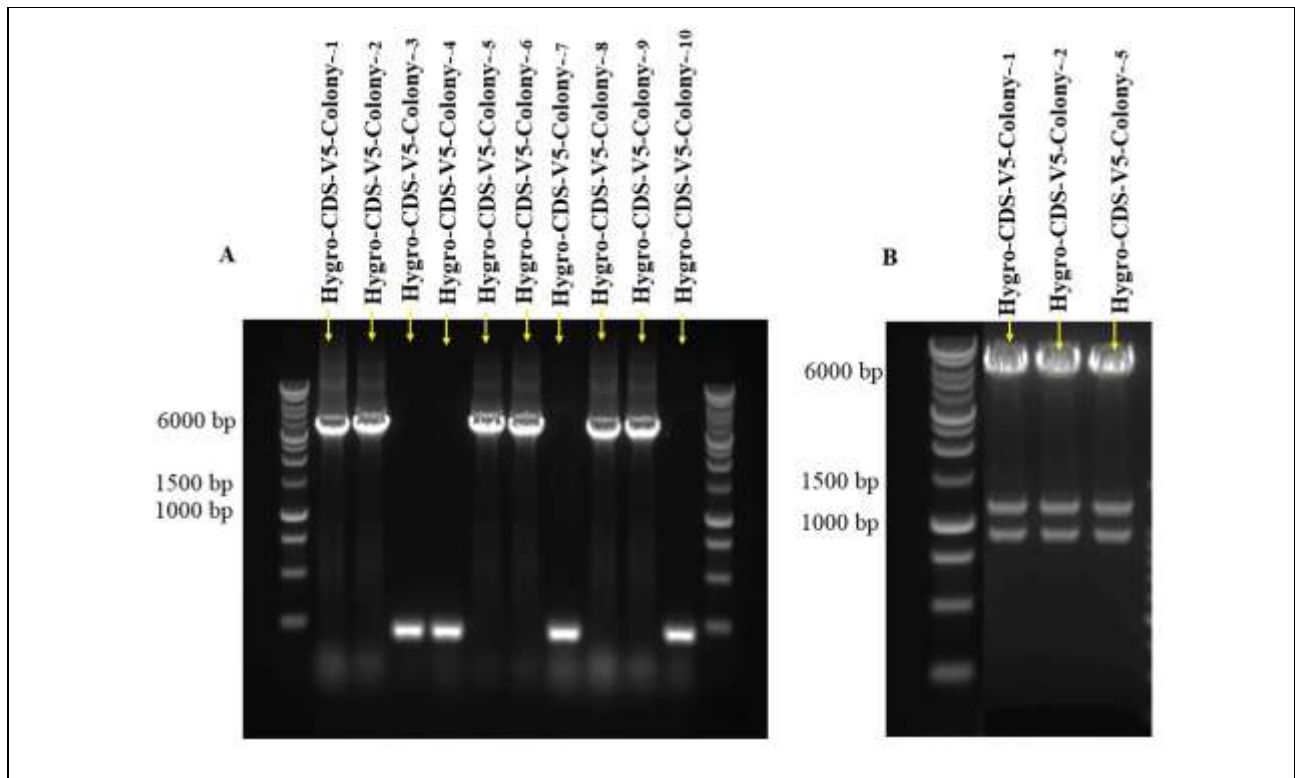


Figure 4.3.14. Agarose gel analysis for single-colony PCR screening and restriction digestion products of plasmid DNA of iNOS-V5 tagged plasmid.

(A) Colony screening PCR of iNOS-V5 tagged plasmid DNA using T7 and BGHR primers and GoTaq DNA polymerase and 1% (w/v) agarose gel analysis to determine the size of bands amplified. The agarose image shows colony screening PCR products of 10 colonies with colonies showing positive colonies (1, 2, 5, 6, 8 and 9) and colonies showing negative colonies or colonies with aberrant insert (3, 4, 7 and 10). (B) Digested products of iNOS-V5 tagged plasmids from the positive colonies 1, 2 and 5 using *ApaI* fast digestive enzyme. Digested bands were observed around the expected sizes of 6796 bp, 1227 bp and 935 bp.

4.3.6. Analysis of transient protein expression of iNOS-V5 and a control eGFP

4.3.6.1. Western blot analysis

BNL CL2 and 3T3 L1 cells were transiently transfected with either iNOS-V5 tagged pcDNA3.1/V5-His-TOPO plasmid, V5-tagged empty pcDNA3.1/V5-His-TOPO vector or eGFP pcDNA3.1/Hygro vector construct and then protein samples collected to confirm transient protein expression of the target proteins. The expected band for iNOS-V5 tagged protein was observed at 131.4 kDa, consisting of iNOS; 130 kDa and the V5 epitope tagged of 14 amino acids (1.42 kDa) in BNL CL2 (Fig 4.3.15 (A)) and 3T3 L1 cells (Fig 4.3.15 (B)). The control (to confirm transfection had worked) reporter eGFP protein expression was observed at 26 kDa (Fig 4.3.16).

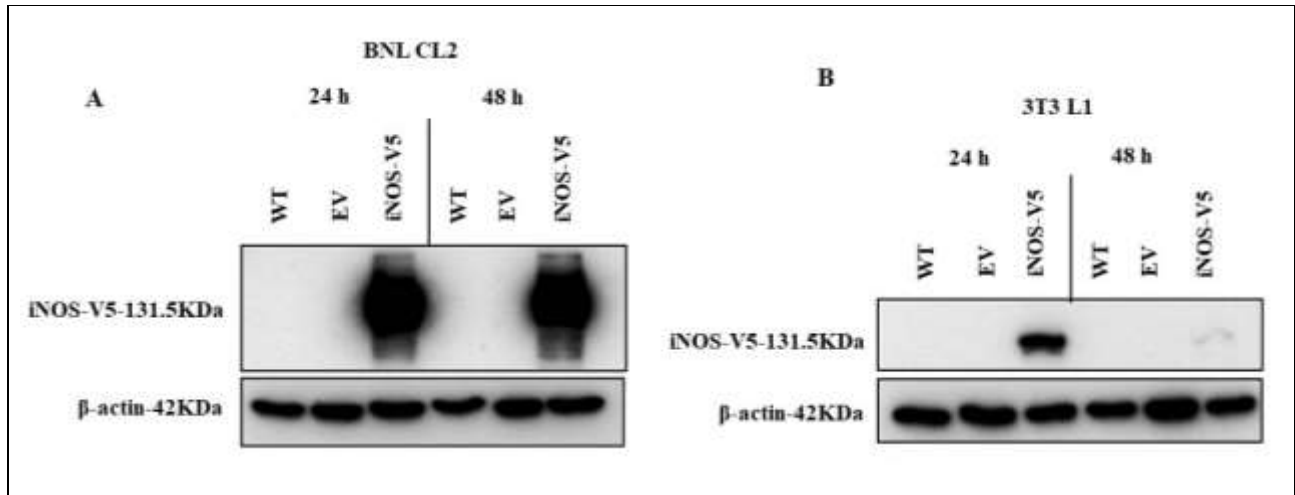


Figure 4.3.15. Western blot of transient expression of iNOS-V5 tagged protein in BNL CL2 (A) and 3T3 L1 cells (B).

The blots display the protein bands for iNOS-V5 tagged protein and the reference protein; β-actin at time points 24 and 48 h in both BNL CL2 and 3T3 L1 cells. The expected band for iNOS-V5 tagged protein was observed at 131.4 kDa. (WT; protein samples prepared from wild type cells, either BNL CL2 or 3T3 L1 cells, EV; 3.1/ Hygro-V5-His-TOPO empty vector transfected in either BNL CL2 or 3T3 L1 cells).

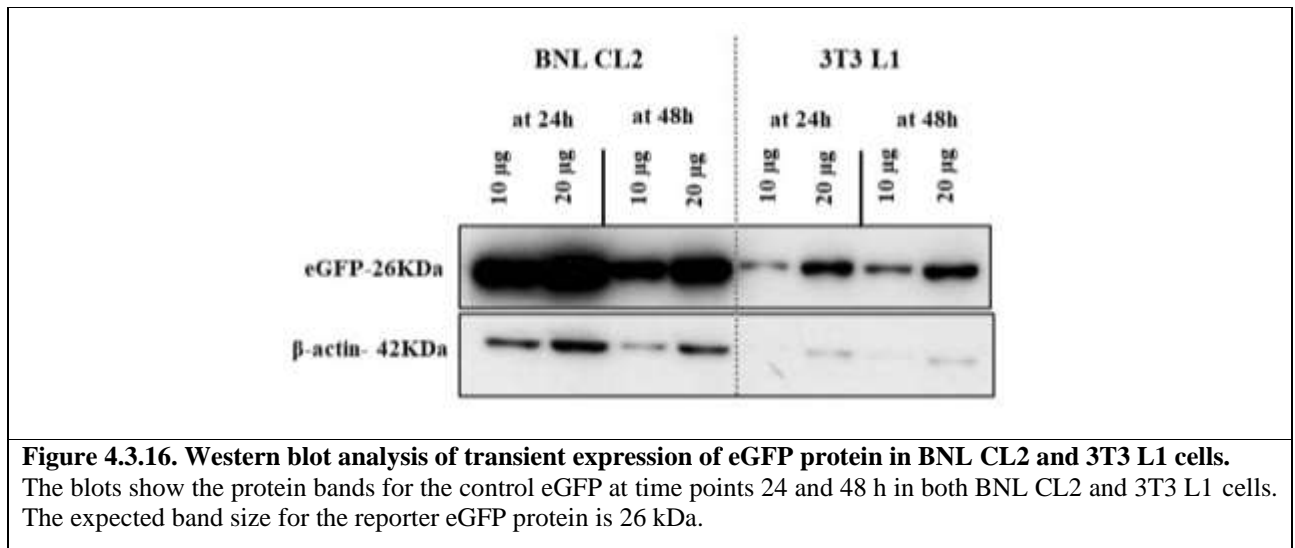


Figure 4.3.16. Western blot analysis of transient expression of eGFP protein in BNL CL2 and 3T3 L1 cells.

The blots show the protein bands for the control eGFP at time points 24 and 48 h in both BNL CL2 and 3T3 L1 cells. The expected band size for the reporter eGFP protein is 26 kDa.

4.3.7. Immunofluorescence analysis of transiently expressed iNOS-V5 in 3T3 L1 cells

To confirm the presence and localisation of the exogenous iNOS, indirect immunofluorescence staining and imaging was performed for iNOS-V5 epitope tagged recombinant protein, native or endogenous AMPK and ACC-1 proteins in 3T3 L1 cells. The resulting fluorescence images are presented in **Fig 4.3.17**.

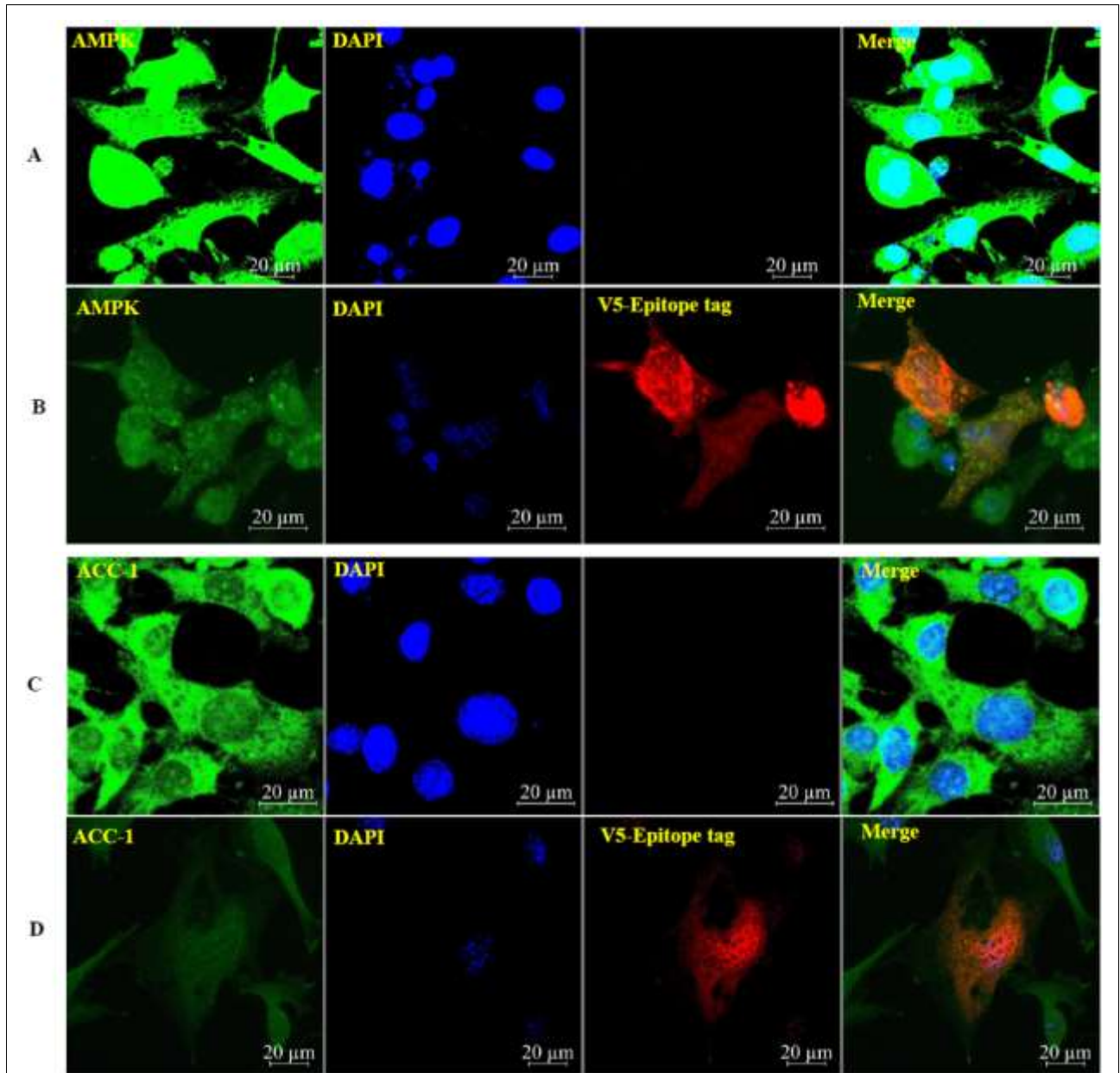


Figure 4.3.17. Combined immunofluorescent images of endogenous AMPK and ACC-1 proteins and V5 tagged iNOS protein in 3T3 L1 cells transfected with iNOS-V5-tagged plasmid and 3.1/V5-His-TOPO empty vector.

3T3 L1 cells were transiently transfected with either iNOS-V5 tagged plasmid or 3.1/V5-His-TOPO Hygro empty vector for a 24 h and then cells were fixed and permeabilized followed by conjugation with FITC (green), TRITC (red) and nuclear stain DAPI (blue) and imaged using a confocal microscopy. Green stain; endogenous AMPK or ACC-1 protein, blue stain; nucleus, red stain; anti-V5. The last merged image shows an overlay of green, blue and red. Stained images of the cells in top panels; **A**, the control empty vector cells staining for endogenous AMPK protein and V5 tag; **B**, the iNOS-V5 tagged cells staining for endogenous AMPK protein and V5 tagged iNOS protein. The images in panels **C**; the control empty vector cells staining for endogenous ACC-1 protein and V5 tag and **D** the iNOS-V5 tagged cells staining for endogenous ACC-1 protein and V5 tagged iNOS proteins.

4.3.8. Nitric oxide (as NO₂⁻) measurement in stably expressing iNOS-3T3 L1 cells upon culturing in different concentrations of L-Arg

As described in the introduction chapter, the L-Arg/NOS/NO pathway is the major source of culture supernatant nitrite. The relative (A) and absolute concentrations (B) of culture supernatant nitrite is shown in Fig 4.3.18.

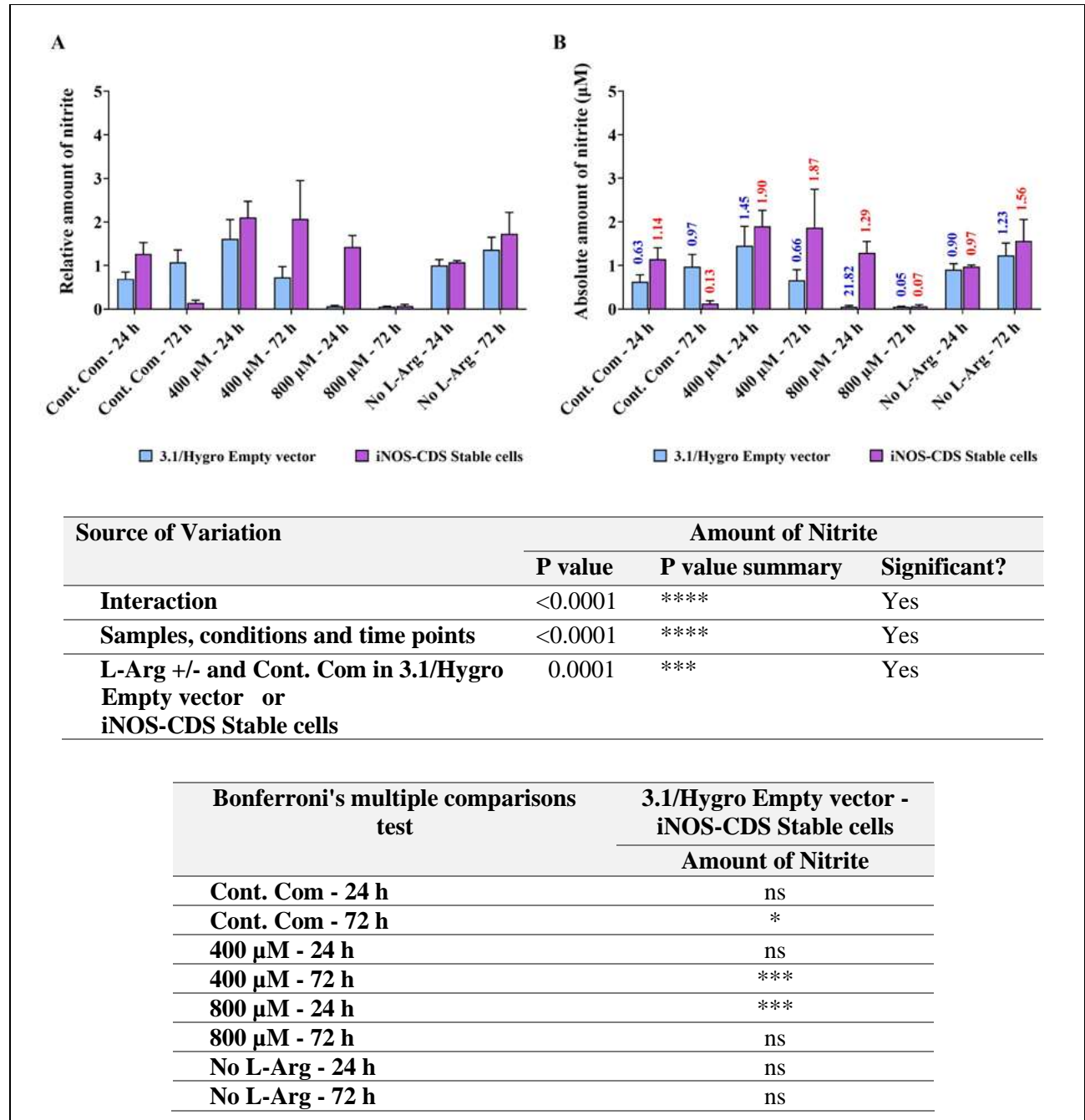


Figure 4.3.18. The effect of exogenous L-arginine concentration on nitrite production in stably expressing iNOS and the control empty vector 3T3 L1 cells.

Cell culture supernatant was obtained from cultured cells grown in the presence of 0, 400 or 800 µM L-arginine and the control complete DMEM for 24 or 72 h. The data are expressed as relative (A) and absolute (B) values. Relative

plasma nitrite values obtained by normalising the quantified nitrite to the nitrite amount presence in empty vector 3T3 L1 cells cultured in no L-arginine SILAC DMEM (0 μ M L-arginine) at 24 h. Data points represent the mean \pm SD. Error bars represent the standard deviation from the mean (n = 3). The tables summarise two-way ANOVA followed by a Bonferroni multiple comparison test using GraphPad Prism 9.4.1. The stars indicate the levels of significance; ns = P > 0.05, * = P \leq 0.05, ** = P \leq 0.01, *** = P \leq 0.001 and **** = P \leq 0.0001.

Supernatant levels of nitrite were significantly higher (P<0.001) in stably expressing iNOS 3T3 L1 cells treated with L-Arg and complete DMEM after 24 h (control; 1.81-fold, 400 μ M; 1.31-fold, 800 μ M; 22.63-fold and 0 μ M; 1.08-fold) compared to the samples cultured in empty vector 3T3 L1 cells at 24 h. When the stable iNOS cells were grown in different L-Arg concentrations (0, 400 and 800 μ M), after 72 h there was generally increased (P<0.0001) nitrite (400 μ M; 2.84-fold, 800 μ M; 1.19-fold and 0 μ M; 1.27-fold). **Figure 4.3.18** summarises the nitrite concentrations observed with the different cells and conditions investigated in the study.

4.3.9. HPLC amino acid analysis in stably expressing iNOS-3T3 L1 cells upon culturing in different concentrations of L-Arg

The effect of L-arginine supplementation on the amount of selected supernatant amino acids L-arginine, L-citrulline and L-ornithine of either stably expressing iNOS or empty vector 3T3 L1 cells cultured in different concentrations of L-Arg (0, 400 and 800 μ M) and the control complete DMEM after 24 h was determined. The relative (**A**) and absolute (**B**) concentrations of selected plasma amino acids are shown in **Fig 4.3.19** and **Fig 4.3.20**. The amount of L-Arg present in the supernatant samples increased (P<0.001) in the stably expressing iNOS cells (control 1.25-fold, 400 μ M; 1.31-fold and 0 μ M; 1.16-fold high in stable cells) compared to the empty vector 3T3 L1 cells, except when the cells were grown in high concentration of L-Arg (800 μ M) after 24 h.

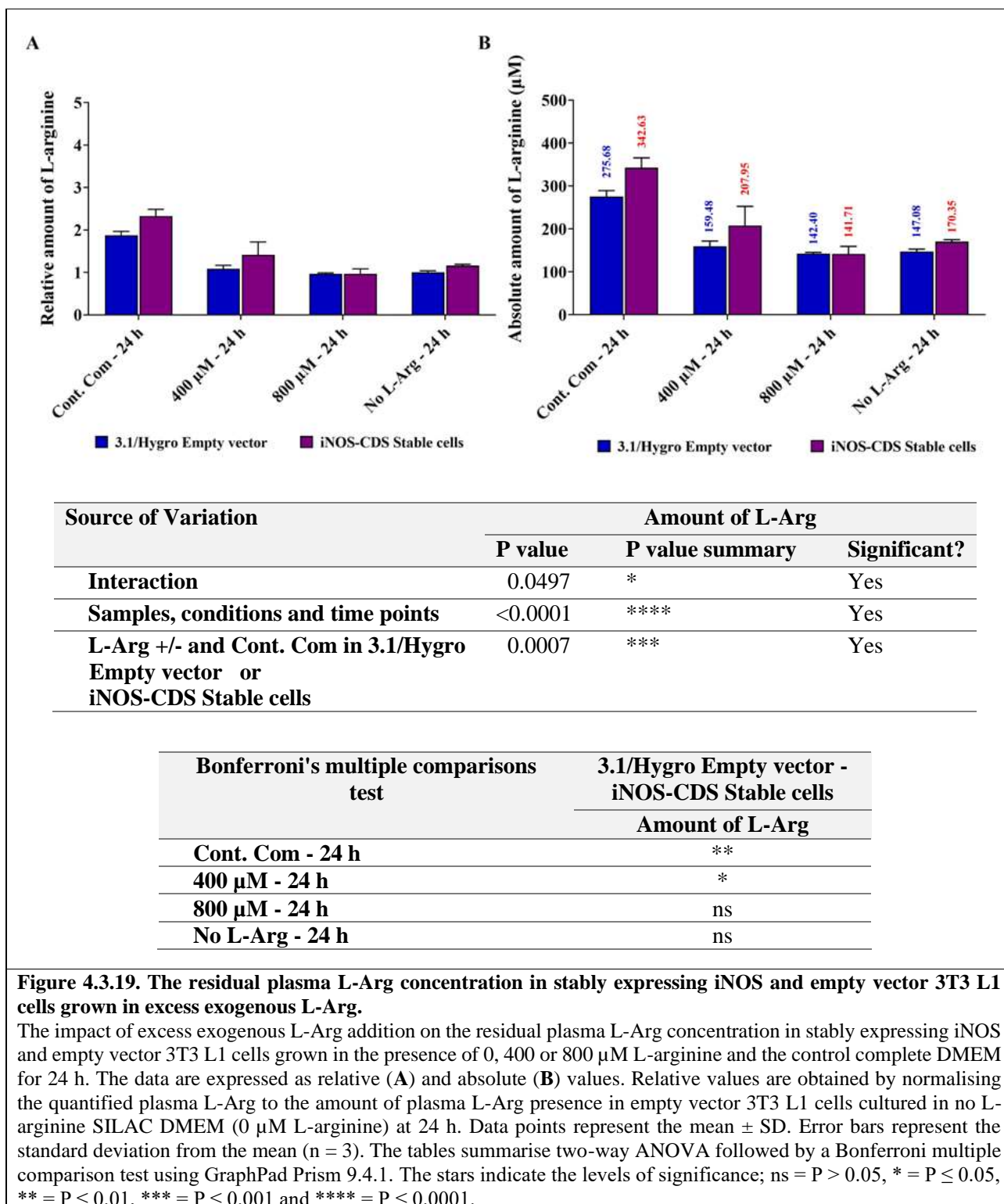
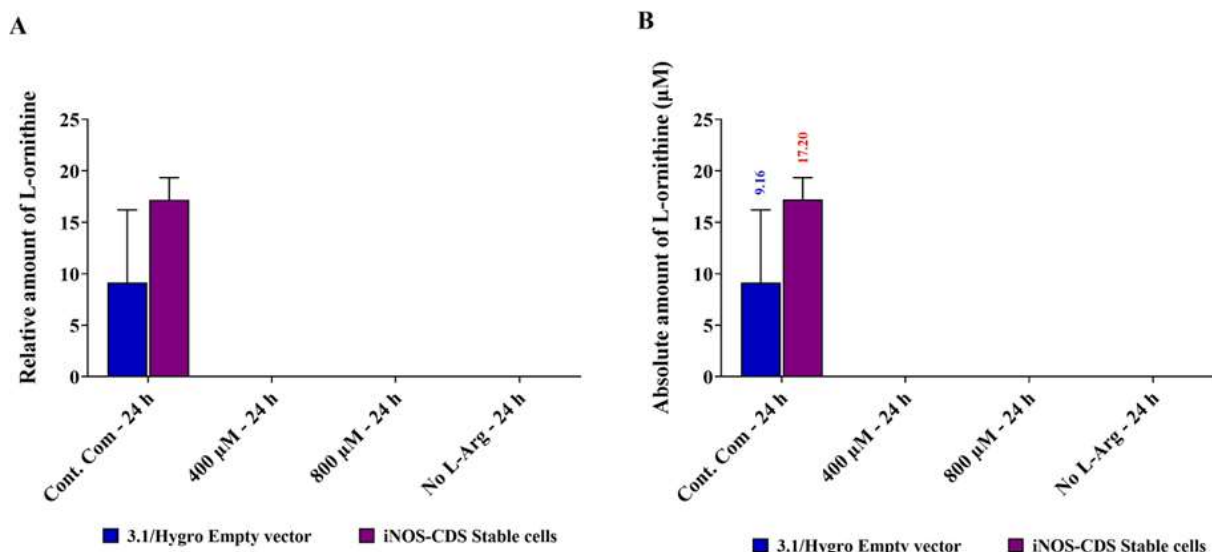


Figure 4.3.19. The residual plasma L-Arg concentration in stably expressing iNOS and empty vector 3T3 L1 cells grown in excess exogenous L-Arg.

The impact of excess exogenous L-Arg addition on the residual plasma L-Arg concentration in stably expressing iNOS and empty vector 3T3 L1 cells grown in the presence of 0, 400 or 800 µM L-arginine and the control complete DMEM for 24 h. The data are expressed as relative (A) and absolute (B) values. Relative values are obtained by normalising the quantified plasma L-Arg to the amount of plasma L-Arg presence in empty vector 3T3 L1 cells cultured in no L-arginine SILAC DMEM (0 µM L-arginine) at 24 h. Data points represent the mean ± SD. Error bars represent the standard deviation from the mean (n = 3). The tables summarise two-way ANOVA followed by a Bonferroni multiple comparison test using GraphPad Prism 9.4.1. The stars indicate the levels of significance; ns = P > 0.05, * = P ≤ 0.05, ** = P ≤ 0.01, *** = P ≤ 0.001 and **** = P ≤ 0.0001.

L-citrulline, the metabolite and precursor of L-Arg/NOS pathways was not detected while for L-ornithine (Fig 4.3.20) there was no detectable amounts in the samples cultured in different L-Arg concentrations (0, 400 and 800 µM).



Source of Variation	Amount of L-Orn		
	P value	P value summary	Significant?
Interaction	0.0374	*	Yes
Samples, conditions and time points	<0.0001	****	Yes
L-Arg +/- and Cont. Com in 3.1/Hygro Empty vector or iNOS-CDS Stable cells	0.0766	ns	No

Bonferroni's multiple comparisons test	3.1/Hygro Empty vector - iNOS-CDS Stable cells
	Amount of L-Orn
Cont. Com - 24 h	**
400 µM - 24 h	ns
800 µM - 24 h	ns
No L-Arg - 24 h	ns

Figure 4.3.20. The residual plasma L-Orn concentration in stably expressing iNOS and empty vector 3T3 L1 cells grown in excess exogenous L-Arg.

The impact of excess exogenous L-Arg addition on the residual plasma L-Orn concentration in stably expressing iNOS and empty vector 3T3 L1 cells grown in the presence of 0, 400 or 800 µM L-arginine and the control complete DMEM for 24 h. The data are expressed as relative (A) and absolute (B) values. Relative values are obtained by normalising the quantified plasma L-Orn to the amount of plasma L-Orn presence in empty vector 3T3 L1 cells cultured in no L-arginine SILAC DMEM (0 µM L-arginine) at 24 h. Data points represent the mean ± SD. Error bars represent the standard deviation from the mean (n = 3). The tables summarise two-way ANOVA followed by a Bonferroni multiple comparison test using GraphPad Prism 9.4.1. The stars indicate the levels of significance; ns = P > 0.05, * = P ≤ 0.05, ** = P ≤ 0.01, *** = P ≤ 0.001 and **** = P ≤ 0.0001.

4.4. Discussion

4.4.1. Trouble shooting of endogenously induced iNOS transcript expression

As explained in the introduction chapter, NOS-2 or inducible NOS (iNOS) is not expressed constitutively and thereby induces by a combination of inflammatory lipopolysaccharide and certain cytokines (McAdam *et al.*, 2012; Tengan, Rodrigues and Godinho, 2012). At first, BNL CL2 and 3T3L1 cells were treated with lipopolysaccharide (LPS), proinflammatory factor (Skrzypczak-Wiercioch and Sałat, 2022) and RNA samples were collected at 24 and 72 h, however in such samples iNOS transcript was not observed. Consequently, the LPS (8 µg) amount was doubled and shorter time points examined to allow for the short half-life of iNOS, therefore, samples were collected at 6, 24 and 48 h. From these samples the expected band and a non-specific band by agarose gel analysis was observed for the amplicon product of one-step qRT-PCR. Two-step qRT-PCR was undertaken to increase the iNOS priming with the template of BNL CL2 and 3T3 L1 RNA. Specific and non-specific bands of the amplicon products were observed constantly in the agarose gel image. Therefore, an attempt to remove the non-specific band was undertaken by running a gradient qRT-PCR and then the 'best' annealing temperature (64.2°C) was used in non-gradient qRT-PCR however the non-specific bands were observed in the agarose gel image. The qRT-PCR analysis with different iNOS primers suggested that there was a strong cross reaction of the iNOS primers with other non-target sequences in mouse. Therefore, the non-specific bands at 250 bp were observed in all iNOS primer testing in BNL CL2 and 3T3 L1 cell RNA. This problem was analysed by checking the similar sequences for iNOS in mouse. One sequence, sialic acid synthase (sequence similarity with iNOS is 80%), may give an amplicon of 367 bp that could produce a possible non-specific band. It is also possible that the *iNOS* gene is not expressed/induced in cells or that the time period when it is present in the cells was not sampled. Therefore, a positive control, pBS-iNOS with the *iNOS* gene cloned was generated to optimise an assay to determine if the assay was specific, if the transcript was present and if over expression of iNOS exogenously in cells impacts downstream targets and responses to different cell culture media L-arginine concentrations.

4.4.2. Over and constitutive expression of iNOS

This study was designed to investigate how stably over-expressed iNOS impacts the L-arginine/iNOS/NO pathway and subsequent signalling pathways. Thus, the aim of this chapter was to clone the iNOS and subsequently generate stably over-expressing 3T3 L1 cells. For iNOS transcript analysis, iNOS constructs were established using a positive control plasmid pBS-iNOS containing the *iNOS* gene. Given the large size of iNOS, the cloning of iNOS was not expected to be straightforward. The first part consisted of a PCR amplification step using two sets of primers. One set of primers covered the region that included the untranslated region (UTR) of the *iNOS* transcript and another set of primers covered the region of the ORF of the iNOS transcript only. Each of these primers contained recognition sites for restriction enzymes for cloning the fragments. The

authenticity of iNOS inserts in pcDNATM3.1/Hygro (+) was confirmed by sequencing using T7 and BGHR universal sequencing primers. Based on the sequence alignments shown in **appendix III**, sequence was as expected.

To identify genes impacted by over-expression of iNOS, qRT-PCR analysis was used. The results reported as relative expression are presented in **Fig 4.3.12**. In stable iNOS 3T3 L1 cells cultured after 24 h, relative iNOS mRNA expression was higher compared to the empty vector 3T3 L1 cells. In both stable iNOS and empty vector 3T3 L1 cells, after 24 h, there was decreased iNOS transcript expression in excess exogenous L-Arg culture samples compared to that of complete DMEM control samples and 0 μ M L-Arg.

It has been demonstrated that the energy sensing gene, AMPK was decreased in stable iNOS 3T3 L1 cells with excess L-Arg at 400 and 800 μ M, but increased in the control complete DMEM, samples cultured with 0 μ M L-Arg after 24 h and untreated samples at T=0, compared to samples cultured in empty vector 3T3 L1 cells. It is noteworthy that the relative gene expression of AMPK in stable cells cultured in L-Arg at 400 and 800 μ M and in the control was very similar. However, when culture supernatant nitrite was investigated, the amount of nitrite observed in the samples cultured in 800 μ M L-Arg in stably expressing iNOS cells at 24 h was high (1.29 μ M) compared to the empty vector cells (0.057 μ M) while 400 μ M L-Arg additions also showed high nitrite after 24 h compared to the control. An iNOS-CDS-V5 tagged construct was also established (**Appendix IV**).

Chapter-5 Overall Summary and Future Directions

5.1. Overall Summary and Discussion

Here the impact of excess exogenous L-Arg in the media of *in-vitro* cultured model cell lines and the subsequent impact on NO signalling and L-Arg metabolism has been investigated. Previous studies have reported that dietary arginine supplementation reduces fat mass in obese animal models (Fu *et al.*, 2005) and humans with type-2 diabetes (Lucotti *et al.*, 2006). The goal of this study was to investigate how excess L-Arg perturbed the L-Arg/NOS/NO metabolic pathways in *in-vitro* cultured insulin sensitive cells from the liver (BNL CL2) and adipocytes (3T3 L1). As outlined elsewhere in the thesis (introduction chapter) synthesis of NO requires a number of co-factors including BH₄ and the biological availability of NO is affected by the iNOS inhibitor L-NAME and the NO donor SNAP. The first part of the study was designed to evaluate the effect of L-arginine on metabolism of the cells, the second part was conducted to investigate the effect of modulators of NO synthesis (L-NAME, BH₄ and SNAP), and the third to investigate the impact of overexpression of iNOS in 3T3 L1 recombinant pools.

Excess L-Arg addition impacted cell culture parameters such as culture viability and viable number of cells. Increasing the concentration of L-Arg generally positively impacted culture viability and the viable number of cells. In BNL CL2 hepatocytes (**Fig 2.3.3A** and **2.3.13**) and 3T3 L1 adipocytes (**Fig 2.3.24A** and **Fig 2.3.34**), transcript and protein levels of AMPK increased in response to elevated extracellular concentrations of L-Arg, whilst AMPK protein phosphorylation was also high in BNL CL2 (**Fig 2.3.13**) but low in 3T3 L1 cells compared to the control (**Fig 2.3.34**). This reflects L-arginine stimulation of AMPK changes in expression and activity, especially in hepatocytes, which have an extremely active intrinsic metabolic activity that can be modulated to adapt to physiological needs. Excess L-Arg addition did not impact on the active form of AMPK (**Fig 2.3.34**) in 3T3 L1 cells, consequently phosphorylated ACC-1 level was low (**Fig 2.3.35**) in the cells over to the control. These results are not consistent with the findings of a previous *in-vivo* study in whole animals where dietary arginine supplementation increased the metabolism of energy substrates in adipose tissue (Fu *et al.*, 2005). This may reflect the difference between *in-vitro* culture cell models and whole animal models.

Phosphorylation of ACC and regulation of β -oxidation are consecutive progresses when AMPK is activated by naturally synthetic compounds (Ahn *et al.*, 2008; Johnson *et al.*, 2016; Dugdale *et al.*, 2018). Along with the activation of AMPK in BNL CL2 cells, protein levels for phosphorylated ACC-1 (**Fig 2.3.14**), which is negatively related to its activity, increased in response to L-arginine treatment, while mRNA (**Fig 2.3.3B**) and protein expression of ACC-1 (**Fig 2.3.14**) were also increased. Previous studies have reported that animals fed on a typical chow diet had a half-life greater than 48 h for ACC-1 turnover in liver and adipose tissue and when gene expression and protein turnover of ACC-1 was investigated there was tight control between mRNA and protein expression (Brownsey, Zhande and Boone, 1997). The work undertaken here shows a time dependent

change in ACC-1 in liver BNL CL2 cells for ACC-1 mRNA (**Fig 2.3.3B**) and protein expression (**Fig 2.3.14**) increased at 400 and 800 μ M after 72 h. There was not, however an obvious link between the mRNA and protein expression of ACC-1 in 3T3 L1 cells (**Fig 2.3.35**).

Another target investigated, CPT-1, is located in the mitochondrial outer membrane. In this study, excess L-arginine did not modulate mRNA (**Fig 2.3.4A**) or protein expression of CPT-1 (**Fig 2.3.15**) in liver BNL CL2 cells. This result is not consistent with the report that NO can stimulate fatty acid oxidation through reducing ACC activity and enhancing CPT-1 activity in rat hepatocytes (García-Villafranca, Guillén and Castro, 2003). In this study ACC-1 protein expression was increased but there was no observable impact on CPT-1 protein expression in excess L-Arg. However, interestingly CPT-1 expression was high at the mRNA (**Fig 2.3.25A**) and protein (**Fig 2.3.36**) level in L-Arg treated samples in adipocyte 3T3 L1 cells, where fatty acid synthesis is essentially high (Kim, Leahy and Freake, 1996). Therefore, presumably L-Arg addition regulates fatty acid content in adipose tissue by decreasing ACC-1 phosphorylation and increasing expression of CPT-1 in L-Arg treated adipose tissues.

Previous reports also suggest that HMG CoA reductase inhibitors may have beneficial effects in atherosclerosis beyond that attributed to the lowering of serum cholesterol by increasing eNOS activity (Laufs *et al.*, 1998). Therefore, presumably HMGCR has significant impact on the NOS/NO signalling pathway. HMGCR (**Fig 2.3.4B**) and SREBP-2 (**Fig 2.3.5B**) involved in cholesterol synthesis were reduced in transcript level in L-Arg treated BNL CL2 cells and also post-translational modifications of the protein such as mature forms of SREBP-2 (**Fig 2.3.20**) and the catalytically inactive N-terminal forms of HMGCR (**Fig 2.3.18**) which were higher than in control samples. Even though the transcript expression was high for HMGCR (**Fig 2.3.25B**) and SREBP-2 (**Fig 2.3.26B**), in 3T3 L1 cells, the catalytically active form of HMGCR (**Fig 2.3.39**) and SREBP-2 (**Fig 2.3.41**) were low in L-Arg treated samples. Lipid intake, transfer and storage are regulated by many genes involved in the glycolytic and lipogenic pathway. One of the vital transcription factors that regulates hepatic lipid metabolism is SREBP-1c (Rui, 2016). In this study, SREBP-1 expression was reduced at the transcript level in both cells (**Fig 2.3.5A and Fig 2.3.26A**), whereas there was an increase in the mature protein form of SREBP-1 in the liver cells (**Fig 2.3.19**), but reduced in adipose cells (**Fig 2.3.40**) cultured with excess L-Arg.

Cells detect changes in amino acid availability and alter signal transduction pathways to respond to the integrated signalling input by also either upregulating or downregulating translation initiation (Kimball and Jefferson, 2004). Protein synthesis has been stimulated in the liver and skeletal muscle of fasted rats, when feeding a meal containing a complete mixture of essential amino acids, but has no effect on eIF2 α phosphorylation or eIF2B activity. In contrast, increases in eIF2 α phosphorylation and decreases in eIF2B activity have been observed in liver when feeding a diet lacking a single essential amino acid (Kimball and Jefferson, 2004). In this study, when BNL CL2 cells were cultured in 400 μ M additional L-Arg, there was no

overall effect on eIF2 α phosphorylation but at 800 μ M this was changed at 24 (high) and 72 h (low) compared to the control (**Fig 2.3.17**). Noticeably, overall, phosphorylation of eIF2 α was moderately (or less) regulated by excess L-Arg in 3T3 L1 cells (**Fig 2.3.38**). These data show that global translation is modified by the cell as it senses different concentrations of exogenous (and presumably intracellular) L-Arg, presumably to ensure that a homeostasis of metabolism is maintained. This is further evidenced by the fact that phosphorylated eIF2 α was high at 800 μ M for 24 h (RE 0.21) in BNL CL2 cells (**Fig 2.3.17**), which would slow global translation and there was also higher phosphorylation of eEF2 under the same condition (RE 5.8) in BNL CL2 cells (**Fig 2.3.16**).

Dietary L-arginine (1%) supplemented into animal models has been shown to increase the level of plasma L-Arg to 500 μ M (Wu *et al.*, 2007). L-Arg is catabolized by multiple pathways to form NO, L-citrulline, L-ornithine and proline in cultured cells (Wu & Morris, 1998). When the BNL CL2 cells were grown in exogenous 800 μ M L-arginine, after 24 h cell culture supernatant nitrite concentrations were high (**Fig 2.3.21**) and the metabolite of L-Arg/arginase pathway L-Orn was also increased (**Fig 2.3.50**). Similar impacts were observed in the 3T3 L1 cells cultured in excess L-Arg at 400 and 800 μ M concentrations (**Fig 2.3.42**).

It has been reported that hypercholesterolemia associated with elevation of LDL cholesterol can be reduced by chronic oral administration of synthetic NO donor which could be interact with metabolism of lipoproteins in the liver. The NO-generating drugs appear to affect metabolism of lipoproteins directly in the liver via a cellular sterol-independent mechanism (Kurowska and Carroll, 1998). Interestingly, in the absence of L-NAME, increasing extracellular concentrations of arginine from 0 to 800 μ M increased NO synthesis and consequently AMPK and ACC-1 mRNA and protein expressions in both BNL CL2 and 3T3 L1 cells. The investigation of the effect and mechanism of action of the NOS inhibitor L-NAME on the expression of AMPK and ACC-1 in BNL CL2 and 3T3 L1 cells revealed that an inhibition of NO synthesis moderately attenuated the effect of L-arginine on the expression of AMPK (and ACC-1) at the mRNA and protein level, but greatly impacted the amount of nitrite in the cell culture supernatant (**Fig 3.3.13** and **Fig 3.3.37**) and residual amino acids in BNL CL2 (**Fig 3.3.16-Fig 3.3.18**) and 3T3 L1 cells (**Fig 3.3.40-Fig 3.3.42**). In addition to modulating AMPK and ACC-1 mRNA and protein expression, BH₄, a co-factor of iNOS and SNAP, an external NO donor regulated the culture concentrations of the metabolites dependent on L-Arg concentration and culture time. From the data presented in this thesis, the proposed mechanisms and cellular responses by which liver cells (BNL CL2) or adipose cells (3T3 L1) respond to excess exogenous L-Arg (400 and 800 μ M) and its modulators (L-NAME, BH₄ and SNAP) are summarised in **Fig 5.1.1** and **Fig 5.1.2**.

whereas it increased after 24 h in samples cultured with 0 μM L-Arg and control complete DMEM empty vector 3T3 L1 cultures (Fig 4.3.12). These results show that iNOS can be modulated by addition of exogenous gene copies and forms the basis for approaches to further investigate iNOS activity and functions in *in-vitro* cultured liver cells.

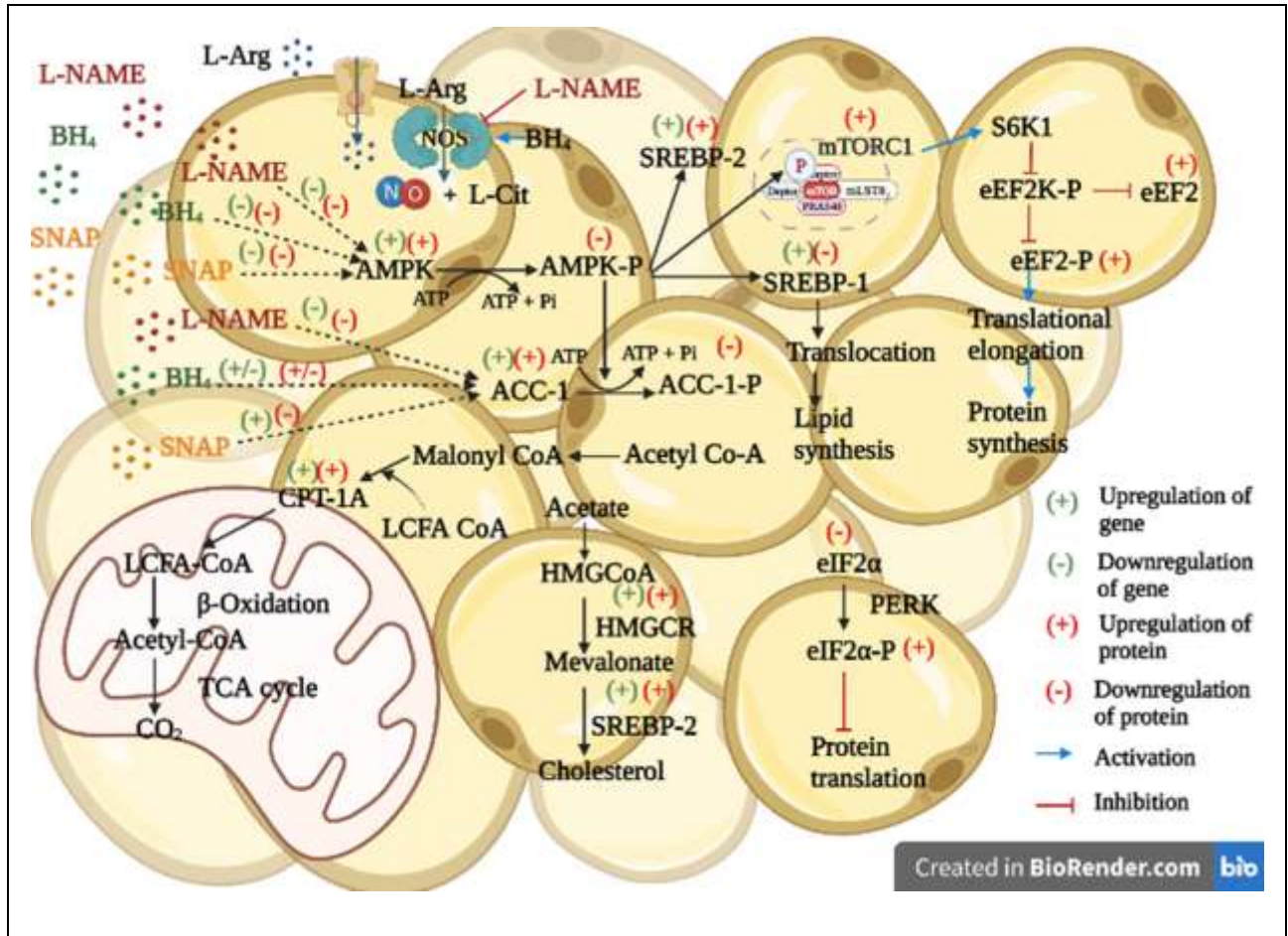


Figure 5.1.2. Putative cell signalling pathway of L-Arg/NOS/NO and regulation of this pathway by the modulators L-NAME, BH₄ and SNAP in adipose cells.

The proposed mechanisms responsible for the beneficial effect of L-Arg/NOS/NO on the metabolic pathways in mammalian adipose cells, 3T3 L1. The symbol (+) denotes an upregulation in gene expression or protein expression. The symbol (-) denotes a downregulation of gene expression or protein expression.

5.2. Future directions

At the transcript (mRNA) and protein levels, the effect of exogenous L-arginine concentrations on AMPK expression was generally similar with a large difference at 400 μM after 72 h and 800 μM after 24 h (Fig 2.4.1). There are several metabolic signalling pathways that cross-talk with AMPK to coordinate responses to nutritional and hormonal signalling of cells (Garcia and Shaw, 2017), which may explain this time-dependent relationship between changes in transcription before changes in protein synthesis were observed. In future studies, it would be interesting to determine if the decrease in transcript levels in 400 μM cultures at 72 h

resulted in a decrease in protein levels at a later time point. AMPK is a heterotrimeric complex composed of a catalytic α -subunit and two regulatory β - and γ -subunits (Kim *et al.*, 2012). Further, in this study AMPK transcript expression was analysed by monitoring one of the catalytic subunits of AMPK isoforms; AMPK α 1. However, in the protein analysis the primary antibody detects both isoforms of AMPK α (AMPK α 1 and AMPK α 2) but does not distinguish the isoforms present in the samples. This may also account for differences between the protein and transcript data. Therefore, in future, to find the isoform specific activity of AMPK and to investigate which isoform is phosphorylated by excess L-Arg would clarify whether L-Arg impacts regulatory or catalytic activity of the energy sensor of the cells; AMPK.

In order to better understand how arginine controls AMPK gene expression and protein phosphorylation in a cell-specific manner, further research is needed. The unique guanidino group in the chemical structure of arginine (**Fig 1.1.1**) may contribute to its action. AMPK expression and phosphorylation may be directly regulated by this amino acid in various cell types. It is possible to address this question by using nonmetabolizable arginine (including D-arginine). It has been reported that upregulating the expression of GTP cyclohydrolase-I in endothelial cells (Shi *et al.*, 2004) and increasing level of phosphorylation of mTOR in intestinal cells (Rhoads *et al.*, 2007) have been directly linked to arginine addition.

The breakdown product of nitric oxide, nitrite, is oxidized within the body to nitrate. It is most common to measure the stable end-products of NO metabolism, nitrite (NO_2^-) and nitrate (NO_3^-). NO can undergo a series of reactions within biological tissues, as described below (**Fig 5.1.3**) (Titherade, 1998).

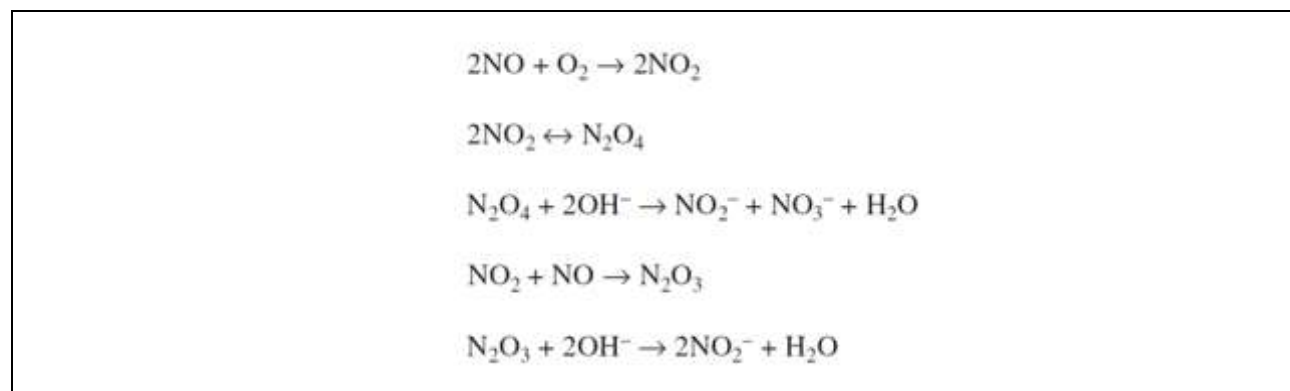


Figure 5.1.3. Series of reaction and oxidized congeners of NO.

Nitrogen dioxide is formed due to the oxidation of nitrogen oxides in the presence of oxygen. Nitrogen dioxide is also a free radical, but in contrast to nitric oxide, does readily dimerise, setting up the equilibrium. In alkaline condition, again there is a production of mixture of NO_2^- and NO_3^- from the oxidised products of NO.

While nitrite is often used alone as a measure of NO metabolism (we measured cell culture supernatant nitrite using Griess assay), nitrate is also formed in these reactions, and haem iron-containing proteins may further oxidize nitrite into nitrate in biological systems (Titherade, 1998). It is therefore difficult to determine the extent of NO metabolism without measuring both nitrite and nitrate, since the ratios of these two end-products

are variable and dependent upon the sample origin (Titherade, 1998). Therefore, it would be useful to measure both nitrite and nitrate in future to analyse the impact of L-Arg on physiological pathways by producing a biomarker NO. There are modified protocols that can be used for identifying nitrite and nitrate. The simultaneous measurement of nitrate and nitrite using the NADPH-nitrate reductase was first described by Wu and Brosnan (Wu and Brosnan, 1992) and is based upon the reduction of nitrate to nitrite using NADPH and measurement of the total nitrite formed with the Griess reagent. This method was subsequently modified by Verdon et al. (Verdon, Burton and Prior, 1995) by the inclusion of a glucose-6-phosphate/glucose-6-phosphate dehydrogenase NADPH-regenerating system to prevent the interference with colour development in the Griess reaction caused by the high concentrations of NADP⁺ (Titherade, 1998).

The arginine-derived products by the NOS and arginase enzyme-catalysed reactions were investigated by HPLC to quantify residual amino acids. HPLC can be employed to identify directly (detect the derivatised amino acid adduct) the products of arginine metabolism. In some cells or tissues, especially in liver cells, however, other pathways of arginine metabolism are present and the products formed may fail to be separated from arginine, from each other, or from citrulline or ornithine using the HPLC method described in this work. For example, the widely distributed enzyme arginase can hydrolyze arginine to ornithine and urea. Using the HPLC method, it is not possible to distinguish ornithine from arginine or citrulline from arginine. Monitoring conversion of radiolabelled arginine to citrulline, the co-product of the nitric oxide synthase (NOS)-catalysed reaction or arginine to ornithine, the co-product of arginase catalysed reaction would distinguish the catabolic products of L-Arg. Therefore, for residual amino acids analysis radiolabelled L-Arg can be used to identify the amount of L-Cit or L-Orn produced from L-Arg metabolic pathway using ion-exchange separation. This separation procedure allows quantification of the relative activities of NOS and arginase in cell and tissue extracts by permitting identification of radiolabelled arginine-derived citrulline and/or ornithine. This method is useful, therefore, as a means to identify arginine-derived citrulline and/or ornithine, to assess the contribution of pathways other than that catalysed by NOS to the generation of arginine-derived products, and to simultaneously monitor NOS and arginase activities in the cells. Further, ornithine and proline are the major products of arginine catabolism via the arginase pathway (Morris, 2009). Analysing the residue proline could also help explain the effect of arginine on metabolism in these cell types. Whether ornithine and/or proline affect metabolic pathway through arginase enzyme in BNL CL 2 hepatocytes and 3T3 L1 adipocytes remains to be determined.

Elongation factor 2 is regulated by phosphorylation of its threonine 56 residue by eEF2K. Phosphorylation of the Thr56 residue deactivates eEF2, blocking its interaction with the ribosome and prevents polypeptide elongation (Ma and Blenis, 2009; Kenney *et al.*, 2014). The activity of this kinase is dependent on calcium ions and calmodulin and eEF2K is the only calcium/calmodulin (Ca/CaM)-activated α -kinase (X. Wang *et al.*,

2014). NOS synthase (eNOS and nNOS) activity is also linked to the calcium and calmodulin pathway (Förstermann and Sessa, 2012). Therefore, it would be useful to investigate a direct link of eEF2K protein expression along with the L-Arg addition.

In-vitro studies such as those described here are important in that they allow laboratory-based studies in cell culture systems. *In-vivo* studies provide further valuable information regarding the effects of a particular substance or disease progression in a whole, living organism. Here it is shown that excess exogenous L-Arg (400 and 800 μ M) impacts metabolism in mammalian liver and adipose tissue. In future, an *in-vivo* study to determine if these concentrations are safe and effective in intact organisms (using mouse as an animal model), when the animal model supplement with different concentrations of L-Arg (400 and 800 μ M) and the controls L-alanine (as a negative control amino acid) and/or saline water would need to be undertaken to confirm the *in vitro* results transfer to a whole animal.

There has been interest in assessing whether delivery of specific amino acids can improve patient outcome under various pathological conditions (Kurokawa *et al.*, 2012). L-glutamine is the most plentiful amino acid in the human body and plays an important role in catabolic states and is a crucial factor in various cellular and organ functions (Kurokawa *et al.*, 2012). L-glutamine and L-arginine, conditionally essential amino acids, are able to work together to improve inflammation response (Lecleire *et al.*, 2008); however, L-arginine reduced L-glutamine's antioxidant properties (El-Sheikh and Khalil, 2011). Although there is a lack of research on the combined effects of L-arginine and L-glutamine, the preliminary data shows that combining the two may benefit those with intestinal inflammation in cultured colonic biopsies from patients with active Crohn's disease (CD) (Lecleire *et al.*, 2008). In the current study, one of the products of L-Arg/NOS pathway; L-Cit was unexpectedly very much high in untreated samples at T=0, when the cells were grown in complete DMEM media, which formulated with high concentration of Glutamine (**Appendix II, Table 5.2.1**). The present study was undertaken to evaluate the effects of an L-arginine, in future comparing this with supplementation with L-glutamine and L-alanine (the latter as a negative control) might be useful to analyse if there is a combination effect of these amino acids in BNL CL2 and 3T3 L1 cells.

L-arginine may be useful as an exercise supplement in different capacities. It has been shown that L-arginine can prolong exercise ability in people suffering from congestive heart failure (Mendes-Ribeiro *et al.*, 2009). In order to increase blood flow to working muscles, L-arginine acts as a vasodilator (Álvares *et al.*, 2012). So, these properties may also increase exercise duration in healthy individuals. The L-arginine supplement may be effective at increasing growth hormone levels (Kanaley, 2008), so it may not only be beneficial for exercise but also to promote good health in general. There is no official recommended daily allowance (RDA) for L-Arg. Our best understanding is that 2-3 grams of L-Arg per day is completely safe dose for a healthy individual to achieve the benefits of L-Arg and maintain good health. Who knows, a novel, safe and effective means of

preventing and treating obesity in mammals may potentially be supported by controlling arginine supplementation.

References

- Abraham, M. H. *et al.* (2000) 'The solvation properties of nitric oxide', *Journal of the Chemical Society. Perkin Transactions 2*, (10), pp. 2067–2070. doi: 10.1039/b004419i.
- De Abreu Costa, L. *et al.* (2017) 'Dimethyl sulfoxide (DMSO) decreases cell proliferation and TNF- α , IFN-, and IL-2 cytokines production in cultures of peripheral blood lymphocytes', *Molecules*, 22(11), pp. 1–10. doi: 10.3390/molecules22111789.
- Abu-Elheiga, L. *et al.* (2000) 'The subcellular localization of acetyl-CoA carboxylase 2', *Proceedings of the National Academy of Sciences of the United States of America*, 97(4), pp. 1444–1449. doi: 10.1073/pnas.97.4.1444.
- Abu-Elheiga, L. *et al.* (2003) 'Acetyl-CoA carboxylase 2 mutant mice are protected against obesity and diabetes induced by high-fat/high-carbohydrate diets', *Proceedings of the National Academy of Sciences of the United States of America*, 100(18), pp. 10207–10212. doi: 10.1073/pnas.1733877100.
- Afinanisa, Q., Cho, M. K. and Seong, H. A. (2021) 'AMPK localization: A key to differential energy regulation', *International Journal of Molecular Sciences*, 22(20). doi: 10.3390/ijms222010921.
- Ahn, J. *et al.* (2008) 'The anti-obesity effect of quercetin is mediated by the AMPK and MAPK signaling pathways', *Biochemical and Biophysical Research Communications*, 373(4), pp. 545–549. doi: 10.1016/j.bbrc.2008.06.077.
- Albrecht, E. W. J. A. *et al.* (2003) 'Protective role of endothelial nitric oxide synthase', *Journal of Pathology*, 199(1), pp. 8–17. doi: 10.1002/path.1250.
- Alderton, W. K., Cooper, C. E. and Knowles, R. G. (2001) 'Nitric oxide synthases: Structure, function and inhibition', *Biochemical Journal*, 357(3), pp. 593–615. doi: 10.1042/0264-6021:3570593.
- Álvares, T. S. *et al.* (2012) 'Acute L-arginine supplementation increases muscle blood volume but not strength performance', *Applied Physiology, Nutrition and Metabolism*, 37(1), pp. 115–126. doi: 10.1139/H11-144.
- Andaya, A. *et al.* (2012) 'Phosphorylation of Human Eukaryotic Initiation Factor 2 γ : Novel Site Identification and Targeted PKC Involvement', *Bone*, 23(1), pp. 1–7. doi: 10.1021/pr200429y.Phosphorylation.
- Arnal, J. F. *et al.* (1995) 'Interactions between L-arginine and L-glutamine change endothelial NO production: An effect independent of NO synthase substrate availability', *Journal of Clinical Investigation*, 95(6), pp. 2565–2572. doi: 10.1172/JCI117957.
- Arriarán, S. *et al.* (2016) 'White adipose tissue urea cycle activity is not affected by one-month treatment with a hyperlipidic diet in female rats', *Food and Function*, 7(3), pp. 1554–1563. doi: 10.1039/c5fo01503k.
- Ayala, A., Muñoz, M. F. and Argüelles, S. (2014) 'Lipid peroxidation: Production, metabolism, and signaling mechanisms of malondialdehyde and 4-hydroxy-2-nonenal', *Oxidative Medicine and Cellular Longevity*, 2014. doi: 10.1155/2014/360438.
- Bae, S. Y. *et al.* (2005) 'Y+ and y+L arginine transporters in neuronal cells expressing tyrosine hydroxylase', *Biochimica et Biophysica Acta - Molecular Cell Research*, 1745(1), pp. 65–73. doi: 10.1016/j.bbamcr.2004.12.006.
- Baldelli, S. *et al.* (2014) 'The role of nNOS and PGC-1 α in skeletal muscle cells', *Journal of Cell Science*, 127(22), pp. 4813–4820. doi: 10.1242/jcs.154229.
- Balligand, J.-L., Feron, O. and Dessy, C. (2009) 'eNOS Activation by Physical Forces: From Short-Term Regulation of Contraction to Chronic Remodeling of Cardiovascular Tissues', *Physiological Reviews*, 89(2), pp. 481–534. doi: 10.1152/physrev.00042.2007.
- Balligand, J. L. and Cannon, P. J. (1997) 'Nitric oxide synthases and cardiac muscle: Autocrine and paracrine influences', *Arteriosclerosis, Thrombosis, and Vascular Biology*, 17(10), pp. 1846–1858. doi: 10.1161/01.ATV.17.10.1846.
- Bastiani, M. and Parton, R. G. (2010) 'Caveolae at a glance', *Journal of Cell Science*, 123(22), pp. 3831–3836. doi: 10.1242/jcs.070102.

- Baur, A. *et al.* (2006) 'Calorie Diet', 444(7117), pp. 337–342. doi: 10.1038/nature05354.Resveratrol.
- Becerril, S. *et al.* (2010) 'Deletion of inducible nitric-oxide synthase in leptin-deficient mice improves brown adipose tissue function', *PLoS ONE*, 5(6), pp. 1–12. doi: 10.1371/journal.pone.0010962.
- Bergen, W. G. and Mersmann, H. J. (2018) 'Comparative Aspects of Lipid Metabolism: Impact on Contemporary Research and Use of Animal Models', *The Journal of Nutrition*, 135(11), pp. 2499–2502. doi: 10.1093/jn/135.11.2499.
- Betz, C. and Hall, M. N. (2013) 'Where is mTOR and what is it doing there?', *Journal of Cell Biology*, 203(4), pp. 563–574. doi: 10.1083/jcb.201306041.
- Bray, G. A. and Bellanger, T. (2006) 'Epidemiology, trends, and morbidities of obesity and the metabolic syndrome', *Endocrine*, 29(1), pp. 109–117. doi: 10.1385/ENDO:29:1:109.
- Bröer, S. and Bröer, A. (2017) 'Amino acid homeostasis and signalling in mammalian cells and organisms', *Biochemical Journal*, 474(12), pp. 1935–1963. doi: 10.1042/BCJ20160822.
- Brosnan, M. E. and Brosnan, J. T. (2004) 'Renal Arginine Metabolism', (9), pp. 2888–2894.
- Browne, G. J., Finn, S. G. and Proud, C. G. (2004) 'Stimulation of the AMP-activated Protein Kinase Leads to Activation of Eukaryotic Elongation Factor 2 Kinase and to Its Phosphorylation at a Novel Site, Serine 398', *Journal of Biological Chemistry*, 279(13), pp. 12220–12231. doi: 10.1074/jbc.M309773200.
- Brownsey, R. W., Zhande, R. and Boone, A. N. (1997) 'Isoforms of acetyl-CoA carboxylase: Structures, regulatory properties and metabolic functions', *Biochemical Society Transactions*, 25(4), pp. 1232–1238. doi: 10.1042/bst0251232.
- Cahová, M., Vavřínková, H. and Kazdová, L. (2007) 'Glucose-fatty acid interaction in skeletal muscle and adipose tissue in insulin resistance', *Physiological Research*, 56(1), pp. 1–15.
- Cai, B. *et al.* (2016) 'Does Citrulline Have Protective Effects on Liver Injury in Septic Rats?', *BioMed Research International*, 2016. doi: 10.1155/2016/1469590.
- Cantó, C. and Auwerx, J. (2013) 'Europe PMC Funders Group AMP-activated protein kinase and its downstream transcriptional pathways', *Cellular and Molecular Life Science*, 67(20), pp. 3407–3423. doi: 10.1007/s00018-010-0454-z.AMP-activated.
- Cao, S. *et al.* (2020) 'Arginase promotes immune evasion of *Echinococcus granulosus* in mice', *Parasites and Vectors*, 13(1), pp. 1–12. doi: 10.1186/s13071-020-3919-4.
- Carroll, B. *et al.* (2016) 'Control of TSC2-Rheb signaling axis by arginine regulates mTORC1 activity', *eLife*, 5(JANUARY2016), pp. 1–23. doi: 10.7554/eLife.11058.001.
- Carruthers, B. M. and Winegrad, A. I. (1962) 'Effects of insulin on amino acid and ribonucleic acid metabolism in rat adipose tissue', *The American journal of physiology*, 202, pp. 605–610. doi: 10.1152/ajplegacy.1962.202.4.605.
- Chang, H. R. *et al.* (2016) 'HNF4 α is a therapeutic target that links AMPK to WNT signalling in early-stage gastric cancer', *Gut*, 65(1), pp. 19–32. doi: 10.1136/gutjnl-2014-307918.
- Cinelli, M. A. *et al.* (2020) 'Inducible nitric oxide synthase: Regulation, structure, and inhibition', *Medicinal Research Reviews*, 40(1), pp. 158–189. doi: 10.1002/med.21599.
- Clemens, M. G. (1999) 'Nitric Oxide in Liver Injury', *American Association for the Study of Liver Diseases.*, pp. 125–127. doi: 10.1016/B978-0-12-804274-8.00008-4.
- Closs, E. I. *et al.* (2006) 'Structure and function of cationic amino acid transporters (CATs)', *Journal of Membrane Biology*, 213(2), pp. 67–77. doi: 10.1007/s00232-006-0875-7.
- Colberg, S. R. *et al.* (1995) '<J. Clin. Invest. 1995 Colberg-1.pdf>', 95(August 1994), pp. 1846–1853.
- Conato, C. *et al.* (2000) 'Copper(II) complexes with L-lysine and L-ornithine: Is the side-chain involved in the coordination? A thermodynamic and spectroscopic study', *Thermochimica Acta*, 362(1–2), pp. 13–23. doi: 10.1016/S0040-6031(00)00633-X.
- Coughlan, K. A. *et al.* (2015) 'Nutrient Excess in AMPK Downregulation and Insulin Resistance.', *Journal of*

endocrinology, diabetes & obesity, 1(1), p. 1008. Available at: <http://www.ncbi.nlm.nih.gov/pubmed/26120590><http://www.pubmedcentral.nih.gov/articlerender.fcgi?artid=PMC4479300>.

Cunningham, R. P., Sheldon, R. D. and Rector, R. S. (2020) 'The Emerging Role of Hepatocellular eNOS in Non-alcoholic Fatty Liver Disease Development', *Frontiers in Physiology*, 11(July), pp. 1–9. doi: 10.3389/fphys.2020.00767.

Cypess, A. M. *et al.* (2009) 'Identification and Importance of Brown Adipose Tissue in Adult Humans', *Clinical Lymphoma Myeloma*, 9(1), pp. 19–22. doi: 10.3816/CLM.2009.n.003.Novel.

DeBose-Boyd, R. A. (2008) 'Feedback regulation of cholesterol synthesis: Sterol-accelerated ubiquitination and degradation of HMG CoA reductase', *Cell Research*, 18(6), pp. 609–621. doi: 10.1038/cr.2008.61.

DeFronzo, R. A. and Tripathy, D. (2009) 'Skeletal muscle insulin resistance is the primary defect in type 2 diabetes.', *Diabetes care*, 32 Suppl 2. doi: 10.2337/dc09-S302.

Dick, B. P. *et al.* (2020) 'Hematopoietic cell-expressed endothelial nitric oxide protects the liver from insulin resistance', *Arteriosclerosis, Thrombosis, and Vascular Biology*, (March), pp. 670–681. doi: 10.1161/ATVBAHA.119.313648.

Dolinsky, V. W. and Dyck, J. R. B. (2006) 'Role of AMP-activated protein kinase in healthy and diseased hearts', *American Journal of Physiology - Heart and Circulatory Physiology*, 291(6). doi: 10.1152/ajpheart.00329.2006.

Dugdale, H. F. *et al.* (2018) 'The role of resveratrol on skeletal muscle cell differentiation and myotube hypertrophy during glucose restriction', *Molecular and Cellular Biochemistry*, 444(1–2), pp. 109–123. doi: 10.1007/s11010-017-3236-1.

Dzambo, N. *et al.* (2008) 'AMPK-independent pathways regulate skeletal muscle fatty acid oxidation', *Journal of Physiology*, 586(23), pp. 5819–5831. doi: 10.1113/jphysiol.2008.159814.

El-Sheikh, N. M. and Khalil, F. A. (2011) 'L-Arginine and l-glutamine as immunonutrients and modulating agents for oxidative stress and toxicity induced by sodium nitrite in rats', *Food and Chemical Toxicology*, 49(4), pp. 758–762. doi: 10.1016/j.fct.2010.11.039.

Elhanati, S. *et al.* (2013) 'Multiple regulatory layers of SREBP1/2 by SIRT6', *Cell Reports*, 4(5), pp. 905–912. doi: 10.1016/j.celrep.2013.08.006.

Engeli, S. *et al.* (2004) 'Regulation of the nitric oxide system in human adipose tissue', *Journal of Lipid Research*, 45(9), pp. 1640–1648. doi: 10.1194/jlr.M300322-JLR200.

Feng, C. (2012) 'Mechanism of Nitric Oxide Synthase Regulation: Electron Transfer and Interdomain Interactions', *Coord Chem Rev*, 23(1), pp. 1–7. doi: 10.1016/j.ccr.2011.10.011.Mechanism.

Fitzgerald, S. J. *et al.* (2018) 'A new approach to study the sex differences in adipose tissue', *Journal of Biomedical Science*, 25(1), pp. 1–12. doi: 10.1186/s12929-018-0488-3.

Förstermann, U. and Sessa, W. C. (2012) 'Nitric oxide synthases: Regulation and function', *European Heart Journal*, 33(7), pp. 829–837. doi: 10.1093/eurheartj/ehr304.

Forzano, I. *et al.* (2023) 'L-Arginine in diabetes: clinical and preclinical evidence', *Cardiovascular diabetology*, 22(1), p. 89. doi: 10.1186/s12933-023-01827-2.

Frayn, K. N. *et al.* (2003) 'Integrative physiology of human adipose tissue', *International Journal of Obesity*, 27(8), pp. 875–888. doi: 10.1038/sj.ijo.0802326.

Frühbeck, G. and Gómez-Ambrosi, J. (2001) 'Modulation of the leptin-induced white adipose tissue lipolysis by nitric oxide', *Cellular Signalling*, 13(11), pp. 827–833. doi: 10.1016/S0898-6568(01)00211-X.

Fu, W. J. *et al.* (2005) 'Dietary L-arginine supplementation reduces fat mass in Zucker diabetic fatty rats', *Journal of Nutrition*, 135(4), pp. 714–721. doi: 10.1093/jn/135.4.714.

García-Villafranca, J., Guillén, A. and Castro, J. (2003) 'Involvement of nitric oxide/cyclic GMP signaling pathway in the regulation of fatty acid metabolism in rat hepatocytes', *Biochemical Pharmacology*, 65(5), pp.

807–812. doi: 10.1016/S0006-2952(02)01623-4.

Garcia, D. and Shaw, R. J. (2017) ‘AMPK: Mechanisms of Cellular Energy Sensing and Restoration of Metabolic Balance’, *Molecular Cell*, 66(6), pp. 789–800. doi: 10.1016/j.molcel.2017.05.032.

Gharavi, N. M. *et al.* (2006) ‘Role of endothelial nitric oxide synthase in the regulation of SREBP activation by oxidized phospholipids’, *Circulation Research*, 98(6), pp. 768–776. doi: 10.1161/01.RES.0000215343.89308.93.

Giorgino, F., Laviola, L. and Eriksson, J. W. (2005) ‘Regional differences of insulin action in adipose tissue: Insights from in vivo and in vitro studies’, *Acta Physiologica Scandinavica*, 183(1), pp. 13–30. doi: 10.1111/j.1365-201X.2004.01385.x.

Göbel, A. *et al.* (2019) ‘Induction of 3-hydroxy-3-methylglutaryl-CoA reductase mediates statin resistance in breast cancer cells’, *Cell Death and Disease*, 10(2). doi: 10.1038/s41419-019-1322-x.

González, A. *et al.* (2020) ‘AMPK and TOR: The Yin and Yang of Cellular Nutrient Sensing and Growth Control’, *Cell Metabolism*, 31(3), pp. 472–492. doi: 10.1016/j.cmet.2020.01.015.

Grahame, H. D. (2013) ‘AMPK: A target for drugs and natural products with effects on both diabetes and cancer’, *Diabetes*, 62(7), pp. 2164–2172. doi: 10.2337/db13-0368.

Griess, P. (1879) ‘P e t e r’, *Bemerkungen zu der Abhandlung der HH. Weselsky und Benedikt “Ueber einige Azoverbindungen.”*, 12., pp. 426–428.

Gwinn, D. M. *et al.* (2014) ‘AMPK phosphorylation of raptor mediates a metabolic checkpoint’, *Bone*, 23(1), pp. 1–7. doi: 10.1016/j.molcel.2008.03.003.AMPK.

Harvey, R. and Ferrier, D. (2011) *Biochemistry*. Available at: <https://books.google.com/books?id=Lhp0ppRYWoC&pgis=1>.

Hawley, S. A. *et al.* (2002) ‘The Antidiabetic Drug Metformin’, *Diabetes*, 51(August), pp. 2420–2425.

Herman, M. A. *et al.* (2010) ‘Adipose tissue Branched Chain Amino Acid (BCAA) metabolism modulates circulating BCAA levels’, *Journal of Biological Chemistry*, 285(15), pp. 11348–11356. doi: 10.1074/jbc.M109.075184.

Hizli, A. A. *et al.* (2013) ‘Phosphorylation of Eukaryotic Elongation Factor 2 (eEF2) by Cyclin A–Cyclin-Dependent Kinase 2 Regulates Its Inhibition by eEF2 Kinase’, *Molecular and Cellular Biology*, 33(3), pp. 596–604. doi: 10.1128/mcb.01270-12.

Hon, W. M., Lee, K. H. and Khoo, H. E. (2015) ‘Nitric oxide in liver diseases’, *Trends in Pharmacological Sciences*, 36(8), pp. 524–536. doi: 10.1016/j.tips.2015.05.001.

Honka, M. J. *et al.* (2018) ‘Insulin-stimulated glucose uptake in skeletal muscle, adipose tissue and liver: A positron emission tomography study’, *European Journal of Endocrinology*, 178(5), pp. 523–531. doi: 10.1530/EJE-17-0882.

Hoppe, S. *et al.* (2009) ‘AMP-activated protein kinase adapts rRNA synthesis to cellular energy supply’, *Proceedings of the National Academy of Sciences of the United States of America*, 106(42), pp. 17781–17786. doi: 10.1073/pnas.0909873106.

Jobgen, W. S. *et al.* (2006) ‘Regulatory role for the arginine-nitric oxide pathway in metabolism of energy substrates’, *Journal of Nutritional Biochemistry*, 17(9), pp. 571–588. doi: 10.1016/j.jnutbio.2005.12.001.

Johanns, M. *et al.* (2017) ‘Direct and indirect activation of eukaryotic elongation factor 2 kinase by AMP-activated protein kinase’, *Cellular Signalling*, 36(December 2016), pp. 212–221. doi: 10.1016/j.cellsig.2017.05.010.

Johnson, R. *et al.* (2016) ‘Aspalathin, a dihydrochalcone C-glucoside, protects H9c2 cardiomyocytes against high glucose induced shifts in substrate preference and apoptosis’, *Molecular Nutrition and Food Research*, 60(4), pp. 922–934. doi: 10.1002/mnfr.201500656.

Kahn, B. B. *et al.* (2005) ‘AMP-activated protein kinase: Ancient energy gauge provides clues to modern understanding of metabolism’, *Cell Metabolism*, 1(1), pp. 15–25. doi: 10.1016/j.cmet.2004.12.003.

- Kanaley, J. A. (2008) 'Growth hormone, arginine and exercise', *Current Opinion in Clinical Nutrition and Metabolic Care*, 11(1), pp. 50–54. Available at: <http://ovidsp.ovid.com/ovidweb.cgi?T=JS&PAGE=reference&D=emed8&NEWS=N&AN=2007618933>.
- Kaul, G., Pattan, G. and Rafeequi, T. (2011) 'Eukaryotic elongation factor-2 (eEF2): Its regulation and peptide chain elongation', *Cell Biochemistry and Function*, 29(3), pp. 227–234. doi: 10.1002/cbf.1740.
- Kenney, J. W. *et al.* (2014) 'Eukaryotic elongation factor 2 kinase, an unusual enzyme with multiple roles', *Advances in Biological Regulation*, 55, pp. 15–27. doi: 10.1016/j.jbior.2014.04.003.
- Kershaw, E. E. and Flier, J. S. (2004) 'Adipose tissue as an endocrine organ', *Journal of Clinical Endocrinology and Metabolism*, 89(6), pp. 2548–2556. doi: 10.1210/jc.2004-0395.
- Kikuchi-Utsumi Kazue *et al.* (1987) 'Enhanced gene expression of endothelial nitric oxide synthase in brown adipose tissue during cold exposure', *Endocrinologia Japonica*, 34(2), pp. 319–323. doi: 10.1507/endocrj1954.34.319.
- KIM, H.-J. *et al.* (2006) 'Sterol Regulatory Element-Binding Proteins (SREBPs) as Regulators of Lipid Metabolism', *Annals of the New York Academy of Sciences*, 967(1), pp. 34–42. doi: 10.1111/j.1749-6632.2002.tb04261.x.
- Kim, M. *et al.* (2012) 'AMPK isoform expression in the normal and failing hearts', *J Mol Cell Cardiol*, 52(1), pp. 1–7. doi: 10.1016/j.yjmcc.2012.01.016.
- Kim, S.-J. *et al.* (2016) 'AMPK Phosphorylates Desnutrin/ATGL and Hormone-Sensitive Lipase To Regulate Lipolysis and Fatty Acid Oxidation within Adipose Tissue', *Molecular and cellular biology*, 36(14), pp. 1961–1976. doi: 10.1128/MCB.00244-16.Address.
- Kim, T., Leahy, P. and Freake, H. C. (1996) 'Promoter Usage Determines Tissue Specific Responsiveness of the Rat Acetyl-CoA Carboxylase Gene', 653, pp. 647–653.
- Kim, Y. M. *et al.* (1998) 'Inhibition of protein synthesis by nitric oxide correlates with cytostatic activity: Nitric oxide induces phosphorylation of initiation factor eIF-2 α ', *Molecular Medicine*, 4(3), pp. 179–190. doi: 10.1007/bf03401915.
- Kimball, S. R. and Jefferson, L. S. (2004) 'Amino acids as regulators of gene expression', *Nutrition and Metabolism*, 1, pp. 1–10. doi: 10.1186/1743-7075-1-3.
- Knight, J. R. P. *et al.* (2015) 'Eukaryotic elongation factor 2 kinase regulates the cold stress response by slowing translation elongation', *Biochemical Journal*, 465, pp. 227–238. doi: 10.1042/BJ20141014.
- Kohjima, M. *et al.* (2008) 'SREBP-1c, regulated by the insulin and AMPK signaling pathways, plays a role in nonalcoholic fatty liver disease', *International Journal of Molecular Medicine*, 21(4), pp. 507–511. doi: 10.3892/ijmm.21.4.507.
- Kohli, R. *et al.* (2018) 'Dietary L-Arginine Supplementation Enhances Endothelial Nitric Oxide Synthesis in Streptozotocin-Induced Diabetic Rats', *The Journal of Nutrition*, 134(3), pp. 600–608. doi: 10.1093/jn/134.3.600.
- Komar, A. A. and Merrick, W. C. (2020) 'A retrospective on EIF2A—and not the alpha subunit of EIF2', *International Journal of Molecular Sciences*, 21(6). doi: 10.3390/ijms21062054.
- Kuo, L. (1998) 'Arginase modulates nitric oxide production in activated macrophages', *American Journal of Physiology*, 274(1 PART 2).
- Kurokawa, T. *et al.* (2012) 'Effect of L-arginine supplement on liver regeneration after partial hepatectomy in rats', *World Journal of Surgical Oncology*, 10(1), p. 1. doi: 10.1186/1477-7819-10-99.
- Kurowska, E. M. and Carroll, K. K. (1998) 'Hypocholesterolemic properties of nitric oxide. In vivo and in vitro studies using nitric oxide donors', *Biochimica et Biophysica Acta - Lipids and Lipid Metabolism*, 1392(1), pp. 41–50. doi: 10.1016/S0005-2760(97)00215-4.
- Lalioitis, G. P., Bizelis, I. and Rogdakis, E. (2010) 'Comparative Approach of the de novo Fatty Acid Synthesis (Lipogenesis) between Ruminant and Non Ruminant Mammalian Species: From Biochemical Level to the

- Main Regulatory Lipogenic Genes', *Current Genomics*, 11(3), pp. 168–183. doi: 10.2174/138920210791110960.
- Langland, J. O. and Jacobs, B. L. (2004) 'Inhibition of PKR by vaccinia virus: Role of the N- and C-terminal domains of E3L', *Virology*, 324(2), pp. 419–429. doi: 10.1016/j.virol.2004.03.012.
- Laplante, M. and Sabatini, D. M. (2009) 'mTOR signaling at a glance', *Journal of Cell Science*, 122(20), pp. 3589–3594. doi: 10.1242/jcs.051011.
- Laplante, M. and Sabatini, D. M. (2012) 'An emerging role of mTOR in lipid biosynthesis', *Curr Biol*, 19(1), p. 22. doi: 10.1016/j.cub.2009.09.058.
- Lau, T. *et al.* (2000) 'Arginine, citrulline, and nitric oxide metabolism in end-stage renal disease patients', *Journal of Clinical Investigation*, 105(9), pp. 1217–1225. doi: 10.1172/JCI7199.
- Laufs, U. *et al.* (1998) 'Upregulation of Endothelial Nitric Oxide Synthase by HMG CoA Reductase Inhibitors', pp. 1129–1135.
- Laurberg, M. *et al.* (2000) 'Structure of a mutant EF-G reveals domain III and possibly the fusidic acid binding site', *Journal of Molecular Biology*, 303(4), pp. 593–603. doi: 10.1006/jmbi.2000.4168.
- Lecleire, S. *et al.* (2008) 'Combined glutamine and arginine decrease proinflammatory cytokine production by biopsies from Crohn's patients in association with changes in nuclear factor- κ B and p38 mitogen-activated protein kinase pathways', *Journal of Nutrition*, 138(12), pp. 2481–2486. doi: 10.3945/jn.108.099127.
- Leclerc, I. and Rutter, G. A. (2004) 'AMP-activated protein kinase: A new β -cell glucose sensor? Regulation by amino acids and calcium ions', *Diabetes*, 53(SUPPL. 3), pp. 67–74. doi: 10.2337/diabetes.53.suppl_3.S67.
- Leclercq, I. A. *et al.* (2007) 'Insulin resistance in hepatocytes and sinusoidal liver cells: Mechanisms and consequences', *Journal of Hepatology*, 47(1), pp. 142–156. doi: 10.1016/j.jhep.2007.04.002.
- Lee, J. *et al.* (2003) 'Translational control of inducible nitric oxide synthase expression by arginine can explain the arginine paradox', *Proceedings of the National Academy of Sciences*, 100(8), pp. 4843–4848. doi: 10.1073/pnas.0735876100.
- Lee, M. S. *et al.* (2011) 'meso-dihydroguaiaretic acid inhibits hepatic lipid accumulation by activating AMP-activated protein kinase in human HepG2 cells', *Biological and Pharmaceutical Bulletin*, 34(10), pp. 1628–1630. doi: 10.1248/bpb.34.1628.
- Letexier, D. *et al.* (2003) 'Comparison of the expression and activity of the lipogenic pathway in human and rat adipose tissue', *Journal of Lipid Research*, 44(11), pp. 2127–2134. doi: 10.1194/jlr.m300235-jlr200.
- Li, F. *et al.* (2019) 'Adipose-specific knockdown of Sirt1 results in obesity and insulin resistance by promoting exosomes release', *Cell Cycle*, 18(17), pp. 2067–2082. doi: 10.1080/15384101.2019.1638694.
- Li, Y. *et al.* (2011) 'AMPK phosphorylates and inhibits SREBP activity to attenuate hepatic steatosis and atherosclerosis in diet-induced insulin-resistant mice', *Cell Metabolism*, 13(4), pp. 376–388. doi: 10.1016/j.cmet.2011.03.009.
- Li, Y. and Wu, S. (2021) 'Curcumin inhibits the proteolytic process of SREBP-2 by first inhibiting the expression of S1P rather than directly inhibiting SREBP-2 expression', *Food Science and Nutrition*, 9(1), pp. 209–216. doi: 10.1002/fsn3.1985.
- Liscum, L. *et al.* (1985) 'Domain structure of 3-hydroxy-3-methylglutaryl coenzyme A reductase, a glycoprotein of the endoplasmic reticulum', *Journal of Biological Chemistry*, 260(1), pp. 522–530. doi: 10.1016/s0021-9258(18)89764-2.
- Liu, X. *et al.* (2017) *Hepatic Metabolism in Liver Health and Disease, Liver Pathophysiology: Therapies and Antioxidants*. Elsevier Inc. doi: 10.1016/B978-0-12-804274-8.00030-8.
- Loh, K. *et al.* (2019) 'Inhibition of Adenosine Monophosphate-Activated Protein Kinase-3-Hydroxy-3-Methylglutaryl Coenzyme A Reductase Signaling Leads to Hypercholesterolemia and Promotes Hepatic Steatosis and Insulin Resistance', *Hepatology Communications*, 3(1), pp. 84–98. doi: 10.1002/hep4.1279.
- López-Lluch, G. *et al.* (2008) 'MITOCHONDRIAL BIOGENESIS AND HEALTHY AGING', *Bone*, 23(1),

pp. 1–7. doi: 10.1038/jid.2014.371.

Lucotti, P. *et al.* (2006) ‘Beneficial effects of a long-term oral L-arginine treatment added to a hypocaloric diet and exercise training program in obese, insulin-resistant type 2 diabetic patients’, *American Journal of Physiology - Endocrinology and Metabolism*, 291(5), pp. 906–912. doi: 10.1152/ajpendo.00002.2006.

Luo, L. and Liu, M. (2016) ‘Adipose tissue in control of metabolism’, *Journal of Endocrinology*, 231(3), pp. R77–R99. doi: 10.1530/joe-16-0211.

Luo, L. and Liu, M. (2018) ‘Adipose tissue in control of metabolism’, *Physiology & behavior*, 176(1), pp. 139–148. doi: 10.1530/JOE-16-0211.Adipose.

Ma, X. M. and Blenis, J. (2009) ‘Molecular mechanisms of mTOR-mediated translational control’, *Nature Reviews Molecular Cell Biology*, 10(5), pp. 307–318. doi: 10.1038/nrm2672.

MacKenzie, A. and Wadsworth, R. M. (2003) ‘Extracellular L-arginine is required for optimal NO synthesis by eNOS and iNOS in the rat mesenteric artery wall’, *British Journal of Pharmacology*, 139(8), pp. 1487–1497. doi: 10.1038/sj.bjp.0705380.

Marini, J. C. *et al.* (2010) ‘Glutamine: Precursor or nitrogen donor for citrulline synthesis?’ *American Journal of Physiology - Endocrinology and Metabolism*, 299(1). doi: 10.1152/ajpendo.00080.2010.

McAdam, E. *et al.* (2012) ‘Inducible nitric oxide synthase (iNOS) and nitric oxide (NO) are important mediators of reflux-induced cell signalling in esophageal cells’, *Carcinogenesis*, 33(11), pp. 2035–2043. doi: 10.1093/carcin/bgs241.

McGee, S. . (2013) ‘Muscle Cramps’, *Journal of Chemical Information and Modeling*, 53(9), pp. 1689–1699. doi: 10.1017/CBO9781107415324.004.

McKnight, J. R. *et al.* (2010) ‘Beneficial effects of L-arginine on reducing obesity: Potential mechanisms and important implications for human health’, *Amino Acids*, 39(2), pp. 349–357. doi: 10.1007/s00726-010-0598-z.

McNaughton, L. *et al.* (2002) ‘Distribution of nitric oxide synthase in normal and cirrhotic human liver’, *Proceedings of the National Academy of Sciences of the United States of America*, 99(26), pp. 17161–17166. doi: 10.1073/pnas.0134112100.

Mendes-Ribeiro, A. C. *et al.* (2009) ‘The Role of Exercise on L-Arginine Nitric Oxide Pathway in Chronic Heart Failure’, *The Open Biochemistry Journal*, 3, pp. 55–65. doi: 10.2174/1874091x00903010055.

Mew, N. A. *et al.* (2018) ‘Urea Cycle Disorders Overview’, pp. 1–13.

Mohamed, M. A., Elkhateeb, W. A. and Daba, G. M. (2022) ‘Rapamycin golden jubilee and still the miraculous drug: a potent immunosuppressant, antitumor, rejuvenative agent, and potential contributor in COVID-19 treatment’, *Bioresources and Bioprocessing*, 9(1). doi: 10.1186/s40643-022-00554-y.

Mohan, S. *et al.* (2013) ‘AMP-activated protein kinase regulates L-arginine mediated cellular responses’, *Nutrition and Metabolism*, 10(1), p. 1. doi: 10.1186/1743-7075-10-40.

Mokdad, A. H. *et al.* (2003) ‘Prevalence of obesity, diabetes, and obesity-related health risk factors, 2001’, *Journal of the American Medical Association*, 289(1), pp. 76–79. doi: 10.1001/jama.289.1.76.

Molinaro, A., Becattini, B. and Solinas, G. (2020) ‘Insulin signaling and glucose metabolism in different hepatoma cell lines deviate from hepatocyte physiology toward a convergent aberrant phenotype’, *Scientific Reports*, 10(1), pp. 1–10. doi: 10.1038/s41598-020-68721-9.

Montero, H. *et al.* (2008) ‘Rotavirus Infection Induces the Phosphorylation of eIF2 α but Prevents the Formation of Stress Granules’, *Journal of Virology*, 82(3), pp. 1496–1504. doi: 10.1128/jvi.01779-07.

Moore, S. J. *et al.* (2018) ‘Rapid acquisition and model-based analysis of cell-free transcription–translation reactions from nonmodel bacteria’, *Proceedings of the National Academy of Sciences of the United States of America*, 115(19), pp. 4340–4349. doi: 10.1073/pnas.1715806115.

Mori, M. (2007) ‘Regulation of nitric oxide synthesis and apoptosis by arginase and arginine recycling’, *Journal of Nutrition*, 137(6), pp. 3–7. doi: 10.1093/jn/137.6.1616s.

Morries, S. (2004) ‘Recent advances in arginine metabolism’, pp. 45–51. doi:

10.1097/01.mco.0000109606.04238.88.

Morris, S. M. (2009) 'Recent advances in arginine metabolism: Roles and regulation of the arginases', *British Journal of Pharmacology*, 157(6), pp. 922–930. doi: 10.1111/j.1476-5381.2009.00278.x.

Munday, M. R. (2002) 'Regulation of mammalian acetyl-CoA carboxylase', *Biochemical Society Transactions*, 30(5), pp. A101–A101. doi: 10.1042/bst030a101c.

Muraleedharan, R. and Dasgupta, B. (2022) 'AMPK in the brain: its roles in glucose and neural metabolism', *FEBS Journal*, 289(8), pp. 2247–2262. doi: 10.1111/febs.16151.

Mustafa, S. B. and Olson, M. S. (1999) 'Effects of calcium channel antagonists on LPS-induced hepatic iNOS expression', *American Journal of Physiology - Gastrointestinal and Liver Physiology*, 277(2 40-2). doi: 10.1152/ajpgi.1999.277.2.g351.

Nguyen, S. T., Nguyen, H. T.-L. and Truong, K. D. (2020) 'Comparative cytotoxic effects of methanol, ethanol and DMSO on human cancer cell lines', *Biomedical Research and Therapy*, 7(7), pp. 3855–3859. doi: 10.15419/bmrat.v7i7.614.

Nijvelde, R. J. *et al.* (2004) 'High plasma arginine concentrations in critically ill patients suffering from hepatic failure', *European Journal of Clinical Nutrition*, 58(4), pp. 587–593. doi: 10.1038/sj.ejcn.1601851.

O'Neill, H. M. *et al.* (2014) 'AMPK phosphorylation of ACC2 is required for skeletal muscle fatty acid oxidation and insulin sensitivity in mice', *Diabetologia*, 57(8), pp. 1693–1702. doi: 10.1007/s00125-014-3273-1.

Oh, W. K. *et al.* (2005) 'Glucose and fat metabolism in adipose tissue of acetyl-CoA carboxylase 2 knockout mice', *Proceedings of the National Academy of Sciences of the United States of America*, 102(5), pp. 1384–1389. doi: 10.1073/pnas.0409451102.

Osowska, S. *et al.* (2004) 'Citrulline increases arginine pools and restores nitrogen balance after massive intestinal resection', *Gut*, 53(12), pp. 1781–1786. doi: 10.1136/gut.2004.042317.

Pahlavani, N. *et al.* (2017) 'L-arginine supplementation and risk factors of cardiovascular diseases in healthy men: A double-blind randomized clinical trial', *F1000Research*, 3(0), pp. 1–11. doi: 10.12688/f1000research.5877.1.

Raghow, R. *et al.* (2008) 'SREBPs: the crossroads of physiological and pathological lipid homeostasis', *Trends in Endocrinology and Metabolism*, 19(2), pp. 65–73. doi: 10.1016/j.tem.2007.10.009.

Rajapakse, N. W. and Mattson, D. L. (2009) 'Role of L-arginine in nitric oxide production in health and hypertension', *Clinical and Experimental Pharmacology and Physiology*, 36(3), pp. 249–255. doi: 10.1111/j.1440-1681.2008.05123.x.

Rath, M. *et al.* (2014) 'Metabolism via Arginase or Nitric Oxide Synthase: Two Competing Arginine Pathways in Macrophages.', *Frontiers in immunology*, 5(October), p. 532. doi: 10.3389/fimmu.2014.00532.

Rhoads, J. M. *et al.* (2007) 'Intestinal ribosomal p70S6K signaling is increased in piglet rotavirus enteritis', *American Journal of Physiology - Gastrointestinal and Liver Physiology*, 292(3), pp. 913–922. doi: 10.1152/ajpgi.00468.2006.

Ribiere, C. *et al.* (1996) 'White adipose tissue nitric oxide synthase: A potential source for NO production', *Biochemical and Biophysical Research Communications*, 222(3), pp. 706–712. doi: 10.1006/bbrc.1996.0824.

Richard, A. J. (2000) 'Adipose Tissue : Physiology to Metabolic Dysfunction introduction : AN Historical Perspective on Adipose Tissue biology', (2), pp. 1–65.

Romero, M., Sabater, D. and Fernández-lópez, J. A. (2015) 'Glycerol Production from Glucose and Fructose by 3T3-L1 Cells: A Mechanism of Adipocyte Defense from Excess Substrate', pp. 1–18. doi: 10.1371/journal.pone.0139502.

Rosen, E. D. and Spiegelman, B. M. (2011) 'Adipocytes as regulators of energy balance and glucose homeostasis', 444(7121), pp. 847–853. doi: 10.1038/nature05483.Adipocytes.

Roy, D., Perreault, M. and Marette, A. (1998) 'Insulin stimulation of glucose uptake in skeletal muscles and

- adipose tissues in vivo is NO dependent', *American Journal of Physiology - Endocrinology and Metabolism*, 274(4 37-4), pp. 692–699. doi: 10.1152/ajpendo.1998.274.4.e692.
- Rui, L. (2016) 'Energy Metabolism in the Liver', *Physiology & behavior*, 176(1), pp. 139–148. doi: 10.1016/j.physbeh.2017.03.040.
- Ruiz, R. *et al.* (2014) 'Sterol regulatory element-binding protein-1 (SREBP-1) is required to regulate glycogen synthesis and gluconeogenic gene expression in mouse liver', *Journal of Biological Chemistry*, 289(9), pp. 5510–5517. doi: 10.1074/jbc.M113.541110.
- de sa, P. M. *et al.* (2017) 'Transcriptional regulation of adipogenesis', *Comprehensive Physiology*, 7(2), pp. 635–674. doi: 10.1002/cphy.c160022.
- Sansbury, B. E. and Hill, B. G. (2014) 'Regulation of obesity and insulin resistance by nitric oxide', *Free Radical Biology and Medicine*, 73(502), pp. 383–399. doi: 10.1016/j.freeradbiomed.2014.05.016.
- Sass, G. *et al.* (2001) 'Inducible nitric oxide synthase is critical for immune-mediated liver injury in mice', *Journal of Clinical Investigation*, 107(4), pp. 439–447. doi: 10.1172/JCI10613.
- Saxton, R. A. and Sabatini, D. M. (2017) 'mTOR Signaling in Growth, Metabolism, and Disease', *Cell*, 168(6), pp. 960–976. doi: 10.1016/j.cell.2017.02.004.
- Schmidt, I. and Herpin, P. (1998) 'Carnitine palmitoyltransferase I (CPT I) activity and its regulation by malonyl-CoA are modulated by age and cold exposure in skeletal muscle mitochondria from newborn pigs', *Journal of Nutrition*, 128(5), pp. 886–893. doi: 10.1093/jn/128.5.886.
- Schreurs, M., Kuipers, F. and Van Der Leij, F. R. (2010) 'Regulatory enzymes of mitochondrial β -oxidation as targets for treatment of the metabolic syndrome', *Obesity Reviews*, 11(5), pp. 380–388. doi: 10.1111/j.1467-789X.2009.00642.x.
- Sell, H., Deshaies, Y. and Richard, D. (2004) 'The brown adipocyte: Update on its metabolic role', *International Journal of Biochemistry and Cell Biology*, 36(11), pp. 2098–2104. doi: 10.1016/j.biocel.2004.04.003.
- Sengupta, J. *et al.* (2011) 'Visualization of the eEF2-80S Ribosome Transition State Complex by Cryo-electron Microscopy', *Bone*, 23(1), pp. 1–7. doi: 10.1016/j.jmb.2008.07.004. Visualization.
- Sessa, W. C. (2004) 'eNOS at a glance', *Journal of Cell Science*, 117(12), pp. 2427–2429. doi: 10.1242/jcs.01165.
- Shi, W. *et al.* (2004) 'Regulation of tetrahydrobiopterin synthesis and bioavailability in endothelial cells', *Cell Biochemistry and Biophysics*, 41(3), pp. 415–433. doi: 10.1385/CBB:41:3:415.
- Shin, S., Mohan, S. and Fung, H. L. (2011) 'Intracellular L-arginine concentration does not determine NO production in endothelial cells: Implications on the "L-arginine paradox"', *Biochemical and Biophysical Research Communications*, 414(4), pp. 660–663. doi: 10.1016/j.bbrc.2011.09.112.
- Siendones, E. *et al.* (2003) 'Role of nitric oxide in D-galactosamine-induced cell death and its protection by PGE1 in cultured hepatocytes', *Nitric Oxide - Biology and Chemistry*, 8(2), pp. 133–143. doi: 10.1016/S1089-8603(02)00182-9.
- Simonsen, U. *et al.* (2019) 'Extracellular L-arginine enhances relaxations induced by opening of calcium-activated SKCa channels in porcine retinal arteriole', *International Journal of Molecular Sciences*, 20(8), pp. 1–14. doi: 10.3390/ijms20082032.
- Singh, K. *et al.* (2019) 'Dietary Arginine Regulates Severity of Experimental Colitis and Affects the Colonic Microbiome', 9(March), pp. 1–15. doi: 10.3389/fcimb.2019.00066.
- Skrzypczak-Wierciach, A. and Sałat, K. (2022) 'Lipopolysaccharide-Induced Model of Neuroinflammation: Mechanisms of Action, Research Application and Future Directions for Its Use', *Molecules*, 27(17). doi: 10.3390/molecules27175481.
- Søndergaard, E. and Jensen, M. D. (2016) 'Quantification of adipose tissue insulin sensitivity', *Journal of Investigative Medicine*, 64(5), pp. 989–991. doi: 10.1136/jim-2016-000098.

- Song, Z., Xiaoli, A. M. and Yang, F. (2018) 'Regulation and metabolic significance of De Novo lipogenesis in adipose tissues', *Nutrients*, 10(10), pp. 1–22. doi: 10.3390/nu10101383.
- Spahn, C. M. T. *et al.* (2004) 'Domain movements of elongation factor eEF2 and the eukaryotic 80S ribosome facilitate tRNA translocation', *EMBO Journal*, 23(5), pp. 1008–1019. doi: 10.1038/sj.emboj.7600102.
- Srivastava, R. A. K. *et al.* (2012) 'AMP-activated protein kinase: An emerging drug target to regulate imbalances in lipid and carbohydrate metabolism to treat cardio-metabolic diseases', *Journal of Lipid Research*, 53(12), pp. 2490–2514. doi: 10.1194/jlr.R025882.
- Su, Y. W. *et al.* (2014) 'Association between phosphorylated AMP-activated protein kinase and acetyl-CoA carboxylase expression and outcome in patients with squamous cell carcinoma of the head and neck', *PLoS ONE*, 9(4). doi: 10.1371/journal.pone.0096183.
- Sujobert, P. and Tamburini, J. (2016) 'Co-activation of AMPK and mTORC1 as a new therapeutic option for acute myeloid leukemia', *Molecular and Cellular Oncology*, 3(4), pp. 1–3. doi: 10.1080/23723556.2015.1071303.
- Sukumaran, A., Choi, K. and Dasgupta, B. (2020) 'Insight on Transcriptional Regulation of the Energy Sensing AMPK and Biosynthetic mTOR Pathway Genes', *Frontiers in Cell and Developmental Biology*, 8(July), pp. 1–16. doi: 10.3389/fcell.2020.00671.
- Sun, J. *et al.* (2003) 'Measurement of Nitric Oxide Production in Biological Systems by Using Griess Reaction Assay', *Sensors*, 3, pp. 276–284. Available at: <http://www.mdpi.net/sensors>.
- Szlas, A., Kurek, J. M. and Krejpcio, Z. (2022) 'The Potential of L-Arginine in Prevention and Treatment of Disturbed Carbohydrate and Lipid Metabolism—A Review', *Nutrients*, 14(5). doi: 10.3390/nu14050961.
- Tan, B. (2012) 'Regulatory roles for L-arginine in reducing white adipose tissue', *Frontiers in Bioscience*, 17(7), p. 2237. doi: 10.2741/4047.
- Tanaka, T. *et al.* (2003) 'Nitric oxide stimulates glucose transport through insulin-independent GLUT4 translocation in 3T3-L1 adipocytes', *European Journal of Endocrinology*, 149(1), pp. 61–67. doi: 10.1530/eje.0.1490061.
- Tao, R. *et al.* (2013) 'Hepatic SREBP-2 and cholesterol biosynthesis are regulated by FoxO3 and Sirt6', *Journal of Lipid Research*, 54(10), pp. 2745–2753. doi: 10.1194/jlr.M039339.
- Taylor, D. J. *et al.* (2007) 'Structures of modified eEF2.80S ribosome complexes reveal the role of GTP hydrolysis in translocation', *EMBO Journal*, 26(9), pp. 2421–2431. doi: 10.1038/sj.emboj.7601677.
- Tengan, C. H., Rodrigues, G. S. and Godinho, R. O. (2012) 'Nitric oxide in skeletal muscle: Role on mitochondrial biogenesis and function', *International Journal of Molecular Sciences*, 13(12), pp. 17160–17184. doi: 10.3390/ijms131217160.
- Testuo, M. *et al.* (1992) 'Stimulation of Nitric Oxide-Cyclic GMP pathway by L-Arginine increases the release of Hepatic Lipase from culture rat hepatocytes', *Chemical Pharmaceutical Bulletin*, 56(5), pp. 845–846.
- Titherade, M. A. (1998) *Nitric Oxide Protocols*. doi: 10.1385/1-59259-749-1:281.
- Tortora, G. J. and Derrickson, B. (2019) *Principles of Anatomy & Physiology, Hilos Tensados*. doi: 10.1017/CBO9781107415324.004.
- Trayhurn, P. (2005) 'Endocrine and signalling role of adipose tissue: New perspectives on fat', *Acta Physiologica Scandinavica*, 184(4), pp. 285–293. doi: 10.1111/j.1365-201X.2005.01468.x.
- Uma, S., Yun, B. G. and Matts, R. L. (2001) 'The heme-regulated eukaryotic initiation factor 2 α kinase. A potential regulatory target for control of protein synthesis by diffusible gases', *Journal of Biological Chemistry*, 276(18), pp. 14875–14883. doi: 10.1074/jbc.M011476200.
- Uyeda, K., Yamashita, H. and Kawaguchi, T. (2002) 'Carbohydrate responsive element-binding protein (ChREBP): A key regulator of glucose metabolism and fat storage', *Biochemical Pharmacology*, 63(12), pp. 2075–2080. doi: 10.1016/S0006-2952(02)01012-2.

- De Vera, M. E., Geller, D. A. and Billiar, T. R. (1995) 'Hepatic inducible nitric oxide synthase: Regulation and function', *Biochemical Society Transactions*, 23(4), pp. 1008–1013. doi: 10.1042/bst0231008.
- Verdon, C. P., Burton, B. A. and Prior, R. L. (1995) 'Sample pretreatment with nitrate reductase and glucose-6-phosphate dehydrogenase quantitatively reduces nitrate while avoiding interference by NADP⁺ when the Griess reaction is used to assay for nitrite', *Analytical Biochemistry*, pp. 502–508. doi: 10.1006/abio.1995.1079.
- Viollet, B. *et al.* (2006) 'Activation of AMP-activated protein kinase in the liver: A new strategy for the management of metabolic hepatic disorders', *Journal of Physiology*, 574(1), pp. 41–53. doi: 10.1113/jphysiol.2006.108506.
- Vos, T. A. *et al.* (1999) 'Expression of inducible nitric oxide synthase in endotoxemic rat hepatocytes is dependent on the cellular glutathione status', *Hepatology*, 29(2), pp. 421–426. doi: 10.1002/hep.510290231.
- Walker, V. and Mills, G. A. (1995) 'Quantitative methods for amino acid analysis in biological fluids', *Annals of Clinical Biochemistry*, 32(1), pp. 28–57. doi: 10.1177/000456329503200103.
- Wang, F. *et al.* (1999) 'Redox imbalance differentially inhibits lipopolysaccharide-induced macrophage activation in the mouse liver', *Infection and Immunity*, 67(10), pp. 5409–5416. doi: 10.1128/iai.67.10.5409-5416.1999.
- Wang, L. *et al.* (2009) 'Mammalian target of rapamycin complex 1 (mTORC1) activity is associated with phosphorylation of raptor by mTOR', *Journal of Biological Chemistry*, 284(22), pp. 14693–14697. doi: 10.1074/jbc.C109.002907.
- Wang, M. *et al.* (2014) 'Effects of Arginine Concentration on the In Vitro Expression of Casein and mTOR Pathway Related Genes in Mammary Epithelial Cells from Dairy Cattle', 9(5). doi: 10.1371/journal.pone.0095985.
- Wang, Q. *et al.* (2018) 'AMPK-mediated regulation of lipid metabolism by phosphorylation', *Biological and Pharmaceutical Bulletin*, 41(7), pp. 985–993. doi: 10.1248/bpb.b17-00724.
- Wang, R. *et al.* (2018) 'L-arginine enhances protein synthesis by phosphorylating mTOR (Thr 2446) in a nitric oxide-dependent manner in C2C12 cells', *Oxidative Medicine and Cellular Longevity*, 2018. doi: 10.1155/2018/7569127.
- Wang, X. *et al.* (2014) 'Eukaryotic Elongation Factor 2 Kinase Activity Is Controlled by Multiple Inputs from Oncogenic Signaling', *Molecular and Cellular Biology*, 34(22), pp. 4088–4103. doi: 10.1128/mcb.01035-14.
- Wang, Y. G. *et al.* (2016) 'Functional differences between AMPK α 1 and α 2 subunits in osteogenesis, osteoblast-associated induction of osteoclastogenesis, and adipogenesis', *Scientific Reports*, 6(September), pp. 1–14. doi: 10.1038/srep32771.
- Weitzberg, E., Hezel, M. and Lundberg, J. O. (2010) 'Implications for Anesthesiology and Intensive Care', *Anesthesiology*, 113(6), pp. 1460–1475.
- Wennmalm, Å. *et al.* (1993) 'Metabolism and excretion of nitric oxide in humans: An experimental and clinical study', *Circulation Research*, 73(6), pp. 1121–1127. doi: 10.1161/01.RES.73.6.1121.
- Widmer, J. *et al.* (1996) 'Identification of a second human acetyl-CoA carboxylase gene', *Biochemical Journal*, 316(3), pp. 915–922. doi: 10.1042/bj3160915.
- Wijnands, K. A. P. *et al.* (2015) 'Citrulline supplementation improves organ perfusion and arginine availability under conditions with enhanced arginase activity', *Nutrients*, 7(7), pp. 5217–5238. doi: 10.3390/nu7075217.
- Willows, R. *et al.* (2017) 'Phosphorylation of AMPK by upstream kinases is required for activity in mammalian cells', *Biochemical Journal*, 474(17), pp. 3059–3073. doi: 10.1042/BCJ20170458.
- Wong, T. Y., Lin, S. M. and Leung, L. K. (2015) 'The flavone luteolin suppresses SREBP-2 expression and post-translational activation in hepatic cells', *PLoS ONE*, 10(8), pp. 1–18. doi: 10.1371/journal.pone.0135637.
- Wu, G. *et al.* (2007) 'Pharmacokinetics and safety of arginine supplementation in animals', *Journal of Nutrition*, 137(6), pp. 1673–1680. doi: 10.1093/jn/137.6.1673s.

- Wu, G. *et al.* (2013) 'Arginine metabolism and nutrition in growth, health and disease', 71(2), pp. 233–236. doi: 10.1038/mp.2011.182.doi.
- Wu, G. (2014) 'Dietary requirements of synthesizable amino acids by animals: A paradigm shift in protein nutrition', *Journal of Animal Science and Biotechnology*, 5(1), pp. 1–12. doi: 10.1186/2049-1891-5-34.
- WU, G. *et al.* (2015) 'Glutamine metabolism to glucosamine is necessary for glutamine inhibition of endothelial nitric oxide synthesis', *Biochemical Journal*, 353(2), pp. 245–252. doi: 10.1042/bj3530245.
- Wu, G. and Brosnan, J. T. (1992) 'Macrophages can convert citrulline into arginine', *Biochemical Journal*, 281(1), pp. 45–48. doi: 10.1042/bj2810045.
- Wu, G. and Meininger, C. J. (2002) 'Regulation of Nitric Oxide Synthesis by Dietary Factors', *Annual Review of Nutrition*, 22(1), pp. 61–86. doi: 10.1146/annurev.nutr.22.110901.145329.
- Wu, G. and Meininger, C. J. (2008) 'Analysis of Citrulline, Arginine, and Methylarginines Using High-Performance Liquid Chromatography', *Methods in Enzymology*, 440(07), pp. 177–189. doi: 10.1016/S0076-6879(07)00810-5.
- Wu, G. and Morris, S. (2008) 'Arginine metabolism: nitric oxide and beyond', 17, pp. 1–17. doi: 10.1016/S0928-4680(98)80513-0.
- Wu, N. *et al.* (2012) 'AMPK-dependent degradation of TXNIP upon energy stress leads to enhanced glucose uptake via GLUT1', *NIH public access*, 23(1), pp. 1–7. doi: 10.1016/j.molcel.2013.01.035.AMPK-dependent.
- Wu, P.-Y. *et al.* (no date) 'Effects of Arginine Deimination and Citrulline Side-Chain Length on Peptide Secondary Structure'.
- Xia, N. *et al.* (2016) 'Uncoupling of Endothelial Nitric Oxide Synthase in Perivascular Adipose Tissue of Diet-Induced Obese Mice', *Arteriosclerosis, Thrombosis, and Vascular Biology*, 36(1), pp. 78–85. doi: 10.1161/ATVBAHA.115.306263.
- Xie, J. *et al.* (2019) 'Regulation of the Elongation Phase of Protein Synthesis Enhances Translation Accuracy and Modulates Lifespan', *Current Biology*, 29(5), pp. 737-749.e5. doi: 10.1016/j.cub.2019.01.029.
- Yamada, M. *et al.* (2000) 'Endothelial nitric oxide synthase-dependent cerebral blood flow augmentation by L-arginine after chronic statin treatment', *Journal of Cerebral Blood Flow and Metabolism*, 20(4), pp. 709–717. doi: 10.1097/00004647-200004000-00008.
- Yamada, S. *et al.* (2019) 'AMPK activation, eEF2 inactivation, and reduced protein synthesis in the cerebral cortex of hibernating chipmunks', *Scientific Reports*, 9(1), pp. 1–11. doi: 10.1038/s41598-019-48172-7.
- Yang, Y. *et al.* (2014) 'Profiling of Plasma Results in Improved Coverage of Metabolome', *Journal of Chromatography A*, pp. 217–226. doi: 10.1016/j.chroma.2013.04.030.New.
- Ye, J. and DeBose-Boyd, R. A. (2011) 'Regulation of cholesterol and fatty acid synthesis', *Cold Spring Harbor Perspectives in Biology*, 3(7), pp. 1–13. doi: 10.1101/cshperspect.a004754.
- Ye, R. Z. *et al.* (2022) 'Fat Cell Size: Measurement Methods, Pathophysiological Origins, and Relationships With Metabolic Dysregulations', *Endocrine reviews*, 43(1), pp. 35–60. doi: 10.1210/endrev/bnab018.
- Yvette C. Luiking, Engelen, M. P. K. J. and Deutz, N. E. P. (2011) 'REGULATION OF NITRIC OXIDE PRODUCTION IN HEALTH AND DISEASE', *Differences*, 13(5 Pt 1), pp. 97–104. doi: 10.1097/MCO.0b013e328332f99d.REGULATION.
- Zhao, Q., Lin, X. and Wang, G. (2022) 'Targeting SREBP-1-Mediated Lipogenesis as Potential Strategies for Cancer', *Frontiers in Oncology*, 12(July), pp. 1–22. doi: 10.3389/fonc.2022.952371.
- Zois, C. E. and Harris, A. L. (2016) 'Glycogen metabolism has a key role in the cancer microenvironment and provides new targets for cancer therapy', *Journal of Molecular Medicine*, 94(2), pp. 137–154. doi: 10.1007/s00109-015-1377-9.

Appendices

Appendix I. Multialignment of NOS isoforms

The following are the isoforms/splice variants of NOS in mouse. Clustal Omega which is a multiple sequence alignment tool was used to align the DNA sequences of the NOS isoforms.

1. Mus musculus nitric oxide synthase 2, inducible (Nos2), transcript variant 2, mRNA
NCBI Reference Sequence: NM_001313921.1
2. Mus musculus nitric oxide synthase 1, neuronal (Nos1), mRNA
NCBI Reference Sequence: NM_008712.3
3. Mus musculus nitric oxide synthase 3, endothelial cell (Nos3), mRNA
NCBI Reference Sequence: NM_008713.4

Multialignment

iNOS	-----	0
nNOS	ATGGAAGAGCACACGTTTGGGGTCCAGCAGATCCAACCCAACGTCATTTCTGTCCGTCTC	60
eNOS	-----	0
iNOS	-----	0
nNOS	TTCAAACGCAAAGTGGGAGGTCTGGGCTTCCTGGTGAAGGAACGGGTCAGCAAGCCCCCG	120
eNOS	-----	0
iNOS	-----	0
nNOS	GTGATCATCTCAGATCTGATCCGAGGAGGTGCCGCGAGCAGAGCGCCTTATCCAAGCC	180
eNOS	-----	0
iNOS	-----	0
nNOS	GGCGACATCATTCTCGCCGTCAATGATCGGCCCTGGTAGACCTCAGCTATGACAGCGCT	240
eNOS	-----	0
iNOS	-----	0
nNOS	CTGGAAGTTCTCAGGGGCATTGCCTCTGAGACCCATGTGGTCCTCATTCTGAGAGGCCCT	300
eNOS	-----	0
iNOS	-----	0
nNOS	GAGGGCTTTACTACACACCTGGAGACCACCTTCACAGGGGATGGAACCCCAAGACCATC	360
eNOS	-----	0
iNOS	-----	0
nNOS	CGTGTGACCCAGCCCCTGGGGACACCCACCAAAGCTGTCGATCTGTCTCGCCAGCCATCA	420
eNOS	-----	0
iNOS	-----	0
nNOS	GCCAGCAAAGACCAGCCATTAGCAGTAGACAGGGTCCCAGGTCCCAGTAACGGACCTCAG	480
eNOS	-----	0
iNOS	-----	0
nNOS	CATGCCAAGGCCGTGGACAGGGACCGGCTCAGTCTCCAGGCTAATGGTGTGGCCATT	540
eNOS	-----	0

nNOS	TGTGGGCAGGATCCAGTGGTCCAAGCTGCAGGTGTTCGATGCCCGAGACTGCACCACAGC	1304
eNOS	TGTGGGCCGGATCCAGTGGGGAAAGCTGCAGGTATTTGATGCTCGGGACTGCAGGACTGC * ** * ***** ** ***** * * * * * * * * * * * * * * * *	608
iNOS	ACAGGAAATGTTTCAGCACATCTGCAGACACATACTTTATGCCACCAACAATGGCAACAT	701
nNOS	CCATGGGATGTTCAACTACATCTGTAACCACGTCAAGTACGCCACCAACAAAGGGAACT	1364
eNOS	ACAGGAAATGTTTCACCTACATCTGTAACCACATTTAAATACGCAACAAATAGAGGCAATCT * * * ***** ***** * * * * * * * * * * * * * * * *	668
iNOS	CAGGTCGGCCATCACTGTGTTCCCCCAGCGGAGTGACGGCAAACATGACTTCAGGCTCTG	761
nNOS	CAGGTCGGCCATCACTATATTCCTCAAAGGACTGATGGCAAGCATGACTTCCGAGTGTG	1424
eNOS	TCGTTCAAGCCATCACAGTGTTCCTCCAGCGCTGCCCTGGCCGGGAGACTTCCGATCTG * ** ***** * ***** * * * * * * * * * * * * * * * *	728
iNOS	GAATTCACAGCTCATCCGGTACGCTGGCTACCAGATGCCCGATGGCACCATCAGAGGGGA	821
nNOS	GAATTCGACAGCTCATCCGCTATGCCGGCTACAAGCAGCCAGATGGCTCTACCTTGGGCGA	1484
eNOS	GAACAGCCAGCTGATACGCTATGCCGGCTATAGGCAGCAGGATGGCTCCGTGCCGAGGGGA *** ***** *	788
iNOS	TGCTGCCACCTTGGAGTTCACCCAGTTGTGCATCGACCTAGGCTGGAAGCCCCGCTATGG	881
nNOS	TCCAGCTAATGTGGAGTTCACAGAGATCTGTATACAGCAGGGCTGGAACCCCCAAGAGG	1544
eNOS	CCCCGCCAACGTGGAGATCACTGAGCTCTGTATCCAACATGGCTGGACCCAGGAAATGG * * * * * ***** *	848
iNOS	CCGCTTTGATGTGCTGCCTCTGGTCTTGCAAGCTGATGGTCAAGATCCAGAGGTCTTTGA	941
nNOS	CCGGTTCGATGTGCTGCCTCTCCTGCTCCAGGCCAATGGCAATGACCCTGAACCTTTTCA	1604
eNOS	CCGCTTTGATGTGCTGCCCTGTTACTCCAGGCTCCTGATGAGCCCCAGAACCTTTTCA *** * * ***** *	908
iNOS	AATCCCTCCTGATCTTGTGTTGGAGGTGACCATGGAGCATCCCAAGTACGAGTGGTTCCA	1001
nNOS	GATCCCCCAGAGCTGGTGTGGAAGTACCCATCAGGCACCCCAAGTTCGACTGGTTTAA	1664
eNOS	TCTGCCCCAGAGATGGTCTCGAGGTGCCTCTGGAGCACCCACGCTCGAGTGGTTGC *	968
iNOS	GGAGCTCGGGTTGAAGTGGTATGCACTGCCTGCCGTGGCCAACATGCTACTGGAGGTGGG	1061
nNOS	GGACCTGGGGCTCAAATGGTATGGCTCCCCGCTGTGTCCAACATGCTGCTGGAGATTGG	1724
eNOS	TGCCCTTGGCCTGCGCTGGTATGCCCTCCAGCTGTGTCCAACATGCTGCTAGAAATCGG *	1028
iNOS	TGGCCTCGAATTCAGCCTGCCCTTCAATGGTTGGTACATGGGCACCGAGATTGGAGT	1121
nNOS	GGCCTGGAGTTCAGCGCTGTCCCTTTAGTGGCTGGTACATGGGCACCGAGATTGGCGT	1784
eNOS	GGCCTGGAGTTTCTGCTGCCCTTTCAGCGCTGGTACATGAGTTCAGAGATTGGCAT ***** *	1088
iNOS	TCGAGACTTCTGTGACACACAGCGCTACAACATCCTGGAGGAAGTGGGCCGAAGGATGGG	1181
nNOS	TCGTGATTACTGTGACAACCTCTCGATAACAACATCCTGGAGGAAGTAGCCAAGAAAATGGA	1844
eNOS	GAGGACCTGTGTGACCCTCACCGCTACAACATACTTGGAGATGTGGCTGTGTGCATGGA * * * ***** * * ***** * * * * * * * * * * * * * * * *	1148
iNOS	CCTGGAGACCCACACACTGGCCTCCCTCTGGAAGACCGGGCTGTACGGAGATCAATGT	1241
nNOS	TTTGGACATGAGGAAGACATCCTCCCTCTGGAAGACCAAGCCCTGGTGGAGATTAACAT	1904
eNOS	TCTGGACACCAGGACAACCTCATCCCTGTGGAAGACAAGGCAGCGGTGGAATTAATGT *** *	1208
iNOS	GGCTGTGCTCCATAGTTTCCAGAAGCAGAATGTGACCATCATGGACCACCACACAGCCTC	1301
nNOS	TGCTGTCTATACAGCTTCCAGAGTGACAAGGTGACCATTGTGGACCACCACTCTGCCAC	1964
eNOS	GGCCGTGTTGCACAGTTACCAGCTGGCCAAAGTGACCATAGTGGACCACCACGCCGCCAC *	1268
iNOS	AGAGTCCTTCATGAAGCACATGCAGAATGAGTACCGGGCCCGTGGAGGCTGCCCGGCAGA	1361
nNOS	CGAGTCCTTCATCAAACACATGGAGAATGAGTACCGCTGCAGAGGGGGCTGTCCCGCCGA	2024
eNOS	AGCTCCTTCATGAAGCACCTGAAAATGAGCAGAGGCCAGAGGGGGCTGCCCTGCCGA * ***** *	1328

iNOS	CTGGATTTGGCTGGTCCCTCCAGTGTCTGGGAGCATCACCCCTGTGTTCCACCAGGAGAT	1421
nNOS	CTGGGTGTGGATTGTGCCCCCATGTGCGGCAGCATCACCCCTGTCTTCCACCAGGAGAT	2084
eNOS	TTGGCCTGGATTGTGCCCCCATCTCAGGCAGCTAACTCCTGTCTTCCATCAAGAGAT *** ** *	1388
iNOS	GTTGAACTATGTCCTATCTCCATTCTACTACTACCAGATCGAGCCCTGGAAGACCCACAT	1481
nNOS	GCTCAACTACCGGCTCACCCCGTCCCTTGTAGTACCAGCCTGATCCATGGAACACCCACGT	2144
eNOS	GGTCAACTATTTCCCTGTCCCTGCCTTCCGCTACCAGCCAGACCCCTGGAAGGGAAGTGC *	1448
iNOS	CTGGCAGAATGAGAAGCTGAGGCCAGG---AGGAGAGAGATCCGATTTAGAGTCTTGTT	1538
nNOS	GTGGAAGGGCACCAATGGGACCCCAAGCGGCAGCCATTGGCTTCAAGAAATTGGC	2204
eNOS	AGCAAAGGGGGCAGGCATC-----ACCAGGAAGAAGACCTTTAAGGAAAGTAGC *	1496
iNOS	GAAAGTGGTGTCTTTGCTTCCATGCTAATGCGAAAGGTCATGGCTTACGGGTCAGAGC	1598
nNOS	AGAGGCCGTCAAGTCTCAGCCAAGCTGATGGGACAGGCCATGGCCAAGAGAGTCAAAGC	2264
eNOS	CAATGCAGTGAAGATCTCTGCCTCACTCATGGGCAGGTGATGGCGAAGCGTGTGAAGGC *	1556
iNOS	CACAGTCTCTTTGCTACTGAGACAGGGAAGTCTGAAGCACTAGCCAGGGACCTGGCCAC	1658
nNOS	GACCATTCTCTACGCCACCGAGACAGGCAAATCCCAAGCCTATGCCAAGACCCCTGTGCGA	2324
eNOS	AACCATTCTGTATGGCTCTGAGACTGGCCGGGCCAGAGCTACGCACAGCAGCTGGGAAG *	1616
iNOS	CTTGTTACAGCTACGCCTTCAACACCAAGGTTGTCTGCATGGACCAGTATAAGGCAAGCAC	1718
nNOS	GATCTTCAAGCATGCCTTCGATGCCAAGGCTATGTCCATGGAGGAATATGACATCGTGCA	2384
eNOS	ACTCTTCCGGAAGGCGTTTGATCCCCGGGTCTGTGCATGGATGAGTATGATGTGGTGTCT *	1676
iNOS	CTTGGAAGAGGAGCAACTACTGCTGGTGGTGACAAGCACATTTGGGAATGGAGACTGTCC	1778
nNOS	CCTGGAGCACGAAGCCCTGGTCTTGGTGGTACCAGCACCTTTGGCAATGGAGACCCCCC	2444
eNOS	CCTAGAGCACGAGGCACTGGTGTGGTGGTGACCAGCACATTTGGCAATGGGGATCTCTCC *	1736
iNOS	CAGCAATGGGCAGACTCTGAAGAAATCTCTGTTCATGCTTAGAGAACTCAAC-----	1830
nNOS	AGAGAATGGGGAGAAATTCGGCTGTGCTTTGATGGAGATGAGGCACCCCA-----A	2495
eNOS	GGAGAATGGAGAGAGCTTTCAGCAGCGCTCATGGAAATGTCAGGCCCGTACAACAGCTC *	1796
iNOS	-----	1830
nNOS	CTCTGTGCAAGAGGAGAGGAAGAGCTACAAGGTCGGATTCAACAGCGTCTCCTCCTATTC	2555
eNOS	CCCTAGGCCTGAGCAGCACAAAGAGCTACAAAATCCGATTCAACAGTGTCTCCTGCTCAGA	1856
iNOS	-----	1830
nNOS	TGACTCCCGCAAGTCATCAGGCGATGGACCAGACCTCAGAGACAACTTTGAAAGTACTGG	2615
eNOS	CCCCTGGTATCCTCTTGGCGGCGCAAGAGGAAGGAGTCTAGCAACACAGACAGTGCAGG	1916
iNOS	-----CACACCTCAGGTATGCTGTGTTGGCCTTGGCTCCAGCATGTACCCTCAGTT	1883
nNOS	ACCGCTGGCCAATGTGAGGTTCTCAGTCTTCGGCTGGGCTCTCGGGCATAACCCTCACTT	2675
eNOS	AGCCCTGGGCACCCTCAGGTTCTGTGTGTTGGCTGGGCTCCCGAGCATAACCCCACTT *	1976
iNOS	CTGCGCCTTTGCTCATGACATCGACCAGAAGCTGTCCCACCTGGGAGCCTCTCAGCTTGC	1943
nNOS	CTGTGCCTTTGGGCACGCAGTGGACTCTCCTGGAGGAGCTGGGCGGGGAGAGGATTCT	2735
eNOS	CTGTGCCTTTGCTCGAGCGGTGGACACAAGGCTGGAGGAGCTGGGCGGGGAGCGACTACT *	2036
iNOS	CCCAACAGGAGAAGGGGACGAACCTCAGTGGGCAGGAGGATGCCTTCCGCAGCTGGGCTGT	2003
nNOS	GAAGATGAGGGAGGGAGATGAGCTCTGCGGACAGGAAGAGGCTTTCAGGACCTGGGCTAA	2795

Appendix III. Sequencing results for iNOS-CDS and iNOS-UTR inserts

Sequencing with BGHR and T7 universal sequencing primers confirmed the authenticity of either iNOS-CDS or iNOS-UTR insert in pcDNATM3.1/Hygro (+) and the nucleic acid sequences of the cloned iNOS fragments were aligned with sequences deposited in multialignment tool and were found to be a high match.

Designed primers

Primers for iNOS-CDS amplification:

iNOS-CDS-ATG-FP-HindIII: 5' **TATAAGCTTGAC**ATGGCTTGCCCCTGGAAGTTTC 3' (T_m 64.2°C)

iNOS-CDS-TGA-RP-XbaI: 5' GCCCAAAGCCACGAGGCTCTGAT**CTAGATAT** 3' (T_m 63.9°C)

Primers for iNOS-UTR amplification:

iNOS-UTR-FP-HindIII: 5' **TATAAGCTT**GAGACTCTGGCCCCACG 3' (T_m 61.8°C)

iNOS-UTR-RP-XbaI: 5' CATTTTATTTTAATCAAAAAAAAAAAGCGCCG**CTAGATAT** 3' (T_m 60.3°C)

Mus musculus nitric oxide synthase 2, inducible (Nos2), transcript variant 2, mRNA

NCBI Reference Sequence: NM_001313921.1

Template DNA sequences of insert iNOS-CDS

atggccttgcccctggaagtttctcttcaaagtc aaatcctaccaaagtgacctgaaagaggaaaaggacattaacaacaa
cgtgaagaaaacccttgtgctgttctcagcccaacaatacaagatgacctaaagagtcacccaaaatggctccccgcagc
tcctcactgggacagcacagaatgttccagaatccctggacaagctgcatgtgacatcgaccctccacagtatgtgagg
atcaaaaactggggcagtgagagatgttgcacacactcttcaccacaaggccacatcgatcttacttgcaagtccaa
gtcttggcttgggggtccatcatgaaccccaagagtttgaccagaggaccagagacaagcctaccctctggaggagctcc
tgcctcatgcccattgagttcatcaaccagatattatggctcctttaaagaggcaaaaatagaggaacatctggccaggctg
gaagctgtaacaaaggaaatagaacaacaggaacctaccagctcactctggatgagctcatcttggccaccaagatggc
ctggaggaatgcccctcgctgcatcggcaggatccagtggtccaacctgcaggctcttggacgctcggaactgtagcacag
cacaggaatgtttcagcacatctgcagacacatactttatgccaccaacaatggcaacatcaggctcgccatcactgtg
ttccccagcggagtgacggcaaacatgacttcaggctctggaattcacagctcatccggtacgctggctaccagatgcc
cgatggcaccatcagaggggatgctgccaccttggagttcaccagttgtgcatcgacctaggctggaagccccgctatg
gccgcttggatgtgctgctcctctggtcttgc aagctgatggtcaagatccagaggtcttggaaatccctcctgatcttgtg
ttggaggtgacctggagcattcccaagtaagtggttccaggagctcggggtgaaagtggtatgcaactggcctgcccgtggc
caacatgctactggaggtgggtggcctcgaattccagcctgcccttcaatgggttggtacatgggaccagcagatggag
ttcgagactctgtgacacacagcgtacaacatcctggaggaagtgggcgaaggatgggctggagaccacacactg
gcctccctctggaaagaccgggctgtcacggagatcaatgtggctgtgctccatagttccagaagcagaatgtgacat
catggaccaccacacagcctcagagtccttcatgaagcacatgcagaatgagtagcgggcccgtggaggctgcccggcag
actggatgtggctggtccctccagtgctctgggagcatcaccctgtgttccaccaggagatggtgaactatgtcctatct
ccattctactactaccagatcgagccctggaagaccacatctggcagaatgagaagctgaggcccaggaggagagagat
ccgatttagagctcttgggtgaaagtggtgttcttggcttccatgctaagtcgaaaggctatggcctcaggggtcagagcca
cagtcctcttggctactgagacaggaagtctgaagcactagccagggacctggccaccttggctcagctacgccttcaac
accaaggttgtctgcatggaccagtataaggcaagcaccttggaaagaggagcaactactgctggtggtgacaagcacatt
tgggaatggagactgtcccagcaatgggcagactctgaagaaatctctgttcatgcttagagaactcaaccacaccttca
ggatgtctgtgttggccttggctccagcatgtacctcagttctgctgcttggctcatgacatcgaccagaagctgtcc
cacctgggagcctctcagcttggcccaacaggagaaggggacgaactcagtgggcaggaggatgccttccgcagctgggc
tgtacaaaccttccgggcagcctgtgagaccttggatgtccgaagcaaacatcacattcagatcccgaacgcttcaact
ccaatgcaacatgggagccacagcaatataggctcatccagagcccggagcctttagacctcaacagagccctcagcagc
atccatgcaagaacgtgtttaccatgaggctgaaatcccagcagaatctgcagagtgaaaagtcagccgcaccacct
cctcgttcagctcaccttgcaggggcagccgagggcccagctacctgctggggaacacctggggatcttcccaggcaacc
agaccgccctggtgcagggaaatcttggagcagattgtggattgtcctacaccacacaaactgtgtgcttggaggttctg
gatgagagcggcagctactgggtcaaagacaagaggctgccccctgctcactcagccaagccctcactacttcttggga
cattacgaccctcccaccagctgcagctccacaagctggctcgcttggccaggacgagacggataggcagagattgg
aggccttgtgtcagccctcagagtaaatgactggaagttcagcaacaacccccacgttccctggaggtgcttgaagagttc

ccttccttgcatgtgcccgtgccttctgctgtgcgagctccctatcttgaagccccgctactactccatcagctcctc
ccaggaccacacccccctcggaggttcacctcactgtggccgtggcaccctaccgcaccccgagatgggcaggggtccctgc
accatgggtgtctgcagcacttggatcaggaacctgaagccccaggaccagtgccctgctttgtgcaagtgtcagtggc
ttccagctccctgaggaccctcccagccttgcacccctcattgggcctggtacgggcattgctcccttccgaagttctg
gcagcagcggctccatgactcccagcacaagggtcaaaggaggccgcatgagcttgggtgtttgggtgccggcaccg
aggaggaccacctctatcaggaagaaatgcaggagatgggtccgcaagagagtgctgttccaggtgcacacaggctactcc
cggtgcccggcaaacccaaggtctacgttcaggacatcctgcaaaagcagctggccaatgaggtactcagcgtgctcca
cggggagcagggccacctctacatttgcggagatgtgcatggtcgggatgtggctaccacattgaagaagctgggtg
ccaccaagctgaacttgagcggaggcaggtggaagactatcttccagctcaagagccagaaacgttatcatgaagat
atcttcgggtgcagctcttttctatggggcaaaaaagggcagcgccttggaggagcccaaacgacagaggctctga

Sequencing result for iNOS-CDS

a. Sequencing results from T7 forward sequencing primer in iNOS-CDS DNA

NNNNNNGGTTAACTTAAGCTTGACATGGCTTGCCCTGGGAAGTTTCTCTTCAAAGTCAAATCCTACCAAAGTGACCTGA
AAGAGGAAAAGGACATTAACAACAACGTGAAGAAAACCCCTTGTGCTGTTCTCAGCCCAACAATACAAGATGACCCTAAG
AGTCACCAAAATGGCTCCCCGCAGCTCCTCACTGGGACAGCACAGAATGTTCCAGAATCCCTGGACAAGCTGCATGTGAC
ATCGACCCGTCCACAGTATGTGAGGATCAAAAAGTGGGGCAGTGGAGAGATTTTGCATGACACTCTTACCACAAGGCCA
CATCGGATTTCACTTGCAAGTCCAAGTCTTGCTTGGGGTCCATCATGAACCCCAAGAGTTTGACCAGAGGACCCAGAGAC
AAGCCTACCCCTCTGGAGGAGCTCCTGCCTCATGCCATTGAGTTCATCAACCAGTATTATGGCTCCTTTAAAGAGGCAAA
AATAGAGGAACATCTGGCCAGGCTGGAAGCTGTAACAAAGGAAATAGAAACAACAGGAACCTACCAGCTCACTCTGGATG
AGTTCATCTTTGCCACCAAGATGGCCTGGAGGAATGCCCCTCGCTGCATCGGCAGGATCCAGTGGTCCAACCTGCAGGTC
TTTGACGCTCGGAACGTGTAGCACAGCACAGGAAATGTTTCAGCACATCTGCAGACACATACTTTATGCCACCAACAATGG
CAACATCAGGTCGGCCATCACTGTGTTCCCCAGCGGAGTGACGGCAAACATGACTTCAGGCTCTGGAATTCACAGCTCA
TCCGGTACGCTGGCTACCAGATGCCGATGGCACCATCAGAGGGGATGCTGCCACCTTGGAGTTCACCCAGTTGTGCATC
GACCTAGGCTGGAAGCCCCGCTATGGCCGCTTTGATGTGCTGCCTCTGGTCTTGCAAGCTGATGGTCAAGATCCAGAGGT
CTTTGAAATCCCTCCTGATCTTGTGTTGGAAGGTGACCATGGAGCATCCCAAGTACGAATGGTTCCAGGAGCTCGGGTTG
AAATGGTATGCACTGCCTGCCGNGGCCAAATGCTACTGGGAGGTGGGTGGGCCTCGAATTCACCCCGGCCCTTCAAGG
GTTGGGACATGGGCCCCAGAATTGGAATTCAGACTTTTGGGAACCCAGCGCTTACAACTCCTGGAGAGAAAGGGGG
GCCCGAAAGNAGGGGCCGGGGGAAACCCCAACCCCGGGGCCCCCNNGAAAAAANCGGGGTGNACGAGANAA
AAAAAGGGGGGTNNGTCCNNAAT

b. Sequencing results from BGHR reverse sequencing primer in iNOS-CDS DNA

NAGGGGCTCTAGAATCAGAGCCTCGTGGGCTTTGGGCTCCTCCAAGGCGCTGCCCTTTTTTGGCCCATAGGAAAAGACT
GCACCGAAGATATCTTCATGATAACGTTTCTGGCTCTTGAGCTGGAAGAAATAGTCTTCCACCTGCTCCTCGCTCAAGTT
CAGCTTGGTGGCCACCAGCTTCTTCAATGTGGTAGCCACATCCCAGCCATGCGCACATCTCCGCAATGTAGAGGTGGC
CCTGCTCCCCGTGGAGCACGCTGAGTACCTCATTGGCCAGCTGCTTTTGCAGGATGTCTGAACGTAGACCTTGGGTTT
CCGGGACCCGGGAGTAGCCTGTGTGCACCTGGAACAGCACTCTCTTGCAGGACATCTCCTGCATTTCTTCTGATAGAG
GTGGTCTCTCCGGGTGCCGGCACCCAAACACCAAGCTCATGCGGCTCCTTTGAGCCCTTTGTGCTGGGAGTCAATGGA
GCCGCTGCTGCCAGAACTTCGGAAGGGGAGCAATGCCCGTACCAGGCCCAATGAGGATGCAAGGCTGGGAGGGTCTCTCA
GGGAGTGGAAGCCACTGACACTTCGCACAAAGCAGGGCACTGGGTCTGGGGCTTCCAGGTTCTGATCCAAGTGTGCA
GACACCATGGTGCAGGGGACCCTGACCATCTCGGGTGCAGGTGACCACGGCCACAGTGAAGTGAACCTCCGAGGGGG
TGTGGTCTGGGAGGAGCTGATGGAGTAGTAGCGGGCTTCAAGATAGGGAGCTGCGACAGCAGGAAGGCAGCGGGCACA
TGCAAGGAAGGGAATCTTCAAGCACCTCCAGGAACGGTGGGGTGTGCTGAACTTCCAGTCATTGTACTCTGAGGGCT
GACACAAGGCCTCCAATCTCTGCCTATCCGTCTCGTCCGTGGCAAAGCGAGCCAGCTTGTGGAGCTGCAGCTGGGTGGGA
AGGGGTCTGTAATGTCCAGGAAGTAGGTGAAGGCTTGGCTGAATGAGCAGGGGGGCGCCTCTTGTCTTTGACCCAGTAGC
TGCCGCTTTCATCCAGAACCTCCAGGCACACAGTTTTGGGGGGGTGGAAGGACAATCCCAAACTCGCTCCAAGATTCCC
TGCCCCAGGGCGGTCTGGTTGCCCGGAAAAATCCCCNNGGGTTCCCCCAGGAAAGGAACTGGGCCCCCNNTGCCCC
CAAAGGGGAAATTAATAAAGGAGGGGGGGGNCCTGGGTATT

Reverse compliments DNA sequences for the sequencing results from BGHR reverse sequencing primer in iNOS-CDS DNA

AATACCCAGCGNCCCCCCCCCTCCTTTTTTTAATTTCCCTTTGGGGGCANNNGGGGGGCCAGTTTCTTTCTGGGGG
AACCCCNNGGGGATTTTTCCCGGGCAACCAGACCGCCCTGGGGCAGGGAATCTTGGAGCGAGTTTGGGATTGTCTTCCAC

CCCCCCCCAAAAGTGTGTGCCTGGAGGTTCTGGATGAAAGCGGCAGCTACTGGGTCAAAGACAAGAGGCTGCCCCCTGCT
 CATTACAGCCAAGCCTTACCTACTTCTGGACATTACGACCCCTTCCCACCCAGCTGCAGCTCCACAAGCTGGCTCGCTT
 TGCCACGGACGAGACGGATAGGCAGAGATTGGAGGCCTTGTGTGAGCCCTCAGAGTACAATGACTGGAAGTTGAGCAACA
 ACCCCACCGTTTCTGGAGGTGCTTGAAGAGTTCCTTTCCTTGCATGTGCCCGCTGCCTTCTGCTGTGCGAGCTCCCTAT
 CTTGAAGCCCCGCTACTACTCCATCAGCTCCTCCCAGGACCACACCCCTCGGAGGTTACCTCACTGTGGCCGTGGTCA
 CCTACCGCACCCGAGATGGTCAGGGTCCCCTGCACCATGGTGTCTGCAGCACTTGGATCAGGAACCTGAAGCCCCAGGAC
 CCAGTGCCTTGTGTCGAAGTGTGAGTGGCTTCCAGCTCCTTGAGGACCCCTCCCAGCCTTGCATCCTCATTGGGCC
 TGGTACGGGCATTGCTCCCTTCCGAAGTTTCTGGCAGCAGCGGCTCCATGACTCCCAGCACAAAGGGCTCAAAGGAGGCC
 GCATGAGCTTGGTGTGTTGGGTGCCGGCACCCGGAGGAGGACCACCTCTATCAGGAAGAAATGCAGGAGATGGTCCGCAAG
 AGAGTGTCTTCCAGGTGCACACAGGCTACTCCCGGTGCCGGCAAACCCAAGTCTACGTTTACAGGACATCCTGCAAAA
 GCAGCTGGCCAATGAGGTACTCAGCGTGTCCACGGGGGAGCAGGGCCACCTCTACATTTGCGGAGATGTGCGCATGGCTC
 GGGATGTGGCTACCACATTGAAGAAGTGGTGGCCACCAAGCTGAACCTGAGCGAGGAGCAGGTGAAGACTATTTCTTC
 CAGCTCAAGAGCCAGAAACGTTATCATGAAGATATCTTCGGTGCAGTCTTTTCTATGGGGCAAAAAGGGCAGCGCCTT
 GGAGGAGCCCCAAGCCACGAGGCTCTGATTCTAGAGGCCCTN

Multialignment of sequencing results for iNOS-CDS using Multalin Interface Page tool

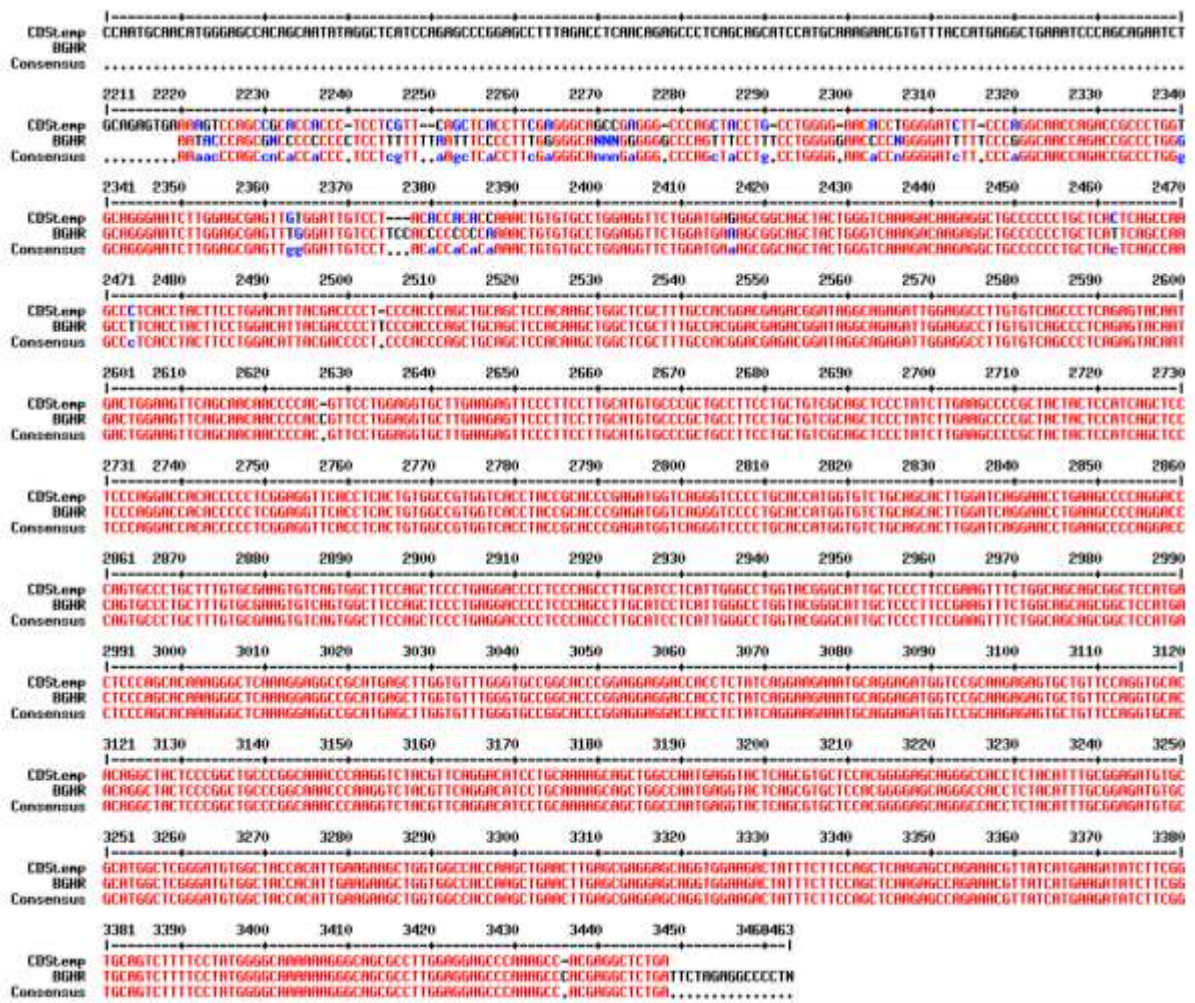
High consensus colour: red

Low consensus colour: blue

Neutral colour: black

High consensus value: 90 % (default: 90%)

Low consensus value: 50% (default: 50%)



Template DNA sequences of insert iNOS-UTR

gagactctggccccacgggacacagtgctcactgggtttgaaacttctcagccaccttgggtgaagggactgagctgtagag
acacttctgagggctcctcacgcttgggtcttgttccactccacggagtagcctagtcactgcaagagaacggagaacggt
ggatttggagcagaagtgcaaagtctcagacat**gggcttggccctggaagtttc**cttcaaagtcaaactcctaccaaagtg
acctgaaagagggaaaaggacattaacaacaacgtgaagaaaaccccttgtgctgttctcagcccaacaatacaagatgac
cctaagagtcacaaaaatggctccccgcagctcctcactgggacagcacagaatgttccagaatccctggacaagctgca
tgtgacatcgaccgctccacagtatgtgaggatcaaaaactggggcagtgagagattttgcacgactctcaccaca
aggccacatcgatttccacttgcaagccaagcttctgcttgggggtccatcatgaaccccaagagtttgaccagaggacc
agagacaagcctaccctctggaggagctcctgcctcatgcccattgagttcatcaaccagattatggctcctttaaaga
ggcaaaaatagaggaacatctggccaggctggaagctgtaacaaaggaaatagaaacaacaggaacctaccagctcactc
tggatgagctcatctttgccaccaagatggcctggaggaatgccctcgctgcatcggcaggatccagtggtccaacctg
caggtctttgacgctcggaaactgtagcacagcacaggaaatgtttcagcacatctgcagacacatactttatgccacaa
caatggcaacatcaggtcggccatcactgtgttccccagcggagtgacggcaaacatgacttcaggctctggaattcac
agctcatccggtagcgtggctaccagatgcccgatggcaccatcagaggggatgctgccaccttggagttcaccagttg
tgcacgacctaggctggaagccccgctatggccgctttgatgtgctgctctggcttgcgaagctgatggccaagatcc
agaggtctttgaaatccctcctgatcttgtgttggaggtgaccatggagcatccaagtacgagtggttccaggagctcg
ggttgaagtggatgcaactgctgcccgtggccaacatgctactggaggtgggtggcctcgaattcccagcctgcccttc
aatgggttggatcatgggcaccgagattggagttcgagacttctgtgacacacagcgtacaacatcctggaggaagtggg
ccgaaggatgggctggagacccacacactggcctccctctggaaagaccgggctgtcacggagatcaatgtggctgtgc
tccatagtttccagaagcagaatgtgaccatcatggaccaccacacagcctcagagtccttcatgaagcacatgcagaat
gagtaccgggcccgtggaggtgcccggcagactggatttggctgggtccctccagtgctctgggagcatcaccctgtgtt
ccaccaggagatgttgaactatgtcctatctccattctactactaccagatcgagccctggaagaccacatctggcaga
atgagaagctgagggcccaggaggagagatccgatttagagctcttgggtgaaagtgggtgttctttgcttccatgctaag
cgaaaggtcatggcttcacgggtcagagccacagtcctctttgctactgagacaggggaagtctgaagcactagccagggg
cctggccactctgttgcagctacgccttcaacccaaggttctgctgcatggaccagtataaggcaagcaccttggagagg
agcaactactgttgggtgcaagcacatttgggaatggagactgtcccagcaatgggcagactctgaagaaatctctg
ttcatgcttagagaactcaaccacaccttcaggatgctgtgttggccttggctccagcatgtaccctcagttctgccc
ctttgctcatgacatcgaccagaagctgtcccacctgggagcctctcagcttggcccaacaggagaaggggacgaactca
gtgggcaggaggatgccttccgcagctgggctgtacaaaccttccgggcagcctgtgagacctttgatgtccgaagcaaa
catcacattcagatcccgaacgcttccacttccaatgcaacatgggagccacagcaatataggctcatccagagcccgga
gccttttagacctcaacagagccctcagcagcatccatgcaagaacgtgtttaccatgaggctgaaatcccagcagaatc
tgcagagtgaaaagtccagccgcaccacctcctcgcttcagctcaccttcgagggcagccgagggcccagctacctgct
ggggaacacctggggatcttcccaggcaaccagaccgcccctgggtgcagggaaatcttggagcaggttgtggattgtcctac
accacaccaaactgtgtgctggaggttctggatgagagcggcagctactgggtcaaagacaagaggctgccccctgct
cactcagccaagccctcacctacttccctggacattacgacccctcccacccagctgcagctccacaagctggctcgctt
gccacggacgagacggataggcagagattggagggccttgtgtcagccctcagagtacaatgactggaagttcagcaacaa
ccccagttcctggaggtgcttgaagagttcccttcccttgcagtggtgcccgtgccttccctgctgtgcagctccctatct
tgaagccccgctactactccatcagctcctcccaggaccacacccccctcggaggttcacctcactgtggccgtggctcacc
taccgcacccgagatggctcaggggtccctgcaccatgggtgtctgcagcacttggatcaggaacctgaagccccaggacc
agtgcctgcttctgtgcaagtgctcagtggttccagctccctgaggacccctcccagccttgcacctcatttgggctg
gtacgggcattgtctcccttccgaagtttctggcagcagcggctccatgactcccagcacaaggggtcaaaggaggccgc
atgagcttgggtgttgggtgcccggcaccggaggaggaccacctctatcaggaagaaatgcaggagatgggtccgcaagag
agtgtgttccaggtgcacacaggctactcccggctgcccggcaacccaaggtctacgttccaggacatcctgcaaaagc
agctggccaatgaggtactcagcgtgctccacggggagcagggccacctctacatttgcggagatgtgcgcatggctcgg
gatgtggctaccacattgaagaagctgggtggcccaagctgaacttgagcagaggagcaggtggaagactatttctcca
gctcaagagccagaaacgttatcatgaagatatcttccggtgcagcttttccctatggggcaaaaaagggcagcgccttgg
aggag**gccc**aaagccagaggctctgacagcccagagttccagcttctggcactgagtaagataatgggtgaggggcttgg
ggagacagcgaatgcaatcccccccagcccctcatgtcattccccctcctccacctaccaagtagtattgtattat
tgtggactactaaatctctctc
ttctccttctcctccttggcctctcactcttcttggagctgagagcagagaaaaactcaacctcctgactgaagcactt
tgggtgaccaccaggaggaccatgccgcccgtctaaacttagctgcactatgtacagatattttatacttcatatttaa
gaaaacagatacttttgtctactcccaatgatggcttgggcttctctgtataattccttgatgaaaaatattttatataa
aatacatttttattttaatacaaaaaaaaaaagcggccgc

Sequencing result for iNOS-UTR

a. Sequencing results from T7 forward sequencing primer in iNOS-UTR DNA

NNCTTAAGCTTGGAGACTCTGGGCCCCACGGGACACAGTGTCACTGGTTTTGAAACTTCTCAGCCACCTTGGTGAAGGGAC
TGAGCTGTTAGAGACACTTCTGAGGCTCCTCACGCTTGGGTCTTGTTCACTCCACGGAGTAGCCTAGTCAACTGCAAGAG
AACGGAGAACGTTGGATTTGGAGCAGAAGTGCAAAGTCTCAGAC**ATGGCTTGCCCTGGAAGTTTC**TCTTCAAAGTCAAA
TCCTACCAAAGTGACCTGAAAGAGGAAAAGGACATTAACAACAACGTGAAGAAAACCCCTTGTGCTGTTCTCAGCCCAAC
AATACAAGATGACCCTAAGAGTCACCAAAATGGCTCCCCGCAGCTCCTCACTGGGACAGCACAGAATGTTCCAGAATCCC
TGGACAAGCTGCATGTGACATCGACCCGTCCACAGTATGTGAGGATCAAAAACCTGGGGCAGTGGAGAGATTTTGCATGAC
ACTCTTCACCACAAGGCCACATCGGATTTCACTTGCAAGTCCAAGTCTTGCTTGGGGTCCATCATGAACCCCAAGAGTTT
GACCAGAGGACCCAGAGACAAGCCTACCCCTCTGGAGGAGCTCCTGCCTCATGCCATTGAGTTCATCAACCAGTATTATG
GCTCCTTTAAAGAGGCCAAAATAGAGGAACATCTGGCCAGGCTGGAAGCTGTAACAAAGGAAATAGAAAACAACAGGAACC
TACCAGCTCACTCTGGATGAGCTCATCTTTGCCACCAAGATGGCCTGGAGGAATGCCCTCGCTGCATCGGCAGGATCCA
GTGGTCCAACCTGCAGGTCTTTGACGCTCGGAACTGTAGCACAGCACAGGAAATGTTTCAGCACATCTGCAGACACATAC
TTTATGCCACCAACAATGGCAACATCAGGTCCGCCATCACTGTGTTCCCCCAGCGGAGTGACGGCAAACATGACTTCAGG
CTCTGGAATTCACAGCTCATCCGGTACGCTAGCTACCAGATGCCCCGATGGCACCATCAGAAGGGGATGCTGCCACCTTGG
AGTTCACCCAGTTGTGCATCGACCTAGGCTGGAAGCCCCTATGGCCGCTTTGATGGGCTGCCTCGGGTCTTGCAAGCTG
AAGGTCAAGAATCAAAGGTCTTTGAAACCCCCCGGATCTNNGGTGGAGGGGACCTGGAGCCTCCAAGTAAAATGGGT
CCCGAACTCCGGTTTTAAAAGGGTTACCC

b. Sequencing results from BGHR reverse sequencing primer in iNOS-UTR DNA

NNNNNNNNNNNNNNNGGCCGCTTTTTTTTTTTTGGATTAAAATAAAATNTATTTTTATATAAAATATTTTTTCATCAAGGAATT
ATACAGGAAAGGCCCAAGCCATCATTGGGAGTAGACAAAAGTATCTGTTTTCTTAAATATGAAGTATAAAATATCTGTACA
TAGTGCAGCTAAGTATTAGAGCGGCGGCATGGTGCCTCCTGGTGGTCACCCAAAGTGCTTCAGTCAGGAGGTTGAGTTTT
TCTCTGCTCTCAGCTCCAAGGAAGAGTGAGAGGCAAAGGAGGAGAAGGAGAAGGAGGGAGCTGGGGAGTGAGAGAAGAAG
GAGGAAAGGGAGAGAGGGGGAGGGAGGAGAGGAGAGA

Reverse compliments DNA sequences for the sequencing results from BGHR reverse sequencing primer in iNOS-UTR DNA

TCTCTCCTCTCCTCCCTCCCCTCTCTCCCTTTCCCTCCCTTCTTCTCCACTCCCCAGCTCCCTCCTTCTCCTTCTCCTCCT
TTGCCTCTCACTCTTCCCTTGGAGCTGAGAGCAGAGAAAACTCAACCTCCTGACTGAAGCACTTTGGGTGACCACCAGGA
GGCACCATGCCGCCGCTCTAATACTTAGCTGCACTATGTACAGATATTTATACTTCATATTTAAGAAAACAGATACTTTT
GTCTACTCCCAATGATGGCTTGGGCCTTTCCCTGTATAATTCCTTGATGAAAAATATTTATATAAAATANATTTTTATTTTA
ATC

Multialignment of sequencing results for iNOS-UTR using Multalin Interface Page tool

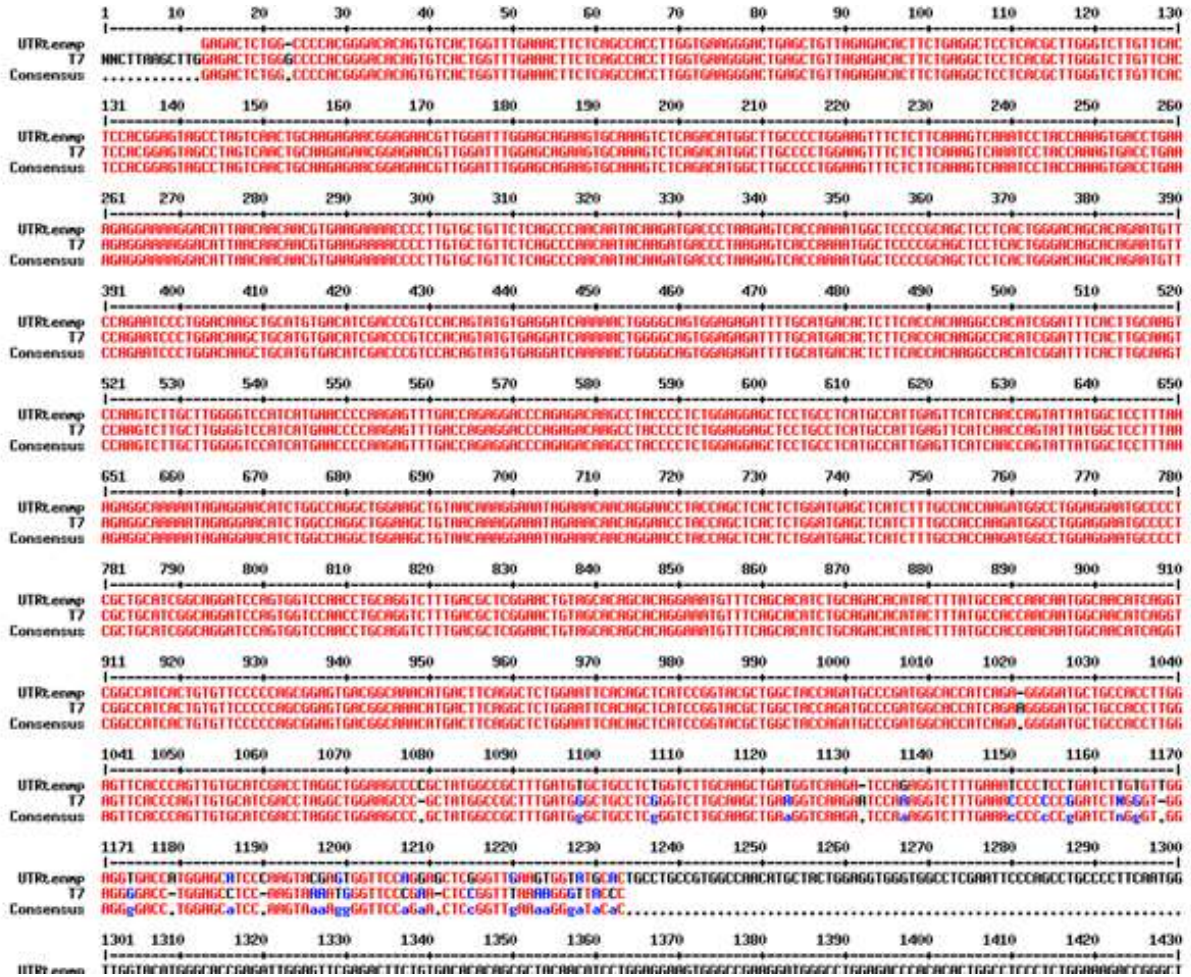
High consensus colour: red

Low consensus colour: blue

Neutral colour: black

High consensus value: 90 % (default: 90%)

Low consensus value: 50% (default: 50 %)



Appendix IV. Sequencing results for iNOS-CDS-in-frame-V5 insert

The authenticity of iNOS-CDS in-frame with V5 insert (**Table 5.2.3**) in the construct iNOS-CDS-V5-tagged 3.1/V5-His-TOPO Hygro (**Fig 4.3.13**) was confirmed by sequencing using T7 and BGHR universal sequencing primers and showed below.

Table 5.1.3. Specification and properties of V5 epitope tag

Specifications of V5 tag	Properties
Epitope	C-terminal
Number of amino acids	14
Amino acid sequence	GKPIP NPLLGLDST
DNA sequence	GGT AAG CCT ATC CCT AAC CCT CTC CTC GGT CTC GAT TCT ACG
Molecular weight (MW)	1.423 Da

Designed primers

iNOS-CDS-ATG-FP-HindIII: 5' **TATAAGCTTGAC**ATGGCTTGCCCCTGGAAGTTTC 3' (T_m 64.2°C)

iNOS-CDS-TGA-RP-XbaI: 5' GCCCAAAGCCACGAGGCTCTG**TCTAGATAT** 3' (T_m 64°C)

Template DNA sequences of insert iNOS-CDS-IF-V5

atggcttgcccctggaagtttctcttcaaagtc aaatcctaccaaagtgacctgaaagaggaaaaggacattaacaacaa
cgtgaagaaaaacccttgtgctgttctcagcccaacaatacaagatgaccctaagagtcacccaaaatggctccccgcagc
tcctcactgggacagcacagaatgttccagaatccctggacaagctgcatgtgacatcgacccgtccacagtatgtgagg
atcaaaaactggggcagtgagagatgttgcacacactctccaccacaaggccacatcggatctcacttgcaagtccaa
gtccttgcttggggccatcatgaaccccaagagtttgaccagaggaccagagacaagcctaccctctggaggagctcc
tgcctcatgcccattgagttcatcaaccagatattatggctcctttaaagaggcaaaaatagaggaacatctggccaggctg
gaagctgtaacaaaggaaatagaaacaacaggaacctaccagctcactctggatgagctcatcttggccaccaagatggc
ctggaggaaatgcccctcgctgcatcggcaggatccagtggtccaacctgcaggctcttggacgctcggaaactgtagcacag
cacaggaaatgttccagcacatctgcagacacatactttagccaccaacaatggcaacatcaggctcggccatcactgtg
ttccccagcggagtgacggcaaacatgacttcaggctctggaattcacagctcatccggtacgctggctaccagatgcc
cgatggcaccatcagaggggatgctgccaccttggagttcaccagttgtgcatcgacctaggctggaagccccgctatg
gccgctttagatgtgctgctcctctggtcttgcaagctgatggtcaagatccagaggtcttggaaatccctcctgatctt
ttggaggtgacctggagcatcccaagtcagagtggttccaggagctcgggttgaagtggtatgacctgctgcccgtggc
caacatgctactggaggtgggtggcctcgaattcccagcctgccccttcaatgggttggtacatgggcaccgagattggag
ttcgagacttctgtgacacacagcgtacaacatcctggaggaaagtgggccgaaggatgggcctggagaccacacactg
gcctccctctggaagaccgggctgtcacggagatcaatgtggctgtgctccatagttccagaagcagaatgtgacct
catggaccaccacacagcctcagagtccttcatgaagcacatgcagaatgagtagcggggcccgtggaggctgcccggcag
actggatcttggctggctccctccagtgctgggagcatcaccctgtgttccaccaggagatggtgaaactatgtcctatct
ccatttactactaccagatcgagccctggaagaccacatctggcagaatgagaagctgaggcccaggaggagagagat
ccgatttagagctcttgggtgaaagtggtgttcttggcttccatgctaagtcgaaaggctcatggcttcacgggtcagagcca
cagtcctcttggctactgagacaggaagtctgaagcactagccaggacctggccaccttggctcagctacgccttcaac
accaaggttgtctgcatggaccagtataaggcaagcaccttggaaagaggagcaactactgctggtggtgacaagcatt
tgggaatggagactgtcccagcaatgggcagactctgaagaaatctctgttcatgcttagagaactcaaccacacctca
ggatgctgtgttggccttggctccagcatgtaccctcagttctgctgcttggctcatgacatcgaccagaagctgtcc
cacctgggagcctctcagcttggcccaacaggagaaggggacgaactcagtgggcaggaggatgccttccgcagctgggc
tgtacaaaccttccgggcagcctgtgagacctttagatgtccgaagcaaacatcacattcagatcccgaacgcttcaact
ccaatgcaacatgggagccacagcaatataggtcctcagagcccggagcctttagacctcaacagagccctcagcagc
atccatgcaaaagacgtgtttaccatgaggctgaaatcccagcagaatctgcagagtgaaaagtcagccgcaccacct
cctcgttcagctcaccttcgagggcagccgagggcccagctacctgctggggaaacacctggggatcttcccagggaacc
agaccgcccctggtgcagggaaatcttggagcagattgtggattgtcctacaccacacaaactgtgtgacctggaggttctg

gatgagagcggcagctactgggtcaaagacaagaggctgccccctgctcactcagccaagccctcacctacttctgga
cattacgacccctcccaccagctgcagctccacaagctggctcgctttgccacggacgagacggataggcagagattgg
aggccttgtgtcagccctcagagtacaatgactggaagttcagcaacaacccacgcttctggagggtgcttgaagagttc
ccttcttgcagtgcccgcgtgccttctgctgctgcagctccctatcttgaagccccgctactactccatcagctcctc
ccaggaccacacccccctcggagggtcacctcactgtggccgtggtcacctaccgacccgagatggtcagggtcccctgc
accatgggtgctcagcacttggatcaggaacctgaagcccaggacccagtgccctgcttgggtgccaaggtgctcagtggc
ttccagctccctgaggacccctcccagccttgcatectcattgggctggtaacgggcattgctcccttccgaagttctg
gcagcagcggctccatgactcccagcacaagggctcaaaggaggccgcatgagcttgggtggttgggtgcccggcaccgg
aggaggaccacctctatcaggaagaaatgcaggagatggctccgcaagagagtgctgttccagggtgcacacagggtactcc
cggctgcccggcaaacccaaggtctacgttcaggacatcctgcaaaagcagctggccaatgaggtactcagcgtgctcca
cggggagcagggccacctctacatttgcggagatgtgcgcagtgctcgggatgtgggtaccacattgaagaagctgggg
ccaccaagctgaacttgagcggaggagcaggtggaagactatttctccagctcaagagccagaacggttatcatgaagat
atcttcgggtcagctcttctcctatggggcaaaaaagggcagcgccttggaggagcccaagccacgaggtctgTCTAGA
GGGCCCGGGTTCGAAGGTAAGCCTATCCCTAACCTCTCCTCGGTCTCGATTCTACGCGTACCGGTCATCATCACCATC
ACCATTGA

Amino acid sequences for NOS-CDS-IF-V5

MACPWKFLFKVKSQSDLKEEKDINNKKTPCAVLSPTIQDDPKSHQNGSPQLLTGTAQNVPESLDKLHVTSTRPQYVR
IKNWGSGEILHDTLHHKATSDFTCKSKSCLGSIMNPKSLTRGPRDKPTPLEELLPHAIIEFINQYYGSFKEAKIEEHLARL
EAVTKEIETTGTYYQLTLELIFATKMAWRNAPRCIGRIQWSNLQVFDARNCSTAQEMFQHIRHILYATNNGNIRSAITV
FPQRS DGKHFRLWNSQLIRYAGYQMPDGTIRGDAATLEFTQLCIDLGWKPRYGRFDVLPVLQADQDPEVFEI PPDLV
LEV TMEHPKYEFQELGLKWIYALPAVANMLLEVGGLFACPFNGWYMGTEIGVRDFCDTQRYNILEEVGRRMGLTHTL
ASLWKDRAVTEINVAVLHSFQKQNVTIMDHHTASESFMKHMONEYRARGGCPADWIWLVPVSGSITPVFHQEMLNIVLS
PFYYYQIEPWKTHIWQNEKLRPRRREIRFRVLVKVVFASMLMRKVMASRVRAVLFATETGKSEALARDLATLFSYAFN
TKVVCMDQYKASTLEEEQLLLVVTSTFGNGDCPSNGQTLKKSFLMRELNHTFRYAVFGLGSSMYPQFCFAHDIQKLS
HLGASQLAPTGGDELSGQEDAFRSWAVQTFRAACETFDVRSKHHIQIPKRFTSNATWEPQYRLIQSPEPLDLNRALSS
IHAKNVFTMRKLSQQNLQSEKSSRTLLVQLTFEGSRGPSYLPGEHLGIFPGNQTALVQGILERVVDCPTPHQTVCLEVL
DESGSYVWKDKRLPPCSLSQALTYFLDITTPPTQLQLHKLARFATDETDRQRLEALCQPSEYNDWKFSSNNPTFLEVLEEF
PSLHVPAAFLLSQLPILKPRYYSISSQDHTPSEVHLTVAVVTYRTRDGGQPLHHGVCSTWIRNLKQDPVPCFVRSVSG
FQLPEDPSQPCILIGPGTGIAPFRSFWQRLHDSQHKLKGGRMSLVFGCRHPEEDHLYQEEMQEMVRKRVLFQVHTGYS
RLPGKPKVYVQDILQKQLANEVLSVLHGEQGHLYICGDVRMARDVATTLKKLVA TKLNLSEEQVEDYFFQLKSQKRYHED
IFGAVFSYGAKKGSAL EEPKATRLCLEGPRFE **GKPIPNLLGLDST**RTGHHHHH

Sequencing result for iNOS-CDS- IF-V5

a. Sequence results from T7 forward sequencing primer

TTTGAATGGGCTTGCCCTGGGAAGTTTCTCTTCAAAGTCAAATCCTACCAAAGTGACCTGAAAGAGGAAAAGGACATTA
ACAACAACGTGAAGAAAACCCCTTGTGCTGTTCTCAGCCCAACAATAACAAGATGACCCTAAGAGTCACCAAAATGGCTCC
CCGACGCTCCTCACTGGGACAGCACAGAATGTTCCAGAATCCCTGGACAAGCTGCATGTGACATCGACCCGTCACAGTA
TGTGAGGATCAAAAAGTGGGACAGTGGAGAGATTTGCATGACACTCTCACCACAAGGCCACATCGGATTTCACTTGCA
AGTCCAAGTCTTGCTTGGGGTCCATCATGAACCCCAAGAGTTTGACCAGAGGACCCAGAGACAAGCCTACCCCTCTGGAG
GAGCTCCTGCCTCATGCCATTGAGTTCATCAACCAGTATTATGGCTCCTTTAAAGAGGCAAAAATAGAGGAACATCTGGC
CAGGCTGGAAGCTGTAACAAAGGAAATAGAAAACAACAGGAACCTACCAGCTCACTCTGGATGAGCTCATCTTTGCCACCA
AGATGGCCTGGAGGAATGCCCTCGCTGCATCGGCAGGATCCAGTGGTCCAACCTGCAGGTCTTTGACGCTCGGAACTGT
AGCACAGCACAGGAAATGTTTCAGCACATCTGCAGACACATACTTTATGCCACCAACAATGGCAACATCAGGTGGCCAT
CACTGTGTTCCCCCAGCGGAGTGACGGCAAACATGACTTCAGGCTCTGGAATTCACAGCTCATCCGGTACGCTGGCTACC
AGATGCCCAGTGGCACCATCAGAGGGGATGCTGCCACCTTGGAGTTCACCCAGTTGTGCATCGACCTAGGCTGGAAGCCC
CGCTATGGCCGCTTTGATGTGCTGCCTCTGGTCTTGCAAGCTGATGGTCAAGATCCAGAGGTCTTTGAAATCCCTCCTGA
TCTTGTGTTGGAGGTGACCATGGAGCATCCAAGTACGAGTGGTTCAGGAGCTCGGGTTGAAGTGGTATGCACTGCCTG
CCGTGGCAACATGCTACTGGAGGTGGGTGGCCTCGAATTCACAGCCTGCCCTTCATGGTTGGTACTGGGCACCGAGAT
TGGAGTTCGAGACTTCTGTGANCCCCAGCGCTACAACATCCTGGAAGAAGGGGGCCGAAGGATGGGCCTGGAAACCCACC
CCTGGCCTCCCCNGGAAAGACGGGCTGTCCGGAAGAAAAGGGGGTGGGTCCCATTTTTCCAAAAAAAAGGGCANNNTGG
GANACCCCAACCCAAAATCTNNGAAAAAAGGGAAAAAGAACGGGGCCGGGGGGGGCCCNAAAAAAGGATTTGGGGGGC
CCCCCGGNNNGGGAAACNNCCCCTGTTTCCCCCAGGNAAGATNTAAATNTTCTCTCTTTTCTTCAANAANNGGAA
AAA

Translation of DNA sequences to a protein sequence using ExPASy Translate tool

LNGLAPGKFLFKVKSYSQSDLKEEKDINNNVKKTPCAVLSPTIQDDPKSHQNGSPQLLTGTAQNVPESLDKLHVTSTRPQY
VRIKNWGSGEILHDTLHHKATSDFTCCKSKSCLGSIIMNPKSLTRGPRDKPTPLEELLPHAEFINQYYGSFKEAKIEEHLA
RLEAVTKEIETTGTYYQLTLELIFATKMAWRNAPRCIGRIQWSNLQVFDARNCSTAQEMFQHCRIHILYATNNGNIRSAI
TVFPQRS DGKHDFRLWNSQLIRYAGYQMPDGTIRGDAATLEFTQLCIDLGWKPRYGRFDVLPVLVQADGQDPEVFEIPPD
LVLEVTMEHPKYEFQELGLKQYALPAVANMLLEVGGLEFPACPFMVGTGHRDWSSRLI

b. Sequence results from BGHR reverse sequencing primer

TTTGGTGATGGTGATGATGACCGGGTACGCGTAGAATCGAGACCGAGGAGAGGGTTAGGGATAGGCTTACCTTCGAACCG
CGGGCCCTCTAGACAGAGCCTCGTGGCTTTGGGCTCCTCCAAGGCGCTGCCCTTTTTTGCCCCATAGGAAAAGACTGCAC
CGAAGATATCTTCATGATAACGTTTCTGGCTCTTGAGCTGGAAGAAATAGTCTCCACCTGCTCCTCGCTCAAGTTCAGC
TTGGTGGCCACCAGCTTCTTCAATGTGGTAGCCACATCCCAGCCATGCGCACATCTCCGCAAATGTAGAGGTGGCCCTG
CTCCCCGTGGAGCACGCTGAGTACCTCATTGGCCAGCTGCTTTTGCAGGATGTCCTGAACGTAGACCTTGGGTTTGCCGG
GCAGCCGGGAGTAGCCTGTGTGCACCTGGAACAGCACTCTCTTGCAGGACCATCTCCTGCATTTCTTCTGATAGAGGTGG
TCCTCCTCCGGGTGCCGGCACCCAAACACCAAGCTCATGCGGCCCTCCTTTGAGCCCTTTGTGCTGGGAGTCATGGAGCCG
CTGCTGCCAGAACTTCGGAAGGGAGCAATGCCCGTACCAGGCCCAATGAGGATGCAAGGCTGGGAGGGGTCTCAGGGA
GCTGGAAGCCACTGACACTTCGCACAAAGCAGGGCACTGGGTCTGGGGCTTCAGGTTCTGATCCAAGTGTGCAGACA
CCATGGTGCAGGGGACCCTGACCATCTCGGGTGCAGTAGGTGACCACGGCCACAGTGAGGTGAACCTCCGAGGGGGTGTG
GTCCTGGGAGGAGCTGATGGAGTAGTAGCGGGCTTCAAGATAGGGAGCTGCGACAGCAGGAAGGCAGCGGGCACATGCA
AGGAAGGAACTCTTCAAGCACCTCCAGGAACGTGGGGTGTGTTGCTGAACCTCCAGTCACTTGTACTCTGAGGGCTGACAC
AAGGCCTCCAATCTCTGCCTATCCGTCTCGTCCGTGGCAAAGCGAGCCAGCTTGTGGAGCTGCACCTGGGTGGGAGGGGT
CGTAATGTCCAGGAAGTAAGTGAAGGCTTGGCTGAATGAGCAGGGGGGCGAGCCTCTTGTCTTTGACCCAGTAGCTGCCGC
TCTNATCCAGAACCTCCAGGCAACCAGTTTGGGGGGGGGGAGGAAAATCCCAACTCCCTCCAGAATTCCTGCCCCAGG
GCGGTTGGGTTGCTGGGAAAATCCCNNGGGTTCCTCCAGGAGGAACTGGGCCCTCCGCTTCCCCCAAANNNGAAACA
AAAAANNAGGGGGGGGGGGGGGGGATTTTTCCCTTGAAATTCNNGGGATTTNNCCCCGGGAAAATTTTTTGGGGGGG
GGGGGNGCTTGNNAGAAAAGGCCCGGCTTGAAAANNAATATTTGTTGGCGCCCCCTTTTTTTNNNAAAAAACT
TCGGNTAAAGAGGGTNNTTTTTCNAAAAAAACCCNGCC

Reverse compliments DNA sequences for the sequence results from BGHR reverse sequencing primer

GGCNGGGGTTTTTTTTNGAAAAANNACCCTCTTTANCCCGAAGTTTTTTTTNNNAAAAAAAAGGGGGCGCCACAAATATTN
NTTTTCCAAGCCGGGGCCTTTTTCTNNNCAAGCNCCCCCCCCCCCCCAAAAATTTTTCCCGGNAAATCCCNGGAATTT
CCAAGGGAAAATCCCGCCCCCCCCCTCNNTTTTTTGTTCNNNTTTGGGGGGAGCGGAGGGCCAGTTCCTCCTGG
GGGAACCCNNGGGATTTTTCCCAGCAACCCAACCGCCCTGGGGCAGGAATTCGGAGGGAGTTGGGGATTTTTCTCCCC
CCCCCAAACCTGGTTGCCTGGAGGTTCTGGATNAGAGCGGCAGCTACTGGGTCAAAGACAAGAGGCTGCCCCCTGCTCA
TTCAGCCAAGCCTTCACTTACTTCTGGACATTACGACCCCTCCCACCCAGGTGCAGCTCCACAAGCTGGCTCGCTTTC
CACGGACGAGACGGATAGGCAGAGATTGGAGGCCTTGTGTGAGCCCTCAGAGTACAATGACTGGAAGTTCAGCAACAACC
CCACGTTTCTGGAGGTGCTTGAAGAGTTCCTTTCCTTGCATGTGCCCCGCTGCCTTCTGCTGTGCGAGCTCCCTATCTTG
AAGCCCCGCTACTACTCCATCAGCTCCTCCCAGGACCACACCCCTCGGAGGTTACCTCACTGTGGCCGTGGTACCTA
CCGACCCCGAGATGGTCAGGGTCCCCTGCACCATGGTGTCTGCAGCACTTGGATCAGGAACCTGAAGCCCCAGGACCCAG
TGCCCTGCTTTGTGCGAAGTGTGAGTGGCTTCCAGCTCCCTGAGGACCCCTCCAGCCTTGCATCCTCATTGGGCCTGGT
ACGGGCATTGCTCCCTTCCGAAGTTTTCTGGCAGCAGCGGCTCCATGACTCCAGCACAAAGGGCTCAAAGGAGGCCGCAT
GAGCTTGGTGTGGGTGCCGGCACCCGGAGGAGGACCCTCTATCAGGAAGAAATGCAGGAGATGGTCCGCAAGAGAG
TGCTGTTCCAGGTGCACACAGGCTACTCCCAGGCTGCCCGGCAAACCCAAGGTCTACGTTCCAGGACATCCTGCAAAAGCAG
CTGGCCAATGAGGTAAGTACTCAGCGTGTCCACGGGGAGCAGGGCCACCTCTACATTTGCGGAGATGTGCGCATGGCTCGGGA
TGTGGCTACCACATTGAAGAAGCTGGTGGCCACCAAGCTGAACTTGAGCGAGGAGCAGGTGGAAGACTATTTCTCCAGC
TCAAGAGCCAGAAACGTTATCATGAAGATATCTTCGGTGCAGTCTTTTCTATGGGGCAAAAAGGGCAGCGCCTTGGAG
GAGCCCAAAGCCAGGAGCTCTGTCTAGAGGGCCCGGTTGAAAGGTAAGCCTATCCCTAACCTCTCCTCGGTCTCGA
TTCTACGCGTACCCGGTTCATCATCACCATCACAAA

Translation of DNA sequences to a protein sequence using ExPASy Translate tool

GIFPSNPTALGQEFWRELGIIFLPPPQTGCLEVLDXSGSYWVKDKRLPPCSFSQAFTYFLDITPPTQVQLHKLARFATDE
TDRQRLEALCQPSEYNDWKFSSNNPTFLEVL EEFPSLHVPAAFLLSQLPILKPRYYSISSSQDHTPSEVHLTVAVVTYRTR
DGQGPLHHGVCSTWIRNLKPQDPVPCFVRSVSGFQLPEDPSQPCILIGPGTGIAPFRSFWQRLHDSQHKGLKGGMSLV

FGCRHPEEDHLYQEEMQEMVRKRVLFQVHTGYSRLPGKPKVYVQDILQKQLANEVLSVLHGEQGHLYICGDVVMARDVAT
TLKKLVATKLNLSSEEQVEDYFFQLKSQKRYHEDI FGAVFSYGAKKGSAL EEPKATRLCLEGPRFEGKPIPNPLLLGLDSTR
TRSSSPSP

Multialignment of sequencing results using Multalin Interface Page tool

High consensus colour: red

Low consensus colour: blue

Neutral colour: black

High consensus value: 90 % (default: 90%)

Low consensus value: 50% (default: 50 %)

